United States Nuclear Regulatory Commission Official Hearing Exhibit
In the Matter of: Entergy Nuclear Operations, Inc.
(Indian Point Nuclear Generating Units 2 and 3)
ASLBP #: 07-858-03-LR-BD01
Docket #: 05000247 | 05000286
Exhibit #: ENT000456-00-BD01
Identified: 10/15/2012
Admitted: 10/15/2012
Withdrawn:
Rejected:
Stricken:
Other:

ENT000456
Submitted: March 30, 2012

U.S.NRC
United States Nuclear Regulatory Commission
Protecting People and the Environment

NUREG/CR-7110, Vol. 1

State-of-the-Art Reactor Consequence Analyses Project

Volume 1: Peach Bottom Integrated Analysis

Office of Nuclear Regulatory Research

AVAILABILITY OF REFERENCE MATERIALS IN NRC PUBLICATIONS

NRC Reference Material

As of November 1999, you may electronically access NUREG-series publications and other NRC records at NRC's Public Electronic Reading Room at http://www.nrc.gov/reading-rm.html.
Publicly released records include, to name a few, NUREG-series publications; *Federal Register* notices; applicant, licensee, and vendor documents and correspondence; NRC correspondence and internal memoranda; bulletins and information notices; inspection and investigative reports; licensee event reports; and Commission papers and their attachments.

NRC publications in the NUREG series, NRC regulations, and *Title 10, Energy*, in the Code of *Federal Regulations* may also be purchased from one of these two sources.

1. The Superintendent of Documents
   U.S. Government Printing Office
   Mail Stop SSOP
   Washington, DC 20402–0001
   Internet: bookstore.gpo.gov
   Telephone: 202-512-1800
   Fax: 202-512-2250
2. The National Technical Information Service
   Springfield, VA 22161–0002
   www.ntis.gov
   1–800–553–6847 or, locally, 703–605–6000

A single copy of each NRC draft report for comment is available free, to the extent of supply, upon written request as follows:
Address: U.S. Nuclear Regulatory Commission
Office of Administration
Publications Branch
Washington, DC 20555-0001
E-mail: DISTRIBUTION.SERVICES@NRC.GOV
Facsimile: 301–415–2289

Some publications in the NUREG series that are posted at NRC's Web site address http://www.nrc.gov/reading-rm/doc-collections/nuregs are updated periodically and may differ from the last printed version. Although references to material found on a Web site bear the date the material was accessed, the material available on the date cited may subsequently be removed from the site.

Non-NRC Reference Material

Documents available from public and special technical libraries include all open literature items, such as books, journal articles, and transactions, *Federal Register* notices, Federal and State legislation, and congressional reports. Such documents as theses, dissertations, foreign reports and translations, and non-NRC conference proceedings may be purchased from their sponsoring organization.

Copies of industry codes and standards used in a substantive manner in the NRC regulatory process are maintained at—
The NRC Technical Library
Two White Flint North
11545 Rockville Pike
Rockville, MD 20852–2738

These standards are available in the library for reference use by the public. Codes and standards are usually copyrighted and may be purchased from the originating organization or, if they are American National Standards, from—
American National Standards Institute
11 West 42nd Street
New York, NY 10036–8002
www.ansi.org
212–642–4900

Legally binding regulatory requirements are stated only in laws; NRC regulations; licenses, including technical specifications; or orders, not in NUREG-series publications. The views expressed in contractor-prepared publications in this series are not necessarily those of the NRC.

The NUREG series comprises (1) technical and administrative reports and books prepared by the staff (NUREG–XXXX) or agency contractors (NUREG/CR–XXXX), (2) proceedings of conferences (NUREG/CP–XXXX), (3) reports resulting from international agreements (NUREG/IA–XXXX), (4) brochures (NUREG/BR–XXXX), and (5) compilations of legal decisions and orders of the Commission and Atomic and Safety Licensing Boards and of Directors' decisions under Section 2.206 of NRC's regulations (NUREG–0750).

United States Nuclear Regulatory Commission

Protecting People and the Environment

NUREG/CR-7110, Vol. 1

State-of-the-Art Reactor Consequence Analyses Project

Volume 1: Peach Bottom Integrated Analysis

Manuscript Completed: January 2012
Date Published: January 2012

Prepared by:
Sandia National Laboratories
Albuquerque, New Mexico 87185
Operated for the U.S. Department of Energy

NRC Job Code N6306

Office of Nuclear Regulatory Research

Sandia National Laboratories is a multi-program laboratory managed and operated by Sandia Corporation, a wholly owned subsidiary of Lockheed Martin Corporation, for the U.S. Department of Energy's National Nuclear Security Administration under contract DE-AC04-94AL85000.

ABSTRACT

The evaluation of accident phenomena and the offsite consequences of severe reactor accidents has been the subject of considerable research by the U.S. Nuclear Regulatory Commission (NRC) over the last several decades. As a consequence of this research focus, analyses of severe accidents at nuclear power reactors are more detailed, integrated, and realistic than at any time in the past. A desire to leverage this capability to address conservative aspects of previous reactor accident analysis efforts was a major motivating factor in the genesis of the State-of-the-Art Reactor Consequence Analysis (SOARCA) project. By applying modern analysis tools and techniques, the SOARCA project developed a body of knowledge regarding the realistic outcomes of severe reactor accidents. To accomplish this objective, the SOARCA project used integrated modeling of accident progression and offsite consequences using both state-of-the-art computational analysis tools and best modeling practices drawn from the collective wisdom of the severe accident analysis community. This study focused on providing a realistic evaluation of accident progression, source term, and offsite consequences for the Peach Bottom Nuclear Power Station. By using the most current emergency preparedness practices, plant capabilities, and best available modeling, these analyses are more detailed, integrated, and realistic than past analyses. These analyses also consider all mitigative measures, contributing to a more realistic evaluation.

PAPERWORK REDUCTION ACT STATEMENT

This NUREG contains and references information collection requirements that are subject to the Paperwork Reduction Act of 1995 (44 U.S.C. 3501 et seq.). These information collection requirements were approved by the Office of Management and Budget, approval number 3150-0011.

PUBLIC PROTECTION NOTIFICATION

The NRC may not conduct or sponsor, and a person is not required to respond to, a request for information or an information collection requirement unless the requesting document displays a currently valid OMB control number.

TABLE OF CONTENTS

ABSTRACT iii

TABLE OF CONTENTS v

LIST OF FIGURES ix

LIST OF TABLES xvii

EXECUTIVE SUMMARY xxi

ACKNOWLEDGEMENTS xxxi

ACRONYMS xxxiii

1.0 INTRODUCTION 1
- 1.1 Background 1
- 1.2 Objective 2
- 1.3 Outline 3

2.0 ACCIDENT SCENARIO DEVELOPMENT 5
- 2.1 Sequences Initiated by Internal Events 5
- 2.2 Sequences Initiated by External Events 6
- 2.3 Mitigation Measures 7

3.0 ACCIDENT SCENARIO DEFINITIONS 9
- 3.1 Long-Term Station Blackout 9
  - 3.1.1 Initiating Event 9
  - 3.1.2 System Availabilities 9
  - 3.1.3 Operator Actions and Mitigation Measures 10
  - 3.1.4 Scenario Boundary Conditions 11
- 3.2 Short Term Station Blackout 16
  - 3.2.1 Initiating Event 16
  - 3.2.2 System Availabilities 17
  - 3.2.3 Mitigative Actions 17
  - 3.2.4 Scenario Boundary Conditions 18
- 3.3 Loss of Vital Alternating Current Bus E-12 19
  - 3.3.1 Initiating Event 20
  - 3.3.2 System Availabilities 20
  - 3.3.3 Mitigative Actions 20
  - 3.3.4 Scenario Boundary Conditions 21

4.0 MELCOR MODEL OF THE PEACH BOTTOM PLANT 25
- 4.1 Reactor Vessel and Coolant System 26
- 4.2 In-vessel Structures and Reactor Core 28
  - 4.2.1 General Configuration of MELCOR In-vessel Nodalization 28
  - 4.2.2 Treatment of Unique Design Features of a BWR Core 32
  - 4.2.3 In-vessel Structures above the Core 35
  - 4.2.4 Leakage through In-core Instrument Tubes 35
- 4.3 Primary Containment and Reactor Building 38
- 4.4 Mechanisms for Induced RPV Depressurization 42

4.4.1 Historical Development of BWR RPV Depressurization Mechanisms 42
4.4.2 Modeling Approach in SOARCA 47
4.5 Behavior of Ex-Vessel Drywell Floor Debris 57
4.6 Containment Failure Model 59
4.7 Radionuclide Inventories and Decay Heat 62
4.8 Other Modeling Issues and Uncertainties 63
4.8.1 Base Case Approach on Important Phenomena 64
4.8.2 Early Containment Failure Phenomena 67

5.0 INTEGRATED THERMAL HYDRAULICS, ACCIDENT PROGRESSION, AND RADIOLOGICAL RELEASE ANALYSIS 69
5.1 Long-Term Station Blackout – Unmitigated Response 69
5.1.1 Thermal Hydraulic Response 71
5.1.2 Radionuclide Release 81
5.2 Long-Term Station Blackout with Mitigation 89
5.2.1 Thermal Hydraulic Response 90
5.2.2 Radionuclide Release 95
5.3 Short-Term Station Blackout with RCIC Blackstart 95
5.3.1 Thermal Hydraulic Response 95
5.3.2 Radionuclide Release 103
5.4 Short-Term Station Blackout- Sensitivity Case without RCIC Blackstart 106
5.4.1 Thermal Hydraulic Response 107
5.4.2 Radionuclide Release 113
5.5 SBO Sensitivity Cases with Alternate SRV Failure Criteria 119
5.5.1 Reasonable variations in failure criteria 120
5.5.2 Extreme variations in failure criteria 128
5.6 Loss of Vital AC Bus E-12 – Sensitivity Cases without B.5.b Equipment 131
5.6.1 Thermal Hydraulic Response 132
5.6.2 Radionuclide Release 135
5.6.3 Sensitivity Analysis 135
5.7 Peer Review 138
5.7.1 Containment Leakage before Failure 138
5.7.2 Atmospheric Mixing in the Drywell 139
5.7.3 Leakage through TIP guide tubes 142
5.8 Barium Release Variations 147

6.0 EMERGENCY RESPONSE 153
6.1 Population Attributes 155
6.1.1 Population Distribution 157
6.1.2 Evacuation Time Estimates 157
6.2 WinMACCS 159
6.2.1 Hotspot and Normal Relocation and Habitability 159
6.2.2 Shielding Factors 160
6.2.3 Potassium Iodide 160
6.2.4 Adverse Weather 161
6.2.5 Modeling Using Evacuation Time Estimates 161
6.2.6 Cohort Modeling 163
6.3 Accident Scenarios 163

6.3.1 Long-Term Station Blackout Unmitigated 163
6.3.2 Short-Term Station Blackout with Reactor Core Isolation Cooling Blackstart..... 167
6.3.3 Short-Term Station Blackout without Reactor Core Isolation Cooling Blackstart. 170
6.4 Sensitivity Studies..... 172
6.4.1 Sensitivity 1 for the STSBO w/o RCIC Blackstart Evacuation to 16 Miles..... 174
6.4.2 Sensitivity 2 for the STSBO without RCIC Blackstart Evacuation to 20 Miles 177
6.4.3 Sensitivity 3 for STSBO w/o RCIC Blackstart - Delay in Protective Actions 179
6.5 Analysis of Earthquake Impact..... 181
6.5.1 Soils Review 181
6.5.2 Infrastructure Analysis..... 182
6.5.3 Electrical Power and Communications..... 185
6.5.4 Emergency Response..... 186
6.5.5 Development of WinMACCS Parameters..... 187
6.5.6 Seismic Short-Term Station Blackout without RCIC Blackstart..... 187
6.6 Accident Response and Mitigation of Source Terms 190
6.6.1 External Resources..... 194
6.6.2 Mitigation..... 195
6.7 Emergency Preparedness Summary and Conclusions 199

7.0 OFF-SITE CONSEQUENCES..... 203
7.1 Introduction..... 203
7.2 Peach Bottom Source Terms..... 204
7.3 Consequence Analyses..... 204
7.3.1 Unmitigated Long-Term Station Blackout Scenario 205
7.3.2 Short-Term Station Blackout with Reactor Core Isolation Cooling Blackstart..... 210
7.3.3 Unmitigated Short-Term Station Blackout without RCIC Blackstart 212
7.3.4 Evaluation of the Effect of Seismic Activity on Emergency Response..... 217
7.3.5 Evaluation of SST1 Source Term 218
7.3.6 Comparison with the 1982 Siting Study 222
7.3.7 Surface Roughness..... 228
7.3.8 Importance of Chemical Classes..... 231

8.0 REFERENCES..... 249

APPENDIX A PEACH BOTTOM RADIONUCLIDE INVENTORY..... A-1

APPENDIX B INPUT PARAMETERS FOR CONSEQUENCE ANALYSIS B-1

LIST OF FIGURES

Figure 4-1 Reactor vessel cross-section detail and MELCOR hydrodynamic nodalization 27
Figure 4-2 Spatial nodalization of reactor pressure vessel and coolant system 29
Figure 4-3 Spatial nodalization of the core and lower plenum 30
Figure 4-4 Local relative power fraction and five ring radial boundaries of core 31
Figure 4-5 Module of Four BWR Fuel Assemblies and Associated Channel Boxes....33
Figure 4-6 BWR Lower Plenum Structures 34
Figure 4-7 Potential containment bypass transport pathway through open TIP guide tubes 36
Figure 4-8 Layout of the TIP system....37
Figure 4-9 Hydrodynamic nodalization of the primary containment....39
Figure 4-10 Hydrodynamic nodalization of the reactor building (a)....40
Figure 4-11 Hydrodynamic nodalization of the reactor building (b)....41
Figure 4-12 Two-stage Target Rock pilot-operated safety relief valve....44
Figure 4-13 Crosby safety relief valve....45
Figure 4-14 Valve stem assembly within valve body....50
Figure 4-15 Arrangement of 1-dimensional safety relief valve heat-up calculation 51
Figure 4-16 Number of safety relief valve cycles from preliminary LTSBO calculation 52
Figure 4-17 Gas velocity through safety relief valve from preliminary LTSBO calculation 52
Figure 4-18 Gas temperature through safety relief valve from preliminary LTSBO calculation 53
Figure 4-19 Gas composition through safety relief valve from preliminary LTSBO calculation 53
Figure 4-20 Thermal response of safety relief valve using simple 1-dimensional models 55
Figure 4-21 Drywell floor regions for modeling molten-core/concrete interactions....58
Figure 4-22 Drywell head flange connection details 61
Figure 4-23 Drywell flange leakage model versus containment pressure 62
Figure 5-1 LTSBO vessel pressure 72
Figure 5-2 LTSBO reactor pressure vessel water level....73
Figure 5-3 LTSBO fuel cladding temperatures at core mid-plane and in-vessel hydrogen generation....75
Figure 5-4 Relocation of core material into the lower plenum during LTSBO 76
Figure 5-5 LTSBO temperature of particulate debris on inner surface of lower head....78
Figure 5-6 LTSBO lower head temperature....78
Figure 5-7 Debris behavior from lower head dryout through lower head failure for LTSBO 79
Figure 5-8 LTSBO containment pressure 80
Figure 5-9 LTSBO suppression pool temperature 80
Figure 5-10 LTSBO In-vessel Fission Product Release from Fuel 82
Figure 5-11 LTSBO Source Term to the Environment 84
Figure 5-12 LTSBO iodine fission product distribution....85
Figure 5-13 LTSBO cesium fission product distribution 85

Figure 5-14 LTSBO tellurium fission product distribution 86
Figure 5-15 LTSBO cerium fission product distribution....86
Figure 5-16 LTSBO ex-vessel debris temperatures....88
Figure 5-17 Reactor Building DF for unmitigated LTSBO....89
Figure 5-18 Mitigated LTSBO vessel pressure 91
Figure 5-19 Mitigated LTSBO coolant level 91
Figure 5-20 Mitigated LTSBO core temperature....92
Figure 5-21 Mitigated LTSBO Suppression Pool Water Temperature 93
Figure 5-22 Mitigated LTSBO containment pressure 94
Figure 5-23 Mitigated LTSBO torus water level 95
Figure 5-24 Reactor pressure for short term station blackout with RCIC blackstart....98
Figure 5-25 Reactor vessel water level for STSBO with RCIC blackstart....99
Figure 5-26 Fuel cladding temperatures at core mid-plane and in-vessel hydrogen generation for STSBO with RCIC blackstart 99
Figure 5-27 Temperatures of core debris along inner surface of lower head for STSBO with RCIC blackstart 100
Figure 5-28 Inner and outer surface temperatures of lower head for STSBO with RCIC blackstart 101
Figure 5-29 Containment pressure history for STSBO with RCIC blackstart....102
Figure 5-30 Environmental source term for STSBO with RCIC blackstart 103
Figure 5-31 Environmental source term for STSBO with RCIC blackstart: details for volatile species 104
Figure 5-32 Iodine fission product distribution for STSBO with RCIC blackstart 105
Figure 5-33 Cesium fission product distribution for STSBO with RCIC blackstart 105
Figure 5-34 Tellurium fission product distribution for STSBO with RCIC blackstart 106
Figure 5-35 Reactor vessel pressure: STSBO without RCIC blackstart....108
Figure 5-36 Reactor vessel water level: STSBO without RCIC blackstart 109
Figure 5-37 Temperatures of fuel cladding at core mid-plane: STSBO without RCIC blackstart 109
Figure 5-38 Mass of core debris in RPV lower plenum: STSBO without RCIC blackstart....110
Figure 5-39 Temperature of debris in RPV lower plenum: STSBO without RCIC blackstart 111
Figure 5-40 Lower head temperature: STSBO without RCIC blackstart 111
Figure 5-41 Suppression Pool Temperature: STSBO without RCIC blackstart....112
Figure 5-42 Containment Pressure: STSBO without RCIC blackstart....113
Figure 5-43 STSBO without RCIC blackstart environmental source term 114
Figure 5-44 STSBO without RCIC blackstart environmental source term: details for volatile species 115
Figure 5-45 Spatial distribution of Iodine: STSBO without RCIC blackstart....115
Figure 5-46 Spatial distribution of Cesium: STSBO without RCIC blackstart....116
Figure 5-47 Spatial distribution of Tellurium: STSBO without RCIC blackstart 116
Figure 5-48 Reactor Building decontamination factor (DF): STSBO without RCIC blackstart 117
Figure 5-49 Water level and temperature of RPV recirculation loop-A piping: STSBO without RCIC blackstart....118

Figure 5-50 CsI deposited on the surface of recirculation loop piping: STSBO without RCIC blackstart 119
Figure 5-51 Comparison of RPV Pressure Response: SRV Failure Sensitivity – LTSBO 122
Figure 5-52 Comparison of RPV Level Response: SRV Failure Sensitivity - LTSBO 122
Figure 5-53 Comparison of RPV Pressure Response: SRV Failure Sensitivity – STSBO with RCIC blackstart 123
Figure 5-54 Comparison of RPV Level Response: SRV Failure Sensitivity – STSBO with RCIC blackstart 123
Figure 5-55 Comparison of RPV Pressure Response: SRV Failure Sensitivity – STSBO without RCIC blackstart 124
Figure 5-56 Comparison of RPV Level Response: SRV Failure Sensitivity – STSBO without RCIC blackstart 124
Figure 5-57 Loss of vital AC bus E-12 reactor vessel pressure 133
Figure 5-58 Loss of vital AC bus E-12 reactor water level 134
Figure 5-59 Sensitivity of station battery duration: Reactor water level- loss of vital AC bus E-12 137
Figure 5-60 Sensitivity of station battery duration: Peak clad temperature- loss of vital AC bus E-12 137
Figure 5-61 Effect of increased containment leakage on the release of iodine to the environment 139
Figure 5-62 Drywell atmospheric temperatures in the baseline LTSBO calculation 141
Figure 5-63 Drywell atmospheric temperatures with imposed drywell circulation 141
Figure 5-64 Effect of modeling circulation flow within the drywell on iodine and cesium release to the environment 142
Figure 5-65 Total Hydrogen Mass in the Reactor Building (TIP Sensitivity calculation versus unmitigated LTSBO baseline) 144
Figure 5-66 Integral Mass of Hydrogen Released to the Reactor Building (TIP Sensitivity calculation versus unmitigated LTSBO baseline) 145
Figure 5-67 Fractional Release of Key Fission Products to the Environment (TIP Sensitivity calculation versus unmitigated LTSBO baseline) 146
Figure 5-68 Iodine and Cesium in the Reactor Building (TIP Sensitivity calculation versus unmitigated LTSBO baseline) 146
Figure 5-69 Early Leakage of Key Fission Products to the Environment (TIP Sensitivity calculation versus unmitigated LTSBO baseline) 147
Figure 5-70 Barium release trends in STSBO compared to LTSBO 148
Figure 5-71 Vapor pressure of Ba metal and BaO (oxide vapor pressure is estimated) 149
Figure 5-72 Relative core damage states for STSBO versus LTSBO. The STSBO damage is slightly more extensive with portions of the core forming molten pools 150
Figure 5-73 Maximum core temperature for STSBO and LTSBO analyses. At the time of lower head failure, core temperatures are somewhat higher in the STSBO case 151
Figure 5-74 Zr content in-vessel 151
Figure 6-1 Peach Bottom 10 and 20 mile analysis areas 154
Figure 6-2 Unmitigated LTSBO emergency response timeline 164
Figure 6-3 Duration of protective actions for unmitigated LTSBO 165

Figure 6-4 STSBO with RCIC blackstart emergency response timeline.....168
Figure 6-5 Protective actions for STSBO with RCIC blackstart 168
Figure 6-6 STSBO without RCIC blackstart emergency response timeline.....170
Figure 6-7 Duration of protective actions for STSBO without RCIC blackstart.....171
Figure 6-8 Evacuation timeline from Peach Bottom for the 10 to 20 mile region 174
Figure 6-9 Sensitivity 1 STSBO without RCIC blackstart - evacuation to 16 miles.....175
Figure 6-10 Duration of protective actions for Sensitivity 1 STSBO w/o RCIC blackstart - evacuation to 16 miles 175
Figure 6-11 Sensitivity 2 STSBO without RCIC blackstart - evacuation to 20 miles.....177
Figure 6-12 Duration of protective actions for sensitivity 2 STSBO w/o RCIC blackstart - evacuation to 20 miles 178
Figure 6-13 Sensitivity 3 STSBO w/o RCIC blackstart - delay in protective actions.....180
Figure 6-14 Protective action durations for sensitivity 3 STSBO w/o RCIC blackstart - delay in protective actions.....180
Figure 6-15 Roadway network identifying potentially affected roadways and bridges 183
Figure 6-16 Bridge along Robert Fulton Highway.....185
Figure 6-17 STSBO w/o RCIC blackstart emergency response timeline (seismic analysis).....188
Figure 6-18 Protective action durations - STSBO w/o RCIC blackstart (seismic analysis).....188
Figure 6-19 Reactor Building 197
Figure 6-20 Volume Needed to Fill the Peach Bottom Reactor Building 198
Figure 6-21 Peach Bottom Pumping Capacity and Time 198
Figure 7-1 Mean, individual, LCF risk per Reactor-Year (1/yr) from the Peach Bottom, unmitigated, LTSBO scenario for residents within a circular area of specified radius from the plant for three values of dose-truncation level 207
Figure 7-2 Mean, individual, LNT, LCF risk per Reactor-Year (1/yr) from the Peach Bottom, unmitigated, LTSBO scenario for residents within a circular area of specified radius from the plant for the emergency and long-term phases.....207
Figure 7-3 Mean, individual, LCF risk per Reactor-Year (1/yr) from the Peach Bottom, STSBO scenario with RCIC blackstart for residents within a circular area of specified radius from the plant for three values of dose-truncation level 211
Figure 7-4 Mean, individual, LNT, LCF risk per Reactor-Year (1/yr) from the Peach Bottom, STSBO scenario with RCIC blackstart for residents within a circular area of specified radius from the plant for emergency and long-term phases 212
Figure 7-5 Mean, individual, LCF risk per Reactor-Year (1/yr) from the Peach Bottom, unmitigated, STSBO scenario without RCIC blackstart for residents within a circular area of specified radius from the plant for three values of dose-truncation level.....214
Figure 7-6 Mean, individual, LNT, LCF risk per Reactor-Year (1/yr) from the Peach Bottom, unmitigated, STSBO scenario without RCIC blackstart for residents within a circular area of specified radius for the emergency and long-term phases 215
Figure 7-7 Mean, individual, LNT, LCF risk per Reactor-Year (1/yr) from the Peach Bottom, unmitigated, STSBO scenario without RCIC blackstart for

residents within a circular area of specified radius from the plant showing the effect of the size of the evacuation zone 217
Figure 7-8 Mean, individual, LNT, LCF Risk per Event (dimensionless) from the SST1 source term for residents within a circular area of specified radius from the Peach Bottom plant using the SOARCA STSBO ER timing and showing the risks from the emergency and long-term phases 221
Figure 7-9 Percentage contribution to total, emergency-phase, and long-term-phase, mean, individual risk for the population within 10 miles by chemical class for the Peach Bottom unmitigated LTSBO based on the LNT hypothesis 233
Figure 7-10 Percentage contribution to total, mean, individual risk for the population within 10 miles by chemical class for the Peach Bottom unmitigated LTSBO based on US BGR dose truncation 234
Figure 7-11 Percentage contribution to total, mean, individual risk for the population within 10 miles by chemical class for the Peach Bottom unmitigated LTSBO based on a truncation level reflecting the HPS Position for quantifying health effects 234
Figure 7-12 Percentage contribution to total, emergency-phase, and long-term-phase, mean, individual risk for the population within 20 miles by chemical class for the Peach Bottom unmitigated LTSBO based on the LNT hypothesis 236
Figure 7-13 Percentage contribution to total, mean, individual risk for the population within 20 miles by chemical class for the Peach Bottom unmitigated LTSBO based on US BGR dose truncation 236
Figure 7-14 Percentage contribution to total, mean, individual risk for the population within 20 miles by chemical class for the Peach Bottom unmitigated LTSBO based on a truncation level reflecting the HPS Position for quantifying health effects 237
Figure 7-15 Percentage contribution to total, emergency-phase, and long-term-phase, mean, individual risk for the population within 50 miles by chemical class for the Peach Bottom unmitigated LTSBO based on the LNT hypothesis 237
Figure 7-16 Percentage contribution to total, mean, individual risk for the population within 50 miles by chemical class for the Peach Bottom unmitigated LTSBO based on US BGR dose truncation 238
Figure 7-17 Percentage contribution to total, mean, individual risk for the population within 50 miles by chemical class for the Peach Bottom unmitigated LTSBO based on a truncation level reflecting the HPS Position for quantifying health effects 238
Figure 7-18 Percentage contribution to total, emergency-phase, and long-term-phase, mean, individual risk for the population within 10 miles by chemical class for the Peach Bottom unmitigated STSBO with RCIC blackstart based on the LNT hypothesis 239
Figure 7-19 Percentage contribution to total, mean, individual risk for the population within 10 miles by chemical class for the Peach Bottom unmitigated STSBO with RCIC blackstart based on US BGR dose truncation 239
Figure 7-20 Percentage contribution to total, mean, individual risk for the population within 10 miles by chemical class for the Peach Bottom unmitigated

STSBO with RCIC blackstart based on a truncation level reflecting the HPS Position for quantifying health effects 240
Figure 7-21 Percentage contribution to total, emergency-phase, and long-term-phase, mean, individual risk for the population within 20 miles by chemical class for the Peach Bottom unmitigated STSBO with RCIC blackstart based on the LNT hypothesis 240
Figure 7-22 Percentage contribution to total, mean, individual risk for the population within 20 miles by chemical class for the Peach Bottom unmitigated STSBO with RCIC blackstart based on US BGR dose truncation 241
Figure 7-23 Percentage contribution to total, mean, individual risk for the population within 20 miles by chemical class for the Peach Bottom unmitigated STSBO with RCIC blackstart based on a truncation level reflecting the HPS Position for quantifying health effects 241
Figure 7-24 Percentage contribution to total, emergency-phase, and long-term-phase, mean, individual risk for the population within 50 miles by chemical class for the Peach Bottom unmitigated STSBO with RCIC blackstart based on the LNT hypothesis 242
Figure 7-25 Percentage contribution to total, mean, individual risk for the population within 50 miles by chemical class for the Peach Bottom unmitigated STSBO with RCIC blackstart based on US BGR dose truncation 242
Figure 7-26 Percentage contribution to total, mean, individual risk for the population within 50 miles by chemical class for the Peach Bottom unmitigated STSBO with RCIC blackstart based on a truncation level reflecting the HPS Position for quantifying health effects 243
Figure 7-27 Percentage contribution to total, emergency-phase, and long-term-phase, mean, individual risk for the population within 10 miles by chemical class for the Peach Bottom unmitigated STSBO without RCIC blackstart based on the LNT hypothesis 244
Figure 7-28 Percentage contribution to total, mean, individual risk for the population within 10 miles by chemical class for the Peach Bottom unmitigated STSBO without RCIC blackstart based on US BGR dose truncation 245
Figure 7-29 Percentage contribution to total, mean, individual risk for the population within 10 miles by chemical class for the Peach Bottom unmitigated STSBO without RCIC blackstart based on a truncation level reflecting the HPS Position for quantifying health effects 245
Figure 7-30 Percentage contribution to total, emergency-phase, and long-term-phase, mean, individual risk for the population within 20 miles by chemical class for the Peach Bottom unmitigated STSBO without RCIC blackstart based on the LNT hypothesis 246
Figure 7-31 Percentage contribution to total, mean, individual risk for the population within 20 miles by chemical class for the Peach Bottom unmitigated STSBO without RCIC blackstart based on US BGR dose truncation 246
Figure 7-32 Percentage contribution to total, mean, individual risk for the population within 20 miles by chemical class for the Peach Bottom unmitigated STSBO without RCIC blackstart based on a truncation level reflecting the HPS Position for quantifying health effects 247

Figure 7-33 Percentage contribution to total, emergency-phase, and long-term-phase, mean, individual risk for population within 50 miles by chemical class for the Peach Bottom unmitigated STSBO without RCIC blackstart based on the LNT hypothesis 247
Figure 7-34 Percentage contribution to total, mean, individual risk for the population within 50 miles by chemical class for the Peach Bottom unmitigated STSBO without RCIC blackstart based on US BGR dose truncation 248
Figure 7-35 Percentage contribution to total, mean, individual risk for the population within 50 miles by chemical class for the Peach Bottom unmitigated STSBO without RCIC blackstart based on a truncation level reflecting the HPS Position for quantifying health effects 248

LIST OF TABLES

Table 3-1 Accident scenarios and frequencies 9
Table 4-1 Important Design Parameters for Peach Bottom 26
Table 4-2 Percent change in strength of stainless steel from value at 600ºF (589K) 56
Table 4-3 Concrete Composition 59
Table 4-4 Decay Power in Peach Bottom MELCOR Model 63
Table 5-1 Timing of Key Events for LTSBO 70
Table 5-2 Timing of Key Events for Mitigated LTSBO 90
Table 5-3 Timing of Key Events for the short term station blackout with successful RCIC blackstart 97
Table 5-4 Timing of Key Events for the STSBO without RCIC blackstart 107
Table 5-5 Key Metrics of the Impact of Reasonable Variations in SRV Failure Criteria 127
Table 5-6 The Effects of Extreme Variations in SRV Failure Criteria on Key Severe Accident Metrics 130
Table 5-7 Timing of Key Events for Loss of Vital AC Bus E-12 132
Table 5-8 Sensitivities for Loss of Vital AC Bus E-12 138
Table 6-1 Scenarios Assessed for Emergency Response 155
Table 6-2 Peach Bottom Cohort Population Values 157
Table 6-3 Peach Bottom Shielding Factors. 160
Table 6-4 Unmitigated LTSBO Cohort Timing 167
Table 6-5 STSBO with RCIC blackstart Cohort Timing. 169
Table 6-6 STSBO without RCIC blackstart Cohort Timing. 172
Table 6-7 STSBO without RCIC blackstart, Sensitivity 1 177
Table 6-8 STSBO without RCIC blackstart, Sensitivity 2. 179
Table 6-9 Cohort Timing for Sensitivity 3 181
Table 6-10 Description of the Potential Evacuation Failure Locations 182
Table 6-11 Cohort Timing for STSBO without RCIC blackstart 190
Table 7-1 Brief Source-Term Description for Unmitigated Peach Bottom Accident Scenarios and the SST1 Source Term from the 1982 Siting Study 204
Table 7-2 Mean, Individual, LCF Risk per Event (Dimensionless) for Residents within the Specified Radii of the Peach Bottom Site for the Unmitigated LTSBO Scenario, which has a Mean, Core Damage Frequency (CDF) of $3x10^{-6}$ pry 206
Table 7-3 Mean, Individual, LCF Risk per Reactor-Year (1/yr) for Residents within the Specified Radii of the Peach Bottom Site for the Unmitigated LTSBO Scenario, which has a Mean, CDF of $3x10^{-6}$ pry 206
Table 7-4 Mean, Individual, LCF Risk per Event (Dimensionless) for Residents within the Specified Radii of the Peach Bottom Site for the STSBO Scenario with RCIC blackstart, which Has a Mean CDF of $3x10^{-7}$ pry 210
Table 7-5 Mean, Individual, LCF Risk per Reactor-Year (1/yr) for Residents within the Specified Radii of the Peach Bottom Site for the Unmitigated STSBO Scenario with RCIC blackstart, which Has a Mean CDF of $3x10^{-7}$ pry 210
Table 7-6 Mean, Individual, LCF Risk per Event (Dimensionless) for Residents within the Specified Radii of the Peach Bottom Site for the Unmitigated STSBO Scenario without RCIC blackstart, which Has a Mean CDF of $3x10^{-7}$ pry 213

Table 7-7 Mean, Individual, LCF Risk per Reactor-Year (1/yr) for Residents within the Specified Radii of the Peach Bottom Site for the Unmitigated STSBO Scenario without RCIC blackstart, which Has a Mean CDF of $3x10^{-7}$ pry 213
Table 7-8 Effect of Size of Evacuation Zone on Mean, Individual, LNT, Latent Cancer Fatality Risk per Reactor-Year (1/yr) for Residents within the Specified Radii of the Peach Bottom Site for the Unmitigated STSBO Scenario without RCIC blackstart 216
Table 7-9 Mean, Individual, LNT, LCF Risk per Event (Dimensionless) for Residents within the Specified Radii of the Peach Bottom Site for the Unmitigated, STSBO Scenario without RCIC blackstart Comparing the Unmodified Emergency Response and Emergency Response Adjusted for the Effect of Seismic Activity on Evacuation Routes and Human Response 218
Table 7-10 Mean, Individual, LCF Risk per Event (Dimensionless) for Residents within the Specified Radii of the Peach Bottom Site for the SST1 Source Term previously used in the 1982 Siting Study. All Parameters Other than for Source Term Are Taken from the Unmitigated STSBO Scenario without RCIC blackstart 219
Table 7-11 Mean, Individual, LNT, LCF Risk per Event (dimensionless) for Residents within the Specified Radii of the Peach Bottom Site for the SST1 Source Term previously used in the 1982 Siting Study Using Emergency Response Parameters from the STSBO Scenario. The Final Column of the Table Shows the SOARCA Results for the Unmitigated STSBO without RCIC blackstart 220
Table 7-12 Mean, Individual, Prompt-Fatality Risk per Event (Dimensionless) for Residents within the Specified Radii of the Peach Bottom Site for the SST1 Source Term previously used in the 1982 Siting Study Using Emergency Response Parameters from the SOARCA STSBO without RCIC blackstart Scenario 222
Table 7-13 Total Release Fractions by Chemical Group Comparison between the SST1 and the SOARCA Unmitigated STSBO without RCIC blackstart Peach Bottom Scenarios 223
Table 7-14 Comparison of Modeling Choices and Parameters Used to Reconstruct 1982 Siting Study Results with the Peach Bottom Unmitigated STSBO without RCIC blackstart from SOARCA 224
Table 7-15 Mean, LNT, LCF Risk per Event (dimensionless) for Residents within the Specified Radii of the Peach Bottom Site for the Recreation of the Siting Study Using the SST1 Source Term and for the Unmitigated STSBO without RCIC blackstart Calculated for SOARCA. CDFs Were Estimated to Be 10^{-5}/yr and $3x10^{-7}$/yr for the SST1 and STSBO without RCIC blackstart Source Terms, Respectively 227
Table 7-16 Mean, LCF Risk per Event (dimensionless) Using US Background (620 mrem/yr) Dose-Truncation for Residents within the Specified Radii of the Peach Bottom Site for the Recreation of the 1982 Siting Study Using the SST1 Source Term and for the Unmitigated STSBO without RCIC blackstart Scenario Calculated for SOARCA. CDFs Were Estimated to Be

10^{-5}/yr and $3x10^{-7}$/yr for the SST1 and STSBO without RCIC blackstart Source Terms, Respectively 227
Table 7-17 Mean, LCF Risk per Event (dimensionless) for Three Levels of Dose Truncation for Residents within the Specified Radii of the Peach Bottom Site for the Recreation of the 1982 Siting Study Using the SST1 Source Term. The CDF for This Sequence of the 1982 Siting Study is 10^{-5}/yr 228
Table 7-18 Surface roughness for various land-use categories for the area surrounding the Peach Bottom site 229
Table 7-19 Deposition Velocities Used for the Base Case Calculations and for the Surface Roughness Sensitivity Study for Each of the Ten Aerosol Bins in the MELCOR Model 230
Table 7-20 Mean, Individual, LCF Risk per Event (Dimensionless) for Residents within the Specified Radii of the Peach Bottom Site for the Unmitigated STSBO Scenario without RCIC blackstart, which has a Mean CDF of $3x10^{-7}$ pry. Risks are shown for the base case (10 cm surface roughness) and the sensitivity case (60 cm surface roughness) 230

EXECUTIVE SUMMARY

The U.S. Nuclear Regulatory Commission (NRC), the nuclear power industry, and the international nuclear energy research community have devoted considerable research over the last several decades to examining severe reactor accident phenomena and offsite consequences. Following the terrorist attacks of 2001, an NRC initiative reassessed severe accident progression and offsite consequences in response to security-related events. These updated analyses incorporated the wealth of accumulated research and used more detailed, integrated, and best-estimate modeling than past analyses. An insight gained from these security assessments was that the NRC needed updated analyses of severe reactor accidents to reflect realistic estimates of the more likely outcomes, considering the current state of plant design and operation and the advances in understanding of severe accident behavior.

The NRC initiated the State-of-the-Art Reactor Consequence Analyses (SOARCA) project to develop best estimates of the offsite radiological health consequences for potential severe reactor accidents for two pilot plants: the Peach Bottom Atomic Power Station in Pennsylvania and the Surry Power Station in Virginia. Peach Bottom is generally representative of U.S. operating reactors using the General Electric boiling-water reactor (BWR) design with a Mark I containment. Surry is generally representative of U.S. operating reactors using the Westinghouse pressurized-water reactor (PWR) design with a large, dry (subatmospheric) containment. SOARCA results, while specific to Peach Bottom and Surry, may be generally applicable to plants with similar designs. Additional work would be needed to confirm this, however, since differences exist in plant-specific designs, procedures, and emergency response characteristics.

The SOARCA project evaluates plant improvements and changes not reflected in earlier NRC publications such as NUREG/CR-2239, "Technical Guidance for Siting Criteria Development," NUREG-1150, "Severe Accident Risks: An Assessment for Five U.S. Nuclear Power Plants," and WASH-1400, "Reactor Safety Study: An Assessment of Accident Risks in U.S. Commercial Nuclear Power Plants." SOARCA includes system improvements, improvements in training and emergency procedures, offsite emergency response, and security-related improvements, as well as plant changes such as power uprates and higher core burnup. To provide perspective between SOARCA results and more conservative offsite consequence estimates, SOARCA results are compared to NUREG/CR-2239, "Technical Guidance for Siting Criteria Development," issued in 1982 and referred to in this report as the Siting Study. Specifically, SOARCA results are compared to the Siting Study siting source term 1 (SST1). SST1 assumes severe core damage, loss of all safety systems, and loss of containment after 1.5 hours. The SOARCA report helps the NRC to communicate its current understanding of severe-accident-related aspects of nuclear safety to stakeholders, including Federal, State, and local authorities, licensees, and the general public.

The SOARCA project sought to focus its resources on the more important severe accident scenarios for Peach Bottom and Surry. The project narrowed its approach by using an accident sequence's possibility of damaging reactor fuel, or core damage frequency (CDF), as a surrogate for risk. The SOARCA scenarios were selected from the results of existing probabilistic risk

assessments (PRAs). Core damage sequences from previous staff and licensee PRAs were identified and binned into core damage groups. A core damage group consists of core damage sequences that have similar timing for important severe accident phenomena and similar containment or engineered safety feature operability. It is important to note that each core damage sequence that belongs to a given core damage group is initiated by a specific cause (for example, a seismic event, a fire, or a flood), and that the frequency of each core damage group was estimated by aggregating the CDFs of the individual sequences that belong to the group. This approach was taken to help ensure that the contributions from all core damage sequences were accounted for during the sequence selection process. During the consequence analysis, the core damage groups for station blackouts were analyzed as if they were initiated by a seismic event. This approach was taken because seismically induced equipment failures occur immediately following the seismic event, which produces the severe challenge to the plant. The groups were screened according to their approximate CDFs to identify the most risk significant groups. SOARCA analyzed scenarios with a CDF equal to or greater than 10^{-6} (1 in a million) per reactor-year. SOARCA also sought to analyze scenarios leading to an early failure or bypass of the containment with a CDF equal to or greater than 10^{-7} (1 in 10 million) per reactor-year, since these scenarios have a potential for higher consequences and risk. This approach allowed a more detailed analysis of accident consequences for the more likely, although still remote, accident scenarios.

The staff used updated and benchmarked standardized plant analysis risk (SPAR) models and available plant-specific external events information in the scenario-selection process and identified two major groups of accident scenarios for analysis. The first group common to both Peach Bottom and Surry includes short-term station blackout (STSBO) and long-term station blackout (LTSBO). Both types of SBOs involve a loss of all alternating current (ac) power. The STSBO also involves the loss of turbine-driven systems through loss of direct current (dc) control power or loss of the condensate storage tank and therefore proceeds to core damage more rapidly (hence "short term"). The STSBO has a lower CDF, since it requires a more severe initiating event and more extensive system failures. SBO scenarios can be initiated by external events such as a fire, flood, or earthquake. SOARCA assumes that an SBO is initiated by a seismic event since this is the most extreme case in terms of both the timing and amount of equipment that fails. Notwithstanding the SOARCA scenario screening process, SBO scenarios are commonly identified as important contributors in PRA because of the common cause of failure for both reactor safety systems and containment safety systems.

SOARCA's second severe accident scenario group, which was identified for Surry only, is the containment bypass scenario. For Surry, two containment bypass scenarios were identified and analyzed. The first bypass scenario is a variant of the STSBO scenario, involving a thermally-induced steam generator tube rupture (TISGTR). The second bypass scenario involves an interfacing systems loss-of-coolant accident (ISLOCA) caused by an unisolated rupture of low-head safety injection piping outside containment. The CDF for the ISLOCA, 3×10^{-8} (3 in 100 million) per reactor-year, falls below the SOARCA screening criterion for bypass events but it is analyzed for completeness because NUREG-1150 identified ISLOCA, in addition to SBO and SGTRs, as principal contributors to mean early and latent cancer fatality risks. This scenario-selection process captured the more important internally and externally initiated core damage scenarios.

SOARCA's analyses were performed with two computer codes, MELCOR for accident progression and the MELCOR Accident Consequence Code System, Version 2 (MACCS2) for offsite consequences. The NRC staff's preparations for the analyses included extensive cooperation from the licensees of Peach Bottom and Surry to develop high-fidelity plant systems models, define operator actions including the most recently developed mitigation actions, and develop models for simulation of site-specific and scenario-specific emergency planning and response. Moreover, in addition to input for model development, licensees provided information on accident scenarios from their PRAs. Through tabletop exercises of the selected scenarios with senior reactor operators, PRA analysts, and other licensee staff, licensees provided input on the timing and nature of the operator actions to mitigate the selected scenarios. The licensee input for each scenario was used to develop assumed timelines of operator actions and equipment configurations for implementing available mitigation measures which include mitigation measures beyond those routinely credited in current PRA models. A human reliability analysis, commonly included in PRAs to represent the reliability of operator actions, was not performed for SOARCA, but instead tabletop exercises, plant walkdowns, simulator runs and other inputs from licensee staff were employed to ensure that operator actions and their timings were correctly modeled.

SOARCA modeled several types of mitigation measures, including those specified in emergency operating procedures (EOPs), severe accident management guidelines (SAMGs), and Title 10 to the *Code of Federal Regulations* (10 CFR) 50.54(hh). The 10 CFR 50.54(hh) mitigation measures refer to additional equipment and strategies required by the NRC following the terrorist attacks of September 11, 2001, to further improve each plant's capability to mitigate events involving a loss of large areas of the plant caused by fire and explosions. To assess the benefits of mitigation measures and to provide a basis for comparison to the past analyses of unmitigated severe accident scenarios, the SOARCA project analyzes the selected scenarios twice: first assuming that the event proceeds unmitigated, and then assuming that mitigation is successful. SOARCA's unmitigated cases assumed neither 10 CFR 50.54(hh) equipment nor a subset of other key operator actions that would prevent core damage were implemented. The subset of operator actions not credited was specific to each individual scenario and included such actions as use of the residual heat removal system for the Surry ISLOCA.

For the LTSBO scenarios for both Peach Bottom and Surry (the most likely severe accident scenario for each plant considered in SOARCA) analyzed assuming no mitigation, core damage begins in 9 to 16 hours, and reactor vessel failure begins at about 20 hours. Offsite radiological release due to containment failure begins at about 20 hours for Peach Bottom (BWR) and at 45 hours for Surry (PWR). The SOARCA analyses therefore show that time may be available for operators to take corrective action and get additional assistance from plant technical support centers even if initial efforts are assumed unsuccessful. For the most rapid events (i.e., the unmitigated STSBO in which core damage may begin in 1 to 3 hours), reactor vessel failure begins at roughly 8 hours, possibly allowing time to restore core cooling and prevent vessel failure. In these cases, containment failure and radiological release begins at about 8 hours for Peach Bottom and at 25 hours for Surry. For the unmitigated Surry ISLOCA, the offsite radiological release begins at about 13 hours and in the other bypass event analyzed, the TISGTR, the radiological release begins at about 3.5 hours but is shown by analyses to be substantially smaller than the 1982 Siting Study SST1 release.

In addition to delayed radiological releases relative to the 1982 Siting Study SST1 case, the SOARCA study demonstrates that the amount of radioactive material released is much smaller as shown in Figures 1 (Iodine-131) and 2 (Cesium-137) below. The Surry ISLOCA iodine release is calculated to be 16 percent of the core inventory, but the results are more generally in the range of 0.5 to 2 percent for iodine and cesium for the other scenarios analyzed. By contrast, the 1982 Siting Study SST1 case calculated an iodine release of 45 percent and a cesium release of 67 percent of the core inventory.

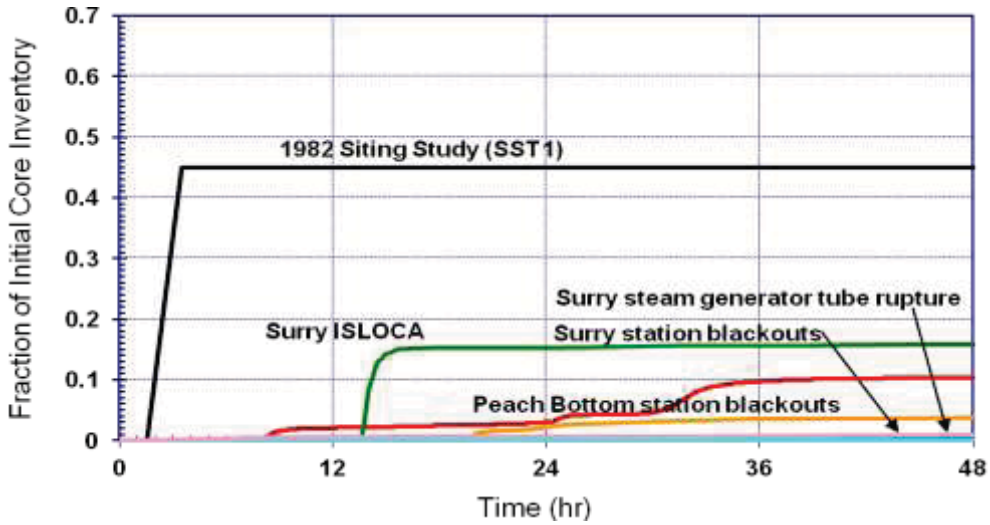

Figure ES-1 Iodine release to the environment for SOARCA unmitigated scenarios and the 1982 Siting Study SST1 case

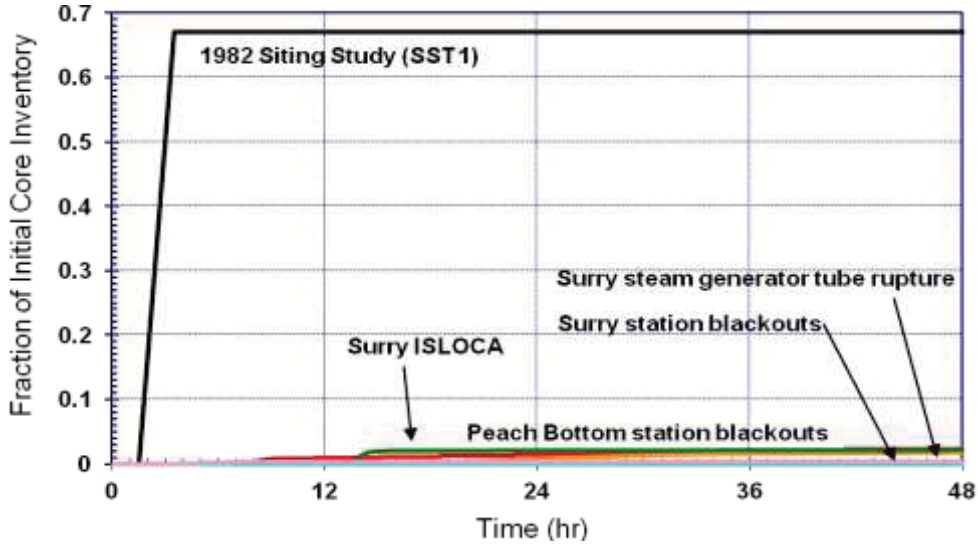

Figure ES-2 Cesium release to the environment for SOARCA unmitigated scenarios and the 1982 Siting Study SST1 case

Past PRAs and consequence studies showed that sequences involving large early releases were important risk contributors. For example, the PWR SBO with a TISGTR was historically believed to result in a large, relatively early release potentially leading to higher offsite consequences. However, MELCOR analysis of Surry performed for SOARCA shows that the release is small, because other reactor coolant system piping inside containment (i.e., hot leg nozzle) fails soon after the tube rupture and thereby retains the fission products within the containment. Additional work would be needed to determine if this result generally applies for all types of PWRs.

The SOARCA results demonstrate the potential benefits of employing 10 CFR 50.54(hh) mitigation enhancements for the scenarios analyzed. MELCOR analyses were used both to confirm the time available to implement mitigation measures and to confirm that those measures, once taken, are effective in preventing core damage or significantly reducing radiological releases. When successful mitigation is assumed, the MELCOR results indicate no core damage for all scenarios except the Surry STSBO and its TISGTR variant. The security-related mitigation measures that provide alternative ac power and portable diesel-driven pumps are especially helpful in counteracting SBO scenarios. For the Surry STSBO and its TISGTR variant, the mitigation is sufficient to flood the containment through the containment spray system to cover core debris resulting from vessel failure. For the ISLOCA scenario, installed equipment unrelated to 10 CFR 50.54(hh) is effective in preventing core damage owing to the time available for corrective action.

For scenarios that release radioactive material to the environment, MACCS2 uses site-specific weather data to predict the downwind concentration of material in the plume and the resulting population exposures and health effects. The analysis of offsite consequences in SOARCA incorporates the improved modeling capability reflected in the MELCOR and MACCS2 codes as well as detailed site-specific public evacuation models. These models were developed for each scenario based on site-specific emergency preparedness programs and State emergency response plans to reflect timing of onsite and offsite protective action decisions and the evacuation time estimates and road networks at Peach Bottom and Surry. Scenarios that are assumed to be initiated by a seismic event consider the earthquake's impact on implementing emergency plans from loss of infrastructure (i.e., long-span bridges, traffic signals, sirens).

The unmitigated versions of the scenarios analyzed in SOARCA have lower risk of early fatalities than calculated in the 1982 Siting Study SST1 case. SOARCA's analyses show essentially zero risk of early fatalities. Early fatality risk was calculated to be ~ 10^{-14} for the unmitigated Surry ISLOCA (for the area within 1 mile of Surry's exclusion area boundary) and zero for all other SOARCA scenarios. In comparison, 92 early fatalities for Peach Bottom and 45 early fatalities for Surry were calculated for the SST1 case in the 1982 Siting Study.

SOARCA results indicate that bypass events (e.g., Surry ISLOCA) do not pose a higher scenario-specific latent cancer fatality risk than non-bypass events (e.g., Surry SBO). While consequences are greater when the bypass scenario happens, this is offset by the scenario being less likely to happen. SOARCA reinforces the importance of external events relative to internal events and the need to continue ongoing work related to external events risk assessment.

Offsite radiological consequences were calculated for each scenario expressed as the average individual likelihood of an early fatality and latent cancer fatality. Tables 1 (Peach Bottom) and 2 (Surry) show, for both mitigated and unmitigated cases, conditional (on the occurrence of the core damage scenario) scenario-specific probabilities of a latent cancer fatality for an individual located within 10 miles of the plant. Tables 1 and 2 show the results using the linear no-threshold (LNT) dose-response model, which assumes that the health risk is directly proportional to the exposure and even the smallest radiation exposure carries some risk. The tables also provide the scenario-specific latent cancer fatality risk for an individual located within 10 miles of the plant, taking into account the scenario's core damage frequency.

Table ES-1 Offsite Consequence Results for Peach Bottom Scenarios Assuming Linear No- Threshold (LNT) Dose-Response Model

Scenario	Core damage frequency [CDF] (per reactor year)	Mitigated		Unmitigated	
		Conditional scenario-specific probability of latent cancer fatality for an individual located within 10 miles	Scenario-specific risk [CDF x Conditional] of latent cancer fatality for an individual located within 10 miles (per reactor year)	Conditional scenario-specific probability of latent cancer fatality for an individual located within 10 miles	Scenario-specific risk [CDF x Conditional] of latent cancer fatality for an individual located within 10 miles (per reactor year)
Long-term SBO	3×10^{-6}	No Core Damage		9×10^{-5}	$\sim 3\times10^{-10}$ ***
Short-term SBO	3×10^{-7}	No Core Damage **		2×10^{-4}	$\sim 6\times10^{-11}$ ***
Short-term SBO with RCIC Blackstart*	3×10^{-7}			7×10^{-5}	$\sim 2\times10^{-11}$ ***

* Blackstart of the reactor core isolation cooling (RCIC) system refers to starting RCIC without any ac or dc control power. Blackrun of RCIC refers to the long-term operation of RCIC without electricity, once it has been started. This typically involves using a portable generator to supply power to indications such as reactor pressure vessel (RPV) level to allow the operator to manually adjust RCIC flow to prevent RPV overfill and flooding of the RCIC turbine.

** If the RCIC system is successfully controlled (i.e., successful blackstart and blackrun) then both mitigated Short-term SBO scenarios would be functionally similar to the mitigated Long-term SBO (i.e., no core damage). This was qualitatively determined based on the timing and equipment availabilities from the other SBO analyses.

*** Estimated risks below 1×10^{-7} per reactor year should be viewed with caution because of the potential impact of events not studied in the analyses and the inherent uncertainty in very small calculated numbers.

Table ES-2 Offsite Consequence Results for Surry Scenarios Assuming LNT Dose-Response Model

Scenario	Core damage frequency [CDF] (per reactor-year)	Mitigated		Unmitigated	
		Conditional scenario-specific probability of latent cancer fatality for an individual located within 10 miles	Scenario-specific risk [CDF x Conditional] of latent cancer fatality for an individual located within 10 miles (per reactor-year)	Conditional scenario-specific probability of latent cancer fatality for an individual located within 10 miles	Scenario-specific risk [CDF x Conditional] of latent cancer fatality for an individual located within 10 miles (per reactor-year)
Long-term SBO	2×10^{-5}	No Core Damage		5×10^{-5}	~ 7×10^{-10} ***
Short-term SBO	2×10^{-6}	No Containment Failure *		9×10^{-5}	~ 1×10^{-10} ***
Short-term SBO with TISGTR	4×10^{-7}	3×10^{-4} **	~ 1×10^{-10} ***	3×10^{-4}	~ 1×10^{-10} ***
Interfacing systems LOCA	3×10^{-8}	No Core Damage		3×10^{-4}	~ 9×10^{-12} ***

* Accident progression calculations were run showing that source terms in the mitigated case are smaller than in the unmitigated case. Offsite consequence calculations were not run since the containment fails at about 66 hours. A review of available resources and emergency plans shows that adequate mitigation measures could be brought on site within 24 hours and connected and functioning within 48 hours. Therefore 66 hours would allow ample time for mitigation via measures brought to the site from offsite.

** Containment failure is delayed by about 46 hours in the mitigated case relative to the unmitigated case. Rounding to one significant figure shows conditional LCF probabilities of 3×10-4 for both mitigated and unmitigated cases, however the original values were 2.8×10-4 for the mitigated case and 3.2×10-4 for the unmitigated case.

*** Estimated risks below 1 x 10^{-7} per reactor year should be viewed with caution because of the potential impact of events not studied in the analyses and the inherent uncertainty in very small calculated numbers.

LCF risks using alternate dose-response models, as well as LCF risks for circular areas out to a radius of 50 miles, are also presented. Using a dose-response model that truncates annual doses below normal background levels (including medical exposures) results in a further reduction to the latent cancer fatality risks (by a factor of 100 for smaller releases and a factor of 3 for larger releases). Latent cancer fatality risk calculations are generally dominated by long-term exposure to small annual doses (~500 mrem per year corresponding to state return criteria) by evacuees returning to their homes after the accident and being exposed to residual radiation over a long period of time. SOARCA's calculated LCF risk results are smaller than extrapolations of 1982 Siting Study SST1 LCF risk results. However, the difference diminishes when considering larger areas, out to a distance of 50 miles from the plant.

Figure 3 compares SOARCA's scenario-specific latent cancer fatality risks for an individual within 10 miles of the plant to the NRC Safety Goal and to an extrapolation of the 1982 Siting Study SST1[1] results.

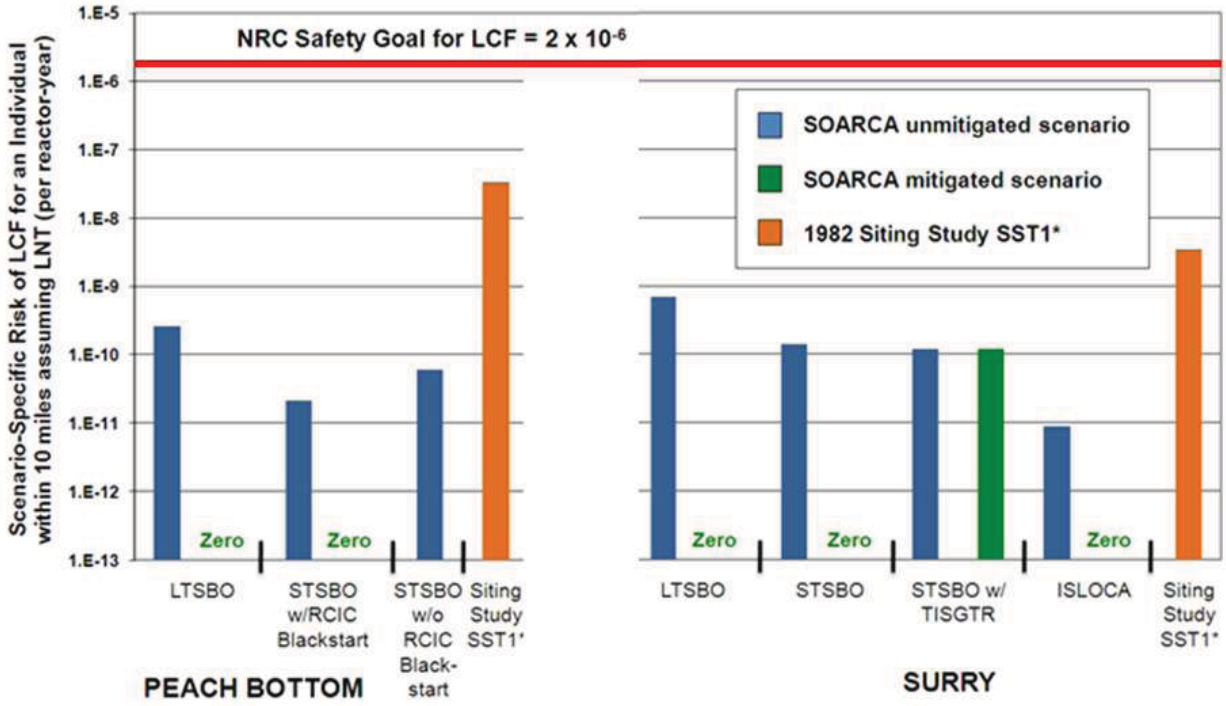

Figure ES-3 Comparison of individual LCF risk results for SOARCA mitigated and unmitigated scenarios to the NRC Safety Goal and to extrapolations of the 1982 Siting Study SST1 *(plotted on logarithmic scale)*

The NRC Safety Goal for latent cancer fatality risk from nuclear power plant operation (i.e., $2x10^{-6}$ or two in one million) is set 1,000 times lower than the sum of cancer fatality risks resulting from all other causes (i.e., $2x10^{-3}$ or two in one thousand). The calculated cancer fatality risks from the selected, important scenarios analyzed in SOARCA are thousands of times lower than the NRC Safety Goal and millions of times lower than the general U.S. cancer fatality risk.

Comparisons of SOARCA's calculated LCF risks to the NRC Safety Goal and the average annual US cancer fatality risk from all causes are provided to give context that may help the reader to understand the contribution to cancer risks from these nuclear power plant accident scenarios. However, such comparisons have limitations for which the reader should be aware. Relative to the safety goal comparison, the safety goal is intended to encompass all accident scenarios. SOARCA does not examine all scenarios typically considered in a PRA, even though

---

[1] The Siting Study did not calculate LCF risks. Therefore, to compare the Siting Study SST1 case to LCF results for SOARCA, the SST1 source term was put into the MACCS2 offsite consequence code files for the Peach Bottom and Surry unmitigated STSBO calculations.

it includes the important scenarios. In fact, any analytical technique, including PRAs, will have inherent limitations of scope and method. As a result, comparison of SOARCA's scenario-specific calculated LCF risks to the NRC Safety Goal is necessarily incomplete. However, it is intended to show that adding multiple scenarios' low risk results in the ~ 10^{-10} range to approximate a summary risk from all scenarios, would yield a summary result that is also below the NRC Safety Goal of $2x10^{-6}$ or two in one million.

Relative to the U.S. average individual risk of a cancer fatality comparison, the sources of an individual's cancer risk include a complex combination of age, genetics, lifestyle choices, and other environmental factors whereas the consequences from a severe accident at a nuclear plant are involuntary and unlikely to be experienced by most individuals.

The SOARCA analyses show that emergency response programs, implemented as planned and practiced, reduce the scenario-specific risk of health consequences among the public during a severe reactor accident. Sensitivity analyses of seismic impacts on site-specific emergency response (e.g., loss of bridges, traffic signals, and delayed notification) at Peach Bottom and Surry do not significantly affect LCF risk.

In summary, the staff believes SOARCA has achieved its objective to develop a body of knowledge regarding detailed, integrated, state-of-the-art modeling of the most important severe accident scenarios for Peach Bottom and Surry. SOARCA analyses indicate that successful implementation of existing mitigation measures can prevent reactor core damage or delay or reduce offsite releases of radioactive material. All SOARCA scenarios, even when unmitigated, progress more slowly and release much less radioactive material than the 1982 Siting Study SST1 case. As a result, the calculated risks of public health consequences from severe accidents modeled in SOARCA are very small.

The SOARCA study was nearing completion when the Fukushima Daiichi accident occurred on March 11, 2011. The Fukushima accident has many similarities and differences with some of the Peach Bottom severe accident scenarios analyzed in SOARCA. While there are significant gaps in information and uncertainties regarding what occurred in the Fukushima reactors, an appendix to this report compares and contrasts the SOARCA study and the Fukushima accident based on currently available information for the following topics: (1) operation of the RCIC system, (2) hydrogen release and combustion, (3) 48-hour truncation of releases in SOARCA, (4) multiunit risk, and (5) spent fuel pool risk.

ACKNOWLEDGEMENTS

The contributions from the following individuals in preparing this document are gratefully acknowledged.

Jon Ake	U.S. Nuclear Regulatory Commission
Terry Brock	U.S. Nuclear Regulatory Commission
Richard Chang	U.S. Nuclear Regulatory Commission
Ata Istar	U.S. Nuclear Regulatory Commission
Robert Prato	U.S. Nuclear Regulatory Commission
Jocelyn Mitchell	U.S. Nuclear Regulatory Commission
Mark Orr	U.S. Nuclear Regulatory Commission
Jason Schaperow	U.S. Nuclear Regulatory Commission
Abdul Sheikh	U.S. Nuclear Regulatory Commission
Richard Sherry	U.S. Nuclear Regulatory Commission
Randolph Sullivan	U.S. Nuclear Regulatory Commission
Charles G. Tinkler	U.S. Nuclear Regulatory Commission
Nathan E. Bixler	Sandia National Laboratories
Shawn P. Burns	Sandia National Laboratories
Randall O. Gauntt	Sandia National Laboratories
Joseph A. Jones	Sandia National Laboratories
Raymond J. Jun	Sandia National Laboratories
Douglas M. Osborn	Sandia National Laboratories
Jesse Phillips	Sandia National Laboratories
Mark T. Leonard	dycoda, LLC
Kenneth C. Wagner	dycoda, LLC

ACRONYMS

AC	Alternating Current
ATWS	Anticipated Transient Without Scram
BWR	Boiler Water Reactor
CD	Core Damage
CDF	Core Damage Frequency
CRDHS	Control Rod Drive Hydraulic System
CRGT	Control Rod Guide Tube
CST	Condensate Storage Tank
DC	Direct Current
DOE	Department of Energy
EAL	Emergency Action Level
EAS	Emergency Alert System
EOF	Emergency Operations Facility
EOP	Emergency Operating Procedure
EP	Emergency Preparedness
EPA	Environmental Protection Agency
EPDM	Ethylene Propylene Diene Methylene
EPZ	Emergency Planning Zone
ERO	Emergency Response Organization
ETE	Evacuation Time Estimate
GE	General Emergency
GNF	Global Nuclear Fuel
HCTL	Heat Capacity Temperature Limit
HPCI	High Pressure Coolant Injection
HPS	Health Physics Society
IPE	Individual Plant Examination
IPEEE	Individual Plant Examination of External Event
LNT	Linear, No-Threshold
LOCA	Loss of Coolant Accident
LPCI	Low Pressure Coolant Injection
LPI	Low Pressure Injection
LTSBO	Long-Term Station Blackout
MACCS2	MELCOR Accident Consequence Code System, Version 2
MCCI	Molten Corium-Concrete Interactions
MSIV	Main Steam Isolation Valve
NG	Noble Gases
NRC	Nuclear Regulatory Commission
NRCS	Natural Resources Conservation Service
NRF	National Response Framework
ORO	Offsite Response Organization
PEMA	Pennsylvania Emergency Management Agency
PRA	Probabilistic Risk Assessment
QHO	Quantitative Health Objective

RAMCAP	Risk Analysis and Management for Critical Asset Protection
RCIC	Reactor Core Isolation Cooling
RHR	Residual Heat Removal
RPF	Relative Power Fraction
RPV	Reactor Pressure Vessel
SAE	Site Area Emergency
SAMG	Severe Accident Management Guidelines
SECPOP	SECtor POPulation and Economic Estimator
SOARCA	State-of-the-Art Reactor Consequence Analysis
SPAR	Standardized Plant Analysis Risk
SRV	Safety Relief Valve
STCP	Source Term Code Package
STSBO	Short-Term Station Blackout
TAF	Top of Active Fuel
TSC	Technical Support Center
UE	Unusual Event

1.0 INTRODUCTION

This document describes the detailed severe accident analyses (i.e., MELCOR and the MELCOR Accident Consequence Code System, Version 2 (MACCS2) code calculations) performed for the Peach Bottom Atomic Power Station as part of the NRC's State-of-the-Art Reactor Consequence Analyses (SOARCA) project. A separate volume of this report describes severe accident analyses for the Surry Power Station.

1.1 Background

The evaluation of accident phenomena and offsite consequences of severe reactor accidents has been the subject of considerable research by NRC, the nuclear power industry, and the international nuclear energy research community. Most recently, with Commission guidance and as part of plant security assessments, updated analyses of severe accident progression and offsite consequences were completed using the wealth of accumulated research. These analyses are more detailed in terms of the fidelity of the representation and resolution of facilities and emergency response, realistic in terms of the use of currently accepted phenomenological models and procedures, and integrated in terms of the intimate coupling between accident progression and offsite consequence models.

An insight gained from these security assessments was that updated analyses of severe reactor accidents were needed to reflect realistic estimates of the more likely outcomes considering the current state of plant design and operation and the advances in our understanding of severe accident behavior. The SOARCA project evaluates plant improvements and changes (either of which can alter safety margins) not reflected in earlier assessments. These include system improvements, improvements in training and emergency procedures, offsite emergency response, and security-related improvements, as well as plant changes such as power uprates and higher core burnup. SOARCA's more realistic modeling updates the more conservative quantifications of offsite consequences found in earlier NRC publications such as NUREG/CR-2239, "Technical Guidance for Siting Criteria Development" referred to in this report as the Siting Study.

In addition to the improvements in understanding and calculational capabilities that have resulted from these studies, numerous influential changes have occurred in the training of operating personnel and the increased use of plant-specific capabilities. These changes include:

- The transition from event-based to symptom-based Emergency Operating Procedures (EOPs) for the boiling-water and pressurized-water reactor designs.

- The performance and maintenance of plant-specific probabilistic risk assessments (PRAs) that cover the spectrum of accident scenarios.

- The implementation of plant-specific, full-scope control room simulators to train operators.

- An industrywide technical basis, owners-group-specific guidance and plant-specific implementation of the Severe Accident Management Guidelines (SAMGs).

- Use of additional safety enhancements, described in Title 10, Section 50.54(hh) of the *Code of Federal Regulations* (10CFR50.54(hh)). These enhancements are intended to be used to maintain or restore core cooling, containment, and spent fuel pool cooling capabilities under the circumstances associated with loss of large areas of the plant due to explosions or fire, to include strategies in the following areas:(i) Fire fighting;(ii) Operations to mitigate fuel damage; and (iii) Actions to minimize radiological release. For the SOARCA scenarios, successful implementation of this equipment and procedures would prevent core damage and/or delay or prevent the release.

- Improved phenomenological understanding of influential processes such as:

    - in-vessel steam explosions,
    - Mark I containment drywell shell attack,
    - dominant chemical forms for fission products,
    - direct containment heating,
    - hot leg creep rupture,
    - reactor pressure vessel failure, and
    - molten core concrete interactions.

1.2 Objective

The overall objective of the State-of-the-Art Reactor Consequence Analysis (SOARCA) project is to develop a body of knowledge regarding the realistic outcomes of severe reactor accidents. Corresponding and supporting objectives are as follows:

- Incorporate the significant plant improvements and updates not reflected in earlier assessments including system improvements, training and emergency procedures, offsite emergency response, and recent security-related enhancements described in Title 10, Section 50.54(hh) of the *Code of Federal Regulations* (10CFR50.54(hh)) as well as plant updates in the form of power uprates and higher core burnup.

- Incorporate state-of-the-art integrated modeling of severe accident behavior that includes the insights of some 25 years of research into severe accident phenomenology and radiation health effects.

- Evaluate the potential benefits of recent security-related mitigation improvements in preventing core damage and reducing or delaying an offsite release should one occur.

- Enable NRC to communicate severe-accident-related aspects of nuclear safety to stakeholders including Federal, State, and local authorities; licensees; and the general public.

- Update quantification of offsite consequences found in earlier NRC publications such as NUREG/CR-2239, "Technical Guidance for Siting Criteria Development."

1.3 Outline

Section 2 briefly summarizes the method used to select the specific accident scenarios subjected to detailed computational analysis. Additional details of this method can be found in summary report (NUREG 1935) in this series. Section 3 describes the results of the mitigation measures assessment process when it was applied to Peach Bottom. Section 4 describes the key features of the MELCOR model of the Peach Bottom Atomic Power Station. Section 5 describes for each case the results of MELCOR calculations of the thermal hydraulics and, when core damage was predicted, the accident progression and radionuclide release to the environment. Section 6 describes the way in which plant-specific emergency response actions were represented in the MACCS2 code calculations of offsite consequences, and Section 7 describes the MACCS2 calculations of offsite consequences for each accident scenario. Section 7 also describes analyses of offsite consequences that compare SOARCA results to consequence results from earlier studies. References cited in this report are listed in Section 8.

2.0 ACCIDENT SCENARIO DEVELOPMENT

The SOARCA project considered accident sequences that have an estimated frequency greater than $1x10^{-6}$ per reactor-year (pry) of reactor operation as candidate sequences for further deterministic evaluations. It also considered sequences with frequency as low as $1x10^{-7}$ pry if they were judged to proceed rapidly enough to have the potential for generating significant early releases of radionuclides to the environment or involve a radiological transport pathway from the reactor to the environment that bypasses the containment pressure boundary (i.e., so-called 'bypass sequences'). Section 2.1 and Section 2.2 summarize the methods used to identify these sequences and the screening process for retaining candidate sequences.

Once candidate accident sequences were identified, the analysts evaluated realistic opportunities for plant personnel to respond to the observed failures of control and safety systems. The manner in which mitigation measures were evaluated for each accident sequence is described in Section 2.3.

The end result of this process was a list of accident scenarios (i.e., event sequence plus options for mitigation) that were subjected to detailed analysis of plant response including, as appropriate, radionuclide release to the environment (described in Sections 4 and 5) and offsite radiological consequence (Sections 6 and 7).

2.1 Sequences Initiated by Internal Events

The following scenario selection process was used to determine the scenarios for further analysis:

1. Identified candidate accident sequences in analyses using plant-specific Standardized Plant Analysis Risk (SPAR) models (Version 3.31).
    a. Initial Screening: Core damage sequences with low frequencies (less than $1x10^{-8}$ pry) were eliminated from consideration. This step affected only 4 percent of the overall core damage frequency (CDF) for Peach Bottom.
    b. Sequence Evaluation: Dominant cutsets for the remaining sequences were reviewed to characterize system and equipment availabilities and accident sequence timing.
    c. Sequence Grouping: Sequence cutsets with similar equipment availabilities and estimated time for the onset of core damage were aggregated into a single 'sequence group' or 'scenario.'
2. The availability of containment systems was evaluated for each sequence, using system dependency tables. These tables delineate the support systems required for containment systems to function. The status of containment systems was then appended to the accident sequence description.
3. Core damage sequences from the licensee's probabilistic risk assessment (PRA) model were compared with the scenarios determined by using the SPAR models. Differences were resolved during meetings with licensee staff.
4. The screening criteria described above were applied to eliminate extremely low frequency sequences from further analyses.

The initial pass through this process identified only one sequence at Peach Bottom that satisfied the $1.x10^{-6}$ pry frequency threshold criteria. The sequence is initiated by the failure of vital alternating current (AC) bus E-12, which disables several (but not all) trains of safety equipment. The estimated frequency of this sequence was initially found to be above the $1x10^{-6}$ pry threshold. As a result, the sequence was forwarded for an assessment of mitigative measures (see Section 2.3) and a deterministic analysis of accident progression and radiological release. However, the SPAR model was later found to incorrectly represent certain features of this sequence, and the sequence's frequency was reduced to below the screening criterion. Further, the MELCOR analysis performed for this sequence determined that it would not, in fact, result in core damage. Despite both of these late conclusions about the characteristics of this sequence, the analysis results provide unique insights into the effectiveness of small capacity non-safety related equipment in the plant to mitigate certain accident sequences. As a result, the calculation of event progression for this sequence was retained in this report (refer to Section 5.6).

This process provided the basic characteristics of each scenario. However, it is necessary when calculating a consistent integrated response to have more detailed information about a scenario than is provided in a PRA model. To capture the additional sequence details, the project conducted further analysis of system descriptions and a review of the normal and emergency operating procedures.

2.2 Sequences Initiated by External Events

External events include internal flooding and fire; seismic events; extreme wind-, tornado-, and hurricane-related events; and other similar events that may be applicable to a specific site. The external event scenarios developed for SOARCA analysis were derived from a review of past studies, such as the NUREG-1150 study, individual plant examination for external event submittals, and other relevant generic information.

Seismic-initiated sequences were found to be the most restrictive in terms of the timing of equipment failure and the ability to successfully implement onsite mitigative measures and offsite protective actions. In addition, the seismic-initiated sequences (as a group) are important contributors to the external event core damage and release frequencies. As a result, plant and offsite response to external event sequences was assumed to be represented by an earthquake of sufficiently large magnitude to result in widespread damage to important plant support systems, such as electric power sources. The seismic events considered in SOARCA result in loss of offsite and onsite AC power (i.e., long-term station blackout (LTSBO)) and, for the more severe seismic events, loss of DC power (i.e., short-term station blackout (STSBO)). The sequence selection process identified the LTSBO, which has an estimated frequency of $1x10^{-6}$ to $5x10^{-6}$ pry. Even though the STSBO, which has an estimated frequency of $1x10^{-7}$ to $5x10^{-7}$ pry, did not meet the screening criterion, we elected to also analyze it to address the impact of the timing of the offsite release on early and latent cancer fatality risks.

The magnitude of the seismic initiating event reflected by these frequencies corresponds to 0.3 to 0.5 peak ground acceleration (pga) for the LTSBO, and 0.5 to 1.0 pga for the STSBO. As noted earlier, the initiating event for all external event sequences was assumed to be represented by a seismic event because it was judged to limit equipment available to prevent, minimize or delay

radiological releases to the environment, and affect offsite response. Seismic PRAs for several BWRs were reviewed to assess the availability of installed systems.

2.3 Mitigation Measures

Actions that would be taken by plant personnel in response to system failures caused by the postulated seismic initiating events were reviewed and incorporated into the development of the accident scenarios evaluated with deterministic calculations. These actions are guided by plant-specific EOPs, severe accident management guidelines (SAMGs) and mitigation measures developed specifically in response to security concerns that arose from the events of September 11, 2001, as codified in 10CFR50.54(hh). Examples of the latter type of measures include portable equipment, such as generators or other power supplies to open or close valves or energize key instrumentation, diesel driven pumps, and air bottles to open air operated valves. Applicable procedures have been written to align and operate these mitigative measures under severe accident conditions.

The SOARCA analysis team developed a timeline for implementing the mitigation measures directed in plant-specific procedures and mobilizing support organizations after discussing each scenario with licensee personnel that have experience in operations, engineering and facility management. Results of preliminary accident progression calculations were used to characterize anticipated changes in plant conditions and describe the signatures of measurable parameters. Estimates were then made for the time needed to assemble necessary personnel, tools and equipment, align and start components, and establish a desired operating condition. The resulting sequence of events and estimated timelines for each scenario are described in the next section.

The seismic events considered in SOARCA result in loss of offsite and onsite AC power (i.e., LTSBO) and, for the more severe seismic events, loss of DC power (i.e., STSBO). Under these conditions, the use of the turbine driven reactor core isolation cooling (RCIC) system is an important mitigation measure. Diverse procedures have been developed for boiling water reactors (BWRs), including a procedure to start and operate the RCIC system without DC control power, which facilitates a managed response to station blackout conditions. These procedures were discussed during site visits. This is known as RCIC *blackstart*. Under 10CFR50.54(hh), mitigation measures also include long-term operation of the RCIC system without electricity (RCIC *blackrun*), using a portable generator to supply power for indications such as reactor pressure vessel (RPV) level to allow the operator to manually adjust RCIC flow to prevent RPV overfill and flooding of the RCIC turbine. For a LTSBO, RCIC can be used to cool the core until battery exhaustion. After battery exhaustion, RCIC black run can be used to continue to cool the core.

The seismic initiating event for the station blackout accident scenarios might rupture the condensate storage tank (CST), which is the primary water reservoir for RCIC. However, the CST is surrounded by a reinforced concrete wall or moat, which could retain water drained from the CST. Therefore, suction from the CST would not necessarily be interrupted by a loss of CST integrity. Plant specific procedures provide plant personnel with instructions for refilling the CST from a variety of possible resources using equipment that is not dependent on availability of AC or DC power (e.g., portable generators, pumps, etc.). Therefore, sustained availability of the

CST is assumed in the current analysis. This assumption is not critical to the calculation of the LTSBO scenario. Operators could also manually re-align RCIC suction to the torus, if necessary. MELCOR calculations for the LTSBO showed that several hours would be available before torus temperature and pressure conditions would reach RCIC isolation setpoints.

3.0 ACCIDENT SCENARIO DEFINITIONS

As discussed in Section 2.0, three scenarios were chosen for analysis. Table 3-1 summarizes the estimated frequency for each of these scenarios. Sections 3.1 and 3.2 provide detailed descriptions of the LTSBO and STSBO, respectively. Section 3.3 describes the loss of vital AC bus E-12 scenario, which was determined to not result in core damage.

Table 3-1 Accident scenarios and frequencies

Scenario Description	**Frequency** **(per reactor year)**
LTSBO	$1x10^{-6}$ to $5x10^{-6}$
STSBO	$1x10^{-7}$ to $5x10^{-7}$
Loss of vital AC bus E-12	$5x10^{-7}$

3.1 Long-Term Station Blackout

Section 3.1.1 describes the status of the plant immediately following the seismic event. Section 3.1.2 then discusses the response of plant systems available to the initiating event. Actions that can be taken by plant personnel to mitigate the effects of failed plant safety functions are described in Section 3.1.3. Section 3.1.4 describes two scenarios that differ in the assumed success (or failure) of the mitigative actions. Mitigated scenarios are defined as those in which the mitigative actions are successful. Unmitigated scenarios are defined as those in which certain key mitigation measures are not successfully implemented.

3.1.1 Initiating Event

The LTSBO scenario is a composite of several similar sequences that differ only by their initiating event. Initiators can be a seismic event, or an internal fire, or flood. The seismic event is the largest contributor to the composite frequency of this scenario, and is used as the basis for defining consequential events and conditions at the plant. Damage caused by the earthquake is assumed to result in a total loss of offsite power. In addition, onsite AC power is unavailable, due to failures of diesel generators to start or run as needed. The diesel generators at Peach Bottom have a shared configuration between the two units, which causes the loss of offsite and onsite AC power failure to affect both units. However, the deterministic analysis of subsequent accident progression described in Section 5.0 considers only the response of one unit.

3.1.2 System Availabilities

Reactor scram, reactor isolation and containment isolation immediately follow the initiating event. Neither active AC nor DC power is necessary for these safety functions to occur. The station blackout electric power line from the hydroelectric station downstream of the plant site is also assumed to be unavailable because of structural damage to the dam and electric station components. The station batteries are assumed to provide DC power for 4 hours following loss of AC power, allowing DC controlled components and systems to operate as required for this period. Instrumentation would also be available using station batteries. This duration of DC power assumes that the batteries are at their end of life and that operators successfully follow procedural actions to shed nonessential loads from the emergency DC bus. As a result, the steam-driven High-Pressure Coolant Injection (HPCI) system and RCIC would be available with

automatic activation for at least the first 4 hours of the scenario. Only RCIC operation is considered in the current analysis because the larger and functionally redundant HPCI system is not needed to respond if RCIC successfully operates. Additionally, remote manual control of the safety relief valves (SRVs) would be available.

3.1.3 Operator Actions and Mitigation Measures

An unmitigated MELCOR calculation was performed for the LTSBO scenario assuming that manual actions to mitigate the loss of vital safety systems are limited to those currently implemented in EOPs[2]. The effects of additional mitigative actions and equipment at the plant (i.e., SAMGs and 10CFR50.54(hh) measures) were then examined in a separate 'mitigated' calculation. Results of the unmitigated calculation are described in Section 5.1, and results of the mitigated accident scenario are described in Section 5.2.

Two operator actions were credited in the unmitigated long-term station blackout calculation[3]. First, operators are assumed to open one SRV to begin a controlled depressurization of the reactor vessel approximately 1 hour after the initiating event. This action is prescribed in station emergency procedures to prevent excessive cycles on the SRV. The target reactor vessel pressure is at or above 125 pounds per square inch (psi), which would permit continued operation of RCIC or HPCI, if necessary. Five SRVs associated with the automatic depressurization system would be available for this operation. These SRVs are provided with accumulators that provide a back-up pneumatic supply for operation of the valves upon loss of the Instrument Nitrogen System. Second, operators are assumed to take manual control of RCIC approximately 2 hours after the initiating event. This involves remote (i.e., from the control room) manipulation of the position of the steam throttle valve at the inlet to the RCIC turbine to reduce and control turbine speed. This action reduces and stabilizes coolant flow from the RCIC pump to maintain the reactor vessel level within a prescribed range.

The mitigated LTSBO calculation credits four additional manual actions. First, two portable AC power supplies (e.g., 10CFR50.54(hh) equipment) are assumed to be connected to restore power to the DC buses delivering power to at least one SRV and (separately) to essential instrumentation (e.g., level indication). The precise time this action is completed is not

---

2 Current procedures for using B.5.b equipment (portable nitrogen bottles, in particular) to open containment vent path isolation valves only address the drywell ventilation system pathway. This path is not desirable under accident conditions in which the vented gas would be comprised of steam and/or hydrogen and/or high levels of radioactivity. The potential for adverse effects to the reactor building have been demonstrated in past NRC research programs concerning containment venting at Peach Bottom (NUREG/CR-4696, for example) and plant-specific emergency procedures caution against using this vent path if an alternative is available, such as the 16-in hardened vent or the 6-in integrated leak rate test (ILRT) line. B5.b equipment could be used to open the isolation valves for either of these paths, but plant-specific procedures have not yet been developed.

3 The action times used in this analysis were based on 'table-top' exercises among NRC staff and licensee personnel, in which the anticipated accident sequence timeline was reviewed to characterize a reasonable time at which action would be taken. If the two actions credited here are completed sooner than the times assumed in these calculations (which is possible), the net effect on the overall hydraulic response of the reactor and containment would be inconsequential.

important, provided it occurs before station battery power is exhausted (i.e., at least 4 hours after the initiating event). This ensures continuous control of RPV pressure and water level, by holding open a single SRV and facilitating operation of the RCIC system after the loss of the onsite emergency DC power supply[4].

The second action involves staging and operation of portable pumping equipment to refill the CST, which is located outside the reactor building. Various equipment and water resources could be used for this purpose. The installed fire protection system is assumed to be disabled as a consequence of the initiating event (i.e., seismic damage). However, the diesel-driven portable pump (i.e., 10CFR50.54(hh) equipment) could be used and/or other mobile equipment. Calculations described in Section 5.2 indicate a pumping capacity of less than 200 gpm would ensure the CST inventory is never depleted for the LTSBO sequence considered here. It is assumed that pumps would take suction from the cooling tower basin or the Susquehanna River.

The third manual action involves opening a containment vent pathway to relieve pressure and prevent structural damage to the containment pressure boundary. Instructions for this action are available in the form of detailed plant-specific procedures, which are outlined in Section 3.1.4.2. These procedures include guidance for selecting an appropriate containment vent path and the actuation criteria for venting.

Procedures also address manual actions to prevent automatic isolation of RCIC by manually defeating trip signals that might be received as plant conditions change in time. For example, the lack of active containment heat removal in the LTSBO scenario, combined with steam discharge from the RPV to the suppression pool, leads to an increase in suppression pool temperature. This in turn, would eventually generate signals for low steam inlet pressure for the RCIC turbine and (possibly) high RCIC room temperature. Among the observations made from the events that occurred at the Fukushima Daiichi Nuclear Power Station in Japan in March 2011 is that during a station blackout accident sequence, RCIC can operate for a considerable period of time (i.e., >24 hrs) beyond the point at which these isolation signals would occur. As a result, the fourth manual action assumed in the MELCOR analysis of the mitigated LTSBO is that operators defeat RCIC trip signals. If these actions are not successful, and the RCIC pump were to trip off coolant makeup is assumed to be provided through low-pressure injection lines by means of re-aligning the portable diesel-driven pump for direct RPV injection.

3.1.4 Scenario Boundary Conditions

Section 3.1.4.1 lists the sequence of events prescribed in the unmitigated LTSBO calculation. Section 3.1.4.2 summarizes the sequence of events in the mitigated LTSBO calculation.

3.1.4.1 Unmitigated Event Sequence

The unmitigated case credits automatic system responses and manual actions that would be directed by plant EOPs, such as operator reactor vessel depressurization and intervention to

---

[4] Attention also needs to be paid to managing pneumatic supply to the SRV accumulators. The limited gas supply in the accumulators can be replenished from multiple sources including alignment to the CAD tank via the instrument nitrogen header or placing the ADS nitrogen bottles in service. An external tanker truck connection can also be made to maintain a long-term pneumatic supply.

control RCIC injection flow (after its automatic actuation) to stabilize and maintain the level within a target range. The unmitigated case did not credit operator actions that are beyond the scope of EOPs – primarily, the mitigation measures installed in response to 10CFR50.54(hh). The effects of such actions were examined in the mitigated scenario, which is described in Section 3.1.4.2.

The following is the timeline of events and operator actions that were credited in the unmitigated case.

Unmitigated Event Timeline

<u>Event Initiation and Initial Plant Response</u>

- Seismic event results in a loss of offsite power.
- All diesel generators assumed to fail to start.
- DC power (station batteries) and associated emergency buses are available.
- Reactor trips (successful scram).
- Reactor pressure vessel isolates (i.e., main steam line isolation valves (MSIVs) close) and containment isolation valves close.
- The control rod drive hydraulic system (CRDHS), low pressure coolant injection (LPCI) mode of the residual heat removal (RHR) system, standby liquid control, condensate, containment cooling and containment spray systems are not available.
- Control room receives indication that plant is in a station blackout condition requiring the operator to enter Special Event Procedure SE-11, "Station Blackout Procedure." RCIC automatically starts when level drops to low-level setpoint with suction aligned to the CST.

<u>10-15 minutes</u>

- Plant operations personnel complete an initial assessment of plant status.
- RCIC auto-starts to make up for coolant losses and maintain RPV level.
- HPCI might auto-start in response to initial transient, but is secured by operations personnel.
- In accordance with SE-11, plant operations personnel initiate the following mitigation measures:
    - Attempt to line up the Conowingo hydroelectric dam (i.e., station blackout line) as an alternative offsite power source, but the line is not available.
    - Attempt manual start of emergency diesel generators, but none is available.
    - Begin to shed non-essential loads from the emergency DC bus.

50 minutes

- Emergency Operation Facility (EOF) is manned. The EOF is located in the Philadelphia area, far away from the plant. Therefore, the timing should not be affected by the seismic event.

1 hour

- Actions to shed non-essential loads from DC bus is complete, battery life extended to an estimated 4 hours.

- Initiate RPV depressurization by opening one SRV. The target reactor coolant system (RCS) pressure is 125 psi.

2 hours

- Operator assumes remote manual control of RCIC flow.

2.25 hours

- Technical Support Center (TSC) is assumed operational.

4 hours

- DC power from station batteries is exhausted. The consequences of a loss of DC power are:
    - Open SRV closes.
    - Remote control of RCIC flow terminates. The system is assumed to continue operate at the conditions it experienced immediately prior to battery exhaustion. This effectively assumes the RCIC pump continues to operate at a constant rate, ultimately flooding the main steam line causing delayed termination of RCIC.

3.1.4.2 Mitigated Event Sequence

The mitigated case credits the same actions assumed in the unmitigated event sequence, but also credits implementation of the mitigation measures installed in response to the requirements outlined in 10CFR50.54(hh). As noted in Section 3.1.3, this includes the staging and alignment of a variety of portable equipment, such as electric power supplies, low-pressure coolant injection pump and gas bottles for air-operated valve control.

It also credits manual opening of a containment vent path when containment pressure reaches unacceptably high levels. In the current analysis, a 16-in. (hard-pipe) vent path is assumed to be opened when containment pressure exceeds 45 psig. This vent path and opening pressure were selected based on a review of plant-specific containment vent procedures. Selection of the vent pathway took two factors into account. One factor is the availability of electric power or other equipment needed to open vent path isolation valves. The loss of all AC power supplies in the

LTSBO sequence demands use of portable 10CFR50.54(hh) equipment for this purpose.[5] A second factor is caution to avoid creating a hazardous environment in the reactor building by using vent pathways involving containment ventilation system ductwork. These factors led to the assumption that the preferred vent path would either be the 2-in hard pipe vent to the standby gas treatment system (SGTS), or the 16-in hard pipe vent pathway would be used. The larger vent path was used in this analysis because it was judged necessary to prevent further increases in containment pressure.

The procedure for containment pressure control recommends opening a vent path if pressure exceeds the 'peak containment pressure limit' (PCPL) of 60 psig. However, a high turbine exhaust pressure isolation signal for RCIC would be received at a pressure of 50 psig. Since RCIC is the only operating coolant injection system available in this scenario,[6] this analysis assumed operators would open the containment vent path at a slightly lower pressure (45 psig), thereby averting termination of RCIC flow.

The following is a timeline for these and other actions after the initiating event.

Mitigated Event Timeline

<u>Event Initiation and Initial Plant Response</u>

- Seismic event results in a loss of offsite power.
- All diesel generators fail to start.
- DC power (station batteries) and associated emergency buses are available.
- Reactor trips (successful scram).
- Reactor pressure vessel isolates (i.e., MSIVs close) and containment isolation valves close.
- The CRDHS, LPCI mode of the RHR system, standby liquid control, condensate, containment cooling and containment spray systems are not available.

---

[5] Current procedures for using B.5.b equipment (portable nitrogen bottles, in particular) to open containment vent path isolation valves only address the drywell ventilation system pathway. This path is not desirable under accident conditions in which the vented gas would be comprised of steam and/or hydrogen and/or high levels of radioactivity. The potential for adverse effects to the reactor building have been demonstrated in past NRC research programs concerning containment venting at Peach Bottom (NUREG/CR-4696, for example) and plant-specific emergency procedures caution against using this vent path if an alternative is available, such as the 16-in hardened vent or the 6-in integrated leak rate test (ILRT) line. B5.b equipment could be used to open the isolation valves for either of these paths, but plant-specific procedures have not yet been developed.

[6] The portable coolant injection pump is considered a viable backup to RCIC, but continued RCIC operation would be the preferred method for coolant injection.

- Control room receives indication that plant is in a station blackout condition requiring the operator to enter Special Event Procedure SE-11, "Station Blackout Procedure."

- RCIC automatically starts when level drops to low-level setpoint with suction aligned to the CST.

- Cooling tower basin is assumed to be undamaged, containing about 3.55 million gallons of water and is a source for refilling the CST.

<u>10-15 minutes</u>

- Plant operations personnel complete an initial assessment of plant status.

- RCIC auto-starts to make up for coolant losses and maintain RPV level.

- HPCI might auto-start in response to initial transient, but is secured by operations personnel.

- In accordance with SE-11, plant operations personnel initiate the following mitigation measures:
    - Attempt to line up the Conowingo hydroelectric dam (i.e., station blackout line) as an alternative offsite power source, but the line is not available.
    - Attempt manual start of emergency diesel generators, but none is available.
    - Begin to shed non-essential loads from the emergency DC bus.

<u>50 minutes</u>

- EOF is manned. The EOF is located in the Philadelphia area, far away from the plant. Therefore, the timing should not be affected by the seismic event.

<u>1 hour</u>

- Actions to shed non-essential loads from DC bus is complete, battery life extended to an estimated 4 hours.

- RPV depressurization is initiated using one SRV. The target RCS pressure is 125 psi.

<u>1.5 hours</u>

- The EOF is operational. The EOF reviews actions taken by Operations and determines the availability of the remotely located trailer-mounted portable diesel-driven pump stored outside of the protected area. Actions recommended by the EOF include the following:
    - Use portable power supply for operating SRVs and for RPV level indication.
    - Perform RCIC blackstart.
    - Use portable diesel driven pump (250 psi, 500 gpm) to provide makeup to RCS, Hotwell, CST, and other locations.
    - Use portable air supply to manually operate containment vent valves.
    - Use pumper truck in place of portable diesel-driven pump.

1.75 hours

- Operators assess and concur with EOF recommendations. Operators prioritize recommendations based on plant conditions and begin implementation.

2 hours

- Operator assumes remote manual control of RCIC flow.

- TSC is manned. Because of the magnitude of the event, loss of causeway, other potential infrastructure failures, and multiple emergency responders located on both sides of the river, a 1-hour delay in minimum manning of the TSC was assumed.

2.25 hours

- TSC is assumed operational.

3.5 hours

- Portable DC power supply (i.e., AC generator operating through an converter) is connected to continue operating the SRV to depressurize the RPV.

- RCIC system is manually controlled to limit the use of site batteries and to continue providing makeup to the RCS.

Before 10 hours

- Portable air supply to manually operate containment vent valves is in place and ready for operation.

- Portable diesel driven pump is staged and available for service.

3.2 Short Term Station Blackout

Section 3.2.1 describes the initial status of the plant following the seismic event. Section 3.2.2 then discusses the availability of plant systems to respond to the initiating event. Actions that can be taken by plant personnel to mitigate the effects of failed plant safety functions are described in 3.2.3. Section 3.2.4 describes two scenarios that differ in the assumed success (or failure) of the mitigative actions. Mitigated scenarios are defined as those in which the mitigative actions are successful. Unmitigated scenarios are defined as those in which certain key mitigation measures are not successfully implemented.

3.2.1 Initiating Event

The STSBO is initiated by the same spectrum of events that lead to the LTSBO, but is more extensive in the amount of consequential damage to plant systems. The most frequent initiators are large seismic events or internal fires or floods. The seismic event is a major contributor to the composite frequency of this sequence and is conservatively used as the basis for defining consequential events and conditions at the plant. Damage caused by the earthquake is assumed to result in a total loss of offsite power. In addition, all diesel generators fail to start or run as

needed, rendering all onsite AC power unavailable. The diesel generators have a shared configuration between the two units, which causes power failure to affect both units. However, this analysis considers only the response to failures at one of the units. Additionally, the earthquake results in failure of all onsite DC power.

3.2.2 System Availabilities

Similar to the LTSBO scenario, reactor scram, reactor isolation and containment isolation immediately follow the initiating event. Neither active AC nor DC power is necessary for these safety functions to occur. The station blackout electric power line from the hydroelectric station downstream of the plant site is also assumed to be unavailable because of structural damage to the dam and electric station components.

The principal difference between this scenario and the LTSBO is that DC power from station batteries is also not available. Thus, a total loss of all onsite and offsite electrical power occurs immediately following the initiating event rather than several hours later, thereby disabling all plant equipment dependent on control or motive power for start-up and operation.

Loss of all DC power disables electronic start-up and control of steam-driven emergency coolant makeup systems (RCIC and HPCI), as well as control and motive power to reactor pressure relief valves, which were available for a few hours in the LTSBO. As described in Section 2.3, however, plant operations personnel would attempt to blackstart RCIC in this situation. The specific actions necessary to accomplish local, manual start-up and operation of RCIC are delineated in plant procedures, and the actions are reviewed as part of routine operator training. Therefore, successful RCIC blackstart is assumed to occur in the baseline calculation for the STSBO. However, a sensitivity calculation was also performed to investigate the ways in which failure of RCIC blackstart (i.e., loss of all coolant injection) alters the chronology of severe accident progression and the resulting source term. Results of this sensitivity case are also useful for comparison to past STSBO analyses.

3.2.3 Mitigative Actions

Manual operation of RCIC under blackstart and blackrun conditions would delay (blackstart) or prevent (blackrun) core damage during an STSBO. A calculation assuming RCIC blackstart (but not blackrun) is described in Section 5.3. This calculation shows RCIC blackstart delays the onset of core damage by more than 5 hours, which is sufficient time to mobilize and align equipment added under 10CFR50.54(hh), i.e., the independent diesel-driven pump. The independent diesel-driven pump would then be used as a means of direct injection into the RPV if RCIC operation could not be sustained via blackrun. Alternatively, long term operation of RCIC could be maintained under blackrun conditions if the portable electric generator energized the instrumentation that measures and indicates RPV water level. Based on the calculation described in Section 5.3, this action would need to be completed within 3.4 hours of the initiating event to prevent failure of RCIC due to RPV overfill. The independent diesel-driven pump could then be aligned to replenish the CST, thereby maintaining RCIC suction from a source that is not adversely affected by the absence of suppression pool cooling and resulting increases suppression pool water temperature. Full mitigation (i.e., prevent core damage and long term containment heat removal) would result if portable equipment necessary to manually open and close a containment vent path is available. This equipment was described in Section 3.1.3 for the

LTSBO accident sequence. The resulting plant response would be very similar to the mitigated LTSBO described in Section 5.2.

Procedures and equipment added under 10CFR50.54(hh) (i.e., the independent diesel driven pump and a portable electric generator) were not explicitly modeled for the unmitigated STSBO (i.e., no blackstart or blackrun) because it was judged that insufficient time is available to mobilize and align the portable equipment prior to the onset of core damage.

3.2.4 Scenario Boundary Conditions

Two variations of the STSBO scenario were considered. The only difference in the two cases is success or failure of actions to manually actuate (blackstart) the steam-driven RCIC system. The base case assumes successful blackstart; a sensitivity case examines the effects of failure to blackstart RCIC.

3.2.4.1 STSBO with RCIC Blackstart

Blackstart of RCIC during a STSBO requires several manual actions by plant operations personnel. These actions include local, manual opening of normally closed valves to admit steam from the main steam lines into the RCIC turbine and pump discharge valves to direct water into the reactor vessel.

The baseline STSBO calculation assumes operators successfully complete these actions within one hour after the initiating event, at which time coolant flow to the reactor vessel begins. Manual actions to regulate steam flow into the RCIC turbine (thereby controlling pump discharge rate) after blackstart is accomplished are not credited in this scenario because electric power to instrumentation needed to monitor reactor coolant level would not be available. As a result, the system effectively operates at a constant flow rate equivalent to the rated capacity of the system (i.e., 600 gpm). Because this flow rate is greater than the rate required to make up for evaporative losses, the reactor water level rises above nominal and eventually overfills the reactor vessel. In this context, 'overfill' means that the reactor water level increases to the elevation of the main steam line nozzles, allowing water to spill into the steam lines and causing them to flood with water. The steam supply line for the RCIC turbine connects to the main steam line at a low elevation (adjacent to the inboard MSIVs). Therefore, water spilling over into the main steam lines blocks or flows toward the RCIC turbine, causing the system to cease functioning. RCIC blackstart without effective RPV level control is therefore a temporary measure for managing reactor coolant inventory, and core damage occurs approximately 6 hrs later than would be observed in a case without RCIC blackstart.

Results of the STSBO with RCIC blackstart are described in Section 5.3.

The following is the timeline of events and operator actions that were credited in the STSBO scenario with successful RCIC blackstart.

Event Timeline for STSBO with Successful RCIC Blackstart

<u>Event Initiation and Initial Plant Response</u>

- Large seismic event results in a loss of offsite power.

- All diesel generators fail to start.

- DC power (station batteries) and/or associated emergency buses are not available.

- Reactor trips (successful scram).

- Reactor pressure vessel isolates (i.e., MSIVs close) and containment isolation valves close.

- The CRDHS, LPCI mode of the RHR system, standby liquid control, condensate, containment cooling and containment spray systems are not available.

- Control room receives indication that plant is in a station blackout condition requiring the operator to enter Special Event Procedure SE-11, "Station Blackout Procedure."

<u>15 minutes</u>

- Plant operations personnel complete an initial assessment of plant status.

- Plant operations personnel begin to implement actions to blackstart RCIC.

- In accordance with SE-11, plant operations personnel initiate the following mitigation measures:
    - Attempt to line up the Conowingo hydroelectric dam (i.e., station blackout line) as an alternative offsite power source, but the line is not available.
    - Attempt manual start of emergency diesel generators, but none is available.

<u>1 hour</u>

- RCIC is successfully started and begins to inject water from the CST at rated capacity (600 gpm).

3.2.4.2 STSBO without RCIC Blackstart

Past NRC severe accident analyses of STSBO scenarios did not credit blackstart of RCIC. A sensitivity calculation without blackstart was therefore performed to provide a basis for comparison to past analyses. Section 5.4 describes results of the sensitivity calculation.

3.3 Loss of Vital Alternating Current Bus E-12

The scenario is initiated by the loss of vital AC bus E-12. It was initially estimated to have a frequency above the SOARCA screening criterion of $1x10^{-6}$ pry. However, after further review of the SPAR model and comparison with the licensee's PRA, the scenario was determined to have a CDF below the screening criteria. Because the MELCOR analysis provided unique insights into the response of the plant to an internal event sequence, the MELCOR analysis was retained.

Section 3.3.1 describes the initial status of the plant following the initiating event. The key system availabilities during the course of the accident are summarized in Section 3.3.2. The pertinent mitigative measures available to address the accident progression are described in Section 3.3.3. Section 3.3.4 describes various scenarios based on the success of the mitigative actions. Mitigated scenarios are defined as those in which the mitigative actions are successful. Unmitigated scenarios are defined as those in which certain key mitigate measures are not successfully implemented.

3.3.1 Initiating Event

The initiating event for this scenario is a loss of Division I vital AC bus E-12. Loss of power through this bus eliminates power that sustains power to the Division I DC bus (through the battery charger). The Division I DC bus would continue to remain energized for the lifetime of the batteries, which is expected to be a minimum of 2 hours.

3.3.2 System Availabilities

Loss of one vital AC bus disables motive or control power to some plant equipment, but not all. For example, power to the instrument and control air system would be lost, and the converters that charge the station batteries would not function. However, other AC buses would direct motive power to the RHR and core spray pumps, permitting use of low-pressure coolant injection. One of the two CRDHS pumps would also remain available.

Steam-driven injection systems (HPCI and RCIC)[7] operate as long as station batteries deliver DC power to control system components. Station batteries also facilitate manual control of SRVs. When battery power is depleted, HPCI, RCIC, and SRV controls are assumed to be lost.

The shut-down cooling mode of RHR would not be available because of loss of AC power disables valves needed to align the system for that configuration. However, the system can be aligned to operate suppression pool cooling and drywell sprays.

The duration of DC power is treated as an uncertain parameter in this scenario. The licensee PRA uses a value of 2 hours, which is the minimum value and represents the worst possible condition. The licensee's engineering judgment is that batteries can last 4 hours with effective DC load shedding. As described in Section 5.6.3, a precise value is not particularly important, provided battery duration is greater than 3 hours.

3.3.3 Mitigative Actions

This event was shown to be satisfactorily mitigated without crediting any of the security related mitigative actions mentioned in Section 3.1.3. Therefore, although scenario boundary conditions were determined for a mitigated case (see Section 3.3.4.2), a thermal-hydraulic accident progression analysis was not performed for the mitigated scenario. Further, the base

---

[7] Although RCIC is available in all the standard plant analysis risk cut sets for this sequence, HPCI is disabled due to independent failures in some of the sequences. Availability of HPCI is not important in this sequence and is neglected.

case among the unmitigated cases, as well as many of the sensitivity calculations described below, did not result in core damage as described later in Section 5.6.

It should also be noted that the licensee ran the Loss of E12 Bus scenario on their plant simulator in November 2011. The licensee offered the following description of the observed response:

> The Training Instructor that ran the simulation determined that the immediate impact of the bus loss did not result in a plant scram, only a one-half logic primary containment isolation (½ PCIS isolation); however, loss of the bus does cause all condenser hotwell indication to fail and condenser hotwell makeup valves to go full open. This eventually results in a loss of vacuum due to the high hotwell level covering the condenser tubes. Attempts to control level manually are not an option because you do not have indication of hotwell level. Additionally, vacuum will eventually be lost due to the 'A" Steam Jet Air Ejector (SJAE) pressure controller failing to 0 (maybe a simulator issue but could be a plant issue also) requiring a manual scram before receipt of the automatic scram (per procedure). During the simulation, attempts were made to swap to the "B" SJAE controller but the "B" SJAE train could not be placed in service apparently due to the loss of power was not allowing the valve interlock logic to work.

3.3.4 Scenario Boundary Conditions

Section 3.3.4.1 lists the sequence of events to be prescribed in the unmitigated accident scenario for loss of AC bus E-12 accident scenario. Section 3.3.4.2 summarizes the sequence of events in the mitigated case.

3.3.4.1 Unmitigated Cases

Several unmitigated cases were considered, which differ only in terms of the assumed duration of station batteries. Unmitigated cases, as noted above, generally did not result in core damage. Variations in station battery duration affected the length of time RCIC was available for controlled coolant makeup and an SRV could be held in the open position to maintain lower RPV pressure. As noted later, all cases in which station batteries continued to provide control power to RCIC for at least 3 hours were found to avoid core damage. The unmitigated cases did <u>not</u> credit mitigation measures developed under the requirements of 10CFR50.54(hh), such as the staging and alignment of a back-up power supply and portable coolant injection pump.

The timeline following the initiating event is summarized below.

Unmitigated Event Timeline

<u>Event Initiation and Initial Plant Response</u>

- Loss of Division I AC bus E-12.
- Loss of all AC powered coolant injection except one CRDHS pump.
- Successful reactor trip, reactor and containment isolation.

- DC power (station batteries) functional.

- RCIC auto-initiates when reactor level drops to low-level setpoint. Suction is initially aligned to the CST.

- When level rises to operating range, operator takes manual control of RCIC to maintain RPV level.

15 minutes
- Initial Operations assessment of plant status is complete.

- RCIC is operating, maintaining RCS level.

- In accordance with SE-11, actions to shed non-essential loads from the emergency DC bus are initiated.

1 hour
- DC load shedding is complete, extending battery life from 2 to 4 hours.

- Also available is access to the CRD throttle valve to increase flow from 110 gpm to 140 gpm without reactor depressurization.

1.25 hours
- TSC is fully operational.
- EOF is fully operational.

1.5 hours
- Operators initiate RPV depressurization by opening one SRV. Target RCS pressure is approximately 125 psi.

4 hours
- DC power from station batteries is exhausted.
- Open SRV re-closes.
- RCIC stops operating due to turbine overspeed trip.

Parameters Varied in Sensitivity Calculations

Section 5.6 describes results of several calculations of plant response to the unmitigated scenario. Several calculations were performed to quantitatively assess the effects of uncertainties in some of the boundary conditions for this scenario. Among the boundary conditions are:

- RPV depressurization: The rate of coolant flow delivered by the single, operating CRDHS pump is affected by RPV pressure. The nominal case assumes operators follow EOP guidance to depressurize the RPV. This assumption increases the delivered CRDHS flow. Sensitivity calculations were performed assuming actions to depressurize the RPV were not successful, resulting in lower CRDHS flow.

- Managing CRDHS flow: plant-specific procedures instruct operators to maximize CRDHS flow if the system serves as an alternate means of RPV injection. In this case, CRDHS is the only system available for coolant injection after station battery exhaustion. Sensitivity calculations were therefore performed to examine the effects of not increasing CRDHS flow from nominal values to maximum flow conditions.

- Duration of DC power: Battery lifetimes of 2, 3, 4, and 6 hours are analyzed to determine the extent to which sustained operation of RCIC is necessary to prevent core damage.

3.3.4.2 Mitigated Case

Implementation the mitigation measures developed in response to 10CFR50.54(hh) provides diverse and redundant means of maintaining coolant injection beyond the systems that continue to operate in the unmitigated cases. The following is a timeline for implementing these and other actions after the initiating event.

Mitigated Event Timeline

Event Initiation

- Loss of Division I AC bus E-12.

- Loss of all AC powered coolant injection except one CRDHS pump.

- Successful reactor trip, reactor and containment isolation.

- DC power (station batteries) functional.

- RCIC auto-initiates when reactor level drops to low-level setpoint. Suction is initially aligned to the CST.

- When level rises to operating range, operator takes manual control of RCIC to maintain RPV level.

- Standby liquid control system is available but neglected because its cooling injection flow of 50 gpm is not necessary.

- Drywell spray is available, but neglected because it is not necessary.

15 minutes

- Initial Operations assessment of plant status is complete.

- RCIC is operating, maintaining RCS level.

- In accordance with SE-11, actions to shed non-essential loads from the emergency DC bus are initiated.

50 minutes

- TSC staffing is underway. Their primary function would be to review initiating event, plant status, and operator action to provide guidance on alternative mitigative measures.

- EOF staffing is underway. Their primary function would be to review initiating event, plant status, and operator action to provide guidance on alternative mitigative measures. The primary users of SAMGs and Extreme Damage Mitigation Guidelines (EDMGs) are the Tech Manager, Operations Manager, and Emergency Director who are trained on SAMGs and EDMGs.

1 hour

- DC load shedding is complete, extending battery life from 2 to 4 hours.

- Also available is access to the CRD throttle valve to increase flow from 110 gpm to 140 gpm without reactor depressurization.

1.25 hours

- TSC is fully operational.
- EOF is fully operational.

1.5 hours

- Operators initiate RPV depressurization by opening one SRV. Target RCS pressure is approximately 125 psi.

- TSC and/or EOF review actions taken by Operations and determines the availability of the remotely located equipment. Recommend the following actions:
    - Portable power supply connected through an converter to the emergency DC bus to ensure power necessary to hold SRV open .
    - Portable diesel driven pump (500 gpm at 250 psi) is available for makeup to the RCS, Hotwell, or CST.
    - Portable air supply is available to manually operate containment vent isolation valves, as required.
    - Portable diesel driven pump is available to inject water into the drywell via RHR or the RCS.

1.75 hours

- Operations staff assesses and concurs with TSC's and/or EOF's recommendations.

- Operations staff prioritizes recommendations based on plant conditions and begins implementation.

4 hours

- Manual operation of the RCIC to sustain RCS level after battery depletion.

4.0 MELCOR MODEL OF THE PEACH BOTTOM PLANT

This section summarizes the MELCOR model of the Peach Bottom Atomic Power Station. A comprehensive description of the model is available in separate documentation.

The MELCOR Peach Bottom model was originally generated for code assessment applications with MELCOR 1.8.0 at Brookhaven National Laboratories. The model was subsequently adopted by J. Carbajo at Oak Ridge National Laboratories to study differences between fission product source terms predicted by MELCOR 1.8.1 and those generated for use in NUREG-1150, "Severe Accident Risks: An Assessment for Five U.S. Nuclear Power Plants," issued December 1990, using the Source Term Code Package [1]. In 2001, Sandia National Laboratories refined the BWR/4 core nodalization to support the developmental assessment and release of MELCOR 1.8.5. These refinements concentrated on the spatial nodalization of the reactor core (in terms of fuel and structural material and hydrodynamic volumes) used to calculate in-vessel melt progression. However, the overall scope of the model also expanded to permit a wider spectrum of accident scenarios to be examined, some of which involved operation or delayed failures of plant safety systems.

These developments culminated in a model that was applied in the reassessment of radiological source terms for high burnup and MOX core designs, and a comparison of their release characteristics [4] to the regulatory prescription outlined in NUREG-1465, "Accident Source Term for Light-Water Nuclear Power Plants," issued February 1995 [5]. These calculations addressed a wide spectrum of postulated accident sequences, which required the following new models to represent diverse plant design features:

- Modifications of modeling features needed to achieve steady-state reactor conditions (e.g., recirculation loops, jet pumps, steam separators, steam dryers, feedwater flow, CRDHS, main steam lines, turbine/hotwell, core power profile),

- New models and control logic to represent coolant injection systems (e.g., RCIC, HPCI, RHR, LPCS) and supporting water resources (e.g., CST with switchover), and

- New models to simulate reactor vessel pressure management (e.g., SRV, safety valves, ADS, and logic for manual actions to affect a controlled depressurization if torus water temperatures exceed the heat capacity temperature limit).

Subsequent work in support of other NRC research programs motivated further refinement and expansion of the model in two broad areas. The first area focused on the spatial representation of primary and secondary containment. The drywell portion of primary containment has been subdivided to distinguish thermodynamic conditions internal to the pedestal from those within the drywell itself. Refinements have also been made to the spatial representation and flow paths within the reactor building (i.e., secondary containment). The second area has focused on bringing the model up to current best practice standards for MELCOR 1.8.6. Table 4-1 provides a brief summary of plant design parameters that are helpful in comparing the configuration of Peach Bottom to other reactors of interest.

Table 4-1 Important Design Parameters for Peach Bottom

Parameter	*Value (SI units)*	*Value (British units)*
Rated Core Power [MW_{th}]	3514	
Number of Fuel Assemblies in Core	764	
Assumed Average Specific Power [MWD/MTU]	25.5	
Fuel (UO_2) Mass [kg / lb]	155,500	342,800
Zircaloy Mass in Fuel Cladding [kg / lb]	40,580	89,500
Zircaloy mass in Fuel Channels [kg / lb]	19,600	43,200
RPV Inner Diameter [m / ft]	6.4	21.0
RPV Height [m / ft]	22.2	72.9
RPV Wall Thickness (core mid-plane) [cm / in]	16.4	6.4
Containment Design Pressure [MPa / psig]	0.49	56
Drywell Free Volume [m^3 / ft^3]	4,980	176,000*
Nom. Wetwell Free Volume (airspace) [m^3 / ft^3]	3,570	126,000
Nom. Suppression Pool Water Volume [m^3 / ft^3]	3,570	126,000
Reactor Building Free Volume [m^3 / ft^3]	75,200	2,655,600
Condensate Storage Tank Water Volume [L / gal]	757,082	200,000
RCIC Rated Flow [tonne per hr / gpm] **	136	600
CRDHS Flow [tonne per hr / gpm]**		
Nominal (during full-power reactor operation)	14	63
Post-scram	25	110
Maximum capacity per pump	32	140

* Including the volume of wetwell-drywell vent pipes
** Values with reactor at nominal pressure.

4.1 Reactor Vessel and Coolant System

Excluding the core region, the RPV is represented by seven hydrodynamic control volumes, nine flow paths, and 24 heat structures. Nodalization for the core region between the core top guide and the bottom of active fuel are described in detail in Section 4.2. Figure 4-1 illustrates the reactor vessel nodalization by comparing the actual vessel design (on the left) to the MELCOR control volume representation (on the right). In Figure 4-1, control volumes are indicated by 'CV' followed by the three-digit control volume number, and flow paths are indicated by 'FL' followed by the three-digit flow path number.

Appended to the MELCOR control volumes representation of the RPV shown in Figure 4-1 are several additional control volumes and flow paths representing a variety of reactor support systems, such as:

- reactor recirculation piping,
- main feedwater and steam lines, and
- connections to emergency coolant injection and heat removal systems.

The MELCOR representation of the entire reactor coolant system is illustrated in Figure 4-2. Collectively, these ancillary systems permit the model to properly calculate steady state, as well

as a wide variety of transient conditions. To optimize numerical performance of this model, some parallel lines or trains of certain systems have been consolidated. For example, the four main steam lines have been represented by two parallel 'lines,' one of which represents the single steam line containing the lead (i.e., lowest set point) SRV, and the second, the composite geometry of the remaining three lines. Isolating the steam line with the lead SRV permits the proper geometry (e.g., internal volume, structural surface area) to be represented for fission product transport from the reactor to the suppression pool during accident sequences in which fuel damage begins while the reactor vessel is at high pressure and pressure relief is accomplished by SRV operation.

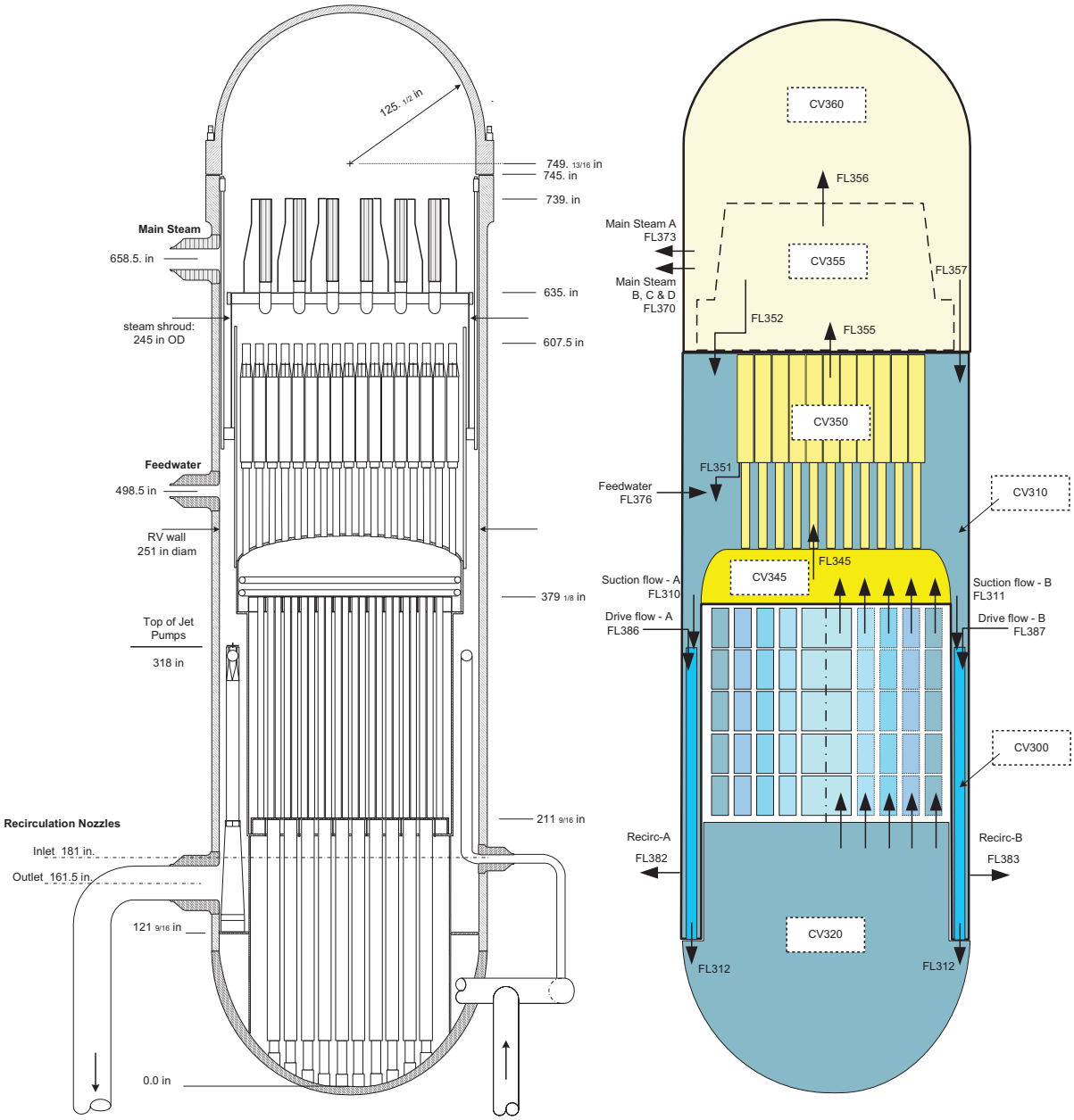

Figure 4-1 Reactor vessel cross-section detail and MELCOR hydrodynamic nodalization

4.2 In-vessel Structures and Reactor Core

Structures within the RPV are described in the next three sections. First, Section 4.2.1 describes the general configuration of the spatial nodalization of the core and structures below the core. Certain aspects of this nodalization, and some characteristics of the MELCOR model of material degradation, are tailored to the unique design features of BWRs. These are briefly summarized in Section 4.2.2. Finally, Section 4.2.3 mentions the manner in which in-vessel structures above the core are treated in the MELCOR model.

4.2.1 General Configuration of MELCOR In-vessel Nodalization

In MELCOR, the region tracked directly by the COR package model includes a cylindrical space extending vertically downward along the inner surface of the core shroud from the core top guide to the reactor vessel lower head. It also extends radially outward from the core shroud to the hemispherical lower head in the region of the lower plenum below the base of the downcomer, preserving the curvature of the lower head from this point back to the vessel centerline.

The core and lower plenum regions are divided into concentric radial rings and axial levels. Each core cell may contain one or more core components, including fuel pellets, cladding, canister walls, supporting structures (e.g., the lower core plate and control rod guide tubes), non-supporting structures (e.g., control blades, the upper tie plate, and core top guide) and once fuel damage begins, particulate and molten debris.

The spatial nodalization of the core is shown in Figure 4-3 and Figure 4-4. The entire core and lower plenum regions are divided into six radial rings. As indicated in Figure 4-4, rings one, two, three, four, and five represent 112, 160, 200, 168, and 124 fuel assemblies, respectively. The radial distance between each of the five rings is not uniform. The radius of each ring was defined so as to preserve the radial power distribution in the Unit 2 core, based on plant operating data from four recent and consecutive operating cycles. Radial ring 6 represents the region in the lower plenum outside of the core shroud and below the downcomer. Ring 6 exists only at the lowest axial levels in the core model.

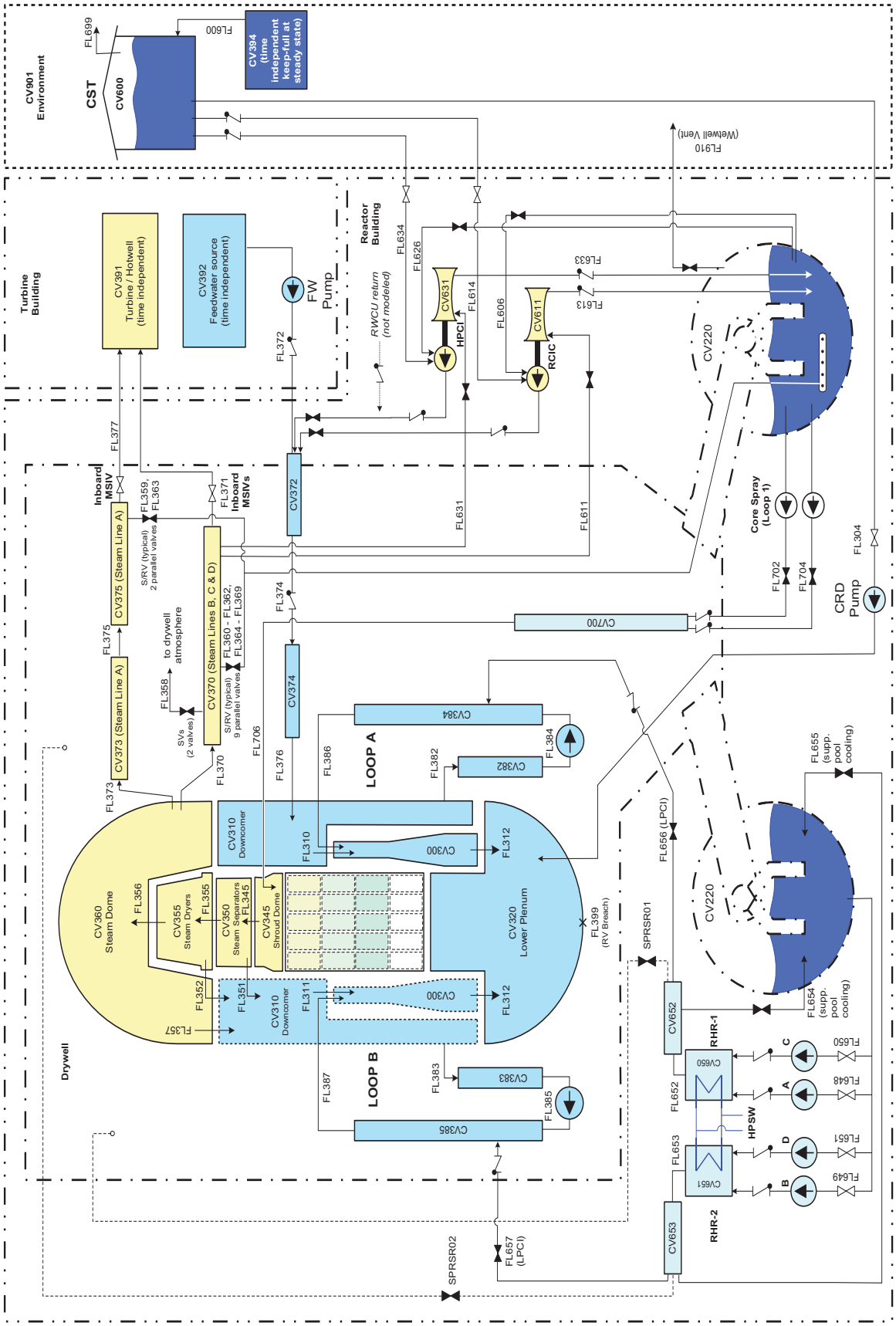

Figure 4-2 Spatial nodalization of reactor pressure vessel and coolant system

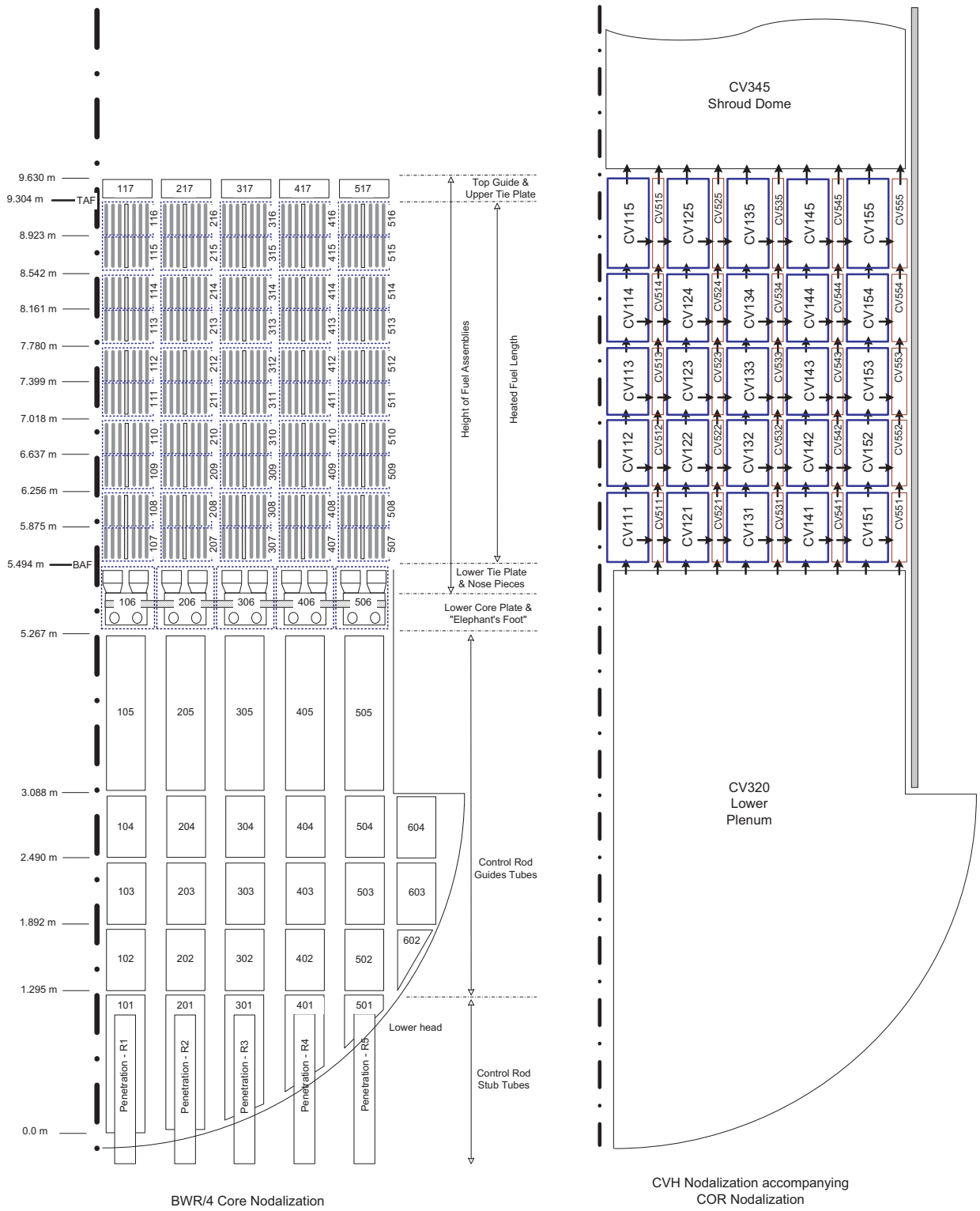

Figure 4-3 Spatial nodalization of the core and lower plenum

radius > v 0	0 center	0.153 16	0.305 17	0.458 18	0.610 19	0.763 20	0.915 21	1.068 22	1.220 23	1.373 24	1.525 25	1.678 26	1.830 27	1.983 28	2.135 29	2.288 30	(m)
0.153	16	0.928	1.306	1.088	1.258	1.045	1.413	1.094	1.344	1.069	1.440	1.090	1.162	0.727	0.528	0.270	
0.305	17	1.305	1.100	1.373	1.065	1.395	1.207	1.468	1.209	1.463	1.303	1.421	1.225	0.818	0.536	0.272	
0.458	18	1.084	1.367	1.156	1.389	1.182	1.471	1.246	1.487	1.208	1.496	1.236	1.273	0.791	0.531	0.268	
0.610	19	1.253	1.044	1.365	1.064	1.341	1.134	1.482	1.215	1.454	1.268	1.403	1.156	0.756	0.510	0.257	
0.763	20	1.040	1.368	1.159	1.335	1.120	1.463	1.242	1.448	1.203	1.465	1.098	1.110	0.704	0.484	0.241	
0.915	21	1.410	1.199	1.460	1.128	1.459	1.246	1.500	1.163	1.480	1.323	1.337	1.121	0.700	0.453	0.215	
1.068	22	1.092	1.462	1.240	1.473	1.233	1.489	1.235	1.455	1.250	1.378	0.995	0.980	0.620	0.336	0.168	
1.220	23	1.343	1.205	1.479	1.206	1.431	1.129	1.417	1.145	1.258	1.139	1.014	0.724	0.450	0.246		
1.373	24	1.068	1.459	1.201	1.443	1.186	1.432	1.203	1.245	0.954	0.945	0.720	0.522	0.295			
1.525	25	1.439	1.299	1.489	1.257	1.447	1.297	1.352	1.128	0.942	0.775	0.498	0.306	0.172			
1.678	26	1.089	1.417	1.231	1.394	1.087	1.320	0.981	1.007	0.716	0.497	0.314					
1.830	27	1.161	1.222	1.268	1.152	1.104	1.112	0.970	0.707	0.517	0.304						
1.983	28	0.727	0.813	0.788	0.754	0.701	0.695	0.615	0.445	0.291	0.171						
2.135	29	0.528	0.532	0.530	0.508	0.482	0.450	0.333	0.244								
2.288	30	0.270	0.271	0.268	0.256	0.240	0.214	0.166									
(m)																	

	# assemblies	3-cycle average RPF
RING 1	112	1.223
RING 2	160	1.313
RING 3	200	1.275
RING 4	168	0.746
RING 5	124	0.295
	764	

Figure 4-4 Local relative power fraction and five ring radial boundaries of core

The core and lower plenum are divided into 17 axially stacked levels. The height of a given level varies but generally corresponds to the vertical distance between major changes in the flow area, structural materials, or other physical features of the core (and below core) structures. Axial levels 1 through 5 represent the open space and structures within the lower plenum. Initially, this region has no fuel and no internal heat source but contains a considerable mass of steel associated with the control rod guide and in-core instrument tubes. During the core degradation process, the fuel, cladding, and other core components displace the free volume within the lower plenum as they relocate downward in the form of particulate or molten debris.

Axial level 6 represents the steel associated with fuel assembly lower tie plates, fuel nose pieces, and the lower core plate and its associated support structures. Particulate and molten debris formed by failed fuel, canister, and control blades above the lower core plate will be supported at this level until the lower core plate yields. Axial levels 7 through 16 represent the active fuel region. All fuel is initially in this region and generates the fission and decay power. Axial level 17 represents the nonfuel region above the core, including the top of the canisters, the upper tie plate, and the core top guide.

4.2.2 Treatment of Unique Design Features of a BWR Core

Several design features of the BWR core, and associated structures located below the core, merit special attention in modeling severe accidents. These are not discussed exhaustively here, but a few are mentioned to illustrate the way in which the modeling approach to this type of reactor differed from the approach used to model a Pressurized Water Reactor (PWR), or other designs.

Fuel Channels and Control Blades

Each BWR fuel assembly in the core is shrouded by a solid rectangular channel box, which confines coolant flow to that single assembly. Therefore, cross-flow between adjacent assemblies is not possible in a BWR unless a pair of adjacent channel boxes fails. Figure 4-5 illustrates this configuration for a module of four fuel assemblies, which surrounds a single control blade. Unlike control rod clusters in a typical PWR, which are inserted directly into certain fuel assemblies, the control blade in a BWR is inserted into the interstitial space between (and outside) adjacent fuel channels.

The MELCOR hydrodynamic model for this configuration recognizes the vertical constraint placed on flow through the core unless or until structural damage to fuel channels occurs. The in-core heat transfer model also accounts for lateral (or radial) differences in the materials adjacent to 'bladed' sides of a channel (i.e., sides neighboring a control blade) versus 'unbladed' sides, which communicate only with a neighboring fuel channel. As fuel temperature rise in the core during an accident simulation, axial and radial heat transfer calculations account for oxidation of Zircaloy fuel cladding and the Zircaloy channels. Separate failure criteria are used to ascertain when highly oxidized fuel rods and highly oxidized channels can no longer maintain their normal upright configuration and collapse into particulate debris. Failure criteria for fuel rods and channels are discussed briefly in Section 4.8.1.

Radial cross-flow from one ring of the core nodalization to a neighboring ring is possible if the channels in both rings melt or collapse to open a flow path in the radial direction. As indicated by in the nodalization diagram on the right-hand side of Figure 4-3, radial flow out of the interior region of the channels within a particular must first flow into the neighboring core bypass area (i.e., the space between channels normally occupied by control blades.) If the stainless steel clad control blades and Zircaloy channel boxes in the neighboring fuel channel also melt or collapse, fluid could continue to flow radially out of the bypass region into the neighboring channel, and so on. Circular, natural circulation flow patterns within the core region can, therefore, only occur after a sufficient number of channel boxes (properly distributed) melt, or otherwise relocate downward, creating open space in the radial direction. Logical control functions in the MELCOR model track the structural status of channel boxes at each cell (node) in the core to determine whether flow paths in the radial direction should be open or closed.

Notable BWR Core Design Features

1. Core top guide

3. Fuel assembly upper tie plate

6. Channel box
7. Cruciform control blade
8. Fuel rod
9. Spacer
10. Core plate

Figure 4-5 Module of Four BWR Fuel Assemblies and Associated Channel Boxes[8]

The axial nodalization of the core is designed, in part, to account changes in material composition and mass along the axial length of a typical fuel assembly. For example, Figure 4-5 does not explicitly show the fact that some BWR fuel assembly designs (modern 10x10 assemblies, for example) incorporate fuel rods of different length within a single assembly. As a result, the amount of UO_2, and other constituents can differ at the top of an assembly from the bottom. Discrete locations of fuel rod spacers along the axial height of an assembly also affect local Zircaloy mass. The distribution of material mass within the axial nodalization of the core takes these variations into account.

Lower Plenum Structures

The COR Package in MELCOR, which models the oxidation, melting, and downward relocation of overheated core materials, extends downward below the lower core plate into the RPV lower plenum. Molten core debris that flows, or particulate debris that falls, under gravity into the lower plenum collects as a mixed debris bed on the inner surface of the lower head. In a BWR, this region is filled with a forest of vertical cylinders that house the drive mechanisms for core control blades as well as in-core instrumentation. Figure 4-6 depicts a typical configuration of a control rod guide tube (CRGT) this region of the RPV.

---

[8] Illustration courtesy of General Electric.

The MELCOR model for Peach Bottom accounts for the structural mass and surface area of the CRGTs, which participate in heat transfer within the debris bed that accumulates around them. The physical space occupied by intact CRGTs displaces volume available for debris to occupy in the lower plenum.[9] Therefore, debris accumulates to an elevation higher than the value that would be calculated by neglecting the volume of the CRGTs. Debris heat transfer, and continued oxidation of metallic components within the lower head, accounts for the heat capacity and stainless steel composition of the CRGTs. The CRTGs are modeled as vertical columns, which fail (buckle) when load carried by the CRGTs exceeds their residual strength, which decreases as heat is transferred from core debris. The calculation of CRGT integrity is performed on a radial ring-by-ring basis, with 5 rings in the Peach Bottom model as indicated in the diagram on the left-hand side of Figure 4-3.

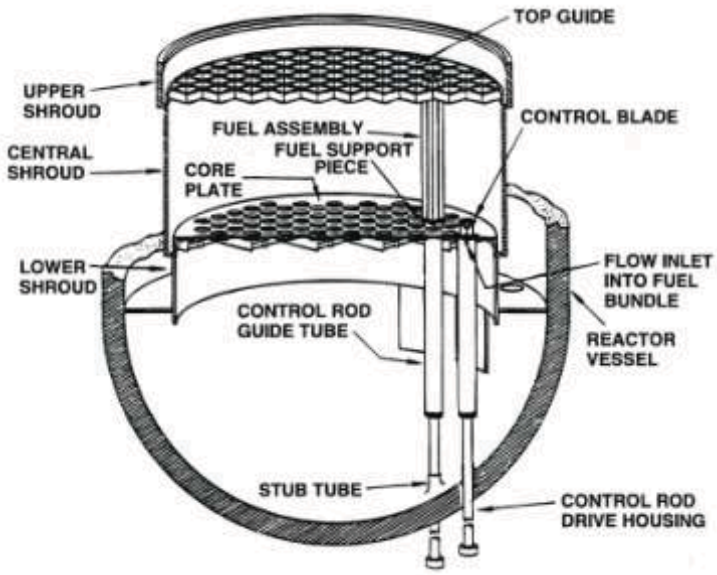

Figure 4-6 BWR Lower Plenum Structures

Collapse of the CRGTs has two important effects on the composition and mass of debris in the lower plenum prior to lower head failure. The first, and most important, is that all core rested on or positioned above the lower core plate within that ring collapses as particulate debris into the lower plenum. This fragmented core debris is not uniformly mixed with the debris bed already in the lower plenum, but is added to the top of the debris bed according to the spatial nodalization shown in Figure 4-3. Therefore, the material composition and porosity of debris within the debris bed can vary considerably within the 2-dimensional spatial nodalization of the lower plenum. Second, the material composition of the CRGTs themselves is added to the debris bed at the location where the intact components were originally positioned. This has the tendency to increase the surface area of metallic components in the lower plenum because the

---

[9] Debris relocating to the lower plenum is assumed to accumulate in the volume between intact CRGTs, and not within them, based on observations from melt relocation experiments for BWR geometries (e.g., see NUREG/CR-6527).

surface area of particulate debris is generally higher than the surface area of the intact CRGT columns.

Thermal interactions between molten core debris and penetrations through the lower head are not explicitly modeled in the Peach Bottom SOARCA calculations. A simple, lumped parameter model for bulk heat transfer to a penetration assembly is available in MELCOR, but the model is not sufficiently refined to calculate multi-dimensional heat transfer and phase change that would occur in the neighborhood of a CRGT or instrument penetration; or to calculate molten material drainage into an open penetration, as could occur in a BWR RPV drain line. This limitation in MELCOR, combined with observations from several large-scale experimental programs that examined failure mechanisms for failure of lower head with penetrations [15], led to a modeling approach that focuses on creep rupture of the hemispherical lower head as the dominant mechanism for lower head failure. This approach is supported by the observation that none of the MELCOR calculations predict elevated RPV pressure at the time debris temperatures are sufficiently high to challenge lower head integrity. That is, detailed analysis of lower head penetration failure [16] suggest internal pressures greater than those obtained in the SOARCA calculations are necessary to eject a penetration assembly from the lower head.

4.2.3 In-vessel Structures above the Core

The COR Package in MELCOR does not explicitly model the mechanical response (i.e., potential material melting or collapse) of structures above the core top guide. This is an inherent limitation in the architecture of MELCOR. As indicated in Figure 4-1, several large steel structures are positioned above the core, which can absorb a substantial amount of energy carried away from the core during the early periods of core damage. They also represent a significant surface area for deposition of fission product aerosols released from the core. These structures most notably include the upper shroud dome, steam dryers and separators.

The thermal response and fission product deposition properties of these structures are modeled using 1-dimensional heat structures. This modeling approach, combined with the nodalization and connectivity of control volumes above the core, provides sufficient spatial resolution to calculate the time-dependent temperature response of each structure. A limitation of this modeling approach is that the mechanical response of these structures, material melting or collapse and the potential for incorporation of steel into core debris, is not modeled. Changes in the flow area through this region of the RPV that might be caused by changes in structure geometry are also not modeled.

4.2.4 Leakage through In-core Instrument Tubes

Among the comments offered by the independent peer review panel that reviewed the models and calculations described in this report was one that questioned whether failure of in-core instrument tubes (i.e., due to melting of neighboring fuel assemblies) could create a pathway for fission product transport outside the containment pressure boundary that should be considered in the SOARCA analyses. The proposed fission product leakage pathway involves leakage through traverse in-core probe (TIP) guide tubes, which run from various locations in the core, through penetrations in the RPV lower head and the containment pressure boundary, and terminate at TIP drive mechanisms located in the reactor building. Leakage through TIP guide tubes would

represent a containment bypass pathway, it the tubes are not isolated. Figure 4-7 illustrates the TIP guide tube pathway.

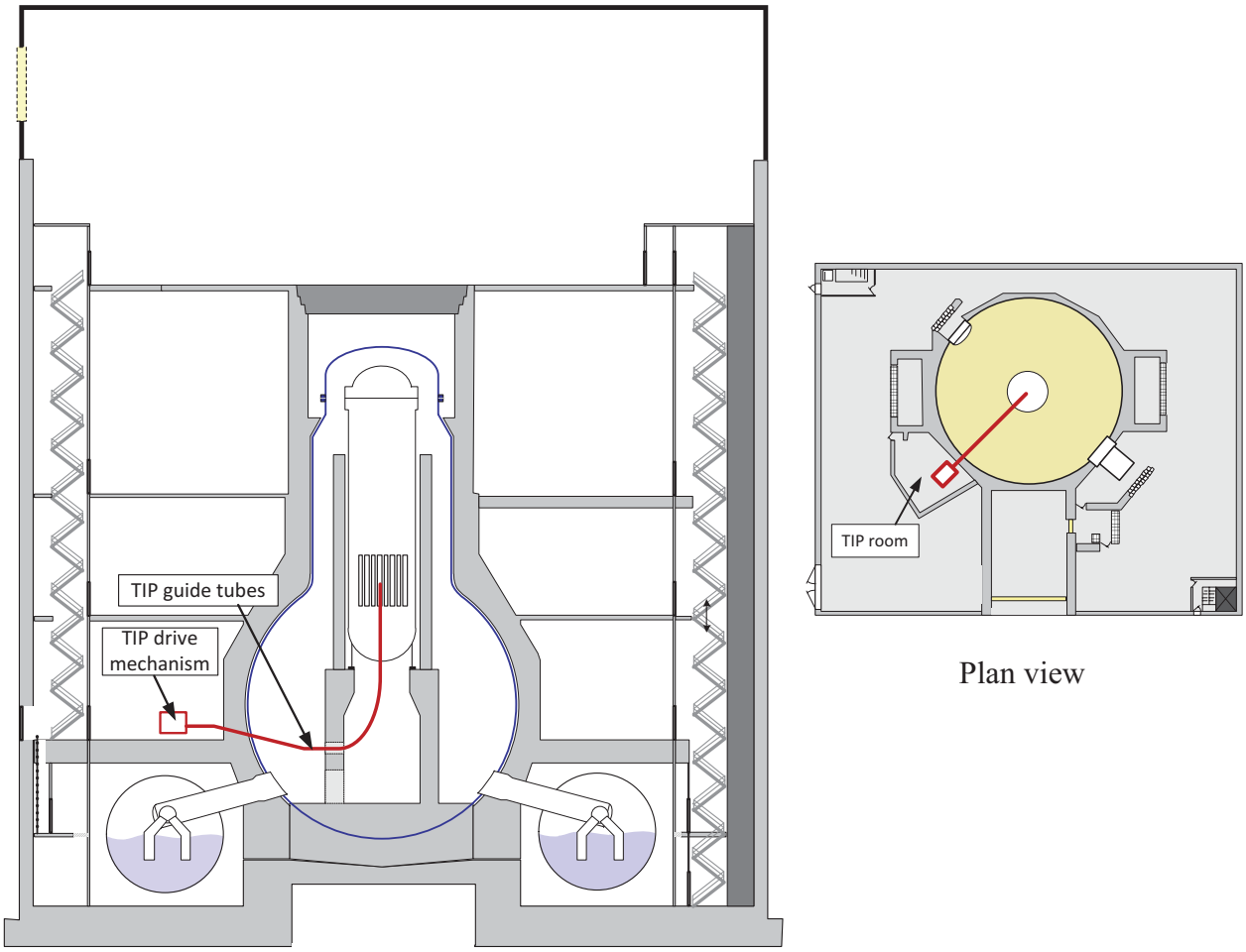

Figure 4-7 Potential containment bypass transport pathway through open TIP guide tubes

TIP Guide Tube Configuration

The TIP system drives three probes of fissile material into various locations in the core to calibrate in-core instrumentation. The probes are normally stored in a shield chamber located outside the containment pressure boundary. As illustrated in Figure 4-8, each probe can be driven out of its shield chamber, through a guide tube, to one of several locations within the core. The probe is pushed through its guide tube by a steel cable. Each TIP guide tube enters an indexing unit located in the drywell. The indexing units guide a TIP probe into one of several exit tubes, each of which are connected to particular local power range monitors (LPRMs) in the core. Therefore, the indexing units serve as TIP tube multipliers, allowing three tubes to serve the calibration needs of multiple in-core instruments.

The diameter of TIP probe is approximately 0.211 inches. The internal diameter of the TIP guide tube is 0.280 inches and the diameter of the drive cable is 0.258 inches. Therefore, the available cross-sectional area for flow through an operating guide is small (0.009 in^2 per tube is the probe is inserted, and 0.06 in^2 if the probe is withdrawn into its shield chamber).

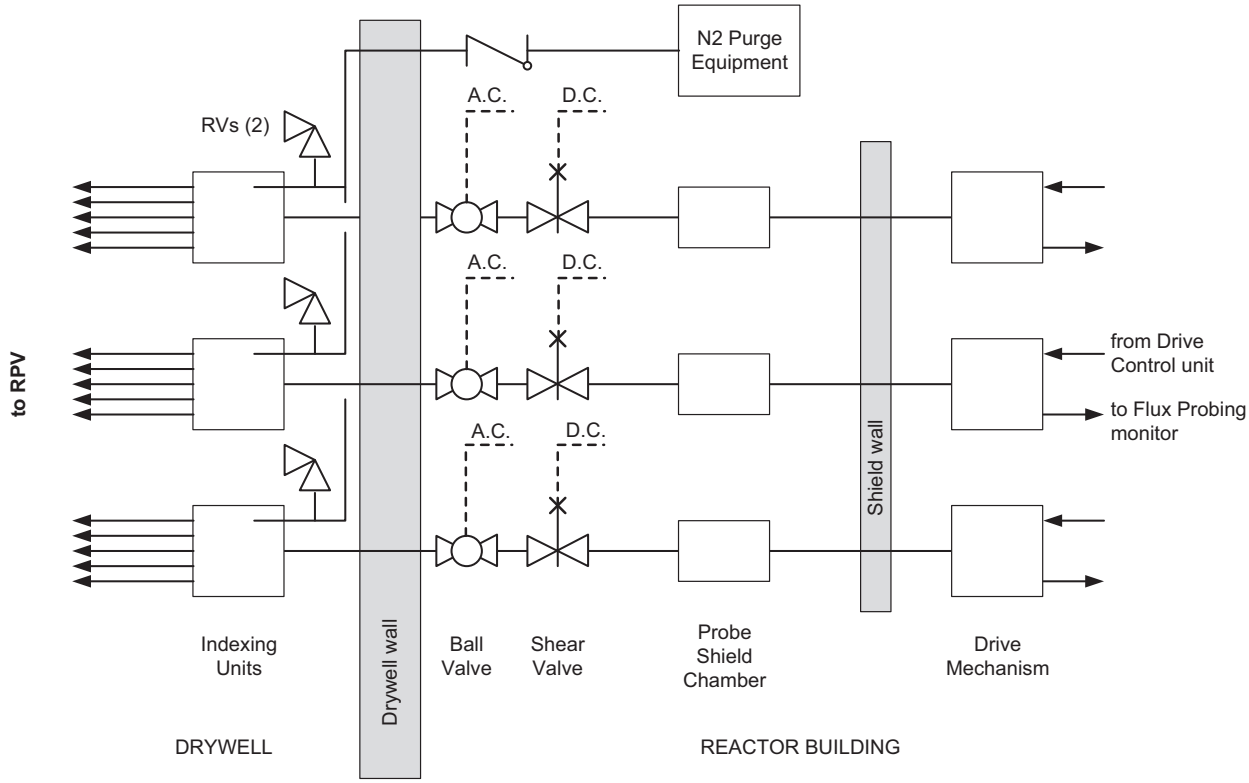

Figure 4-8 Layout of the TIP system

The TIP guide tubes can be isolated with either a motor-operated (AC powered) globe valve or a squib-actuated shear valve. The globe valve functions only when the TIP probe is fully withdrawn because the drive cable for the in-core probe runs through the valve body. If, for some reason, the probe cannot be retracted, the squib (explosive) operators on the shear valves can be manually actuated to shear the drive cable and seal the guide tube. The squib actuators require DC power to operate. The explosive operators on the squib valves could, in principle, be actuated locally using a portable dc power supply. However, procedures for this action are not formally implemented for this action.

TIP System Operation

Operating experience at Peach Bottom suggests the TIP system is used to calibrate in-core instrumentation once every four months. The calibration exercise takes approximately 1 hour to complete and involves simultaneous operation of all three TIP probes. Therefore, an individual TIP guide tube is open (i.e., not insolated), on average, a small fraction of the time (i.e., 1/2920 hours). Over a typical operating cycle, this represents a conditional probability of an open TIP tube of approximately 3.4E-4.

MELCOR Model of TIP Guide Tubes

The baseline MELCOR calculations of accident progression and source terms did not consider leakage of steam, hydrogen or fission products from the RPV to the reactor building through the

TIP guide tubes. The conditional probability of the TIP system being in operation at the time of a severe accident initiating event was well below the truncation limit for accident sequence selection.

However, a sensitivity calculation was performed to evaluate the effects of open (unisolated) TIP guide tubes on accident progression and the radionuclide source term for the LTSBO accident sequence. The MELCOR model for leakage through the TIP guide tube accounts for internal geometry of the tubes and flow resistance due to wall friction along the length of the tubes (approx. 150 ft). As shown in Figure 3, a single control volume is used to represent the total internal volume of the guide tube(s) and flow paths connect each end of the tube coolant space within the core and the reactor building. Heat transfer between flowing gas and the guide tube(s) is accounted for; and the tube internal wall represents an aerosol deposition surface. Results of the sensitivity calculation using this additional feature to the Peach Bottom MELCOR model are described in Section 5.7.3.

4.3 Primary Containment and Reactor Building

The primary containment of the BWR Mark I design consists of two separate regions: a drywell and a wetwell. As shown in Figure 4-9 each region is explicitly represented in the MELCOR model with distinct hydrodynamic control volumes, flow paths, and heat structures to preserve the geometric configuration and major functional features of the Mark I design (e.g., steam pressure suppression, fission product scrubbing, and surface deposition). The drywell is further divided into four connected volumes to account for non-uniformities in the temperature and composition of the atmosphere during late phases of a severe accident.

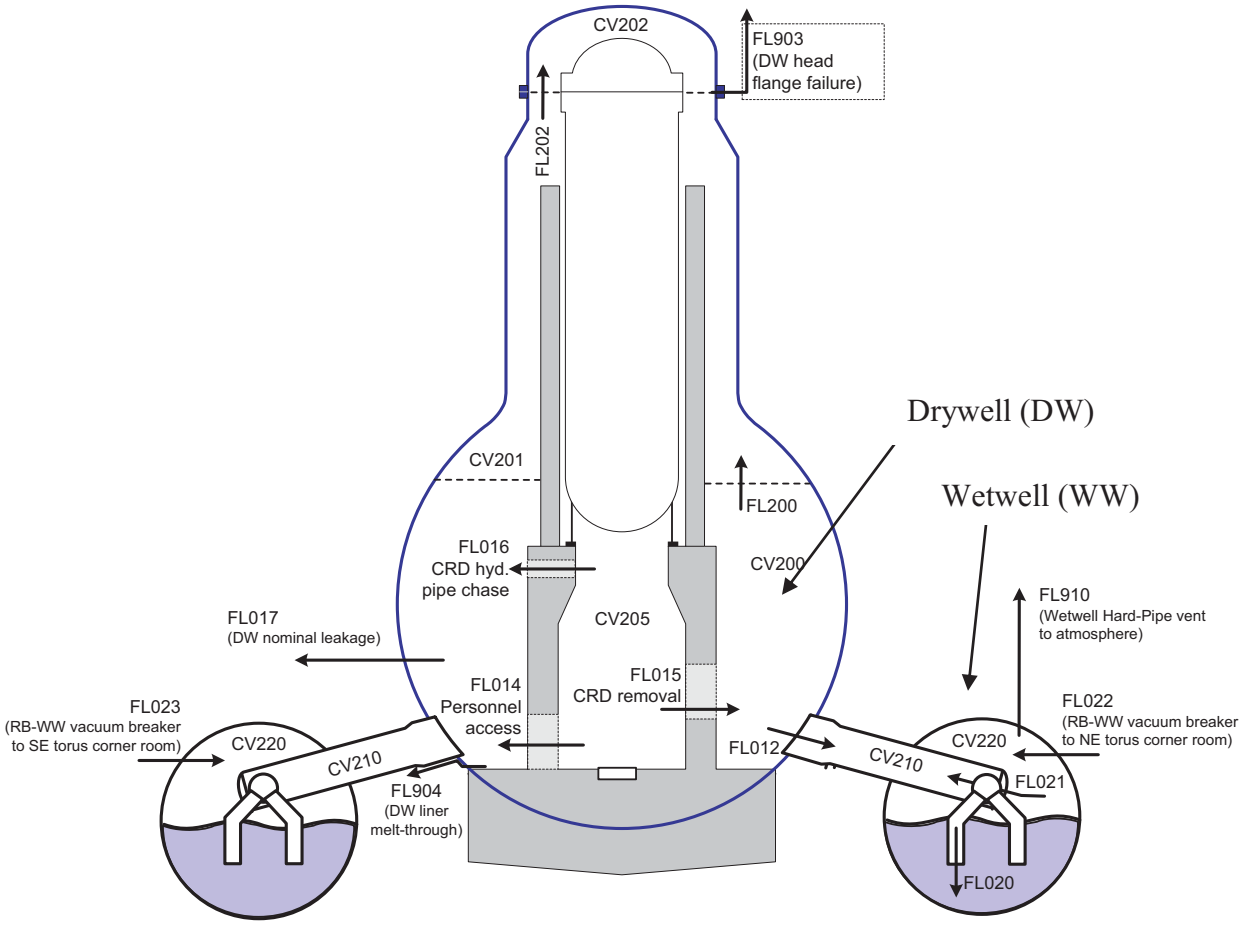

Figure 4-9 Hydrodynamic nodalization of the primary containment

The internal volume, airflow flow pathways, and structures of the reactor building are modeled in considerable detail as illustrated in Figure 4-10 and Figure 4-11. The reactor building fully encloses the primary containment and participates in the release pathway of fission products from the containment to the environment by offering a large volume within which an airborne radionuclide concentration can be diluted by expansion into and mixing with the building atmosphere.

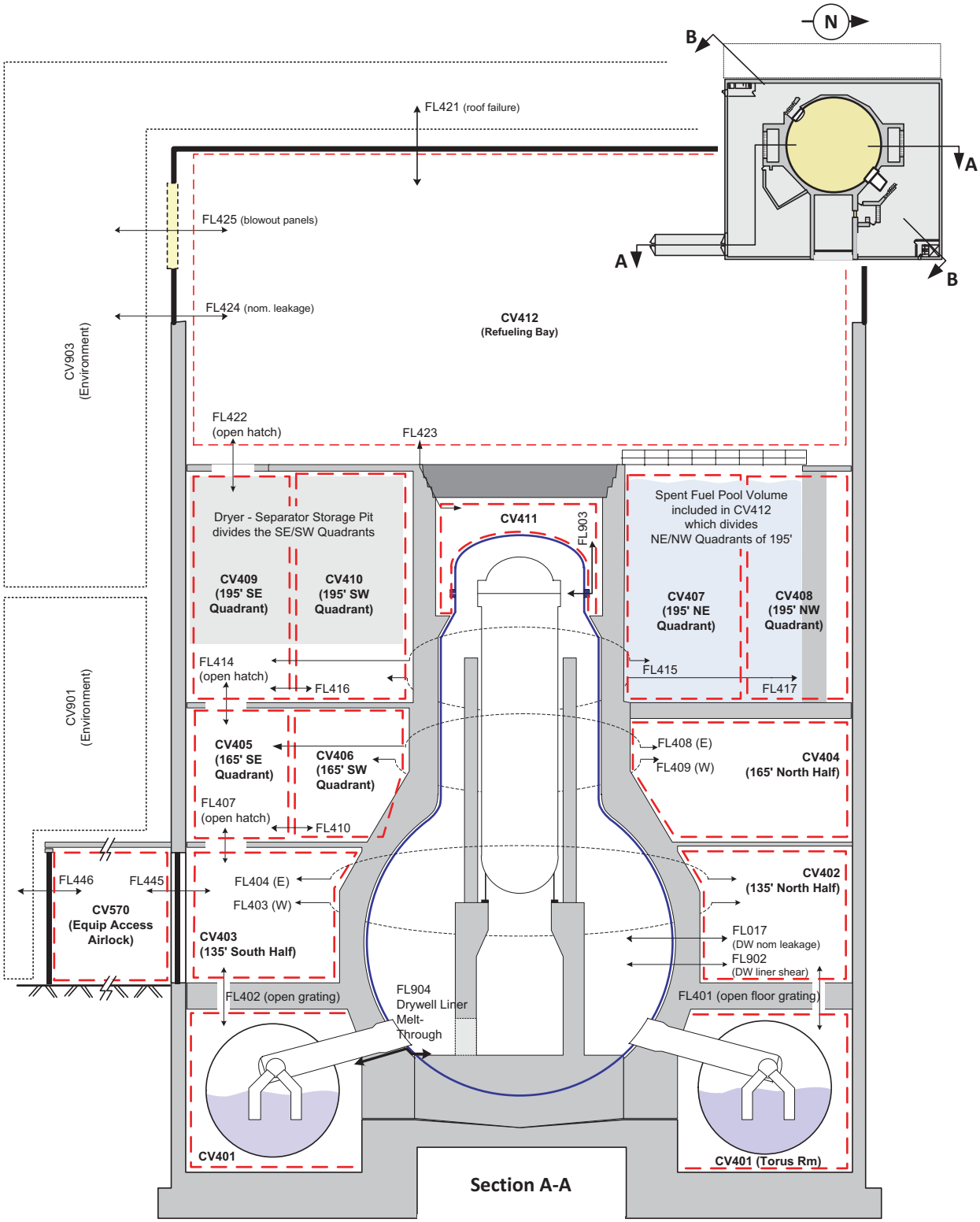

Figure 4-10 Hydrodynamic nodalization of the reactor building (a)

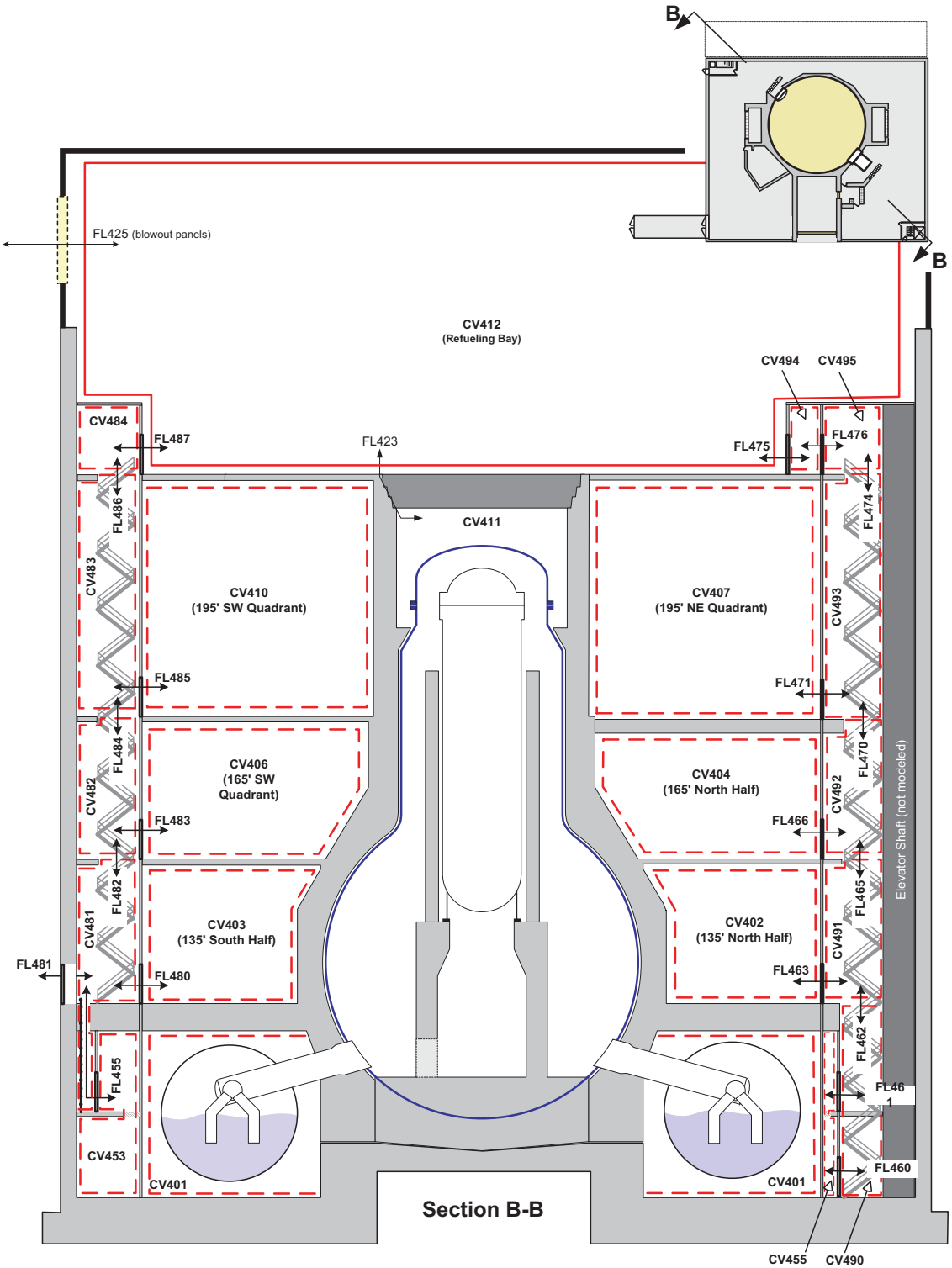

Figure 4-11 Hydrodynamic nodalization of the reactor building (b)

The airborne concentration of fission product aerosols within the reactor building is attenuated by gravitational settling and other natural deposition mechanisms. The building is also equipped with a ventilation system with aerosol and charcoal filters, which would greatly aid in reducing an airborne radioactive release. However, these systems would not be available during the particular accident scenarios examined in this work, because of a loss of electrical power or other equipment failures. Therefore, the reactor building is occasionally referred to as a secondary containment, although it has a negligible capacity for internal pressure.

4.4 Mechanisms for Induced RPV Depressurization

Mechanisms for induced depressurization of the RPV in BWR severe accident sequences were first introduced to the U.S. NRC MELCOR models in the calculations performed for the reactor security assessment in 2002-2003. The principal motivation at the time was to correct previous calculations of high pressure accident sequences (e.g., SBO), which allowed SRVs to continue cycling for several hours after the onset of core damage, when gas discharge temperatures exceeded values at which material damage to moving valve components would challenge normal valve behavior. Specific values at which this could occur are discussed later. Data were not available to support a deterministic valve degradation model. As a result, an intuitive approach was used to capture the basic idea that moving valve components would eventually break or seize when sufficient heat was transferred from the flow gas stream to the valve body. Eventually other mechanisms for RPV depressurization were added to the MELCOR model. Section 4.4.1 summarizes the historical development of this aspect of BWR severe accident modeling practices. The specific modeling approach used in the current SOARCA calculations is then described in Section 4.4.2.

4.4.1 Historical Development of BWR RPV Depressurization Mechanisms

Within this section a summary of SRV seizures at high temperatures is discussed in Section 4.4.1.1. Section 4.4.1.2 provides a discussion on the stochastic failure for a cycling SRV, and Section 4.4.1.3 discusses the potential for creep rupture of a BWR main steam line pipe or RPV nozzle.

4.4.1.1 Valve Seizure at High Temperatures

An initial criterion for high-temperature valve failure was based on manufacturers' information describing the strength of stainless steel, published by the Stainless Steel Information Center.[10] Softening or loss of strength of stainless steel (300 series) was described as *"about 1000 ºF"* (811 K). The same reference also suggested the maximum service temperature for intermittent exposure of stainless steel components is 1600 ºF (1100 K). It was assumed that 'service temperature' referred to the temperature of thermal environment within which steel components operate. In the case of a valve, this was assumed to be the internal gas temperature. Therefore, in earlier analyses, a cycling valve was judged to cease functioning properly when the internal gas temperature exceeded a value between the two referenced values (i.e., somewhere between 811 K and 1100 K). In particular, valve seizure (failure to reclose) was assumed to occur if the valve was exposed to discharge gas temperatures greater than ~1000 K for several cycles.

---

[10] Reference: www.ssina.com/composition/temperature.html

The response of valve components to high temperature gas strongly depends on valve design and operation. For example, different thermal failure criteria were developed for the Peach Bottom and Grand Gulf MELCOR models because the two plants have different types of SRVs. Three-stage Target Rock SRVs are installed at Peach Bottom, and Dikkers SRVs are installed at Grand Gulf. Other valve designs in the BWR fleet include the two-stage Target Rock, which is modified version of the earlier three-stage valve, and another SRV is manufactured by Crosby (now a subsidiary of Tyco). Figure 4-12 depicts the cross-section of a typical two-stage Target Rock valve; Figure 4-13 shows the cross-section of a Crosby valve, which is similar in design to the Dikkers valves.

Valve design and operating features are important for several reasons. First, the way in which the valve opens to relieve pressure differs between the Target Rock and Dikkers/Crosby designs. Target Rock SRVs are pilot-operated valves, which lift to a full-open position when pressure within the SRV exceeds a setpoint. When pressure decreases below another setpoint, the valve fully re-seats. Movement of the main valve disc is controlled by a pilot valve, which is distinct from, but integral to, the main SRV valve body. Movement of the pilot valve re-aligns gas flow through small ports and vent lines within the valve body (see Figure 4-12), allowing RPV pressure to help keep the valve fully-seated when pressure is within desired values, and to help lift the valve if pressure gets too high. In contrast, the Dikkers/Crosby SRV design is a spring-loaded valve that 'pops' open to relief RPV pressure, and then gradually recloses as internal pressure decreases. The variable valve stem position (or valve open fraction) allows RPV pressure to be maintained close to a target value until RPV pressure reduces below a minimum setpoint when the valve recloses.

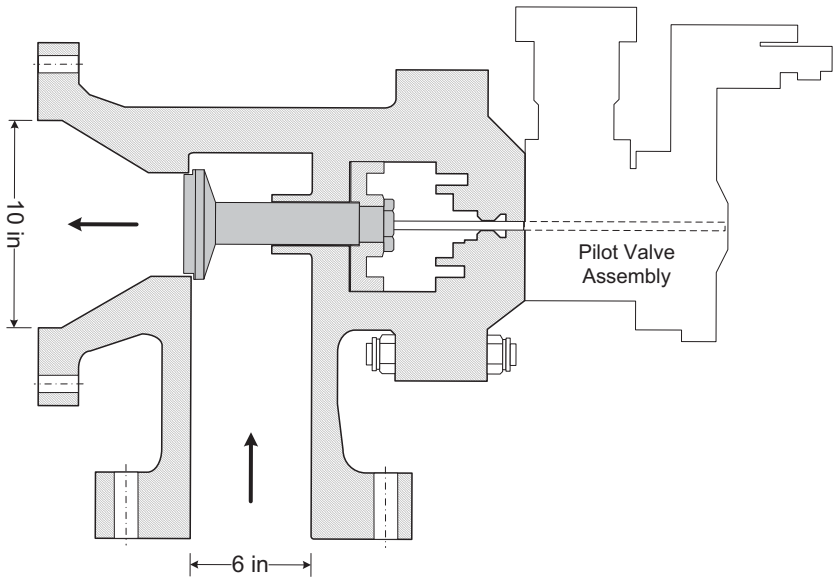

Closed Position

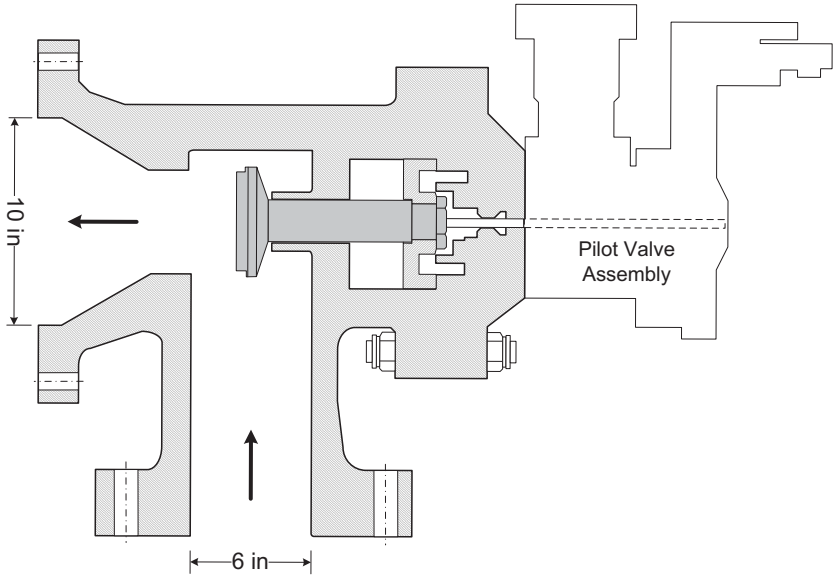

Open Position

Figure 4-12 Two-stage Target Rock pilot-operated safety relief valve
(Taken from Target Rock Corporation drawing M-1-R-213)

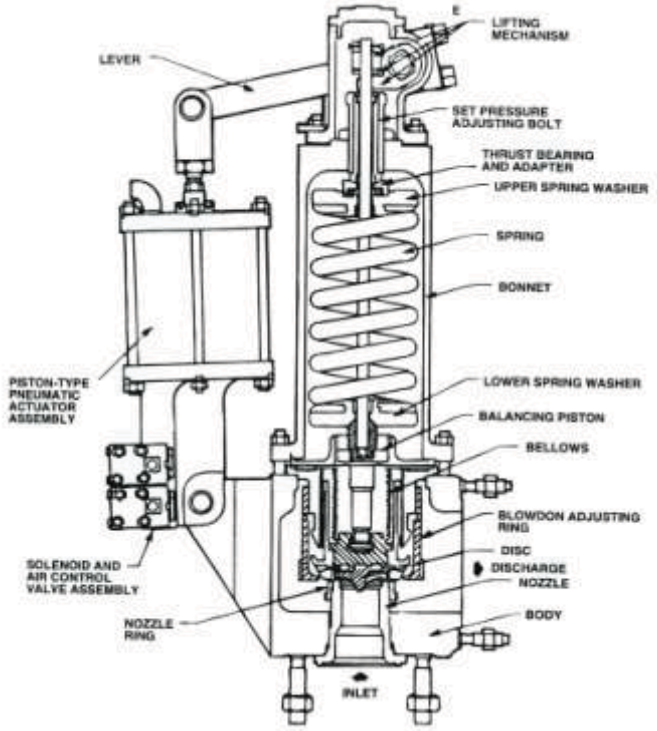

Figure 4-13 Crosby safety relief valve

These differences in valve design and operation led to different criteria for valve seizure at high temperatures in the Peach Bottom and Grand Gulf MELCOR models. In both cases, seizure was assumed to occur when sufficient heat was transferred from discharged gas to the valve body for internal valve components to cease functioning. In the absence of data on valve performance at high temperatures, or detailed calculations of valve heat up, the following simple assumptions were made:

1. The number of times a Target Rock valve could cycle at temperatures at or above 1000 K wasn't known. A value of 10 cycles was chosen to represent the expectation that several cycles would be necessary to transfer enough heat to valve internal components to deform or expand valve components, causing failure. It was recognized that although convective heat transfer from the gas would only occur when the valve was open, heat transfer within the valve body would continue after the valve stem reseated. Therefore, it was postulated that non-uniform thermal expansion could reduce clearances of valve components and cause the valve seize in the closed position; or material softening and deformation could cause the valve to fail in the open position. Uncertainties in both failure mechanisms (i.e., thermal expansion and material softening/deformation) were also reflected in the number of cycles used to characterize failure to reclose. That is, if the lowest set point SRV seized closed after 2 or 3 cycles with gas temperatures above 1000 K, the next lowest set point SRV would pick up the load and begin cycling without significant pre-heating. A nominal valve failure (seize open) criterion was defined as: 10 cycles with gas temperatures, prior to opening, above 1000 K. This was judged to be

a reasonable approximation of conditions under which one of the 11 Target Rock valves at Peach Bottom would seize in the open position.

2. Tracking the number of valve cycles was judged to not be a meaningful method for characterizing heat up and seizure of a Dikkers/Crosby valve. Instead, seizure was assumed to occur if the valve discharged high temperature gas for a sufficiently long period of time. A failure criterion was developed based on the concept of a cumulative damage function, which tracked the amount of time high temperature gas was discharged through the valve and compared it to a time limit. The time limit was assumed to be inversely proportional to temperature, and the valve was assumed to seize in the position it held at the time the failure limit was reached. This was often a few percent of full open. The specific values used in this time-at-temperature criterion were:

    a. 60 minutes at temperatures of 1000 K.
    b. 30 minutes above 1500 K.

These criteria were used in the calculations of severe accident progression for Peach Bottom and Grand Gulf in the 2002 security assessment as well as the 2005 analyses of fission product source terms for high burnup fuels for both plants. The valve failure criterion which was used for Grand Gulf has not been benefitted from the additional work done for Peach Bottom, and may be examined in the future. The thermal criterion for the Target Rock SRVs was modified after a more detailed assessment as described in Section 4.4.2.2.

4.4.1.2 Stochastic Failure

The possibility that a cycling SRV would randomly fail to open, or to reclose after opening, was not represented in the security assessment calculations, nor in the high burnup fuel source term analyses. However, several hundred cycles were calculated for some accident sequences, such as station blackout, which raised concerns that random failures should not be ignored. The Peach Bottom Individual Plant Examination (IPE) cites a plant-specific failure rate (to reclose) for an SRV of 3.7×10^{-3}/demand .[11]

It must be noted that the NRC assessment of component reliability in nuclear systems suggests a failure lower than the value cited in the Peach Bottom IPE. An NRC analysis of industry average data for SRV performance in NUREG-/CR-6928 [17], for example, estimated a mean value of approx. 8×10^{-4}/demand with 5th and 95th percentile values of 4.3×10^{-5} and 3.1×10^{-3}/demand, respectively.[12] Therefore, the Peach Bottom value is slightly larger than the 95th percentile of the industry-average value.[13]

---

[11] Reference: Philadelphia Electric Co., Individual Plant Examination, Peach Bottom Units 2 and 3, Vol., 2, §4.6.5.3.1.

[12] The 5th and 95th percentiles are not reported in NUREG/CR-6928, but can be readily calculated from the Beta distribution parameters listed in Table 5-1.

[13] Significant reductions in the observed rate of spurious valve opening were achieved by various modifications to the Target Rock SRV through a BWR Owners Group initiative coordinated under General Safety Issue (GSI) B-55. The extent to which these modifications would also affect the expected rates for failure to reclose is not known. However, this might contribute to the difference in the current (NRC)

Control logic was added to the Peach Bottom MELCOR model to calculate the cumulative probability of random failure of a cycling SRV to reclose based on the IPE failure rate. Failure was assumed to occur when the cumulative probability (i.e., confidence of failure) reached 90%. The high confidence level was used in recognition of the principal in PRA system reliability analysis that credit should not be taken for 'benevolent' failures of components. That is, failure of a reactor component should not be assumed if it has a potentially beneficial effect on the accident sequence.[14] Therefore, rather than use an 'expected value' condition for predicting failure, valve failure was assumed to occur only if the number of cycles was sufficiently large that the failure probability was high (0.9).

4.4.1.3 Main Steam Line Creep Rupture

The potential for creep rupture of a BWR main stream line (i.e., piping or RPV nozzle) was not evaluated in the MELCOR calculations performed for the security assessment, nor was it represented in the high burnup source term calculations. This feature was added to the Peach Bottom model developed for SOARCA. Initially the model was implemented for the sole purpose of monitoring the potential for conditions that would suggest the possibility of creep rupture. Flow paths to represent the rupture of main steam line piping were added relatively late in the SOARCA model development process, in response to comments received from the SOARCA peer review panel.

The creep rupture model is a direct translation of the hot leg creep rupture model used in the Surry MELCOR calculations. The Larson-Miller control function available in MELCOR is applied to a heat structure representing the RPV nozzle to main steam Line A and (separately) to the heat structure representing the horizontal section of the main steam line piping immediately adjacent to the RPV nozzle (approx. 3.5 m in length). The nozzle is assumed to have twice the thickness of the main steam line pipe.

4.4.2 Modeling Approach in SOARCA

Within this section a summary of SRV stochastic failure to reclose is discussed in Section 4.4.2.1. Section 4.4.2.2 provides a discussion on the thermal failure mechanism for a cycling SRV, and Section 4.4.2.3 discusses the differential thermal expansion for materials in a SRV. Section 4.4.2.4, Section 4.4.2.5, and Section 4.4.2.6 discuss material deformation, SRV pilot valve failure, and SRV spring softening respectively.

4.4.2.1 Stochastic Failure to Reclose

The SOARCA Peer Review Panel agreed with the basic method used to represent stochastic failure of an SRV in the MELCOR calculations. One panel member noted, however, that a

---

estimate of SRV failure rate (to reclose) and the older (circa 1990) failure rate reflected in the Peach Bottom IPE.

[14] In Level 1 PRA, this principal primarily applies to components that would enable the operation of alternate or backup safety systems. An example would be failure of a cycling SRV to reclose would depressurize the RPV and enable the use of low-pressure coolant injection systems for makeup. Refer to requirement SY-A12 in ASME/ANS RA-Sa-2009, "Standard for Level 1/Large Early Release Frequency Probabilistic Risk Assessment for Nuclear Power Plant Applications."

recent EPRI study of SRV performance, which is undocumented at the time of the review, suggests the failure rate cited in the plant-specific IPE and the value in the generic data base are probably too low, especially when valve temperatures begin to rise above the design value. This view was acknowledged as an opinion, and is not supported by failure data that would supplant the information used to calculate the IPE or generic failure rates. Therefore, the failure rate obtained from the plant-specific IPE is retained in the SOARCA calculations. Deterioration in valve performance at temperatures above design is represented by a separate, and independent, failure model described in the next section.

It should be noted, however, that the failure rate reflected in the generic data base and the value obtained from the Peach Bottom IPE are conceptually different from the situation modeled here. In simple terms, the rate at which an SRV fails to reclose is calculated by dividing the number of observed valve failures (to reclose) by the number of valve demands. This ratio, therefore, reflects the conditional probability that a valve would fail to reclose, given a successful demand to open. However, the failure events that represent the numerator of this ratio occurred after only a few valve cycles. The precise number is difficult to determine from the raw data documented in NUREC/CR-6928. However, it is clear that valve failure data after numerous cycles are extremely rare (perhaps non-existent) primarily because events involving numerous, continuous valve cycling are not observed. It is, therefore, debatable whether the failure rate used to calculate the (low) probability of failure to reclose after a few cycles should be extrapolated to estimate the (higher) probability of failure after a large number of cycles. Other unknown failure mechanisms would likely overwhelm those that lie behind the nominal failure rate. This qualitative observation is consistent with the opinion expressed by members of the peer review panel that the valve failure rates obtained from the PRA data base are too low. Also, it should be noted that comments provided by the licensee on this analysis indicated the early failure rate reported in their IPE was not based on plant-specific performance data, and they have since replaced this value with the industry value reported in NUREG/CR-6928.

Accident progression modeling in SOARCA reflects best estimate values for uncertain parameters. Therefore, the conditions at which random valve failure would occur reflect the expected value, or mean, number of cycles at which the valve fails to reclose. This number is the inverse of the failure rate ($1/\lambda$), or $1/(3.7\text{x}10^{-3}$ per demand), which is 270 consecutive cycles.

4.4.2.2 Thermal Failure Mechanisms

Several members of the SOARCA Peer Review Panel expressed the opinion that the criteria used to represent conditions at which a cycling SRV would seize in the open position due to thermal effects (described earlier) were too severe. They agreed that seizure due to physical deformation of moving valve components would be expected before the temperature of valve components reached 1000 K. They also expressed the opinion that multiple valve cycles above 1000 K was not credible.

Four thermal failure mechanisms were examined to refine the criteria for valve seizure. Each is described below. These mechanisms are assumed to operate independently of the mechanisms causing stochastic failure.

4.4.2.3 Differential Thermal Expansion

Heat transfer from hot gases discharged through an open SRV to internal surfaces of the valve body would gradually increase the temperature of valve components. The internal geometry of the valve is complex and the temperature distribution within the valve would not be uniform, causing differential thermal expansion of valve components. If displacements are sufficiently large, the clearances required for moving components to operate could close, resulting in valve seizure.

The extent to which differential expansion might reduce valve stem clearances is examined very simplistically. First, the differential expansion of the valve stem from its surrounding sleeve and valve body, due solely to differences in material properties was considered. That is, the stainless steel stem will expand at a slightly faster rate than its carbon steel enclosure due to differences in the linear coefficient of expansion for stainless verses carbon steel. Second, the effects of temperature gradient within the valve body were considered.

Differences in material properties: The mean linear expansion coefficient for the valve body (ASTM A216 Gr WCB steel)[15] is 8.3 x 10^{-6} in/in ºF; the coefficient for the valve stem and disc (A276 Type 304 stainless steel)[15] is 11 x10^{-6} in/in ºF. Therefore, if the temperature of the entire valve increased to 1000 ºF (425 ºF greater than the design value), outward radial displacement of the valve stem (approx. 2.5-in diameter) would be greater than the surrounding valve body by approximately 1.4 mil:

$$dr = (11x10^{-6} – 8.3x10^{-6})\ \text{in/in- ºF} * 2.5/2\ \text{in} * 425\text{ºF} = 1.4x10^{-3}\ \text{inches}$$

The valve stem is a solid cylinder, surrounded by a thermal sleeve, as illustrated in Figure 4-14. This is probably not sufficient to cause seizure of the valve stem.

<u>Effects of temperature gradient</u>
In the absence of mechanistic, multi-dimensional calculations of the transient thermal response of the valve body to cyclic heating, it is difficult to judge whether temperature gradients within the valve would be sufficiently large for adjacent valve components to bind against each other due to differential thermal expansion. However, the rates at which major components within the valve would heat up can be estimated using some simple, but reasonable geometric models. In particular, the response times of major valve components were estimated by representing them as a geometric shape that can be modeled using a one-dimensional heat transfer model.

The main portion of the valve body, which encloses the gas flow stream, was approximated as a cylinder with an internal diameter of 6 inches (i.e., the approximate valve throat diameter) and length to diameter ratio (L/D) of 5. The outer diameter, or wall thickness, of the cylinder was treated parametrically because, as indicated in Figure 4-12, the shape of the valve body is not a perfect cylinder. Two alternatives were considered. The first alternative examined a 1-in wall thickness, which represents the approximate wall thickness of the entrance and exit portion of the valve body. The second alternative attempts to capture the effects of the large steel mass

---

[15] Reference: Peach Bottom UFSAR, 4.4-4.

appended to one side of the main valve body, and houses the pilot valve operator. The wall thickness in this case was 3 in, which is the equivalent (uniform) thickness of a cylinder with one-half the weight of a fully-assembled SRV.[16] Calculating the thermal response of a cylinder with this range of material masses (or wall thicknesses) to cyclic heating by gas flowing within it provides an indication of the rate at which the main valve body would respond to heat transfer from gas flow when the SRV opens.

A specific internal component of interest is the main valve stem that must slide along a cylindrical sleeve that is integral to the valve body to seat and unseat the disc. Also, the upper portion of the valve stem is mounted to a ring piston that slides within a hollow cavity within the main valve body. These components are highlighted in Figure 4-14. If the valve stem and attached ring piston were to expand at a faster rate than the surrounding valve body, mechanical binding could occur, and the valve would stick or seize in the open position. Seizure in the open position is judged more likely than the closed position because gas flow through the valve (i.e., the heat source) only operates when the valve is open. Since the disc and a portion of the valve stem are directly immersed in the high temperature gas flow stream, one would expect these components to heat faster than the surrounding valve body. The thermal response of the valve stem was therefore estimated by modeling it as a solid 3-in diameter cylinder with an L/D=3. This diameter represents the combined dimension of the valve stem (~2.5-in.) plus the exposed portion of the surrounding valve stem sleeve.

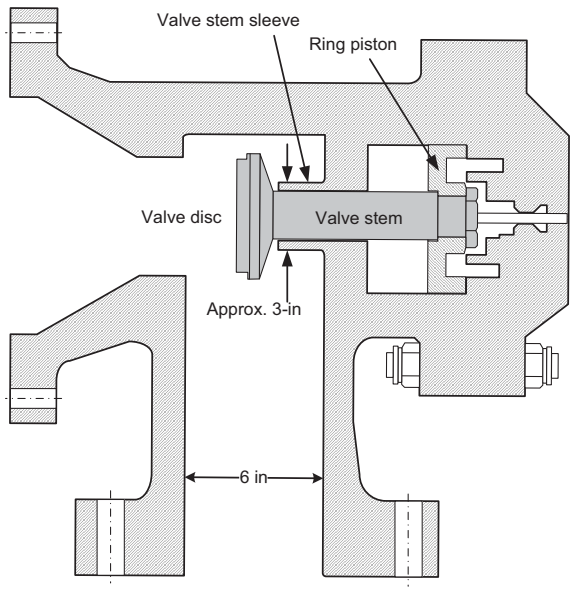

Figure 4-14 Valve stem assembly within valve body
(Taken from Target Rock Corporation drawing M-1-R-213)

Boundary conditions for each of the 1-dimensional conduction models (i.e., the two valve body models and the valve stem model) were taken from a preliminary MELCOR calculation of the

---

16 Total weight of a fully-assembled valve is given as 1500 lbs in an EPRI SRV Testing and Maintenance Guide (TR-105872s, Aug 1996).

long-term station blackout accident sequence. The calculated temperature history, composition of gases passing through the SRV, and the time-dependent (cyclic) gas velocity through the valve were tabulated and applied as a boundary condition for the simple flow model illustrated in Figure 4-15.

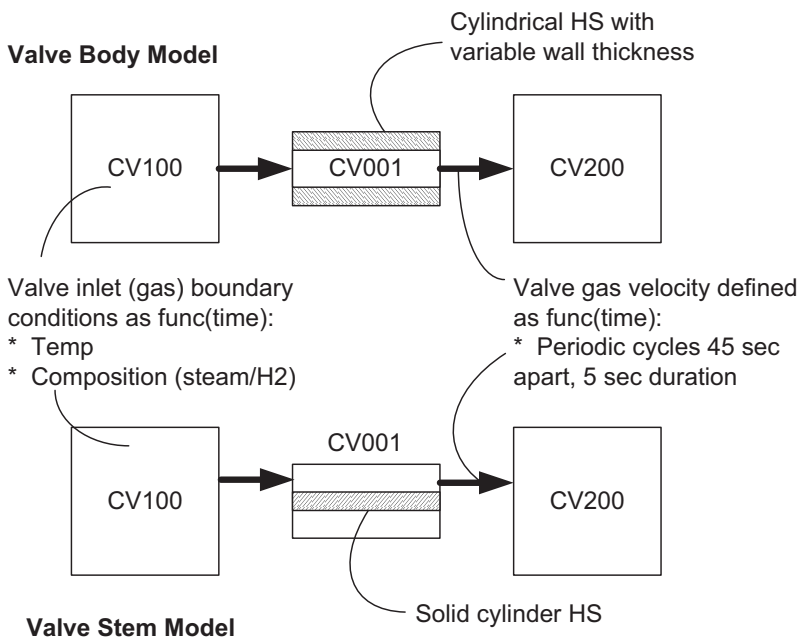

Figure 4-15 Arrangement of 1-dimensional safety relief valve heat-up calculation

The boundary conditions are illustrated in Figure 4-16 through Figure 4-19 as follows:

- Figure 4-16: Gas flow through the valve is based on a cycle period of 45 seconds with an open cycle duration of 5 seconds.

- Figure 4-17: Gas velocity during an open cycle is constant during a single 5-second cycle, but increases from 420 m/s to 500 m/s as the gas temperature (Figure 14) increases from 600 K to 1100 K.

- Figure 4-18: Gas temperature as a function of time. Approximately 100 K temperature changes between the beginning and end of a cycle were neglected. The mid-point values were used as shown in the table adjacent to the figure.

- Figure 4-19: The Steam and hydrogen mole fractions were specified as a function time as indicated in the figure and adjacent table.

System pressure was assumed to be constant at 1150 psia.

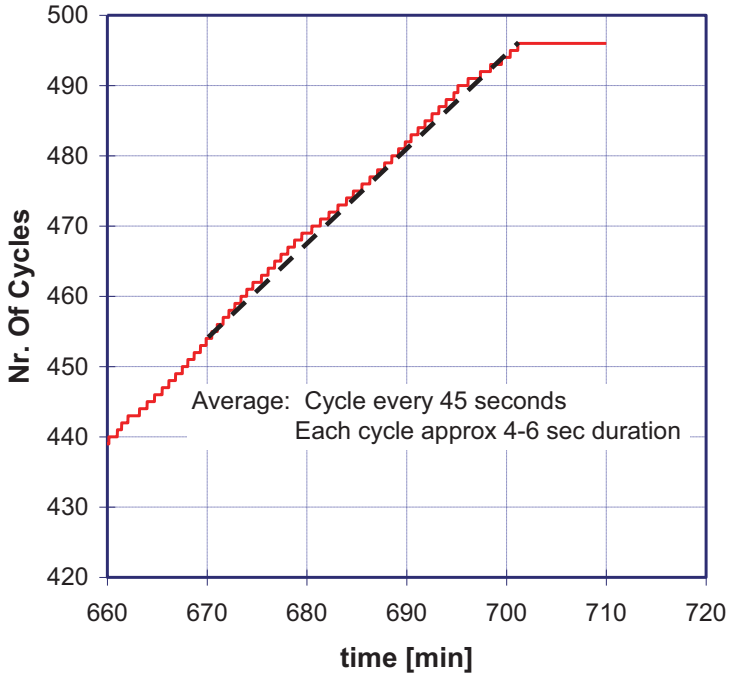

Figure 4-16 Number of safety relief valve cycles from preliminary LTSBO calculation

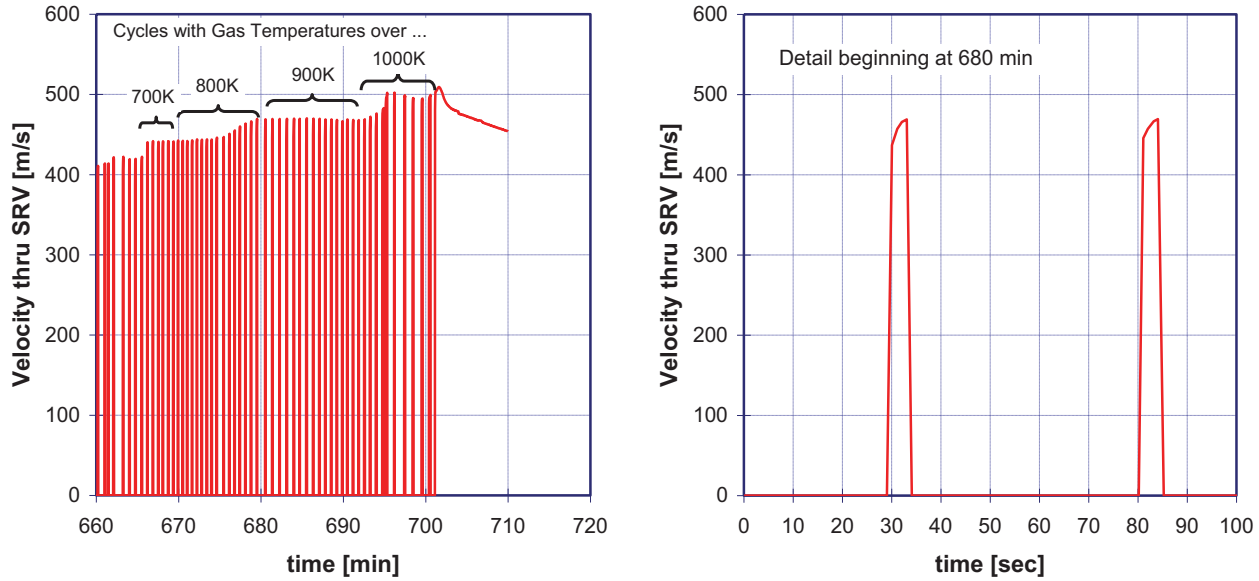

Figure 4-17 Gas velocity through safety relief valve from preliminary LTSBO calculation

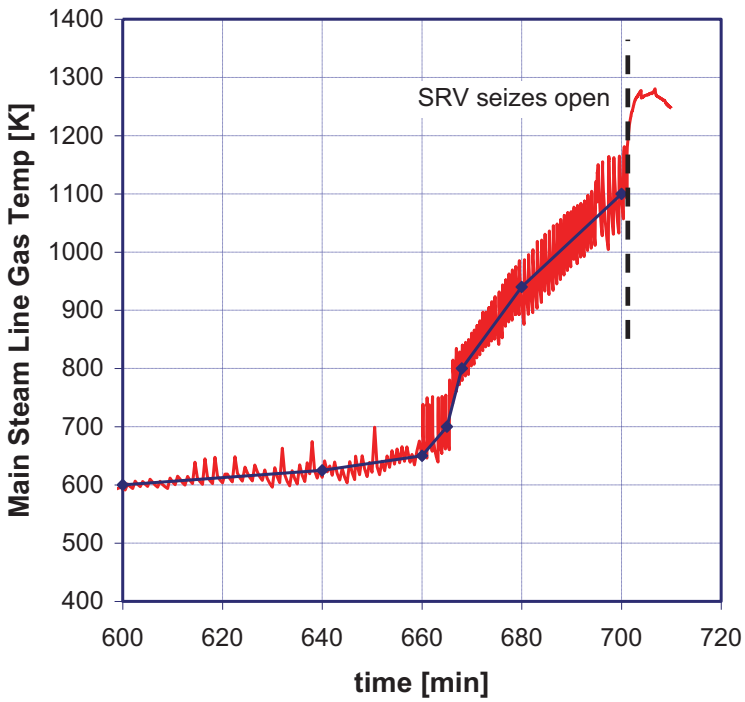

Time (sec)	Ave Temp (K)
36000.	600.
38400.	625.
39600.	650.
39900.	700.
40080.	800.
40800.	940.
42000.	1100.

Figure 4-18 Gas temperature through safety relief valve from preliminary LTSBO calculation

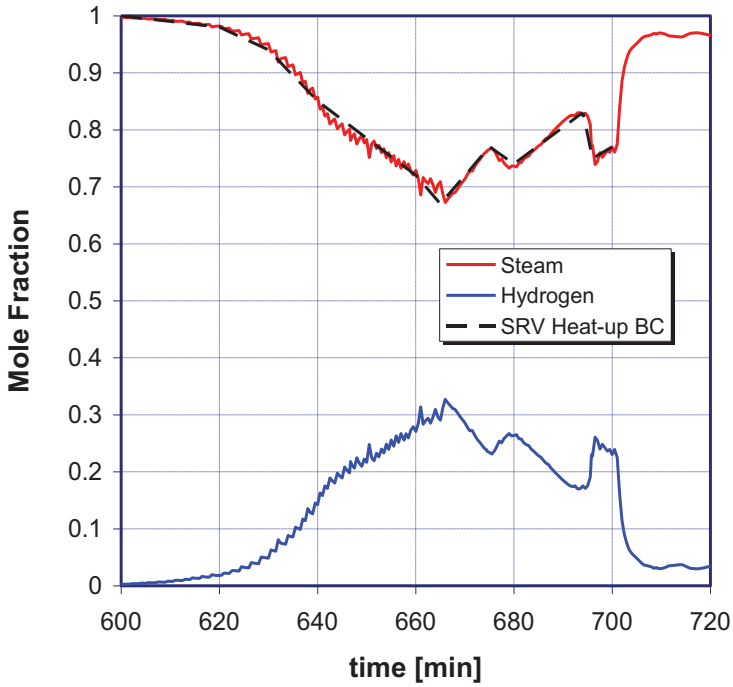

Time (sec)	Steam v/o
36000.	1.0
37200.	0.98
37800.	0.94
38400.	0.85
39600.	0.72
39900.	0.67
40500.	0.77
40800.	0.74
41640.	0.83
41760.	0.75
42000.	0.77

Figure 4-19 Gas composition through safety relief valve from preliminary LTSBO calculation

The calculated thermal response of the 1-dimensional conduction models are compared in Figure 4-20. As expected, the relatively small thermal mass of the 3-in diameter shaft responds

more quickly to increasing gas temperature than the heavier valve body. The centerline temperature of the 3-in diameter cylinder, representing the valve stem, lags the gas temperature by approximately 4 minutes. In comparison, the 1-in thick cylinder lags by approximately 6 minutes and the 750 lb cylinder, each represent the valve body, by almost 20 minutes, when the internal gas temperature reaches 850 K.

From the perspective of thermal expansion, the principal result of these calculations is the temperature difference between the valve body and the valve stem when gas temperatures exceed 800 K. This difference depends on the geometry and mass of steel attributed to the valve body. However, based on the two simple options examined here (i.e., a 1-in versus 3-in wall thickness), the valve body temperature is 20 to 140 K (11 to 78 ºF) less than the valve stem temperature. A bounding estimate of the resulting differential expansion of the valve stem within the cooler valve body is obtained by assuming the maximum of this range. The resulting differential radial expansion is 1.1 mil:

$$11 \times 10^{-6} \text{ in/in-ºF} * 2.5/2 \text{ in} * 78 \text{ ºF} = 1.1\text{x}10^{-3} \text{ inches}$$

If this value is added to the difference associated with material properties (estimated earlier), the combined radial expansion is less than 3 mil. This is within the range of possible values for the gap between sliding metal components, but is not sufficiently large to confidently conclude, without more detailed analysis, that thermal expansion alone would cause valve seizure with gas temperatures up to approximately 1000 K.

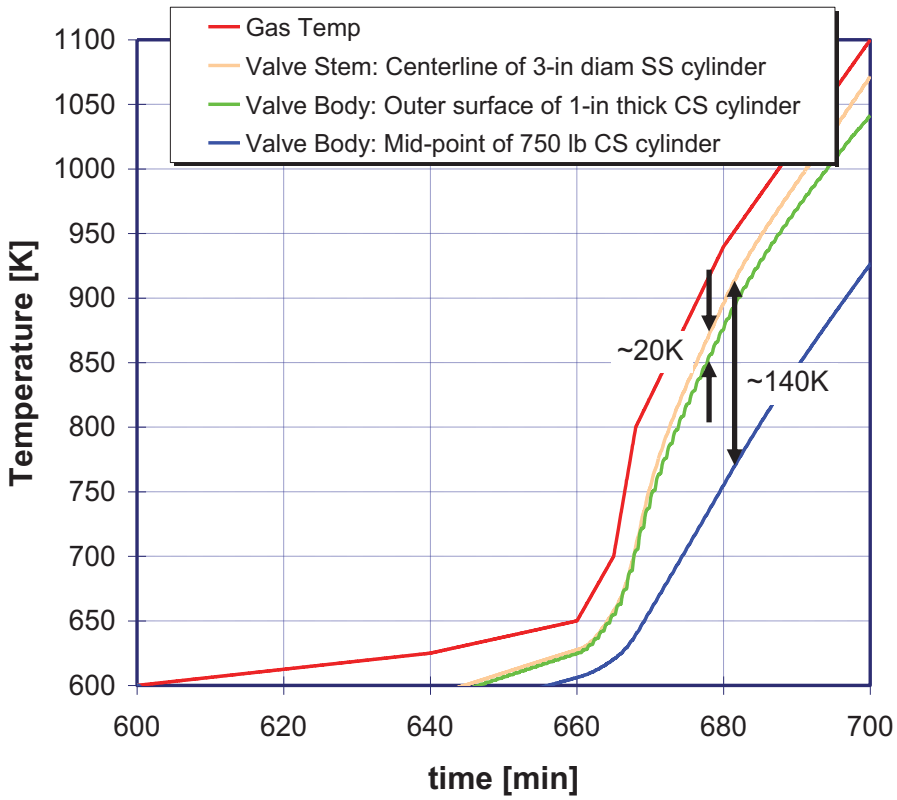

Figure 4-20 Thermal response of safety relief valve using simple 1-dimensional models

4.4.2.4 Material Deformation

Mechanical properties of stainless steel at very high temperatures described by a trade association for the specialty steam industry[17] were used to estimate the temperature at which SRV failure would occur in early (preliminary) MELCOR calculations for the SOARCA Program. However, two aspects of this evaluation merit re-consideration. First, the 'failure temperature' was applied to the calculated temperature of gases flowing through the valve. As indicated in Figure 4-20, the temperature of at least some valve components lags the gas temperature by a relatively small amount (e.g., perhaps as little as 20 K). Therefore, the 'error' introduced by this simplification is not significant in comparison to the temperature at which failure is likely to occur.

The second aspect is more important; namely, the temperature at which material deformation occurs is lower than the value used in the early calculations (i.e., 1000 K). As noted earlier, this value was selected primarily to reflect the 'service temperature' for stainless steel components, as reported by the steel industry trade association. However, a review of vendor literature on material properties of 304 stainless steel clearly indicates the maximum service temperature of approximately 1600 ^{o}F (~1100 K) is based on the scaling properties (or resistance to corrosion)

---

[17] Reference: High Temperature Properties of Stainless Steel, published by the Specialty Steel Industry of North America. Available at: www.ssina.com/composition/temperature.html

of 300 series stainless steel, rather than its mechanical properties. Spec sheets for 304/304L stainless steel from several vendors suggest a more appropriate temperature at which mechanical strength begins to deteriorate is 1000 ºF (811 K).

Table 4-2 compares the tensile and yield strength of 304 stainless steel at elevated temperature to values at the design temperature of the reactor coolant system (~600 ºF). The reduction in ultimate tensile strength doubles for every 200 ºF increase in temperature. This provides a quantitative measure of the qualitative statement given in a steel industry Spec Sheet, which states that stainless steel experiences a loss of strength at temperatures above 1000 ºF.

Engineering judgment is needed to apply the information in Table 4-2 for the purposes of estimating when moving valve components would cease to function due to material deformation. If one assumes valve components continue to function up to a temperature 1000 ºF, where material softening begins, the valve stem and other internal components would have already endured a reduction in tensile strength of approximately 18%, and a reduction in yield strength of 28%. If material temperature increases another 200 ºF, however, the ultimate tensile strength reduces by another 22% (below its already reduced value at 1000 ºF). At a temperature above 1000 ºF but below 1200 ºF (i.e., approximately 900 K), the ultimate tensile strength and yield strength are 30% lower than their values at the SRV design temperature. It is unreasonable to expect moving valve components to continue functioning with this deterioration in mechanical properties. A maximum material temperature of 900 K is, therefore, recommended as a reasonable limit to valve operation.

Table 4-2 Percent change in strength of stainless steel from value at 600ºF (589K) [18]

Temperature ºF (K)	***Change in ultimate tensile strength relative to value at 600ºF***	***Change in 0.2% yield strength relative to value at 600ºF***
600 (589)	0.0	0.0
800 (700)	-6.0%	-14.9%
1000 (811)	-17.7%	-27.6%
1200 (922)	-35.4%	-34.3%
1400 (1033)	-57.4%	-43.3%

4.4.2.5 Pilot Valve Failure

A third possible failure mechanism results from heating of the pilot valve, which actuates the main valve. Small low-flow ports within the valve body direct flow from gas upstream of the main valve disc to the pilot valve, which is comprised of a machined bellows. According to the Target Rock manual, the machined bellows, "acts as a combination piston, spring and hermetic seal." Expansion or extension of the bellows due to high internal pressure and movement of the pilot valve stem is the normal means by which the pilot valve realigns itself, and causes the main valve to open. It's conceivable that thermal expansion of the bellows might cause the same

[18] AK Steel Corporation, West Chester, OH, "Product Data Bulletin: 304/304L Stainless Steel," 394/394L-B-08-01-07 (2007).

effect. However, the flow rate to the pilot valve is not known and, therefore, the heat up rate cannot be estimated.

4.4.2.6 Spring Softening

It is also conceivable that flow of gases through the ports into the pilot assembly could heat the main valve spring or the smaller spring encapsulated in the pilot valve assembly. This might result in softening of the spring and a loss of valve stem closing force. The rate at which heat could be carried into this portion of the valve is not known for the same reasons described above for pilot valve failure.

4.5 Behavior of Ex-Vessel Drywell Floor Debris

The drywell floor is subdivided into three regions for the purposes of modeling molten-core/concrete interactions. The first region, which receives core debris exiting the reactor vessel, corresponds to the reactor pedestal floor and sump areas (CAV 0). Debris that accumulates in CAV 0 can flow out through a doorway in the pedestal wall[19] to a second region representing a 90 degree sector of the drywell floor (CAV 1). If debris accumulates in this region to a sufficient depth, it can spread further around the annular drywell floor into the third region (CAV 2). This discrete representation of debris spreading is illustrated in Figure 4-21.

Two features of debris relocation within the three regions are modeled. The first represents bulk debris spill over or movement from one region to another. A control system monitors the debris elevation and temperature within each region, both of which must satisfy user-defined threshold values for debris to move from one region to its neighbor. More specifically, when debris in a cavity is at or above the liquidus temperature of concrete, all material that exceeds a predefined elevation above the floor/debris surface in the adjoining cavity is relocated (i.e., 6 inches for CAV 0 to CAV 1 and 4 inches for CAV 1 to CAV 2). When debris in a cavity is at or below the solidus temperature of concrete, no flow is permitted. Between these two debris temperatures, restricted debris flow is permitted by increasing the required elevation difference in debris between the two cavities (i.e., more debris head required to flow).

The second control system manages the debris spreading radius across the drywell floor within CAVs 1 and 2. Debris entering CAV 1 and CAV 2 is not immediately permitted to cover the entire surface area of the cavity floor. The maximum allowable debris spreading radius is defined as a function of time. If the debris temperature is at or above the concrete's liquidus temperature, then the maximum transit velocity of the debris front to the cavity wall is calculated

---

[19] Although the drawing provided by the licensee seems to indicate the presence of a swing-door in the personnel opening at the base of the reactor pedestal, the analysis described here assumes this door does not actually exist. Years of research on the issue of drywell liner melt-through never acknowledged the presence of a door (e.g., NUREG/CR-5423 and NUREG/CR-6025.) It is noted in the introduction to NUREG/CR-5423 that the geometry of the Peach Bottom configuration was used as the template for the analysis. The flow of debris from the pedestal onto the outer drywell floor would not be impeded in any way by an obstacle in the concrete 'doorway' in the pedestal wall. As a result, the current SOARCA analysis applied the same rationale and assumed molten debris would freely flow from the pedestal onto the drywell floor.

(i.e., results in 10 minutes to transverse CAV 1 and 30 minutes to transverse CAV 2). When the debris temperature is at or below the concrete solidus, the debris front is assumed to be frozen, and lateral movement is precluded (i.e., debris velocity is 0 meters per second). A linear interpolation is performed to determine the debris front velocity at temperatures between these two values.

Full mixing of all debris into a single mixed layer is assumed in each of these debris regions. The specific properties for concrete composition, ablation temperature, density, solidus temperature, and liquidus temperature are specified. The concrete composition represented in the MELCOR model is listed in Table 4-3. The drywell floor concrete composition includes 13.5% rebar.

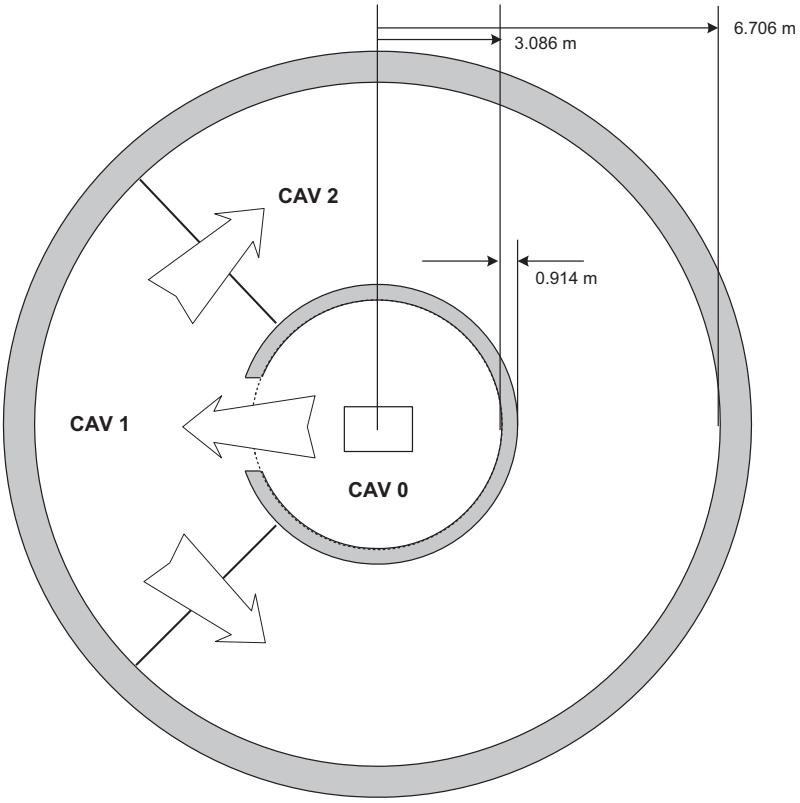

CAV	FLOOR AREA	EQUIV RADIUS
0	29.92	3.086
1	22.75	2.691
2	68.25	4.661

Figure 4-21 Drywell floor regions for modeling molten-core/concrete interactions

Other key user-defined concrete properties are selected to match defaults for limestone-common sand concrete including the following:

- Ablation temperature of 1,500 K
- Solidus temperature of 1,420 K
- Liquidus temperature of 1,670 K
- Density of 2,340 kilograms (kg) per cubic meter
- Emissivity of 0.6

Table 4-3 Concrete Composition

Species	Mass Fraction
Al_2O_3	0.0091
Fe_2O_3	0.0063
CaO	0.3383
MgO	0.0044
CO_2	0.2060
SiO_2	0.3645
H_2O_{evap}	0.0449
H_2O_{chem}	0.0265

It must be noted that lateral debris mobility is strongly affected by geometric details of the drywell floor design, and these design features vary among BWRs with a Mark I containment. The volume of debris that can be sequestered in the sump (and, therefore, not available for lateral movement toward the drywell liner) spans a wide range. Further, the steel liner at the periphery of the drywell floor is protected or elevated above the surface of the floor by a concrete curb in some plants. The volume of the sump at Peach Bottom (located within the pedestal region) and the location at which the steel liner intersects the drywell floor were taken into account in the MELCOR model described above.

4.6 Containment Failure Model

The MELCOR model of the Peach Bottom Mark I containment incorporates criteria for opening leak pathways through the containment pressure boundary by two distinct mechanisms. The first mechanism, which occurs in all the calculations involving sufficient core damage and breach of the RPV lower head, is drywell liner melt-through. The second mechanism is leakage through the drywell head flange during when high internal temperatures and pressure develop within the containment. Each is briefly discussed in the following.

<u>Drywell liner melt-through</u>
If debris flows out of the reactor pedestal and spreads across the drywell floor, as described in Section 4.5, and contacts the outer wall of the drywell, the steel liner will fail, opening a release pathway to the lower reactor building. Heat transfer between the steel liner and molten core debris is not explicitly calculated in the MELCOR model, due to limitations of the CAV Package, which addresses ex-vessel model debris behavior. The model assumes an opening in the drywell liner occurs 15 minutes after debris first contacts the drywell wall. This time delay

represents an average of estimates for failure time discussed in NUREG/CR-5423 [11] for situations in which the drywell floor is not covered with water.

Containment over-pressure

Peach Bottom has a Mark I containment that consists of a drywell and a toroidal-shaped wetwell, which is half full of water (i.e., the pressure suppression pool). The drywell has the shape of an inverted light bulb. The drywell head is removed during refueling to gain access to the reactor vessel. The drywell head flange is connected to the drywell shell with 68 bolts of 2 ½ inch diameter (Figure 4-22). The flanged connection also has two ¾ inch wide and ½ inch thick ethylene propylene diene methylene (EPDM) gaskets. The torque in the 2 ½ inch diameter bolts range from 817 to 887 foot-pounds (ft-lb) [18][19]. An average bolt torque of 850 ft-lb was used in this study.

The 68 drywell head flange bolts (see Figure 4-22) are pre-tensioned during reassembly of the head. This pre-tension also compresses the EPDM gaskets in the head flange. During an accident condition, the containment vessel may be pressurized internally. The internal pressure would counteract the pre-stress in the bolts. At a certain internal pressure, all of the pre-stressing force from the bolts would be eliminated, and the EPDM gaskets would be decompressed. Further increase in the internal pressure would result in leakage at the flanged connection.

The EPDM gasket manufacturers recommend a maximum squeeze (compression) of 30 percent for a static-seal joint. The gaskets recover about 15 percent of the total thickness after the compressive load is removed from the flange. However, the licensee engineers informed the SOARCA personnel that the gaskets for the drywell head flange are squeezed to 50 percent to have a metal to metal contact to ensure no leakage at a design pressure of 56 psig. In addition, the gaskets are exposed to constant temperature and radiation, which contribute to early degradation. For this reason, the gaskets are replaced during each reassembly of the reactor vessel head. Based on this information and actual observations, the Peach Bottom licensee engineers recommended a gasket recovery of 0.03 inch.

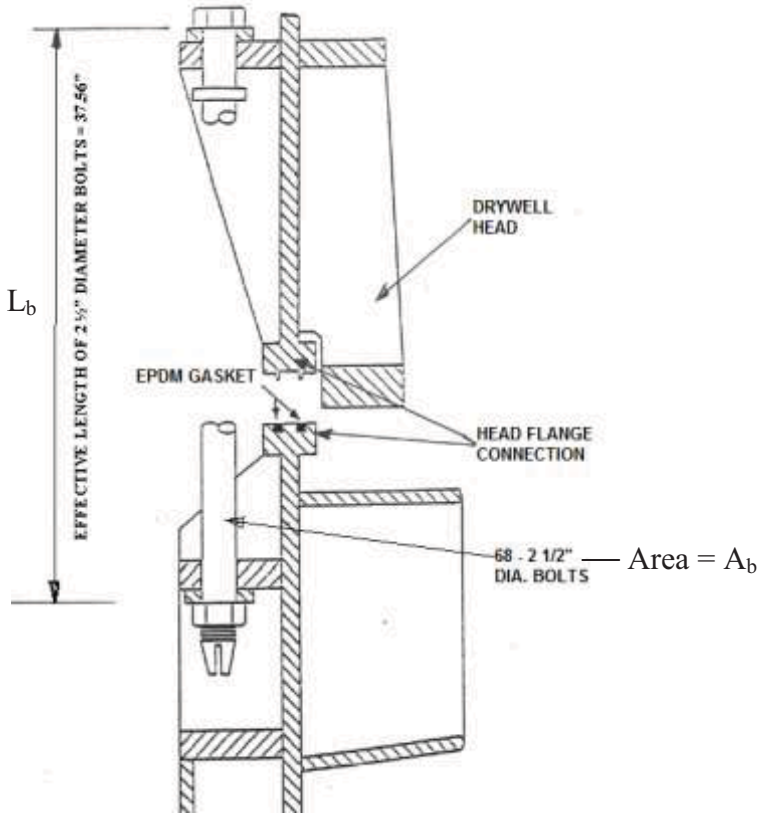

Figure 4-22 Drywell head flange connection details

Leakage areas for different internal pressures are shown in Figure 4-23 based on a gasket recovery of 0.03 inches. The drywell head flange does not leak until the internal accident pressure is 0.660 megapascal (MPa) (i.e., $P/P_D = 1.35$ or 82 psig). Thereafter, there is a gradual increase in the leakage area.

At high temperatures (greater than 755 K, or greater than 900 ^oF), upward and radial thermal growth of the drywell would lead to binding of small and large penetrations against the biological shield wall and failure. In addition, radial growth of the containment may also cause the seismic stabilizers to punch through the upper portion of the drywell at high temperatures [14]. This observation is consistent with the results of previous studies that show that the drywell is likely to fail at the low pressure range of 0-65 psig [14]. Therefore, it can be concluded that the drywell is likely to fail under any appreciable pressure load at structure temperatures of 900 ^oF or greater.

Finally, the containment can fail by drywell shell melt-through containment failure (see relevant discussions in Sections 4.5 and 4.8.2).

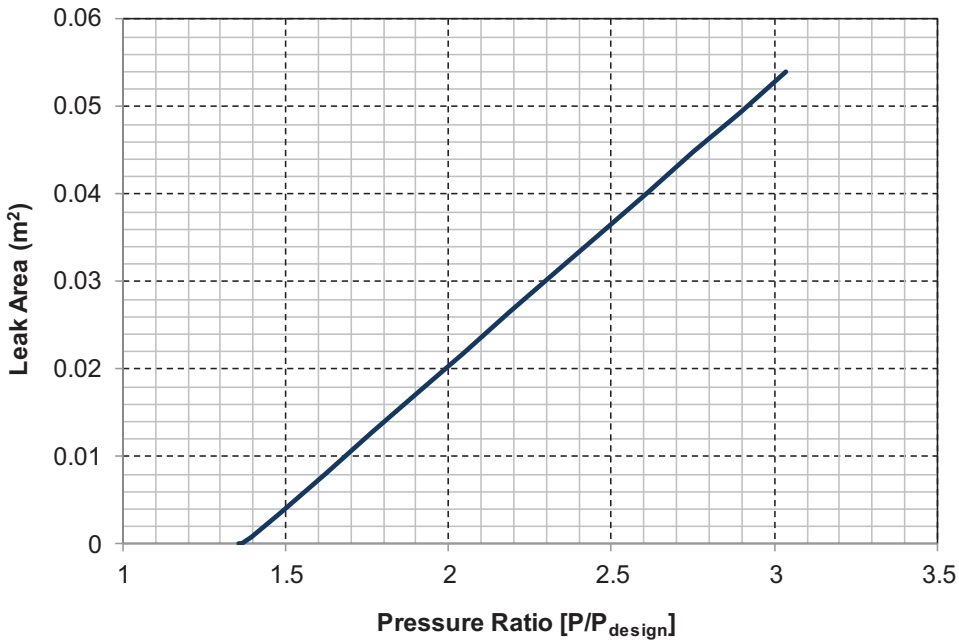

Figure 4-23 Drywell flange leakage model versus containment pressure

4.7 Radionuclide Inventories and Decay Heat

One important input to MELCOR is the initial concentration of radionuclide groups in the fuel and their associated decay heat. These values are important to the timing of initial core damage and the location and concentration of the initial radioactive source. The radionuclide groups in a nuclear reactor come from three primary sources:

1. Fission products are the result of fissions in either fissile or fissionable material in the reactor core.

2. Actinides are the product of neutron capture in the initial heavy metal isotopes in the fuel.

3. Other radioisotopes are formed from the radioactive decay of these fission products and actinides.

Integrated computer models, such as the TRITON sequence in SCALE, exist to capture all of these interrelated physical processes, but they are intended primarily as reactor physics tools [13]. As such, their standard output does not provide the type of information needed for MELCOR [6]. It is important to note that changes to the TRITON sequence in SCALE were not needed for this analysis. The BLEND3 post- processing software extracts output from the TRITON sequence and combines it in a way that makes it useful for MELCOR [6].

A Global Nuclear Fuel 10x10 (GE-14C) fuel assembly was used as a typical fuel element for the Peach Bottom analysis. Information about assembly dimensions, enrichments, and operating characteristics was obtained from the licensee (with permission from the fuel vendor) and used for a realistic evaluation. Twenty-seven different TRITON runs were performed to model three different cycles of fuel at nine specific power histories. The specific power histories ranged from

2 megawatt-days per metric ton uranium (MWD/MTU) to 45 MWD/MTU, which bounded all expected BWR operational conditions. For times before the cycle of interest, an average specific power of 25.5 MWD/MTU was used. For example in the use of a second fuel cycle, the fuel was burned for its first cycle using 25.5 MWD/MTU and, allowed to decay for an assumed 30 day refueling outage. Then nine different TRITON calculations were performed with specific powers ranging from 2 to 45 MWD/MTU. The BLEND3 code was applied to each of the 50 core nodes[20] in the MELCOR model using average specific powers derived from data for three consecutive operating cycles and appropriate nodal volume fractions. Once new libraries for each of the 50 nodes in the model were generated, the final step in the procedure was to deplete each node for 48 hours. The decay heats, masses, and specific activities as a function of time were processed and applied as input data to MELCOR to define decay heat and the radionuclide inventory. Values used in the MELCOR calculations corresponded to those generated for equilibrium conditions, in the middle of an operating cycle. A summary of the total (core-wide) decay power generated by this process is listed in Table 4-4.

Table 4-4 Decay Power in Peach Bottom MELCOR Model

Time	Decay Power (MW)
0.0 sec	221.36
1.0 sec	204.13
3.0 sec	185.90
7.0 sec	167.306
13.0 sec	152.86
27.0 sec	136.18
54.0 sec	120.87
1.8 min	105.85
3.7 min	92.61
7.4 min	80.96
14.8 min	69.46
29.8 min	57.51
60.0 min	46.19
2.0 hr	37.18
12.0 hr	22.69
24.0 hr	18.59
48.0 hr	14.97

4.8 Other Modeling Issues and Uncertainties

The SOARCA project is intended to provide a body of knowledge regarding the realistic outcomes of severe reactor accidents. To accomplish this objective, the SOARCA project used integrated modeling of accident progression and offsite consequences using both state-of-the-art computational analysis tools and best modeling practices drawn from the collective wisdom of the severe accident analysis community.

---

[20] The 50 core nodes are in five radial rings by ten axial levels

The MELCOR 1.8.6 computer code [6] embodies much of this knowledge and was used for the accident and source-term analysis. MELCOR includes capabilities to model the two-phase thermal-hydraulics, core degradation, fission product release, transport, deposition, and containment response. The SOARCA analyses include operator actions and equipment performance issues as prescribed by the sequence definition and mitigative actions. The MELCOR models are constructed using plant data and the operator actions were developed based on discussions with operators during site visits. The code models and user-specified modeling practices represent the current best practices.

Uncertainties remain in our understanding of the phenomena that govern severe accident progression and radionuclide transport. Consistent with the best-estimate approach in SOARCA, all phenomena were modeled using best-estimate characterization of uncertain phenomena and events. Important severe accident phenomena and the proposed approach to modeling them in the SOARCA calculations were presented to an external expert panel during a public meeting sponsored by the NRC on August 21 and 22, 2006 in Albuquerque, New Mexico. A summary of this approach is described in Section 4.8.1. These phenomena are singled out because they are important contributors to calculated results and have uncertainty.

Section 4.8.2 briefly describes the two other topics, steam explosions, and drywell shell melt-through on a wet drywell floor, that have been previously included in lists of highly uncertain phenomena.

Finally, a systematic evaluation of phenomenological uncertainties for a particular sequence is a separate task and not discussed in this report. That task will evaluate the importance and impact of alternative settings or approaches for key uncertainties.

4.8.1 Base Case Approach on Important Phenomena

Sandia National Laboratories conducted a review of severe accident progression modeling for the SOARCA project at a public meeting in Albuquerque, NM on August 21-22, 2006 [7]. This review focused primarily on best modeling practices for the application of the severe nuclear reactor accident analysis code MELCOR for realistic evaluation of accident progression, source term, and offsite consequences. The scope of the meeting also included consideration of potential enhancements to the MELCOR code as well as consideration of the SOARCA project in general.

The review was conducted by five panelists[21] with demonstrated expertise in the analysis of severe accidents at commercial nuclear power plants. The panelists were drawn from private industry, the U.S. Department of Energy national laboratory complex, and a company working on behalf of German-government ministries. The review was coordinated by Sandia National Laboratories and attended by NRC staff. A separate task in the SOARCA project is planned to address the importance of uncertainties in these modeling parameters.

---

[21] The expert panel that was convened in 2006 to review the best-estimate modeling approach is a different panel from the peer review panel convened toward the end of the program to review calculated results and program documentation. The objectives and results of the latter are described elsewhere in this report.

The following important uncertain modeling practices were presented to the expert panel. The expert panel provided written comments and suggestions, which were incorporated into the subsequent analyses. Base case approaches were identified for these uncertain and typically important parameters.

- Fuel degradation and relocation treatment: An additional model has been added to characterize the structural integrity of the fuel rods under highly degraded conditions. The new model acknowledges a thermal-mechanical weakening of the oxide shell as a function of time and temperature. As the local cladding oxide temperature increased from the Zircaloy melting temperature (i.e., represented as 2098 K in MELCOR) towards 2500 K, a thermal lifetime function accrues increasing damage from 10 hours to 1 hour until a local thermo-mechanical failure. Similar time-at-temperature failure criteria are applied to oxidized channel boxes, but at any point in time channel temperatures and degree of material oxidation differ from those associated with adjacent fuel assemblies. Therefore, the collapse of channel boxes into particulate debris typically occurs at a different time from the collapse of fuel assemblies in the same radial ring of the core.

- Lower plenum debris/coolant heat transfer: Following the fuel-debris slump into the lower plenum, there may be fuel-coolant interactions. The lower plenum heat transfer settings were updated to reflect the end-state thermal condition of the debris in the deep pool FARO tests (i.e., significant thermal interaction with the water). The resultant behavior results in debris fragmentation and cooling if there is a pool of water in the lower plenum. Debris temperatures can subsequently increase after the pool of water evaporates, which in turn heats up the reactor vessel lower head.

- Core plate failure: The timing of core plate failure affects the relocation of the degraded core materials from the core region into the lower plenum. The local thermal-mechanical failure of the lower core plate, the flow mixer plate, and the lower support forging are calculated within MELCOR using the Roark engineering stress formulae. The yield stress is calculated based on the loading and local temperature.

- Fission product release, speciation, and volatility: First, a new ORNL-Booth fission product release model is used that was adjusted to match the measured responses from the VERCORS Test 4. VERCORS Test 4 is representative of modern, high burn-up fuel. The previous default model was not representative of the high burn-up release physics.

  Second, the predominant speciation of cesium was changed based on detailed analysis of the deposition and transport of the volatile fission products in the Phebus facility tests. The analysis revealed molybdenum combined with cesium and formed cesium molybdate. Previously, the default predominant chemical form cesium was cesium hydroxide. As consistent with past studies, all the released iodine combines with the cesium. Applications of this information to the MELCOR models used in the SOARCA calculations are described in SAND2010-1633, "Synthesis of VERCORS and Phebus Data in Severe Accident Codes and Applications" [9].

Gaseous iodine remains an uncertain source term issue, especially with respect to long-term radioactive release mitigation issues after the comparatively much larger airborne aerosol radioactivity has settled from the atmosphere. The mechanistic modeling treatment for gaseous iodine behavior is a technology still under development with important international research programs underway to determine the dynamic behavior of iodine chemistry with respect to paints, wetted surfaces, buffered and unbuffered water pools undergoing radiolysis, and gas phase chemistry. The base case treatment under the best practices recommendation are sufficient for the mean effects addressed in this report, and it is planned to investigate parameterization of the gaseous iodine fraction of total iodine releases in the context of the uncertainty quantification phase of this work.

- Vessel lower head failure and debris ejection: The base case approach of modeling the vessel lower head failure and debris ejection included some modifications in MELCOR. First, all particulate debris in the lower plenum is permitted to be in contact with water, if present. In previous versions of the code, a restrictive one dimensional counter-current flooding limitation (CCFL) criterion prevented water from penetrating a deep debris bed. This restriction has been removed, effectively assuming water steam rising upward from the debris bed does not totally preclude water from entering lower regions of the bed (e.g., via lateral flow from peripheral regions of the lower plenum). Second, the mechanical response of the vessel lower head is modeled using a one dimensional creep rupture model. A Larson-Miller failure criterion is calculated based on the one dimensional conduction and stress profile through the lower head. Failure of a lower head penetration prior to gross head failure was not explicitly modeled in the SOARCA calculations because it was judged unlikely based on observations from experimental studies at Sandia National Laboratories lower head failure (LHF) tests and prior analyses of BWR lower head failure mechanisms [16]. Refer to the discussion in Section 4.2.2 for more information on this subject.

- Ex-vessel phenomena – Molten Corium-Concrete Interactions (MCCI): An evaluation of typical MELCOR calculations of ex-vessel debris behavior when debris is submerged in a pool of water concluded the default treatment of heat transfer between debris and an overlying pool of water was not consistent with observations from the MACE tests. The default value for the debris-water interface heat transfer coefficient in MELCOR did not account for multi-dimensional effects of fissures, other surface non-uniformities, and side heat fluxes. An enhancement to the default value was used to more closely replicate heat transfer rates observed in the MACE tests.

- Hydrogen combustion: The default MELCOR hydrogen combustion model was used in control volumes representing the Peach Bottom reactor building. This model assumes ignition of a flammable mixture occurs at a volume-average hydrogen concentration of 10%, provided sufficient oxygen is present. Ignition at this concentration reflects the absence of a strong ignition source that might be present in accident sequences involving active AC power. Modeling options were also exercised to calculate horizontal and vertical propagation of combustion flames between neighboring control volumes, after a time delay that accounts for the time required for a flame front to span the width of the control volume. The time associated with flame propagation assumes a volume-centered distance between

neighboring volumes; therefore, the propagation time varies with the size of the control volume.

4.8.2 Early Containment Failure Phenomena

Two phenomenological issues not explicitly modeled in the best-estimate approach used in SOARCA are: (1) alpha-mode containment failure, and (2) drywell liner melt-through in the presence of water leading to containment failure. These phenomena, if they occurred, would result in early failure of containment, and were included in the probabilistic studies documented in NUREG-1150 to quantify the risks from nuclear reactors.

The alpha-mode event is characterized by the supposition that an in-vessel steam explosion might be initiated during core meltdown by molten core material falling into the water-filled lower plenum of the reactor vessel. The concern was that the resulting steam explosion could impart sufficient energy to separate the upper vessel head from the vessel itself and form a missile with sufficient energy to penetrate the reactor containment. This would produce an early failure of the containment building at a time when the largest mass of fission products is released from the reactor fuel. In the following years, significant research was focused on characterizing and quantifying this hypothesized response in order to attempt to reduce the significant uncertainty. A group of leading experts ultimately concluded in a position paper published by the Nuclear Energy Agency's Committee on the Safety of Nuclear Installations that the alpha-mode failure issue for Western-style reactor containment buildings can be considered resolved from a risk perspective, posing little or no significance to the overall risk from a nuclear power plant. Therefore, the complex processes leading to this failure mode were not explicitly modeled in the BWR MELCOR calculations.

The issue of Mark I drywell liner melt-through at Peach Bottom was assessed by the NUREG-1150 molten core-containment interaction panel. The results of expert panel elicitation are reported in NUREG/CR-4551, Volume 2, Revision 1, Part 2, "Evaluation of Severe Accident Risks: Quantification of Major Input Parameters, Experts' Determination of Containment Loads and Molten Core Containment Interaction Issues," issued April 1991[10]. Analyses performed by the group of experts identified several areas of uncertainty in the phenomena governing debris transport out of the reactor pedestal toward the drywell liner. Subsequent to the completion of NUREG-1150, the NRC sponsored analytical and experimental programs to resolve the "Mark I liner attack" issue. The results of an assessment of the probability of Mark I containment failure by melt attack of the liner were published in NUREG/CR-5423, "The Probability of Liner Failure in a Mark I Containment," issued in 1989 [11] and NUREG/CR-6025, "The Probability of Mark I Failure by Melt-Attack of the Liner," issued in 1993 [12]. This work concluded that, in the presence of water, the probability of early containment failure by melt-attack of the liner is so low as to be considered physically unreasonable. In contrast, liner melt-through was determined to be likely under conditions in which the volume and temperature of core debris released to the drywell floor would support lateral debris movement toward, and contact with, the drywell liner.

None of the scenarios examined in the SOARCA BWR evaluation generate a pool of water on the drywell floor prior to vessel breach. Therefore, it was not necessary to model the effects of boiling heat transfer between core debris and on over-lying pool of water, and the resulting

effects on debris mobility. However, lateral flow of a slurry of molten metallic and particulate oxides across a dry floor is modeled within the MELCOR framework, as described earlier in Section 4.5.

5.0 INTEGRATED THERMAL HYDRAULICS, ACCIDENT PROGRESSION, AND RADIOLOGICAL RELEASE ANALYSIS

This section describes the MELCOR accident progression analysis for the internal and external event scenarios described in Section 3.0 of this report. Version 1.8.6 of the MELCOR severe accident analysis code was used in the accident progression and radiological release calculations.

5.1 Long-Term Station Blackout – Unmitigated Response

The unmitigated scenario event progression for the LTSBO accident progression analysis assumes that the operators follow the actions described in Special Event Procedure SE-11 [2]. This document provides guidelines for managing the plant with degraded AC power sources. Initial operator actions would concentrate on assessing plant status. Successful reactor scram, containment isolation, and automatic actuation of RCIC for reactor level control would be verified. These checks would take approximately 15 minutes. One or more SRVs would cycle to control the RPV pressure.

Special Event Procedure SE-11 directs operators to align the station blackout line from Conowingo Dam in the event of failure of offsite power combined with the failure of all diesel generators to start. If this action fails to restore AC power to the plant, as assumed in this analysis, operators are directed to de-energize all non-essential DC loads. By removing as many unnecessary loads as possible from the DC bus, the station battery lifetime is extended. This load shedding would not affect or disable control logic to the RCIC, HPCI, main control room instrumentation, or SRV control.

The load shedding is expected to begin 15 minutes into the event and take approximately 15 minutes to complete. Plant system engineers estimate the effect of load shedding would be to extend station battery duration from 2 to 4 hours.

One consequence of station blackout is the loss of cooling to the RCIC and HPCI corner rooms. Heat losses from system piping and equipment to the room atmosphere would cause these areas to overheat. In such an event, a step of the Special Event Procedure SE-11 is applicable. It directs operators to block open doors to these rooms and facilitate cross ventilation, which would slow the rate of room heat up. These actions are assumed to successfully prevent system isolation from high room temperature for the entire period of system operation.[22] A subsequent step of the procedure directs operators to defeat high torus temperature isolation signals for HPCI and RCIC (if operating). MELCOR calculations presented in Section 5.1.1 indicate these signals would not be received before the station batteries exhaust; therefore, these actions are not important for the LTSBO scenario. Another step of the Special Event Procedure directs the operators to monitor the inventory in the CST and take actions to refill the tank[23] via gravity feed

---

[22] Heat loss from RCIC (or HPCI) systems to their enclosure corner rooms is not explicitly represented in the MELCOR model.

[23] If the seismic initiating event ruptured the CST, water would be retained in the reinforced concrete moat surrounding the tank and suction would continue to be available. The total (integral) volume of coolant drawn from the CST during the entire period of RCIC operation in the LTSBO sequence is approximately 110,000 gal, which is considerably less than the tank capacity (approximately 200,000 gal).

from other sources if necessary. Long-term viability of the CST is therefore assumed in the MELCOR calculations.

Table 5-1 lists the calculated timing of key events that follow from all of these actions. The time at which core damage begins strongly depends on the duration of station batteries. The difference in time between loss of DC power and the onset of core damage increases as battery lifetime increases because of reductions in decay heat levels with time. In the absence of effective manual intervention, core damage eventually proceeds to melting and relocation of core material into the reactor vessel lower head, reactor vessel lower head failure, and release of molten core debris to the drywell floor.

Table 5-1 Timing of Key Events for LTSBO

Event	LTSBO with 4 hr DC power (time in hours unless noted otherwise)
Station blackout loss of all onsite and offsite AC power	0.0
Low-level 2 and RCIC actuation signal	10 minutes
Operators manually open SRV to depressurize the reactor vessel	1.0
RPV pressure first drops below LPI setpoint (400 psig)	1.2
Battery depletion leads immediate SRV re-closure	4.0
RCIC steam line floods with water RCIC flow terminates	5.2
SRV sticks open because of excessive cycling	8.2
Downcomer water level reaches top of active fuel	8.4
First hydrogen production	8.9
First fuel-cladding gap release	9.1
First channel box failure	9.3
Reactor vessel water level reaches bottom of lower core plate	9.3
First localized failure of lower core plate	9.6
First core cell collapse because of time at temperature	9.8
Beginning of large-scale relocation of core debris to lower plenum	10.5
Lower head dries out	13.3
Ring 5 CRGT column collapse (failed at axial level 2)	15.8
Ring 1 CRGT column collapse (failed at axial level 2)	17.4
Ring 4 CRGT column collapse (failed at axial level 2)	17.4
Ring 3 CRGT column collapse (failed at axial level 2)	17.5
Ring 2 CRGT column collapse (failed at axial level 2)	18.6

Table 5-1 Timing of Key Events for LTSBO (continued)

Event	LTSBO with 4 hr DC power (time in hours unless noted otherwise)
Lower head failure	19.7
Drywell head flange leakage begins	19.9
Hydrogen burns initiated in drywell enclosure region of reactor building	20.0
Refueling bay to environment blowout panels open	20.0
Hydrogen burns initiated in reactor building refueling bay	20.0
Drywell shell melt-through initiated and drywell head flange re-closure	20.0
Hydrogen burns initiated in lower reactor building	20.1
Door to environment through railroad access opens because of overpressure	20.1
Refueling bay roof fails due to overpressure	20.2
Time iodine release to environment exceeds 1% of initial core inventory	23.6
Calculation terminated	48.0

The absence of water on the drywell floor in a transient scenario like a station blackout[24] allows core debris ejected from the reactor vessel after lower head failure to spread laterally across the floor and contact the drywell wall. Past calculations have predicted drywell shell melt-through to occur relatively soon after vessel failure (i.e., within 30 minutes.) Fission product release from the containment to the reactor building and with a very short delay to the environment will begin at this point in time. Several release points to the environment are possible, depending on the response of the reactor building. Past calculations have shown that hydrogen combustion leads to nearly immediate opening of the refueling bay blow-out panels and the railroad doorway at grade level. Blow-out panels into the turbine building and personnel access doorways out of the reactor building might also open. However, the dominant flow path for fission products to the environment is through the refueling bay blowout panels.[25]

5.1.1 Thermal Hydraulic Response

When plant conditions are stabilized, Special Event Procedure SE-11 calls for a controlled depressurization of the RPV to 125 psig using the instructions in the RC/P leg of Trip Procedure T-101. Depressurization would be accomplished by opening one or more SRVs or, if necessary, by manually opening other steam vent pathways, such as main steam line drains. The cooldown rate would be limited to less than 100 °F per hour. A controlled depressurization is initiated at 1 hour by opening a single SRV. As shown in Figure 5-1, this results in a

---

24 As opposed to a loss-of-coolant accident, where reactor coolant effluent accumulates on the drywell floor.

25 A stable flow of air is calculated to enter the building through the open railroad doorway, rise upward through the open equipment hatches from grade level to the refueling bay and exit the building to the environment through the open blow-out panels.

stable pressure of approximately 125 psig. Reactor vessel pressure remains near this pressure for approximately 2 hours, while active DC power permits a SRV to hold in the open position. Four hours into the scenario, however, DC power from the station batteries is exhausted, and the solenoid valve regulating control air to the SRV operator closes, causing the SRV itself to reclose.[26] SRV closure causes reactor vessel pressure to gradually increase back to its automatic (safety) lift setpoint. Reactor vessel pressure subsequently cycles about its lift setpoint for approximately the next 2 hours.

During the first 12 hours of the accident scenario, the reactor vessel water level is also undergoing significant changes (see Figure 5-2). The hydraulic transient immediately following reactor scram and isolation results in a gradual decrease in water level because of coolant evaporation and discharge through a cycling SRV to the suppression pool. RCIC automatically starts 10 minutes after the initiating event and begins to restore reactor water level. Two hours into the scenario, operators take manual control of RCIC and maintain level within the indicated range of +5 to +35 inches (i.e., 16 feet above the top of active fuel – TAF).

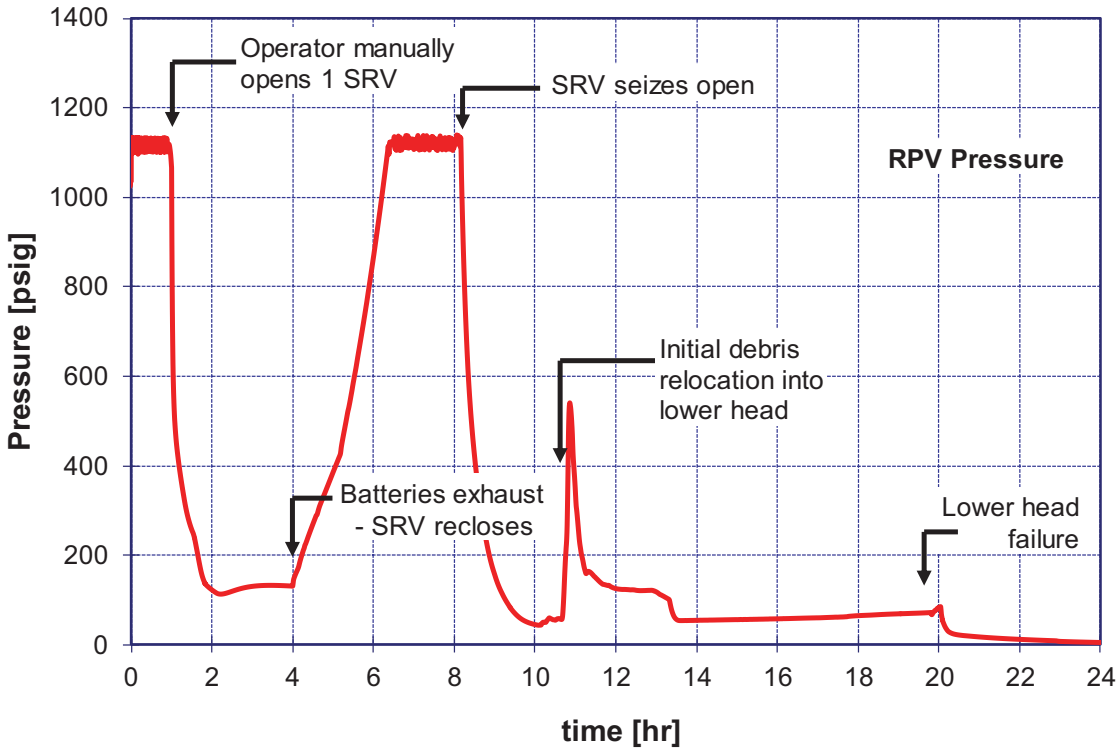

Figure 5-1 LTSBO vessel pressure

[26] Loss of control air pressure to the valve operator might take a few minutes to affect valve position, but this short time is ignored in this analysis.

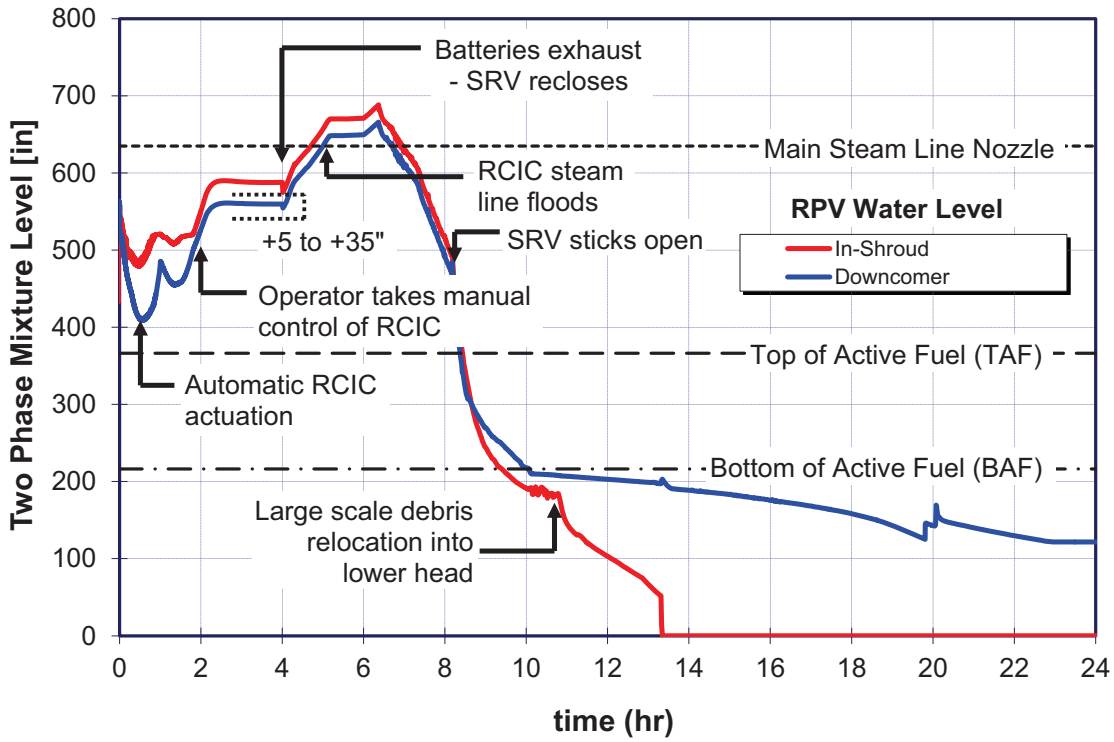

Figure 5-2 LTSBO reactor pressure vessel water level

When DC power from the station batteries expires 4 hours into the scenario, RCIC turbine speed is assumed to remain fixed at a nearly full-open position. The loss of electric (DC) power would cause the turbine inlet throttle valve to move to a full-open position. If RPV pressure is above approximately 400 psig, the additional steam flow resulting from further opening of the steam throttle valve would result in an automatic trip of the system due to steam turbine overspeed. At the time of battery exhaustion in this scenario, however, RPV pressure is well below 400 psig, and the steam inlet valve would already be positioned at or near its full-open position to permit a sufficient flow of steam into the RCIC turbine. As a result, a change in valve position is not anticipated in this situation, and a turbine overspeed trip would not be an immediate consequence of the loss of DC power. The functional effect of this response is that, for more than 1 hour (i.e., until RPV pressure increases above 400 psig), the RCIC system continues to deliver coolant flow at approximately the same flow rate it had at the time DC power expired.[27] However, closure of the SRV at 4 hours means that coolant losses from the reactor vessel are temporarily terminated. Therefore, the reactor vessel level begins to rise (i.e., coolant injection continues, but losses are terminated.) A continuous rise in level is evident in Figure 5-2, between 4 hours and approximately 5.2 hours.

---

[27] Steam flow to the RCIC turbine increases as RPV pressure increases following closure of the SRV. Based on conversations with licensee system engineers, this would lead to a turbine over-speed trip of the system above a pressure of approximately 400 psig. However, results of the MELCOR calculation for this scenario indicate flooding of the main steam line and attendant termination of RCIC operation would occur before RPV pressure reached this point.

At 5.1 hours, the water level in the reactor vessel increases above the elevation of the main steam line nozzles. Water subsequently spills over into the main steam lines causing the steam line to the RCIC turbine to flood within a few minutes. The resulting termination of RCIC operation at 5.2 hours causes the reactor water level to stabilize. Approximately one hour later, the average water temperature in the reactor vessel increases to saturation. When that occurs, the reactor vessel pressure is above 1000 psia and increasing. This increasing reactor vessel pressure causes a slight increase in the effective level of water because of decreasing average coolant density.[28] At 6.4 hours, reactor vessel pressure returns to the SRV lift pressure, and coolant losses through the cycling SRV resume. Without any form of coolant makeup, the reactor water level continuously decreases at a rate of 2 inches per minute. At 8.2 hours, the lead SRV fails to reclose after opening for the 270th time (refer to Section 4.4.2.1 for the technical basis for this event.) The stuck-open SRV reduces RPV pressure below 200 psia within one hour, and to equilibrium with the containment pressure in two hours.[29] The enhanced rate of coolant discharge from the reactor vessel causes the rate at which reactor water level decreases to accelerate. Water level decreases below TAF approximately 15 minutes after SRV seizure. One hour later, the level decreases below the bottom of the lower core plate. Within the first 10 hours of station battery exhaustion, the entire inventory of water in the reactor vessel is evaporated (see Figure 5-2 and Table 5-1).

The thermal response of fuel in the core is illustrated in Figure 5-3, which shows the calculated temperature of fuel cladding across the core mid-plane. Temperatures of fuel cladding at the top of the core begin to rise when the mixture level decreases below approximately two-thirds of the core height. As the mixture level decreases toward the bottom of the core, fuel temperatures increase rapidly due to runaway oxidation of Zircaloy cladding. The close relationship between the rate at which fuel cladding temperature increase and Zircaloy oxidation is shown in Figure 5-3, which compares clad temperatures (left-hand scale) to total in-vessel hydrogen generation (right-hand scale). Mechanical failure of fuel at the top of the core occurs when Zircaloy clad material either melts and drains to lower regions of the core, or oxides to form a thin, fragile ZrO_2 shell around over-heated fuel. This mechanically weak material fragments into particulate debris, which relocate toward the lower core plate as rubble.

---

[28] The density of saturated water decreases by 4 to 5 percent as pressure increases from 900 psia to 1,150 psia. This causes the entire body of water within the core shroud to expand slightly, resulting in an increase in effective (swollen) water level.

[29] If RPV depressurization did not occur due to seizure of the cycling SRV, low RPV pressure prior to vessel breach could be achieved by invoking plant-specific procedures in SAMG-1 (T-252), which offer means of depressurization that do not require electric power to position valves (i.e., manual operation).

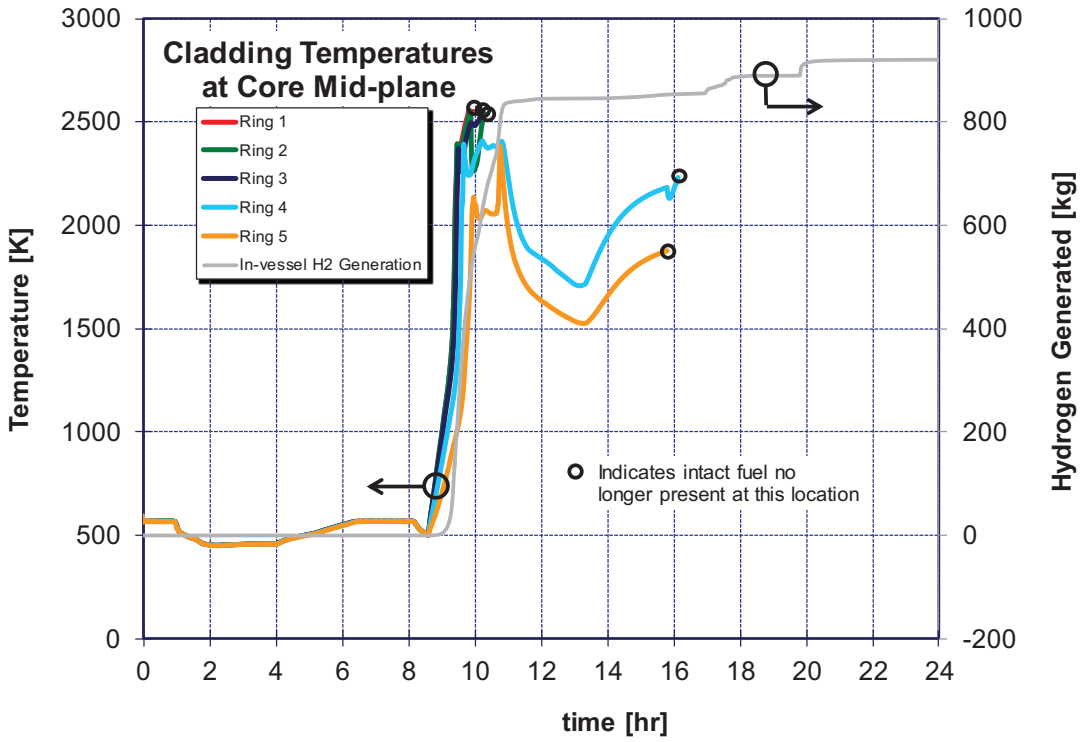

Figure 5-3 LTSBO fuel cladding temperatures at core mid-plane and in-vessel hydrogen generation

Particulate and molten debris continue to move downward in the core until 10.5 hours, when the lower core plate yields, releasing molten core debris into the reactor vessel lower head. The interaction between hot debris and residual water in the lower head increases the rate of coolant evaporation, as indicated in Figure 5-2 with the increased (negative) slope of the in-shroud water level. It also causes the molten debris to freeze on surfaces of the control rod guide tubes, which are submerged in the large body of water that remains in the lower plenum. The changes in core geometry during this time frame, which are caused by the formation and downward relocation of molten and particulate debris, are illustrated in Figure 5-4.

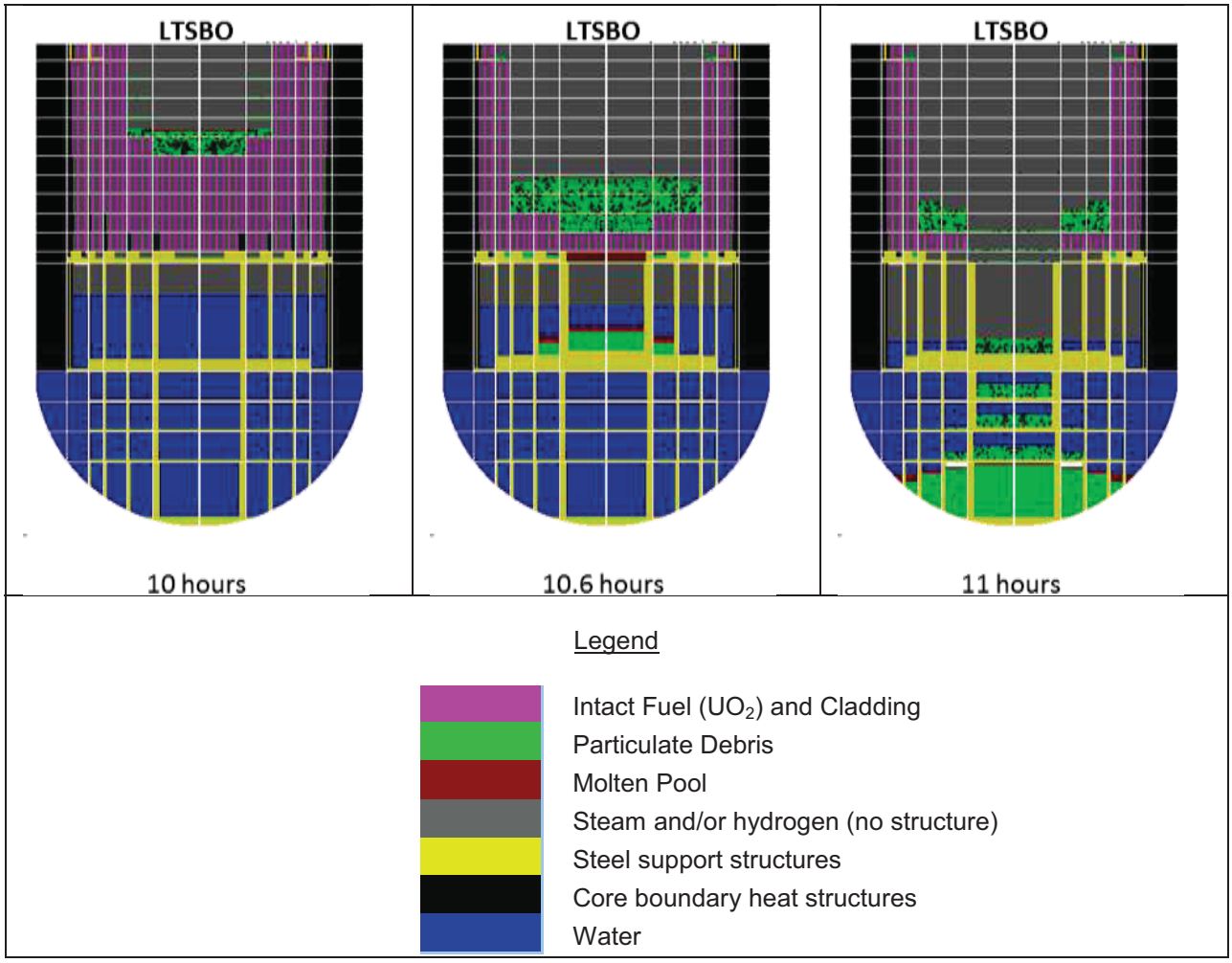

Figure 5-4 Relocation of core material into the lower plenum during LTSBO

The cooling of core debris as it enters the water-filled lower plenum is also evident in Figure 5-5, which shows the calculated temperature of debris along the inner surface of the lower head. When residual water in the lower plenum is completely evaporated at 13.3 hours, debris temperatures begin to increase. Heat transfer from debris to the inner surface of the lower head causes the lower head temperature to increase as well. This is illustrated in Figure 5-6, which depicts the calculated temperature on the inner and outer surfaces of the lower head across all five rings of the MELCOR model. Because reactor vessel pressure is relatively low during the

heat up of debris in the lower plenum, the failure of the lower head is more strongly influenced by thermal rather than mechanical stresses.[30]

Figure 5-7 illustrates changes in the configuration of core debris and lower plenum structures between the time of RPV dryout (~13.3 hrs) and lower head failure (19.7 hours). At the time of lower head dryout, approximately 60% of the core fuel assemblies (i.e., the central three of five radial rings in the MELCOR model) have collapsed into the lower plenum. Highly oxidized, but vertically intact assemblies remain standing in the outer two rings of the core. Debris in the lower plenum surrounds a forest of intact control rod guide tubes (CRGTs). As indicated in Figure 5-5, the temperature of lower plenum debris steadily increases, eventually causing structural failure of the CRGTs, which collapse and are mixed into the growing debris bed. Collapse of the CRGTs supporting the outer two rings of fuel in the core causes this material to also fall into the debris bed. Immediately prior to lower head failure, the debris bed represents the mass of nearly the entire core plus structural materials below the core. This debris bed is composed of a mixture of molten stainless steel (~32% by mass), unoxidized zirconium (~12%) and particulate debris containing uranium dioxide and metallic oxides (the remainder). Failure of the lower head (19.7 hours) results in the rapid ejection of over 300 metric tons of core debris onto the floor of the reactor pedestal in the drywell.

---

[30] The inner surface temperature of the lower head (i.e., MELCOR rings 1-3) is above the melting point of steel at the time failure occurs.

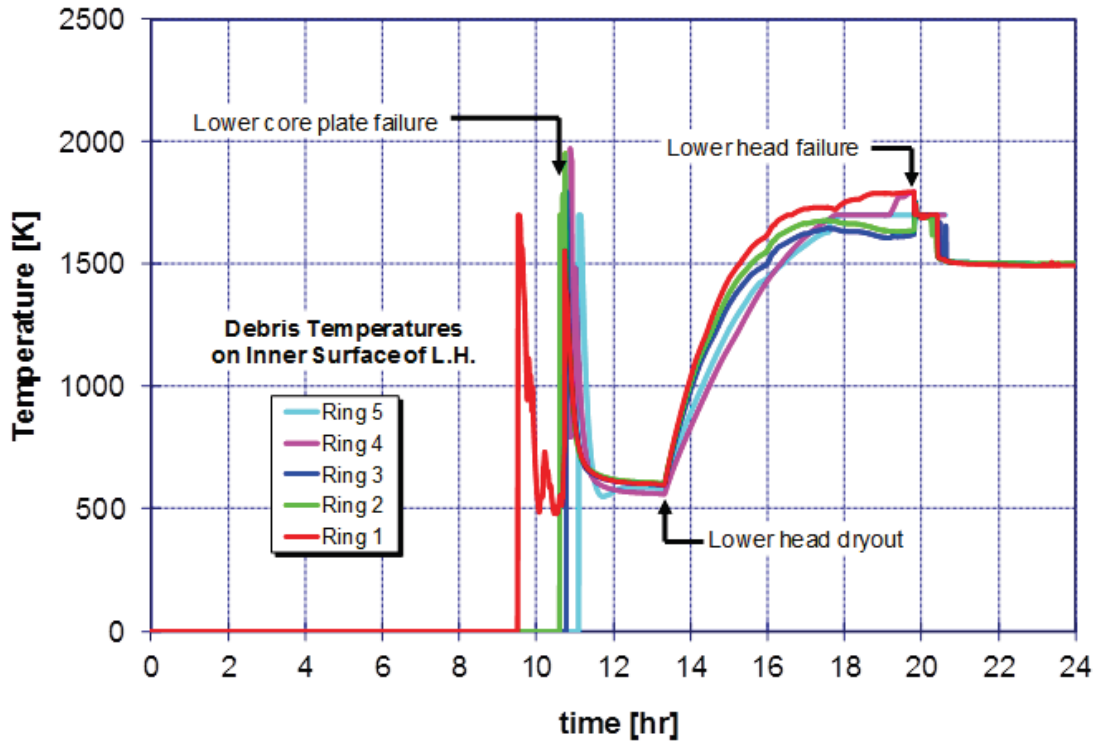

Figure 5-5 LTSBO temperature of particulate debris on inner surface of lower head

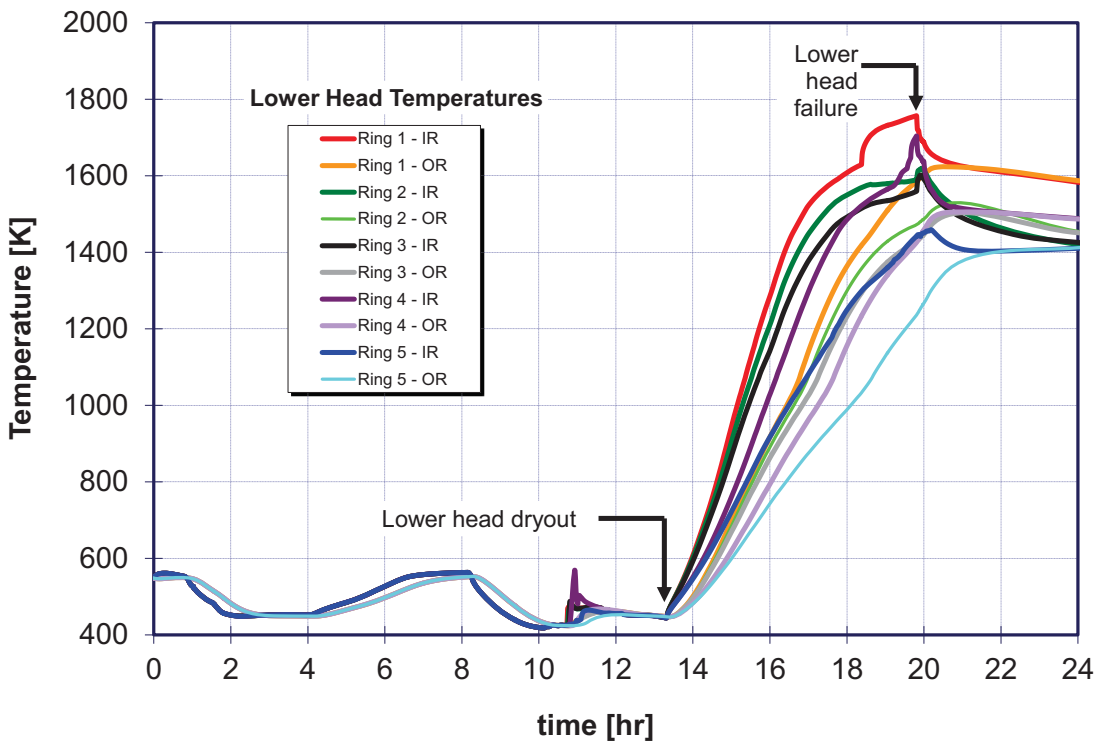

Figure 5-6 LTSBO lower head temperature

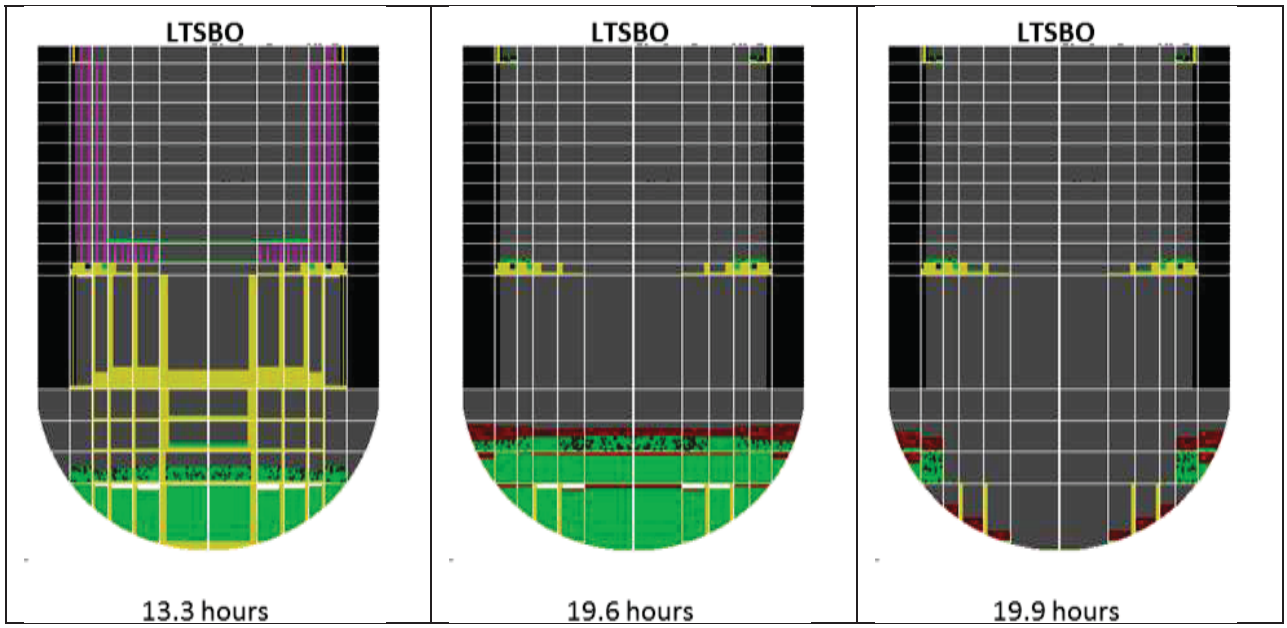

Figure 5-7 Debris behavior from lower head dryout through lower head failure for LTSBO

Before the reactor vessel lower head fails, thermodynamic conditions in the containment are governed by the gradual release of hydrogen through the SRV to the torus. The large quantity of hydrogen (i.e., over 900 kg between 9 and 19 hours – see Figure 5-3), combined with the small free volume of the containment, results in significant increases in pressure. The containment pressure history is shown in Figure 5-8. Eighteen hours after the initiating event (i.e., 13 hours after the loss of all coolant injection), the containment pressure increases above the design pressure of 56 psig. Immediately before lower head failure (19.7 hours), containment pressure increased by a small amount more, to 58 psig.

Containment atmosphere temperatures remain modest throughout the period of early increases in pressure because the steam/hydrogen mixture cools as it bubbles through the suppression pool. Changes in suppression pool temperature through the first 24 hours of the accident are shown in Figure 5-9. Immediately following vessel breach, containment atmosphere pressure and temperature increase dramatically from the accumulation of molten core debris on the reactor pedestal and drywell floors. The atmosphere temperature in the pedestal increases to over 1500 K and the atmosphere in the drywell increases to a stable temperature of approximately 490 K (420 ºF). The combination of elevated pressure and temperature near the top of the drywell results in short-term leakage through the head flange. The leak area and discharge rate are assumed to be proportional to the differential pressure across the flange.[31] Drywell head flange leakage begins almost 20 hours after the initial loss of offsite power. The initial leak rate is relatively small and is quickly overwhelmed by a different containment failure mode.

[31] The flange leak area, which is based on a structural analysis based on the containment internal pressure, is described in Section 4.6.

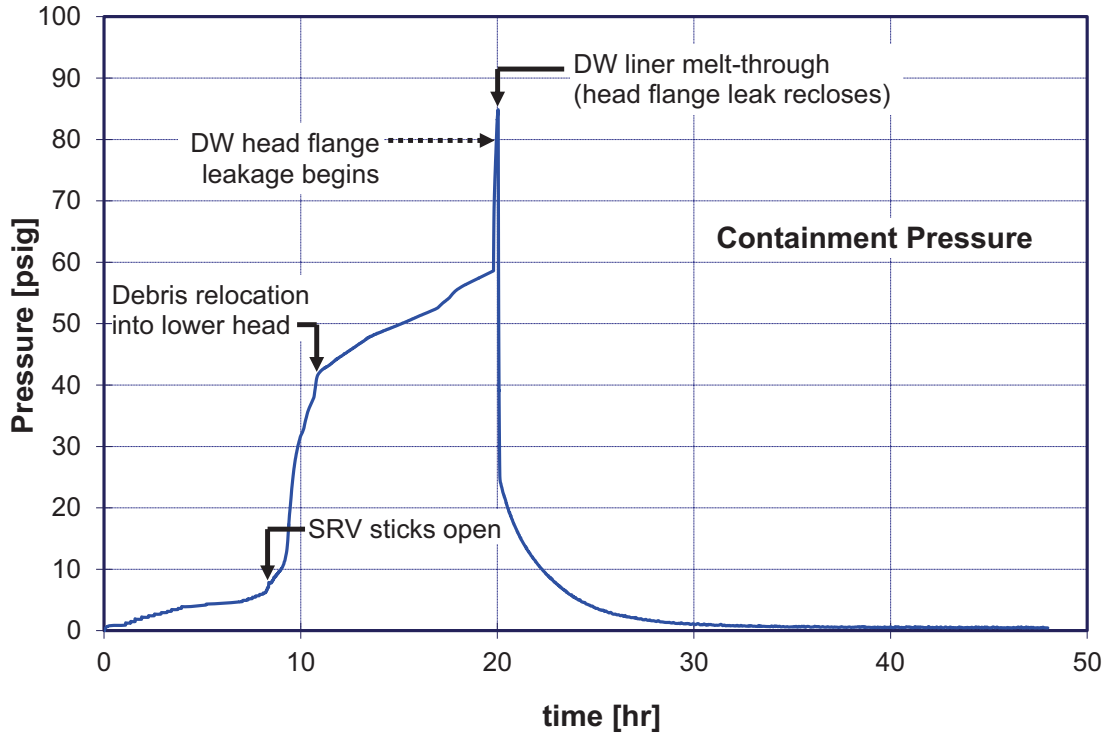

Figure 5-8 LTSBO containment pressure

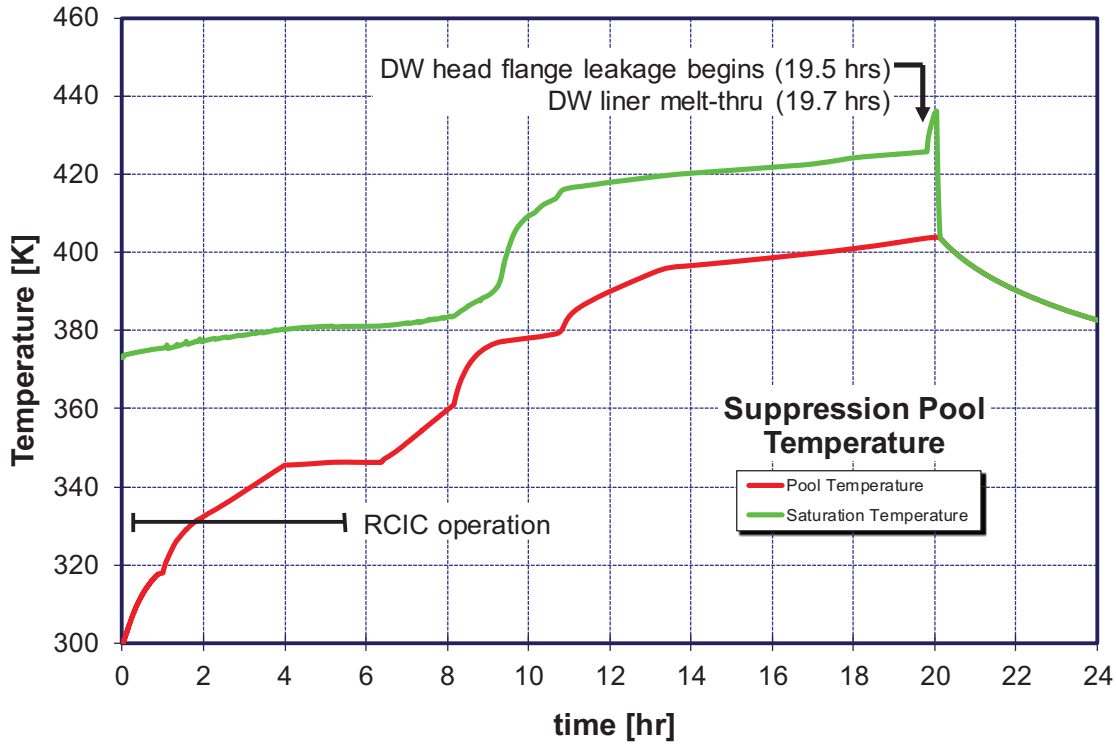

Figure 5-9 LTSBO suppression pool temperature

Soon after debris is released onto the reactor pedestal floor, it flows laterally out of the cavity through the open personnel access doorway and spreads out across the main drywell floor. Lateral movement and spreading of debris across the drywell floor allows debris to reach the steel shell at the outer perimeter of the drywell within 10 minutes. Five minutes later, thermal attack of the molten debris against the steel shell results in shell penetration and opening of a release pathway for fission products into the basement (i.e., torus room) of the reactor building. The combined leakage through the drywell head flange and the ruptured drywell shell results in a rapid depressurization of the containment to approximately 25 psig, and then a gradual long-term depressurization, through the opening in the drywell liner.[32] Before drywell shell melt-through occurs, hydrogen leaks through the drywell head flange and accumulates in the reactor building refueling bay.[33] Within a few minutes, a flammable mixture develops and is assumed to ignite when local hydrogen concentrations exceed 10 vol-%. The resulting increase in pressure within the building causes the blow-out panels in the side walls of the refueling bay to open, creating a release pathway to the environment. Small increases in internal pressure (0.25 psig) cause the blowout panels to open. Therefore, the panels in the sidewalls of the refueling bay offer a release pathway to the environment immediately after a hydrogen burn occurs within the building.

Several minutes after melt-through of the drywell liner, additional hydrogen is released from the drywell into the basement of the building (i.e., torus room) and is transported upward through open floor gratings into the ground level of the reactor building. Flammable mixtures quickly develop in several regions of the building, causing a sequence of several discrete combustion events. The pressure rise within the building causes several doorways to open, including the large equipment access doorway at grade level. Several other doorways also open within the building, including personnel access doorways into the building stairwells. The large opening at grade level, coupled with the open blow-out panels in the refueling bay at the top of the building, creates an efficient transport pathway to the environment for material released from containment. That is, a vertical column of airflow is created within the building whereby fresh air from outside the building enters through the open equipment doors at grade level, rises upward through the open equipment hatches at every intermediate floor within the building, and exits through the blow-out panels at the top of the building. As the next section will show, this chimney effect reduces the effectiveness of the reactor building as an area for fission product retention.

5.1.2 Radionuclide Release

Volatile fission product release from fuel begins at 9.1 hours, when a portion of the fuel gap inventory is released due to early fuel cladding failures. As fuel temperatures rise (see Figure 5-3), diffusion-driven release of fission products out of the fuel matrix rapidly increases the amount of volatile species released into the reactor coolant system. The cumulative release of several volatile species from the fuel is shown in Figure 5-10.

---

[32] Reduction in drywell internal pressure causes the drywell head flange leak pathway to reclose.

[33] The precise leak pathway includes intermediate transport through the drywell head flange to the drywell head enclosure. Leakage from the enclosure into the refueling bay occurs through gaps in the concrete shield blocks on the refueling bay floor. This complex leak pathway is explicitly represented in the MELCOR model.

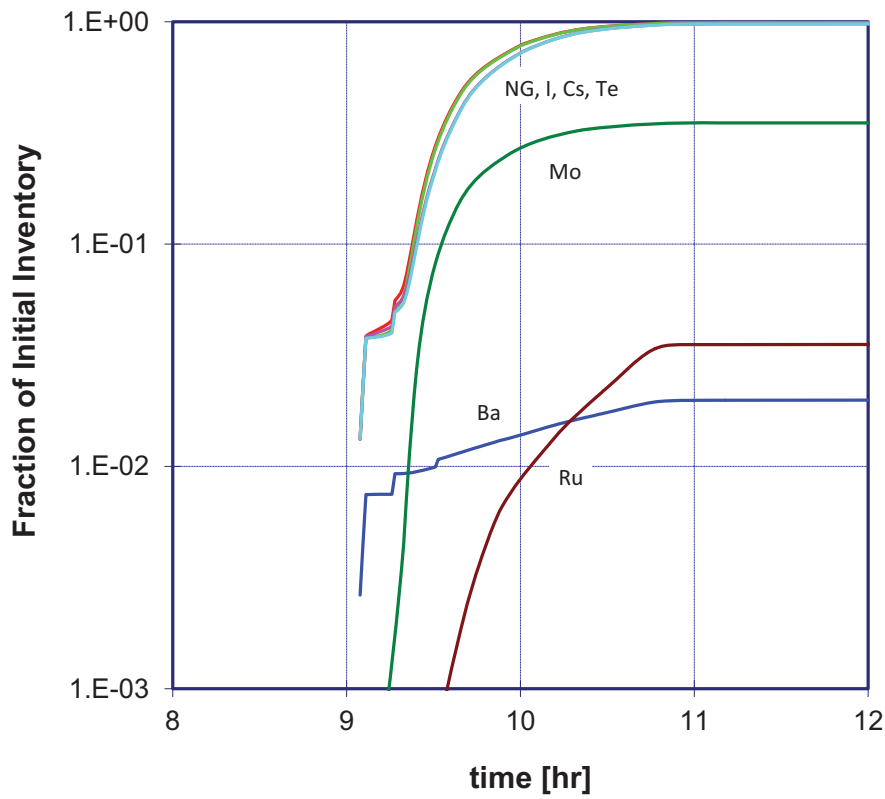

Figure 5-10 LTSBO In-vessel Fission Product Release from Fuel

The release of radionuclides that follows containment failure is shown in Figure 5-11 (see Appendix A for a detailed radionuclide core inventory). This release occurs in two steps because of sequential breaches in the containment boundary by two distinct failure modes. The first appearance of significant release to the environment begins at 19.9 hours, when leakage begins through the drywell head flange. The leak area associated with this failure mode is small and the leak pathway is open for a short time because within 5 minutes a larger leak[34] develops when molten debris flows across the drywell floor and penetrates the steel liner after lower head failure. The two phases of release are, therefore, indistinguishable in Figure 5-11, which appears to show a single large 'puff' release at approximately 20 hours.

The amount (fraction of initial core inventory) of several important radionuclide species released to the environment continues to increase for several hours after the puff release that accompanies containment failure. Two processes cause the protracted release that occurs over a 4 to 6 hour period after containment failure, which is highlighted in the expanded view of the release signature shown in Figure 5-11(b). First, molten corium-concrete interactions (MCCI) on the drywell floor drive the residual quantity of volatile fission products from fuel debris, and release

---

34 The maximum containment pressure that occurs prior to drywell liner melt-through is approximately 85 psig. Therefore, based on the head flange leakage evaluation described in Section 4.6, the maximum leak area through the flange is approximately 2 in^2 (0.001 m^2). In comparison, the assumed opening created by molten debris penetration of the drywell liner is 1 ft^2 (0.1 m^2).

a relatively small fraction of all nonvolatile species. Second, the combination of high drywell atmosphere temperatures generated as a byproduct of MCCI and heating of reactor vessel internal structures because of decay heating of deposited radionuclides results in a late revaporization release of volatile species from within the containment and RCS. The latter is described in greater detail below.

Figure 5-12 depicts the fraction of the initial iodine inventory that is captured in the suppression pool, deposited or airborne within the RPV and the drywell, and released to the environment as a function of time. Similar information is shown in Figure 5-13 for cesium, in Figure 5-14 for tellurium, and in Figure 5-15 for non-volatile cerium. Collectively, these figures provide useful information about the mobility of different radionuclide species and the temporal changes in their spatial distribution. For example, next to noble gases, iodine is the most volatile radionuclide group. In the SOARCA calculations, iodine is assumed to be transported in the form of cesium iodine (CsI), which vaporizes at relatively modest temperatures for a severe accident. As a result, CsI is released from fuel during the early phases of in-vessel core damage progression, and a significant fraction remains airborne because of the relatively high temperatures of structures within the reactor vessel. Airborne iodine is efficiently transported to the wetwell through the open SRV. In particular (see Figure 5-12), approximately 60 percent of the initial core inventory of iodine is discharged from the RPV to the suppression pool during the blowdown of the reactor vessel that occurs during the same time that volatile fission products are released from the fuel (see Figure 5-10). At approximately 10.5 hours, an additional 30% of the iodine inventory is purged from the RPV to the suppression pool by steam that is generated in the RPV lower plenum when a large quantity of core debris collapses into the pool of water in the lower head. During the succeeding 6 hours, the majority of CsI that remains deposited on reactor vessel internal structures after RPV blowdown evaporates from these surfaces as a result of decay heating, and is also carried into the suppression pool.

The release of iodine (CsI) and tellurium to the environment increases beginning after 23 hours after initially stabilizing at values below 1% of the initial core inventory (refer to Figure 5-11). The source of this delayed release is CsI and Te aerosol that was initially captured in water trapped in the RPV downcomer (i.e., below the top of the jet pumps.) As indicated in Figure 5-2, the rate at which this water evaporates reduces dramatically when core debris relocates from the core region to the lower plenum at approximately 10.5 hours (i.e., heat losses through the core shroud are reduced when debris falls into the lower plenum after lower core plate failure). Total dryout of the downcomer occurs at 23 hours, and is indicated in Figure 5-2 by a plateau in downcomer level at an elevation of approximately 122 in, which corresponds to the elevation of the floor or 'baffle plate' of the downcomer. When water is totally evaporated from a control volume, MELCOR deposits all radioactive aerosols captured in water on the heat structure representing the 'floor' of the control volume -- in this case, the heat structure representing the baffle plate. Subsequent heat up of this structure due to decay heating increases the structure temperature, and results in the evaporation of CsI and Te into the RPV (downcomer) atmosphere. At the time this occurs, the RPV lower head has failed allowing airborne fission products to be carried directly into the drywell, and the drywell liner has failed allowing airborne fission products in the drywell to be transported to the environment. Therefore, late revolatilization of iodine and tellurium from the downcomer results in a direct increase in the environmental release for these species.

(a)

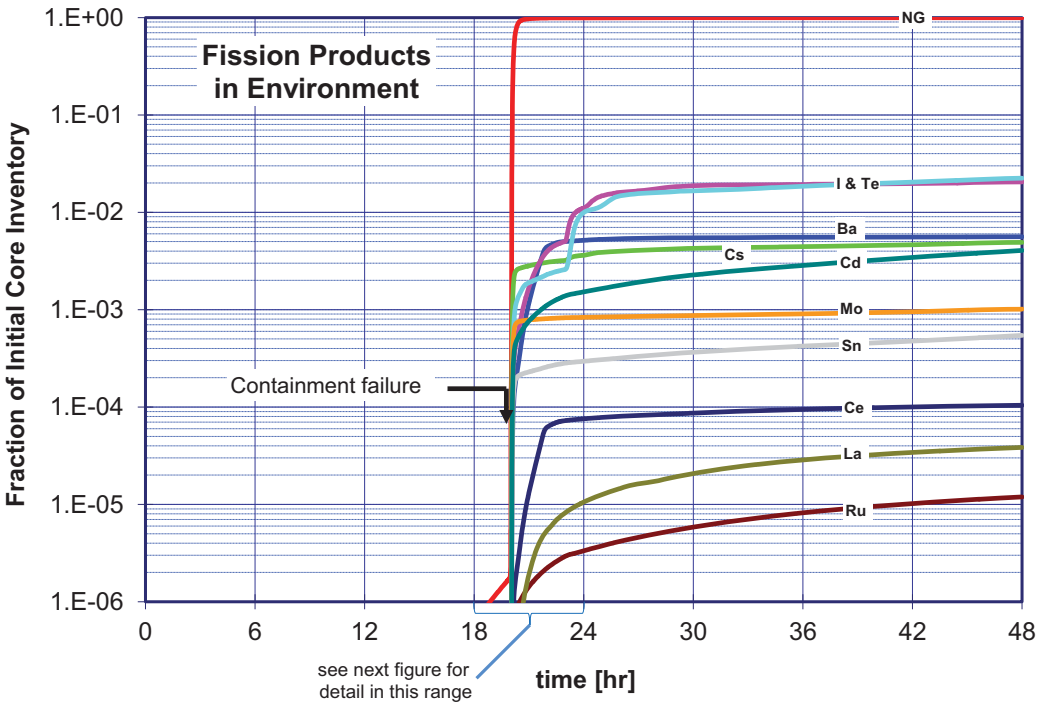

(b)

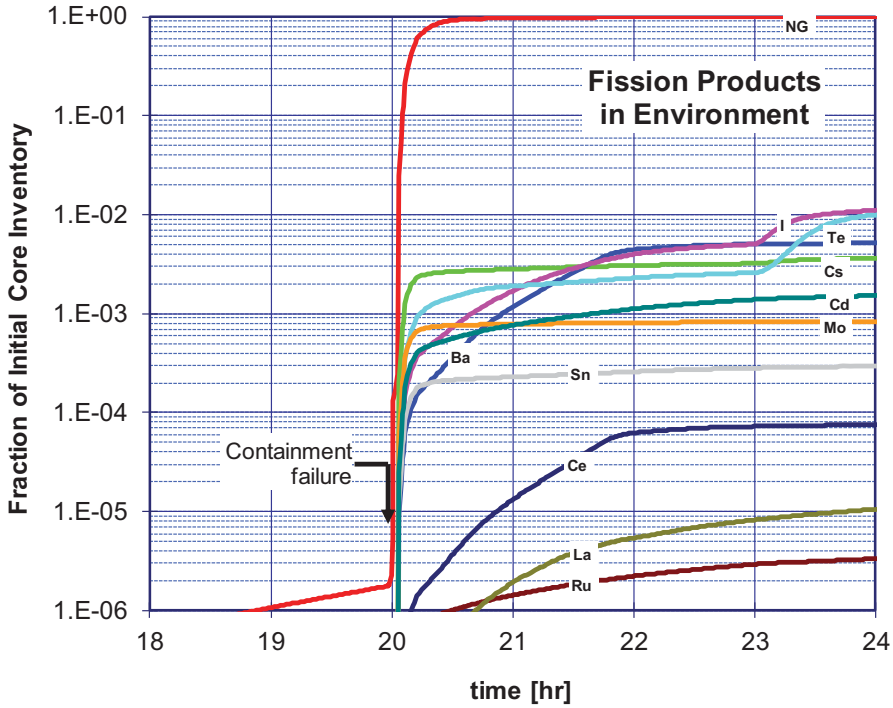

Figure 5-11 LTSBO Source Term to the Environment

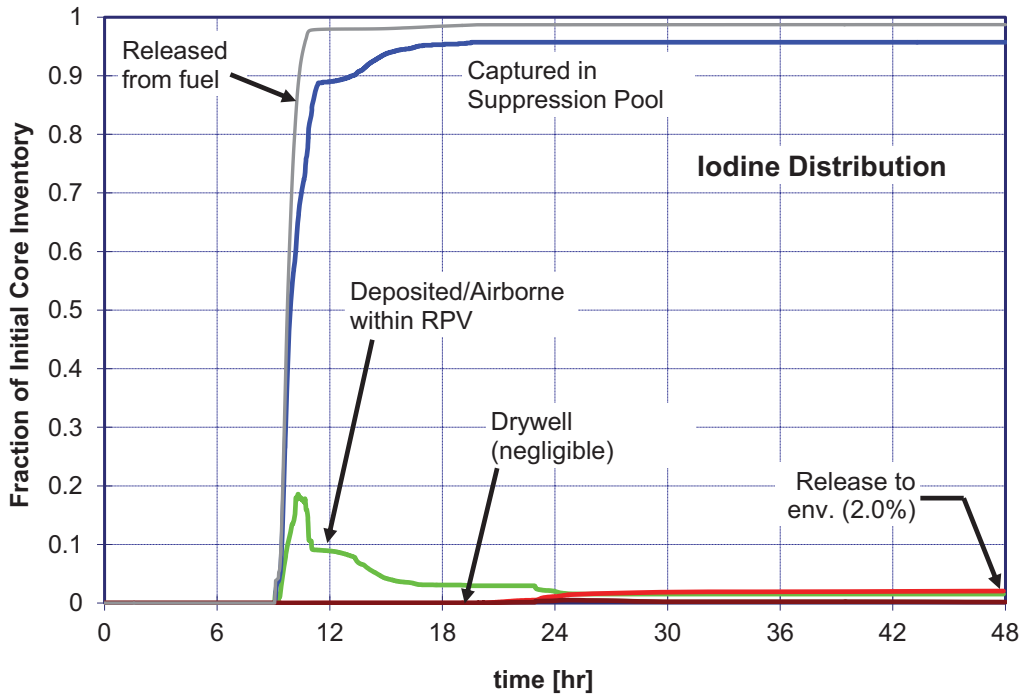

Figure 5-12 LTSBO iodine fission product distribution

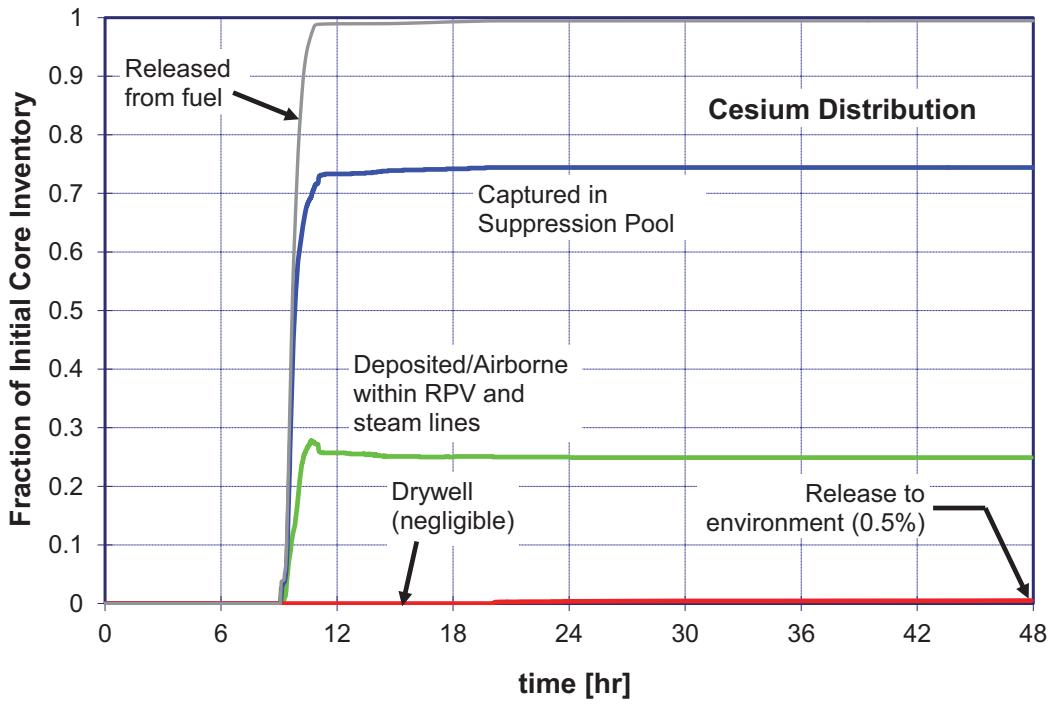

Figure 5-13 LTSBO cesium fission product distribution

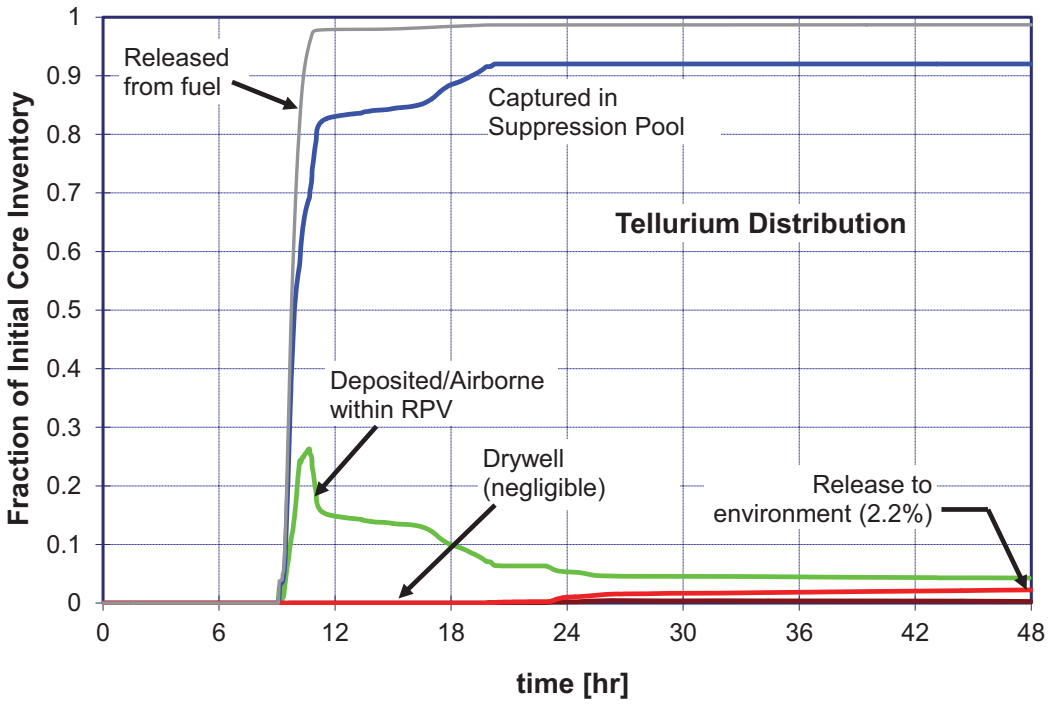

Figure 5-14 LTSBO tellurium fission product distribution

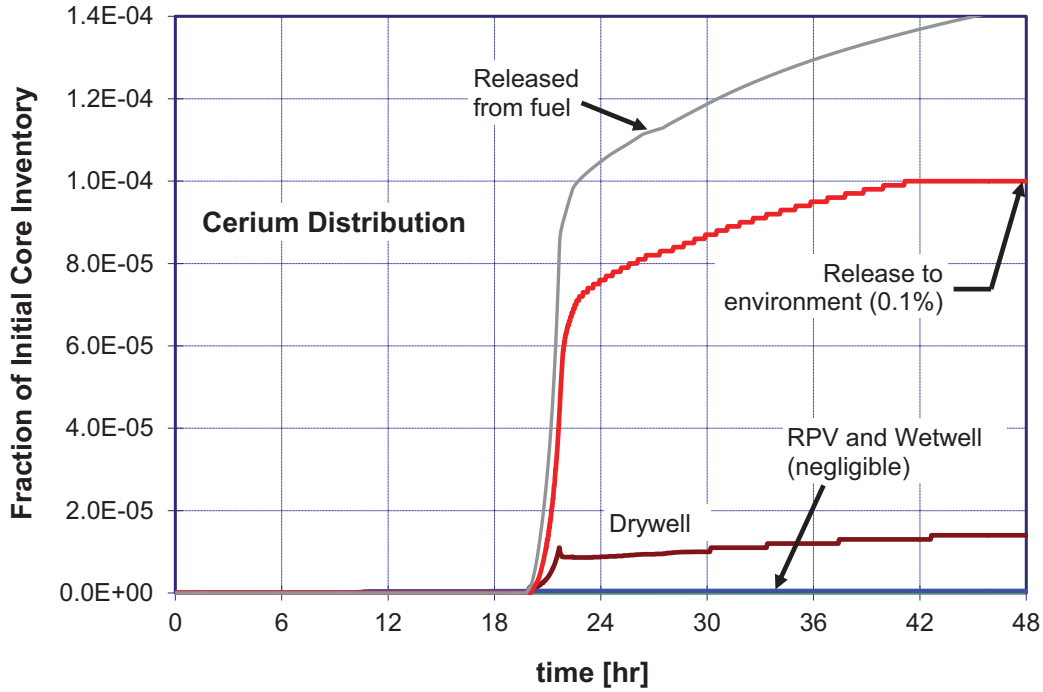

Figure 5-15 LTSBO cerium fission product distribution

The spatial distribution of cesium does not change with time in the same way the distribution changed for iodine. This is evident in Figure 5-13, and also in the relatively small changes in release to the environment relative to the initial puff release at containment failure (i.e., compare, for example, the release signatures for iodine and cesium in Figure 5-11). A slightly larger fraction of the cesium released from fuel deposits on the steam separators and dryers above the core in the RPV than is observed for iodine (i.e., 28% versus 18%). More importantly, however, a larger proportion of deposited cesium is retained on these structures as in-vessel damage progression proceeds over time.

These differences in iodine and cesium behavior can be attributed to differences in the physical properties of their dominant chemical forms. As mentioned earlier, iodine is transported as CsI. The cesium contribution to CsI represents only 6 percent of the total cesium inventory. The vast majority (approximately 90 percent)[35] of the cesium inventory is transported in the form of cesium molybdate (Cs_2MoO_4). Cesium molybdate is less volatile than the iodide and remains deposited on in-vessel structures at significantly higher temperatures. The in-vessel temperature history calculated for the LTSBO creates a thermal environment that promotes a greater evaporation of CsI relative to that of Cs_2MoO_4. Therefore, iodine is preferentially transported to the torus, but cesium remains deposited on in-vessel structures.

The suppressed mobility of cesium compared to iodine also affects the ultimate quantity transported to the environment in the first few hours after containment failure. A large fraction of iodine (CsI) initially captured on in-vessel structure surfaces evaporates and is released directly into the drywell atmosphere through the ruptured RPV lower head and to the environment through the failure in the drywell liner. Conversely, the vast majority of cesium molybdate deposited on in-vessel structures remains there throughout the late phases of accident progression.

The behavior of tellurium (Figure 5-14) is similar to that described above for iodine, and is not described in further detail here. Release of the heavy non-volatile species (e.g., cerium) differs substantially from the trends described above for any of the volatile species. As indicated in Figure 5-15, the release of the non-volatile refractory metals does not begin until after vessel breach, when MCCI occurs on the drywell floor. Release of cerium and other similar species (e.g., lanthanum (La) and ruthenium (Ru)) from fuel debris begins soon after vessel breach when MCCI is most aggressive. As indicated in Figure 5-16, the temperature of ex-vessel debris decreases significantly as it spreads across the drywell floor from its initial point of arrival in the reactor pedestal. This greatly reduces the rate at which the non-volatile species are released.

---

[35] The remaining fraction is cesium located in the fuel cladding gap.

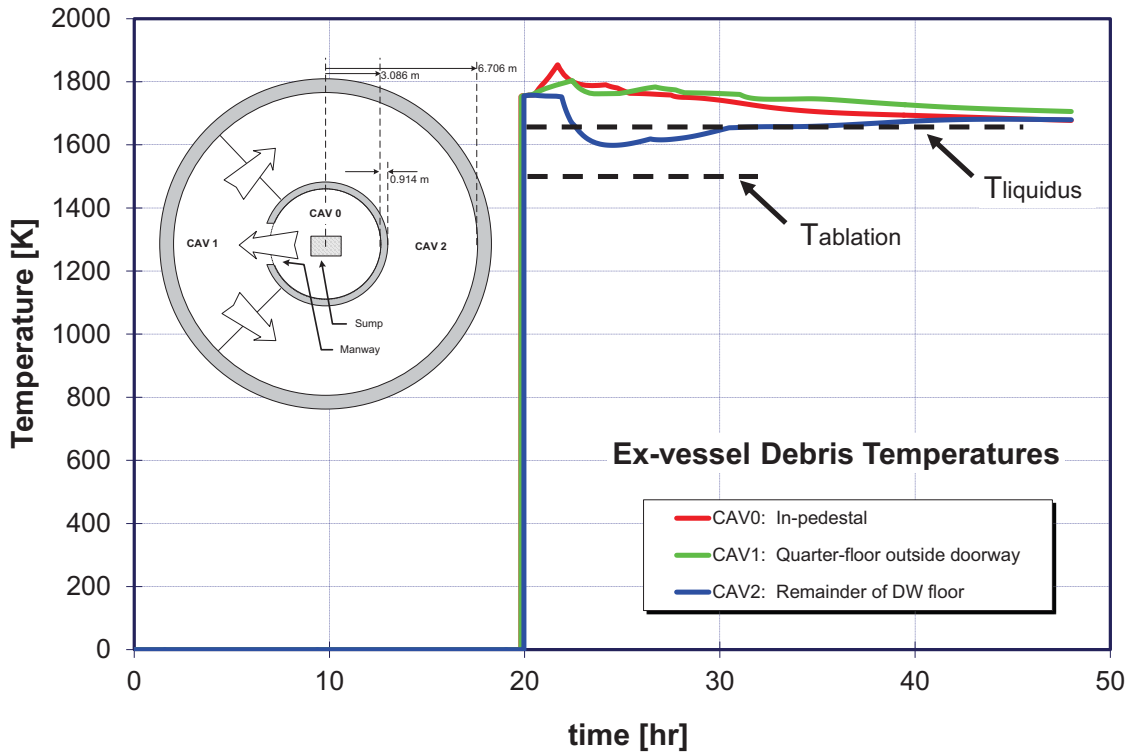

Figure 5-16 LTSBO ex-vessel debris temperatures

An earlier discussion of the physical response of the reactor building (Section 5.1.1) noted that hydrogen burns greatly reduce the effectiveness of building to retain fission products released after containment failure. The principal cause of low residence time in the building after containment failure is combustion of hydrogen released from containment, which generates an increase in internal pressure large enough to open blowout panels at the top of the reactor building and fail the large equipment access doorway at grade level as well as several doors within the building. Flow through these openings in the reactor building creates a pathway for air to enter the building through the open equipment access doorway, rise through the vertical equipment hatches through the multiple floors of the building, and out the open blowout panels. Relatively large flow rates along this pathway during the peak period of fission product release reduce the average residence time for aerosols in the building below values that permit gravitational setting to operate. Therefore, negligible attenuation of fission product aerosols released from the containment occurs before release to the environment.

Later in time when containment depressurization is complete and hydrogen release rates reduce to levels that no longer support combustion, a smaller but stable flow of air along the same flow path is sustained by buoyancy effects. The temperature of gases released from the drywell to the reactor building is between 700 and 1100 K.[36] This hot gas enters the reactor building at a low elevation[37] and rises through the same vertical flow path created by the original hydrogen

---

36 Refer to Section 5.7.2 for details on the calculation of drywell atmosphere temperature.

37 The opening in the drywell shell would likely create a flow path into the basement of the reactor building where the torus vent pipes are located.

combustion events. The thermal plume created by this buoyant gas rises at a velocity of 2 to 3 m/s, which is large enough to sweep the vast majority of airborne aerosols to the environment with little opportunity for deposition. This low residence time created by this persistent air flow is compounded by the fact that the aerosol particles released late in time, due to revaporization from RCS surfaces, are very small. The calculated mass median diameter of airborne aerosols transported from the drywell through the reactor building after containment depressurization is less approximately 0.5 micron. These two factors combine to produce a global decontamination factor (DF) for the reactor building barely over 1.0. Figure 5-17 shows the calculated reactor building DF for iodine and cesium.

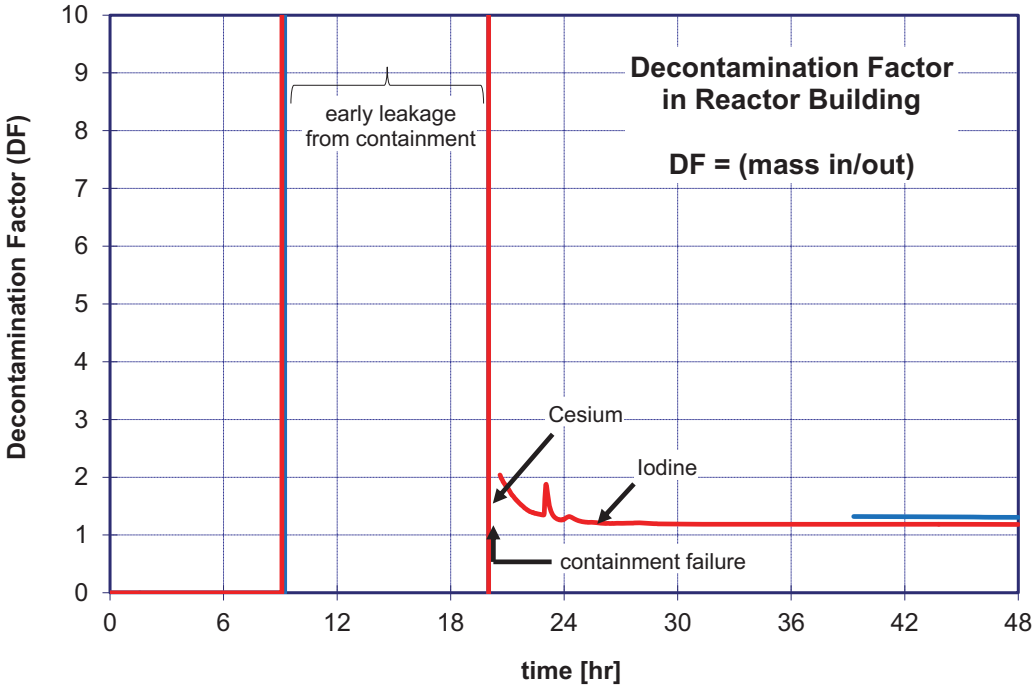

Figure 5-17 Reactor Building DF for unmitigated LTSBO

5.2 Long-Term Station Blackout with Mitigation

Table 5-2 outlines the key events for LTSBO with mitigative actions (discussed in Section 3.1.3).

Table 5-2 Timing of Key Events for Mitigated LTSBO

Event	Mitigated LTSBO with 4 hr DC power (Time in hours unless noted otherwise)
Station blackout loss of all onsite and offsite AC power.	0.0
Automatic reactor scram and containment isolation	0.0+
Low-level 2 and RCIC actuation signal	10 minutes
Operators manually open SRV to depressurize the reactor vessel	1.0
RPV pressure first drops below LPI setpoint (400 psig)	1.2
Operators take manual control of RCIC; flow throttled to maintain level within range (+5 to +35 in)	2.0
Portable electric generator positioned, started, and connected to remote panel	1.0 to 4.0
Station batteries depleted	4.0
Operators position, align, and start portable pump to replace RCIC as injection source, if needed	4.0 to 10.0
Portable electric power and gas bottles staged near isolation valves for containment hard pipe vent line	10.0
Hard pipe containment vent line opened/closed at containment pressures of 45/25 psig	22.4 / 23.3 29.6 / 30.5 37.1 / 38.0 44.4 / 46.2
Calculation terminated	48

5.2.1 Thermal Hydraulic Response

The thermal hydraulic response during the first four hours of the mitigated case matches the response of the unmitigated case. RCIC automatically actuates to restore reactor water level. Operators manually open an SRV to reduce pressure in the RPV (see Figure 5-18), then assume manual control of RCIC flow to maintain water level within a specified range. Beyond four hours, however, the sequence of events for the mitigated case differs from the unmitigated case.

Before DC power from the station batteries expires at 4 hours, a portable generator is engaged to maintain a long-term supply of control power. This permits the open SRV to remain open, maintaining reduced pressure in the RPV according to Special Event Procedure SE-11. Using the RPV water level information, which is available by use of a portable generator, operators manually control (locally) RCIC to maintain a stable water level in the RPV, as shown in Figure 5-19, and maintain fuel cooling as indicated in the plot of peak clad temperature shown in Figure 5-20.

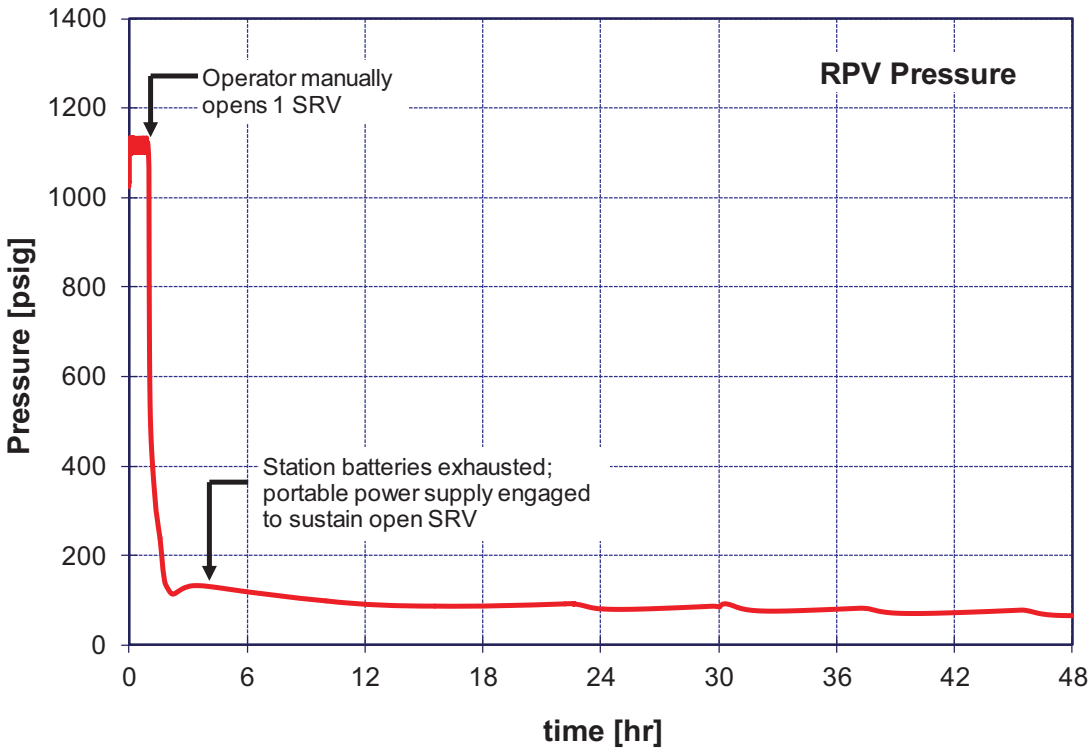

Figure 5-18 Mitigated LTSBO vessel pressure

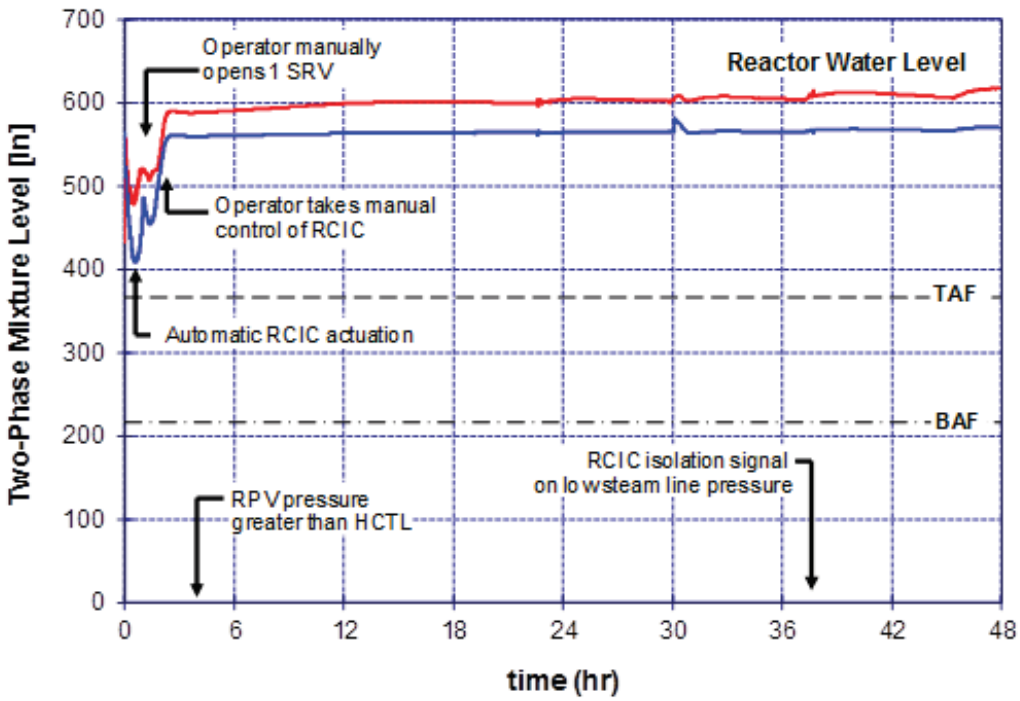

Figure 5-19 Mitigated LTSBO coolant level

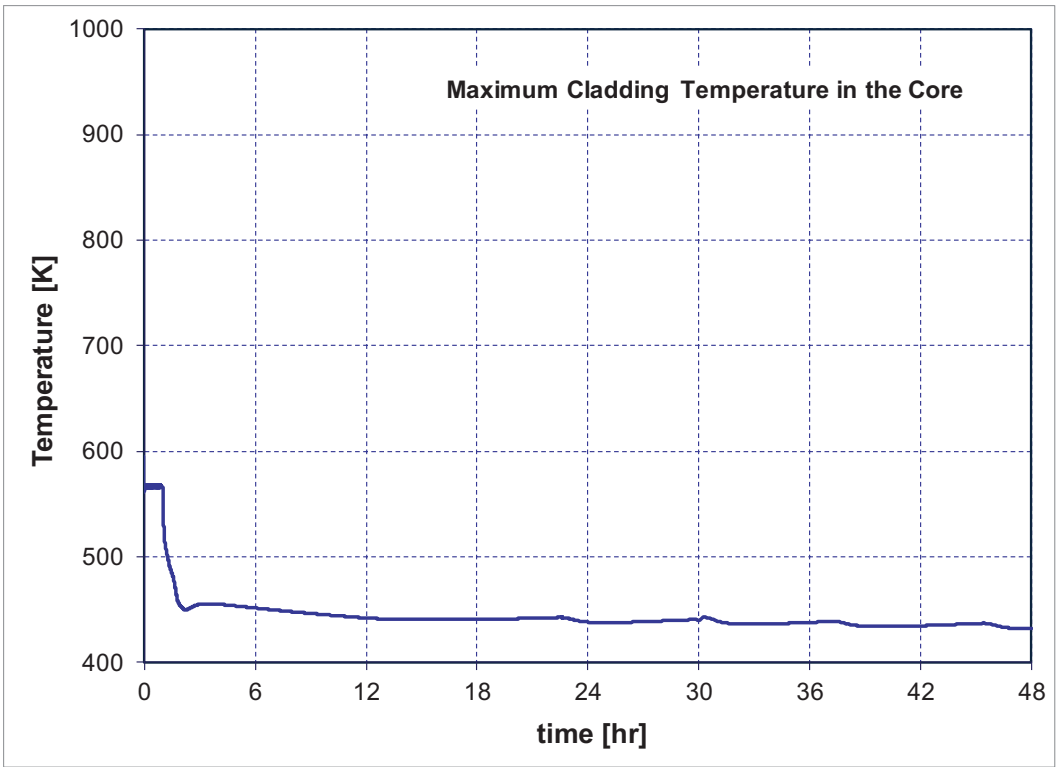

Figure 5-20 Mitigated LTSBO core temperature

The mitigation measures do not restore function to systems that provide containment heat removal. Therefore, energy discharged from the RPV through the open SRV gradually increases the temperature of water in the suppression pool. As shown in Figure 5-21, the temperature of water in the torus reaches saturation conditions in approximately 16 hours, which increases the rate at which containment pressure (see Figure 5-22) rises. Prior to this point in time, however, suppression pool temperature and pressure increase to values that would either trigger isolation signals for the RCIC system or invoke instructions for further RPV depressurization. For example, as indicated in Figure 40, RPV pressure exceeds the Heat Capacity Temperature Limit (HCTL) within approximately 5 hours, and would reduce below RCIC isolation setpoint for low steam line pressure in approximately 38 hours. Operators are instructed to take actions to ensure continued operation of RCIC under station blackout conditions, such as defeating isolation signals if they occur. The time at which one example signal is calculated to occur is indicated in Figure 5-19. Heating of the suppression pool reduces the HCTL, which would normally demand further reductions in RPV pressure. However, RPV pressure must be maintained above the minimum operating conditions for RCIC to ensure a sufficient steam supply to the RCIC turbine. Therefore, it is assumed no actions are taken to further reduce RPV pressure. Approximately 10 hours into the scenario, pool temperatures increase above 378 K (220 °F). Above this temperature, RCIC isolation on loss of Net Positive Suction Head or inadequate cooling of RCIC pump bearings would be possible if suction were taken from the torus. However, the mitigation measures assumed in this calculation maintain RCIC suction from the CST, thereby, eliminating challenges to RCIC operation due to high suppression pool temperature.

The timeline for implementing the mitigation measures (see Section 3.1.4.2) suggests portable electric power sources and gas bottles needed to open isolation valves on the 16-in hard pipe vent line would be staged for use as early as 10 hours after the initiating event. Therefore, the hard pipe vent is assumed to open at approximately 20 hrs, when containment pressure reaches 45 psig, and is closed at 23 hours when containment pressure is reduced to approximately 25 psig. Several open/close cycles of the containment vent isolation valves are necessary with a period of approximately 8 hours to manage containment pressure within this range.

The principal basis for the containment venting criteria is based in part from comments received from the licensee during a verbal walk-through of LTSBO mitigation, which was part of a site visit in 2007. Based on these comments and others received from the Peer Review Panel, the venting criterion assumes the hard-pipe vent path will be opened at 45 psig and reclosed at 25 psig (Figure 5-22). These values were selected based on a review of plant-specific procedures for containment pressure control, but also taking into consideration isolation setpoints for RCIC, which are sensitive to containment thermodynamic conditions. Most important in this regard is the setpoint for high turbine exhaust pressure.

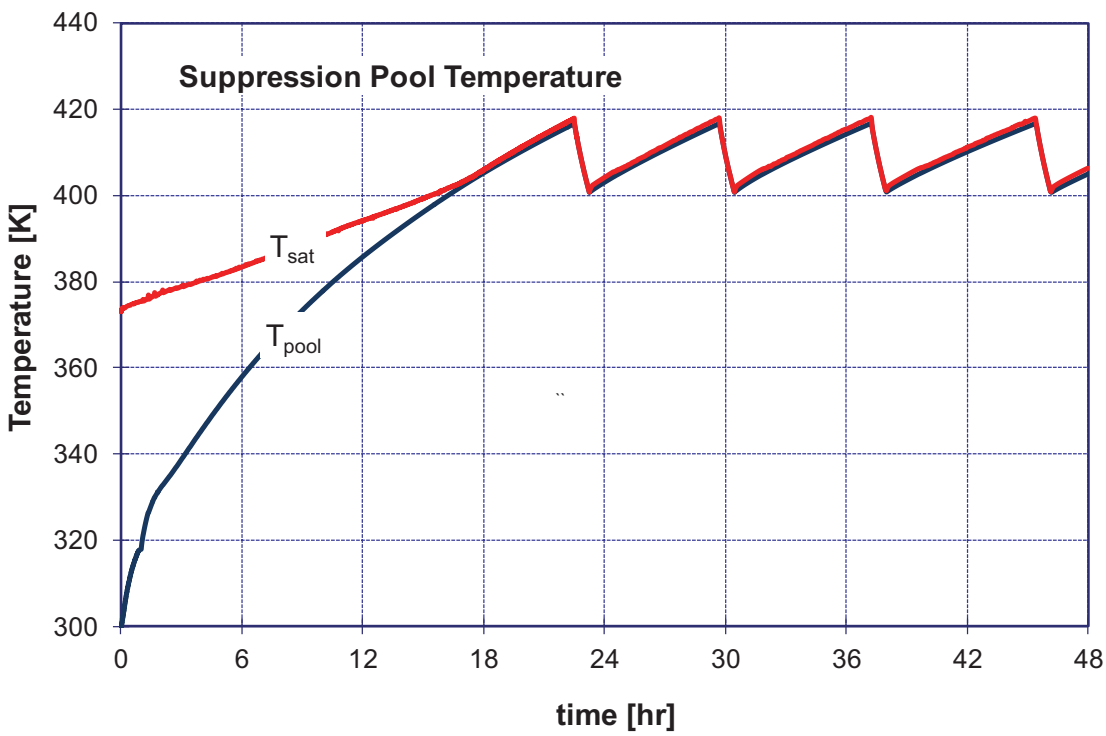

Figure 5-21 Mitigated LTSBO Suppression Pool Water Temperature

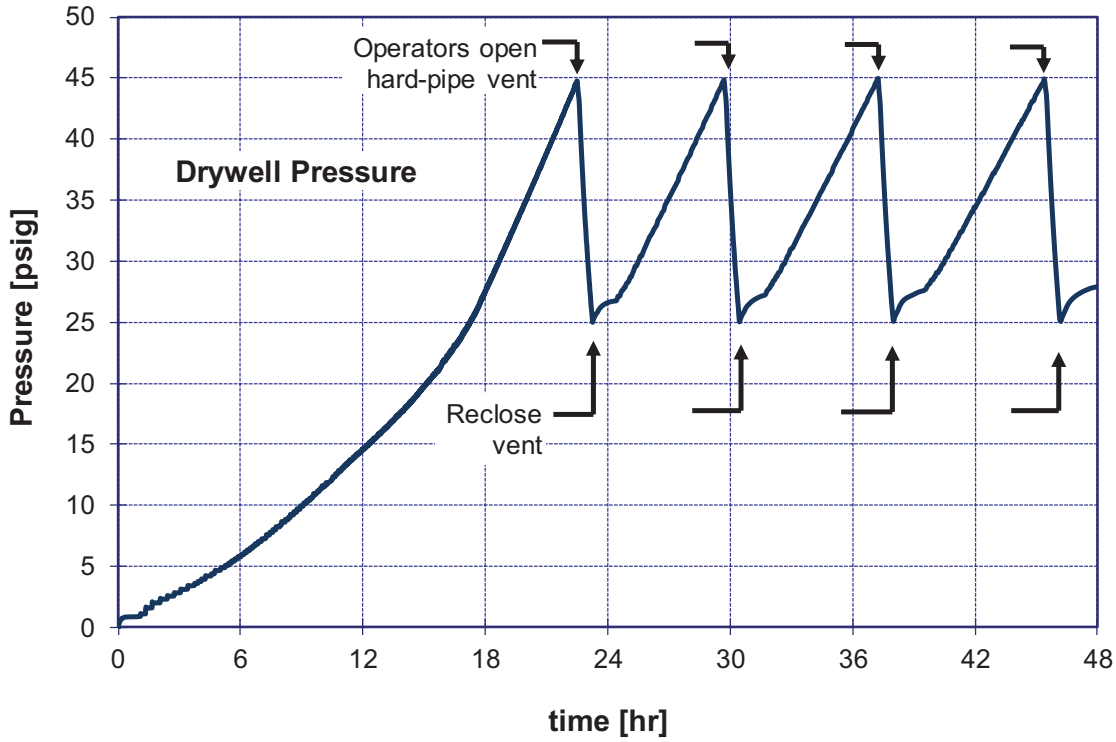

Figure 5-22 Mitigated LTSBO containment pressure

The Peak Containment Pressure Limit (PCPL) mentioned in containment pressure control procedures is 60 psig. However, a high turbine exhaust pressure isolation signal for RCIC would be received at a pressure of 50 psig. Since RCIC is the only operating coolant injection system available in this scenario, it was assumed operators would open the containment vent path at 45 psig, thereby averting RCIC isolation. Long term containment pressure control would be managed by periodically opening and reclosing the vent line. The effects of vent line operation are clearly indicated in the pressure response shown in Figure 5-22.

The total quantity of water transferred from the CST to the RPV by continuous (throttled) operation of RCIC exceeds the nominal CST inventory in approximately 15 hours. Makeup water provided by the portable pump maintains the CST inventory for an indefinite period of time. The continuous supply of water from outside the containment pressure boundary ensures stable control of core cooling, but it also results in an accumulation of water in the torus. Steam evaporated from the RPV is discharged to the torus through the open SRV, where it is condensed. As indicated in Figure 5-23, this results in a slow increase in the suppression pool water level the time containment venting begins. Depressurization of the containment due to venting causes the torus water level to swell by approximately 1.5 ft. The torus level then collapses down to a value below the pre-vent level when the vent line recloses. This general behavior is repeated during subsequent periods of containment venting, resulting in a fluctuating water level that oscillates between approximately 18.4 and 20.5 ft. Although this value is well above target values for the torus water level (i.e., 14.5 to 15.5 ft), the peak value lies below the elevation at which the SRV solenoids would be flooded (~21 ft), thereby preventing any interference with manual SRV control.

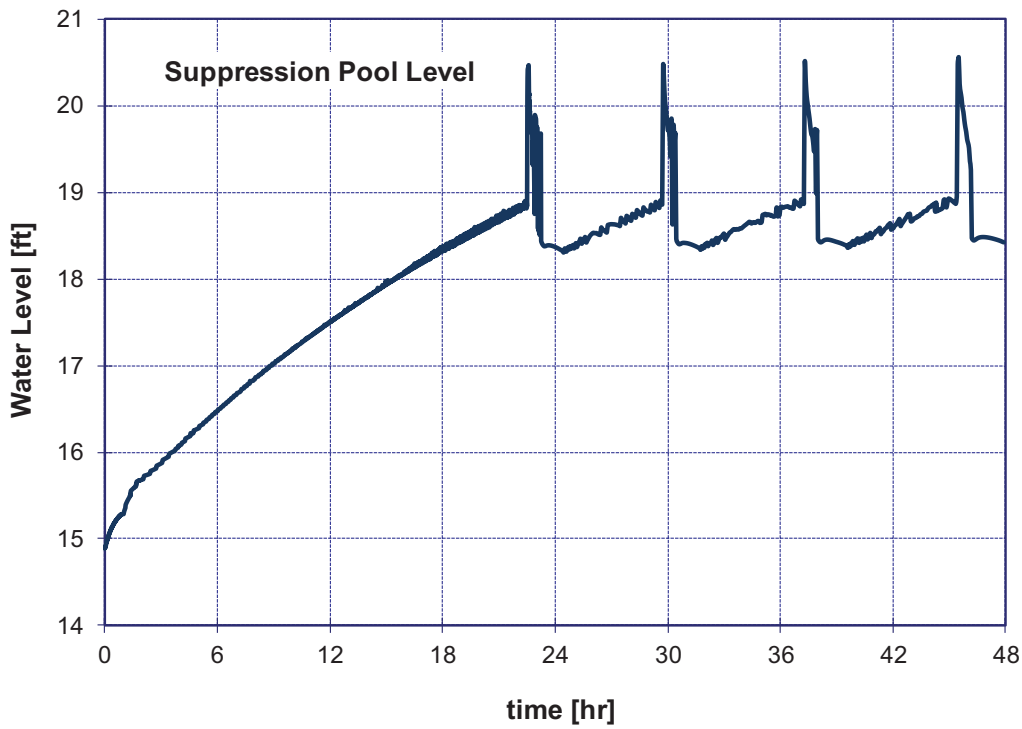

Figure 5-23 Mitigated LTSBO torus water level

5.2.2 Radionuclide Release

No plots are presented for the iodine fission product distribution history, cesium fission product distribution history, barium fission product distribution history, cerium fission product distribution history, or environmental release history of all fission products resulting from mitigated LTSBO because the mitigated case does not result in core damage.

5.3 Short-Term Station Blackout with RCIC Blackstart

The general response of plant equipment and operating personnel to the STSBO resembles the unmitigated LTSBO scenario. The reader is referred to Section 5.1 for a description of the actions that plant personnel would take in response to this type of event. However, a key difference is the assumed immediate failure of DC power, which significantly reduces the time available for intervention and accelerates the time line of damage progression. Successful manual actions to blackstart RCIC compensates for effects of the additional loss of DC power for a period of time. That is, the delayed (manual) actuation of coolant injection restores RPV water level, but RPV water level control via RCIC throttling is assumed not to be achieved. Therefore, although many similarities are observed in plant response between this scenario and the LTSBO discussed earlier, some important differences arise as well. The calculated timing of key events that follow is listed in Table 5-3.

5.3.1 Thermal Hydraulic Response

The initiating event causes a prompt failure of all AC and DC power supplies to plant equipment and instrumentation. Reactor control blades, MSIVs, and containment isolation valves would all move to their fail-safe positions (inserted and closed). Isolation of the RCS causes reactor

pressure to rise to the set point of the SRVs, which open and direct coolant to the pressure suppression pool. As shown in Figure 5-24, reactor pressure is maintained at approximately 1,100 psig, as the SRV with the lowest set point cycles open and closed for nearly 2.5 hours.[38] Actions taken by plant operations personnel to manually reduce reactor pressure and prevent frequent cycling of the SRVs are assumed to not be successful.

Actions by plant personnel to blackstart the RCIC pump take one hour to accomplish, at which time coolant flow into the reactor vessel begins. As shown in Figure 5-25, the coolant inventory lost to evaporation during the first hour of the transient is quickly replenished and reactor water level is restored. The minimum reactor water level prior to RCIC actuation is approximately midway between the top and bottom of active fuel. The brief period of core uncovery allows fuel cladding temperatures to increase above 1000 K (see Figure 5-26) and a small portion of the cladding near the top of the core begins to oxidize. Restoration of coolant injection quenches the overheated fuel before clad failure occurs and temperatures throughout the core are quickly restored to equilibrium with reactor coolant.

---

[38] A second SRV periodically opens during the first 45 minutes of the transient, when decay heat levels remain high. However, after this point in time, only one valve is cycling.

Table 5-3 Timing of Key Events for the short term station blackout with successful RCIC blackstart

Event	Time (hours, unless otherwise noted)
Station blackout – loss of all onsite and offsite AC power	0.0
Low-level 2 and RCIC actuation signal (no RCIC response)	10 min
Downcomer water level reaches TAF	30 min
Hydrogen production begins	55 min
RCIC started manually and begins injection at full flow	1.0
Fuel cladding quenched and oxidation terminated (<2% oxidation)	1.2
RPV water temperature subcooled; depressurization begins	2.4
RPV pressure first drops below LPI set point (400 psig)	2.9
RPV water level above main steam line nozzles – RCIC stops due to steam turbine flooding	3.4
SRV sticks open due to excessive number of cycles	4.8
Downcomer water level decreases permanently below TAF	5.7
Hydrogen production begins again	6.6
First fuel-cladding gap release	6.8
First channel box failure	6.9
First core support plate localized failure in supporting debris	7.2
Reactor vessel water level reaches bottom of lower core plate	7.2
First core cell collapse due to time at temperature	7.4
Beginning of large-scale debris relocation into lower plenum	7.7
Lower head dries out	10.9
Ring 5 CRGT Column Collapse [failed at axial level 2]	13.2
Ring 1 CRGT Column Collapse [failed at axial level 2]	14.4
Ring 3 CRGT Column Collapse [failed at axial level 2]	14.6
Ring 4 CRGT Column Collapse [failed at axial level 2]	15.2
Ring 2 CRGT Column Collapse [failed at axial level 2]	15.6
Lower head failure	16.7
Drywell liner melt-through	16.9
Refueling bay to environment blowout panels open	16.9
Hydrogen burns initiated in lower reactor building	16.9
Doors to stairwell open due to overpressure	16.9
Door to environment through railroad access opens due to overpressure	16.9
Time Iodine release to environment exceeds 1%	23.6
Calculation terminated	48.0

Introduction of a large quantity of cold water to the RPV causes the average RPV water temperature to decrease below saturation conditions at approximately 2.4 hours. This reduces steam generation below levels necessary to sustain RPV pressure at the SRV set point. Valve cycling ceases at this time, and RPV pressure decreases below 400 psig within an hour. Steam supply to the RCIC turbine is assumed to be sufficient to permit the pump to continue operating at full capacity until 3.4 hours, when the RPV water level increases above the elevation of the main steam lines nozzles and water pours into the main steam lines. Flooding of the main steam line chokes the steam supply to the RCIC turbine, and pump operation ceases at 3.4 hours.

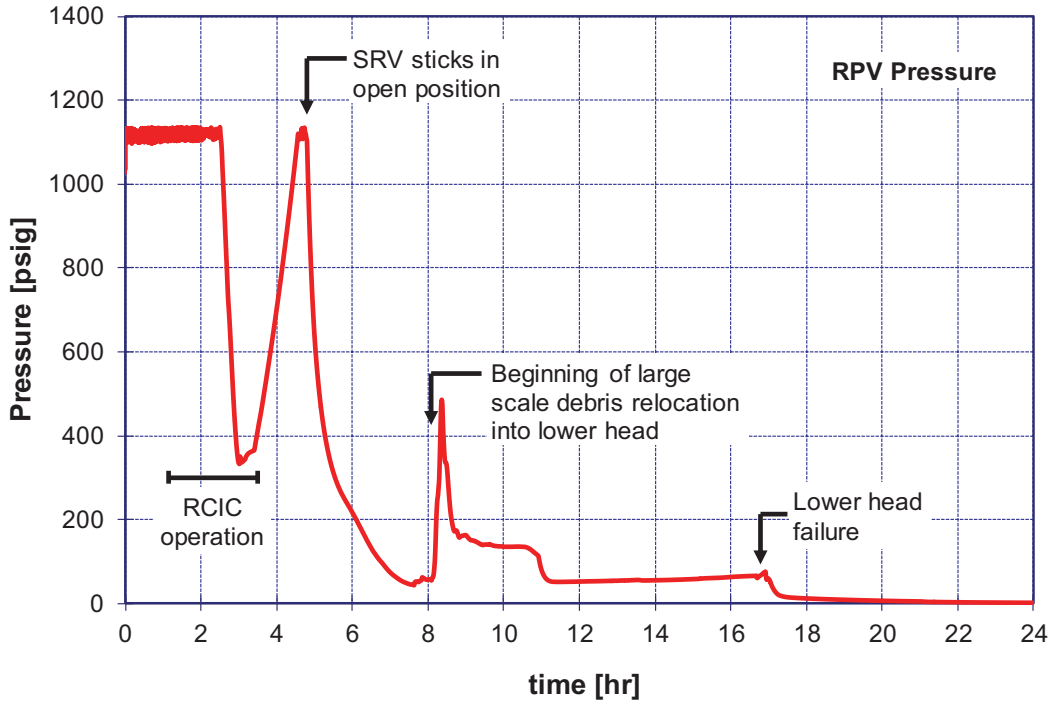

Figure 5-24 Reactor pressure for short term station blackout with RCIC blackstart

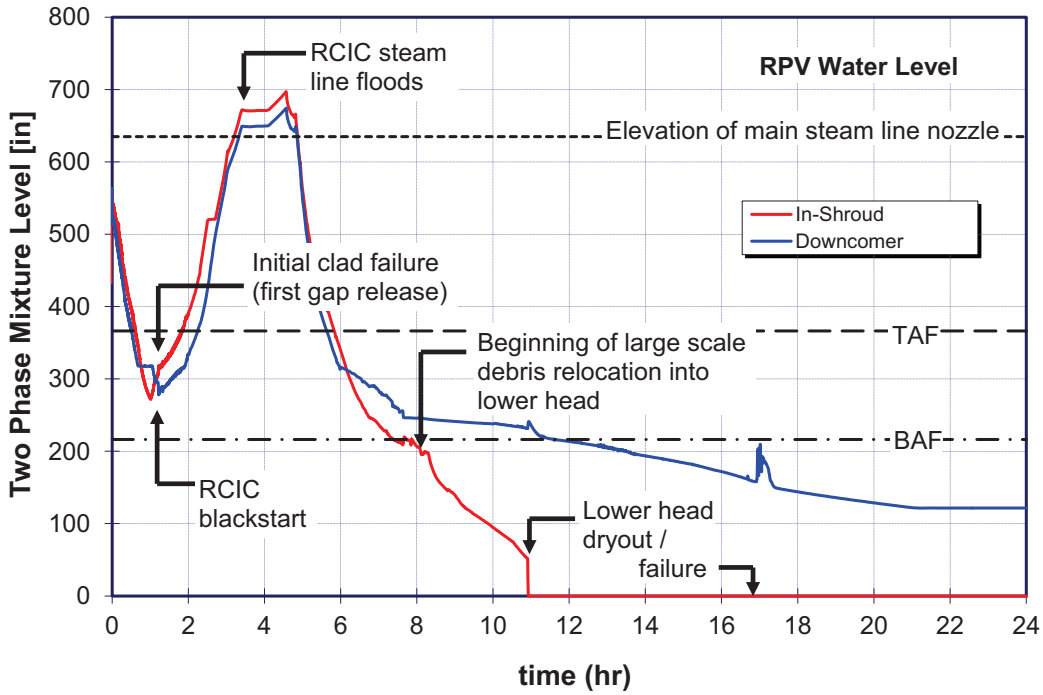

Figure 5-25 Reactor vessel water level for STSBO with RCIC blackstart

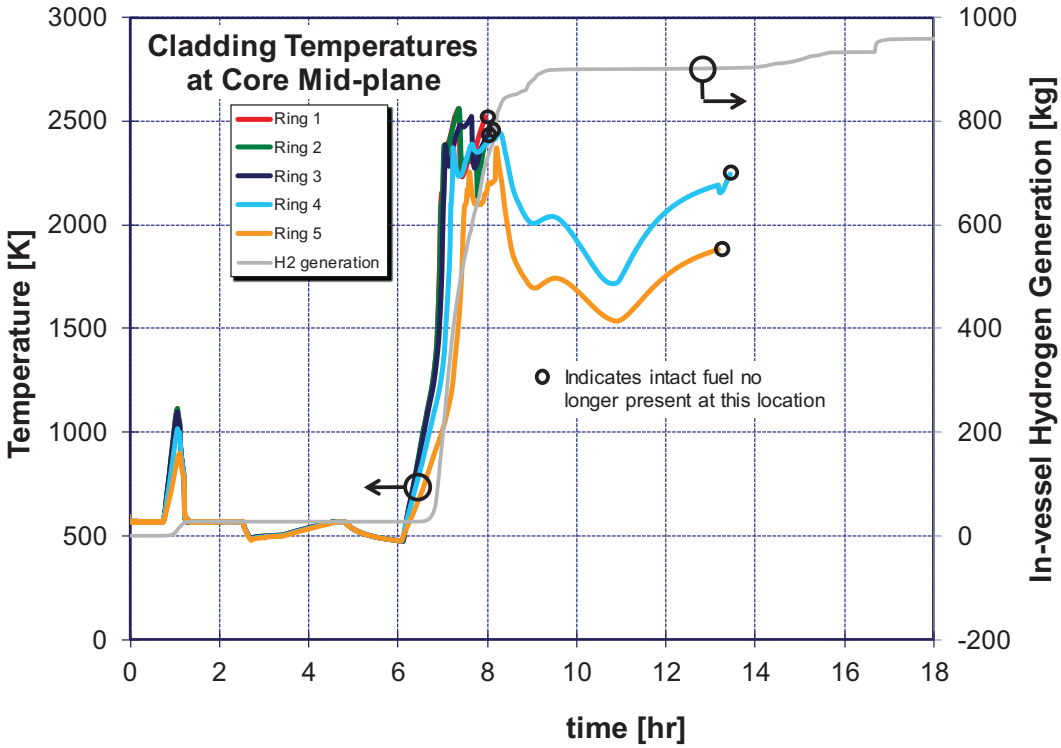

Figure 5-26 Fuel cladding temperatures at core mid-plane and in-vessel hydrogen generation for STSBO with RCIC blackstart

Termination of steam flow to the RCIC turbine, combined with the loss of (cold) coolant injection to the RPV, results in a steady increase in RPV pressure. Figure 5-24 shows RPV pressure returning to the SRV setpoint approximately one hour after the main steam line floods and RCIC operation ceases. Afterward, the lead SRV begins to cycle again. However, within 15 minutes, the cycling SRV sticks in the open position. This occurs due to stochastic failure, when the valve experienced a total of 270 cycles, as described in Section 4.4.2.1. RPV pressure decreases again as a result of the open SRV.

The permanent loss of coolant makeup following termination of RCIC operation causes the RPV water level to decrease below the top of active fuel at approximately 5.7 hours. Clad oxidation is renewed and, as shown in Figure 5-26, fuel temperatures begin to rise rapidly at approximately 7 hours when clad temperature increase above 1500 K. Molten core debris forms near the top of the core and relocates downward in a configuration similar to images shown in Figure 5-4 and Figure 5-7 for the LTSBO scenario. Molten and particulate debris accumulates in the lower plenum and are initially quenched by the large body of residual water below the lower core plate. This water is entirely evaporated by 11 hours into the STSBO sequence and debris temperatures begin to rise (see Figure 5-27). Heat transferred from high temperature core debris causes the lower head structure to heat up as illustrated in Figure 5-28.

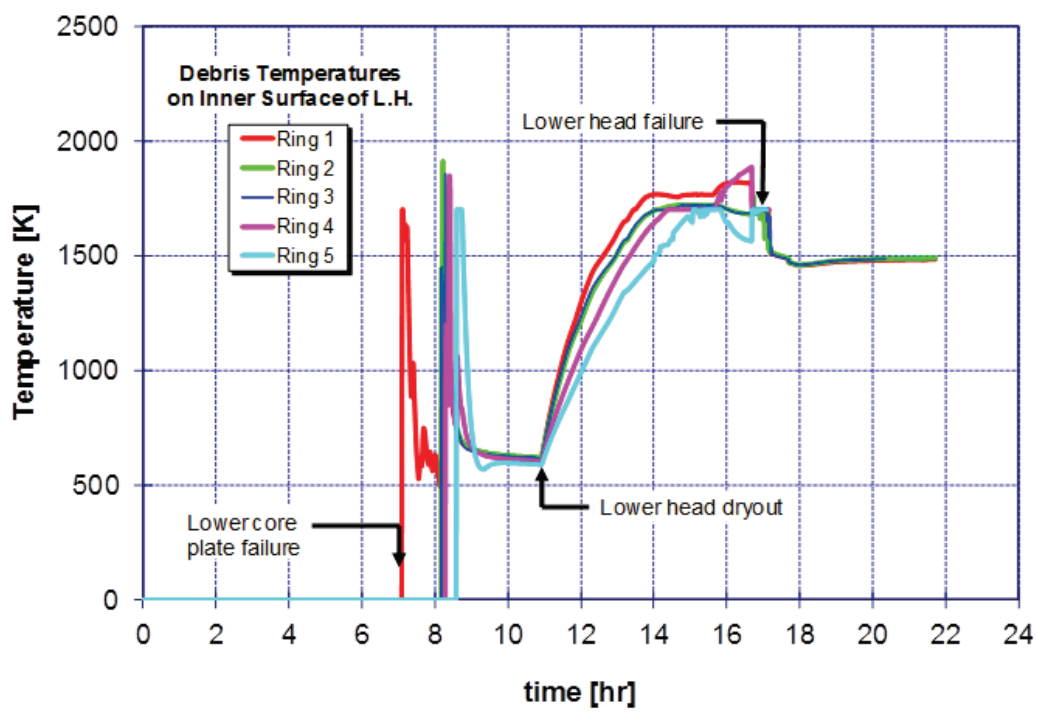

Figure 5-27 Temperatures of core debris along inner surface of lower head for STSBO with RCIC blackstart

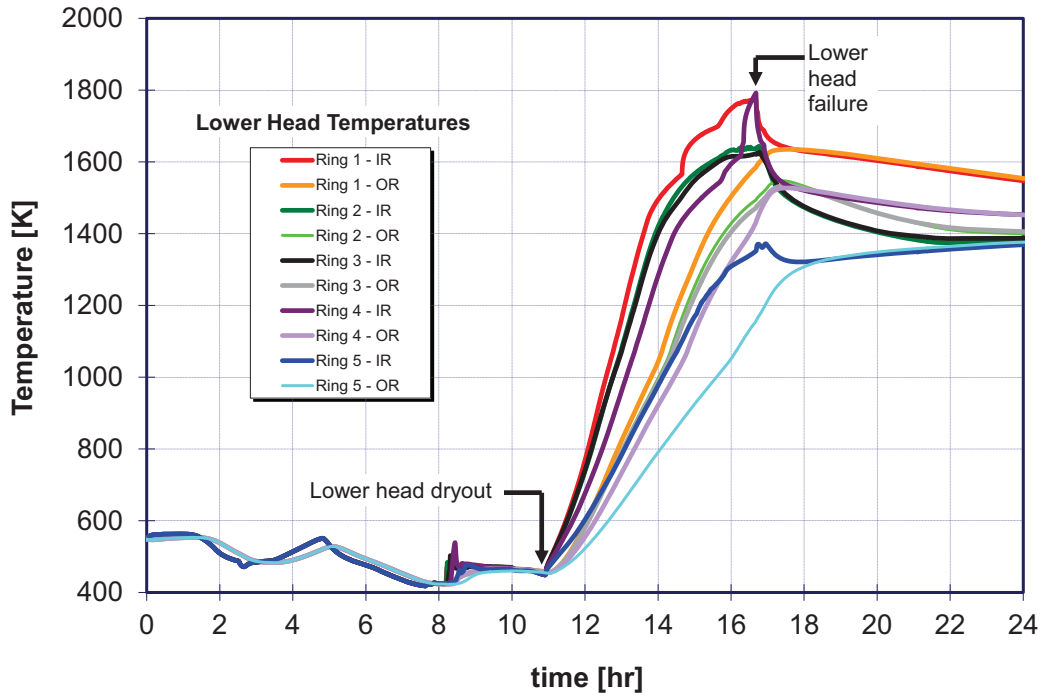

Figure 5-28 Inner and outer surface temperatures of lower head for STSBO with RCIC blackstart

Failure of the lower head (at 16.7 hours) results in the rapid ejection of over 300 metric tons of core debris onto the floor of the reactor pedestal in the drywell. The composition of this debris at the time of head failure is a mixture of molten stainless steel (about one-third by mass), unoxidized zirconium (~12%), and particulate debris containing uranium dioxide and metallic oxides (the remainder).

Before the reactor vessel lower head fails, thermodynamic conditions in the containment are governed by the release of hydrogen through the open SRV to the torus. The large quantity of hydrogen (i.e., over 960 kg within 10 hours), combined with the small free volume of the containment, results in a significant increase in pressure. The containment pressure history is shown in Figure 5-29. Immediately before lower head failure, containment pressure is approximately 53 psig, which is slightly lower than the corresponding base pressure in the LTSBO scenario. The energy accompanying the discharge of molten core debris after lower head failure causes this pressure to increase to 75 psig before containment failure occurs due to thermal failure of the drywell shell as discussed below.

In contrast to the LTSBO (refer to Section 5.1.1), containment pressure immediately following reactor vessel failure is below the threshold for induced leakage through the drywell head flange (80 psig). Therefore, leakage from containment does not occur by this mechanism. This is due primarily to the slightly lower base pressure (i.e., prior to vessel breach) in the short-term scenario, which results from the shorter period of reactor steaming to the suppression pool (i.e., before to the onset of core damage).

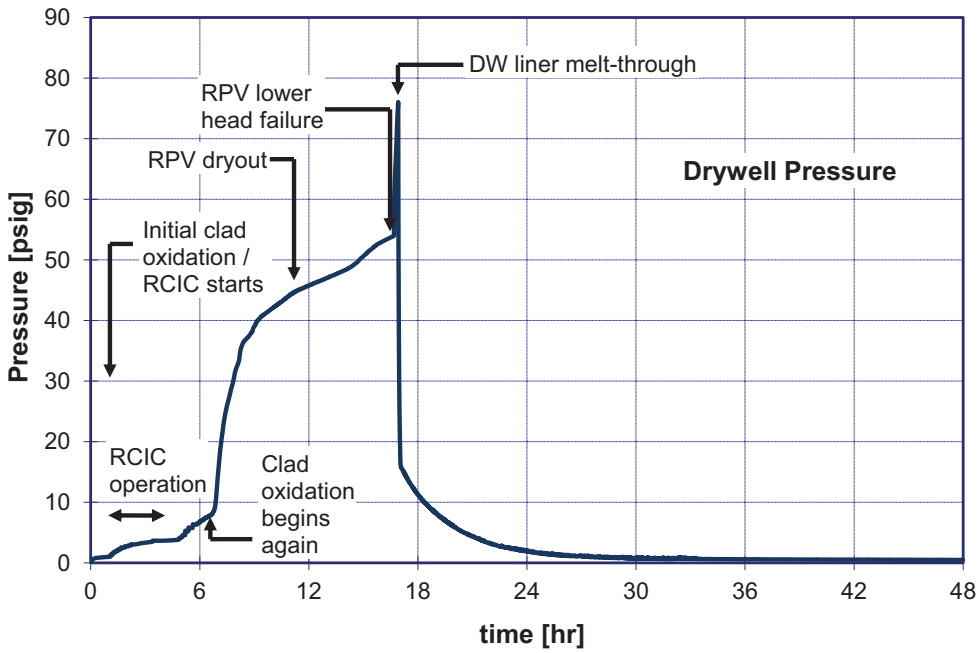

Figure 5-29 Containment pressure history for STSBO with RCIC blackstart

Containment conditions change dramatically, when debris is released onto the reactor pedestal floor following lower head failure. The absence of water on the drywell floor allows debris to flow laterally out of the cavity through the personnel access doorway and spread out across the main drywell floor. Lateral movement and spreading of debris across the drywell floor allow debris to reach the steel shell at the outer perimeter of the drywell within 10 minutes.
Five minutes later, thermal attack of the molten debris against the steel shell results in shell penetration and opening of a release pathway for fission products into the basement (i.e., torus room) of the reactor building. This results in a rapid depressurization of the containment to atmospheric conditions in a short time (less than 1 hour).

Immediately following drywell shell melt-through, hydrogen is released from the drywell into the basement of the building (i.e., torus room) and is transported upward through open floor gratings into the ground level of the reactor building. Flammable mixtures quickly develop in these regions, which are assumed to ignite from high flammable gas concentration and high gas effluent temperatures exceeding 1500 K near the floor of the drywell. The resulting pressure rise within the building causes several doorways within the building to open, including the large equipment access doorway at grade level and the blow-out panels in the side walls of the refueling bay near the top of the building. This combination of two large openings in the reactor building creates an efficient transport pathway for material released from containment to the environment. That is, a vertical column of airflow is created within the building, whereby fresh air from outside the building enters through the open equipment doors at grade level, rises upward through the open equipment hatches at every intermediate floor within the building, and exits through the blowout panels at the top of the building. As was described earlier (Section 5.1.2), retention of fission products in the reactor building is small for most species because of the chimney effect that is created by this flow pattern.

5.3.2 Radionuclide Release

The time-dependent release fraction for all radioactive species to the environment is shown in Figure 5-30. The release of radionuclides immediately accompanying containment failure (i.e., the puff release) is the dominant contributor to the release of activity to the environment. However, as indicated in the expanded view of the release fractions for volatile species shown in Figure 5-31, the release of some important species, iodine and tellurium in particular, continues for several hours. The initial 'puff' release accompanying containment failure primarily results from the discharge of fission products that were airborne in the containment atmosphere at the time of drywell liner melt-through.

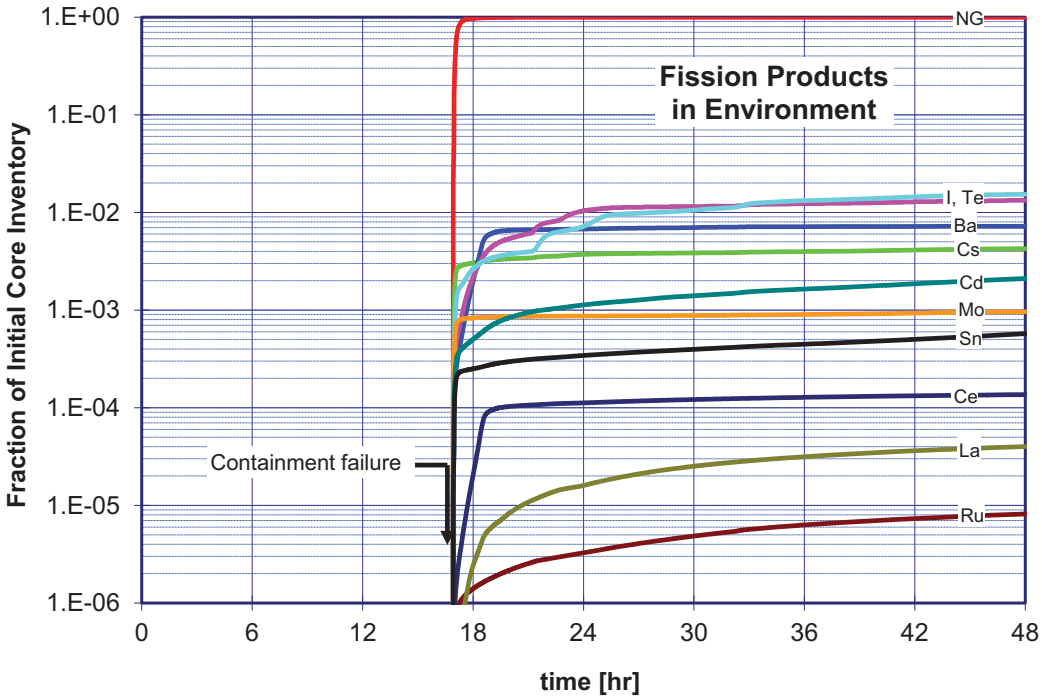

Figure 5-30 Environmental source term for STSBO with RCIC blackstart

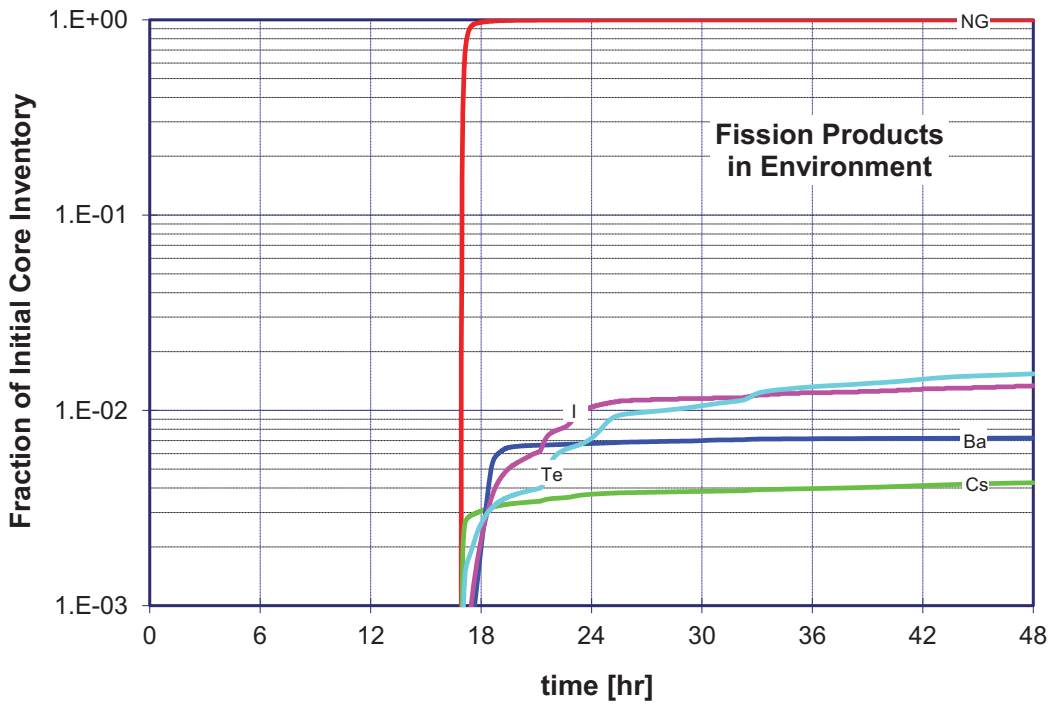

Figure 5-31 Environmental source term for STSBO with RCIC blackstart: details for volatile species

Figure 5-32 summarizes the spatial distribution of the total iodine inventory as a function of time. Similar information is shown in Figure 5-33 for cesium and Figure 5-34 for tellurium. Collectively, these figures highlight differences in the mobility of different radionuclide species and temporal changes in their location. For example, all iodine is assumed to be transported in the form of CsI, which vaporizes at relatively modest temperatures for a severe accident and is readily swept from the RPV to the wetwell by the hydrogen/steam mixture that flows through the open SRV. The fractions of iodine, cesium, and tellurium swept into the suppression pool immediately are roughly in proportion to their relative volatility: iodine (90%); tellurium (83%); and cesium (75%). During the succeeding 6 hours, most CsI initially deposited on reactor vessel internal structures after RPV blowdown evaporates from the surfaces because of decay heating, and is swept into the suppression pool. Deposited tellurium behaves in a similar manner, but over a much longer time frame. Most of the cesium (i.e., the molybdate) deposited on in-vessel structures remains there for the duration of the 48 hour calculation.

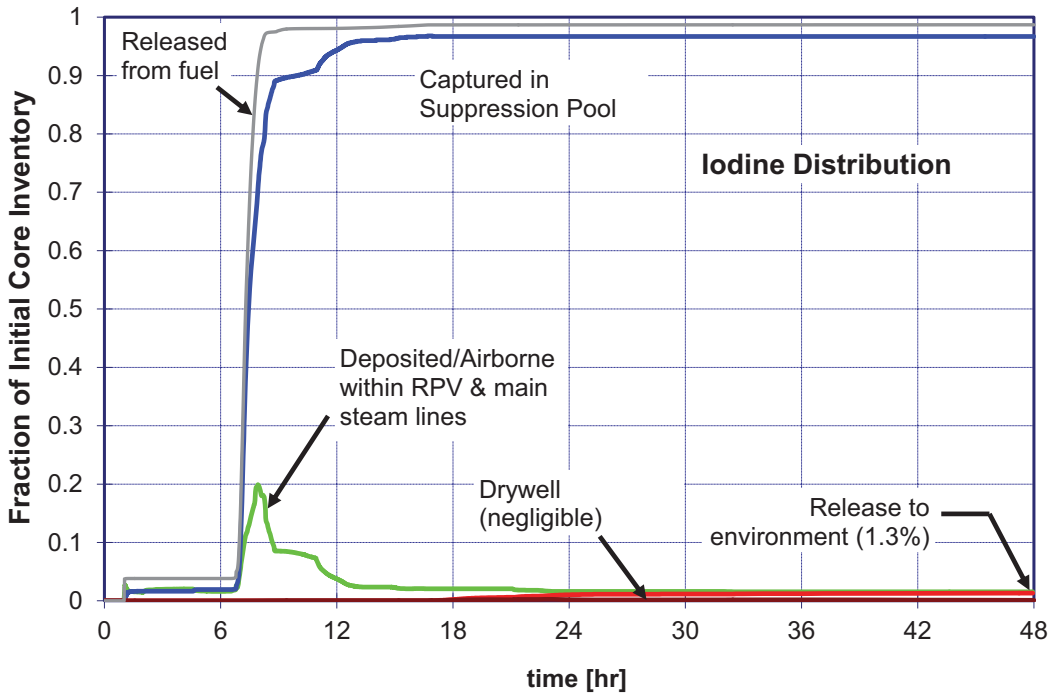

Figure 5-32 Iodine fission product distribution for STSBO with RCIC blackstart

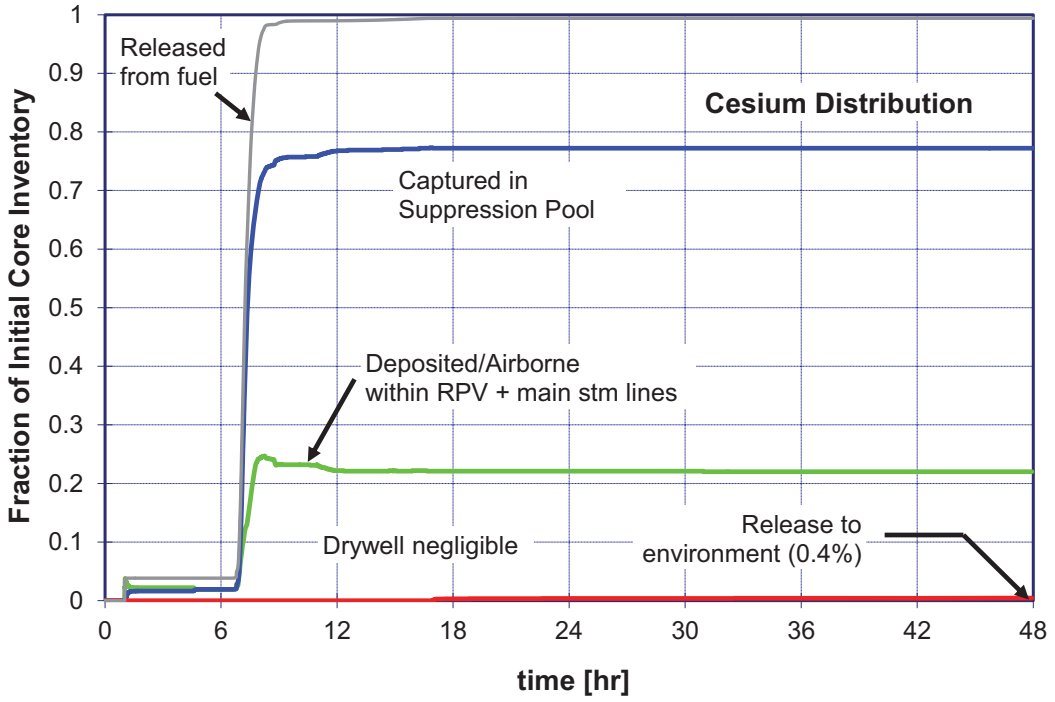

Figure 5-33 Cesium fission product distribution for STSBO with RCIC blackstart

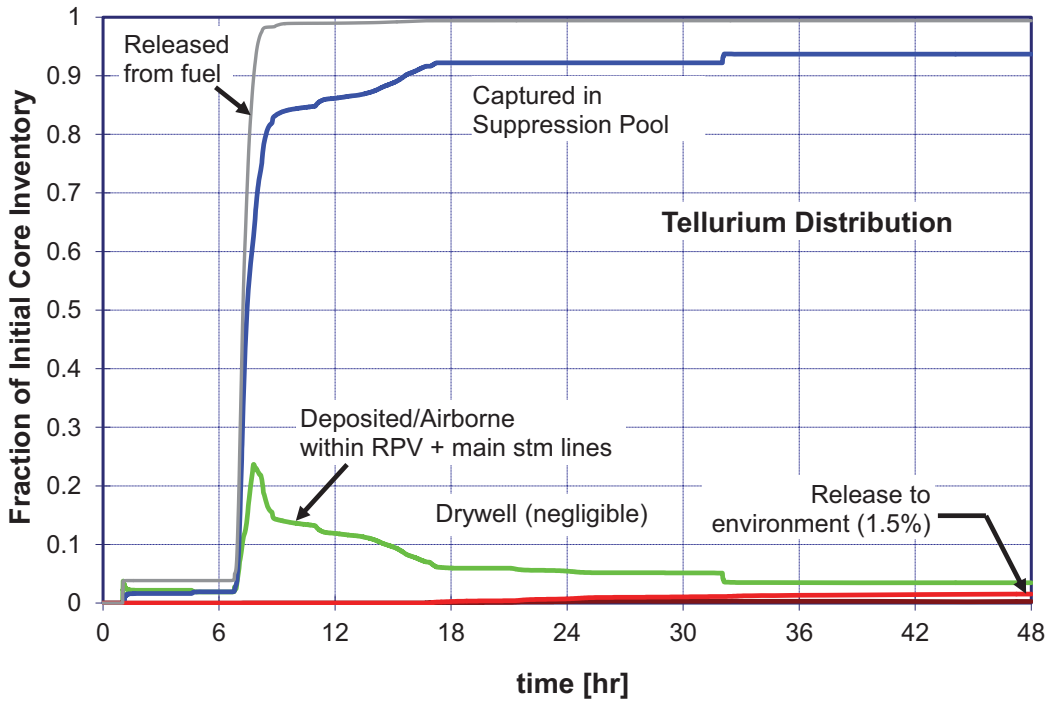

Figure 5-34 Tellurium fission product distribution for STSBO with RCIC blackstart

5.4 Short-Term Station Blackout- Sensitivity Case without RCIC Blackstart

Another form of a STSBO scenario and a variation commonly found in BWR PRAs is one that does not credit actions by plant personnel to manual start steam-driven coolant injection systems (i.e., RCIC or HPCI). Immediate loss of all onsite and offsite electric power defeats all sources of emergency coolant injection, reactor pressure control and containment heat removal. As a result, the timeline of events in this version of a STSBO is accelerated in comparison to a STSBO with RCIC blackstart and the LTSBO. The calculated chronology of events for the STSTO without RCIC blackstart is listed in Table 5-4.

The onset of fuel damage occurs in approximately one hour. That is, oxidation of Zircaloy cladding in the upper region of the core leads to the release of the gap inventory of fission products in about one hour. Large-scale relocation of core debris to lower elevations of the core begins within two hours and core debris is released into the lower plenum at 2.4 hours. Lower head failure occurs in 8.2 hours, which releases molten core debris to the drywell floor and drywell liner melt-through in 8.5 hours. Significant fission product release to the environment,[39] therefore, begins at roughly ten hours of the initiating event.

[39] 'Significant' in this context means the release of greater than 1% of the initial core inventory of iodine.

Table 5-4 Timing of Key Events for the STSBO without RCIC blackstart

Event	Time (hours, unless noted otherwise)
Station blackout – loss of all onsite and offsite AC power	0.0
Low-level 2 and RCIC actuation signal (no RCIC response)	10 min
Downcomer water level reaches TAF	30 min
First hydrogen production	55 min
First fuel-cladding gap release	1.0
First channel box failure	1.3
First core cell collapse due to time at temperature	1.6
SRV sticks open due to cycling at high temperatures	1.8
Reactor vessel water level reaches bottom of lower core plate	1.9
RPV pressure first drops below LPI setpoint (400 psig)	2.1
First core support plate localized failure in supporting debris	2.4
Lower head dries out	3.3
Ring 5 CRGT Column Collapse [failed at axial level 2]	4.9
Ring 3 CRGT Column Collapse [failed at axial level 2]	5.8
Ring 1 CRGT Column Collapse [failed at axial level 2]	6.0
Ring 2 CRGT Column Collapse [failed at axial level 2]	6.1
Ring 4 CRGT Column Collapse [failed at axial level 2]	6.3
Lower head failure	8.2
Drywell liner melt-through	8.5
Refueling bay to environment blowout panels open	8.5
Hydrogen burns initiated in lower reactor building	8.5
Doors to stairwell open due to overpressure	8.5
Door to environment through railroad access opens due to overpressure	8.5
Time Iodine release to environment exceeds 1%	9.7
Calculation terminated	48.0

5.4.1 Thermal Hydraulic Response

The loss of all AC and DC power supplies to plant equipment and instrumentation causes reactor control blades, MSIVs, and containment isolation valves to move to their fail-safe positions (i.e., inserted and closed). Isolation of the RCS causes reactor pressure to rise to the set point of the SRVs, which opens and directs coolant to the pressure suppression pool. As shown in Figure 5-35, reactor pressure is maintained at approximately 1,120 psia, as the SRV with the lowest set point cycles open and closed for approximately 2 hours.[40] Actions taken by plant operations personnel to manually reduce reactor pressure and prevent frequent cycling of the

[40] A second SRV periodically opens during the first 45 minutes of the transient, when decay heat levels remain high. However, after this point in time, only one valve is cycling.

SRVs are assumed to not be successful. This is because control power (i.e., B.5.b portable generator and converter) to necessary equipment (e.g., SRV solenoid control valves) is assumed not to be available and manual actions to open alternative steam relief paths[41] are assumed not to be taken.

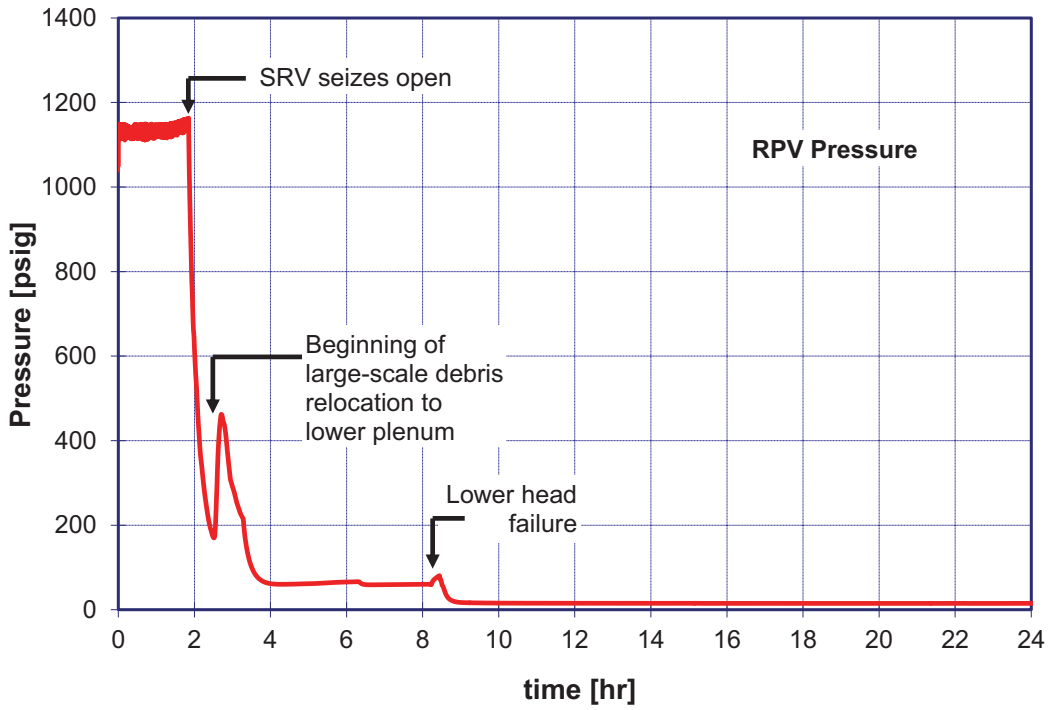

Figure 5-35 Reactor vessel pressure: STSBO without RCIC blackstart

Two hours after the initiating event, the single cycling SRV sticks in the open position due to thermal seizure of internal valve components.[42] This initiates a rapid depressurization of the RCS. The continuous discharge of steam through the open SRV accelerates the rate at which the coolant inventory is depleted from the RPV. Figure 5-36 shows the two-phase reactor mixture level in the downcomer and within the core shroud. Both levels show a sharp decrease at two hours, corresponding to the time of reactor blowdown through the open SRV. The steam flow produced by the flashing of residual water into steam temporarily cools over-heated fuel and in-core debris as shown in Figure 5-37, but also reduces the in-shroud mixture level well below the elevation of the lower core plate. Within an hour (i.e., less than 3 hours after the initiating event), the lower core plate yields, and debris begins to relocate into the lower plenum.

---

41 For example, SAMP-1 (RC/P-11) lists opening main steam line drains or HPCI and RCIC steam line drains as options for reducing RPV pressure.

42 Refer to Section 4.4 for details of this failure mechanism.

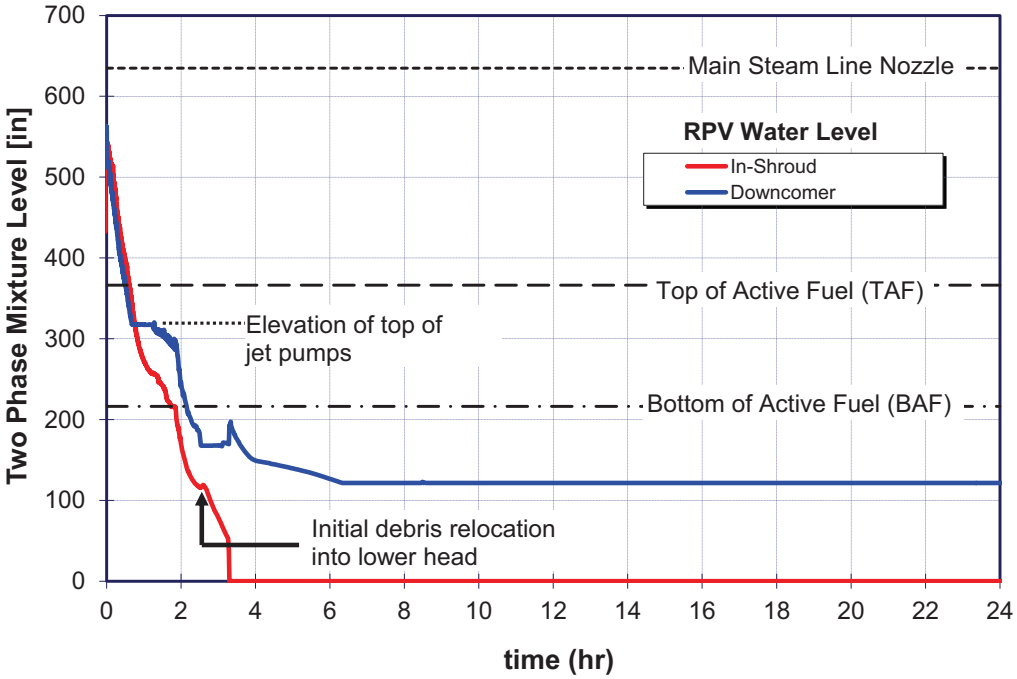

Figure 5-36 Reactor vessel water level: STSBO without RCIC blackstart

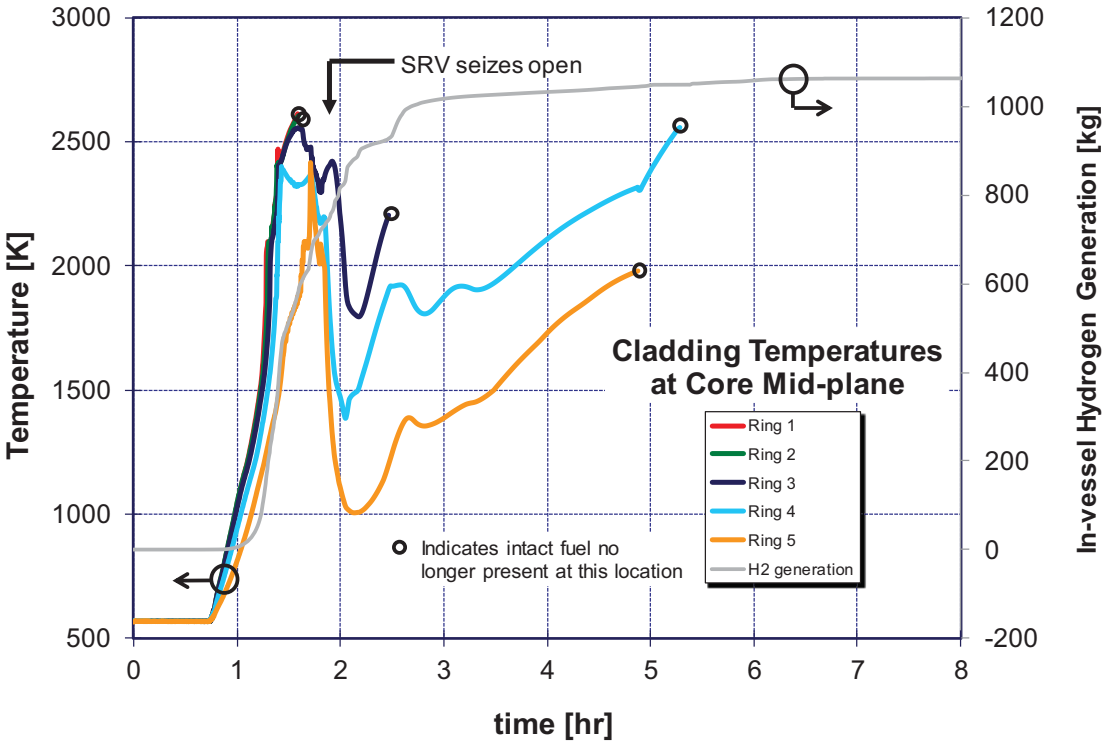

Figure 5-37 Temperatures of fuel cladding at core mid-plane: STSBO without RCIC blackstart

Debris that pours into the body of water in the lower head is cooled because of fragmentation as it travels through water and is then cooled by bulk boiling on surfaces of the resulting debris bed. This effect is shown in Figure 5-38 and Figure 5-39, which give the calculated mass and temperature[43] of debris in the lower head, respectively. When residual water in the lower plenum is completely evaporated, debris temperatures begin to rise, exceeding the melting temperature of stainless steel (1700 K) in approximately 1.5 hours. Rising debris temperatures also cause the temperature of the lower head to increase, as indicated in Figure 5-40. Because reactor vessel pressure is relatively low during this heat up, failure of the lower head is from creep rupture at high temperature.[44]

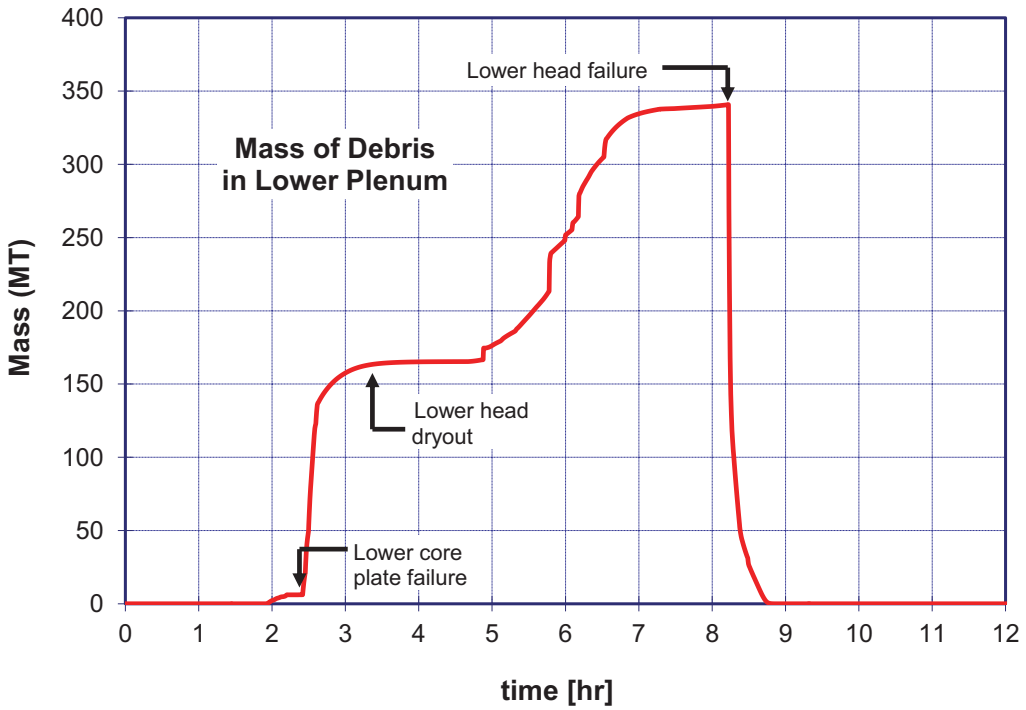

Figure 5-38 Mass of core debris in RPV lower plenum: STSBO without RCIC blackstart

---

43 The signatures shown in Figure 4-3 represent the temperature of debris along the vertical axis of the debris bed in the lower plenum. The axial nodalization of the lower plenum is shown in Figure 4-3.

44 The inner surface temperature of the central region of the lower head (i.e., MELCOR rings 1-4) is above the melting point of steel at the time failure occurs.

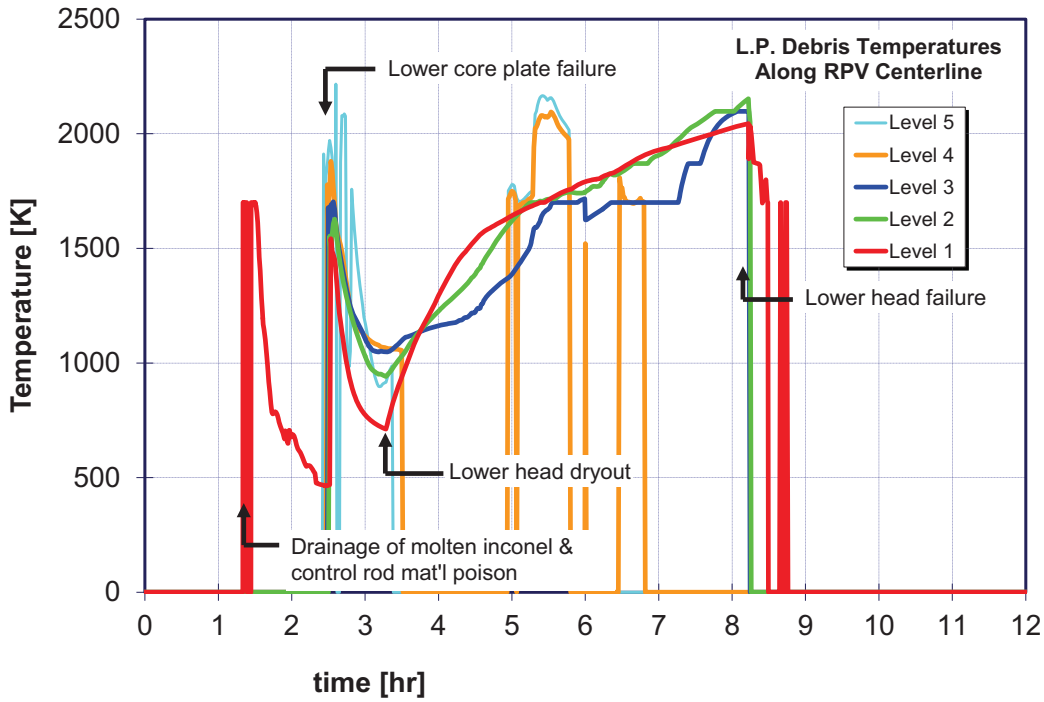

Figure 5-39 Temperature of debris in RPV lower plenum: STSBO without RCIC blackstart

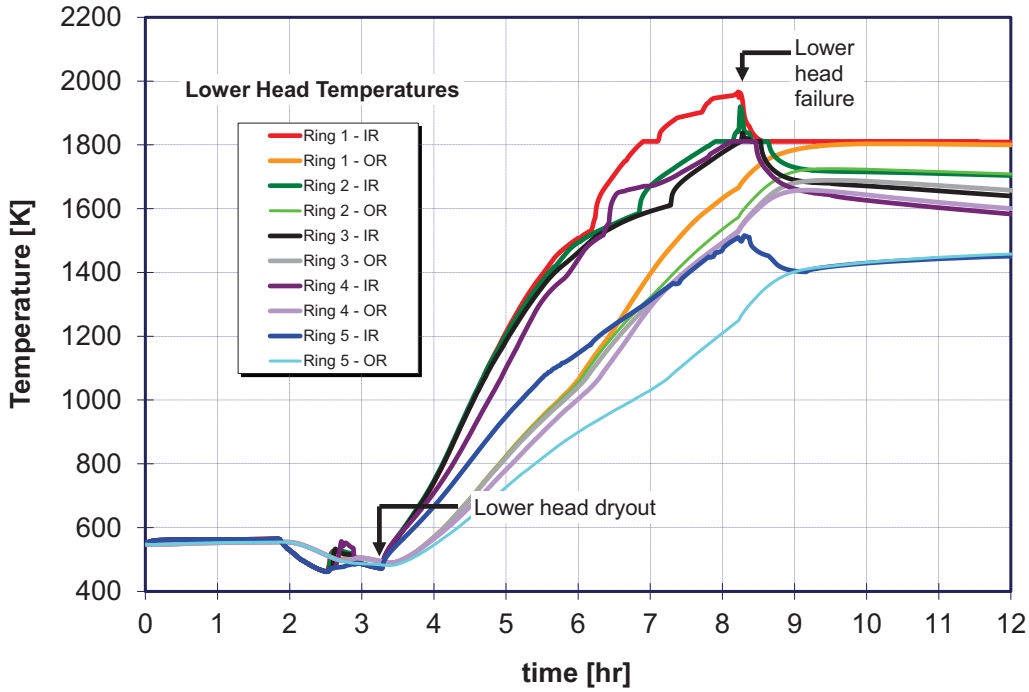

Figure 5-40 Lower head temperature: STSBO without RCIC blackstart

In contrast to the LTSBO (refer to Section 5.1.1), containment pressure immediately following reactor vessel failure is well below the threshold for induced leakage through the drywell head flange (80 psig). Therefore, leakage from containment does not occur by this mechanism. The lower pressure in the short-term scenario is the result of a reduced period of reactor steaming to the suppression pool before to the onset of core damage. Torus water temperature remains sub cooled, relative to atmospheric conditions, throughout the entire period of in-vessel core damage progression (see Figure 5-41). Therefore, steam contributions to containment pressure are negligible. Figure 5-42 shows the containment pressure for this short-term station blackout scenario.

Containment conditions change dramatically, when debris is released onto the reactor pedestal floor following lower head failure. The absence of water on the drywell floor allows debris to flow laterally out of the cavity through the open personnel access doorway and spread out across the main drywell floor. Lateral movement and spreading of debris across the drywell floor allow debris to reach the steel shell at the outer perimeter of the drywell within 10 minutes.
Five minutes later, thermal attack of the molten debris against the steel shell results in shell penetration and opening of a release pathway for fission products into the basement (i.e., torus room) of the reactor building. This results in a rapid depressurization of the containment to atmospheric conditions in a short time (i.e., less than 1 hour).

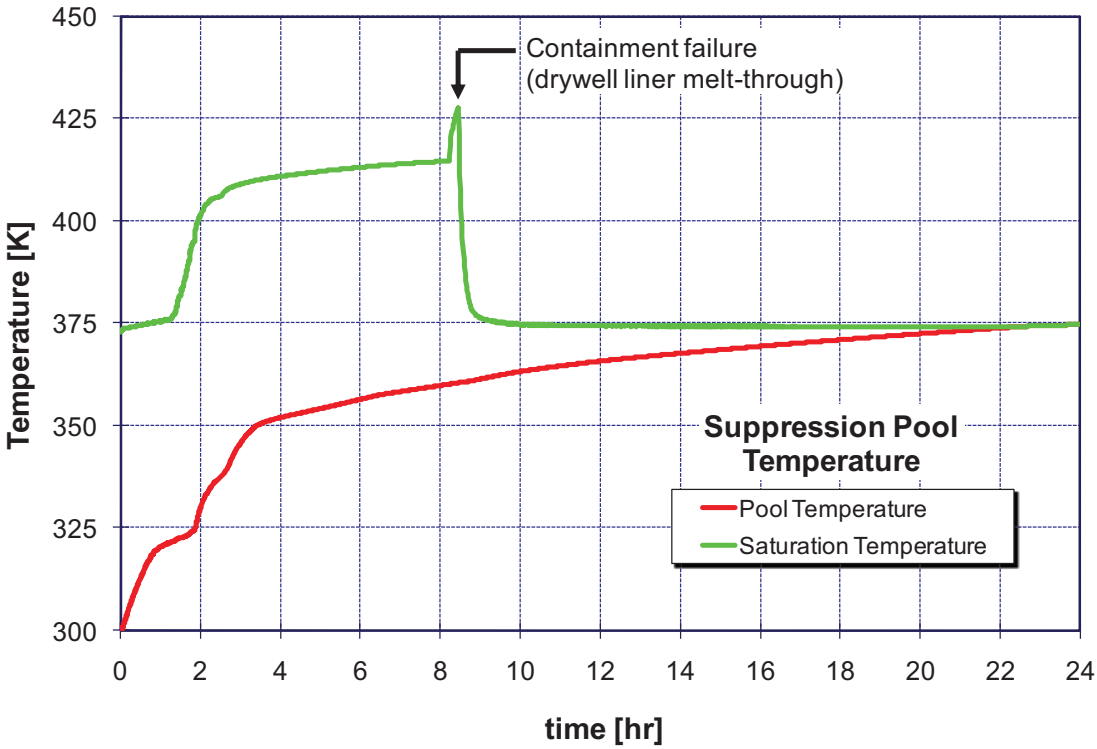

Figure 5-41 Suppression Pool Temperature: STSBO without RCIC blackstart

Immediately following drywell shell melt-through, hydrogen is released from the drywell into the basement of the building (i.e., torus room) and is transported upward through open floor gratings into the ground level of the reactor building. Flammable mixtures quickly develop in

these regions, which are assumed to ignite from high flammable gas concentration and high gas effluent temperatures exceeding 1500 K near the floor of the drywell. The resulting pressure rise within the building causes several doorways within the building to open, including the large equipment access doorway at grade level and the blow-out panels in the side walls of the refueling bay near the top of the building. This combination of two large openings in the reactor building creates an efficient transport pathway for material released from containment to the environment. That is, a vertical column of airflow is created within the building, whereby fresh air from outside the building enters through the open equipment doors at grade level, rises upward through the open equipment hatches at every intermediate floor within the building, and exits through the blowout panels at the top of the building. As was described earlier (Section 5.1.2), retention of fission products in the reactor building is small for most species because of the chimney effect that is created by this flow pattern.

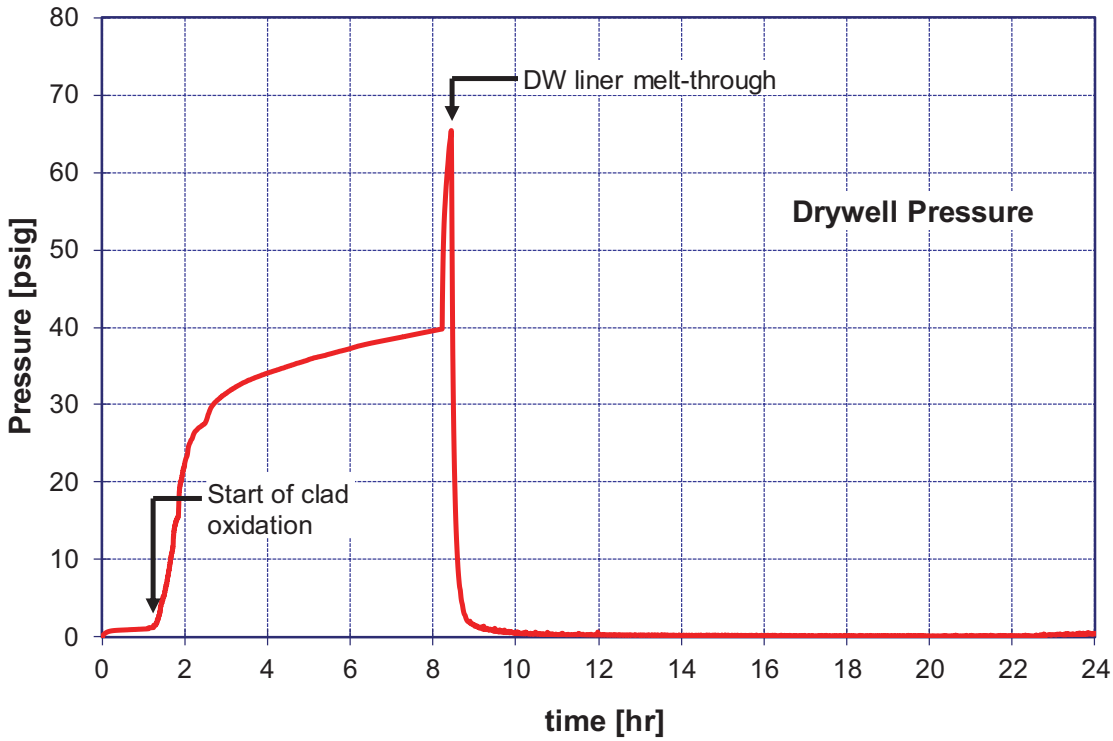

Figure 5-42 Containment Pressure: STSBO without RCIC blackstart

5.4.2 Radionuclide Release

The release of radionuclides to the environment occurs in two important phases. The first phase is very short and is characterized by the discharge of airborne fission products from the containment immediately following containment failure. A later and protracted release of begins 24 hours into the sequence as a result of revaporization of CsI and tellurium initially deposited on surfaces within the RCS. Both phases are clearly evident in Figure 5-43, which shows the fractional release to the environment for all radioactive species. An expanded view of the release fractions for volatile species is shown in Figure 5-44.

Figure 5-45 through Figure 5-47 indicate changes in the spatial distribution of iodine, cesium and tellurium that result in the environmental releases shown in Figure 5-44. In particular, Figure 5-45 and Figure 5-47 clearly indicate the delayed, gradual release of iodine and tellurium, which begins 16 hours after containment failure,[45] is due to the movement of these species away from surfaces within the RCS, through the drywell to the environment. Although the transport pathway to the environment also involves the reactor building, retention within the building is negligible. Airborne fission products have a short residence time in the building due to hydrogen combustion immediately follows containment failure and a persistent buoyancy-driven flow through the building in the long term. This behavior was described earlier for the unmitigated LTSBO scenario (Section 5.1) and results in very low DFs for the reactor building, as illustrated in Figure 5-48.

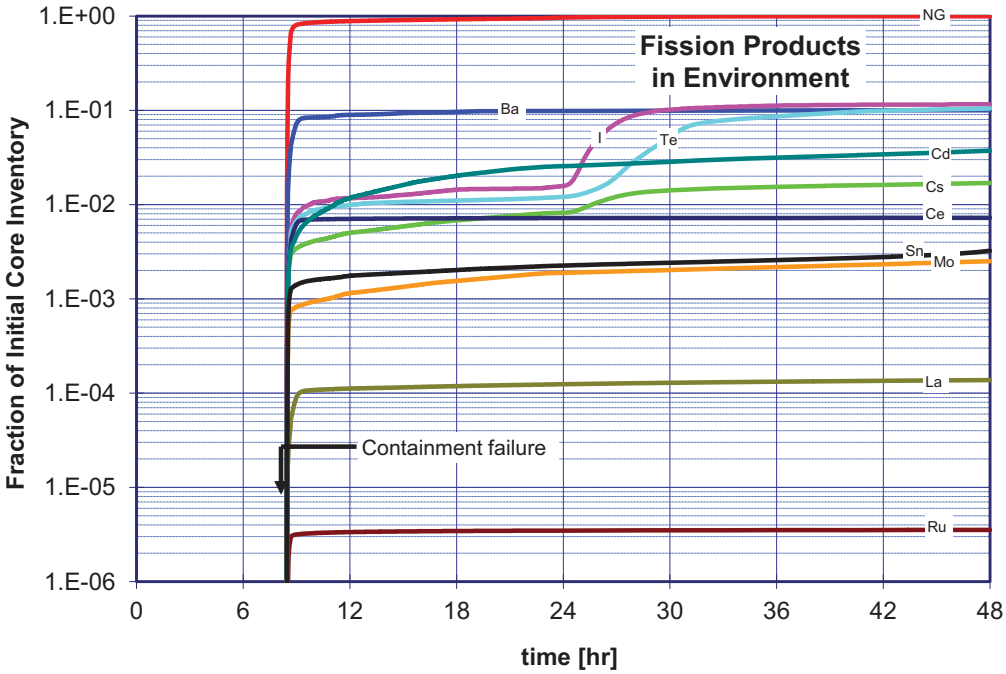

Figure 5-43 STSBO without RCIC blackstart environmental source term

[45] 24 hours after the initiating event.

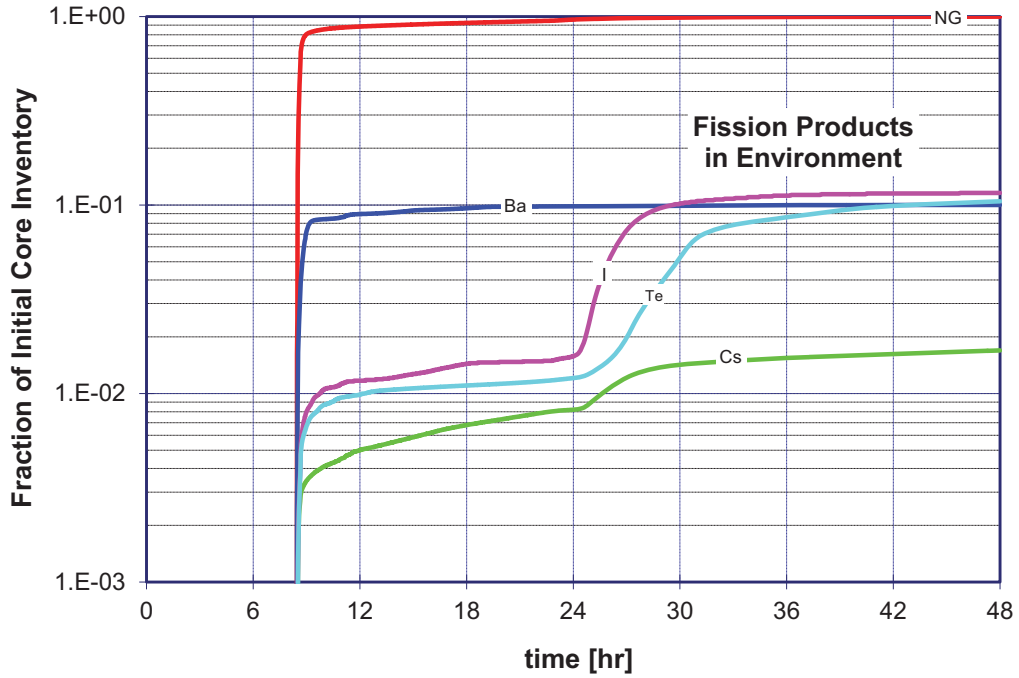

Figure 5-44 STSBO without RCIC blackstart environmental source term: details for volatile species

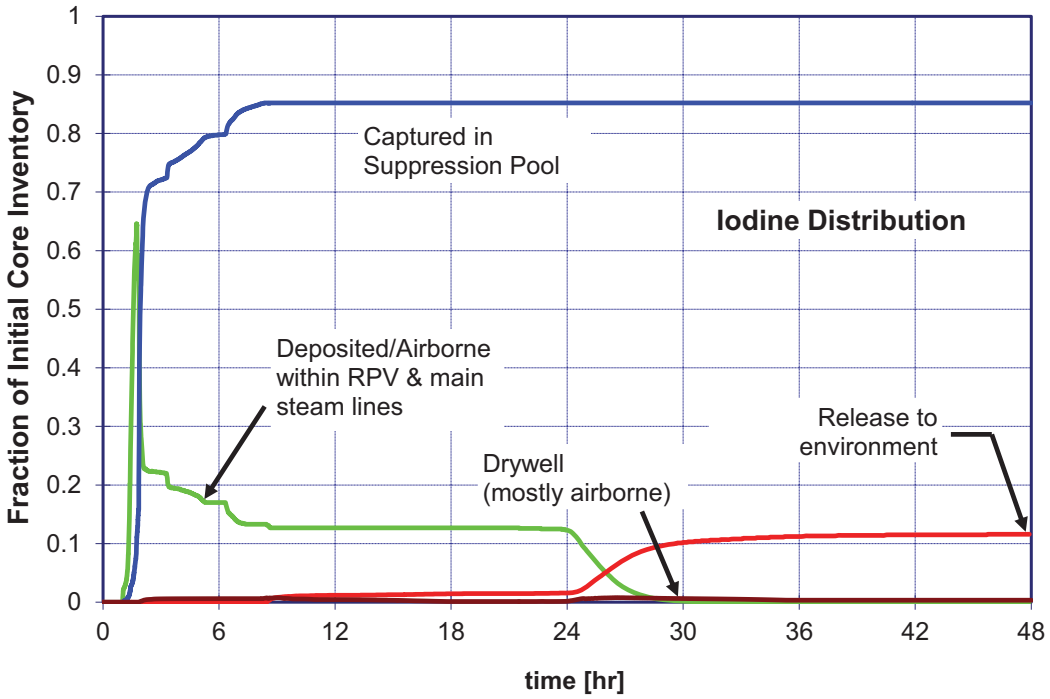

Figure 5-45 Spatial distribution of Iodine: STSBO without RCIC blackstart

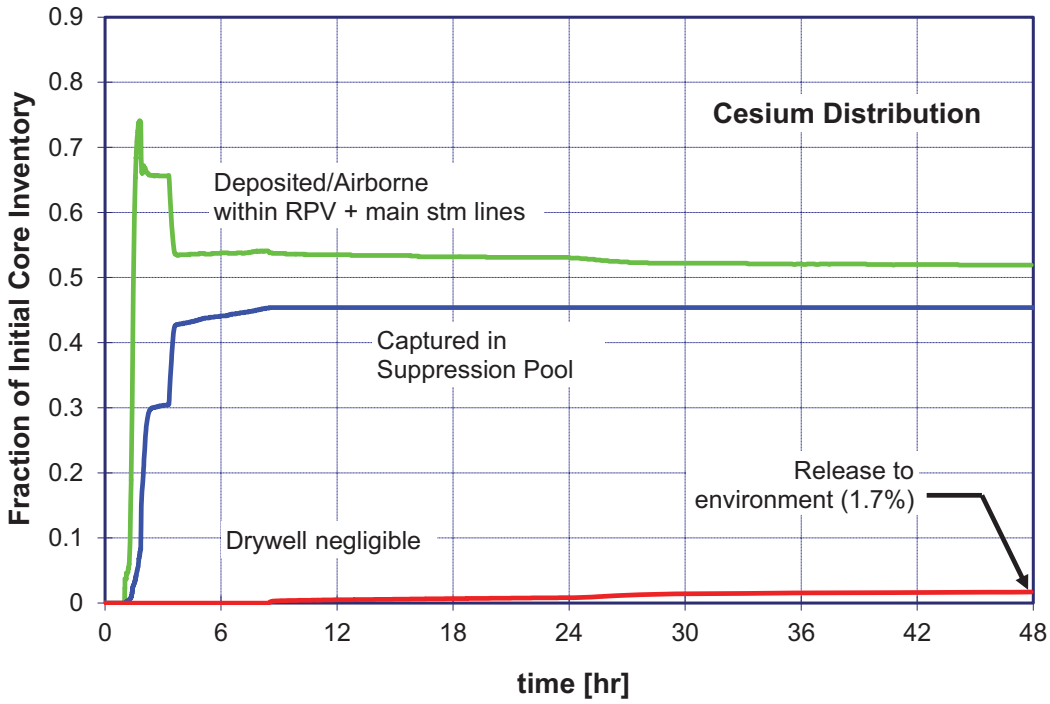

Figure 5-46 Spatial distribution of Cesium: STSBO without RCIC blackstart

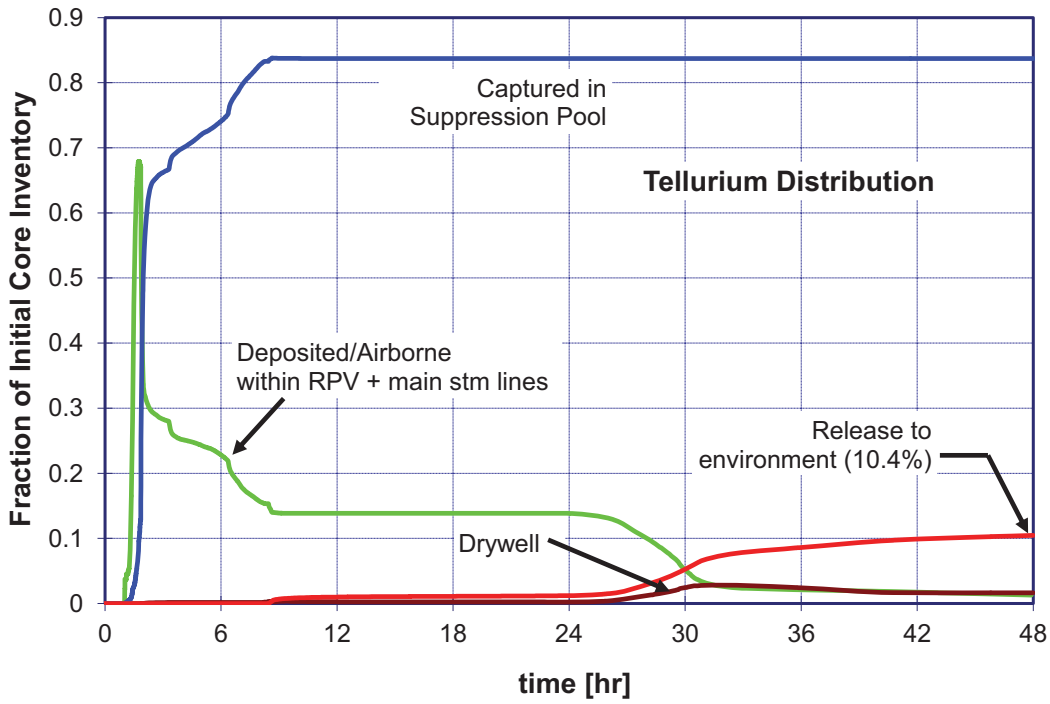

Figure 5-47 Spatial distribution of Tellurium: STSBO without RCIC blackstart

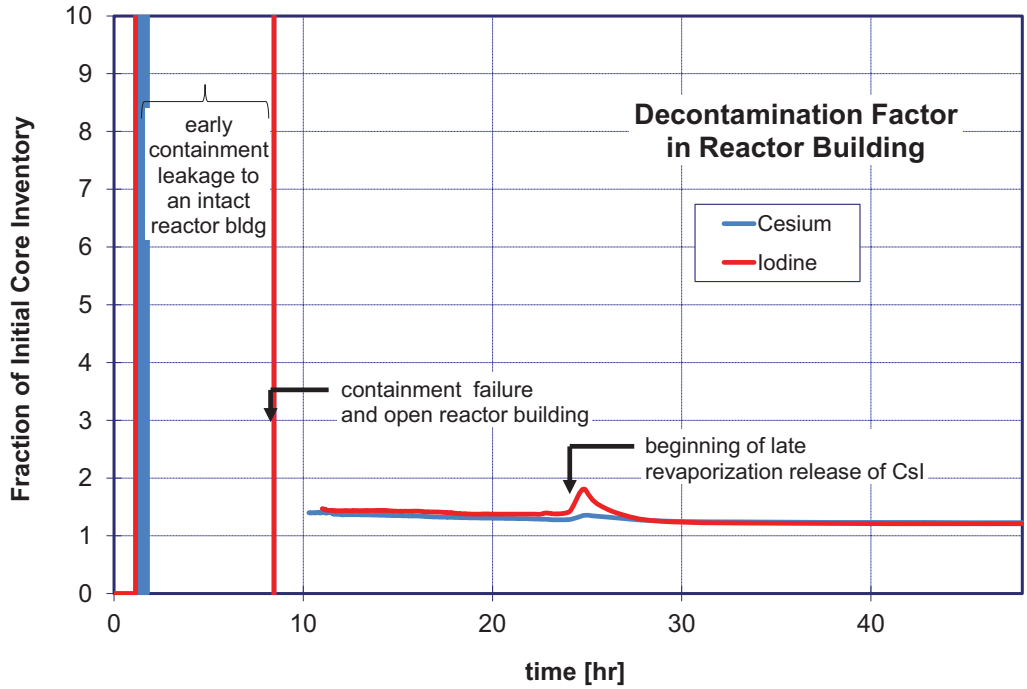

Figure 5-48 Reactor Building decontamination factor (DF): STSBO without RCIC blackstart

Figure 5-45 indicates that iodine that deposits on surfaces within the RCS during the first 6 to 10 hours of damage progression is subsequently released from these surfaces to the environment. High atmosphere temperatures in the drywell prevent CsI from depositing on surfaces in the containment. It was noted earlier that a long-term stable flow of air through the reactor building prevents airborne CsI from depositing in the building. Nearly all material released from the RPV after 24 hours is, therefore, transported to the environment. The source of this late release of iodine and tellurium (shown in Figure 5-45 and Figure 5-47, respectively) within the RPV can be traced to the delayed evaporation of water from reactor recirculation loop piping.

Forced circulation flow through the reactor vessel is maintained by two recirculation loops external to the RPV (see Figure 4-2). The diagram shown in the lower right-hand corner of Figure 5-49 shows the hydrodynamic nodalization of fluid in these loops, as represented in the MELCOR model shown in Figure 4-2. Water in recirculation loop piping only partially participates in depletion of reactor coolant (see Section 5.4.1) due to boiling in the core. Gradual evaporation of water in the recirculation loop piping results in significant increases in the surface area of recirculation loop piping. The level of water in the recirculation loops 'risers' (i.e., discharge piping between the recirculation pumps and top of the jet pumps) initially follows the decline in water level in the RPV downcomer (see Figure 5-36). Residual water in the downcomer (i.e., outside the jet pump diffusers) evaporates at approximately 6 hours; but approximately 4 meters of water is trapped in the bottom of the recirculation loop piping when RPV lower head failure occurs. This water in both recirculation loops retains approximately 4.4 kg of CsI, or nearly 11% of the initial core inventory, representing over 10% of the initial core inventory of iodine.

It is also instructive to compare the amount of iodine and tellurium captured on in-vessel surfaces and in water in the recirculation loop piping in the STSBO to the amount that was indicated earlier for the LTSBO scenario. In-vessel retention of these species is larger in the STSBO than the LTSBO. At the time of RPV lower head failure, the amount of iodine retained in the RPV is approximately 13% for the STSBO (without RCIC blackstart) versus 3% for the LTSBO. This difference affects the extent to which late revaporization from the RCS affects the environmental release in the two scenarios. That is, more iodine and tellurium are available for late revaporization in the STSBO than in the LTSBO, and thus the late release from the recirculation loop piping observed in the STSBO has a measureable impact on the total release to the environment but does not impact the LTSBO. For completeness, it should be noted that total evaporation of water from the recirculation loop piping does not occur until long after 48 hours in the LTSBO scenario. However, as shown in Figure 5-12 and Figure 5-14 respectively, the amount of volatile iodine and tellurium that is available for release (i.e., retained within the RCS) is not sufficiently large to significantly impact the environmental release even if it occurred earlier.

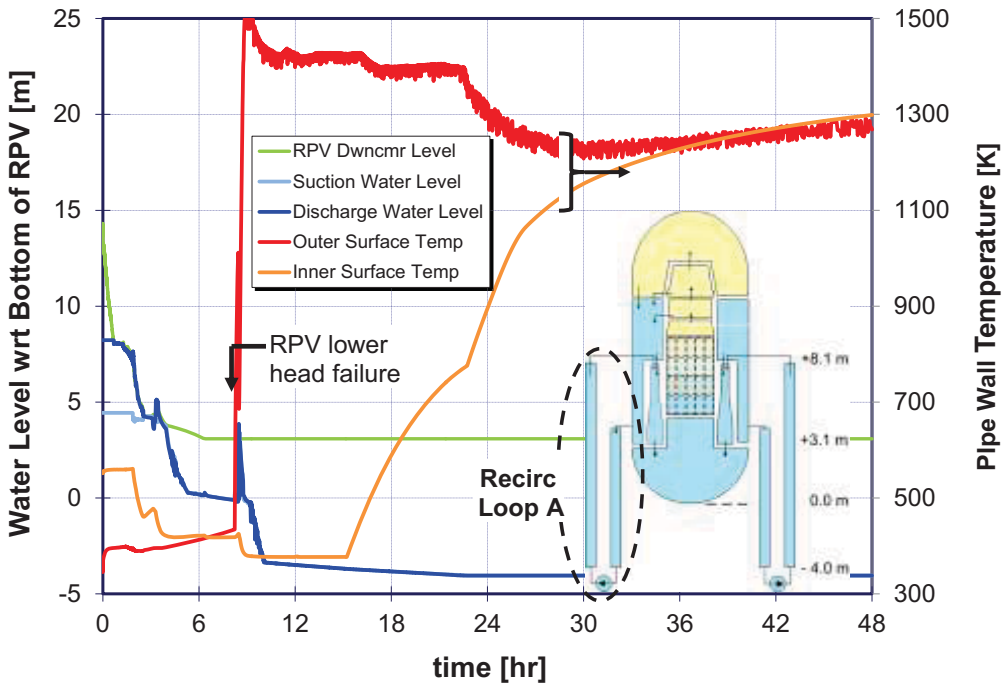

Figure 5-49 Water level and temperature of RPV recirculation loop-A piping: STSBO without RCIC blackstart

After RPV lower head failure, this piping is exposed (optically) to molten core debris that spreads across the drywell floor. This causes the outer temperature of the outer surface of recirculation loop piping increase dramatically, as indicated in Figure 5-49. Conduction heat transfer through the recirculation loop piping evaporates residual water within the pipe, which dries out at approximately 22.5 hours.

MELCOR assumes that fission products retained in an evaporating pool of water remain in or on the surface of the pool until it fully evaporates. At that point in time, the material is transferred

to the surfaces of neighboring heat structures – in this case, heat structures representing the recirculation loop piping. Figure 5-50 shows the accumulation of CsI in water within recirculation loop piping during the early period of in-vessel damage progression and transfer of the solute onto the inner surface of the recirculation loop piping walls when the water is completely evaporated (at approximately 22 hours). The figure also shows the gradual evaporation of the deposited CsI aerosol away from the walls over the succeeding 5 hours due to the very high surface temperatures generated by heat transfer from neighboring core debris (pipe wall temperature is shown in Figure 5-49.) The total quantity of re-vaporized CsI (approximately 11% of the initial core inventory) corresponds directly to the amount released to the environment over the same time frame. The same relationship between retention and late revaporization from recirculation loop piping is observed with tellurium. Although similar fractional quantities of the dominant form of cesium (cesium molybdate) are captured in recirculation loop piping, sufficiently high pipe wall temperatures are not calculated within the 48 hour time frame of these calculations to revaporize this material due to its chemical form with a higher vapor pressure.

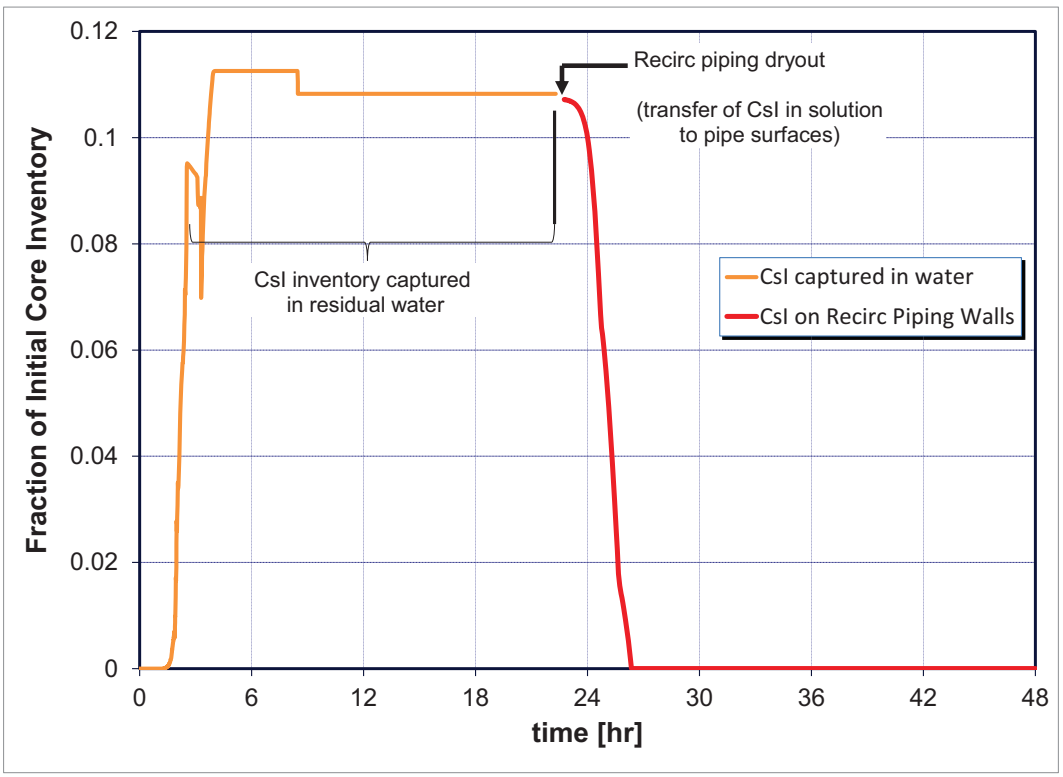

Figure 5-50 CsI deposited on the surface of recirculation loop piping: STSBO without RCIC blackstart

5.5 SBO Sensitivity Cases with Alternate SRV Failure Criteria

The chronology of events for each of the SBO calculations described in previous sections includes failure of a cycling SRV. At some point in time, a continuously cycling SRV sticks in the open position either due to stochastic or thermally-induced failure mechanisms described in Section 4.4.2. The criterion for valve failure, and therefore the precise time at which valve

seizure would occur, is uncertain. Analyses of severe accident progression frequently identify RPV pressure as an important parameter affecting severe accident progression and fission product source term. Therefore, sensitivity calculations were conducted to quantitatively measure the impact of uncertainties in SRV failure criteria and discern how they affect calculated source terms.

The calculations separately addressed uncertainties in stochastic and thermal failure criteria. Reasonable variations in these criteria were examined first, and results are described in Section 5.5.1. In this context, 'reasonable variations' means the alternate failure criteria are judged to fall within 1- or 2-sigma range of credible values for a normal distribution (i.e., they differ from the best estimate, but do not lie outside the 5th and 95th percentile values). The calculations were not explicitly designed to span this entire range, but provide a sufficient sampling to understand the extent to which the time of SRV seizure affects results.

As noted in the next section, all of the calculations performed within this range depressurized the RPV before creep rupture of the reactor coolant system pressure boundary occurred. Therefore, energetic containment loads associated with rapid RPV blowdown from high pressure did not result from any of the sensitivity calculations. Additional calculations were, therefore, performed to examine the manner in which creep rupture and attendant energetic loads on the containment pressure boundary would affect calculated source terms. Creep rupture in this context involves structural failure in one of two locations: reactor vessel lower head due to direct heating by molten core debris or main steam line (MSL) piping due to heat transfer from hot gases transported through cycling SRV(s). For creep rupture at either location to occur at high pressure, extreme values of SRV failure criteria must be defined. Section 5.5.2 describes results of sensitivity calculations that apply these extreme SRV failure conditions.

5.5.1 Reasonable variations in failure criteria

Alternate stochastic and thermal failure criteria for a cycling SRV were examined as follows:

- The best-estimate stochastic failure criterion of 270 cycles was changed downward as low as the 50th percentile (or 187 cycles) and upward to the 90th percentile (or 620 cycles)[46].

- The best-estimate valve-stem temperature failure criterion of 900 K (1160 °F) was reduced to 811 K (1,000 °F) and as high as 1,100 K (1,500 °F).

- The best-estimate position at which the valve is expected to fail is full open. The possibility of valve stem seizure at positions less than full open were examined by reducing the flow area after seizure by 50%.

---

[46] 620 cycles is never observed in the sensitivity calculations because the SRV seizes open due to thermal failure criteria before this large number is reached. More discussion on this is provided later.

Also included in the comparison of results from these sensitivity variations to the best estimate results are preliminary calculations in which the SRV thermal failure criterion was defined on the basis of high gas temperatures, rather than the temperature of a simulated internal valve component. These results are included here primarily to document the effects of changes in calculation methods that resulted from the independent peer review process. The peer review panel recommended a more rigorous assessment of SRV failure criteria as part of their review of preliminary MELCOR results.

Changes in SRV failure criteria alter the time at which RPV blowdown begins, and therefore affect the RPV pressure and water level signatures. Sample results of a few sensitivity calculations are compared in the following figures for each version of the SBO scenario:

- LTSBO: Figure 5-51 and
- Figure 5-52
- STSBO with RCIC Blackstart: Figure 5-53 and
- Figure 5-54
- STSBO without RCIC Blackstart: Figure 5-55 and Figure 5-56

Changes in the failure criteria for a cycling SRV have a large impact on the transient pressure signature for all cases. Within a reasonable range of alternate failure criteria, the time SRV depressurization begins can shift by several hours. However, these changes in the RPV pressure signatures have a smaller impact on the coolant boiloff (water level) signature, and a very small effect on RPV failure time. The time at which the RPV water level decreases below TAF shifts by less than 30 minutes in the STSBO without RCIC blackstart and less than one hour in the LTSBO. The impact on the STSBO with RCIC blackstart is more complicated. Late SRV failure generally occurs long after RCIC flow terminates by over-filling the RPV with water. However, early SRV failure can result in premature RCIC failure on low steam turbine inlet pressure. This difference in pressure response changes the amount of water in the RPV at the time RCIC flow terminates and, therefore, also impacts the coolant boiloff signature.

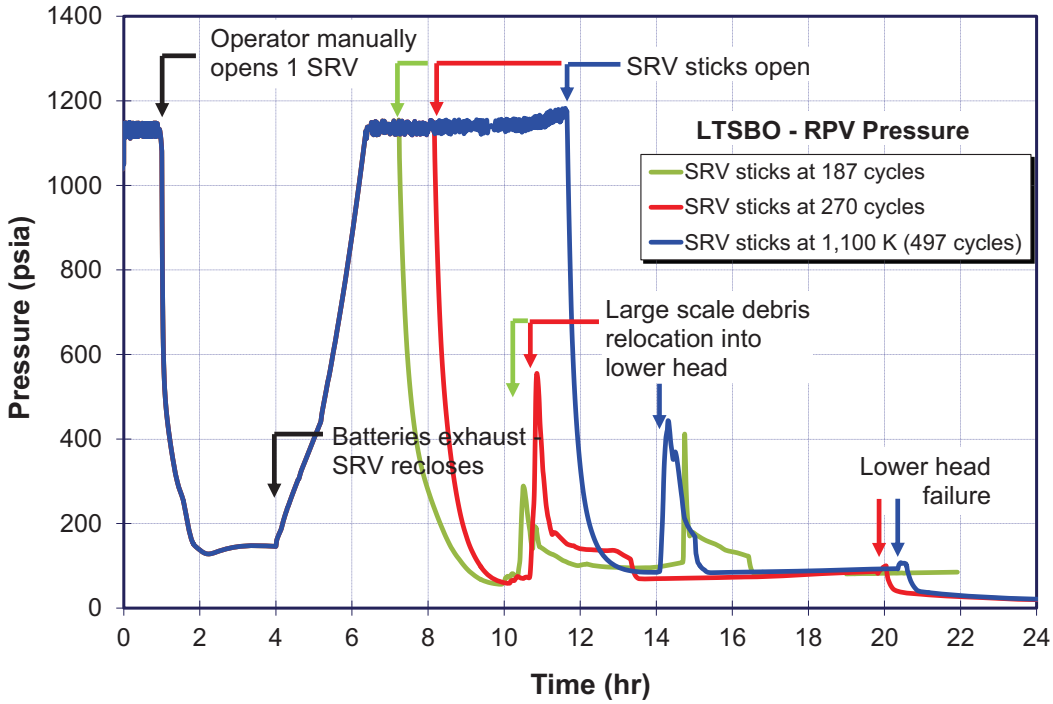

Figure 5-51 Comparison of RPV Pressure Response: SRV Failure Sensitivity – LTSBO

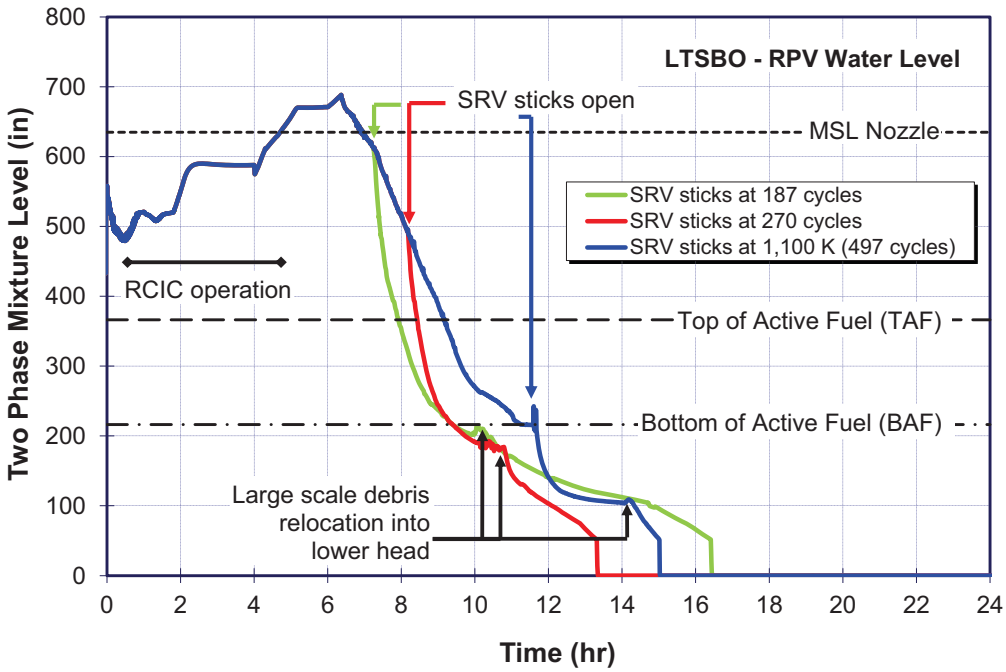

Figure 5-52 Comparison of RPV Level Response: SRV Failure Sensitivity - LTSBO

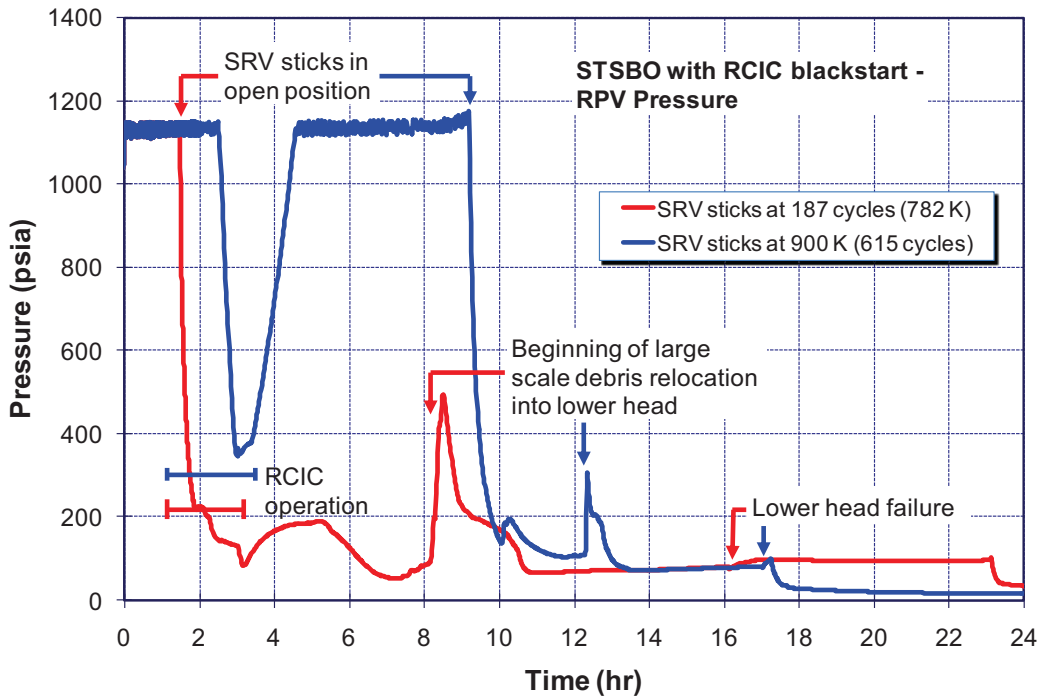

Figure 5-53 Comparison of RPV Pressure Response: SRV Failure Sensitivity – STSBO with RCIC blackstart

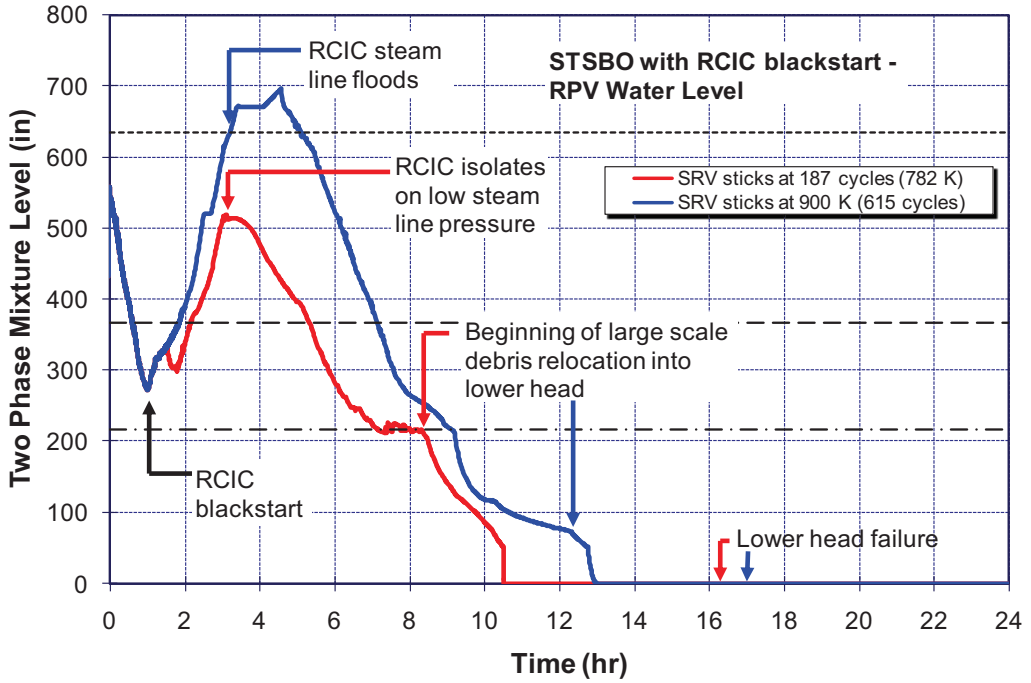

Figure 5-54 Comparison of RPV Level Response: SRV Failure Sensitivity – STSBO with RCIC blackstart

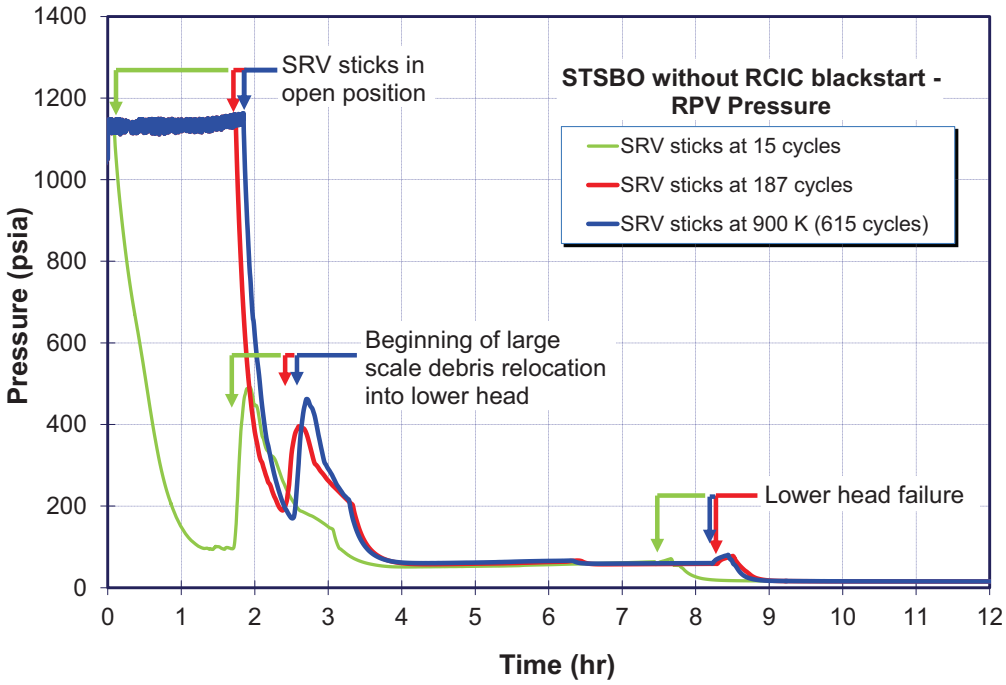

Figure 5-55 Comparison of RPV Pressure Response: SRV Failure Sensitivity – STSBO without RCIC blackstart

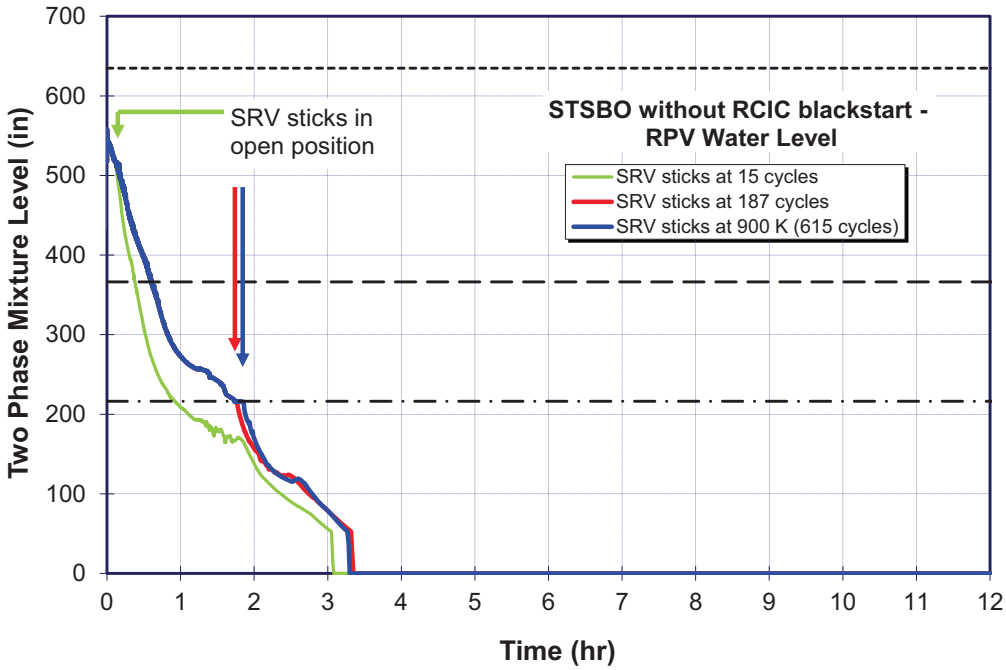

Figure 5-56 Comparison of RPV Level Response: SRV Failure Sensitivity – STSBO without RCIC blackstart

Differences in the details of parameters that reflect the calculated progression of fuel damage, material relocation and debris temperature are observed among the SRV sensitivity cases examined here. For example, the time at which large scale debris relocation into the lower plenum begins from above the lower core plate is shown in Figure 5-51 through Figure 5-55 to span a relatively wide range (i.e., 2 to 4 hours, depending on the scenario). This is due, in part, to the relationship between steam flow through the debris bed that accumulates above the lower core plate and debris temperatures. If SRV seizure occurs early in time (i.e., before RPV water level reaches TAF), RPV depressurization is complete before large quantities of debris accumulate on the lower core plate. Consequently, debris temperatures are reduced by boiling heat transfer near the base of the core, and lower core plate failure occurs very soon after RPV water level decreases below the lower core plate. Conversely, if SRV seizure occurs late in time (i.e., after RPV water level is close to the bottom of active fuel, lower core plate failure is delayed by steam cooling of debris during RPV depressurization. Significant differences in the debris temperature signatures are, therefore, observed among these sensitivity cases. These differences, in turn, affect the calculated time between dryout of the lower head (i.e., total evaporation of water from the RPV) and lower head failure. The time between RPV dryout and lower head failure tends to be longer for cases involving early SRV seizure than those for later seizure. However, it is interesting to note that differences in the details of in-vessel debris temperature signatures and material relocation have a small effect on the calculated time of lower head failure. As indicated in Table 5-5, the calculated time of lower head failure does not vary significantly among the sensitivity cases for a particular scenario. The integral effects of differences in in-vessel damage behavior appears to have a small effect on the time at which lower head failure occurs.

Table 5-5 compares calculated values of several key metrics of the sensitivity calculations to the best estimate results for all three versions of the SBO sequence described in previous section. The listed metrics are:

- SRV failure mode: This indicates the failure criterion that occurred first in each calculation. 'S' indicates stochastic failure; 'T' thermal failure

- Cycles at seizure: This indicates the total number of cycles experienced by the SRV at the time failure occurs.

- Time of SRV seizure: This is time into the accident (after the initiating event).

- Max MSL L-M Damage Index: The maximum value of the Larson-Miller creep damage index calculated for the heat structure representing the SRV valve stem. A value of unity indicates sufficient creep for failure.

- RPV lower head failure: This is the time at which lower head failure is calculated.

- Iodine release to Env > 1%: The time at which the cumulative release of iodine to the environment exceeds 1% of the initial core inventory.

- Fraction of Inventory in Environment at 48 hours: The cumulative release fractions of iodine, cesium and barium to the environment throughout the 48 hour duration of the calculations.

Two important conclusions can be drawn from the results outlined in this table. First and foremost, however, is that reasonable variations in the criteria for SRV failure lead to relatively minor changes in the characteristics of the environmental source term. Over the range of SRV failure criteria considered here, the start time at which fission products are released to the environment varies from the best estimate value by only 2 hours. With only one exception, changes in the cumulative magnitude of fission product release to the environment are negligibly small.[47] This observation enhances confidence that the best estimate result is robust against uncertainties in the SRV failure criteria.

The second conclusion is that the margin from MSL creep rupture is large. The only condition in which the calculated value of the Larson-Miller (L-M) creep damage index for the MSL piping is close to unity is one that was judged by the SOARCA Peer Review panel to be unreasonable (i.e., SRV seizure occurs when the valve experiences 10 cycles with internal gas temperatures above 1000 K). As noted in Section 4.4, this modeling approach was replaced by one that explicitly calculated the thermal response of an SRV internal component. A large margin from MSL creep rupture is observed in all cases using the refined model. This margin can be expressed in at least two ways. One is the low (maximum) values of the L-M damage index for the MSL pipe wall. The second is the very large number of cycles that the valve experiences if stochastic failure is effectively neglected (i.e., if failure occurs only if the valve experiences over 500 cycles, or twice the expected value for failure).

---

[47] The single exception is the case with very early SRV seizure (15 cycles) in the STSBO, in which case the total environmental release fractions are much smaller than other cases.

Table 5-5 Key Metrics of the Impact of Reasonable Variations in SRV Failure Criteria

ENVIRONMENTAL RELEASE FRACTIONS

LTSBO *SRV seizure criterion*	SRV failure mode	Nr of cycles at Seizure	Time of SRV Seizure (hr)	Max MSL L-M Damage Index	RPV lower head failure (hr)	Iodine Release to Env > 1% (hr)	Fraction of Inventory in Environment at 48 hrs: Iodine	Cesium	Ba
Valve Stem > 900K; Stochastic 50%	S	187	7.2						
Valve Stem > 900K; Stochastic 63%	S	270	8.2	5.4E-08	19.8	23.5	2.0%	0.5%	0.6%
Valve Stem > 811K; Stochastic 90%	T	466	11.2	1.2E-05	19.5	21.8	3.2%	3.2%	1.3%
Valve Stem > 900K; Stochastic 90%	T	475	11.4	7.0E-04	19.8	21.2	4.8%	1.8%	0.8%
Valve Stem > 900K; Stochastic 90% (1/2 open area)	T	475	11.4	0.0290	20.2	20.6	3.3%	2.3%	0.8%
Valve Stem > 1000K; Stochastic 90%	T	486	11.5	0.0047	19.7	21.0	5.8%	1.6%	1.5%
Valve Stem > 1100K; Stochastic 90%	T	497	11.7	0.53	20.3	21.0	3.5%	1.9%	1.5%
10 cycles with Gas Temp > 1000K; Stochastic 90%	T	498	11.7	1.0 **	19.5	20.0	3.7%	1.8%	1.6%
STSBO									
Valve Stem > 900K; Stochastic 5%	S	15	5.5 min	2.4E-06	7.4	12.1	1.7%	0.5%	4.3%
Valve Stem > 900K; Stochastic 50%	S	187	1.7	1.6E-05	8.3	9.2	11.4%	1.7%	6.3%
Valve Stem > 811K; Stochastic 90%	T	187	1.7	1.6E-05	8.3	9.2	11.4%	1.7%	6.3%
Valve Stem > 900K; Stochastic 63%	T	195	1.8	0.001	8.2	9.7	11.6%	1.7%	9.6%
Valve Stem > 900K; Stochastic 90%	T	195	1.8	0.001	8.2	9.7	11.6%	1.7%	9.6%
10 cycles with Gas Temp > 1000K; Stochastic 90%	T	211	2.1	0.133	8.1	8.8	11.1%	2.0%	8.4%
STSBO with 1-hr RCIC Blackstart									
Valve Stem > 900K; Stochastic 50%	S	187	1.5	1.9E-04	16.1	24	1.5%	1.4%	1.0%
Valve Stem > 900K; Stochastic 63%	S	270	4.8	5.0E-08	16.7	23.6	1.3%	0.4%	0.7%
Valve Stem > 811K; Stochastic 90%	T	606	9.1	4.1E-05	17.3	17.9	3.8%	1.7%	1.2%
Valve Stem > 900K; Stochastic 90%	T	615*	9.2	6.0E-04	17.0	17.6	3.6%	6.8%	0.4%

Indicates "Best Estimate" Case

S=stochastic
T=Thermal

* The cumulative prob of failure for 615 cycles in nearly 90% (0.897)

** Conditions for creep rupture were calculated, but pipe failure is not modeled in this case.

5.5.2 Extreme variations in failure criteria

If a cycling SRV does not stick in the open position and in-vessel damage progression continue at high pressure, the potential for high pressure creep failure of the RCS becomes a concern. As noted earlier, high pressure creep rupture can either occur in the RPV lower head due to direct heat transfer from molten core debris or by overheating of main steam line piping as hot gases flow to the cycling SRV. Either mechanism of high pressure failure of the RCS has the potential of imparting significantly higher thermodynamic loads on the containment pressure boundary than those observed in calculations described in earlier sections of this report. High containment loads could result from high pressure creep rupture of the RCS because rapid discharge of high temperature, non-condensable gases to the containment would not be efficiently mitigated by the suppression pool in the wetwell.

To investigate this issue, sensitivity calculations was performed to determine the amount by which best estimate SRV failure criteria must be exaggerated for high pressure creep rupture of the RCS pressure boundary to occur. In particular, stochastic SRV failure occurs with 90% confidence if the valve cycles 615 times. The sensitivity calculations described in the previous section suggest thermal failure mechanisms occur well before this number of cycles would occur. In addition, thermal seizure of an SRV was assumed to result with one of the following two extreme conditions:

1. SRV cycling would continue until valve stem temperatures reached a value greater than 1100 K – i.e., greater than the maximum value considered in the sensitivity calculations described in the previous section, or

2. The valve stem seizes in a position that is sufficiently large to prevent further increases in RPV pressure (and therefore preclude pressure relief by another available SRV), but also sufficiently small to maintain pressure above values necessary for MSL creep rupture to occur.

Trial-and-error determined that valve stem temperatures greater than 1175 K satisfied condition-1 for the LTSBO[48] sequence, and valve open fractions of 10% of the nominal flow area satisfied condition-2 for the LTSBO and STSBO sequences.

Table 5-6 summarizes the same metrics listed in Table 5-5, but compares results of the best estimate calculations for LTSBO and STSBO to the extreme situations needed to result in MSL creep rupture. MSL creep rupture was calculated to occur well before lower head failure in each case, so MSL creep rupture is the only high pressure failure mechanism examined here. The comparisons shown in Table 5-5 suggest that if a MSL rupture were to occur, the environmental source terms would be more severe in two respects. First, significant fission product release to environment begins in nearly one-half the time observed in the best-estimate calculations. Iodine release to the environment exceed one percent of the initial core inventory in approximately 24 hours in the best estimate LTSBO calculation, but is reduced to approximately 13 hours in the

---

[48] The STSBO calculation with an assumed SRV failure temperature of 1175 K did not result in MSL creep rupture, as indicated in Table 5-6. Temperatures greater than 1250 K were necessary for the STSBO, which is not considered credible.

cases with MSL creep rupture. The same metric moves forward from nearly 10 hours in the best estimate STSBO calculation to 5.5 hours in the case with MSL creep rupture. This time occurs well before RPV lower head failure in the MSL creep rupture cases for both sequences. Fission product release to the environment begins, in such cases, immediately following MSL creep rupture because the calculated containment pressure is much larger than the failure criterion described in Section 4.6 for drywell head flange leakage. The second way in which the source terms are more severe for the creep rupture cases is the magnitude of the release. The 48-hour release fractions for iodine and cesium are substantially larger than the best estimate values.

It should be noted that the calculations involving creep rupture of an MSL assumed the structural response of the MSL is a fully offset, guillotine break of one MSL. This is considered a conservative assumption because the large break area maximizes the hydrodynamic load to the containment pressure boundary and facilitates fission product transport from the RCS. Alternative credible responses, such as a smaller crack or fissure in the MSL or rupture at an alternative location (i.e., the tailpipe of the open SRV) were not considered in these sensitivity calculations.

Table 5-6 The Effects of Extreme Variations in SRV Failure Criteria on Key Severe Accident Metrics

ENVIRONMENTAL RELEASE FRACTIONS

LTSBO *SRV seizure criterion*	SRV failure mode	Nr of cycles at Seizure	Time of SRV Seizure (hr)	Max MSL L-M Damage Index	RPV lower head failure (hr)	Iodine Release to Env > 1% (hr)	Iodine Release to Env > 1% Rel to Onset of CD (Clad Ox > 1%) (hr)	Fraction of Inventory in Environment at 48 hrs		
								Iodine	Cesium	Ba
Valve Stem > 900K; Stochastic 63%	S	270	8.2	5.4E-08	19.8	23.5	14.4	2.0%	0.5%	0.6%
Valve Stem > 900K; Stochastic 90% (1/10 open area)	T	475	11.4	1.0	19.4	12.8	2.7	17.8%	5.3%	1.5%
Valve Stem > 1175K; Stochastic 90%	T	506	11.8	1.0	19.0	12.9	2.8	15.6%	4.4%	1.4%
STSBO										
Valve Stem > 900K; Stochastic 63%	T	195	1.8	0.001	8.2	9.7	8.6	11.6%	1.7%	9.6%
Valve Stem > 900K; Stochastic 90% (1/10 open area)	T	195	1.8	1.0	8.0	5.5	4.4	18.4%	8.0%	4.7%
Valve Stem > 1175K; Stochastic 90%	T	212	2.1	0.15	8.1	8.9	7.8	12.0%	2.0%	9.0%

Indicates "Best Estimate" Case

S=stochastic
T=Thermal

Grey indicates cases in which MSL creep rupture occurs.

5.6 Loss of Vital AC Bus E-12 – Sensitivity Cases without B.5.b Equipment

This scenario's event progression (Table 5-7) assumes that operators follow the actions directed in Trip Procedure T-101 [3] (RPV control). The estimates of the time at which actions would be taken are based on a table-top exercise with plant operations personnel during a site visit in June 2007. The plant operations personnel would take approximately 15 minutes to assess the situation before taking action. During this time, the RCIC system would actuate and cycle as needed to maintain level. Additionally, one or more SRVs would cycle to control RPV pressure. These systems are assumed to operate automatically based on nominal actuation and termination/closure set points; manual intervention is assumed unnecessary and is not credited within this initial time period. It should be noted that reactor and equipment operators train on taking manual control of RCIC and would likely do so earlier than is assumed in this analysis.

The loss of vital electric power (i.e., the initiating event) results in reactor scram, closure of the MSIV, and containment isolation. In response to this scenario, the operator would be directed, in part, by Trip Procedure T-101. This procedure provides instructions for managing reactor power, water level, and pressure.

Within Trip Procedure T-101, a specific step directs the operators to restore and maintain level between +5 and +35 inches (+177 to +206 inches above TAF) using the following, in order of priority:

- feedwater
- CRDHS
- RCIC
- HPCI
- condensate
- core spray
- low pressure coolant injection

Feedwater is not available in this scenario. However, the CRDHS continues to operate at its nominal (post-scram) flow rate without operator intervention.[49] RCIC is also available and would start automatically upon receipt of a 'low-level 2' signal (i.e., level less than -66 inches relative to instrument zero).[50] Long-term operation of these two systems alone provides sufficient makeup to maintain level. However, RCIC flow terminates in 4 hours when power

---

[49] The procedure directs operators to maximize the CRDHS flow using procedure T-246, but the second pump is not available in this scenario. The only action that can be taken to increase flow is to open the pump discharge throttle valve, which is assumed to occur 1 hour after the initiating event. The licensee estimates this would increase maximum flow (at full pressure) from 110 gpm to 140 gpm.

[50] If the MELCOR reference point is adjusted to use TAF as the reference point, Low-Level-2 corresponds to +106 inches above TAF. This value does not match the value of +124 inches provided by the licensee in response to a 'fact check' of this report requested by the NRC. Correcting this discrepancy would not change the fundamental hydraulic response of the MELCOR model to the Bus E-12 sequence or the SBO sequences because actuation of RCIC fully-restores RPV water level in a very short time. If the time of RCIC actuation is delayed slightly (i.e., based on the 18 inch difference in the modeled versus actual value of 'low-level-2' signal) the minimum value of RPV water level would change, but full level recovery would be nonetheless be calculated.

from station batteries depletes. Parametric MELCOR calculations (described in Section 5.6.3) indicate that battery durations (i.e., RCIC operation) greater than 3 hours are sufficient for long-term operation because after this time, the CRDHS alone can prevent core damage. Therefore, best-estimate MELCOR analysis concludes that this scenario would not lead to core damage as (conservatively) identified in the NRC SPAR model. Additional details of the calculation are provided below.

Table 5-7 Timing of Key Events for Loss of Vital AC Bus E-12

Event Description	Time (hr)
Loss of vital AC bus E-12	0.0
MSIV closure, reactor scram and containment isolation	0.0+
RCIC automatically starts because of low Rx water level	0.2
Operators begin manual depressurization (open 1 SRV)	1.5
Operators take manual control of RCIC to maintain level within range	2.0
Station battery supply exhausted, SRV recloses and RCIC operation terminates*	4.0
Operators secure the single CRDHS pump to prevent reactor overfill	4.3
Reactor pressure back to SRV relief setpoint (SRV automatically cycles)	6.0
Operator restarts single control rod drive hydraulic system pump to restore level	7.0
Cycling SRV fails to reclose after several hundred cycles; reactor depressurizes	13.5
Reactor water level briefly decreases below top of active fuel	13.8
Level restored above top of active fuel	16.0
Level fully recovered to nominal (sequence terminated)	21.0

* As noted in the text, termination of RCIC system operation immediately following a loss of DC power is a conservative assumption when the RPV is at low pressure. At low RPV pressure, it is more probable that the system would continue operating until reactor vessel pressure increased above approximately 400 psig.

5.6.1 Thermal Hydraulic Response

A specific step of Trip Procedure T-101 directs operators to take manual control of the SRVs if they are cycling (i.e., opening automatically at their lift setpoint). Another step further directs operators to open the SRV until the RPV pressure decreases below 950 psig. A quantitative target for the RPV pressure is not prescribed in the procedure, particularly if reduced pressure would not challenge the viability of coolant injection.[51] Preliminary MELCOR calculations indicated that the lead SRV would cycle approximately 50 times before automatic actuation of the RCIC system at approximately 20 minutes into the event. Cycling would temporarily cease and the RPV would briefly depressurize while the RCIC system operated because of the steam flow to the RCIC turbine. RCIC operation automatically and temporarily terminates at 45 minutes when reactor water level is restored to the high-level setpoint. Subsequently, RPV pressure increases and SRV cycling resumes.

Based on this information, operators are assumed to initiate manual depressurization of the reactor vessel 1.5 hours into the event to prevent further cycling of the SRVs. As shown in

[51] It is important to note that manual SRV control requires DC power. Therefore, manual opening of a SRV is viable only while station batteries remain active or with a B.5.b portable power supply.

Figure 5-57, reactor vessel pressure decreases below 200 psig in approximately 1 hour. Reactor vessel pressure stabilizes near 150 psig until 4 hours, when DC power is lost (i.e., station batteries exhaust), and the open SRV recloses. Reactor vessel pressure increases back to the minimum SRV setpoint in 2 hours. For the next 7.5 hours, reactor vessel pressure is maintained at approximately 1100 psig by continuous cycling of the lowest setpoint SRV.

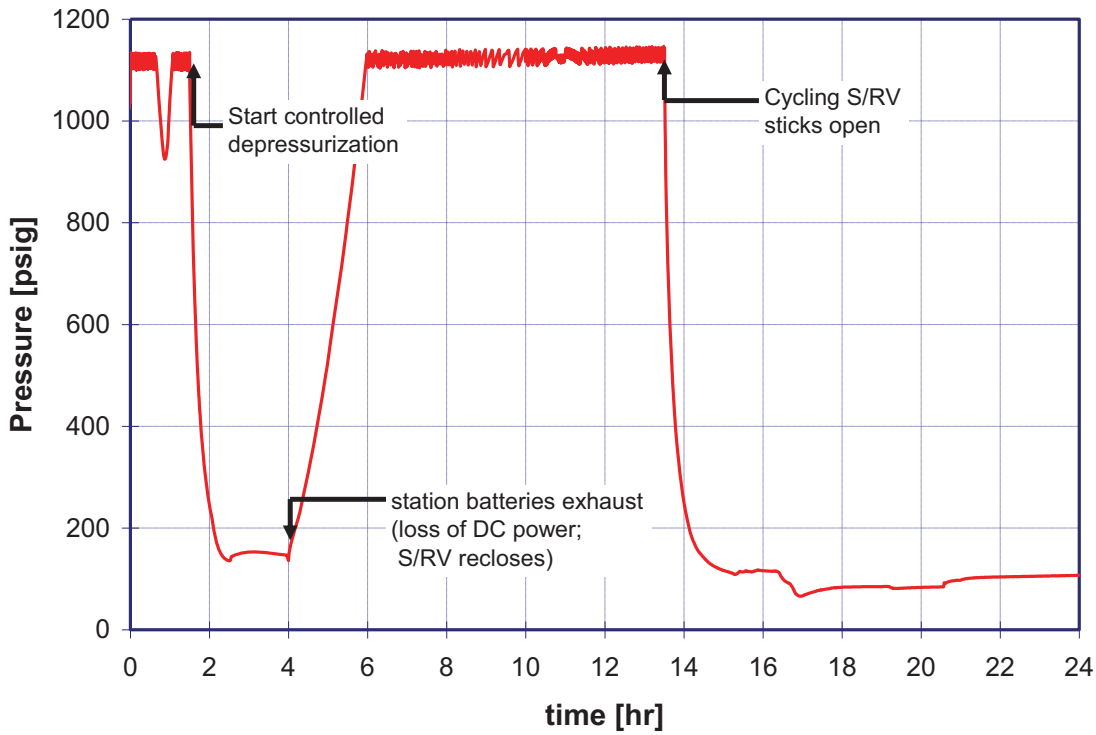

Figure 5-57 Loss of vital AC bus E-12 reactor vessel pressure

At 13.5 hours, after several hundred cycles, the SRV fails to reclose and the reactor vessel again depressurizes. This event represents a random failure of the SRV to reclose, which is calculated by MELCOR based on the number of valve cycles, a failure rate of 3.7×10^{-3} per demand, and a 90 percent confidence level for failure.

Figure 5-58 shows the calculated reactor water level during the entire 24 hour calculation. Water level initially decreases in response to reactor isolation and termination of reactor feedwater. Twelve minutes later, the RCIC system automatically starts and begins to refill the reactor vessel. RCIC flow is automatically terminated at 48 minutes when the water level reaches the high-level setpoint. The water level subsequently decreases slowly because of evaporation resulting from decay heat in the core.

At 1.5 hours, when operators open an SRV to depressurize the reactor, the increased coolant discharge rate through the open SRV accelerates the rate at which reactor water level decreases. The RCIC system automatically starts a second time, briefly stabilizing water level near the low-level setpoint. Two hours into the event, operators take manual control of RCIC turbine speed to reduce injection flow as needed to maintain the water level within range. When the

depressurization transient is completed at approximately 2 hours, the coolant effluent rate through the open SRV is reduced, and reactor water level increases back to the target range. Operators take manual control of RCIC flow during this transient and subsequently maintain the water level within range for approximately 1.5 hours.

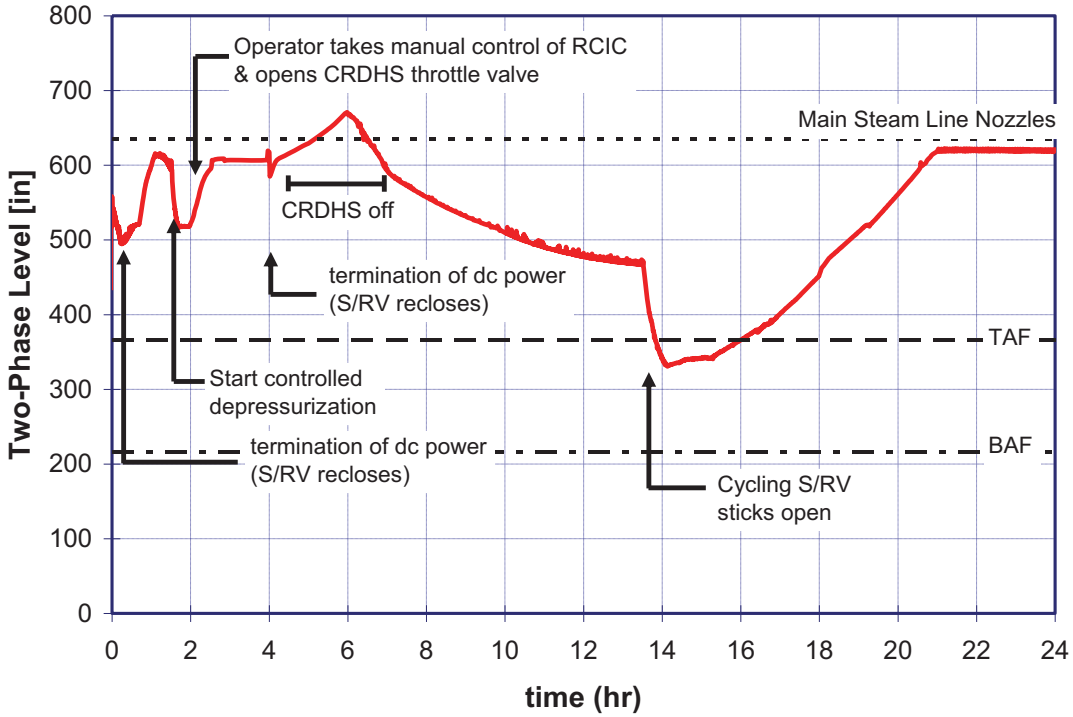

Figure 5-58 Loss of vital AC bus E-12 reactor water level

Four hours into the sequence, DC power from station batteries is exhausted. As noted earlier, this causes the open SRV to reclose, but it is also assumed to result in termination of RCIC system operation. Loss of DC power would cause the RCIC turbine inlet throttle valve to move to a full-open position. If RPV pressure is above approximately 400 psig, the additional steam flow resulting from the change in steam throttle valve position would result in an automatic trip of the system due to steam turbine overspeed. At the time of battery exhaustion in this scenario, however, the steam inlet valve would already be positioned at or near its full-open position to permit adequate steam flow into the RCIC turbine at low RPV pressure. As a result, steam flow to the RCIC turbine would not increase enough to cause an immediate system trip due to turbine over-speed. However, as RPV pressure increases following closure of the SRV, steam flow would increase and an overspeed trip would eventually occur. It is conservatively assumed in this analysis that the overspeed trip occurs immediately following station battery exhaustion.

Between 4 and 6 hours, the reactor vessel pressure slowly increases as shown in Figure 5-57. During this period, coolant losses cease, but CRDHS flow continues. This causes the reactor vessel water level to increase above the upper limit of the target range specified in emergency procedures. Observing this trend, operations personnel are assumed (based on training) to manually secure the CRDHS pump to slow or terminate the increase in reactor water level with the objective of preventing water from spilling over into the main steam lines. As indicated in

Figure 5-58, the MELCOR calculation indicates that this objective would not be met because of expansion of the RCS volume as energy is gradually absorbed by the isolated RCS inventory. The steam lines begin to flood with water approximately one hour after DC power terminates and the open SRV recloses.

Approximately 1 hour after steam line flooding begins, reactor vessel pressure reaches the relief set point of the SRVs, and cycling with its associated discharge of reactor coolant begins anew. The discharge of coolant through the cycling SRV and the absence of any form of active coolant injection (i.e., the CRDHS remains inactive) cause the reactor vessel water level to decrease, eventually reducing below the elevation of the main steam lines and approaching the nominal range. When the level reaches the upper end of the target range (7 hours), the single available CRDHS pump is restarted to compensate for coolant inventory lost through the cycling SRV.

From this point forward in the scenario, the CRDHS operates continuously as the only resource of coolant makeup to the reactor vessel. The coolant delivery rate is approximately 140 gpm (i.e., maximum system flow) while the reactor vessel remains at full pressure. However, following reactor vessel depressurization at 13.5 hours because of SRV failure to reclose, the coolant flow rate increases to over 180 gpm, thereby allowing the reactor water level to increase back to the desired range.

The minimum water level observed in the core is well above the minimum steam cooling water level and fuel heat up, and damage is averted. The reason that this sequence was identified in the SPAR model as a 'core damage' sequence, but the results computed here conclude otherwise, is that the CRDHS system is not credited in the SPAR model. Operation of this system has a significant impact on plant response to the initiating event and a realistic examination of reactor hydraulic behavior leads to a conclusion of 'no core damage.'

5.6.2 Radionuclide Release

Because core damage is averted in this scenario, a release of radionuclides from fuel does not occur and no environmental source term is generated.

5.6.3 Sensitivity Analysis

The analysts performed several sensitivity calculations to examine the effects of alternative assumptions about key features of system performance. Several sensitivity calculations were performed to confirm the conclusion that adequate core cooling would be maintained in this scenario if alternative credible assumptions were made about key features of system performance. This section describes the results of these calculations. In particular, the sensitivity calculations studied following uncertainties:

- Duration of station batteries (DC power): As noted in Section 3.3.2, the actual duration of DC power from station batteries depends on several factors, including battery age and the effectiveness of actions taken by plant personnel to shed nonessential loads from the DC bus. The minimum duration required by plant technical specifications (TS) is 2 hours. However, durations longer than the 4 hour estimate are also possible. Therefore, sensitivity calculations were performed to evaluate the minimum battery duration needed to ensure adequate core cooling in this scenario.

- CRDHS coolant delivery rate: The baseline calculation described in Section 5.6.1 assumes that operators increase the flow rate from the single available CRDHS pump to its maximum capacity. This involves manual actions to open a locked throttle valve in the pump discharge line. Sensitivity calculations were performed to evaluate plant response if this action is not taken.
- Manual depressurization: Plant emergency procedures call for manual depressurization of the reactor vessel, which is assumed to occur 1.5 hours after the initiating event in the baseline calculation. This action has two competing effects on hydraulic behavior in the RPV. Reducing reactor vessel pressure increases the coolant delivery rate from the CRDHS pump, but it also increases the rate at which coolant is discharged from the vessel during the blowdown period. The importance of this action is examined in a single bounding (i.e., worst case) sensitivity calculation, which assumes that manual depressurization does not occur and that operators fail to open the CRDHS throttle valve to permit maximum flow.

The results of the sensitivity calculations examining alternative values of station battery duration are summarized in and Figure 5-59 and Figure 5-60. The calculations considered four distinct values of assumed station battery duration: 2, 3, 4, and 6 hours. These calculations differ slightly from the baseline analysis in two ways. First, the RCIC system is assumed to operate entirely as an automatic system; operator actions to take control of the system to maintain water level within range are not credited. Second, manual actions to maximize CRDHS flow are not credited. The single available CRDHS pump is assumed to operate according to nominal system flow rates.

The calculated reactor water level for these sensitivity cases is shown in Figure 5-59 and the calculated peak cladding temperature in the core is shown in Figure 5-60. The minimum reactor water level is shown to dip below core mid-plane in the case with 2 hour battery duration, with gradually higher values for longer durations. The bounding thermal response of fuel in the core (i.e., maximum cladding temperature) is also improved with increasing battery duration. Fuel cladding failure and accompanying release of the gap inventory of radionuclides occurs in cases with 3 hour battery duration or less. Peak temperatures in cases with battery duration greater than 3 hours are below values at which clad failure would be anticipated (~1200 K).

Results of sensitivity calculations for the other parameters noted above are listed in Table 5-8. Neglecting the beneficial effects of operator actions to control CRDHS flow rate (i.e., maximize flow or secure the system at high reactor water levels) does not alter the conclusion of no core damage. The effects of manual depressurization, on the other hand, are potentially important. If operators fail to maximize CRDHS flow and fail to reduce reactor vessel pressure, core damage would not be avoided even if station batteries sustain RCIC flow for as much as 6 hours. However, in this case the damaged core is reflooded and vessel failure would not occur.

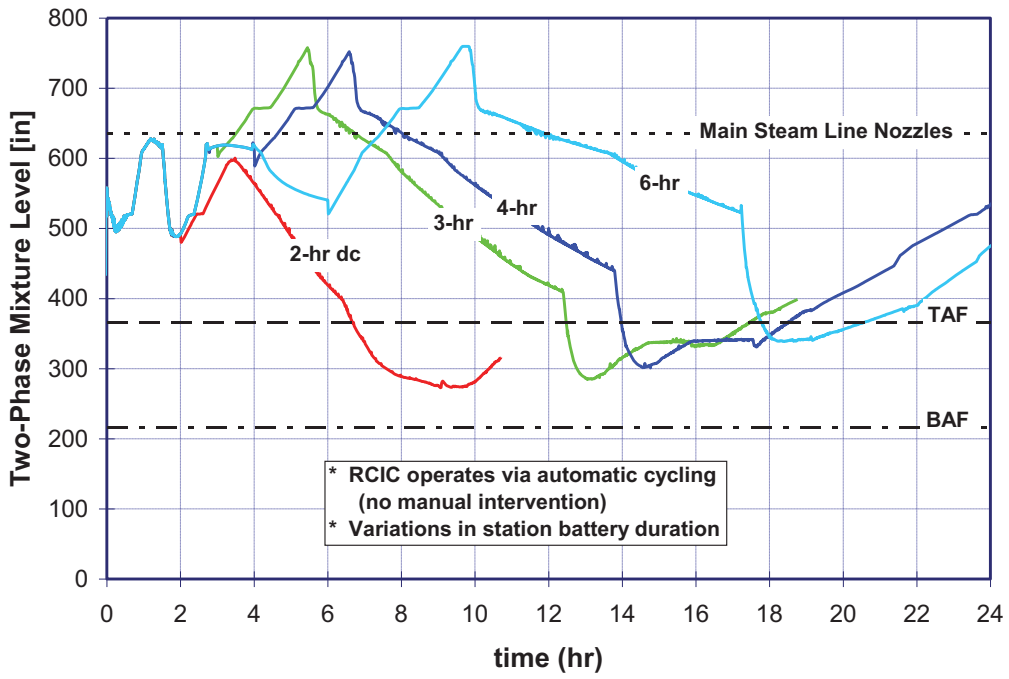

Figure 5-59 Sensitivity of station battery duration: Reactor water level- loss of vital AC bus E-12

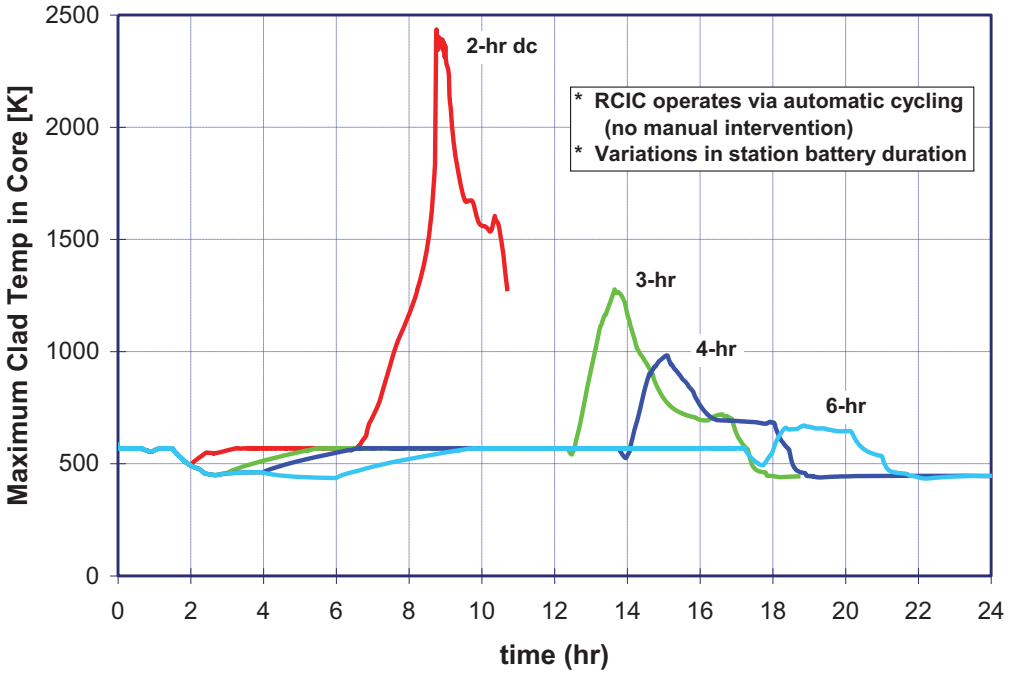

Figure 5-60 Sensitivity of station battery duration: Peak clad temperature- loss of vital AC bus E-12

Table 5-8 Sensitivities for Loss of Vital AC Bus E-12

Sensitivity	RCIC Duration	Maximize CRDHS Flow (Mitigative Action)	CRDHS Off to Prevent RPV Overfill	Depressurize (Open SRV)	Re-pressurize (SRV Closes)	Results*
Base Case	4 hrs	1 hr	4.3 – 7 hrs.	1.5 hrs	4 hrs	No CD
CRD Flow	4 hrs	Not Done	4.3 – 7 hrs.	1.5 hrs	4 hrs	No CD
CRD Flow Battery Life	4 hrs	Not Done	Not Done	1.5 hrs	4 hrs	No CD
	Several cases spanning the range of 2-6 hrs	Not Done	Not Done	1.5 hrs	2-6 hrs	> 3 hr life averts CD
Depressurize	≥3 hrs	Not Done	Not Done	Not Done	N/A	CD, no VF

* Where, CD = core damage. VF = vessel failure.

5.7 Peer Review

The SOARCA peer review panel identified a few issues that motivated sensitivity calculations to investigate their effects. Results of many of these calculations have already been discussed in earlier sections of this report. Most notable is the sensitivity of core damage progression and fission product source terms to SRV behavior after the onset of core damage (Section 5.5). Sensitivity calculations were performed to examine the importance of three additional issues and are described below.

1. Containment leakage before failure
2. Atmospheric mixing in the drywell.
3. Leakage through TIP guide tubes

In all cases, an early (preliminary) version of the LTSBO calculation[52] was used as the basis for investigating these issues. The following sections summarize the results of the sensitivity calculations for each issue.

5.7.1 Containment Leakage before Failure

The initiating event for the station blackout accident scenarios (i.e., both long- and short-term) is assumed to be a large beyond design-basis seismic event. The baseline calculations assume that containment leakage is limited to the maximum allowable by plant-specific TS. This assumption represents more leakage than would be anticipated during normal operation, because routine testing of containment leak tightness strives to control leakage well below the TS limit. However, this assumption does not directly account for the possibility that leakage greater than the TS limit could be caused by a large seismic event.

Two sensitivity calculations were performed to examine the impact of seismically induced increased leakage on radiological release to the environment. One case assumed a leak area

---

[52] The 'base case' calculation described in the following two sections differs slightly from the best estimate calculation of the LTSBO scenario described in Section 5.1. The difference lies solely in the assumed conditions for SRV failure. As described in Section 5.5, small differences in SRV failure criteria have a negligible effect on calculated source terms.

three times larger than the TS limit;[53] a second case assumed an area 10 times the TS limit. Increased levels of containment leakage have a very small impact on the final environmental source term, as shown in Figure 5-61. Prior to containment failure (i.e., zero to 19.5 hours in the LTSBO scenario), increased leakage has a small, but noticeable impact on the release of volatile iodine and cesium to the environment. However, the magnitude of release during this period of leakage is negligibly small in comparison to releases that occur shortly after containment failure.

Increased levels of containment leakage do not affect the long term release of iodine or cesium because the vast majority of volatile species are swept to the suppression pool through the open SRV. Section 5.1.2 discusses this topic in more detail. Increases in containment leakage also have a negligible effect on the long-term release of iodine and cesium to the environment.

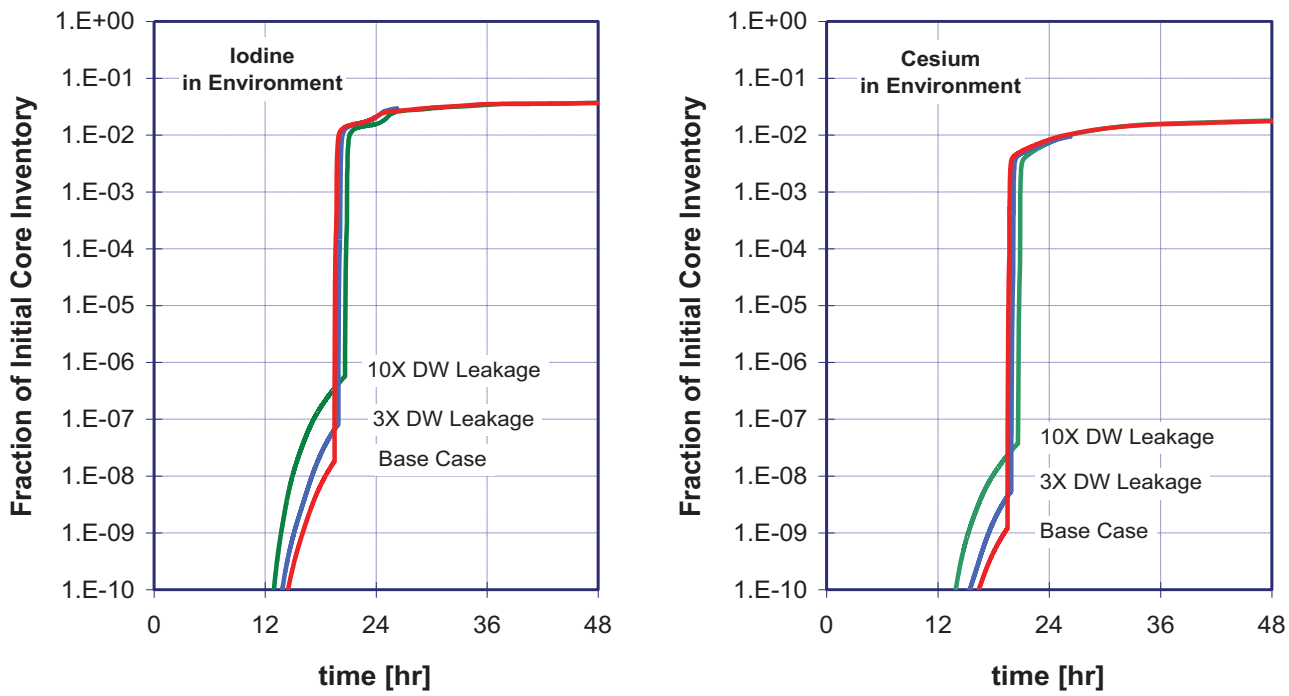

Figure 5-61 Effect of increased containment leakage on the release of iodine to the environment

5.7.2 Atmospheric Mixing in the Drywell

The hydrodynamic model of the containment cannot explicitly calculate buoyancy-driven natural circulation flow patterns. The spatial representation of the drywell, in particular, is a simple series of three vertically-stacked control volumes, each connected by a single flow path. The possibility of rising hot gases and descending cooler gases within this region of the containment cannot be rigorously represented in the current MELCOR modeling framework. The absence of

---

53 Containment leakage is modeled as a constant area opening in the containment pressure boundary. The actual leak rate, therefore, varies with internal pressure. Leakage corresponding to the TS limit is based on the area that would produce a leak rate of 0.5 percent of the containment free volume per day at an internal pressure of 56 psig. The leakage is assumed to be located in the drywell, where the largest number of penetrations through the containment pressure boundary is located.

natural circulation in the MELCOR calculations results in an inverted, stratified temperature profile within the drywell after RPV lower head failure as indicated in Figure 5-62. This configuration is possible if the buoyancy-driven natural circulation within the drywell is inhibited by flow resistance associated with piping and other equipment within the drywell.[54] Further, depressurization of the containment through the opening created in the drywell shell near the elevation of the drywell floor (i.e., the base of region D in Figure 5-62) would preferentially discharge a high-temperature atmosphere near the bottom of the drywell, perhaps supporting a high-temperature region near the drywell floor.

On the other hand, the vertical temperature differences between the top and bottom of the drywell reflected in Figure 5-62 represents a very strong driving force for upward flow. If a return (downward) flow path for cooler air from the top of the drywell is established, the resulting flow pattern would enhance mixing of the drywell atmosphere before being discharged to the reactor building. Analytical models for properly calculating buoyancy-driven natural circulation flow patterns with a large volume, such as a BWR Mark I drywell, are not available within MELCOR. However, the effects of atmospheric mixing can be examined by imposing a flow path configuration in the MELCOR model that encourages flow among the three vertically-stacked control volumes representing the main body of the drywell atmosphere. This configuration involves replacing the single flow path connecting adjacent control volumes with two parallel flow paths and defining the endpoints of parallel flow paths to be slightly asymmetric.

This adjustment to the baseline modeling approach was made in a sensitivity calculation. The result was a nearly continuous circulation velocity within the drywell of approximately 0.5 meters per second and, as shown in Figure 5-63, a merging of atmospheric temperatures in the control volumes representing the main body of the drywell. The atmospheric temperature within the reactor pedestal (i.e., region D in Figure 5-63) is not significantly affected by this modeling adjustment. However, the impact of drywell atmospheric mixing on the radiological source term to the environment is small as indicated in Figure 5-64. The final release fractions of iodine are nearly the same in the baseline and sensitivity calculation. The long-term cesium release fraction increases by a small amount in the sensitivity calculation.

---

[54] Unlike the idealized image shown on the right-hand side of Figure 5-62, a large fraction of the internal free volume and horizontal cross-sectional area of the drywell is displaced by piping, valves, electrical control and instrument cabling and several layers of work platform grating.

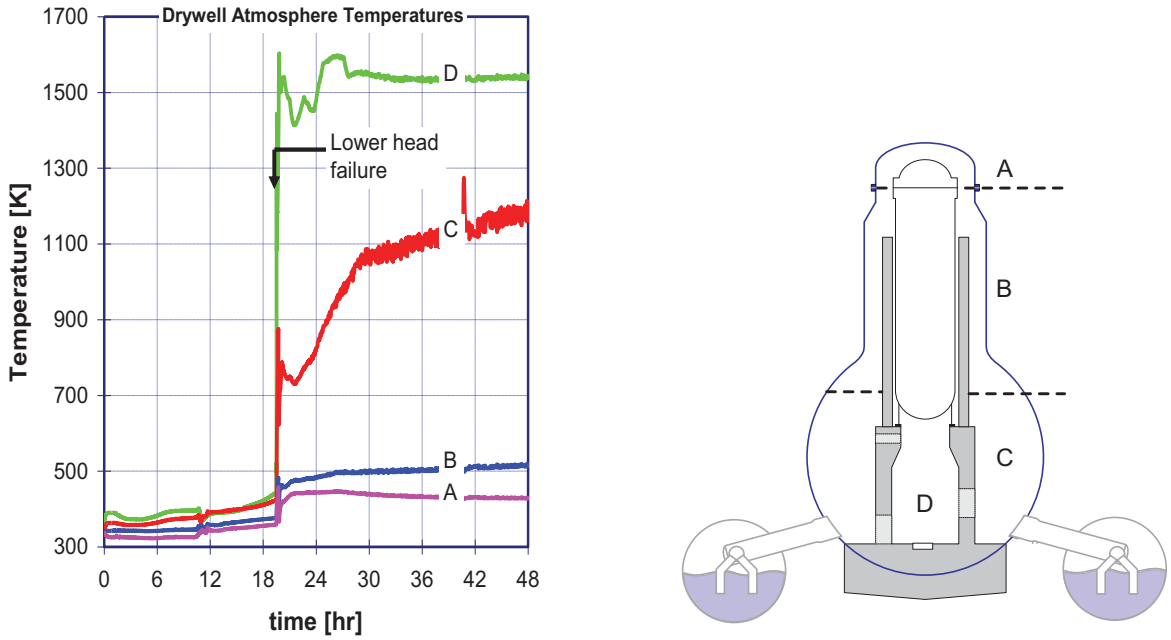

Figure 5-62 Drywell atmospheric temperatures in the baseline LTSBO calculation

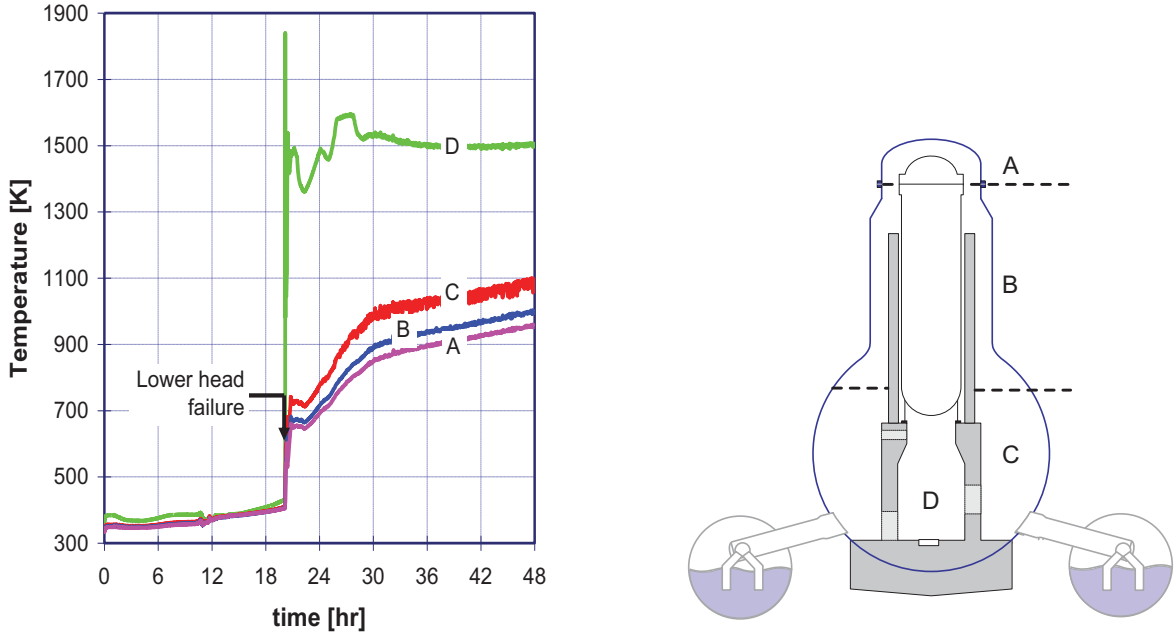

Figure 5-63 Drywell atmospheric temperatures with imposed drywell circulation

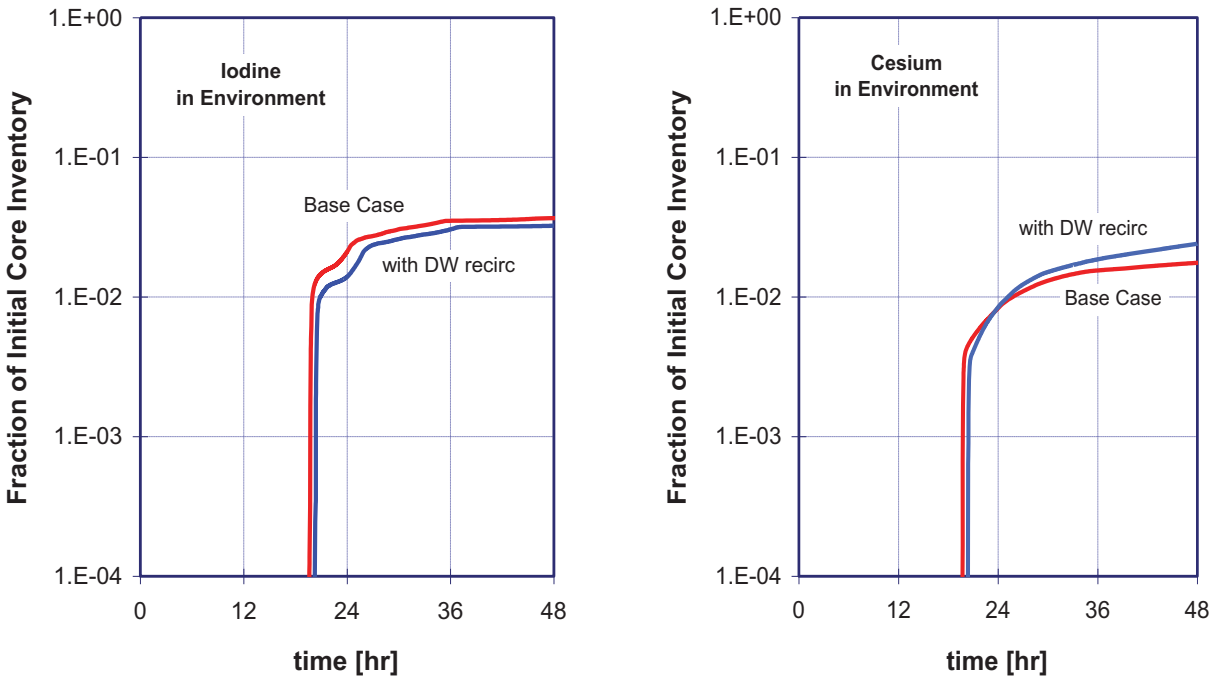

Figure 5-64 Effect of modeling circulation flow within the drywell on iodine and cesium release to the environment

5.7.3 Leakage through TIP guide tubes

The description of the Peach Bottom MELCOR model in Section 4.2.4 mentioned that the TIP system operates for approximately one hour every four months. As a result, the baseline SOARCA calculations assume this system is isolated at the time the postulated accident occurs. However, because the TIP guide tubes offer a pathway for hydrogen and fission products to bypass the containment pressure boundary, a sensitivity calculation was performed to examine the potential consequences of leakage through the system, if it was in operation. The sensitivity calculation applied the additional features to the Peach Bottom MELCOR model described in Section 4.2.4. In particular, a hydrodynamic control volume and associated flow paths and heat structures were added to represent the internal volume, cross-sectional (flow) area and internal surfaces of the TIP guide tubes. The sensitivity calculation examines a bounding case, in which all three guide tubes are assumed to be active (i.e., the isolation valves are open) and all three probes are fully withdrawn into their respective shield chambers. This represents a physical configuration with maximum plausible leakage through the guide tubes.

Flow through the guide tubes begins when the instrument tubes in the core have melted, exposing the internal volume of the tubes to RPV pressure. The MELCOR model represents in-core instrumentation tubes as miscellaneous steel structure within the core, which typically begins to melt when local clad oxidation reaches levels that challenge the physical integrity of fuel. Therefore, the MELCOR flow path from the RPV to the TIP guide tubes opens when damage to fuel in the center of the core exceeds the failure criterion for erect fuel (i.e., fuel pins collapse into particulate debris.) The actual area through which material would be released into the reactor building is difficult to define, as it is characterized by gaps and mechanical clearances in moving components within the probe shield chamber and drive mechanisms, which can

deteriorate if subjected to very high temperature gases (as would be expected in this case). The sensitivity calculation assumed the leak area in the reactor building is equivalent to the cross sectional area of the tubes. Or viewed another way, the leak rate into the reactor building is limited by flow resistance in the tube itself, not by the open area at the terminus of the guide tube. It should also be noted that the MELCOR model accounted for diversion of flow from the TIP guide tubes into the drywell through relief valves (or blowout valves) located in the indexing units. The valves are designed to open at a small differential pressure (a few psi), to protect the tubes and indexing units from over-pressure by the nitrogen purge system. These valves will, therefore, open when the tube is exposed to RPV pressure, allowing hydrogen and fission products to leak into the containment as well as the reactor building.

The sensitivity calculation is a permutation of the unmitigated LTSBO accident scenario described in Section 5.1. With the single exception of the modeling features described above to represent leakage through open TIP guide tubes, the MELCOR model is identical to the one used for the baseline unmitigated LTSBO calculation.

The calculated thermal-hydraulic response of the RPV and containment are not affected by the small amount of steam and hydrogen that leaks through the open TIP guide tubes. The signatures for RPV pressure and water level, containment pressure and temperature, as well as the in-vessel core damage parameters are essentially identical to those described in Section 5.1. Although hydrogen and fission products leak through the relief valves in the TIP indexing unit to the drywell atmosphere, the amounts transported to containment by this leak path are negligible in comparison to the amounts transported to containment through the SRV on the main steam line SRV.

Differences in calculated results are observed, however, in the reactor building. Leakage through the TIP guide tubes begins after significant oxidation of Zircaloy cladding in the core has begun. As a result, hydrogen enters the open TIP tubes and is slowly discharged directly to the reactor building. Figure 5-65 compares total mass of hydrogen in the reactor building in the sensitivity calculation to the amount in the baseline LTSBO calculation. The slow accumulation of hydrogen in the building due to TIP tube leakage is clearly evident in the sensitivity calculation. In contrast, the building is nearly free of hydrogen until containment failure occurs in the baseline (unmitigated) LTSBO calculation.

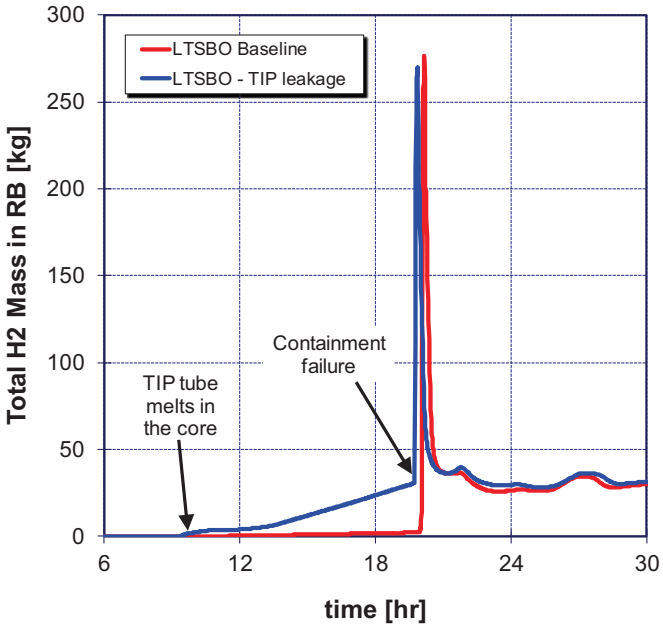

Figure 5-65 Total Hydrogen Mass in the Reactor Building (TIP Sensitivity calculation versus unmitigated LTSBO baseline)

Approximately 30 kg of hydrogen is released to the reactor building over a period of 10 hours before containment failure. This hydrogen accumulates primarily in the atmosphere of the ground level floor of the building, but is also carried upward through the open equipment chase due to buoyancy. Although sufficient oxygen is available to react with the hydrogen, maximum hydrogen concentrations in these regions of the building are well below the flammability criterion of 10%. The maximum concentration calculated (just prior to containment failure) is approximately 2% in the volume closest to the release point at the TIP room. As a result, combustion of hydrogen in the reactor building is not observed in the sensitivity calculation until after containment failure.

Low hydrogen concentrations during the early period of TIP tube leakage are partly due to the assumption of uniform mixing within the large control volumes used to represent the building atmosphere. Although the reactor building is sub-divided into several hydrogen dynamic control volumes (two are used to represent the north and south halves of the building where the TIP release point is located, for example), the free volume of building is rather large. On the other hand, the total amount of hydrogen released (30 kg) is very small in comparison to the amounts released from the containment when drywell head flange leakage or (more importantly) liner melt-through occurs. This is evident in Figure 5-66, which compares the integral quantity of hydrogen released to the reactor building. The amount released prior to containment failure in the TIP leakage sensitivity calculation is overwhelmed by the amount released as a consequence of containment failure.

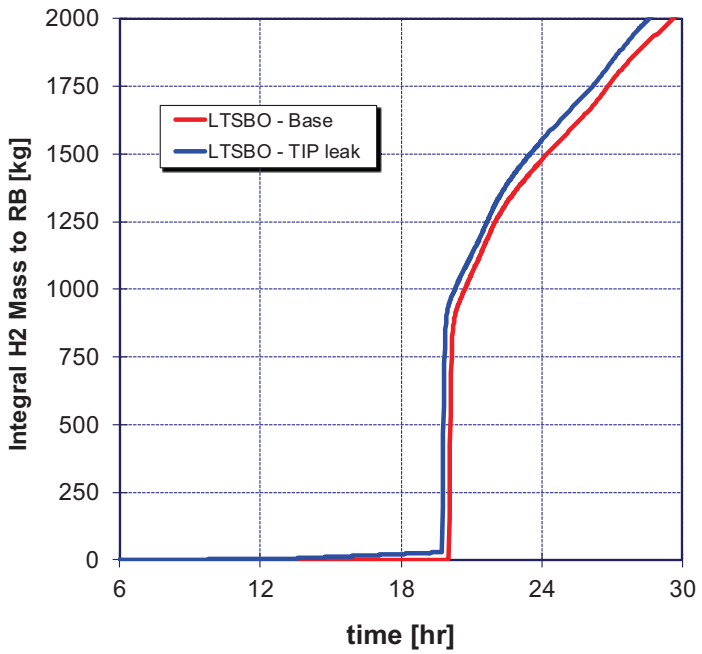

Figure 5-66 Integral Mass of Hydrogen Released to the Reactor Building (TIP Sensitivity calculation versus unmitigated LTSBO baseline)

Fission products are also released through the leaking TIP tubes. Figure 3 shows the long-term release of fission products to the environment is affected only slightly by the early release through leaking TIP tubes. As shown in Figure 5-67, the amount of volatile aerosol species released to the environment immediately following containment is larger in the sensitivity calculations than the baseline calculation. Early leakage of iodine, cesium and (to a lesser extent) molybdenum to the reactor building through the open TIP tubes creates a stable airborne concentration of volatile fission product aerosols in the building. For example, Figure 5-68 compares the amount of iodine in the reactor building (airborne plus deposited) in the sensitivity calculation to the amounts observed in the baseline LTSBO calculation. The airborne mass of fission product is swept out of the building by the relatively large discharge of gas accompanying containment failure and subsequent hydrogen burns. This increases the amount released to the environment immediately following containment failure, but (as indicated in Figure 5-67) has a negligible effect on the larger, long-term integral release of iodine to the environment.

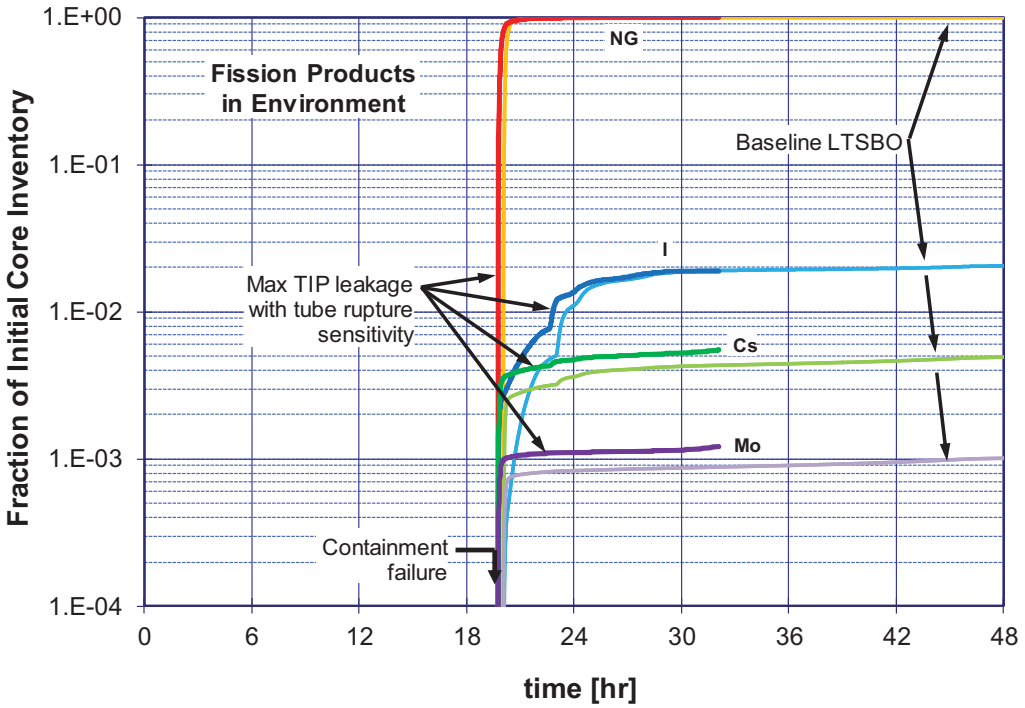

Figure 5-67 Fractional Release of Key Fission Products to the Environment (TIP Sensitivity calculation versus unmitigated LTSBO baseline)

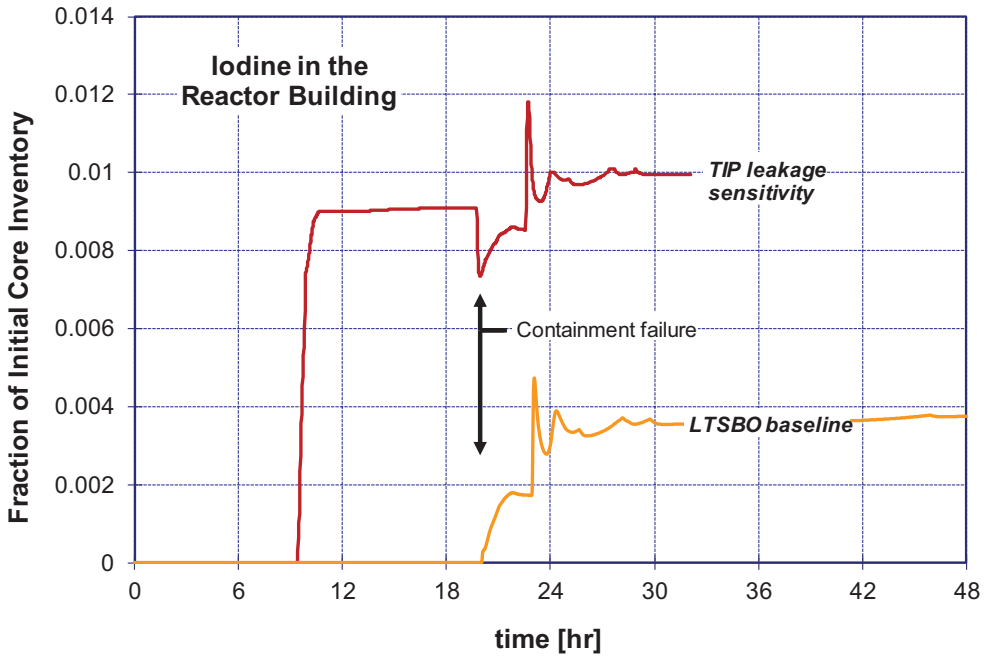

Figure 5-68 Iodine and Cesium in the Reactor Building (TIP Sensitivity calculation versus unmitigated LTSBO baseline)

Early leakage of fission products through the open TIP guide tubes shifts the time at which radioactive aerosols are released to the environment by several hours. As indicated in Figure 5-69, noble gases begin to leak to the environment in small quantities soon after core damage begins. The baseline unmitigated LTSBO calculation assumes the containment leaks at the design basis leak rate of approximately 0.5 volume percent per day. This results in a very small, but steady, release of noble gas starting as early as 11 hours after the initiating event in the baseline unmitigated LTSBO calculation, and approximately one hour earlier in the sensitivity case with TIP tube leakage. The temporal effect on leakage of radioactive aerosols is much more significant. Iodine, cesium and other volatile species are released to the environment at rates comparable to noble gases (in terms of the fraction of core inventory released) for many hours prior to the time of containment failure.

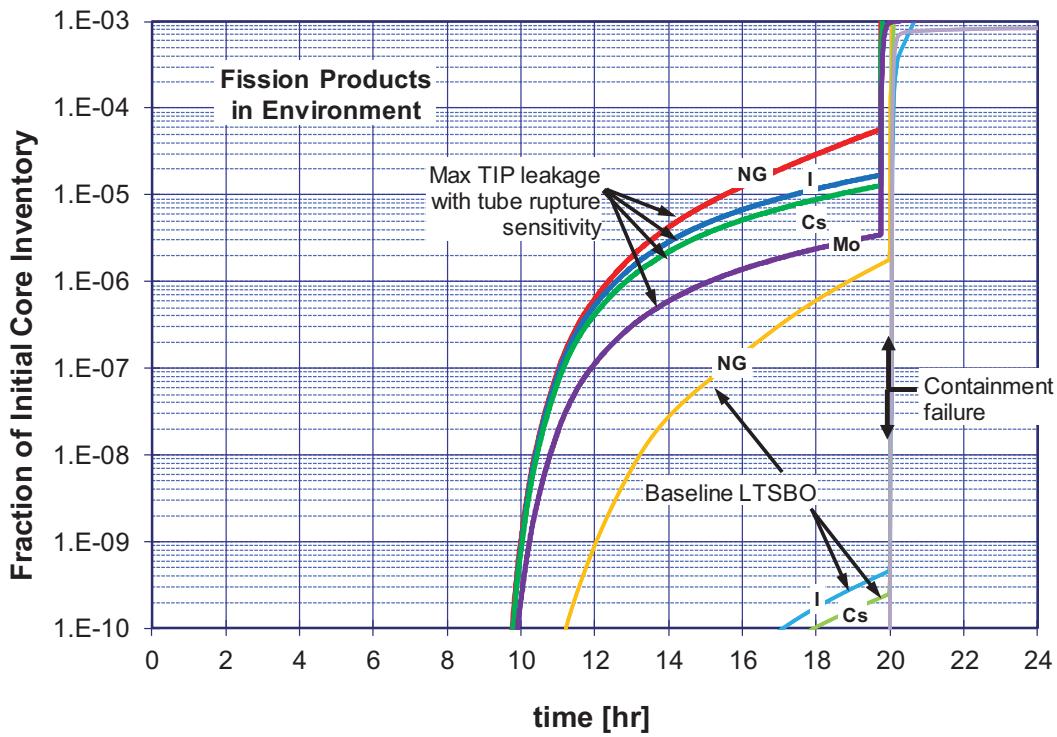

Figure 5-69 Early Leakage of Key Fission Products to the Environment (TIP Sensitivity calculation versus unmitigated LTSBO baseline)

5.8 Barium Release Variations

In the preceding sections, some considerable variability is observed with respect to Barium releases, with a general trend that environmental releases for the short-term SBO are on the order of 8% to 10% and for the long-term SBO, on the order of 0.5% to 1%, as illustrated in Figure 5-70. The observed moderately large and consistent trend is due mainly to differences in release rate from fuel during the ex-vessel molten core-concrete interaction (MCCI) phase of the accidents, which in turn is strongly influenced by the MCCI temperatures realized during the respective MCCI phases. As seen in Figure 5-70, the MCCI temperatures are moderately higher in the short term SBO cases, in part due to higher in-vessel core material temperatures associated with the comparatively higher decay heat levels in STSBO versus LTSBO. This bias also favors

a more vigorous initial MCCI reaction rate which also drives MCCI temperatures upwards. Finally, the Ba release rate is strongly affected by the chemical form of Barium, with the reduced form of Ba metal being significantly more volatile than the oxidized form BaO. These effects are explained as follows.

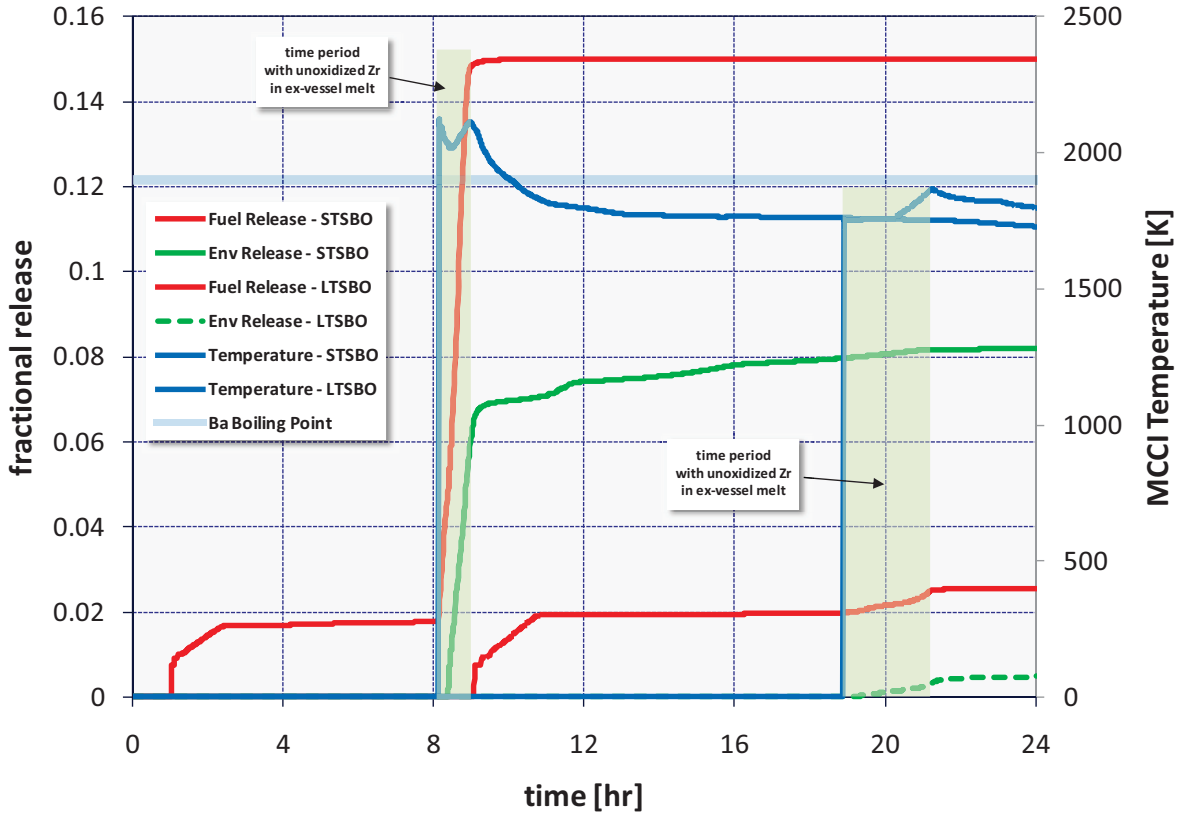

Figure 5-70 Barium release trends in STSBO compared to LTSBO

The speciation of the Barium during MCCI between the metallic and oxide forms is strongly influenced by the reduction/oxidation conditions in the ex-vessel core melt mixture, and this in turn is strongly coupled to the presence of (*or lack of*) Zr metal in the melt, Zirconium being one of the strongest reducing agents in the periodic table. On exiting the failed vessel, the core material contains significant quantities of unoxidized zirconium metal. This is especially true for BWRs because of the large mass of Zr associated with the fuel channel boxes in comparison with PWRs. This Zr metal relatively quickly oxidizes to ZrO_2 during the early stages of the MCCI, and therefore is short-lived in the overall duration of the MCCI phase; however, during the time that metallic Zr persists in the MCCI, the speciation of Barium is shifted towards favoring the reduced metallic Ba form. The speciation tendency can be roughly expressed by the following highly simplified net chemical reaction,

$$Zr + 2\,BaO \;\rightarrow\; ZrO_2 + 2Ba$$

At the same time, Zr is also reacting with steam from concrete decomposition, producing hydrogen gas,

$$Zr + 2\,H_2O \;\rightarrow\; ZrO_2 \;+ 2H_2$$

further driving chemically reducing conditions as suggested by the following reaction

$$BaO + \;H_2 \;\rightarrow\; Ba \;+ H_2O$$

All of these reactions have negative Gibbs energy changes that drive the reactions in the direction indicated. Moreover, the high volatility of the reaction product Ba and the sparging effect of the evolving gases facilitate mass transfer and work to ensure that the reaction continues in the direction indicated in the reaction by keeping the concentration of Ba in the melt at a low value. As the Zr metal in the MCCI is consumed, principally by reaction with the steam evolved from the dehydration of the concrete, the reduction of BaO to Ba dissipates and thereafter BaO is thermodynamically favored.

The importance of the chemical form for Ba, determined by the presence of (*or lack of*) metallic Zr, is with the differing volatility of the metallic versus oxide form, as illustrated in Figure 5-71, where estimates for the vapor pressures for Ba and BaO are shown. In this graph, the Ba vapor pressure is taken from the MELCOR material properties, whereas the trend for BaO is simply approximated by interpolating between the Ba melting point and boiling point taken from chemical handbook data.

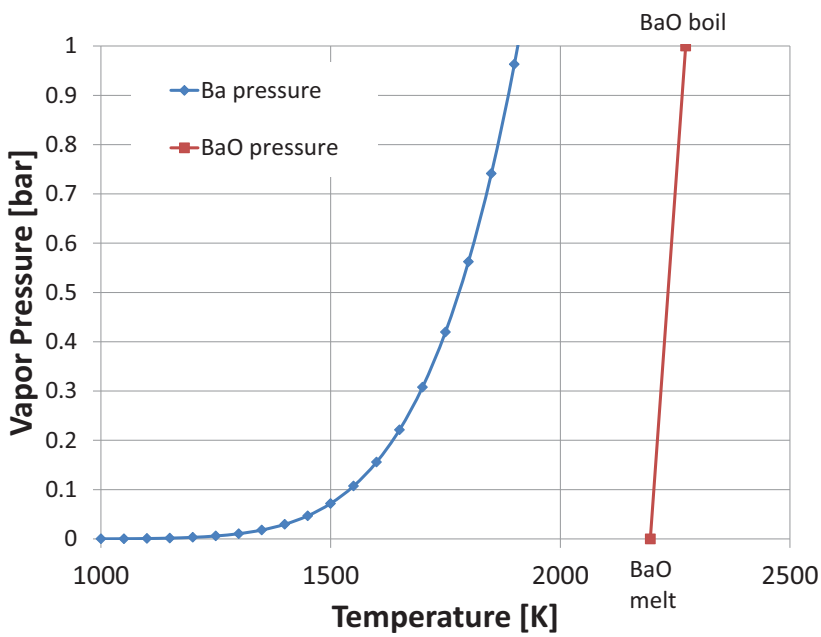

Figure 5-71 Vapor pressure of Ba metal and BaO (oxide vapor pressure is estimated)

As seen in Figure 5-71, the Ba metal shows a wide range of volatility between the range of temperatures typical of MCCI (1600 K to 2000 K), whereas, the BaO form does not have high volatility until temperatures exceed roughly 2250 K.

The trends observed in Figure 5-70 can now be explained. For both the LTSBO and the STSBO, prior to vessel failure, the fractional release of Barium *in-vessel* are nearly identical at about 2% of the core inventory. Following lower head failure, in both the short term and long term SBO, there is a brief period of time when unoxidized Zr is present in the *ex-vessel* MCCI indicated by the light green shaded regions in Figure 5-70. During that time, the Ba release is seen to increase over the in-vessel released quantity. This renewed release is made possible by the Zr-reduction of BaO to the metallic form which shows significant volatility in the range of temperatures driven by the MCCI; however, the ex-vessel release for the STSBO case is significantly greater than for the LTSBO. This is because MCCI temperatures for the STSBO actually exceed the boiling point of the Barium metal. This difference in MCCI temperature is attributable to the temperatures attained by the core materials prior to lower head failure and largely attributable to the significantly larger decay heat level associated with the STSBO compared with the LTSBO, when the decay heat has dropped significantly. These trends are suggested in Figure 5-72 and Figure 5-73. Finally, metallic Zr release from the vessel to the drywell cavity is larger in the STSBO case in comparison to the LTSBO case where relocation takes place over a more protracted time frame and in two stages. These factors in combination would appear to explain the higher Ba releases in the STSBO cases relative to the LTSBO case.

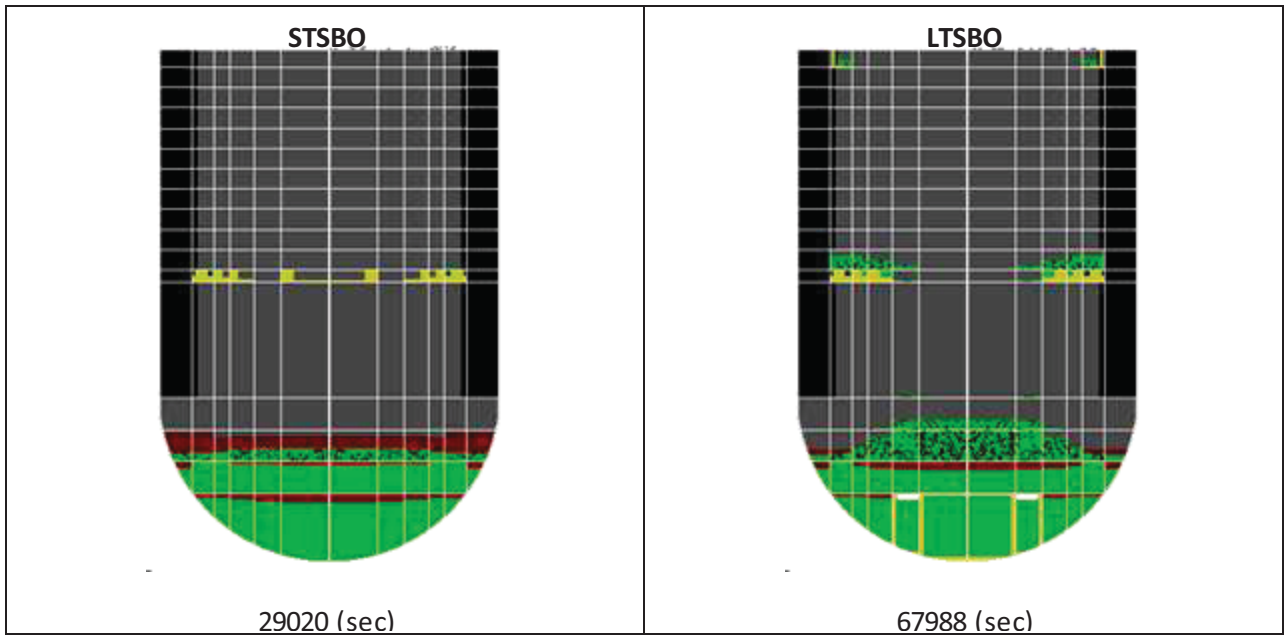

Figure 5-72 Relative core damage states for STSBO versus LTSBO. The STSBO damage is slightly more extensive with portions of the core forming molten pools

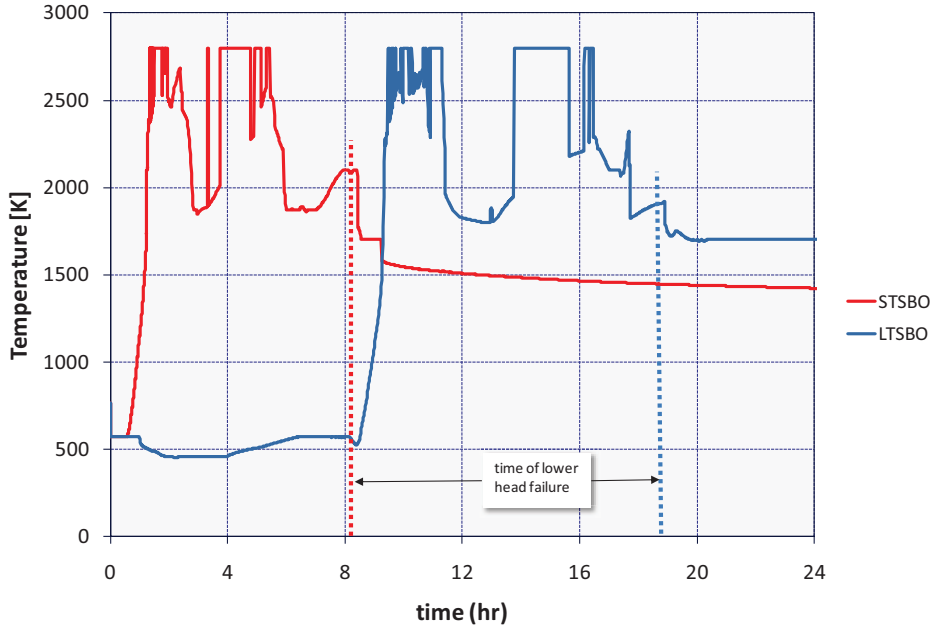

Figure 5-73 Maximum core temperature for STSBO and LTSBO analyses. At the time of lower head failure, core temperatures are somewhat higher in the STSBO case

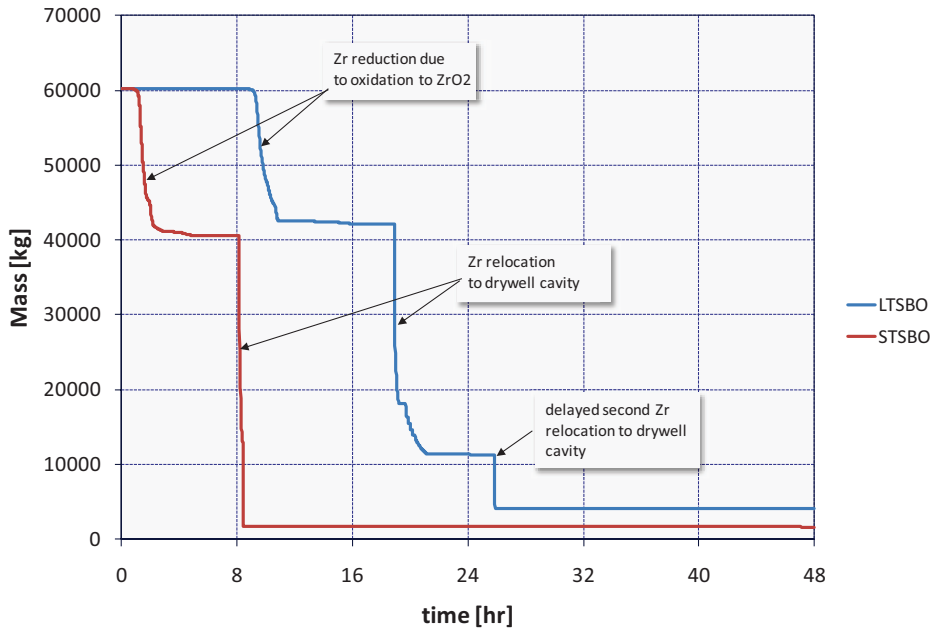

Figure 5-74 Zr content in-vessel

As shown in Figure 5-74, relocations to cavity are evident at just after 8 hours in the STSBO and just before 20 hours in the LTSBO. More unoxidized Zr is released promptly in the STSBO case, whereas two relocations events are evident in the LTSBO case.

After the metallic Zr has been depleted from the MCCI, both cases show the release of Ba to drop significantly, essentially ceasing as the thermodynamics thereafter favor the lower volatile BaO chemical form. The environmental releases simply follow the release trends from the fuel, mainly the MCCI-driven Ba release. In closing this discussion, it should be noted that the ex-vessel release of Barium is treated by the VANESA module of MELCOR, which considers the thermodynamic effects on Barium speciation, albeit in the context of a much larger system of chemical elements. This sophisticated treatment enables MELCOR to capture this transient high volatility of Ba during the Zr-rich phase of the MCCI. In contrast, in-vessel releases of Ba are treated using the less sophisticated CORSOR-Booth model for release from fuel. The in-vessel releases from the degrading fuel rods predicted using the Booth model are well validated against experimental data from testing programs. It could be argued however releases from the lower head molten fuel mixture are not well studied and could warrant a thermodynamic treatment as in VANESA as opposed to the Booth treatment as currently employed in MELCOR. That said, low surface to volume ratio for the in-vessel molten pool stages of core melt progression do not favor large release rates mainly from mass transport limitations. For this reason, a full thermodynamic modeling treatment is not warranted in this stage of the accident.

6.0 EMERGENCY RESPONSE

Emergency response planning is in place to protect the public health and safety in the unlikely event of an accident at a nuclear power plant. Advancements in the consequence model now allow more detailed and more realistic treatment of emergency response when performing consequence analyses. This includes the ability to model protective action decisions from offsite response organizations (OROs) and the implementation of protective actions by individual population segments. These advancements are significant because they facilitate more realistic modeling of response activities, timing of decisions, and implementation of protective actions across different population segments.

Emergency response programs are developed, tested, evaluated, and established as defense in-depth. To support a state-of-the art approach and integrate realism into the analyses, the modeling of the emergency response was based on the site-specific emergency planning documentation. The information developed in this emergency response section was used to support the MACCS2 consequence analyses for the accident scenarios. These analyses are conducted for the unmitigated accident sequences only. Many of these response actions would be similar for the mitigated case because response officials initiate protective actions upon notification, which as described herein occurs very early in the incident, even before mitigation actions have been implemented. This is because emergency planning is designed to be proactive to remove the public prior to plume arrival when possible. For each accident scenario, evacuation of the plume exposure pathway emergency planning zone (EPZ) was assessed. This included consideration of a shadow evacuation to a distance of 20 miles from the plant. Including a shadow evacuation, which occurs when members of the public evacuate from areas that are not under official evacuation orders, provides realism because these are observed in large-scale evacuations and have the potential to slow down the evacuation from the affected area. Also, for each scenario, members of the public were modeled as being relocated from any area where doses are projected, based on the consequence analysis model, to exceed established criteria. Figure 6-1 identifies the location of the Peach Bottom plant and radial distances of 10 and 20 miles from the plant.

Sensitivity analyses were completed to evaluate evacuating the public to distances of 16 miles and 20 miles from the plant. The sensitivity analysis of an evacuation to 20 miles is different than the shadow evacuation to 20 miles described above, because the sensitivity analysis evaluates the conditions under which residents of the entire 20 mile area are notified to evacuate and leave the area. A sensitivity analysis was also completed to assess the effect of a delay in the implementation of protective actions, as suggested by the peer review committee. An analysis was also conducted to evaluate the effects on infrastructure, emergency response, and response of the public due to a seismic event.

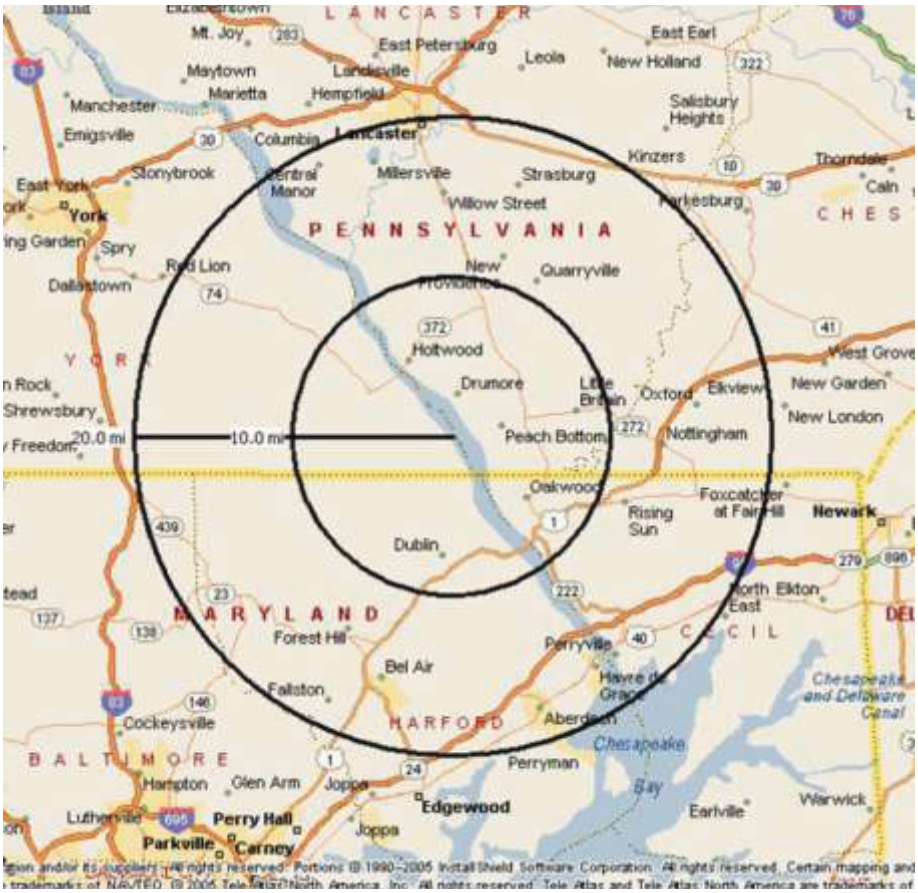

Figure 6-1 Peach Bottom 10 and 20 mile analysis areas

As required by 10 CFR Part 50, "Domestic Licensing of Production and Utilization Facilities," OROs develop emergency response plans for implementation in the event of a nuclear power plant accident. These plans are regularly drilled and inspected biennially through a demonstration exercise performed with the licensee. In biennial exercises, (every 2 years) ORO personnel demonstrate timely decision making and the ability to implement public protective actions. Emergency plans escalate response activities in accordance with a classification scheme based on emergency action levels (EALs). Preplanned actions are implemented at each classification level, including Unusual Event, Alert, Site Area Emergency (SAE), and General Emergency (GE). Public protective actions are required at the GE level, but ORO plans commonly include precautionary protective actions at the SAE level and sometimes at the Alert level. For example, at Peach Bottom sirens are sounded at the SAE to inform the public that an incident has occurred and they should monitor Emergency Alert System (EAS) stations for updated information.

The plume exposure pathway EPZ is identified in NUREG-0654/FEMA-REP-1, Revision 1, "Criteria for Preparation and Evaluation of Radiological Emergency Response Plans and Preparedness in Support of Nuclear Power Plants," issued November 1980 [20], as the area of about 10 miles around a nuclear power plant. Within the EPZ, detailed emergency plans are in place to reduce the risk of public health consequences in the unlikely event of an accident. Emergency planning within the EPZ provides a substantial basis for expansion of response

efforts if necessary [20]. During the inspected biennial exercises, ORO personnel have repeatedly demonstrated the ability to implement protective actions within the EPZ. Modeling of the expected protective action responses described in this section is consistent with exercise performance data. The analysis includes the State of Pennsylvania position that, if an evacuation is ordered, it will include the entire EPZ. This position differs from other states, where evacuation of downwind areas would be implemented rather than the full EPZ. For the analyses in this report, a full evacuation was modeled assuming that the State of Maryland OROs would agree with the Pennsylvania protective action decisions. Analyses were conducted for the accident scenarios identified in Table 6-1.

Table 6-1 Scenarios Assessed for Emergency Response

Section #	Scenario
6.3.1	LTSBO- unmitigated
6.3.2	STSBO- with RCIC blackstart
6.3.3	STSBO- without RCIC blackstart
6.4.1	Sensitivity 1 for the STSBO (without RCIC blackstart) and evacuation to 16 miles
6.4.2	Sensitivity 2 STSBO (without RCIC blackstart) and evacuation to 20 miles
6.4.3	Sensitivity 3 for the STSBO (without RCIC blackstart) with a delay in implementation of protective actions
6.5.6	Seismic analysis - STSBO without RCIC blackstart

Analysis was conducted for the accident scenarios identified in Table 6-1. As indicated in the table, a seismic analysis was completed for the STSBO without RCIC blackstart. This analysis included the effects of damage to infrastructure, such as roadway impacts, loss of traffic signalization, and emergency responder priorities. The remaining analyses completed in this section evaluate the expected response of the public and emergency responders without regard to issues related to the initiating event.

6.1 Population Attributes

The population near the Peach Bottom plant was modeled using six cohorts. A cohort is a population group that mobilizes or moves differently from other population groups. Cohorts were established to represent members of the public who may evacuate early, evacuate late, those who refuse to evacuate, and those who evacuate from areas not under an evacuation order (e.g., the shadow evacuation). The consequence model does not constrain the number of cohorts, but there is no benefit to defining an excessive number of cohorts with little difference in response characteristics. The following cohorts were established for SOARCA analyses:

<u>Cohort 1: 0 to 10 Public.</u> This cohort includes the public residing within the EPZ.

Cohort 2: 10 to 20 Shadow. This cohort includes the shadow evacuation from the 10 to 20 mile area beyond the EPZ. A shadow evacuation occurs when members of the public evacuate from areas that are not under official evacuation orders and typically begin when a large scale evacuation is ordered [21]. Although shadow evacuations are often reported and observed there is little quantitative data available. In a national telephone survey of residents of EPZs, questions were asked about evacuation, about 20 percent of people that had been asked to evacuate had also evacuated for situations in which they were asked not to evacuate [31]. Additional information used to develop a value for use in the SOARCA analysis included a review of more than 20 nuclear power plant evacuation time estimates (ETEs). Although not currently required, most of these ETEs included an analysis of a shadow evacuation. Typically, a shadow evacuation of 30 percent of the public outside the EPZ to a distance of 15 miles was included and often sensitivity analyses were provided that varied the shadow evacuation percentage to values as high as 60 percent. Review of these ETEs showed that increasing the shadow evacuation to 60 percent typically did not affect the ETE. Using the above information, combined with the early decision in the SOARCA project to consider effects beyond the EPZ to a distance of 20 miles, a shadow evacuation of 20 percent of the public from the area 10 to 20 miles from the plant was modeled. For this primarily rural area, a 20 percent shadow evacuation from the area beyond the EPZ has no effect on the evacuation of the EPZ residents.

Cohort 3: 0 to 10 Schools and 0 to 10 Shadow. This cohort includes elementary, middle, and high school student populations within the EPZ. Schools receive early and direct warning from OROs and have response plans in place to support busing of students out of the EPZ. A shadow evacuation from within the EPZ is included with this cohort because sirens are sounded at SAE. This is expected to stimulate an evacuation of some of the residents from within the EPZ beginning about the same time as the evacuation of the schools. Because the 0 to 10 Shadow would evacuate at about the same time as the schools, only one cohort was used to represent the two population groups.

Cohort 4: 0 to 10 Special Facilities. The special facilities population includes residents of hospitals, nursing homes, assisted living communities, and prisons. Special facility residents are assumed to reside in robust facilities such as hospitals, nursing homes, or similar structures that provide additional shielding. Shielding factors for this population group consider this fact.

Cohort 5: 0 to 10 Tail. The 0 to 10 tail is defined as the last 10 percent of the public to evacuate from the 10 mile EPZ. The approach to modeling the tail is an analysis simplification to support inclusion of this population group. The Tail takes longer to evacuate for many reasons such as the need to return home from work to evacuate with the family, pick up children, shut down farming or manufacturing operations or performing other actions prior to evacuating. It also includes those who may miss the initial notification.

Cohort 6: Non-Evacuating Public. This cohort represents a portion of the public from 0 to 10 miles who may refuse to evacuate. It is assumed to be 0.5 percent of the population who are modeled as though they are performing normal activities. Research on large scale evacuations has shown that a small percentage of the public refuses to evacuate [21]; this cohort accounts for this potential group. It is important to note that emergency planning is in place to support evacuation of 100 percent of the public.

6.1.1 Population Distribution

The total Peach Bottom population for the 0 to 20 mile area was obtained from SECPOP for the year 2000. That population value was projected to 2005 using a national level multiplier of 1.0533 obtained from the Census Bureau. The Peach Bottom ETE presents a detailed estimate of the population within the 0 to 10 mile region, and was used to develop population fractions which are used in MACCS2. Table 6-2 summarizes the populations for each cohort used for the SOARCA analyses of the Peach Bottom site.

Table 6-2 Peach Bottom Cohort Population Values

Cohort	Description	Population
1	Public (0 to 10)	24,110
2	Shadow (10 to 20)	82,661
3	Schools (0 to 10) and Shadow (0 to 10)	16,160
4	Special Facilities (0 to 10)	261
5	Tail (0 to 10)	2,693
6	Non-Evacuating Public (0 to 10)	217

6.1.2 Evacuation Time Estimates

As provided in Appendix E, "Emergency Planning and Preparedness for Production and Utilization Facilities," to 10 CFR Part 50 and 10 CFR 50.47, "Emergency Plans", each licensee is required to estimate the time to evacuate the EPZ. Appendix 4 to NUREG-0654/FEMA-REP-1, Revision 1 [20], provides information on the requirements of ETEs, and NUREG/CR-6863, "Development of Evacuation Time Estimate Studies for Nuclear Power Plants," issued January 2005 [23], provides detailed guidance on the development of ETEs. A typical ETE includes many evacuation scenarios to help identify the combination of events for normal and off-normal conditions[55] and provides emergency planners with estimates of the time to evacuate the EPZ under varying conditions [23]. The ETE study provides information on population characteristics, mobilization of the public, special facilities, transportation infrastructure and other information used to estimate the time to evacuate the EPZ. Some of the population values used in SOARCA do not directly align with ETE values because populations were grouped differently in the SOARCA study than in the ETE. For instance, the special facilities population in the ETE represents schools, nursing homes, and hospitals with an estimated total population of 12,989 persons for a winter weekday. In the SOARCA study, the schools and special facilities were represented as separate cohorts. The school population was combined with the 0 to 10 Shadow evacuation cohort in the SOARCA study because the school and shadow evacuation populations mobilize at the same time. The schools and shadow cohort population value used was 16,160.

The SOARCA project used a normal weather winter weekday scenario that includes schools in session. This scenario was selected because it presents several challenges to timely protective

---

[55] The term "off-normal condition" includes unique weather, sporting or entertainment events or other occurrences that would significantly disrupt normal population movements.

action implementation, including evacuating while residents are at work and mobilizing buses to evacuate children at school.

The most recent ETE available from the licensee was used to establish evacuation speeds and delay times within the EPZ [29]. The following ETEs, rounded to the nearest quarter hour, were used to develop evacuation speeds. These ETEs correspond to the normal weather winter weekday scenario:

- 100-percent evacuation: 5 hours and 15 minutes
- 90-percent evacuation: 4 hours and 15 minutes.

The summer weekend ETE and the winter weeknight ETE were also provided in the licensee's most recent ETE study [29] and were considered for use; however, the ETEs for these two scenarios were each approximately 4 hours and 45 minutes for the 100 percent evacuation. The winter weekday scenario with an ETE of 5 hours and 15 minutes can be considered the bounding ETE case for the analysis. The evacuation speed, which is an input into the consequence model, was developed from the ETE and is primarily influenced by population density and roadway capacity.

When using ETE information, it is important to understand the components of the time estimate. The ETE includes mobilization activities that the public undertakes upon receiving the initial notification of the incident [23]. These actions include receiving the warning, verifying information, gathering children, pets, belongings, packing, securing the home, and other evacuation preparations. Thus, a 5 hour ETE does not indicate that all of the vehicles are en route for 5 hours; rather, it is the end of a 5 hour period in which the public mobilizes and evacuates the area. An evacuation population does not enter the roadway system at once. Rather an ideal model would include a 'road loading function' that represents the expected movement. Most ETE studies use such a model. However, MACCS2 does not currently have the capability to move populations in this manner. This being the case, cohorts are modeled to begin moving together at a specific time after notification. To represent the movement of the cohort evacuating together, a single linear value of distance divided by time (the ETE) was used. This distance over ETE ratio provides a slightly slower average speed than would be expected in an evacuation and adds some conservatism to the analysis. Adjustment factors within the consequence model were used to increase or decrease speeds for each cohort at the grid level.

The time to complete an evacuation can be represented as a curve that is relatively steep at the beginning and tends to flatten as the last members of the public exit the area. A review of more than 20 existing ETE studies indicated that the point at which the curve tends to flatten occurs when approximately 90 percent of the population has evacuated. This is consistent with research that has shown that a small portion of the population takes a longer time to evacuate than the rest of the general public and is the last to leave the evacuation area. This last 10 percent of the population is identified as the evacuation tail. For the analyses in this study, the 90 percent ETE value was used to develop evacuation speeds, and the 10 percent evacuation tail was analyzed as a separate cohort.

6.2 WinMACCS

WinMACCS, a user interface for the MACCS2 code, was used to generate input for MACCS2 model runs. WinMACCS integrates the information described above into the consequence analysis. The evacuation area was mapped onto the WinMACCS radial sector grid network. The roadway network was reviewed against site-specific evacuation plans to determine the likely evacuation direction in each grid element. The results of the ETE were reviewed to determine localized areas of congestion and areas where no congestion would be expected. Speed adjustment factors were applied at the grid element level to speed up vehicles in the rural uncongested areas and to slow vehicles in more urban settings where the modeling indicates that speeds are lower than the average values used in the analyses.

6.2.1 Hotspot and Normal Relocation and Habitability

In the unlikely case of a severe accident and radiological release, protective actions in addition to evacuation may be implemented. For instance, residents would be relocated from areas where the dose exceeds protective action criteria. OROs would base this determination on dose projections using State, utility, and Federal agency computer models as well as measurements taken in the field. Hotspot relocation and normal relocation models are included in the MACCS2 code to reflect this activity and include dose from cloudshine, groundshine, direct inhalation, and resuspension inhalation. Within the MACCS2 calculation, individuals who would be relocated because their projected total committed dose from these pathways is projected to exceed the protective action criteria are prevented from receiving any additional dose during the emergency phase. The emergency phase is the 7 day period after the start of the release. This reflects the impact of the relocation of these individuals that would take place in the event of an actual radiological release. This relocation dose criterion is applied at a specified time after plume arrival at the affected area. Relocation is applied to the entire population within the analysis area to a distance of 50 miles, including the non-evacuating cohort within the EPZ, even though this small fraction of the population does not comply with previous evacuation orders. It is assumed these individuals will evacuate when they understand that a release has in fact occurred and they are informed that they are located in high dose areas.

For hotspot relocation, individuals are relocated 12 hours after plume arrival if the total lifetime dose commitment for the weeklong emergency phase exceeds 0.05 sievert (Sv) (5 rem). For normal relocation, such individuals are relocated 24 hours after plume arrival if the total lifetime dose commitment exceeds 0.005 Sv (0.5 rem). The relocation times of 12 hours for hotspot and 24 hours for normal relocation were established based on review of the emergency response time lines, which suggest that OROs may not be available earlier to assist with relocation because of higher priority tasks in the evacuation area. Relocation is a process that requires identification of the affected areas and notification of residents within those areas. The time values represent the average time expected to implement each action.

Habitability is the consequence model parameter that is used to establish the dose level at which residents are allowed to return to the EPZ to live. Site-specific criterion are used for long-term habitability, and most states adhere to the U.S. Environmental Protection Agency (EPA) guidelines which specify a dose of 2 rem in the first year and 500 millirem per year thereafter. The EPA recommendation has traditionally been implemented in MACCS2 as a cumulative 4 rem over the first 5 years (2 rem in the first year + 4 years x 0.5 rem/year) of exposure.

Pennsylvania has a more strict habitability criterion of 500 mrem per year beginning in the first year, and this value was used in the Peach Bottom analysis. The hotspot and normal relocation values used in NUREG-1150 were 0.5 Sv (50 rem) and 0.25 Sv (25 rem) respectively. The long term habitability criteria used in NUREG-1150 was 0.04 Sv (4 rem) over a 5 year period. The values used in SOARCA were established to align with site specific response expectations and EPA protective action guidelines.

6.2.2 Shielding Factors

Shielding factors vary by geographical region across the United States; those used in the Peach Bottom analysis are shown in Table 6-3 and are appropriate for the region. The factors represent the fraction of dose that a person would be exposed to when performing normal activities, evacuating, or staying in a shelter in comparison to a person outside with full exposure. These shielding factors are applied to all cohorts. Special facilities are typically larger and more robust structures than residential housing stock and therefore have better shielding factors, as identified in Table 6-3.

Table 6-3 Peach Bottom Shielding Factors.

	Groundshine			Cloudshine			Inhalation/Skin		
Cohort	**Normal**	**Evac.**	**Shelter**	**Normal**	**Evac.**	**Shelter**	**Normal**	**Evac.**	**Shelter**
Non-special facilities	0.18	0.50	0.10	0.60	1.00	0.50	0.46	0.98	0.33
Special facilities	0.05	0.50	0.05	0.31	1.00	0.31	0.33	0.98	0.33

The site specific values for sheltering were obtained from NUREG-1150 [8]. An updated inhalation/skin evacuation shielding factor was obtained from NUREG/CR-6953, Volume 1, "Review of NUREG-0654, Supplement 3, 'Criteria for Protective Action Recommendations for Severe Accidents'," issued January 2005 [22]. The normal activity shielding factors have been adjusted to account for the understanding that people do not spend a great deal of time outdoors. The normal activity values are all weighted averages of indoor and outdoor values based on being indoors 81 percent of the time and outdoors 19 percent of the time [32]. The shielding factor value for indoor activities was assumed to be the same as the shielding factor value for sheltering shown in Table 6-3.

6.2.3 Potassium Iodide

The State of Pennsylvania potassium iodide (KI) program distributes KI tablets through several different means. The Pennsylvania Department of Health district offices are responsible for coordinating with county emergency management agency officials to make KI available to residents living and working within the EPZ. The distribution of KI occurs on an annual basis for the Peach Bottom EPZ and is preceded by public announcements.

The purpose of the KI is to saturate the thyroid gland with stable iodine so that further uptake of radioactive iodine by the thyroid is diminished. If taken at the right time and in the appropriate dosage, KI can nearly eliminate doses to the thyroid gland from inhaled radioiodine. Factors that contribute to the effectiveness of KI include its availability, the timing of ingestion, and the

degree of pre-existing stable iodine saturation of the thyroid gland, which already inhibits absorption of inhaled radioiodine by the thyroid. The analysis assumes that some residents will not remember where they have placed their KI or may not have it available and will therefore not take KI. It is also assumed some residents will not take their KI when directed (i.e., they may take it early or late which reduces the efficacy). To account for these factors, the analysis modeled KI as taken by 50 percent of the public, and the efficacy of the KI was set at 70 percent.

6.2.4 Adverse Weather

Adverse weather is typically defined as rain, ice, or snow that affects the response of the public during an emergency. The affect of adverse weather on the mobilization of the public was not directly considered in establishing emergency planning parameters for this project because such a consideration approximates a worst-case evacuation scenario. However, adverse weather was addressed in the movement of cohorts within the analysis. The evacuation speed multiplier (ESPMUL) parameter in WinMACCS is used to reduce travel speed when precipitation is occurring as indicated from the meteorological weather file. The ESPMUL factor was set at 0.7, which effectively slows down the evacuating public to 70 percent of the established travel speed when precipitation exists.

6.2.5 Modeling Using Evacuation Time Estimates

The purpose of using the ETE to develop evacuation parameters for the consequence modeling is to better approximate the real time actions expected of the public. Although consequence modeling has evolved to allow the use of many cohorts and can address many individual aspects of each cohort, the approach to modeling evacuations is not direct. As stated earlier, evacuations include mobilizing and evacuating the public over a period of time, which is best modeled as a distribution of data. WinMACCS requires this distribution of data be converted into discrete events. For example, upon the sounding of the sirens and issuance of the EAS messaging, in the SOARCA analysis all members of the public are sheltered and 1 hour later all members of the public enter the roadway network together at the same time and begin to evacuate. Research on existing evacuations for technological hazards has shown that the evacuating public would actually enter the roadway network over a period of time. It is not realistic that all vehicles would load simultaneously; however, this treatment within the model is necessary because of the current modeling abilities of WinMACCS.

Considering the above modeling requirement, reasonable speeds, developed from the ETE, were established for each cohort. The following elements factor into these speeds:

- time to receive notification and prepare to evacuate (mobilization time),
- time to evacuate, and
- distance of travel.

The time to receive notification was based on the assumption that sirens will sound when needed. The NRC Reactor Oversight Program data for siren performance for Peach Bottom shows an average siren performance indicator of 99.8 percent, indicating that sirens will perform when needed. It is recognized that loss of power accidents will result in the loss of power to some offsite areas of the EPZ. However, there is no reason to expect that the power will be out in the

entire 10 mile EPZ. For this analysis, it is assumed that the offsite sirens would be sounded within much of the EPZ. For those areas where the power outage affects sirens, it is assumed societal notification and route alerting by OROs would alert residents within the same mobilization time period as estimated for the EPZ.

A simple ratio of distance to time would show that evacuation of the 0 to 10 Public cohort from the 10 mile EPZ at Peach Bottom which has an ETE of 4 hours and 15 minutes, would move at a speed of 2.4 miles per hour (mph). However, as indicated above, notification and preparation to evacuate are included in the ETE.

For the general public, a 1-hour delay to shelter is assigned to reflect the mobilization time in which residents receive the warning and prepare to evacuate. If the 1-hour mobilization time is subtracted from the ETE (4 hours and 15 minutes minus 1 hour) there remains 3 hours and 15 minutes to travel a maximum of 10 miles. Roadways are not radial out of the EPZ and actual travel distance is estimated, based on review of local mapping, to be 30 to 50 percent greater than the radial distance.

During the evacuation, roadway congestion occurs rather quickly, and traffic exiting the EPZ begins to slow. A review of ETE studies shows that roadway congestion typically occurs in 1 to 2 hours, depending on the population density and roadway capacity of the EPZ. In the SOARCA analysis, the 0 to 10 Public is sheltered and preparing to evacuate for 1 hour. The public is then loaded onto the roadway and congestion is assumed to occur within 15 minutes. This total time of 1 hour and 15 minutes for congestion to occur was established to be consistent with observed data from ETE studies.

The calculation of the speed of evacuees includes the first 15 minutes to the point when congestion occurs. For this first 15 minutes, evacuees are assumed to travel at 5 mph. The speed is slow to account for the model loading all members of a cohort at one time. In the first 15 minutes at 5 mph, a distance of 1.25 miles has been traveled. At that time congestion is heavy and speeds slow for the next 8.75 miles.

The ETE is 4 hours and 15 minutes for this cohort. Having sheltered and prepared to evacuate for 1 hour and then traveled the first 15 minutes at 5 mph, the remaining time is 3 hours (4:15 minus 1 hour shelter minus 15 minutes at 5 mph). To determine the speed of travel for the remaining 8.75 miles, the distance is divided by the time (8.75 miles / 3 hours), which provides a speed of 2.9 mph. The calculated speed used in the analysis for this cohort was rounded to 3 mph. The values were rounded to avoid implying that speeds are precise and because the speeds represent an average for the cohort. This approach applies to evacuees travelling 10 miles. Most evacuees would travel less distance and some travel a greater distance because the roadways are not radial away from the plant. Adjustments were made to the speeds based on review of population densities and aerial photos of roadways. The baseline speed of 3 mph was assigned to the general public cohort and was then adjusted using speed adjustment factors, ranging from 75 percent to 150 percent of the average speed, as appropriate for the rural and urban areas.

6.2.6 Cohort Modeling

The WinMACCS parameters for the cohorts are stored in multi-dimensional arrays. The dimensions of the arrays are defined by geographical area. WinMACCS requires the maximum dimensions be established with the first cohort. All subsequent cohorts must be defined within these array dimensions, meaning that they can extend from the origin to any distance equal to or less than the maximum distance established with the first cohort.

The 0 to 10 Public was expected to be the cohort of greatest interest; therefore, Cohort 1 was defined as the 0 to 10 Public and has the same response characteristics as Cohort 2. The cohort that extends the greatest distance and defines the limits of the array is the shadow evacuation, which is Cohort 2. Thus, within the WinMACCS input file, Cohorts 1 and 2 were defined to meet the requirement that maximum distance be established with the first cohort. The WinMACCS model input parameters for Cohort 1 were extended from the plant out to the maximum array distance of 20 miles, and Cohort 2 extends from the plant out to 10 miles. In the WinMACCS input file, Cohort 1 is input as 20 percent of the population from 0 to 20 miles. This captures the 20 percent of the population between 10 and 20 miles involved in the shadow evacuation beyond the EPZ. As noted earlier, for this site the shadow evacuation has no affect on the evacuation of the residents of the EPZ. The combination of Cohorts 1 and 2 from 0 to 10 miles in the WinMACCS model represent the 0 to 10 Public cohort defined above. For the remaining cohorts, application of parameters in the WinMACCS model is direct, and the population fractions directly correspond to the cohort descriptions.

6.3 Accident Scenarios

An emergency response timeline was developed for each accident scenario using information from the MELCOR analyses, expected timing of emergency classification declarations, and information from the ETE. The timeline identifies points at which cohorts would receive instruction from OROs to implement protective actions. In practice, initial evacuation orders are based on the severity of the accident and in Pennsylvania would likely include an evacuation of the entire EPZ. The emergency planning parameters use a normal workday event, whereas the MELCOR analyses assumes minimum staffing consistent with an off-hours event. This adds some conservatism to the analysis because an off-hours, nighttime evacuation would typically occur a little faster because most residents are at home and schools are not in session.

6.3.1 Long-Term Station Blackout Unmitigated

The timing of emergency classification declarations was based on Table PBAPS 3-1, "Emergency Action Level (EAL) Matrix," contained in site emergency plan implementing procedures. The emergency classification timing was reviewed with the licensee for accuracy. MS1 of the SAE EAL specifies that an SAE is declared 15 minutes after the initiating event (loss of all AC power). Sirens sound about 45 minutes after the SAE is declared. An EAS message is broadcast at this time providing notification to residents and transients within the EPZ that there is an incident and instructing them to monitor the situation for further information. A GE is declared, based on EAL MG1, 45 minutes into the event (coincidentally 15 minutes before the issue of the first EAS message related to the SAE) when it is assumed that operators have determined that offsite power will not be restored within 2 hours. An EAS message for the GE is then broadcast, and sirens sound again 45 minutes after the GE declaration which is 30 minutes

after the siren and initial EAS message for the SAE (see Figure 6-2). The EAS message for the GE would include instructions for implementing protective actions.

Discussions with site representatives were held to help ensure SOARCA staff properly understood the EALs for each accident scenario and emergency response practices. In addition, staff reviewed information from formally evaluated emergency response exercise timelines that show the times for notification of an emergency declaration, siren activation, and broadcast of EAS messaging for Peach Bottom. The timing in the exercises shows approximately 50 minutes from notification to sirens sounding. As indicated in Figure 6-2, the analysis used an estimate of 45 minutes from SAE declaration to SAE siren, which closely approximates the exercise values. The offsite emergency plans for Peach Bottom include sounding sirens for declaration of both SAE and GE. The emergency response timeline for the LTSBO scenario is shown in Figure 6-2. The first fuel cladding gap release occurs about 9 hours into the event and release to the environment begins about 20 hours into the event. The duration of specific protective actions for each cohort is summarized in Figure 6-3.

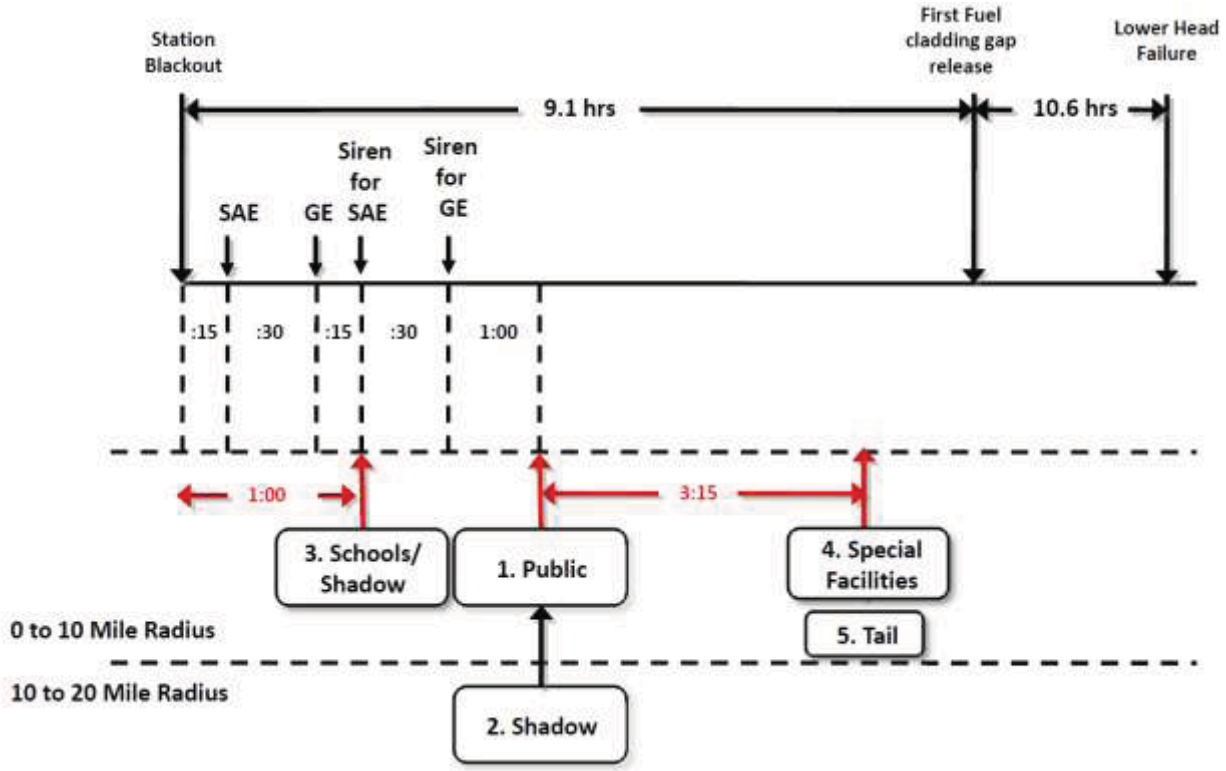

Figure 6-2 Unmitigated LTSBO emergency response timeline

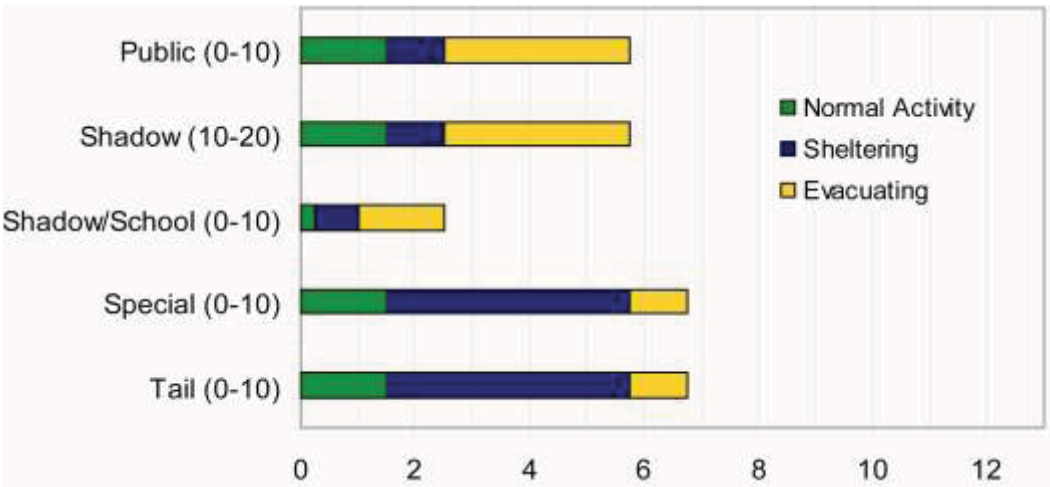

Figure 6-3 Duration of protective actions for unmitigated LTSBO

Cohort 1: 0 to 10 Public. Following declaration of the SAE, sirens are sounded to alert the public. Sirens are again sounded following the declaration of GE, at which time the public is assumed to shelter. The time for the public to receive the warning and prepare to evacuate is assumed to be 1 hour after the siren sounds for the GE which is consistent with empirical data from previous evacuations [25].

Cohort 2: 10 to 20 Shadow. This cohort is assumed to begin movement at the same time as the 0 to 10 Public cohort, once widespread media broadcasts are underway. Residents in the 10 to 20 mile area begin seeing large numbers of people evacuating and initiate a shadow evacuation. There is no warning or notification for the public residing in this area, and the area is not under an evacuation order.

Cohort 3: 0 to 10 Schools and 0 to 10 Shadow. Schools are the first to take action. Upon receipt of the site's declaration of an SAE, county emergency management agencies would notify the schools in accordance with the offsite emergency response plan. The analysis assumes that schools begin sheltering when notified and that this notification occurs about 15 minutes after the emergency declaration. Buses would be mobilized, but in accordance with the offsite emergency plan, evacuation would not begin until a GE is declared. The preliminary action to mobilize buses in response to the SAE allows for a prompt evacuation. It is assumed that schools begin evacuating 15 minutes after GE, and it is only coincidence that this occurs about the same time as the sounding of the sirens in response to the SAE. At this time in the event, roads are uncongested and school buses are able to exit the EPZ quickly. It is assumed that the sounding of sirens and broadcast of the EAS message for the SAE causes a shadow evacuation of residents within the EPZ (e.g., 0 to 10 Shadow cohort). Because the shadow population is grouped with the schools (see Section 6.1), the shadow population is also treated as if it shelters at 15 minutes after the declaration of SAE.

Cohort 4: 0 to 10 Special Facilities. Special facilities can take longer to evacuate than the general public because transportation resources, some of which are specialized such as wheelchair vans and ambulances, must be mobilized. Special facilities evacuate individually with each facility responsible for obtaining resources. These resources are required to be

established during emergency planning; therefore, it is a reasonable assumption that the resources will be available. These types of vehicles sometimes must make return trips until everyone is evacuated. For modeling convenience, the conservative assumption was made that the residents of these facilities remain sheltered and evacuate in a single wave beginning when the tail cohort begins to evacuate. It is recognized that some facilities would actually mobilize and evacuate earlier in the event.

Cohort 5: 0 to 10 Tail. Using the evacuation data provided in the Peach Bottom ETE study [29], the analysis assumes that 90 percent of the evacuation of the EPZ is complete at approximately 4 hours and 15 minutes. This corresponds to the departure time for the 0 to 10 Tail cohort.

Cohort 6: Non-Evacuating Public. This cohort group represents a portion of the public who may refuse to evacuate. It is assumed to be 0.5 percent of the population. Any member of the public who does not evacuate the EPZ is still subject to the hotspot and normal relocation criterion discussed earlier.

The evacuation timing and speeds for each cohort are presented in Table 6-4. Selected input parameters for WinMACCS are provided in Table 6-4 to support detailed use of this study. More detailed information about modeling parameters is available in the MACCS2 user's guide [26]. The following is a brief description of the parameters:

- Delay to shelter (parameter DLTSHL) represents a delay from the time of the start of the accident until cohorts enter the shelter. DLTSHL is generally referenced to alarm time, but the value (OALARM) is set to zero in the SOARCA analyses.

- Delay to evacuation (parameter DLTEVA) represents the length of the sheltering period from the time a cohort enters the shelter until the point at which it begins to evacuate.

- The speed (parameter ESPEED) is assigned for each of the three phases used in WinMACCS including Early, Middle, and Late. Average evacuation speeds were derived from the Peach Bottom ETE report. Speed adjustment factors were then used in the WinMACCS application to represent free flow in rural areas and congested flow in urban areas.

- Duration of beginning phase (parameter DURBEG) is the duration assigned to the beginning phase of the evacuation and may be assigned uniquely for each cohort.

- Duration of middle phase (parameter DURMID) is the duration assigned to the middle phase of the evacuation and may also be assigned uniquely for each cohort.

For the 0 to 10 Public and the 0 to 10 Tail cohorts, by definition the sum of the DLTEVA, DURBEG and DURMID is equal to the ETE. This is because the ETE does not include shelter time.

Table 6-4 Unmitigated LTSBO Cohort Timing

Cohort	Delay to Shelter DLTSHL (hr)	Delay to Evacuation DLTEVA (hr)	DURBEG (hr)	DURMID (hr)	ESPEED* (early) mph	ESPEED* (mid) mph
0 to 10 Public	1.5	1	0.25	3	5	3
10 to 20 Shadow	1.5	1	0.25	3	5	3
0 to 10 Schools and Shadow	0.25	0.75	1	0.5	20	20
0 to 10 Special Facilities	1.5	4.25	0.5	0.5	3	20
0 to 10 Tail	1.5	4.25	0.5	0.5	3	20
Non-Evac	0	0	0	0	0	0

* 20 mph was used for the late phase evacuation speed for all cohorts.

6.3.2 Short-Term Station Blackout with Reactor Core Isolation Cooling Blackstart

The timing of emergency classification declaration for the STSBO with RCIC Blackstart was based on Table PBAPS 3-1 in the site emergency plan implementing procedures. The analysts reviewed the emergency classification timing with the licensee for accuracy. This scenario is an immediate GE. With loss of offsite power and loss of DC power, operators cannot determine whether water level is above TAF, and a GE is declared based on EAL MG1. The emergency response timeline for the STSBO scenario is shown in Figure 6-4 and protective action durations for each cohort are shown in Figure 6-5. Core damage, as evidenced by the first fuel cladding gap release, is calculated at 6.8 hours into the event, with a significant radioactive release from containment beginning 16.7 hours into the event as indicated by the lower head failure in Figure 6-4.

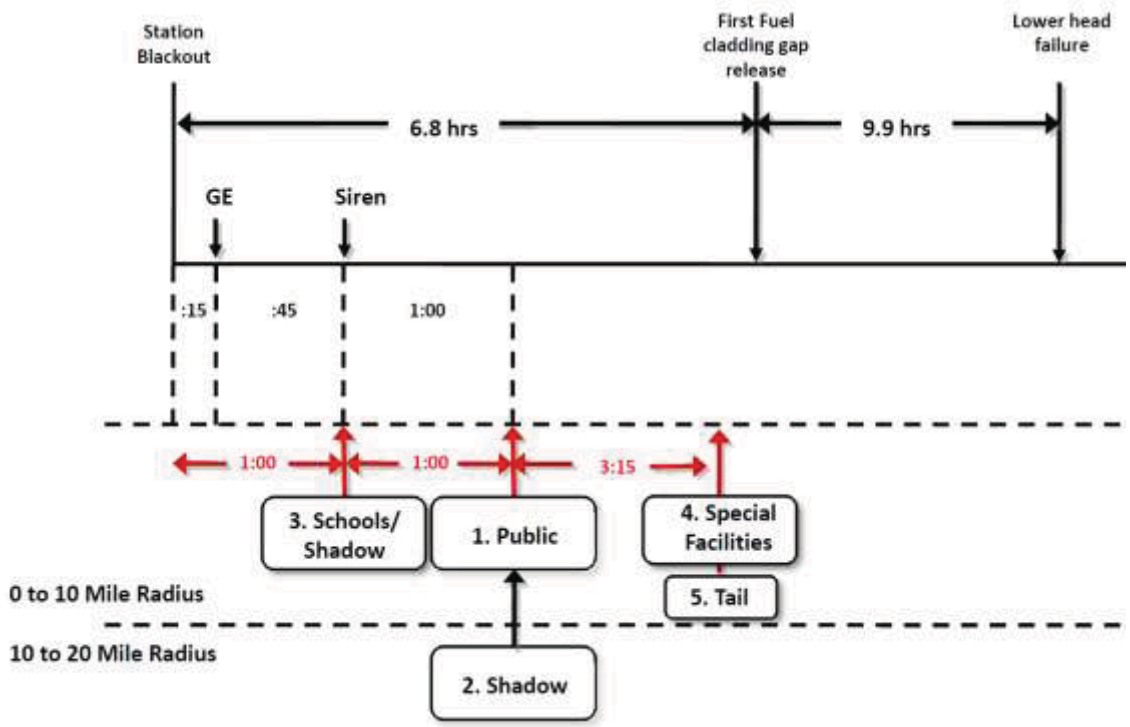

Figure 6-4 STSBO with RCIC blackstart emergency response timeline

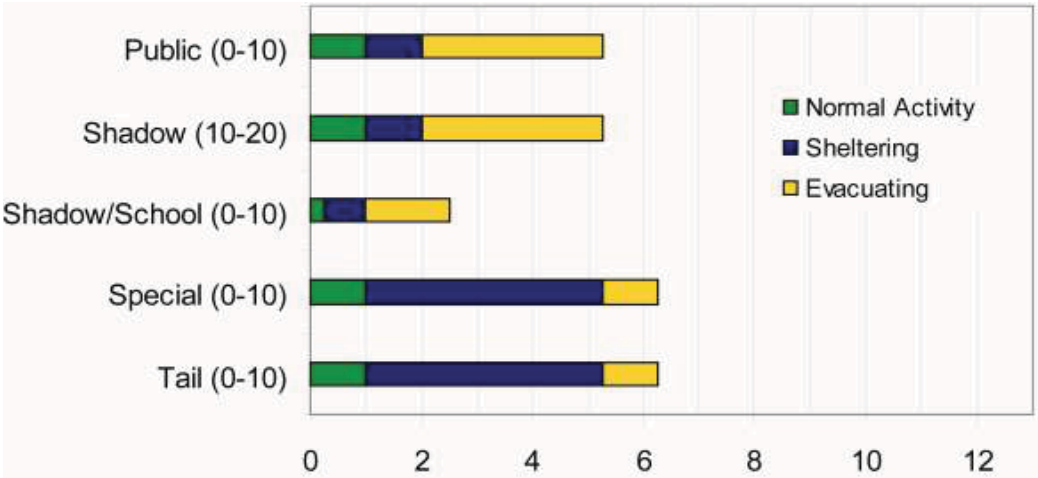

Figure 6-5 Protective actions for STSBO with RCIC blackstart

Cohort 1: 0 to 10 Public. It is assumed to take 45 minutes for OROs to sound sirens following declaration of a GE, at which point the public is assumed to shelter. The time for the public to receive the warning and prepare to evacuate is assumed to be 1 hour after the siren sounds.

Cohort 2: 10 to 20 Shadow. This cohort is assumed to begin movement at the same time as the 0 to 10 Public once widespread media broadcasts are underway. Residents in the 10 to 20-mile

area begin seeing large numbers of people evacuating and initiate a shadow evacuation. There is no warning or notification for the public residing in this area, and area is not under an evacuation order.

Cohort 3: 0 to 10 Schools and 0 to 10 Shadow. This cohort is the first to take action. Upon receipt of the declaration of GE, county emergency management agencies would notify the schools in accordance with the emergency response plan. It is assumed that schools begin sheltering when notified, buses are mobilized, and evacuation begins about 45 minutes after the GE is declared. It is coincidence that evacuation of the schools occurs at the same time that sirens are assumed to sound. The sounding of the sirens for GE is not directly linked to evacuation of the schools.

It is noted that the schools begin to evacuate in 1-hour, which is the same as in the LTSBO scenario. For the LTSBO, school buses are mobilized at the SAE and ready for deployment. Once the GE is declared, the evacuation begins within about 15 minutes because the resources have been prepared. For the STSBO, buses begin to be mobilized when the GE is declared, and the evacuation begins about 45 minutes later.

Cohort 4: 0 to 10 Special Facilities. Special facilities are assumed to depart at the same time as the evacuation Tail.

Cohort 5: 0 to 10 Tail. The tail begins to evacuate approximately 4 hours and 15 minutes after notification to evacuate.

Cohort 6: Non-Evacuating Public. This cohort group represents a portion of the 0 to 10 Public who may refuse to evacuate. It is assumed to be 0.5 percent of the population.

The delay to shelter identified in Table 6-5 represents a delay from the start of the accident, until people enter the shelter, and the delay to evacuation represents the length of the sheltering period before initiating evacuation. These delays correspond to the different shielding factors that would be applied to each cohort during these timeframes. The speeds in this table represent average movements for the cohorts as derived from the ETEs. These speeds are adjusted within each grid element, where appropriate, when developing the WinMACCS model.

Table 6-5 STSBO with RCIC blackstart Cohort Timing.

Cohort	Delay to Shelter DLTSHL (hr)	Delay to Evacuation DLTEVA (hr)	DURBEG (hr)	DURMID (hr)	ESPEED * (early) (mph)	ESPEED * (mid) (mph)
0 to 10 Public	1.00	1.00	0.25	3.00	5	3
10 to 20 Shadow	1.00	1.00	0.25	3.00	5	3
0 to 10 Schools and Shadow	0.25	0.75	1.00	0.50	20	20
0 to 10 Special Facilities	1.00	4.25	0.50	0.50	3	20
0 to 10 Tail	1.00	4.25	0.50	0.50	3	20
Non-Evac	0	0	0	0	0	0

* 20 mph was used for the late-phase evacuation speed for all cohorts.

6.3.3 Short-Term Station Blackout without Reactor Core Isolation Cooling Blackstart

The timing of the emergency classification declaration for the STSBO without RCIC blackstart was based on Table PBAPS 3-1 in site emergency plan implementing procedures. The analysts reviewed the emergency classification timing with the licensee for accuracy. This scenario is an immediate GE. With loss of offsite power and loss of DC power, operators cannot determine whether water level is above TAF, and a GE is declared based on EAL MG1. The emergency response timeline for the STSBO without RCIC blackstart scenario is shown in Figure 6-6; protective action durations for each cohort are shown in Figure 6-7. Core damage, as evidenced by the first fuel cladding gap release, is calculated at 1 hour into the event, with a significant radioactive release from containment beginning 8 hours into the event, as indicated by the lower head failure in Figure 6-6.

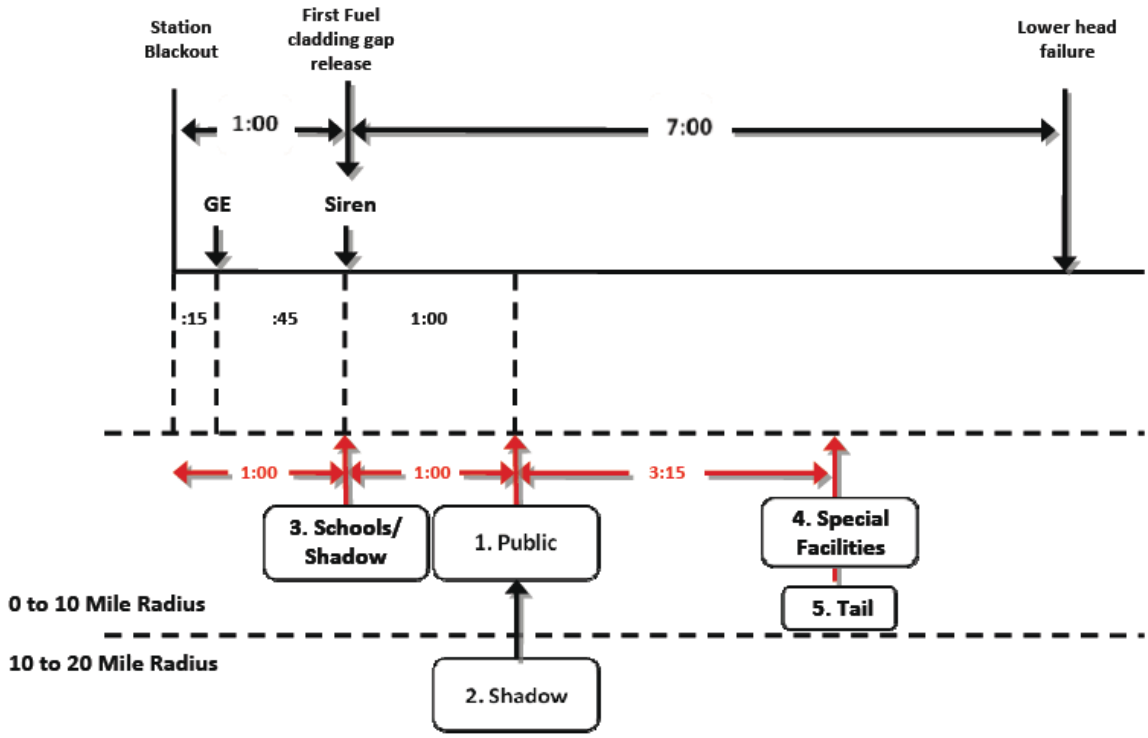

Figure 6-6 STSBO without RCIC blackstart emergency response timeline

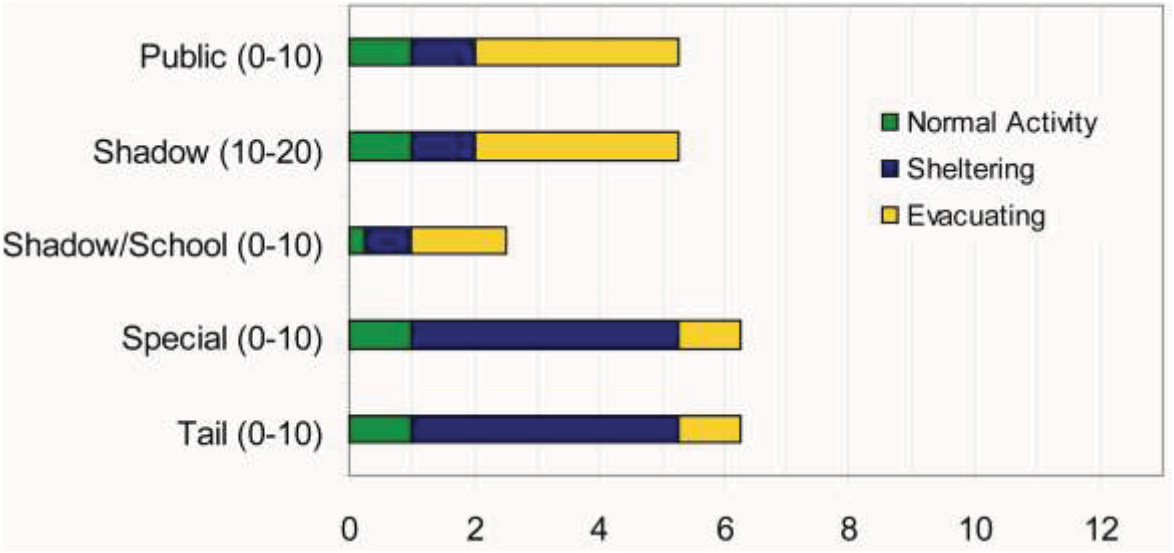

Figure 6-7 Duration of protective actions for STSBO without RCIC blackstart

The implementation of protective actions for the STSBO without RCIC blackstart is the same as implementation for the STSBO with RCIC blackstart.

Cohort 1: 0 to 10 Public. It is assumed to take 45 minutes for OROs to sound sirens following declaration of a GE, at which point the public is assumed to shelter. The time for the public to receive the warning and prepare to evacuate is assumed to be 1 hour after the siren sounds for the GE.

Cohort 2: 10 to 20 Shadow. This cohort is assumed to begin movement at the same time as the 0 to 10 Public cohort once widespread media broadcasts are underway. Residents in the 10 to 20-mile area begin seeing large numbers of people evacuating and initiate a shadow evacuation. There is no warning or notification for the public residing in this area, and area is not under an evacuation order.

Cohort 3: 0 to 10 Schools and 0 to 10 Shadow. This cohort is the first to take action. Upon receipt of the site's declaration of a GE, county emergency management agencies would notify the schools in accordance with the emergency response plan. It is assumed that schools would begin sheltering when notified, buses would be mobilized, and evacuation would begin about 45 minutes after the GE is declared. It is coincidence that this occurs at the same time that sirens are assumed to sound.

Cohort 4: 0 to 10 Special Facilities. Special facilities are assumed to depart at the same time as the evacuation tail.

Cohort 5: 0 to 10 Tail**.** The tail begins to evacuate approximately 4 hours and 15 minutes after notification to evacuate.

Cohort 6: Non-Evacuating Public. This cohort group represents a portion of the 0 to 10 Public who may refuse to evacuate. It is assumed to be 0.5 percent of the population.

The delay to shelter, identified in Table 6-6 represents a delay from the start of the event until people enter the shelter. Delay to evacuation represents the length of the sheltering period before initiating evacuation. These delays correspond to the different shielding factors that would be applied to each cohort during these timeframes. The speeds in this table represent average movements for the cohorts. These values are adjusted within each grid element when developing the WinMACCS model.

Table 6-6 STSBO without RCIC blackstart Cohort Timing.

Cohort	Delay to Shelter DLTSHL (hr)	Delay to Evacuation DLTEVA (hr)	DURBEG (hr)	DURMID (hr)	ESPEED * (early) (mph)	ESPEED * (mid) (mph)
0 to 10 Public	1.00	1.00	0.25	3.00	5	3
10 to 20 Shadow	1.00	1.00	0.25	3.00	5	3
0 to 10 Schools and Shadow	0.25	0.75	1.00	0.50	20	20
0 to 10 Special Facilities	1.00	4.25	0.50	0.50	3	20
0 to 10 Tail	1.00	4.25	0.50	0.50	3	20
Non-Evac	0	0	0	0	0	0

* 20 mph was used for the late phase evacuation speed for all cohorts.

6.4 Sensitivity Studies

Analysis of emergency preparedness and response parameters, such as demographics, infrastructure, and timing, provides many opportunities for further evaluation through sensitivity studies. The project team selected three additional calculations to assess variations in the implementation of protective actions. Each of the sensitivity studies was conducted using the STSBO without RCIC blackstart scenario, which was selected because it represents an earlier release than the other scenarios.

- Sensitivity 1 – evacuation of a 16-mile area and a shadow evacuation from within the 16 to 20 mile area.
- Sensitivity 2 – evacuation of the 0 to 20-mile area.
- Sensitivity 3 – delay in implementation of protective actions for the public within the EPZ.

Sensitivity cases 1 and 2 assessed the effects of expanding the initial protective actions to distances of 16 and 20 miles respectively. The objective of these sensitivity analyses was to determine whether consequences might be reduced if the initial evacuation area were larger. Twenty miles was selected because it is twice the distance of the EPZ. A middle distance was also desired. The 16 mile distance was selected because a 'ring' had been established in the underlying nodalization network in WinMACCS. An existing ring was not available at 15 miles.

Sensitivity 3 assessed a delay in the implementation of protective actions for the public. Although there is high confidence that the licensees and OROs will respond promptly and,

follow their procedures, the SOARCA peer review committee suggested that a delay be considered. Such a delay might be caused by a delay in communication, a delay in the decision process (by licensee or OROs), or other factors. The 30-minute period was selected based on review of response data from exercises at Peach Bottom, which show that the response times and actions typically varied by only a few minutes among different exercises.

For the sensitivity analyses, the modeling of the area beyond the EPZ includes a full-scale evacuation, although this does not reflect likely protective action decisions. To support the assessment of implementing protective actions outside of the EPZ, an evacuation model was developed using data obtained for the 10 to 20 mile area around the nuclear power plant. Evacuation speeds for the cohorts in the 10 to 20 mile area were developed using OREMS Version 2.6. OREMS is a Windows based application used to simulate traffic flow that was designed specifically for emergency evacuation modeling [24]. The main features of OREMS used in the analyses include the following:

- determining the length of time associated with complete or partial evacuation of the population at risk within an emergency zone, or for specific sections of the highway network or sub-zones

- determining potential congestion areas in terms of traffic operations within the emergency zone.

The OREMS model considers special conditions that may be imposed during an emergency evacuation. For example, intersections that normally have pre-timed controllers are assumed to be manned by emergency personnel to facilitate traffic flow. This function is consistent with the emergency response actions that would be implemented during an evacuation. Detail for road networks was obtained from available mapping and was input into OREMS using the standard intersection functions available in the model. Judgment and experience were applied in determining the number of nodes established for the model. OREMS can manage hundreds of nodes, but there is a point at which the addition of nodes and links provides little change in the total times. For an urban area, a nodal network would be heavily populated; for a rural area, the network would be lightly populated. The nodal network established for this analysis would be considered a moderately populated network for this code because the area is primarily rural mixed with some urban areas such as Lancaster, Pennsylvania.

For the Peach Bottom 10 to 20-mile ETE, 232,053 vehicles were loaded onto 118 nodes of a 442 node network. The network loading was distributed over a 5-hour period to account for the trip generation time. The following evacuation times were produced from the OREMS calculation as plotted in Figure 6-8:

- 100 percent evacuation: 19 hours;
- 90 percent evacuation: 12 hours and 15 minutes

These times were used to develop the evacuation speeds input into the WinMACCS model. The evacuation modeling conducted for the Peach Bottom plant was developed consistent with the characteristics observed in prior evacuations conducted for non-nuclear incidents. As described earlier, the analysis includes the common phenomenon of evacuations in which travelers who

depart the threat zone the earliest experience shorter delays because the routes have yet to become fully used during the emergency. Evacuees who depart during the middle part of the evacuation, when the greatest numbers of people are seeking to depart, generally experience the highest congestion and longer delays because the demand on the roadway network is at its greatest, exceeding the available capacity in many areas. Evacuees who depart the hazard zone later enter the network as the demand nears, or goes below, the roadway capacity are able to avoid the delays associated with the peak evacuation demand period. The ETE modeling indicates that most congestion occurs in the more populous areas in the north near Lancaster, PA, and in the south near Forest Hill, Bel Air, and Fallston, MD.

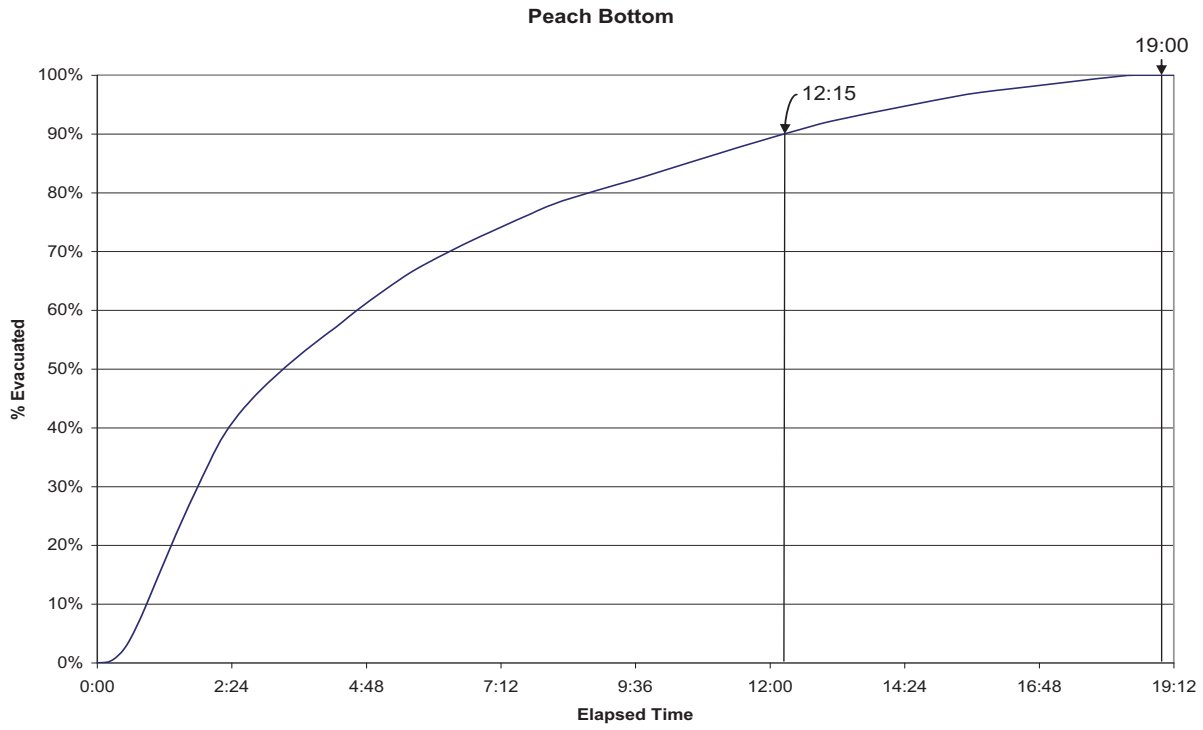

Figure 6-8 Evacuation timeline from Peach Bottom for the 10 to 20 mile region

The initial accident scenarios were evaluated for protective actions within the EPZ. Expanding the protective actions to distances beyond the EPZ is not readily accommodated using the modeling approach selected for these analyses. Therefore, although OROs may request that the 10 to 20-mile population shelter, this population group is treated as performing normal activities throughout the emergency. The normal activity shielding factors are weighted averages of indoor and outdoor values based on being indoors 81 percent of the time and outdoors 19 percent of the time [32]. The hotspot and normal relocation model within MACCS2 will move affected individuals out of the area if the dose criteria apply.

6.4.1 Sensitivity 1 for the STSBO w/o RCIC Blackstart Evacuation to 16 Miles

For Sensitivity 1, evacuation of a 16-mile area around the nuclear power plant is assessed. A shadow evacuation is assumed to occur from within the 16 to 20-mile area, and the remaining members of the public in the 16 to 20-mile area were modeled as performing normal activities as

described above. Figure 6-9 identifies the cohort timing for Sensitivity 1, and Figure 6-10 shows the durations of protective actions for each cohort.

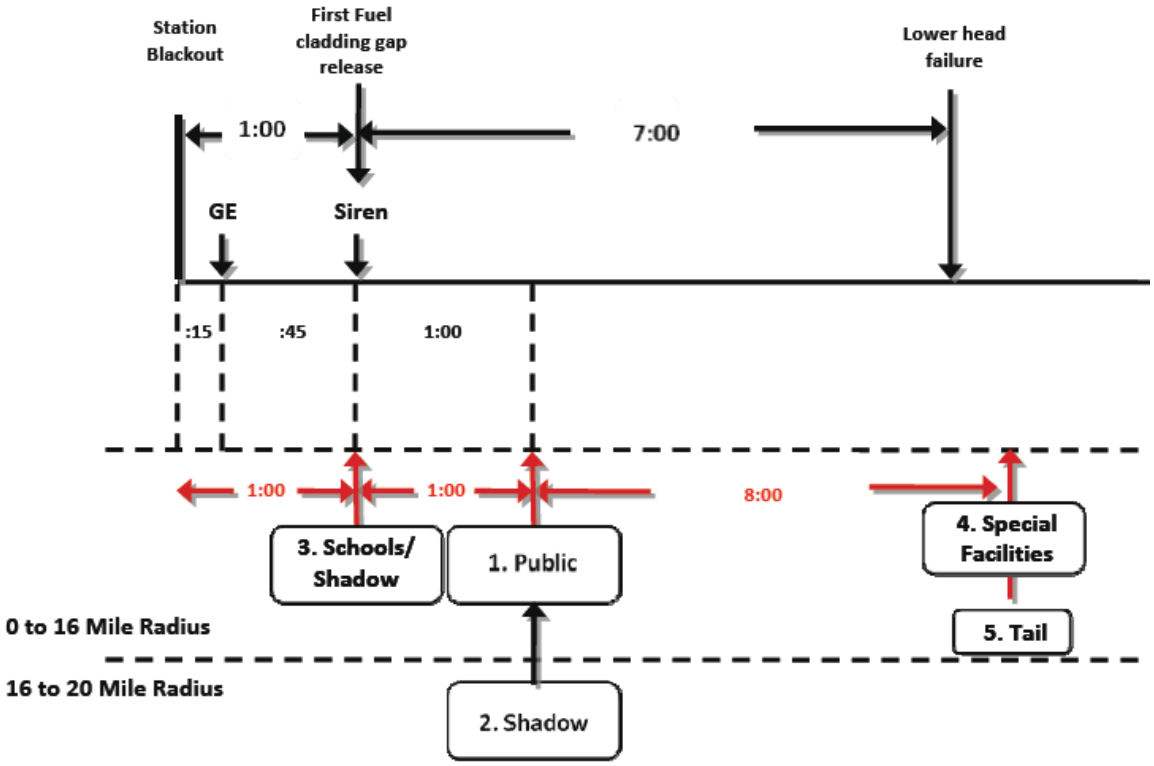

Figure 6-9 Sensitivity 1 STSBO without RCIC blackstart - evacuation to 16 miles

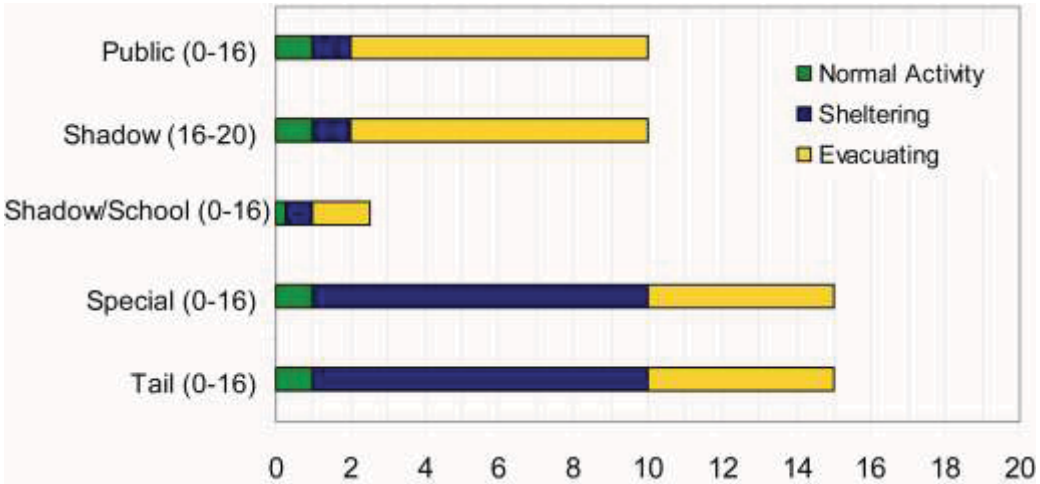

Figure 6-10 Duration of protective actions for Sensitivity 1 STSBO w/o RCIC blackstart - evacuation to 16 miles

Cohort 1: 0 to 16 Public. Following declaration of a GE, sirens are sounded and an EAS message is broadcast to the affected areas within the EPZ. The analysis assumes that the public shelters when the sirens sound and that the time to receive the warning and prepare to evacuate is 1 hour. Another assumption in this sensitivity analysis is that the population from 10 to 16 miles would be notified within the same timeframe as the EPZ via EAS messaging and route alerting. The ETE for the public was estimated as a linear projection between the Peach Bottom ETE study and the 10 to 20-mile ETE developed for the Sensitivity 2 analysis. Therefore, although the evacuation of the public starts at the same time as the base case, it takes longer to evacuate the area as indicated in Table 6-7, which shows longer travel times and slower speeds.

Cohort 2: 16 to 20 Shadow. This cohort is assumed to begin movement at the same time as the 0 to 16 Public cohort once widespread media broadcasts are underway. Residents in the 16 to 20-mile area begin seeing large numbers of people evacuating and initiate a shadow evacuation.

Cohort 3: 0 to 16 Schools and 0 to 16 Shadow. This cohort is the first to take action. Upon receipt of the site's GE declaration, county emergency management agencies would notify the schools in accordance with the emergency response plan. It is assumed that schools begin sheltering in about 15 minutes and begin evacuating 45 minutes after GE. The sounding of sirens in response to the GE provides warning and notification to all residents and transients within the EPZ that there is an incident, and EAS messaging will request that people monitor the situation for further information. It is assumed that these actions cause a shadow evacuation from within the 0 to 16-mile area.

Schools routinely practice fire drills and have call lists to quickly notify parents of an emergency. In the sensitivity study, it is assumed that the initial projections indicate a need for protective actions to a distance of 16 miles. It is assumed that within 1 hour, schools beyond the EPZ would notify parents and mobilize evacuation efforts.

Cohort 4: 0 to 16 Special Facilities. Special facilities are required to have evacuation plans, and this scenario assumes that the facilities within the 0 to 16-mile area would evacuate following these plans. The special facilities cohort is modeled to depart at the same time as the evacuation tail, although, in reality, facilities would be evacuating as resources become available. As shown in Table 6-7, the delay to evacuation is longer than the base case and the speed is slower.

Cohort 5: 0 to 16 Tail. An estimate of the departure for the evacuation tail is established as a linear projection between the Peach Bottom ETE and the OREMS 10 to 20-mile ETE developed for evacuation to a distance of 20 miles from the plant.

Cohort 6: Non-Evacuating Public. This cohort group represents a portion of the public within the 0 to 16-mile area who may refuse to evacuate. It is assumed to be 0.5 percent of the population.

Table 6-7 identifies the cohort timing for Sensitivity 1.

Table 6-7 STSBO without RCIC blackstart, Sensitivity 1

Cohort	Delay to Shelter DLTSHL (hr)	Delay to Evacuation DLTEVA (hr)	DURBEG (hr)	DURMID (hr)	ESPEED* (early) (mph)	ESPEED* (mid) (mph)
0 to 16 Public	1.00	1.00	0.25	7.75	5	2
16 to 20 Shadow	1.00	1.00	0.25	7.75	5	2
0 to 16 Schools and Shadow	0.25	0.75	1.00	0.50	20	20
0 to 16 Special Facilities	1.00	9.00	4.00	1.00	2	20
0 to 16 Tail	1.00	9.00	4.00	1.00	2	20
Non-Evac	0	0	0	0	0	0

* 20 mph was used for the late-phase evacuation speed for all cohorts.

6.4.2 Sensitivity 2 for the STSBO without RCIC Blackstart Evacuation to 20 Miles

Sensitivity 2 assesses the evacuation of a 20 mile area around the nuclear power plant. Because the initial evacuation is extended to 20 miles, no further shadow evacuation was considered. Table 6-8 identifies the cohort timing for Sensitivity 2. For this sensitivity case, the cohort timing and protective action durations are shown in Figure 6-11 and Figure 6-12.

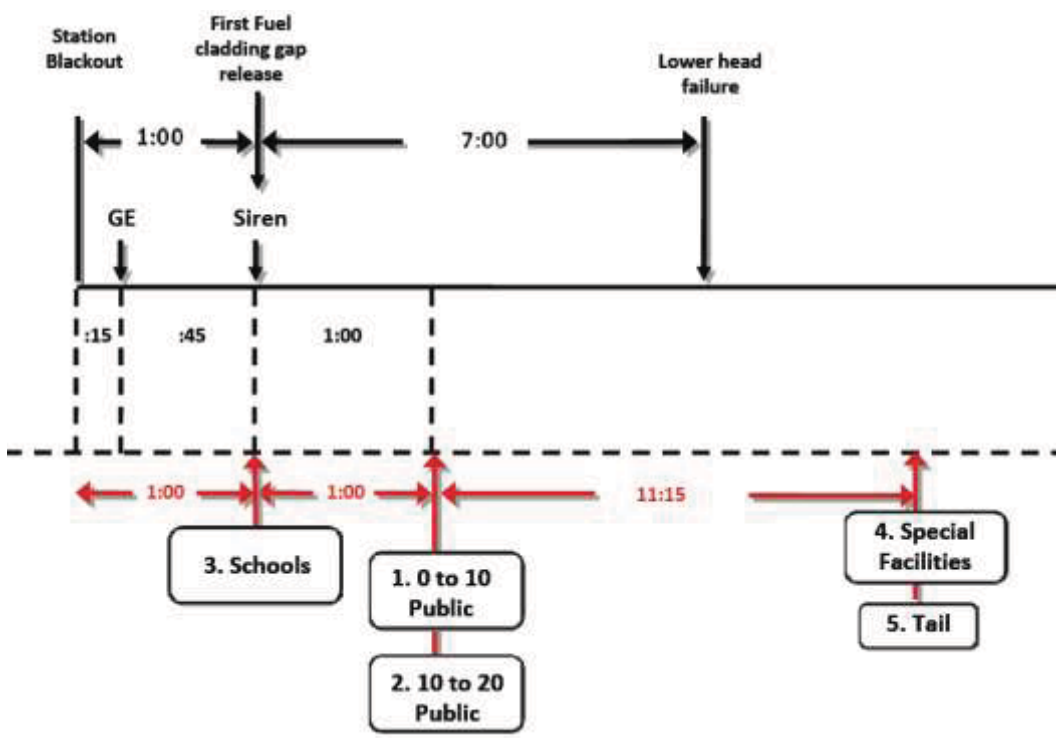

Figure 6-11 Sensitivity 2 STSBO without RCIC blackstart - evacuation to 20 miles

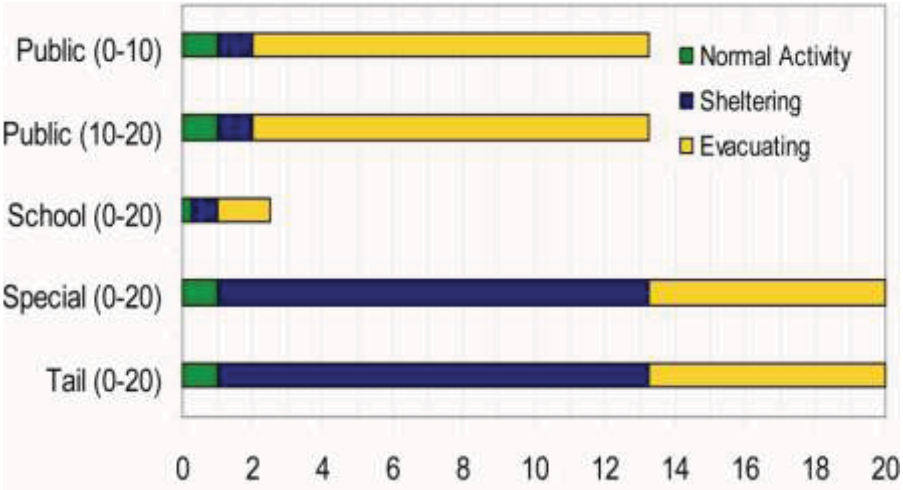

Figure 6-12 Duration of protective actions for sensitivity 2 STSBO w/o RCIC blackstart - evacuation to 20 miles

Cohort 1: 0 to 10 Public. Following declaration of a GE, sirens would be sounded within the EPZ and an evacuation order would be issued for the EPZ. The time for this cohort to receive the warning and prepare to evacuate is assumed to be 1 hour. Although the evacuation of the public starts at the same time as in the base case, it takes longer to evacuate the area as indicated in Table 6-8 which shows longer travel times and slower average speeds. Speeds were adjusted using consequence model speed adjustment factors ranging from 75 percent to 150 percent of the average speed, as appropriate for the rural and urban areas.

Cohort 2: 10 to 20 Public. This sensitivity analysis considers that the 10 to 20 Public cohort would be notified at the same time as the EPZ via EAS messaging and route alerting. The time to receive the warning and prepare to evacuate is still assumed to be 1 hour after the initial notification. The ETE for the 10 to 20 Public cohort was calculated using OREMS.

Cohort 3: 0 to 20 Schools. Upon receipt of the site's declaration of GE, county emergency management agencies would notify the schools within the EPZ in accordance with the emergency response plan. This sensitivity study assumed that schools beyond the EPZ would decide, based upon media information that it is prudent to evacuate or close schools immediately. It is assumed that within 1 hour, schools beyond the EPZ would notify parents and mobilize evacuation efforts.

Cohort 4: 0 to 20 Special Facilities. This sensitivity study assumed that special facilities beyond the EPZ would decide, based on media information that it is prudent to evacuate. The 0 to 20 Special Facilities cohort is modeled to depart at the same time as the evacuation tail. As shown in Table 6-8, the delay to evacuation is longer than in the base case and the speed is slower.

Cohort 5: 0 to 20 Tail. The ETE for the evacuation tail was estimated based on the OREMS analysis. This cohort shelters upon hearing the sirens and begins evacuating 12 hours and

15 minutes later. As shown in Table 6-8, the delay to evacuation is longer than in the base case and the speed is slower.

Cohort 6: Non-Evacuating Public. This cohort group represents a portion of the public within the 0 to 20-mile area who may refuse to evacuate and is assumed to be 0.5 percent of the population.

Table 6-8 identifies the cohort timing for Sensitivity 2.

Table 6-8 STSBO without RCIC blackstart, Sensitivity 2.

Cohort	Cohort Number#	Delay to Shelter DLTSHL (hr)	Delay to Evacuation DLTEVA (hr)	DURBEG (hr)	DURMID (hr)	ESPEED* (early) (mph)	ESPEED* (mid) (mph)
0 to 10 Public	1	1.00	1.00	0.25	11.00	5	1.8
10 to 20 Public	2	1.00	1.00	0.25	11.00	5	1.8
0 to 20 Schools	3	0.25	0.75	1.0	0.5	20	20
0 to 20 Special Facilities	4	1.00	12.25	5.75	1.00	1.8	20
0 to 20 Tail	5	1.00	12.25	5.75	1.00	1.8	20
Non-Evac	6	0	0	0	0	0	0

* 20 mph was used for the late-phase evacuation speed for all cohorts.

6.4.3 Sensitivity 3 for STSBO w/o RCIC Blackstart - Delay in Protective Actions

At the initiation event for the STSBO without RCIC blackstart, a GE is declared based on EAL MG1. Although there is a high level of confidence about the actions expected from control room operators and the ORO response, the peer review committee suggested that the analysis consider a delay in the implementation of protective actions. Such a delay could be from delayed communication to the public about implementation of protective actions, or other reasons. To address the potential for delay, an additional protective active timeline has been developed for the STSBO without RCIC blackstart. This timeline reflects a delay in the implementation of protective actions by the public within the EPZ. Because protocols and procedures are in place, exercised, and tested frequently, it is assumed that a delay of 30 minutes is adequate for this sensitivity study. The cohort timing and protective action durations are shown in Figure 6-13 and Figure 6-14 for this sensitivity case.

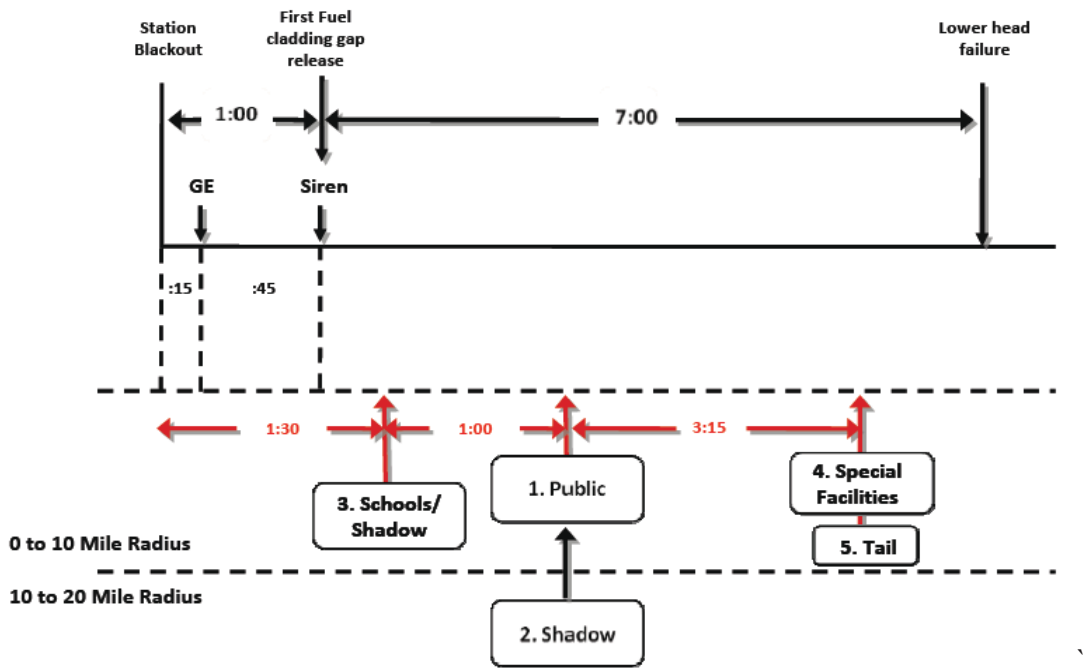

Figure 6-13 Sensitivity 3 STSBO w/o RCIC blackstart - delay in protective actions

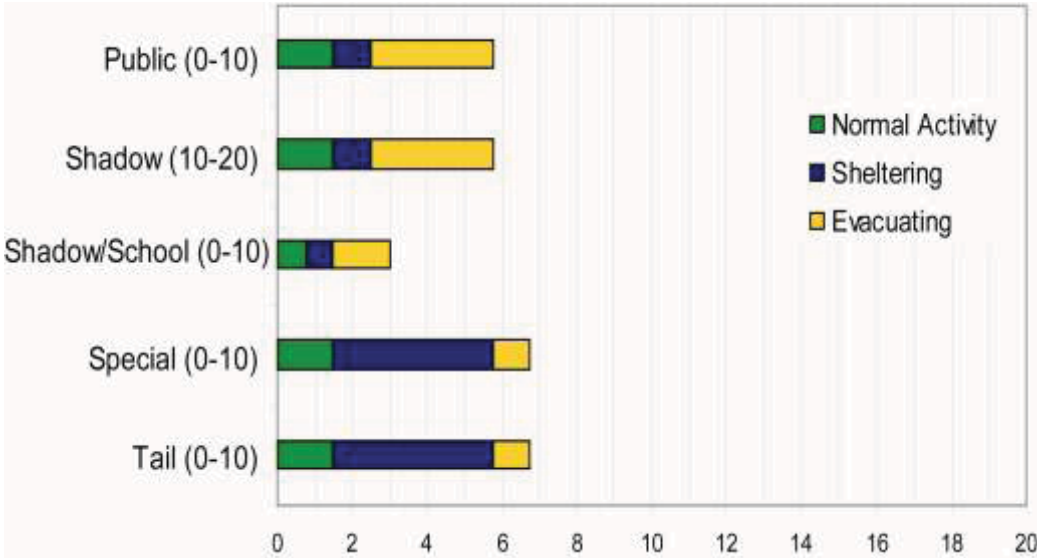

Figure 6-14 Protective action durations for sensitivity 3 STSBO w/o RCIC blackstart - delay in protective actions

The 30 minute delay was added to the 'Delay to Shelter' parameter for all cohorts. The remaining delay and speed parameters were unchanged from the base case. With the delay allocated to this point, all cohort actions move to the right on the timeline by 30 minutes and the sum of DLTEVA, DURBEG, and DURMID still equates to the ETE for the public and the tail.

Table 6-9 identifies the cohort timing for Sensitivity 3.

Table 6-9 Cohort Timing for Sensitivity 3

Cohort	Delay to Shelter DLTSHL (hr)	Delay to Evacuation DLTEVA (hr)	DURBEG (hr)	DURMID (hr)	ESPEED* (early) (mph)	ESPEED* (mid) (mph)
0 to 10 Public	1.50	1.00	0.25	3.00	5	3
10 to 20 Shadow	1.50	1.00	0.25	3.00	5	3
0 to 10 Schools/Shadow	0.75	0.75	1.00	0.50	20	20
0 to 10 Special Facilities	1.50	4.25	0.50	0.50	3	20
0 to 10 Tail	1.50	4.25	0.50	0.50	3	20
Non-Evac	0	0	0	0	0	0

* 20 mph was used for the late phase evacuation speed for all cohorts.

6.5 Analysis of Earthquake Impact

A seismic analysis was developed to assess the potential effects on local infrastructure (e.g., roadways and bridges), communications, and emergency response in the event of a large scale earthquake. The accident scenario used in the earthquake analysis is the STSBO without RCIC blackstart, which was selected because this scenario represents an earlier release than the other scenarios. Integrating the effects of the earthquake into the analysis required assessing the damage potential of the earthquake, identifying parameters that would be affected, and determining the new values for affected parameters.

The potential for an earthquake is largely identified by the occurrence of previous earthquakes in the region. Understanding of where earthquake faults exist in the eastern United States is not robust, unlike in the West, where geological fault lines can be identified on the surface. Faults in the east are usually buried below layers of soil and rock and not identifiable, making prediction of earthquake location and magnitude difficult. The earthquakes hypothesized in SOARCA are assumed to be close to the plant site, and it may be assumed that severe damage is largely localized. Housing stock would mostly survive the earthquake, with some damage. The local electrical grid is assumed to be out of service from the failure of lines, switch yard equipment, or other impacts. As there is currently no backup power system for the sirens at Peach Bottom, the analysis assumed that OROs would perform route alerting to notify the population of the need to take protective actions. This is a routine and effective method of notifying the public to implement protective actions [21]. Under these postulated conditions, the analysis considered the potential for such an earthquake to affect emergency response and public evacuation.

6.5.1 Soils Review

To approximate the extent of damage, NRC seismic experts conducted an evaluation of the potential failure of infrastructure to determine which, if any, roadways or bridges may fail under the postulated earthquake conditions. The assessment was performed using readily available information and professional judgment. Existing information on the basic bedrock geology of the region was developed from reports and papers from the United States Geological Service, Pennsylvania Geological Survey, Maryland Geological Survey, and the final safety analysis

report for the Peach Bottom plant. Generalized soils information was developed from Natural Resources Conservation Service (NRCS) soil survey information for York and Lancaster counties in Pennsylvania. This analysis assumed that the generalized soil characteristics are applicable to the entire region.

The NRCS reports break the soils into several distinct, descriptive units. The units of interest to the present evaluation are the Chester-Gleneig, Mt. Airy-Manor, Grenville, and Codorus soil groups. These are typically well-drained soils, with the Chester-Gleneig and Mt. Airy-Manor units (mostly residuum from saprolite) existing on the ridges and uplands and the Glenville and Codorus soils (mostly alluvium and colluvium) in the low regions and valley bottoms. Based on the engineering properties contained in the NRCS reports, these units of interest would be either 'potentially liquefiable' or 'liquefiable' if the water content in the soils were sufficiently high. Initial assumptions for the analysis included the following: (1) the general soil characteristics described above exist at all locations at the time of any large earthquake and the water table is sufficiently high that liquefaction and loss of strength would result, and (2) liquefaction of soils beneath a roadway in flat topography would not result in any significant damage or otherwise compromise the evacuation route.

The region around Peach Bottom is generally flat to rolling topography with a relatively small number of streams and watercourses, resulting in few bridges and overpasses. The general region of interest near the Peach Bottom site does not have a large number of locations where earthquake damage would render the evacuation routes nonfunctional. Information is not readily available on the specific engineered features of bridges and other infrastructure with which to make specific assessments on the likelihood of failure in an earthquake scenario. Therefore, the analysis assumes that: (1) all of the bridges across the Susquehanna River fail within 20 miles of the plant, and (2) the road across the Conowingo Dam would be unavailable.

6.5.2 Infrastructure Analysis

The seismic evaluation of the potential failure of roadway infrastructure identified 12 bridges and roadway segments that could fail under the postulated conditions.

Table 6-10 provides a brief description of each area assumed to fail, and Figure 6-15 shows the transportation network and the locations of the affected roadway segments and bridges.

Table 6-10 Description of the Potential Evacuation Failure Locations

Location	Description
A	PA Highway 372 upstream of Susquehanna River. Two single span bridges along a single roadway segment.
B	PA 372 bridge across the Susquehanna River north of the plant. Two lane multi-span bridge.
C	US 222 Robert Fulton Highway. Two lane single span bridge.
D	PA 74 (Delta- bypass/Pylesville Road) south of Holtwood Road (PA 372). Single span two-lane bridge.
E	MD 136 - Whiteford Road. Two lane segment along lakeside. Potential for slumping into lake.
F	US 1 (Conowingo Road) east of Susquehanna River and US 222. Two lane

	single-span bridge.
G	US 1 across Conowingo Dam. Two lane road.
H	US 1 west of Susquehanna River, west of MD 136. Two lane road, single span bridge.
I	MD 136 south of US 1. Two lane road, single span bridge.
J	MD 222 Susquehanna River Road north of Main Street. Two lane road runs along river edge. Potential for slumping into river.
K	I-95. Six lane multi span bridge.
L	US 40. Four lane multi span bridge across Susquehanna River.

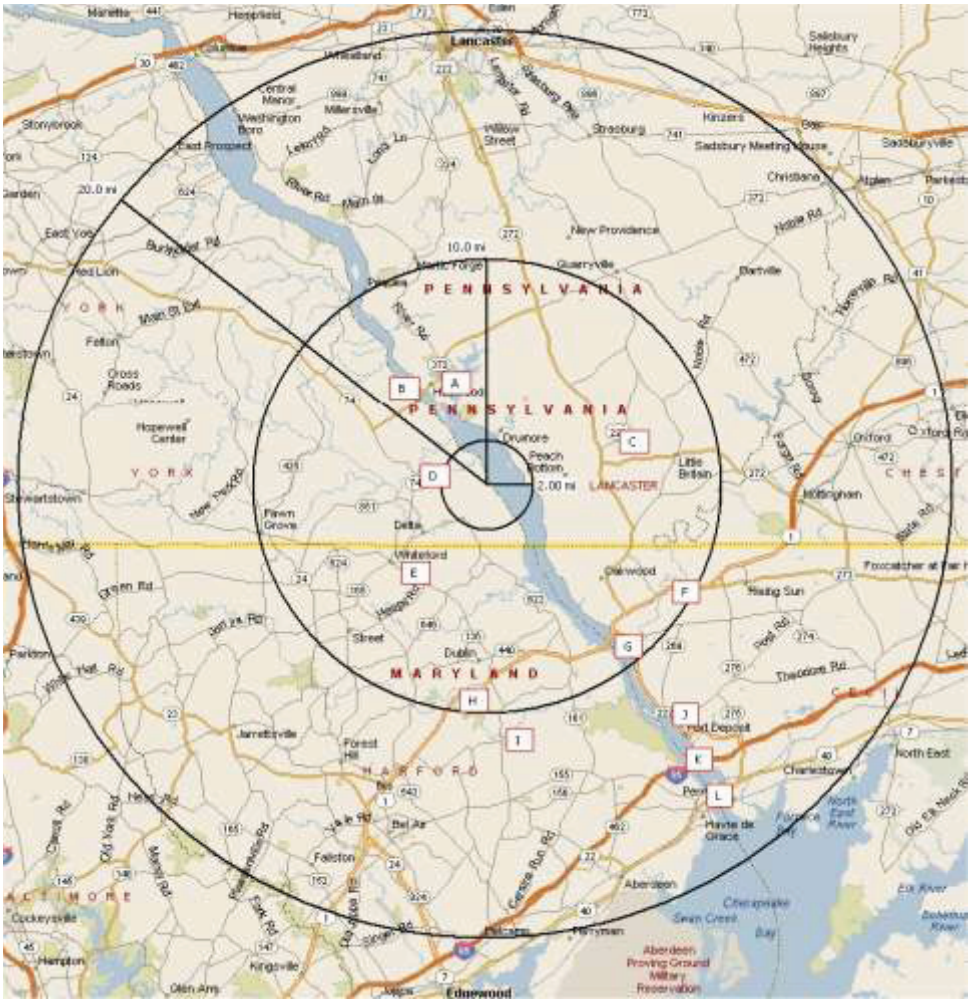

Figure 6-15 Roadway network identifying potentially affected roadways and bridges

Evacuations are planned and conducted to move the public radially away from the nuclear power plants. Evacuation routes are designated in emergency planning brochures, but all roadways within the EPZ serve the evacuees. Some of the bridges identified in the seismic analysis will have a negligible effect on the evacuation because of their location within the roadway network, while others may have a more pronounced effect.

The loss of bridges and the Conowingo Dam Road crossing the Susquehanna River does not affect the ETE. These crossings are represented as B, G, K, and L on Figure 6-15. The EPZ evacuation routes identified in the emergency plan indicate that evacuees west of the river would typically evacuate in a westerly or southerly direction, and evacuees east of the river would evacuate in a northerly or easterly direction. The only river crossing (i.e., location G) identified as a Peach Bottom evacuation route is U.S. Route-1 (US 1) across the Conowingo Dam. Although this road is an evacuation route, the evacuation map indicates that travel west of the river would proceed westerly, and travel east of the river would proceed easterly; therefore, failure of the river crossing would have no effect on the ETE.

Bridges A, C, D, and E in Figure 6-15, serve sparsely populated areas and have additional roads available, supporting a conclusion that evacuation delay because of loss of these bridges is minimal. Along Whiteford Road (i.e., location E in Figure 6-15) there is a potential for part of the roadway to slump into the lake. This is the only roadway failure in this area and there are many alternative routes north, west, and south of the location; therefore, no appreciable delay would be expected due to this failure. Travel along Maryland Route 136 (MD 136) may be diverted to multiple alternative roadways in the event the single span bridge I fails.

Bridges H and I in Figure 6-15 are two lane single span bridges located south of the plant in an area where local roadways are available as alternate routes. Pennsylvania Route 222 (PA 222) becomes MD 222 at the State line; and the MD 222 part may potentially slump off into the river at location J in Figure 6-15. As indicated on the map, there are alternatives to route around this area if the roadway does slump into the river. Failure of these bridges should not appreciably affect the ETE.

The two bridges with the greatest potential to affect the ETE are F and H because they are located along the edge of the EPZ and serve larger areas. The total population identified in the ETE report for the area served by bridge H is about 18,000 corresponding to approximately 6,000 passenger cars using the vehicle population factor applied in the ETE report. For this volume of vehicles, only about 1,200 vehicles per hour would need to exit the EPZ to stay within the 5 hour and 15 minute ETE. For this type of two lane roadway, a service volume of 1,700 passenger cars per hour may be achieved [30]. The alternate routes out of the EPZ have more than sufficient capacity to support the evacuating population.

The total population identified in the ETE report for the area served by bridge F on U.S. 1 is about 6,790, which equates to approximately 2,300 passenger cars. The Susquehanna River Road (PA 222) and other local roadways nearby are available as alternate routes out of the EPZ; therefore, no appreciable delay would be expected.

Based on a review of the ETE report, the EPZ subareas affected by loss of bridges, and a detailed review of the roadway network, the analysts concluded that loss of the identified bridges will not increase the total ETE. This is consistent with the Peach Bottom ETE, report which shows that evacuation of the northeast quadrant of the EPZ controls the evacuation time for the entire EPZ. Only bridge B is located in this area, crossing the river as described above. Figure 6-16 shows an example of a bridge (i.e., Bridge C on US 222 Robert Fulton Highway) that could potentially fail under the earthquake conditions.

Figure 6-16 Bridge along Robert Fulton Highway

6.5.3 Electrical Power and Communications

The seismic event causes the loss of all onsite and offsite power, which can affect the response timing and actions of the public. Typically, sirens would sound following the declaration of an SAE and GE. The loss of power will affect the number of sirens that sound; however, it is expected that many of the sirens within the EPZ will still function. Where sirens are inoperable, the initial alert and notification of the public may take longer. The loss of power affects the number of residents receiving instructions via EAS messaging. Televisions, household radios, and some telephones will not operate, although battery-operated radios and car radios will operate. The residents within the EPZ will have felt the earthquake which will instill a sense of emergency. It may be expected that the residents will use multiple methods of communication, such as cell phones, telephones, websites, and direct interface to communicate the emergency message. The alert and notification will be supplemented by route alerting, which is a planned backup form of communication for the EPZ.

The loss of power will cause traffic signals to default to a four-way stop mode, which is less efficient than normal signalization [30]. Typically, emergency response personnel would respond to these intersections and direct traffic. A review of the roadway network within the EPZ indicates that there are only a few traffic signals within the EPZ and that most intersections are controlled with stop signs. Table 7-1, "Recommended Traffic Control Management Locations," in the ETE report identified 12 key locations for emergency management traffic control to expedite traffic out of the EPZ [29]. As indicated in the ETE report, these 12 locations are included in the county plans. The analysis assumes that the OROs will be able to provide the staff needed to support the few locations where traffic signals are not working; therefore, the analysis also concludes that the loss of signalization will not increase the total ETE.

6.5.4 Emergency Response

The analysis assumed that event timing is a mid-week winter day when residents are at work and children are at school. In Maryland, the primary shift of emergency responders would be on duty and immediately available at the time of the incident. Most of the Pennsylvania emergency responders are volunteers and would be at their normal place of employment. After the earthquake, there will be an initial need to assess damage and respond to life-threatening needs. These initial priorities for emergency response personnel may delay implementation of traffic control to support an evacuation. It is assumed that responders will realize early that damage to local infrastructure is not severe, because there are very few bridges or large structures within the EPZ, and will focus efforts on communicating with the public via route alerting, where necessary. Route alerting would not be appreciably delayed because damage to local infrastructure is not severe.

During large scale emergencies, OROs routinely supplement staff with on call and off duty personnel. Although communications are assumed to be initially limited, radios are available to contact the needed staff, and off duty responders may be expected to report for duty during such emergencies, particularly if they have experienced the earthquake. It is expected by the time an evacuation is ordered, OROs would have been augmented with additional staff.

6.5.4.1 Evacuation Time Estimate

Roadway capacity is a key parameter in developing ETEs. Reducing the number of roadways will reduce the available capacity. The evacuation times can be affected when bridges fail, traffic signals do not operate effectively, and EAS messaging is not disseminated in a timely manner to inform evacuees of protective actions and preferred evacuation routes. Although there are a number of factors that can increase evacuation time, the effect on the ETE is expected to be limited. This is because residents will have experienced the magnitude of the earthquake, therefore they have some level of understanding that an emergency exists, prior to any formal warning. Secondly, emergency response personnel would begin route alerting and establish traffic control.

The roadway network beyond the EPZ was also evaluated to determine if loss of infrastructure might delay evacuees traveling through this area. How this loss of infrastructure affects the evacuation time depends on the location of the facilities and the evacuating public who may be expected to use these routes. As described earlier, loss of the bridges and roadways identified in Table 6-10 are not expected to appreciably affect the ETE. This is because only 12 locations in the 20 mile radius around the plant, (1,256 square miles) were identified as potentially failing. Within such a large area, there are many alternate routes for evacuation.

Another consideration in this analysis is that no large-scale evacuation is expected for the 10 to 20 mile area. Therefore, the roadways are assumed to be substantially available to serve the evacuating public from the EPZ. Furthermore, almost all of the bridges and the roadway sections that are assumed to fail are located in the southern section of the 10 to 20 mile area beyond the EPZ. This area has a smaller population than the area to the north of the plant. The results of the OREMS analysis used to develop the ETE for the 10 to 20 mile area demonstrated that longer evacuation times occurred in the northern section because of congestion experienced near Lancaster, Pennsylvania.

The ETE was used to develop the speeds for the evacuating public. The following ETEs provided for Peach Bottom were used for the base case analyses:

- 100 percent evacuation: 5 hours and 15 minutes
- 90 percent evacuation: 4 hours and 15 minutes

For the seismic analysis, it was assumed that because the earthquake is felt by the public, the 0 to 10 Shadow cohort evacuation increased from the 20 percent used in the base case to 30 percent of the population. This effectively removes 30 percent of the total vehicles from the roadway network shortly after the incident, which reduces potential for traffic congestion. The wide availability of roadway infrastructure at these distances from the plant provides ample access for evacuees leaving the EPZ and should not appreciably affect evacuation times.

6.5.5 Development of WinMACCS Parameters

Modeling the effects of seismic events required adjusting additional parameters. To account for the potential loss of bridges and roadway sections, the routing patterns in the WinMACCS model were adjusted to divert traffic around these locations by using routes not impacted by damaged bridges. This adjustment was completed for each grid element with an impacted roadway. Routing was manually adjusted to travel around rather than through the impacted grid elements.

The relocation parameters used in the earthquake analysis are the same as those used in the base case analyses. Shielding factors are also the same as those used in the base case analyses. It may be expected that the damage to structures caused by an earthquake of this magnitude would include broken windows and some structural damage. However, because residents within the seismic area are assumed to shelter only for a short period of time, any adverse affect on sheltering protection factors is irrelevant because evacuation begins before the plume arrives.

6.5.6 Seismic Short-Term Station Blackout without RCIC Blackstart

The timing of emergency classification declarations for the STSBO without RCIC blackstart was based on the EALs contained in the site emergency plan implementing procedures. The timing of emergency classification declarations for the STSBO without RCIC blackstart was based on Table PBAPS 3-1 in the site emergency plan implementing procedures. The analysts reviewed emergency classification timing with the licensee for accuracy, and this scenario was identified as an immediate GE. With loss of offsite power and loss of DC power, operators cannot determine whether water level is above TAF, and a GE is declared based on EAL MG1. The emergency response timeline for the STSBO without RCIC blackstart scenario is shown in Figure 6-17. The duration of specific protective actions for each cohort is shown in Figure 6-18. Core damage, as evidenced by the first fuel cladding gap release, is calculated at 1 hour into the event, with a significant radioactive release from containment beginning 8 hours into the event as indicated by the containment failure.

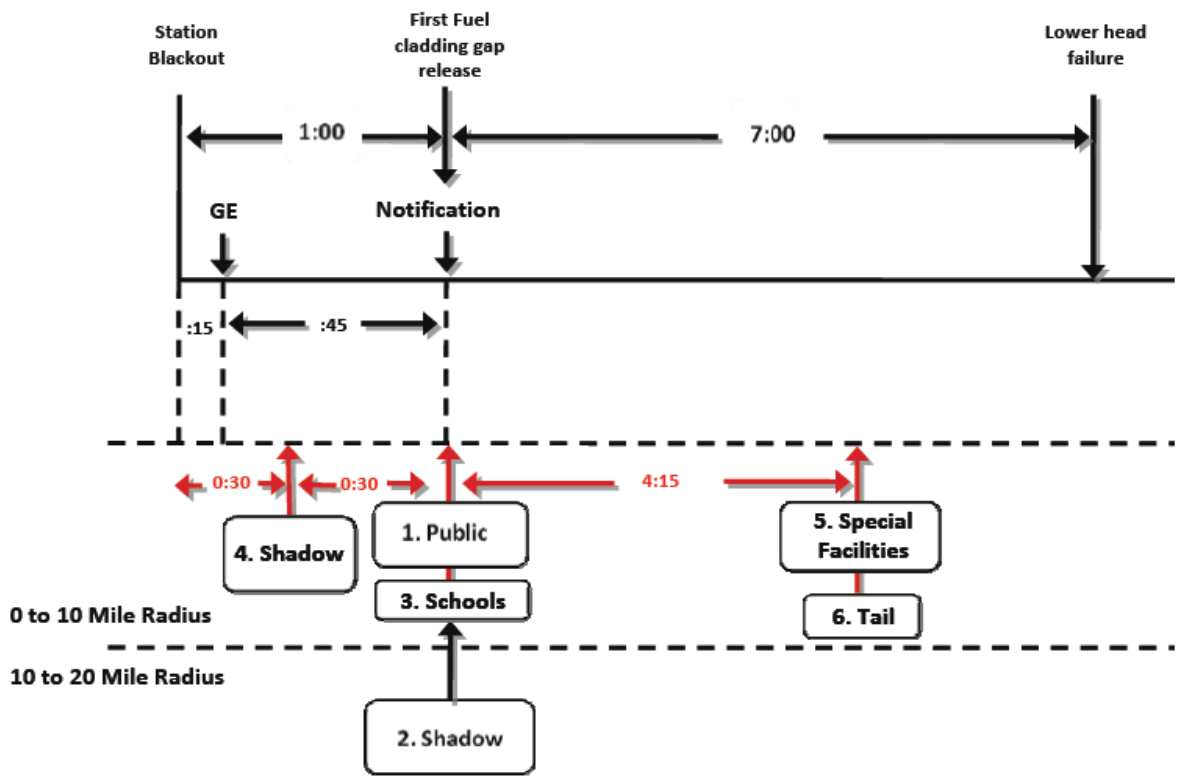

Figure 6-17 STSBO w/o RCIC blackstart emergency response timeline (seismic analysis)

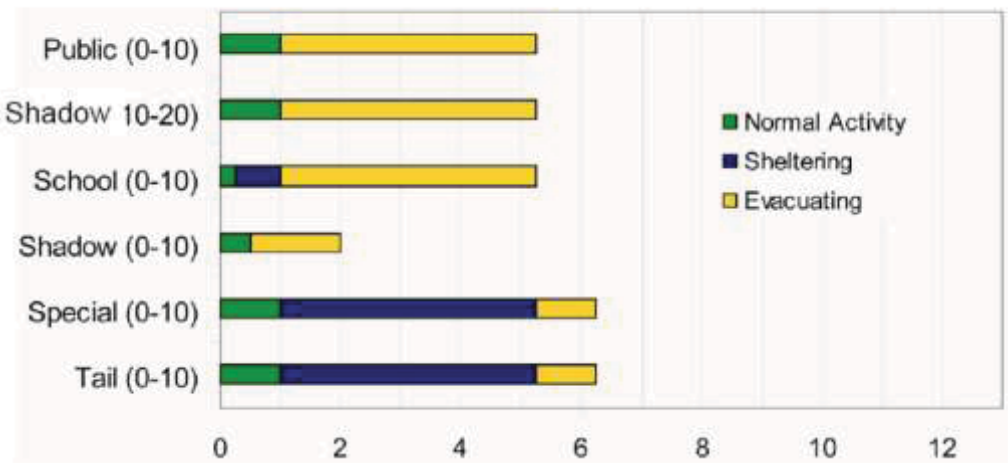

Figure 6-18 Protective action durations - STSBO w/o RCIC blackstart (seismic analysis)

The timeline identifies points at which cohorts would receive instruction from OROs to implement protective actions. Cohorts would then implement the protective actions. While protective actions within the EPZ can be modeled in accordance with procedures, the analysts made assumptions that approximate those actions that could be taken due to the effects of the earthquake. The evacuation is assumed to include the full EPZ, which is consistent with

emergency planning in Pennsylvania. For this analysis, a full evacuation was modeled assuming that the State of Maryland OROs would agree with the Pennsylvania protective action decisions.

The analysis assumed that the large earthquake will be felt by everyone within the EPZ, instilling a heightened preparedness. It is assumed that the public is ready to respond to protective actions once they receive information, and that some individuals will begin to prepare for an evacuation before receiving official notice.

Cohort 1: 0 to 10 Public. The 0 to 10 Public cohort is assumed to begin evacuating upon receipt of notification which is provided primarily by route alerting. The analysis assumes that the effects of the earthquake are so severe that members of the public, knowing they live within an EPZ, begin preparations for evacuation shortly after the earthquake.

Cohort 2: 10 to 20 Shadow. This cohort is assumed to begin movement at the same time as the 0 to 10 Public cohort once widespread media broadcasts are underway. The analysis assumes that the shadow population increases to 30 percent (from 20 percent for the base case calculations) of the public in the area beyond the EPZ.

Cohort 3: 0 to 10 Schools. Although communication systems may have been affected, this analysis assumes that, after receipt of the GE declaration, county emergency management agencies notify the schools promptly. The analysis also assumes that, having felt the earthquake, schools take the initiative to prepare to evacuate as they would for an emergency. Buses would be mobilized, and it is assumed that schools would begin evacuating about 1 hour after the start of the incident. The limited effect on infrastructure within the EPZ is not expected to appreciably delay bus mobilization. The analysis also assumed that, given the magnitude of the earthquake, parents in the vicinity of the schools would pick up their children, reducing the need for a full complement of buses.

Cohort 4: 0 to 10 Shadow. This cohort is assumed to begin movement first. They experience the earthquake and quickly begin to evacuate, avoiding the traffic congestion.

Cohort 5: 0 to 10 Special Facilities**.** The special facilities cohort is assumed to depart at the same time as the evacuation tail. Inbound lanes on roadways will be useable for emergency support vehicles, but localized congestion will delay the arrival of specialized vehicles. Special facilities are assumed to leave at the same time as the evacuation tail; however, as discussed earlier for other scenarios, this is a simplification of the analysis because special facilities would realistically evacuate individually as resources are available.

Cohort 6: 0 to 10 Tail. The tail takes longer to evacuate for many reasons, such as the need to return home from work to evacuate with the family; the need to shut down farming or manufacturing operations before evacuating, and for the earthquake, the need to move rubble or other items before evacuating.

Cohort 7: Non-Evacuating Public. This cohort represents the portion of the 0 to 10-mile Public who may refuse to evacuate. It is assumed to be 0.5 percent of the population.

Table 6-11 summarizes the evacuation timing for each cohort. In general, the cohorts in the seismic study have faster mobilization times because of their immediate awareness and have the same evacuation speeds.

Table 6-11 Cohort Timing for STSBO without RCIC blackstart

Cohort	Delay to Shelter DLTSHL (hr)	Delay to Evacuation DLTEVA (hr)	DURBEG (hr)	DURMID (hr)	ESPEED * (early) (mph)	ESPEED * (mid) (mph)
0 to 10 Public	1.00	0.00	0.25	4.00	5	3
10 to 20 Shadow	1.00	0.00	0.25	4.00	5	3
0 to 10 Schools	0.25	0.75	0.25	4.00	5	3
0 to 10 Shadow	0.50	0.00	1.00	0.50	20	20
0 to 10 Special Facilities	1.00	4.25	0.50	0.50	3	20
0 to 10 Tail	1.00	4.25	0.50	0.50	3	20
Non-Evac	0	0	0	0	0	0

* 20 mph was used for the late-phase evacuation speed for all cohorts.

6.6 Accident Response and Mitigation of Source Terms

The Peach Bottom SOARCA study has concluded that scenarios can be mitigated by the licensee through the use of safety and security enhancements, including SAMGs and 10CFR50.54(hh) mitigation measures. Analyses were conducted of the consequences that may result if the onsite emergency response organization (ERO) takes insufficient mitigative action to prevent core damage and radiological release to the environment. It is expected that mitigative actions would be attempted. The staff believed it appropriate to perform the consequence analyses to develop an understanding of core melt sequences, source term evolution, and offsite response dynamics and to compare this to previous studies. However, neither a human reliability assessment nor a detailed seismic damage assessment for implementation of mitigative measures were performed. The following analysis describes an expected national level response to a severe nuclear power plant accident and provides a basis for truncating the release no later than 48 hours after the accident begins. Note that past studies, including PRA such as NUREG-1150, typically truncated releases after 24 hours.

Mitigative actions during an accident are intended to:

- prevent the accident from progressing;
- terminate core damage if it begins;
- maintain the integrity of the containment as long as possible; and
- minimize the effects of offsite releases.

Response to a General Emergency would begin with the onsite ERO and would expand as needed to include utility corporate resources, State and local resources, and resources available from the Federal government, should these be necessary. It is most likely that plant personnel

would attempt to mitigate the accident before core melt, but if their efforts were unsuccessful the national level response would provide resources to support mitigation of the source term. This discussion presents a timeline for bringing resources onto the Peach Bottom site to support mitigative actions, including as a last effort, flooding the reactor building to a level above a hypothetical hole in containment to minimize the effects of an offsite release. The approach described herein also discusses, to the extent practical at this time, the NRC Task Force review of the response to the nuclear power plant accident at the Fukushima Diaichi facility in Japan.

On March 11, 2011, the Great East Japan Earthquake caused a large tsunami estimated to have exceeded 14 meters (45 feet) in height at the Fukushima Daiichi nuclear power plant site. The earthquake and tsunami produced widespread devastation across northeastern Japan, resulting in approximately 25,000 people dead or missing, displacing tens of thousands of people, and significantly impacting the infrastructure and industry in the northeastern coastal areas of Japan. The earthquake and tsunami caused accidents at Units 1, 2 and 3 of the Fukushima Daiichi nuclear power plant facility and caused concern for the remaining units and spent fuel pools at the site. Amid the vast devastation and competing health and safety priorities in the region, onsite and offsite response agencies worked diligently to bring the accidents under control. This effort took many weeks.

Shortly after the nuclear accident, the NRC established a task force to conduct a methodical and systematic review of the NRC's processes and regulations to determine whether the agency should make additional improvements to its regulatory system. The Task Force report, "Recommendations for Enhancing Reactor Safety in the 21st Century," [35] identified that prolonged SBO and multiunit events present challenges to Emergency Preparedness facilities that were not considered when the NRC issued NUREG–0696, "Functional Criteria for Emergency Response Facilities," in 1981. The Task Force report also states that an overarching lesson is that major damage to infrastructure in the area surrounding the plant might challenge an effective emergency response. A number of recommendations are presented in the report that address physical, administrative, and regulatory enhancements to further reduce the risk of similar challenges occurring among the US fleet of nuclear power plants. As a state-of-art analyses, the SOARCA project included a degree of depth in the analyses beyond the scope of many previous studies. In this regard, some of the recommendations of the Task Force report had already been considered in SOARCA.

For instance, SOARCA investigated the challenges of potential damage to infrastructure within and beyond the EPZ as a result of an earthquake. The site specific analysis showed that 12 bridges may fail. Four of these bridges were located beyond the EPZ and the remaining eight were dispersed within the 10 mile EPZ (314 square miles). The analysis showed that because there were relatively few bridge failures within such a large area, use of the roadways would be relatively unimpeded. The seismic analysis described in Section 6.5 quantified the offsite effects of challenges to both infrastructure and resources within the Peach Bottom EPZ. The Task Force report also recommends further enhancement of current capabilities for onsite emergency actions by requiring that licensee's modify the EOP technical guidelines to include SAMGs. This would enhance current capabilities, but would not change the manner in which SAMGs have already been considered in SOARCA.

With regard to the emergency response, the Peach Bottom analyses applied the emergency classification scheme identified in the site EAL matrix. For Peach Bottom the declaration of a GE would occur at 15 minutes for the STSBO scenarios. For the LTSBO scenario, declaration of an SAE occurs at 15 minutes and declaration of a GE would occur about 30 minutes later. Licensees are required by regulation to notify OROs within 15 minutes of declaring an emergency, and the OROs then initiate a planned response by offsite agencies who are able to direct necessary resources upon request, such as fire trucks, to support mitigation of the accident. The declaration by the licensee is not only a notification, this declaration initiates an ongoing communication between the control room, licensee staff, OROs, NRC, and other response agencies.

As supported by the SOARCA analyses, it is shown that the accidents evaluated could be mitigated through the actions of the onsite and offsite response agencies. The evaluation of the mitigation of source term and truncation of the accident at 48 hours further expands upon the response resources through identification of corporate, local, State, and Federal offsite resources. The responsibilities and resources of each of these organizations are described in onsite and offsite emergency response plans. These response organizations would mobilize upon request and as needed to support a severe nuclear power plant accident. These resources are in addition to the mitigative actions by the licensee through the use of safety and security enhancements, including SAMGs and 10CFR50.54(hh) mitigation measures.

Although the response to the Fukushima Daiichi accident has taken weeks and challenges still remain, it is expected that the regulatory structure, protocols, and resources available to support a response in the US are sufficient to mitigate the release of the accident scenarios identified in this study within 48 hours. Implementation of recommendations from the Task Force report would further improve the capabilities to mitigate the accident itself in a timely manner to help prevent a release from occurring.

For purposes of this analysis, the timeline begins when the plant has declared an emergency. The State would be notified by the plant within 15 minutes after the emergency declaration and the plant would also notify their corporate headquarters. The NRC would be notified, following plant procedures, within one hour of the declaration; although, for a seismic event, it may be assumed that the NRC would be informed sooner than one hour by the onsite NRC resident inspectors, if not the licensee. The NRC resident inspectors are available to provide knowledge of accident conditions and would recognize the urgency of the situation should an earthquake occur. There are multiple onsite communications systems available to make these notifications and the communication paths are exercised and tested. The NRC headquarters would notify other Federal agencies as appropriate.

Upon receipt of notification of the emergency classification, the NRC would activate the Headquarters Operations Center (HOC). NRC response teams reporting to the HOC include the Reactor Safety Team, Protective Measures Team, Executive Team, and other teams that support response related activities. Plant drawings and procedures are available in the HOC. Data that is typically communicated to the HOC via the Emergency Response Data System (ERDS), the Emergency Notification System bridge line, and other communication bridges, would likely be communicated via the resident inspectors satellite phones and via site battery operated systems.

Licensees are required to provide guaranteed power to the emergency communications equipment per NRC Bulletin 80-15, "Possible Loss of Emergency Notification System (ENS) with Loss of Offsite Power."The NRC Region 1 office would activate, with similar response teams, and would mobilize and deploy a Site Team to the licensee's response facilities to independently review response actions. The Site Team would include reactor safety engineers to review actions taken to mitigate the accident and protective measures specialists to review protective action recommendations to assure that the most appropriate actions are taken. Arrival of the Site Team may take several hours. The HOC, Regional Operations Center, and Site Team include liaisons to support coordination of resources when requested by the licensee.

Once notified, the plant corporate headquarters would activate the corporate response resources. Peach Bottom is part of the Exelon fleet, which includes a remote EOF that would be activated. Exelon has access to fleet-wide emergency response personnel and equipment, including equipment from sister plants, following 10CFR50.54(hh) reactor security requirements to mitigate the effects of large fires and explosions. This equipment would support multiple response needs and include such items as generators, pumps, compressed gas, etc. In addition, the Institute for Nuclear Power Operations (INPO) and the Nuclear Energy Institute (NEI) would activate their emergency response centers to assist the site. These organizations would make available additional knowledgeable personnel and an extensive array of equipment.

Concurrent with the NRC and industry response, the National Response Framework (NRF) which establishes a coordinated response of national assets would be implemented. As described in the Nuclear/Radiological Incident Annex to the NRF, NRC is typically the Coordinating Agency for incidents occurring at NRC-licensed facilities. As Coordinating Agency, NRC has technical leadership for the Federal Government's response to the incident. Under established agreement with the NRC, the Department of Homeland Security (DHS) would be the Coordinating Agency[56] for an event in which a GE is declared. In this case, NRC retains the Federal technical leadership role but does not coordinate overall Federal response. Under the NRF, the DHS would likely deploy the radiological monitoring and radiological response assets of the Department of Energy (DOE) for this type of an emergency. Some of the other agencies cooperating in an incident include the EPA, the Federal Emergency Management Agency, the U.S. Department of Health and Human Services, and any other federal agency that may be needed.

The above organizations would be developing onsite and offsite mitigation strategies with different objectives. These strategies would be implemented concurrently. An onsite mitigation strategy relies upon onsite resources and is expected to be immediate in order to prevent core melt and radiological release. As mentioned earlier, for the unmitigated cases the SOARCA project assumes onsite mitigative efforts are not effective. Offsite mitigation strategies utilize onsite and offsite equipment and resources and take more time to develop.

---

[56] The coordinating agency supports the U.S. Department of Homeland Security incident management mission by providing the leadership, expertise, and authorities to implement critical and specific aspects of the response.

6.6.1 External Resources

The initiating event for the reactor accident is a beyond design-basis earthquake close to the plant. A General Emergency is declared shortly after the event, and the DHS would be the Coordinating Agency bringing to bear any needed Federal resources. The State remains responsible for protecting the public health and safety and remains directly involved in the response. State, local and Federal resources would be available for use in mitigating the accident. This review describes how resources within the region might be acquired and used to support accident mitigation.

The States and counties have road departments with access to heavy equipment to clear debris from roadways and facilitate plant access, if needed. The EPZ is largely agricultural, and there are multiple access roads to the plant. The six-lane I-95 and four-lane U.S. 40 bridges south of the Peach Bottom site that cross the Susquehanna River are assumed to fail in the earthquake. There are equipment suppliers on both sides of the river; therefore, loss of these bridges would only have a limited affect on delivery of equipment. A heavy airlift capacity is also available in the region if needed to support prompt delivery of equipment.

It is expected that primary equipment needs for accident mitigation would be electrical generators and additional pumps to deliver water to the facility. Response staff will have identified that these resources must be obtained from offsite. There are numerous fire stations in the region with water trucks and pumper trucks that would respond. This would be the first option for portable water and pumping resources if onsite systems are not functional. Local fire trucks could be onsite within minutes of a request, and larger regional fire station resources could be onsite within 2 to 3 hours based on the proximity of these resources to the plant and the time of the request. The local fire departments are primarily volunteer rural fire departments that are familiar with operating in areas without public water supplies and are experienced with drafting water from ponds and rivers should this be necessary.

For additional or larger capacity resources, Philadelphia is approximately 70 miles east and Baltimore is about 50 miles south of the plant. A review of heavy equipment supply companies in these cities has found that electrical generators and pumping equipment are widely available. As equipment needs are identified, INPO, NEI and utility personnel would be coordinating acquisition and delivery of industry resources or commercially available resources, as needed. It is assumed that large portable generators and pumps, if needed, could be obtained and transported via truck to the site within 8 hours of the start of the accident.

If roadways were inaccessible, the Pennsylvania National Guard air wing in Fort Indiantown Gap, PA, is less than 100 miles from the site and has Chinook-47 helicopters rated to lift about 26,000 pounds. Trailer mounted 600 kilowatt generators weigh about 22,000 pounds and may be the largest generators that can be airlifted to the site in a timely manner. These generators are large enough to support a variety of onsite power needs, including pumps. The Public Information Officer for the air wing confirmed that there are typically five to 25 operational helicopters available, and there are other air wings in the region. Given national response to a GE, it is assumed heavy lift helicopters would be made available within about 6 hours to support delivery of electrical generators, piping, heavy equipment, and other resources that may be

needed. It would take additional time for the helicopters to pick up and deliver the equipment to the site.

6.6.2 Mitigation

The above evaluation explains why it is expected that the management of the emergency, technical expertise, and resources likely needed to mitigate the accident will be available. The next step is applying these resources to mitigate the accident. If other actions are not effective, the mitigative actions identified in the plant Severe Accident Management Plan (SAMP) ultimately direct primary containment flooding to a level of 4 feet above the drywell floor. The EROs for the site and utility will be identifying methods to achieve the primary containment flooding, and the NRC would be independently reviewing the approaches being considered. At this stage of the accident, there are many parallel activities underway which focus on injecting water into the drywell. The current analysis assumes efforts to restore coolant injection directly to the drywell are not successful. Ad hoc means are considered for flooding the reactor building to mitigate the release to the environment. The flooding actions would provide some scrubbing of the source term and would reduce the release.

Several strategies are envisioned for flooding the reactor building. The mitigation strategy considered in this evaluation is one that floods the Reactor Building with water to cover the release pathway out of containment, thereby mitigating the release by scrubbing fission products that emerge through the failed drywell liner. If the opening in the liner is sufficiently large, water could also flow into the containment, covering and cooling core debris. This particular strategy would utilize portable pumps and fire hoses to transfer water from the cooling tower basin or other nearby sources to the basement of the reactor building. Direct access to the basement is not necessary. The compartments in the lower portion of the Reactor Building, such as the Torus room and ECCS pump rooms, are designed for internal flooding to an elevation of approximately 111 feet, which is below the drywell floor elevation. Under normal operations, the Torus room doors are open. If the Torus room is flooded and doors are closed, water that rises above an elevation of 111 feet may flow into adjacent rooms through openings in the walls. This could result in the flooding of compartments that contain the major coolant pumps, such as Core Spray and might also result in leakage into adjacent buildings such as the Radwaste Building. Leakage to adjacent buildings would need to be controlled[57].

The approach to flooding the Reactor Building lower elevations described here includes directing fire hose streams through the open truck bay doors. This would result in the water entering the Torus room through the open grating at elevation 135-ft of the Reactor Building (see Figure 6-19). This approach avoids the need for Core Spray pumps and the need to enter the building to align the Core Spray system valves. The outside equipment hatch to the Torus room on the west side of the building could also be removed to provide an additional location for injection and monitoring of the water level. Calculations developed using building dimensions and depth of water show that approximately 2.5 million gallons would be necessary to fill the building to a level sufficiently deep to generate a static head for water to flow onto the drywell

---

[57] The mitigation scheme examined here assumes no leakage out of the reactor building into adjacent buildings. It is assumed that the initiating event does not cause subterranean structural damage to the building, nor would other leak paths out of the building preclude flooding up to grade level

floor via the opening in the drywell liner, if containment failure occurred as calculated in the STSBO or LTSBO scenarios evaluated in Section 5.

There are three potential water sources available. The primary source would be the onsite 3.55 million gallon cooling tower basin, which is assumed to survive the earthquake. The structure is made of reinforced concrete and is designed to Seismic Class I requirements. Water would also be available from the Susquehanna River. Water tanker trucks supplied by local fire departments could also augment water supplies, but is not a significant source. If the river recedes due to downstream affects from the earthquake, water would need to be drafted from existing or man-made pools that may be away from the existing shoreline. This may require field fabrication of pontoons or temporary platforms to support suction piping across the now exposed river bottom. This could be accomplished with local equipment and available supplies. There are no physical impediments to prevent installation of these temporary fixtures; therefore, it is reasonable to assume this could be in place within a few hours of the decision to draft water from the river.

Portable pumps and fire trucks would be used to deliver water into the building. Piping and hoses may be directed through the open truck bay doors. If radiation dose is an issue, placement may require remote techniques, such as pushing pipe segments through the doorway from a distance, but it is reasonable to expect that mechanical expertise is onsite to accomplish these actions and that in-field designs are developed while plant staff are awaiting delivery of offsite resources. Materials are staged onsite to control radiological runoff from a 10CFR50.54(hh) event that could be used to promote water flowing into the lower elevations, rather than draining out the open doorway. A monitor nozzle could be used on one of the hose lines set on the fog spray mode of operation to provide some scrubbing of the release as it progressed from the Torus room up through the open equipment hatches in the vicinity of the truck bay.

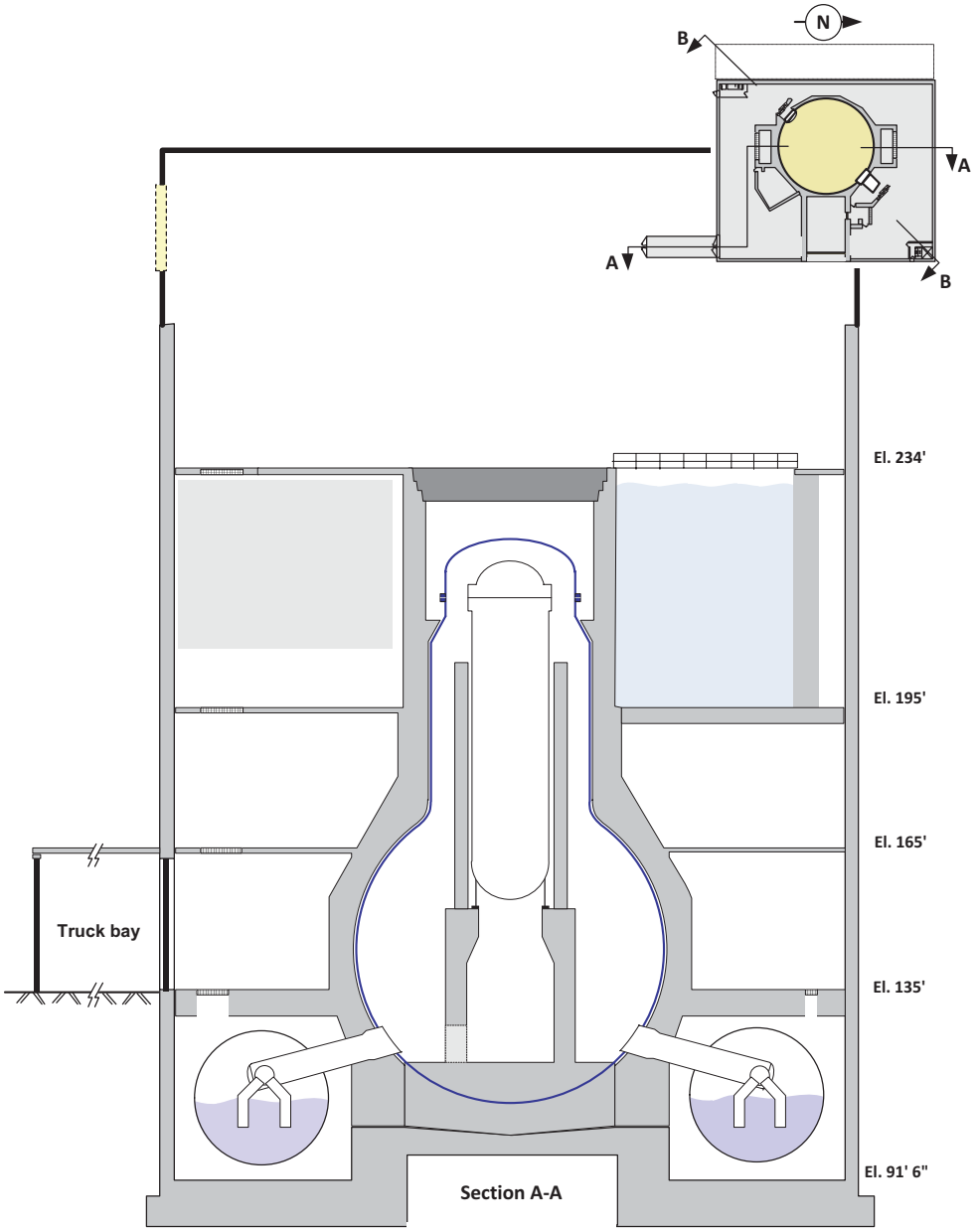

Figure 6-19 Reactor Building

The water would flood the Torus Room and adjacent rooms until it reaches a level above the hole in the reactor. At this point, the water may enter the reactor vessel and continue rising until it covers the molten core on the drywell floor, mitigating the accident. Alternately, there may be pressure from the core melt that could prevent water from entering the hole. In this case, the water would continue rising outside of the reactor vessel and the hole would become submerged. Any release would then be scrubbed through the water covering the hole. As indicated in Figure 6-20, about 2,500,000 gallons would be necessary to fill the building sufficiently to cover the molten core in the Peach Bottom reactor building. With a pumping capacity of 6,000 gpm, equivalent to four to six pumps, 2,500,000 gallons of water could be delivered in about 7 hours after pumping starts as shown in Figure 6-21. This would be sufficient to submerge the molten

core to a depth of about one meter and mitigate the release. If the onsite water tank is available, a greater flow rate may be achieved and the pumping time would be less. If water must be drafted from the river, six pumps/pumper trucks could be configured in a reasonable time.

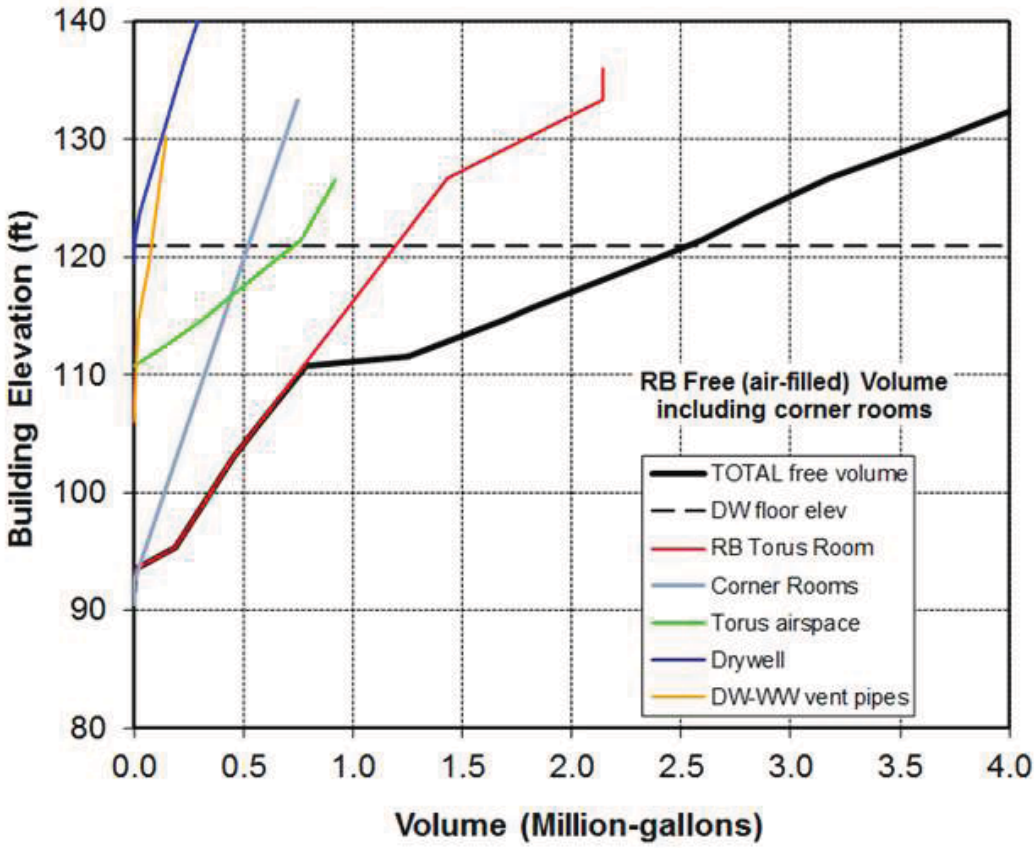

Figure 6-20 Volume Needed to Fill the Peach Bottom Reactor Building

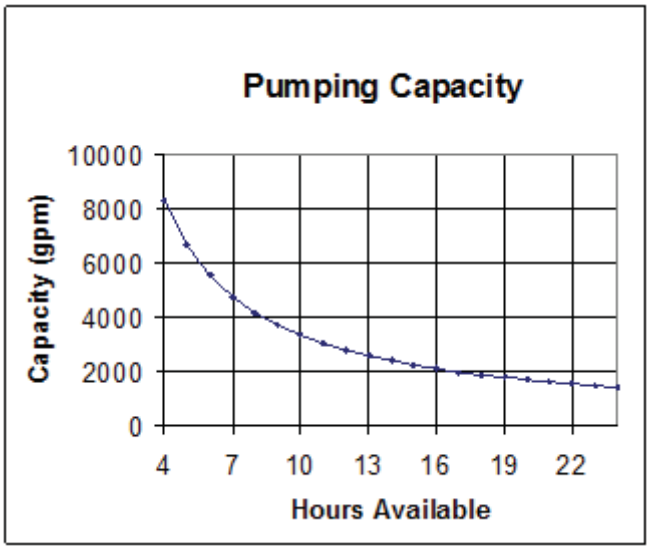

Figure 6-21 Peach Bottom Pumping Capacity and Time

The above assessment is not definitive and describes a response that may occur should all onsite efforts to mitigate the accident fail. Some of the actions taken are ad hoc and the availability of equipment is likely but not certain. It should be recognized that the proceduralized mitigative actions can be successful in preventing core damage. In summary, the key activities and associated timing described above include:

- Fire trucks will be onsite within minutes with additional support available from nearby towns and cities;
- Large capacity pumps and electrical generators transported to the site within a few hours;
- Flooding the Reactor Building at 6,000 gpm takes approximately 6 hours from the time pumping begins.

The types of resources needed are multi-use and would begin being acquired or established early in the response to support restoration of cooling, depressurizing the RCS, injecting into the RCS, etc. Based on the above, flooding of the Reactor Building would need to begin about 40 hours after the start of the accident. It is reasonable to assume that within 40 hours response personnel would be prepared to make a decision to flood the Reactor Building. The approach described provides a supporting basis for truncating the release at 48 hours.

6.7 Emergency Preparedness Summary and Conclusions

Advancements in consequence modeling provide an opportunity to include detailed emergency planning and response activities in the assessment of an accident. This includes the ability to model protective action decisions from OROs and the implementation of these decisions by individual population segments. To support the modeling effort, detailed demographic data was obtained from local and regional sources, and emergency response planning information was obtained from offsite emergency response plans and through discussions with OROs. This information supported the evaluation of differences in the implementation of protective actions for the population segments.

The modeling advancements are significant because they now allow detailed modeling of response activities, timing of decisions, and implementation of protective actions across different population segments. The Peach Bottom EALs were obtained from site procedures for each of the accident scenarios. This provides the best estimate for the timing of the declaration of an SAE and a GE. The response of OROs with regard to sounding sirens, notifying the public, coordinating the evacuation efforts, and establishing return criteria, was obtained from discussions with the OROs and review of emergency plans. The response timing for the public was based on emergency plans, the site specific ETE [29], and research of public actions in response to large scale evacuations [21]. Previous consequence analyses, such as Sample Problem A [26], NUREG-1150 [8], and NUREG-6953 Volume 1 [22], typically used only one cohort to represent the EPZ public and one cohort for the non-evacuating public. In the NUREG-1150 analysis, the EPZ population was first sheltered and then evacuated as a single group at one speed.

The SOARCA analyses included multiple cohorts and considers sheltering and speeds representative of each specific cohort:

- For the general public, shielding factors appropriate for the region were applied for normal activities, sheltering, and evacuation times. Evacuation speeds were developed from the Peach Bottom ETE study.

- Schools were modeled assuming they are notified directly in accordance with offsite emergency response plans.

- Special facilities were modeled assuming they are notified early, but respond differently than schools because of the need to mobilize specialized transportation resources including wheelchair vans and ambulances. In actual practice, evacuation of these facilities would be on a facility-by-facility basis as resources become available. In SOARCA, these facilities were modeled as evacuating together after an extended sheltering period. The shielding protection values for these facilities are better than those for standard housing, and this was considered in the analysis.

- The evacuation tail includes those members of the public who take longer to evacuate and are the last to leave the area. Indoor shielding values were applied to this cohort. They were evacuated late in the emergency and move at faster speeds because of the lower volume of traffic on the roadways at the latter stages of the evacuation. The timing of the evacuation tail was developed from the ETE.

- A shadow evacuation, which occurs when people evacuate from areas that are not under an evacuation order, was represented in the area beyond the EPZ to account for additional vehicles on the roadway network. Including a shadow evacuation adds realism to the analysis and allows consideration of the impact of the shadow evacuation vehicles on the evacuation of the EPZ.

- A non-evacuating cohort representing 0.5 percent of the population was modeled in the analysis consistent with NUREG-1150. Normal activity shielding values were applied to this cohort.

- For the seismic analysis, it was assumed that a shadow evacuation of residents from within the EPZ occurs before the issuance of an evacuation order. This additional shadow evacuation cohort was included in the analysis.

Three sensitivity analyses were performed to understand the effects of expanding the limits of the evacuation and to understand any effects caused by a delay in implementation of protective actions. The sensitivity analyses were performed using the STSBO without RCIC blackstart scenario because this has an earlier release than other scenarios. In the first two sensitivity analyses, the limits of the evacuation were extended to 16 miles and 20 miles. An ETE was developed using OREMS to establish evacuation response parameters for the consequence model. A third sensitivity analysis was conducted maintaining all of the base case parameters

and increasing the delay of response actions by 30 minutes. The peer review committee had suggested the sensitivity of the response timing be evaluated.

An analysis of the effects of a seismic event was also completed and showed that at this site there are relatively few roadway sections and bridges that fail in an earthquake. The roadway sections and bridges that might fail were dispersed enough that local traffic would be able to detour around these areas and exit the area without appreciable delay. The six-lane I-95 and four-lane U.S. 40 bridges south of the Peach Bottom site that cross the Susquehanna River are assumed to fail in the earthquake; however, this would only have a minor affect on the evacuation. Because the public is immediately aware of the earthquake, having experienced it, when notification to evacuate is received, they are prepared and respond promptly. As a result, timing of the public response occurs more quickly because the delay to evacuation is reduced while the travel time is about the same.

The staff expects that plant actions would be successful in mitigating the important severe accident scenarios considered in this study. The truncation evaluation describes some of the types of resources, potential response times, and a conceptual approach that might be considered to mitigate an accident should onsite mitigation not be successful.

The parameters developed for the base case and sensitivity analyses developed in this section provide input to the MACCS2 consequence model presented in Section 7.

7.0 OFF-SITE CONSEQUENCES

7.1 Introduction

The MACCS2 consequence model (Version 2.5.0.0) was used to calculate offsite doses and their effect on members of the public. Updates to the current version of the MACC2 code used for SOARCA offsite consequence predictions are discussed NUREG-1935, Section 5. MACCS2 was developed at Sandia National Laboratories for the NRC for use in PRAs for commercial nuclear reactors to simulate the impact of accidental atmospheric releases of radiological materials on humans and on the surrounding environment. The principal phenomena considered in MACCS2 are atmospheric transport using a straight-line Gaussian plume model of short-term and long-term dose accumulation through several pathways including cloudshine, groundshine, inhalation, deposition onto the skin, and food and water ingestion. The ingestion pathway was not treated in the analyses reported here because uncontaminated food and water supplies are abundant within the United States and it is unlikely that the public would eat radioactively contaminated food. The following doses are included in the reported risk metrics:

- cloudshine during plume passage
- groundshine during the emergency and long-term phases from deposited aerosols
- inhalation during plume passage and following plume passage from resuspension of deposited aerosols. Resuspension is treated during both the emergency and long-term phases.

The SOARCA project made additional enhancements to MACCS2 [7]. In general, these enhancements reflect recommendations obtained during the SOARCA external review and also reflect needs identified by the broader consequence analysis community. The code enhancements done for SOARCA were primarily to improve fidelity and code performance and to enhance existing functionality. These enhancements are anticipated to have a significant effect on the fidelity of the analyses performed under the SOARCA project.

MACCS2 previously allowed up to three emergency-phase cohorts. Each emergency-phase cohort represents a fraction of the population who behave in a similar manner, although response times can be a function of radius. For example, a cohort might represent a fraction of the population who rapidly evacuate after officials instruct them to do so. To create a high-fidelity model for SOARCA, the number of emergency-phase cohorts was increased, as described in Section 6 of this report. This allowed significantly more variations in emergency response (e.g., variations in preparation time before evacuation to more accurately reflect the movement of the public during an emergency). In a similar way, modeling evacuation routes using the network-evacuation model added a greater degree of realism than in previous analyses that used the simpler, radial-evacuation model.

7.2 Peach Bottom Source Terms

Brief descriptions of the source terms for the Peach Bottom accident scenarios are provided in Table 7-1. For comparison, the largest source term (SST1) from the 1982 NUREG/CR-2239, "Technical Guidance for Siting Criteria Development" (referred to hereafter as "The 1982 Siting Study" or just "The Siting Study") [27] is also shown. Of the Peach Bottom source terms shown in the table, the unmitigated STSBO without RCIC blackstart is the largest in terms of release fractions and the release begins at the earliest time; the unmitigated STSBO with RCIC blackstart and the unmitigated LTSBO are comparable in terms of release fractions; the release begins at the latest time for the LTSBO; the mitigated STSBO with RCIC blackstart is intermediate in terms of timing but slightly lower in terms of release fractions, with the exception of barium, which is slightly greater than the release fraction for the unmitigated LTSBO.

The fission product inventory used in these analyses is presented in Appendix A. The inventory data were evaluated specifically for the SOARCA work and reflect realistic fuel cycle data from Peach Bottom. The inventory data are consistent with those used in MELCOR for decay heat values and for fission product masses.

In comparison, the SST1 source term is significantly larger in magnitude, especially for the cesium group, than any of the Peach Bottom source terms. Moreover, it begins only 1.5 hours after accident initiation. The current understanding of accident progression has led to a very different characterization of release signatures than was assumed for the 1982 Siting Study.

Table 7-1 Brief Source-Term Description for Unmitigated Peach Bottom Accident Scenarios and the SST1 Source Term from the 1982 Siting Study

Scenario	CDF (Events/yr)	Integral Release Fractions by Chemical Group									Atmospheric Release Timing	
		Xe	Cs	Ba	I	Te	Ru	Mo	Ce	La	Start (hr)	End (hr)
PB LTSBO	$3x10^{-6}$	0.978	0.005	0.006	0.020	0.022	0.000	0.001	0.000	0.000	20.0	48.0
PB STSBO w/ BS	$3x10^{-7}$	0.979	0.004	0.007	0.013	0.015	0.000	0.001	0.000	0.000	16.9	48.0
PB STSBO w/o BS	$3x10^{-7}$	0.947	0.017	0.095	0.115	0.104	0.000	0.002	0.007	0.000	8.1	48.0
SST1	$1x10^{-5}$	1.000	0.670	0.070	0.450	0.640	0.050	0.050	0.009	0.009	1.5	3.5

For comparison, a set of consequence analyses using the old SST1 source term is presented in this chapter. This allows a direct comparison, using the same modeling options and result metrics, of the SST1 source term and the current, best-estimate source terms.

7.3 Consequence Analyses

The results of the consequence analyses are presented in terms of risk to the public for each of the three accident scenarios identified for Peach Bottom. Both conditional and absolute risks are tabulated. The conditional risks assume that the accident occurs and show the risks to individuals as a result of the accident. The absolute risks are the product of the CDF and the conditional risks. The absolute risks are the likelihood of receiving a fatal cancer or early fatality for an average individual living within a specified radius of the plant per year of plant operation.

The risk metrics are latent-cancer-fatality and early-fatality risks to residents in circular regions surrounding the plant. They are averaged over the entire residential population within the circular region. The risk values represent the predicted number of fatalities divided by the population for four choices of dose-truncation level. These risk metrics account for the distribution of the population within the circular region and for the interplay between the population distribution and the wind rose probabilities.

Risk results are presented for three dose-response assumptions including: 1) linear no threshold (LNT); 2) US average natural background dose rate combined with average annual medical exposure as a dose truncation level (US BGR), which is 620 mrem/yr; and 3) a dose truncation level based on the Health Physics Society's Position that there is a dose below which, due to uncertainties, a quantified risk should not be assigned (HPS), which is 5 rem/yr with a lifetime limit of 10 rem. A 10 mrem/yr dose truncation level was investigated, but it produced results that were just slightly lower than with the LNT assumption, and thus were not included in the final version of this document.

In addition to the base case mitigated and unmitigated accident scenarios, four additional sensitivity analyses are reported in this chapter. A sensitivity analysis for the unmitigated STSBO without RCIC blackstart scenario shows the influence of the size of the evacuation zone or a delay in evacuation on predicted risk. Another sensitivity analysis considers the effect of seismic activity on emergency response. This sensitivity is considered because the base case results account for the effect of the seismic event on the plant but do not account for its effects on evacuation. This sensitivity analysis takes the latter effects into account as well. A separate analysis of the SST1 source term [27] (summarized in Table 7-1) allows older source-term assumptions to be compared with the current state-of-the-art methods for source-term evaluation using otherwise equivalent assumptions and models. This analysis does not try to reproduce the 1982 Siting Study results; it merely overlays the older source term onto what are otherwise SOARCA assumptions for dose-response modeling, emergency response, and other factors. The final sensitivity analysis attempts to replicate the 1982 Siting Study using the current version of MACCS2.

In this section, the risk tables represent rounded values obtained from the full data sets. The plots were developed from the full data sets and slight differences may be noticed due to this rounding.

7.3.1 Unmitigated Long-Term Station Blackout Scenario

Table 7-2 displays the conditional, mean, latent-cancer-fatality (LCF) risks to residents within a set of concentric circular areas centered at the Peach Bottom site for the unmitigated LTSBO scenario. Three values of dose-truncation level are shown in the table: linear, no threshold (LNT); the average, annual, US-background radiation (including average medical radiation) of 620 mrem/yr (US BGR); and a dose truncation level based on the Health Physics Society's Position that there is a dose below which, due to uncertainties, a quantified risk should not be assigned (HPS), which is 5 rem/yr with a lifetime dose limit of 10 rem.

Dose-truncation based on the HPS Position is more complex than the US BGR truncation because it involves both annual and lifetime limits. According to the recommendation, annual doses below the 5-rem truncation level do not need to be counted toward health effects; however, if the lifetime dose exceeds 10 rem, all annual doses, no matter how small, count toward health effects. Because of the 10 rem lifetime limit, risks predicted with the criterion based on the HPS Position can sometimes exceed those using the background radiation level for dose truncation.

Table 7-2 Mean, Individual, LCF Risk per Event (Dimensionless) for Residents within the Specified Radii of the Peach Bottom Site for the Unmitigated LTSBO Scenario, which has a Mean, Core Damage Frequency (CDF) of $3x10^{-6}$ pry

Radius of Circular Area (mi)	LNT	US BGR	HPS
10	$8.9x10^{-5}$	$7.4x10^{-7}$	$3.7x10^{-7}$
20	$7.6x10^{-5}$	$1.9x10^{-5}$	$2.2x10^{-6}$
30	$5.3x10^{-5}$	$1.1x10^{-5}$	$8.9x10^{-7}$
40	$3.3x10^{-5}$	$5.0x10^{-6}$	$3.7x10^{-7}$
50	$2.7x10^{-5}$	$3.4x10^{-6}$	$2.4x10^{-7}$

Table 7-3 is analogous to Table 7-2, but displays the absolute rather than the conditional risks. In the case of the Peach Bottom LTSBO, the mean CDF of $3x10^{-6}$ pry is used, a frequency that is based on the assumption that B.5.b mitigation does not succeed (see Section 3.1.4). The absolute risk is the product of the conditional risk and this CDF.

Table 7-3 Mean, Individual, LCF Risk per Reactor-Year (1/yr) for Residents within the Specified Radii of the Peach Bottom Site for the Unmitigated LTSBO Scenario, which has a Mean, CDF of $3x10^{-6}$ pry

Radius of Circular Area (mi)	LNT	US BGR	HPS
10	$2.7x10^{-10}$	$2.2x10^{-12}$	$1.1x10^{-12}$
20	$2.3x10^{-10}$	$5.8x10^{-11}$	$6.5x10^{-12}$
30	$1.6x10^{-10}$	$3.3x10^{-11}$	$2.7x10^{-12}$
40	$1.0x10^{-10}$	$1.5x10^{-11}$	$1.1x10^{-12}$
50	$8.0x10^{-11}$	$1.0x10^{-11}$	$7.1x10^{-13}$

The values in Table 7-3 are shown in Figure 7-1. The figure shows that for LNT, the risks are greatest for those closest to the plant and diminish monotonically as distance increases. On the other hand, for either of the dose-truncation levels, the risk reaches a maximum outside the 10 mile evacuation zone. The explanation for this counterintuitive trend is provided in the following discussion of the risks incurred during the emergency versus the long-term phases.

Figure 7-2 shows the absolute LNT risks for the Peach Bottom unmitigated LTSBO for the emergency and long-term phases. The entire height of each column shows the combined (total) risk for the two phases. The emergency response is very effective within the evacuation zone (10 miles) during the early phase, so those risks are very small and entirely represent the 0.5 percent of the population that are modeled as refusing to evacuate. The peak emergency phase risk is at 20 miles, which is the first location in the plot outside of the evacuation zone.

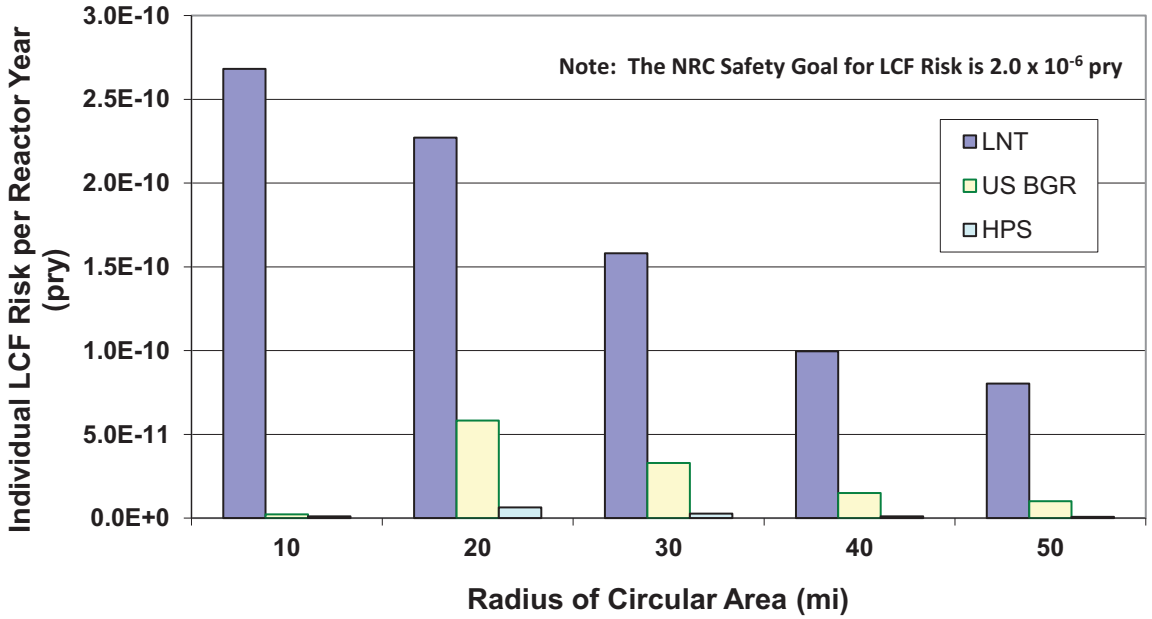

Figure 7-1 Mean, individual, LCF risk per Reactor-Year (1/yr) from the Peach Bottom, unmitigated, LTSBO scenario for residents within a circular area of specified radius from the plant for three values of dose-truncation level

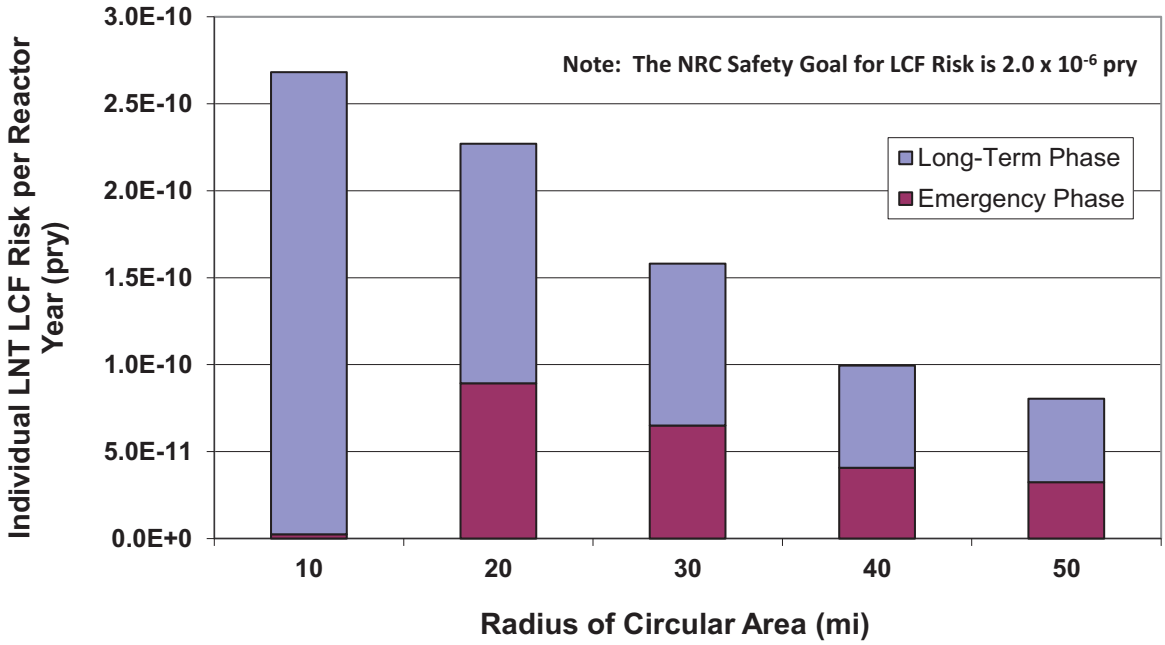

Figure 7-2 Mean, individual, LNT, LCF risk per Reactor-Year (1/yr) from the Peach Bottom, unmitigated, LTSBO scenario for residents within a circular area of specified radius from the plant for the emergency and long-term phases

The long-term phase risks dominate the total risks for the accident scenario when the LNT dose-response assumption is made. These long-term risks are controlled by the habitability (return) criterion, which is the dose rate at which residents are allowed to return to their homes following the emergency phase. For Peach Bottom, the habitability criterion is an annual dose rate of 500 mrem/yr. This dose rate is below the truncation levels based on US background (620 mrem/yr) and based on the HPS Position; therefore, most of the doses received during the long-term phase are below the dose-truncation limit and are not counted toward health effects when using these criteria. Thus, most of the risks associated with either of the truncation levels are from doses received during the first year.

To better understand this explanation, it is important to understand the differences between exposure periods, commitment periods, and the periods of time when doses are actually received. For external dose pathways, the time over which doses are received is concurrent with the exposure period. External dose pathways include cloudshine and groundshine.

The exposure period for internal pathways, inhalation and ingestion, is the period of time when the inhalation or ingestion occurs; however, doses continue to be received over a person's entire lifetime following the exposure. A person's lifetime is obviously variable, depending upon the age of the person at the time of exposure among other things. The period of time over which doses are received from an internal pathway is accounted for in the construction of dose conversion factors by integrating the doses over a finite period called a dose commitment period, which is usually taken to be 50 years when calculating internal-pathway dose conversion factors for adults. The implicit assumption is that the average adult lives for an additional 50 years following the exposure, which is most likely a conservative assumption.

Since ingestion doses are taken to be negligible in SOARCA, inhalation is the only internal pathway that is treated. A significant portion of the exposures during the emergency phase are from inhalation. As explained above, these exposures are assumed to lead to doses over the commitment period, which is the next 50 years following the exposure. However, depending on the isotope inhaled, the doses received may diminish rapidly and become negligible for most of the dose commitment period.

Most of the exposures during the long-term phase are from groundshine; a small fraction is from inhalation of resuspended aerosols. Since groundshine is an external pathway, doses received are concurrent with the exposure. On the other hand, exposures from inhalation during each year of the long-term phase contribute to doses received over the subsequent 50-yr commitment period.

Doses received in the first year thus correspond to:

- all of the dose from external exposure during the emergency phase,
- most of the dose from internal exposure during the emergency phase,
- all of the dose from external exposure during the first year of the long-term phase, and
- most of the dose from internal exposure during the first year of the long-term phase.

Doses received in the second and subsequent years correspond to:

- a fraction of the dose from internal exposure during all previous years plus most of the dose from internal exposure during that year, and

- all of the dose from external exposure during that year.

Following a single exposure, internal doses decrease more slowly from one year to the next when the isotopic half life is relatively long (i.e., on the order of a year or longer) and the solubility of the dominant chemical form of the isotope is low so that the removal rate from the human body is low (i.e., the biological half life is long). A good example is ^{90}Sr, for which the second-year effective dose from inhalation is 60% of the first-year dose. The isotopic half life is 29 years, so most of the reduction from year one to year two results from the biological half life. The internal doses decrease more rapidly from one year to the next when either the isotopic half life is short or when the solubility of the dominant chemical form of the isotope is high so that the human body tends to excrete it rapidly. A good example of this is ^{131}I, for which the second-year effective dose from inhalation is essentially zero. This isotope has a short isotopic half life (i.e., 8 days) and a short biological half life because of its high solubility. For comparison, the second-year effective dose from inhalation for ^{137}Cs is about 10% of the first-year dose, so it is intermediate between the previous examples.

Because the internal doses from inhalation diminish with time, most of the doses in the second and subsequent years are from the exposures during that year. But these doses are limited by the habitability criterion to be less than 500 mrem in any year. The 500 mrem limit is for all dose pathways, in this case groundshine and inhalation from resuspended aerosols. The inhalation dose used in this criterion is a committed dose (i.e., it accounts for doses received over the next 50 years). Because the annual doses allowed by the habitability criterion are less than truncation levels based on US background and the HPS Position, nearly all of the risk is from doses received during the first year. These doses include most of emergency-phase doses and a fraction of the long-term phase doses. This explains why the risk profiles for these dose-truncation criteria in Figure 7-1 are similar to the emergency-phase profile in Figure 7-2.

The prompt-fatality risks are zero for this accident scenario. This is because the release fractions (shown in Table 7-1) are too low to produce doses large enough to exceed the dose thresholds for early fatalities, even for the 0.5 percent of the population that are modeled as refusing to evacuate. The largest value of the mean, acute dose for the closest resident (i.e., 0.5 to 1.2 kilometers from the plant) for this scenario is about 0.1 gray (Gy) to the red bone marrow, which is usually the most sensitive organ for prompt fatalities, but the minimum acute dose that can cause an early fatality is about 2.3 Gy to the red bone marrow. Clearly, the calculated doses are all well below this threshold. Estimated risks below 1×10^{-7} per reactor year should be viewed with caution because of the potential impact of events not studied in the analyses and the inherent uncertainty in very small calculated numbers.

7.3.2 Short-Term Station Blackout with Reactor Core Isolation Cooling Blackstart

Table 7-4 displays the conditional, mean, latent-cancer-fatality risks to residents within a set of concentric circular areas centered at the Peach Bottom site for the STSBO scenario with successful RCIC blackstart. The RCIC blackstart delays the beginning of release and provides more time for evacuation before release than in the subsequent scenario, in which RCIC blackstart is not attempted or fails.

Table 7-4 Mean, Individual, LCF Risk per Event (Dimensionless) for Residents within the Specified Radii of the Peach Bottom Site for the STSBO Scenario with RCIC blackstart, which Has a Mean CDF of $3x10^{-7}$ pry

Radius of Circular Area (mi)	LNT	US BGR	HPS
10	$7.1x10^{-5}$	$6.5x10^{-7}$	$3.0x10^{-7}$
20	$6.5x10^{-5}$	$1.6x10^{-5}$	$1.2x10^{-6}$
30	$4.6x10^{-5}$	$9.2x10^{-6}$	$4.4x10^{-7}$
40	$2.9x10^{-5}$	$4.4x10^{-6}$	$1.8x10^{-7}$
50	$2.4x10^{-5}$	$3.0x10^{-6}$	$1.1x10^{-7}$

Table 7-5 is analogous to Table 7-4 but shows absolute rather than conditional risks. These risks are shown graphically in Figure 7-3. In the case of the Peach Bottom STSBO with RCIC blackstart, the mean CDF of $3x10^{-7}$ pry is used, a frequency that is based on the assumption that B.5.b mitigation does not succeed (see Section 3.2.4).

Table 7-5 Mean, Individual, LCF Risk per Reactor-Year (1/yr) for Residents within the Specified Radii of the Peach Bottom Site for the Unmitigated STSBO Scenario with RCIC blackstart, which has a Mean CDF of $3x10^{-7}$ pry

Radius of Circular Area (mi)	LNT	US BGR	HPS
10	$2.1x10^{-11}$	$2.0x10^{-13}$	$9.0x10^{-14}$
20	$2.0x10^{-11}$	$4.8x10^{-12}$	$3.6x10^{-13}$
30	$1.4x10^{-11}$	$2.8x10^{-12}$	$1.3x10^{-13}$
40	$8.8x10^{-12}$	$1.3x10^{-12}$	$5.3x10^{-14}$
50	$7.1x10^{-12}$	$8.9x10^{-13}$	$3.4x10^{-14}$

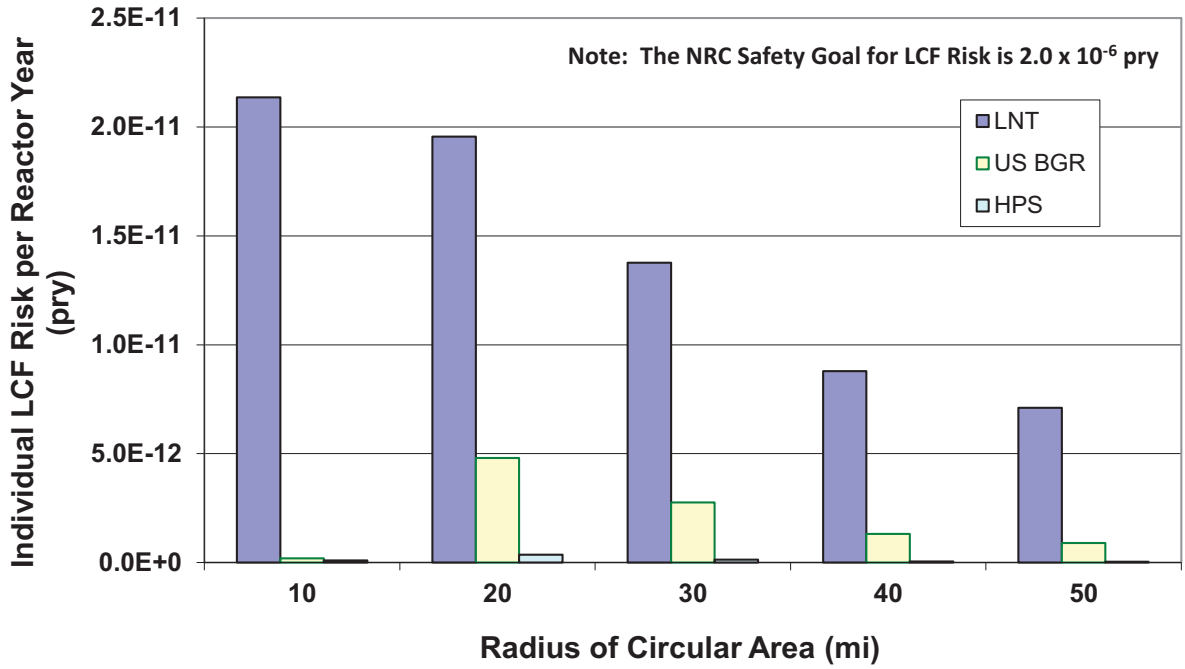

Figure 7-3 Mean, individual, LCF risk per Reactor-Year (1/yr) from the Peach Bottom, STSBO scenario with RCIC blackstart for residents within a circular area of specified radius from the plant for three values of dose-truncation level

Figure 7-4 shows the individual, LNT, LCF risks for the Peach Bottom STSBO with RCIC blackstart for the emergency and long-term phases. The height of each column indicates the combined (total) risk for the two phases. The emergency response is very effective within the evacuation zone (10 miles) during the emergency phase, so those risks are very small and entirely represent the 0.5 percent of the population that are modeled as refusing to evacuate. The peak in the EARLY risk curve is at 20 miles, which is the first location in the plot outside of the evacuation zone.

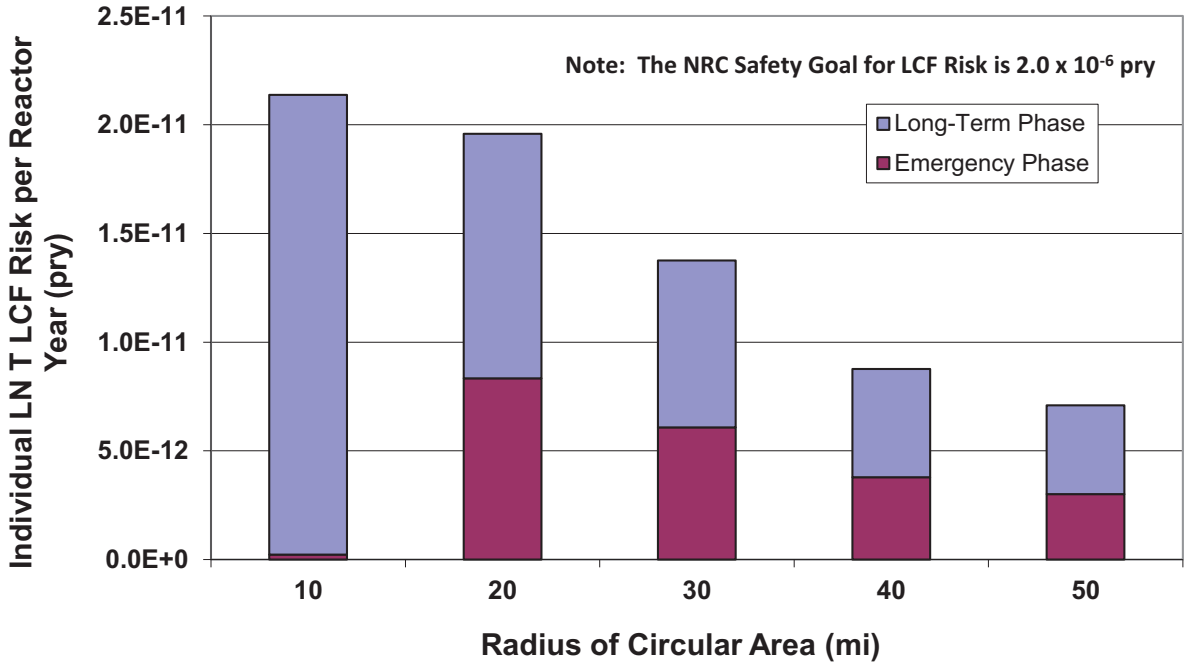

Figure 7-4 Mean, individual, LNT, LCF risk per Reactor-Year (1/yr) from the Peach Bottom, STSBO scenario with RCIC blackstart for residents within a circular area of specified radius from the plant for emergency and long-term phases

The trends for this accident scenario are very similar to those for the unmitigated LTSBO scenario. The long-term-phase risks for this scenario are greater than the emergency-phase risks, especially within the evacuation zone (10 miles), where the emergency-phase risks are very small. The long-term risks are controlled by the habitability or return criterion, which is an annual dose limit of 500 mrem.

Because the annual dose limit of the habitability criterion (500 mrem/yr) is lower than the dose truncation levels based on the US background (620 mrem/yr) and HPS Position, those two risk profiles (shown in Figure 7-3) are similar to the emergency-phase profile shown in Figure 7-4. In other words, the long-term doses are largely excluded by either of the dose-truncation criteria, so the health effects are dominated by doses received during the emergency phase. As a result, those risk profiles are similar to the emergency-phase profile in Figure 7-4.

The prompt-fatality risks are identically zero for this accident scenario. This is because the release fractions are too low to produce doses large enough to exceed the dose thresholds for early fatalities, even for the 0.5 percent of the population that are modeled as refusing to evacuate.

7.3.3 Unmitigated Short-Term Station Blackout without RCIC Blackstart

Table 7-6 displays the conditional, mean, latent-cancer-fatality risks to residents within a set of concentric circular areas centered at the Peach Bottom site for the unmitigated STSBO scenario

without RCIC blackstart. The releases for this scenario are larger and earlier than those for either of the previous ones.

Comparing Table 7-4 and Table 7-6 reveals that the risks are larger for the STSBO when RCIC blackstart does not succeed. Table 7-7 is analogous to Table 7-6 but shows absolute rather than conditional risks. In the case of the Peach Bottom STSBO without RCIC blackstart, the mean CDF of $3x10^{-7}$ pry is used, a frequency that is based on the assumption that B.5.b mitigation does not succeed (see Section 3.2.4).

Table 7-6 Mean, Individual, LCF Risk per Event (Dimensionless) for Residents within the Specified Radii of the Peach Bottom Site for the Unmitigated STSBO Scenario without RCIC blackstart, which Has a Mean CDF of $3x10^{-7}$ pry

Radius of Circular Area (mi)	LNT	US BGR	HPS
10	$2.1x10^{-4}$	$1.2x10^{-5}$	$1.3x10^{-5}$
20	$5.7x10^{-4}$	$3.7x10^{-4}$	$3.7x10^{-4}$
30	$3.9x10^{-4}$	$2.4x10^{-4}$	$2.2x10^{-4}$
40	$2.4x10^{-4}$	$1.3x10^{-4}$	$1.1x10^{-4}$
50	$1.9x10^{-4}$	$9.7x10^{-5}$	$7.3x10^{-5}$

Table 7-7 Mean, Individual, LCF Risk per Reactor-Year (1/yr) for Residents within the Specified Radii of the Peach Bottom Site for the Unmitigated STSBO Scenario without RCIC blackstart, which Has a Mean CDF of $3x10^{-7}$ pry

Radius of Circular Area (mi)	LNT	US BGR	HPS
10	$6.2x10^{-11}$	$3.7x10^{-12}$	$3.8x10^{-12}$
20	$1.7x10^{-10}$	$1.1x10^{-10}$	$1.1x10^{-10}$
30	$1.2x10^{-10}$	$7.3x10^{-11}$	$6.6x10^{-11}$
40	$7.1x10^{-11}$	$4.0x10^{-11}$	$3.2x10^{-11}$
50	$5.6x10^{-11}$	$2.9x10^{-11}$	$2.2x10^{-11}$

Table 7-7 is plotted in Figure 7-5. Due to rounding of the full data set, the plot does not align precisely with the table values. The plot shows that predicted risks reach a maximum beyond the EPZ (10 miles) for all choices of dose truncation level. Risks within the 10 mile evacuation zone are very small for either of the dose-truncation criteria because long-term annual doses are below these truncation levels.

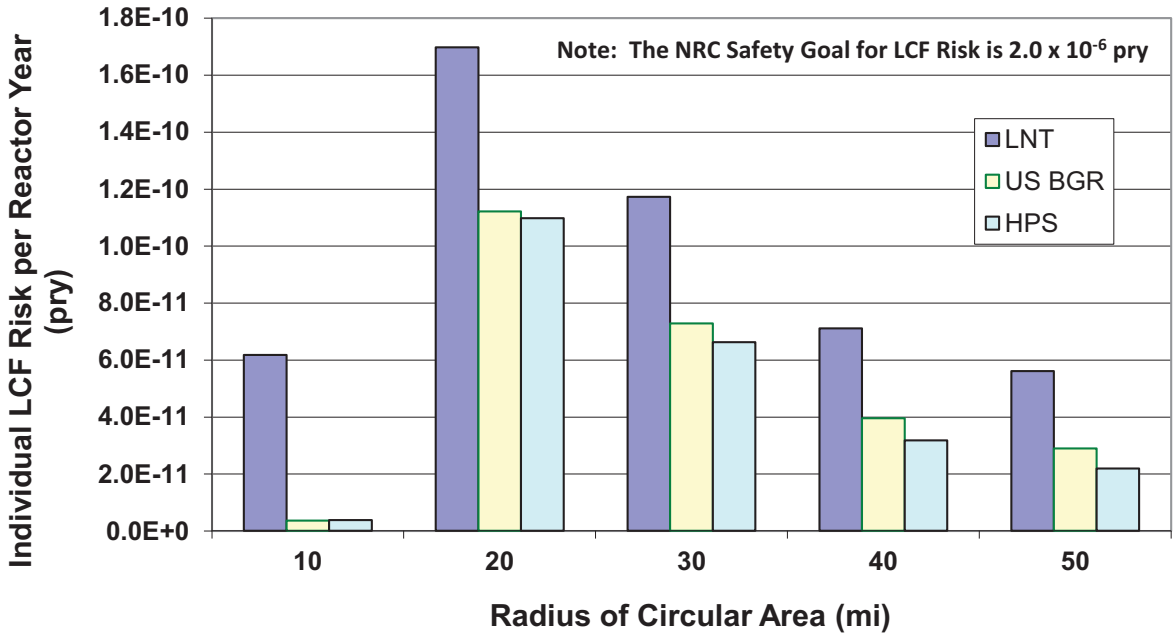

Figure 7-5 Mean, individual, LCF risk per Reactor-Year (1/yr) from the Peach Bottom, unmitigated, STSBO scenario without RCIC blackstart for residents within a circular area of specified radius from the plant for three values of dose-truncation level

Figure 7-6 shows the LNT latent-cancer fatality risks for the Peach Bottom unmitigated STSBO scenario without RCIC blackstart for the emergency and long-term phases. The height of each of the columns shows the combined (total) risk for the two phases. The emergency response is very effective within the evacuation zone (10 miles) during the emergency phase, so those risks are very small and mostly represent the 0.5 percent of the population that are modeled as refusing to evacuate. The peak in the emergency-phase risk profile is at 20 miles, which is the first location in the plot outside of the evacuation zone.

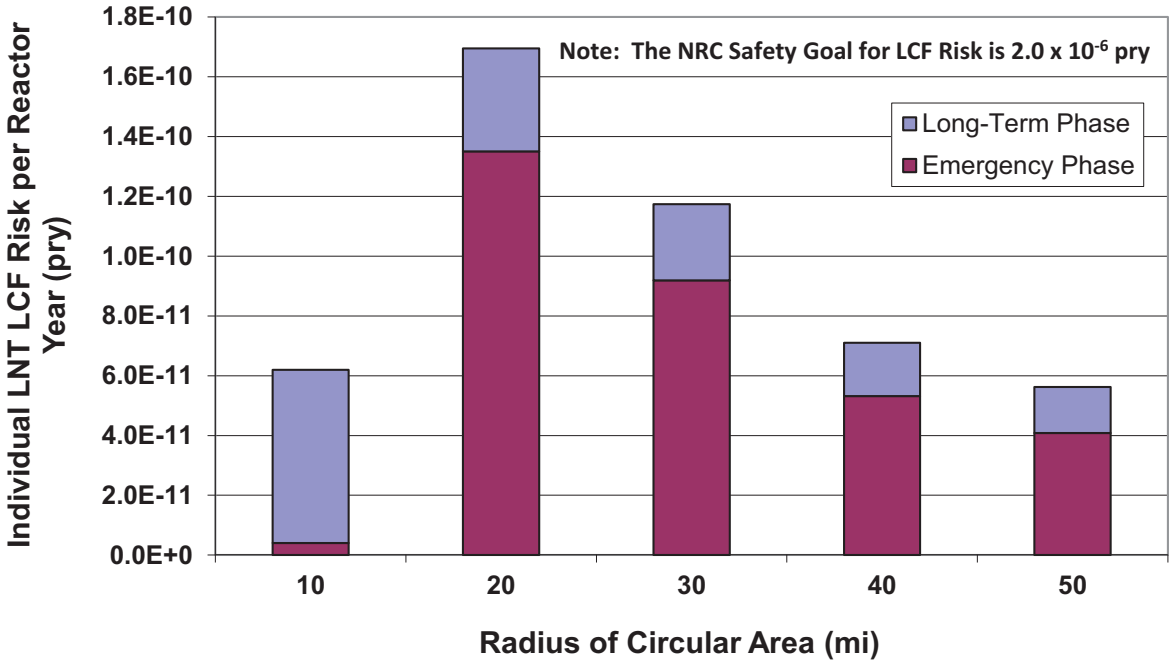

Figure 7-6 Mean, individual, LNT, LCF risk per Reactor-Year (1/yr) from the Peach Bottom, unmitigated, STSBO scenario without RCIC blackstart for residents within a circular area of specified radius for the emergency and long-term phases

The long-term phase risks for this scenario are significantly smaller than the emergency-phase risks except within the evacuation zone (10 miles), where emergency-phase risks are very small. The long-term risks are controlled by the habitability or return criterion, which is an annual dose limit of 500 mrem. Because the overall risks are dominated by the emergency-phase risks, the risk profiles for all truncation levels have peaks at 20 miles, as shown in Figure 7-5.

Because the annual dose limit for the habitability criterion is lower than either of the dose truncation levels, those two risk profiles (shown in Figure 7-5) are mainly influenced by risks during the emergency phase, as shown in Figure 7-6 and explained in more detail in Section 7.3.1.

The contribution of the emergency phase to the overall risk is much greater for the Peach Bottom unmitigated STSBO without RCIC blackstart than for other Peach Bottom scenarios discussed above and for all of the Surry Power Station scenarios presented in Section 7 of the companion Surry report. The uniqueness of the unmitigated STSBO without RCIC blackstart scenario appears to be related to the relatively large releases for the Ba, I, Te, and Ce classes compared with the Cs class for this scenario (see Table 7-1). While the Cs class release fraction is about a factor of 3 greater than the other Peach Bottom scenarios, the Ba class release fraction is more than an order-of-magnitude greater. The cesium group, especially ^{137}Cs, tends to dominate the long-term doses following an accident. Most of the other isotopes, e.g., the iodine, tellurium, and barium isotopes, tend to contribute more to short-term doses.

The prompt-fatality risks are zero for this accident scenario. This is because the release fractions are too low to produce doses large enough to exceed the dose thresholds for early fatalities, even for the 0.5 percent of the population are modeled as refusing to evacuate.

7.3.3.1 Sensitivity Analyses on the Size of the Evacuation Zone and the Evacuation Start Time

The base case analysis included evacuation of the 10-mile EPZ and a shadow evacuation cohort between 10 and 20 miles. For the unmitigated STSBO scenario without RCIC blackstart, three additional calculations were performed to assess variations in the protective actions.

Sensitivity 1 - Evacuation of a 16-mile Circular Area
In this calculation, the evacuation zone is expanded to 16 miles. Shadow evacuation occurs from within the 16 to 20 mile area.

Sensitivity 2 - Evacuation of a 20-mile Circular Area
In this calculation, the evacuation zone is expanded to 20 miles. No shadow evacuation beyond the evacuation zone is considered.

Sensitivity 3 – Delayed Evacuation of a 10-mile Circular Area
This calculation is identical to the base case described above except that implementation of protective action is delayed by 30 minutes.

The results of all three sensitivity analyses are compared with the base case in Table 7-8. The results for the case with delayed evacuation are identical to those for the base case; the other two sensitivities are slightly different than the base case, especially within 10 and 20-mile radii. These results are also shown in Figure 7-7. Since the delayed evacuation case is identical to the base case, it is omitted from the figure.

Table 7-8 Effect of Size of Evacuation Zone on Mean, Individual, LNT, Latent Cancer Fatality Risk per Reactor-Year (1/yr) for Residents within the Specified Radii of the Peach Bottom Site for the Unmitigated STSBO Scenario without RCIC blackstart

Radius of Circular Area (mi)	Base Case 10-mile Evacuation	Sensitivity 1 16-mile Evacuation	Sensitivity 2 20-mile Evacuation	Sensitivity 3 10-mile Delayed Protective Action
10	6.2×10^{-11}	1.8×10^{-10}	1.7×10^{-10}	6.3×10^{-11}
20	1.7×10^{-10}	1.3×10^{-10}	7.2×10^{-11}	1.7×10^{-10}
30	1.2×10^{-10}	1.0×10^{-10}	8.4×10^{-11}	1.2×10^{-10}
40	7.1×10^{-11}	6.6×10^{-11}	5.7×10^{-11}	7.2×10^{-11}
50	5.6×10^{-11}	5.1×10^{-11}	4.8×10^{-11}	5.7×10^{-11}

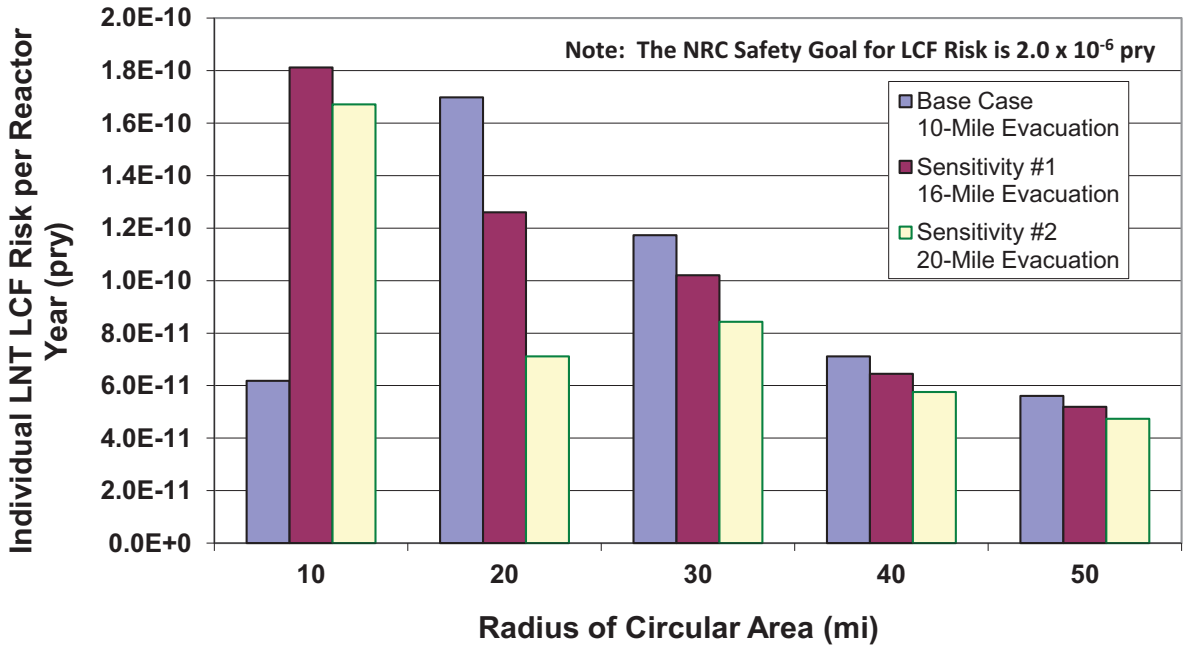

Figure 7-7 Mean, individual, LNT, LCF risk per Reactor-Year (1/yr) from the Peach Bottom, unmitigated, STSBO scenario without RCIC blackstart for residents within a circular area of specified radius from the plant showing the effect of the size of the evacuation zone

Although expanding the size of the evacuation zone decreases the latent cancer fatality risk beyond the 10 mile radius for the unmitigated STSBO without RCIC blackstart, the risk within 10 miles increases with this change. This is because evacuating a larger area increases the time to evacuate the 10-mile region due to increased traffic congestion. For circular areas with greater than a 20-mile radius, the risk reduction associated with increasing the size of the evacuation zone is slight. Prompt-fatality risk remains zero for all three of these sensitivity cases.

7.3.4 Evaluation of the Effect of Seismic Activity on Emergency Response

Earlier sections of this chapter provide offsite health consequence estimates for unmitigated sensitivity cases that reflect the effects of the seismic event on emergency response for mitigation of the accident. However, these earlier sections do not reflect the effects of the seismic event on public evacuation. This section provides consequence estimates that also include the effects of the seismic event on public evacuation. These consequence estimates were developed for the STSBO without RCIC blackstart. Although this is the lowest frequency and lowest absolute risk scenario, this scenario was chosen because it was believed to be the most likely to show an increase in risk. Seismic effects on emergency response (ER) are site-specific but, as the results in Table 7-9 demonstrate, they have no substantial effect on health consequences at Peach Bottom. Although sirens fail, alternative notification is adequate and a larger shadow evacuation is expected. Although bridges fail, they are not significant for evacuation; an adequate road network remains, and evacuation speeds are unchanged. In addition, accident progression timing predicted by realistic analysis is relatively slow so that there is some margin for emergency preparedness activation and execution.

The risk of a prompt fatality is unaffected in this sensitivity analysis and remains zero.

Table 7-9 Mean, Individual, LNT, LCF Risk per Event (Dimensionless) for Residents within the Specified Radii of the Peach Bottom Site for the Unmitigated, STSBO Scenario without RCIC blackstart Comparing the Unmodified Emergency Response and Emergency Response Adjusted for the Effect of Seismic Activity on Evacuation Routes and Human Response

Radius of Circular Area (mi)	Unmodified ER	ER Adjusted for Seismic Effects
10	2.1×10^{-4}	2.1×10^{-4}
20	5.7×10^{-4}	5.1×10^{-4}
30	3.9×10^{-4}	3.7×10^{-4}
40	2.4×10^{-4}	2.3×10^{-4}
50	1.9×10^{-4}	1.8×10^{-4}

7.3.5 Evaluation of SST1 Source Term

An objective of the SOARCA project is to update and compare the quantification of consequences reported in earlier studies, such as the 1982 Siting Study. One of the dramatic differences between the SOARCA study and the 1982 Siting Study is the character of the radiological releases in terms of magnitude and timing. Because of these dramatic differences, it is useful to characterize and compare the risk to the public that derives from these releases.

The project evaluated the updated effects of the SST1 source term previously used in the 1982 Siting Study, and then compared these effects to the most severe accidents in SOARCA. Although previous studies believed that the SST1 source term was important, we now understand the accident progressions leading to such large early releases are either much more unlikely than previously thought or physically impossible.

The approach used in this section is to substitute the SST1 source term in place of the SOARCA source term into the MACCS2 input files for the unmitigated STSBO without RCIC blackstart scenario. This comparison does not attempt to replicate NUREG/CR-2239; nor is it a comparison to its results. Such a comparison is provided in the next section, 7.3.6. Because it is true that many of the parameters and models used at the time of NUREG/CR-2239 differed from those being used in the current SOARCA study, this sensitivity is intended to focus solely on the influence of the source term on predicted consequences.

The MACCS2 input files chosen were the ones developed for the unmitigated LTSBO and STSBO without RCIC blackstart scenarios. These sensitivity analyses show the impact of the improvements made in the source term methods and practices on the consequence results.

The characteristics of the SST1 source term as previously described in the 1982 Siting Study report are as follows:

- severe core damage
- essentially involves loss of all installed safety features
- severe direct breach of containment

An exact scenario and containment failure mechanism (e.g., hydrogen detonation, direct containment heating, or alpha-mode failure) are not specified in the report.

Notification time (i.e., sounding a siren to notify the public that a GE has been declared) for the Peach Bottom unmitigated STSBO without RCIC blackstart occurs at 1.0 hour, as shown in Figure 6-6. Evacuation of the general public begins 1 hour later, or 2 hours after accident initiation, which is the same time as the first cohort was assumed to evacuate in the 1982 Siting Study. The beginning of release for the SST1 source term (see Table 7-1) occurs 1.5 hours after accident initiation, which is 30 min. before evacuation of the general public.

While the 1982 Siting Study treated emergency response very simplistically, a major emphasis of the SOARCA project is to treat all aspects of the consequence analysis as realistically as possible. No attempt was made in this sensitivity analysis to reproduce the treatment of emergency response used in the 1982 Siting Study.

Table 7-10 shows the conditional latent-cancer-fatality risks for a release corresponding to the SST1 source term occurring at Peach Bottom based on the unmitigated STSBO scenario without RCIC blackstart. This comparison shows that dose truncation level has a very minor influence on predicted risk. That is because the doses with the SST1 source term are large enough to exceed the dose truncation levels for most of the affected population.

Table 7-10 Mean, Individual, LCF Risk per Event (Dimensionless) for Residents within the Specified Radii of the Peach Bottom Site for the SST1 Source Term previously used in the 1982 Siting Study. All Parameters Other than for Source Term Are Taken from the Unmitigated STSBO Scenario without RCIC blackstart

Radius of Circular Area (mi)	LNT	US BGR	HPS
10	3.3×10^{-3}	3.2×10^{-3}	3.1×10^{-3}
20	1.8×10^{-3}	1.6×10^{-3}	1.5×10^{-3}
30	1.0×10^{-3}	9.0×10^{-4}	8.2×10^{-4}
40	6.1×10^{-4}	4.9×10^{-4}	4.2×10^{-4}
50	4.6×10^{-4}	3.5×10^{-4}	3.0×10^{-4}

Table 7-10 compares the LNT risks using the SST1 source term with those for the largest source term calculated for Peach Bottom in this study, the unmitigated STSBO. The LNT risk within 10 miles for the SST1 source term using the STSBO ER timing is about a factor of 15 higher than the risk for the unmitigated STSBO. The 10-mile risk using a US BGR dose-truncation criterion is a factor of 250 higher when comparing the SST1 result using the STSBO ER timing with the unmitigated STSBO. At larger distances, the risks are less disparate. For example, the ratio is about a factor of 2.5 for a 50-mile area when comparing the LNT risks for the SST1 source term using the STSBO ER parameters with those for the unmitigated STSBO.

Table 7-11 Mean, Individual, LNT, LCF Risk per Event (dimensionless) for Residents within the Specified Radii of the Peach Bottom Site for the SST1 Source Term previously used in the 1982 Siting Study Using Emergency Response Parameters from the STSBO Scenario. The Final Column of the Table Shows the SOARCA Results for the Unmitigated STSBO without RCIC blackstart

Radius of Circular Area (mi)	SST1 Using STSBO w/o RCIC Blackstart ER	Unmitigated STSBO w/o RCIC Blackstart
10	3.3E-03	2.1E-04
20	1.8E-03	5.7E-04
30	1.0E-03	3.9E-04
40	6.1E-04	2.4E-04
50	4.6E-04	1.9E-04

The maximum risk is within 10 miles for the SST1 source term, which is largely because the release is very early and emergency response is not rapid enough to prevent exposures within the EPZ during the emergency phase.

A notable feature of the risks presented in Table 7-10 is that the choice of dose truncation criterion has a minor influence on risk. This is very different than the SOARCA accident scenarios discussed in preceding sections. Figure 7-8 provides some insights into this behavior. For the SST1 source term, nearly all of the risk, especially at short distances from the plant, is from exposures that occur during the emergency phase. Because a significant fraction of these doses are received over a short period of time, and the doses are large due to the large source term, the range of dose truncation values considered in this study have little influence on predicted risks. Again, this is a very different trend than is observed for the current, state-of-the-art source terms.

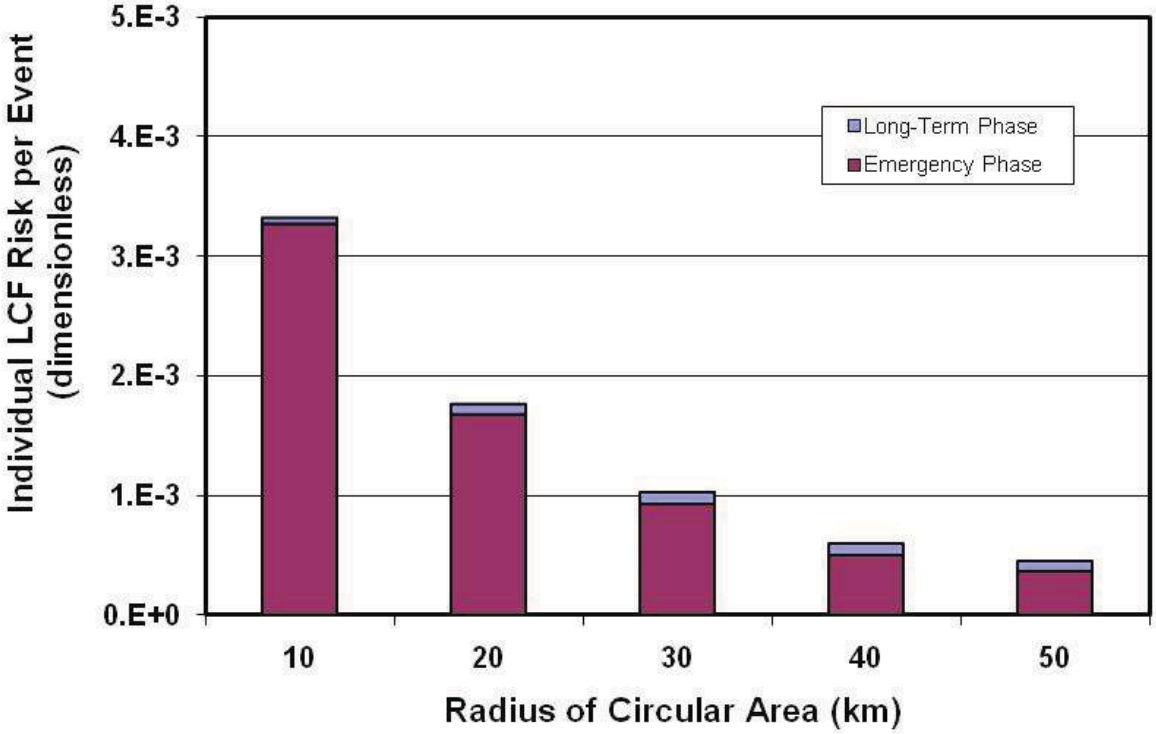

Figure 7-8 Mean, individual, LNT, LCF Risk per Event (dimensionless) from the SST1 source term for residents within a circular area of specified radius from the Peach Bottom plant using the SOARCA STSBO ER timing and showing the risks from the emergency and long-term phases

Table 7-12 shows the individual early fatality risk for several circular areas of specified radii centered at the plant for the two SST1 cases. The individual early fatality risk is approximately $1x10^{-2}$ near the plant. Unlike the source terms presented in the preceding sections, the predicted prompt-fatality risks are greater than zero. The SST1 release fractions are more than large and early enough to induce prompt fatalities for members of the public who live close to the plant. Early fatality risks for the unmitigated SOARCA scenarios are zero, as discussed earlier.

The NRC quantitative health object (QHO) for prompt fatalities ($5x10^{-7}$ pry) is generally interpreted as the absolute risk within 1 mile of the exclusion area boundary (EAB). For Peach Bottom, the EAB is 0.5 mile from the reactor building from which release occurs, so the outer boundary of this 1-mile zone is at 1.5 miles. The closest MACCS2 grid boundary to 1.5 miles used in this set of calculations is at 1.3 miles. Evaluating the risk within 1.3 miles should reasonably approximate the risk within 1 mile of the EAB. The core damage frequency stated for the SST1 source term in the 1982 Siting Study [27] is 10^{-5} pry, so the absolute risk of a prompt fatality for this source term is approximately $1.4x10^{-7}$ pry using the LTSBO ER model and $9.8x10^{-8}$ pry using the STSBO ER model. Even for this very large source term, the prompt fatality risk is below the QHO value of $5x10^{-7}$ pry.

Table 7-12 Mean, Individual, Prompt-Fatality Risk per Event (Dimensionless) for Residents within the Specified Radii of the Peach Bottom Site for the SST1 Source Term previously used in the 1982 Siting Study Using Emergency Response Parameters from the SOARCA STSBO without RCIC blackstart Scenario

Radius of Circular Area (mi)	Probability of a Prompt Fatality Using LTSBO ER (dimensionless)	Probability of a Prompt Fatality Using STSBO ER (dimensionless)
1.0	$1.4x10^{-2}$	$9.9x10^{-3}$
1.3	$1.4x10^{-2}$	$9.8x10^{-3}$
2.0	$7.1x10^{-3}$	$4.2x10^{-3}$
2.5	$4.9x10^{-3}$	$2.8x10^{-3}$
3.0	$3.3x10^{-3}$	$1.8x10^{-3}$
3.5	$1.8x10^{-3}$	$1.0x10^{-3}$
5.0	$5.0x10^{-4}$	$2.8x10^{-4}$
7.0	$2.2x10^{-4}$	$1.2x10^{-4}$
10.0	$9.7x10^{-5}$	$5.4x10^{-5}$

7.3.6 Comparison with the 1982 Siting Study

This subsection discusses the results of a comparison of scenario-specific risk between SOARCA and the 1982 Siting Study analysis for the SST1 source term. Since the 1982 Siting Study does not provide latent cancer results at distances that are meaningful and comparable to those provided in the SOARCA study or to the NRC safety goal, an effort was made to reproduce the Sandia Siting Study results for Peach Bottom using the SST1 source term in order to produce results that are directly comparable to the SOARCA results. An exact reproduction of those results was not feasible because the CRAC2 code is no longer available and some of the models and modeling choices used in the 1982 Siting Study cannot be readily reconstructed. The current successor to the CRAC2 code, MACCS2, shares a number of models with its ancestor, but other models have been improved and therefore produce different results. However, those model parameters that were known or presumed to have been used in the 1982 Siting Study were chosen in an effort to reproduce the results of that study. The results presented in this report were all computed with MACCS2 version 2.5.

The motivation for this calculation is to establish a point of comparison between the 1982 Siting Study and SOARCA. This subsection seeks to compare the results of the 1982 Siting Study and SOARCA by attempting to reproduce all aspects of the 1982 Siting Study, as best as can be done. Key aspects of the modeling are discussed in the following subsection, Section 7.3.6.1.

Table 7-13 compares the release fractions from the Peach Bottom unmitigated STSBO scenario without RCIC blackstart and the SST1 source term. The unmitigated STSBO without RCIC blackstart scenario was chosen for this comparison because it is the largest of the source terms for Peach Bottom that were evaluated as part of the SOARCA investigation. Its frequency is only $3x10^{-7}$/yr compared with the frequency assigned to the SST1 source term of 10^{-5}/yr, about a factor of 30 lower.

Table 7-13 Total Release Fractions by Chemical Group Comparison between the SST1 and the SOARCA Unmitigated STSBO without RCIC blackstart Peach Bottom Scenarios

	Xe	Cs	Ba	I	Te	Ru	Mo	Ce	La
SOARCA	0.9470	0.017	0.095	0.115	0.104	0.000	0.002	0.007	0.000
SST1	1.000	0.670	0.070	0.450	0.640	0.050	0.050	0.009	0.009

7.3.6.1 Comparison of Modeling Choices

Table 7-14 compares key modeling choices and parameters used in the 1982 Siting Study with those used in SOARCA for Peach Bottom. This table reflects our understanding of the differences in key modeling aspects between these two studies. Some of the modeling choices listed in the table could be established with a reasonable degree of certainty from the 1982 Siting Study documentation; others represent best judgments as to how consequence analyses were performed at the time of the 1982 Siting Study. Generally, those judgments were based on NUREG-1150 or WASH-1400 modeling practices. Best judgments or approximations are denoted with an asterisk in the table. Each of the modeling choices shown in the table are discussed below.

Weather Sampling: The exact strategy that was used in the 1982 Siting Study is unknown. The Siting Study does show a binned representation of each of the weather files used in the study, so it is highly likely that weather binning was used. Also, the exact weather data that were used in the study are unknown. The 1982 Siting Study used meteorological data files from 29 regional weather stations to represent the weather at the 91 sites considered in the study. The consequence analysis for Peach Bottom used one of these files, but the documentation does not specify which one. Weather sampling used in this reconstruction uses the current Peach Bottom weather file and the NUREG-1150 choices for weather bin structure and samples per bin.

Habitability Criterion: The habitability criterion used in the Siting Study was 25 rem over an exposure period of 30 years. This criterion leads to higher long-term doses than the one used in SOARCA for Peach Bottom, which is 500 mrem over 1 year.

Emergency Response: Emergency response was treated simplistically and conservatively in the 1982 Siting Study; the SOARCA treatment of emergency response is more detailed and realistic. For example, 30% of the population began to evacuate by 2 hours after accident initiation in the 1982 Siting Study; whereas, almost 93% of the population have begun to evacuate by 2 hours in the STSBO scenario. Also, SOARCA uses the more realistic network evacuation model to represent traffic on designated emergency routes. This model was not developed until after the Siting Study. The evacuation speed, 10 MPH, used in the Siting Study, however, is faster than the travel speed used in the SOARCA representation of Peach Bottom once evacuation begins.

KI Ingestion: KI was not distributed at the time of the 1982 Siting Study. Because it was not distributed, no model for the effect of KI ingesting had been developed. Distribution of KI is relatively common now and is realistically accounted for in the SOARCA study.

Number of Sectors: The only option available at the time of the 1982 Siting Study was to model wind directions using 16 compass sectors. That capability has been extended, and SOARCA takes advantage of the full 64-sector capability in the current version of MACCS2.

Table 7-14 Comparison of Modeling Choices and Parameters Used to Reconstruct 1982 Siting Study Results with the Peach Bottom Unmitigated STSBO without RCIC blackstart from SOARCA

Modeling Choice or Parameter	Siting Study	SOARCA
Weather Sampling	142 Trials*	984 Trials
Habitability Criterion	25 rem in 30 yr	0.5 rem in 1 yr
Emergency Response	3 Cohorts	6 Cohorts
	30% Evacuate at 2 hr	37.2% Evacuate at 1.0 hr
	40% Evacuate at 4 hr	55.5% Evacuate at 2.0 hr
	30% Evacuate at 6 hr	6.8% Evacuate at 5.25 hr
		0.5% Do Not Evacuate
KI Ingestion	No One Takes KI	50% Take KI with 70% Efficacy
Number of Sectors	16	64
Fission Product Inventory	Low Burnup	Mid-Cycle High Burnup
Deposition Velocity	1 cm/s	0.05 to 1.7 cm/s
Mixing Height	Annual Ave.	Day & Night Seasonal Ave.
Risk Factors for Cancers	BEIR III*	BEIR V
Population Basis Year	1970	2005
Groundshine Weathering	WASH-1400*	MACCS2
Relocation Criteria		
Normal	25 rem / 24 hr*	1 rem / 24 hr
Hot Spot	50 rem / 12 hr*	5 rem / 12 hr
Plume Meander Model	MACCS2*	None
Dose Conversion Factors	ICRP-26, -30*	FGR-13
Food Ingestion Model	COMIDA2*	None

Fission Product Inventory: Burnups at the time of the 1982 Siting Study were much lower than today. The Siting Study report provides the fission product inventory used in that study. The inventory used for the SOARCA evaluation of Peach Bottom was based on current fuel cycle practices at Peach Bottom and assumes that the accident occurs mid-cycle. The values are laid out in Appendix A. For comparison, the inventory of ^{137}Cs, the most important isotope for long-term doses, using in the 1982 Siting Study was about 65% of that used for Peach Bottom in the SOARCA study.

Deposition Velocity: Dry deposition of aerosol particles is represented through a set of aerosol size bins. Each size bin represents a range of aerosol sizes, usually characterized by a mass median diameter. Each aerosol bin is assigned a dry deposition velocity. The set of dry deposition velocities are used by MACCS2, along with airborne aerosol concentrations that are calculated using the Gaussian plume approximation, to determine the ground concentrations.

Common practice from the time of the 1982 Siting Study through NUREG-1150 was to treat a single aerosol bin using a representative deposition velocity of 1 cm/s. This single-bin practice is still common today. The practice, used in SOARCA is to use all of the aerosol data from MELCOR. These data are for 10 aerosol bins, each representing a range of aerosol sizes. The representative deposition velocities for the 10 bins range from 0.05 cm/s for the smaller particles to 1.7 cm/s for the larger ones. The dominant or average deposition velocity in SOARCA is about 0.3 cm/s, a factor of 3 lower than the single value used in the 1982 Siting Study.

Mixing Height: The 1982 Siting Study report shows mean annual daytime mixing heights for each representative weather station. Apparently, a single mixing height was used to represent the entire year. In SOARCA, seasonal average daytime and nighttime mixing heights are used.

Risk Factors for Cancer: Cancer risk factors used in the 1982 Siting Study are presumed to have come from the BEIR III report, which would have been the latest available at the time. Cancer risk factors in the SOARCA study are based on BEIR V. BEIR V was chosen rather than BEIR VII because the treatment of tissues is consistent with the FGR-13 dose conversion factors. The BEIR V risk factors are about a factor of 2.7 higher than those from BEIR III.

Population Basis Year: To simplify recreation of the Siting Study results for Peach Bottom, the NUREG-1150 site file, which is for 1980, was used. Data provided in the Siting Study report give population densities at low resolution and would have been difficult to convert into a site file. This NUREG-1150 site file is based on the year 1980 rather than basis year for the Siting Study, which is believed to be 1970. However, individual risks only depend on the relative locations of the population, not on the total population. From that standpoint, using the 1980 population data to reconstruct the Siting Study should have a minor effect on the comparison presented below provided that the locations of the population centers did not change much.

Groundshine Weathering: The Siting Study report did not document the parameters used in the groundshine weathering model. It was judged that the model might have been the same as the one used in WASH-1400, which predated the Siting Study. The SOARCA model for groundshine weathering is the same as the one used in NUREG-1150. The specific model used turns out to play a small role for a large, early release like the SST1 source term because most of the doses are during the emergency phase. Weathering occurs during the long-term phase.

Relocation Criteria: The values used for normal and hot-spot relocation were not described in the Siting Study report, so the values were assumed to be the same as those used in NUREG-1150. The SOACA dose values to trigger relocation were much smaller, but the relocation times were the same.

Plume Meander Model: The plume meander model used in the Siting Study was assumed to be the same as the one used in NUREG-1150. Plume meander was not treated in SOARCA. We considered using the NRC Reg. Guide 1.145 plume meander model, but it would have had a minimal impact on the predicted doses for even the closest residents to the Peach Bottom site because this model only affects the plume dimensions at relatively short distances.

Dose Conversion Factors: The original version of MACCS2 was distributed with a set of dose conversion factors (DCFs) using tissue weighting factors from ICRP-26 and organ-specific DCFs from ICRP-30. These publications predated the 1982 Siting Study, so it is reasonable to expect that they were also used in the Siting Study. These DCFs were used in the reconstruction of the Siting Study SST1 results.

Food Ingestion Model: No details of the ingestion pathway are provided in the Siting Study report, but it does mention that ingestion of contaminated food and milk were treated. The food ingestion model that would have been used certainly predates the implementation of the COMIDA2 food model, which first became available in MACCS2. Since the food model used in the Siting Study would be difficult or impossible to reconstruct, the COMIDA2 model was used as a stand in. For comparison, the food pathway was not treated in the SOARCA analyses.

Making all of the changes listed above plus replacing the Peach Bottom unmitigated STSBO source term with the SST1 source term resulted in a best-effort attempt to reproduce the 1982 Siting Study results. However, this effort over-predicted the Siting Study latent cancer results using the SST1 source term for Peach Bottom by about a factor of 2 at long distance (e.g., 500 miles). Thus, there are other changes in the models and parameter choices that were not captured in the attempt to reproduce this result. Nonetheless, even with this imprecision in recreating the 1982 Siting Study and a residual factor-of-2 bias in the results, this characterization of the Siting Study at shorter distances that can be compared directly with the SOARCA results provides a useful comparison.

7.3.6.2 Comparison of Results

Table 7-15 compares the 1982 Siting Study conditional probabilities of an excess, individual latent cancer fatality using the SST1 source term with those for the unmitigated STSBO scenario without RCIC blackstart evaluated in SOARCA. The comparison shows that the ratio of conditional probabilities within 10 miles of the plant is about 36. Accounting for a potential factor-of-2 bias, the ratio is about 20 within a 10-mile radius. Therefore, at the distance associated with the NRC Safety Goal for latent cancers, the risk predicted for SOARCA is substantially smaller than that predicted in the 1982 Siting Study. This ratio diminishes with increasing radius, becoming about a factor of 2 within a 50-mile radius and beyond. Again, accounting for a potential bias, the ratio may be more like a factor of unity. Therefore overall, when all exposed individuals are considered (i.e., regardless of their proximity to the site), little difference in conditional latent cancer fatality risk is expected between the Peach Bottom STSTBO from the current work and the SST1 source term from the 1982 Siting Study.

The decrease in the ratio from 20 to 1 occurs because the plume is expected to carry radioactive material farther from the site, relocation of the population beyond the 10-mile EPZ limits exposures during the emergency phase, and the habitability criterion limits exposures during the long-term phase. However, implementing the habitability requirement requires significantly greater decontamination and condemnation of land in the case of the 1982 Siting Study than for SOARCA.

The 1982 Siting Study was a consequence analysis and purposefully did not report absolute risk, because as the study states, “Probability times consequence is not an adequate representation of

risk," possibly because, "very large variations (factors of 10 to 100) in the accident probabilities associated with a specific design." However, if a comparison was made using the suggested "representative probabilities" at the time, the factors would be much larger since the frequency of the Unmitigated STSBO without RCIC blackstart is about a factor of 30 lower than the frequency estimated for the SST1 source term. The ratios on the basis of risk (1/reactor year) are therefore about 600 for residents living within 10 miles of the plant and about 30 for residents living within 50 miles of the plant.

Table 7-15 Mean, LNT, LCF Risk per Event (dimensionless) for Residents within the Specified Radii of the Peach Bottom Site for the Recreation of the Siting Study Using the SST1 Source Term and for the Unmitigated STSBO without RCIC blackstart Calculated for SOARCA. CDFs Were Estimated to Be 10^{-5}/yr and $3x10^{-7}$/yr for the SST1 and STSBO without RCIC blackstart Source Terms, Respectively

Radius of Circular Area (mi)	SST1	PB STSBO	Ratio SST1 to STSBO
10	$7.4x10^{-3}$	$2.1x10^{-4}$	36
20	$2.1x10^{-3}$	$5.7x10^{-4}$	4
30	$9.1x10^{-4}$	$3.9x10^{-4}$	2
40	$5.3x10^{-4}$	$2.4x10^{-4}$	2
50	$4.2x10^{-4}$	$1.9x10^{-4}$	2

Table 7-16 is similar to Table 7-15, but compares results calculated with the US background (620 mrem/yr) truncation level. The ratio at 10 miles is larger than the one in Table 7-15 because more of the doses exceed the truncation level in the case of the SST1 result. The ratio beyond 10 miles does not change significantly.

Table 7-16 Mean, LCF Risk per Event (dimensionless) Using US Background (620 mrem/yr) Dose-Truncation for Residents within the Specified Radii of the Peach Bottom Site for the Recreation of the 1982 Siting Study Using the SST1 Source Term and for the Unmitigated STSBO without RCIC blackstart Scenario Calculated for SOARCA. CDFs Were Estimated to Be 10^{-5}/yr and $3x10^{-7}$/yr for the SST1 and STSBO without RCIC blackstart Source Terms, Respectively

Radius of Circular Area (mi)	SST1	PB STSBO	Ratio SST1 to STSBO
10	$6.2x10^{-4}$	$1.2x10^{-5}$	50
20	$8.1x10^{-4}$	$3.7x10^{-4}$	2
30	$4.2x10^{-4}$	$2.4x10^{-4}$	2
40	$2.8x10^{-4}$	$1.3x10^{-4}$	2
50	$2.3x10^{-4}$	$9.7x10^{-5}$	2

Table 7-17 shows the conditional latent cancer fatality risks at three dose truncation levels for the recreation of the 1982 Siting Study results. Predicted LCF risks only vary by about an order of magnitude or less over the range of dose truncation levels considered.

Table 7-17 Mean, LCF Risk per Event (dimensionless) for Three Levels of Dose Truncation for Residents within the Specified Radii of the Peach Bottom Site for the Recreation of the 1982 Siting Study Using the SST1 Source Term. The CDF for This Sequence of the 1982 Siting Study is 10^{-5}/yr

Radius of Circular Area (mi)	LNT	US BGR	HPS
10	7.4×10^{-3}	6.2×10^{-4}	7.2×10^{-4}
20	2.1×10^{-3}	8.1×10^{-4}	9.3×10^{-4}
30	9.1×10^{-4}	4.2×10^{-4}	5.0×10^{-4}
40	5.3×10^{-4}	2.8×10^{-4}	3.5×10^{-4}
50	4.2×10^{-4}	2.3×10^{-4}	3.0×10^{-4}

7.3.7 Surface Roughness

All of the SOARCA analyses presented above use a surface roughness length that represents a typical value for the US, which is 10 cm. This value was used in the 1982 Siting Study and NUREG-1150 and has become a de facto default for most if not all license-related consequence analyses, (e.g., SAMA) analyses for license extension. However, this value of surface roughness is not necessarily the best choice for all regions of the country. In this section, we examine a more site-specific value of surface roughness as a sensitivity analysis to determine whether this parameter is significant for estimated risk.

The effect of increased surface roughness is twofold: It increases vertical mixing of the plume and it increases deposition velocities for all aerosol sizes. Both effects are treated in this sensitivity analysis and are discussed in the subsequent paragraphs.

Peach Bottom is located on the Susquehanna River near the southern border of Pennsylvania. The area surrounding the Peach Bottom Atomic Power Station is characterized by a mosaic of forests, farmland mostly used to grow corn, suburban areas, and several stone quarries. Farmland and forests are the major land-use categories. Each of these land-use types correspond to a typical surface roughness or a range of surface roughness as shown in Table 7-18 [36].

Table 7-18 Surface roughness for various land-use categories for the area surrounding the Peach Bottom site

Land-Use Category	Surface Roughness (cm)
Farmland recently plowed	1
Farmland with mature corn	10
Suburban housing	5 to 20
Suburban institutional buildings	70
Woodland forests	20 to 100
Stone quarries	50 to 200

Determining the best choice of surface roughness to represent the range of land-use categories is not a simple task. The value of 10 cm used in the base case is representative of the corn fields that make up a significant fraction of the countryside surrounding the Peach Bottom site. Woodland forests also make up a large fraction of the area and have a mean surface roughness of about 60 cm. An intermediate choice representing the average between cornfields and woodland forest, about 30 to 35 cm, would also be a reasonable choice for this area. For this sensitivity analysis, a mean value representing typical woodland forest, 60 cm, was chosen to determine whether the results are sensitivity to this input parameter. Results for this sensitivity analysis are based on the STSBO without RCIC blackstart, which is the accident scenario with the largest consequences of those considered in SOARCA for Peach Bottom.

The effect on vertical mixing has traditionally been modeled by means of a multiplicative factor on vertical dispersion. The empirical expression for this factor is the ratio of surface roughness at the site in question to a standard value of surface roughness to the $1/5^{th}$ power. Most of the data upon which empirical dispersion models have been based were taken at a site characterized by prairie grass [33], which was estimated to have a surface roughness of 3 cm. Thus, the empirical equation used to scale vertical dispersion uses the actual surface roughness divided by 3 cm to the $1/5^{th}$ power. The standard multiplicative factor corresponding to a 10-cm surface roughness is $(10 / 3)^{0.2} = 1.27$, which is the value used in all of the calculations presented above. A surface roughness length of 60 cm corresponds to a multiplicative factor of 1.82, which was used in this sensitivity analysis.

The effect of surface roughness on deposition velocity has been characterized by Bixler et al. [34] based on expert elicitation data [28]. Bixler et al. provides a set of correlations for estimating deposition velocity as a function of aerosol diameter, wind speed, surface roughness, and percentile representing degree of belief by the experts. Here, we use the 50th percentile from the experts to get a best estimate deposition velocity. The 50th percentile correlation is as follows:

$$\ln(v_d) = -3.112 + 0.992 \cdot ln(d_p) + 0.190 \cdot [ln(d_p)]^2 - 0.072 \cdot [ln(d_p)]^3 + 5.922 \cdot z_0 - 6.314 \cdot {z_0}^2 + 0.169 \cdot v$$

where

v_d = deposition velocity (cm/s)
d_p = aerosol diameter (μm)
z_0 = surface roughness (m)
v = mean wind speed (m/s)

Table 7-19 shows the aerosol deposition velocities calculated with the above equation that were used in this study for each aerosol bin in the MELCOR model. A mean wind speed of 2.2 m/s was used to obtain the results in the table. The column of deposition velocities corresponding to a surface roughness of 10 cm were used for all of the results shown in the preceding subsections. The column of deposition velocities corresponding to a surface roughness of 60 cm were used in this sensitivity analysis. Increasing surface roughness from 10 to 60 cm roughly doubles the deposition velocity. Because the correlation only extends to aerosol diameters of about 20 μm, the same depositions velocities are used for the top two aerosol bins.

Table 7-19 Deposition Velocities Used for the Base Case Calculations and for the Surface Roughness Sensitivity Study for Each of the Ten Aerosol Bins in the MELCOR Model

Mass Median Aerosol Diameter (μm)	**Deposition Velocity (cm/s) for Specified Surface Roughness**	
	10 cm	**60 cm**
0.15	0.053	0.11
0.29	0.049	0.10
0.53	0.064	0.14
0.99	0.11	0.23
1.8	0.21	0.45
3.4	0.43	0.92
6.4	0.84	1.8
11.9	1.4	2.9
22.1	1.7	3.7
41.2	1.7	3.7

Table 7-20 compares the base case results presented in Subsection 7.3.3 (10-cm surface roughness) with the sensitivity results (60-cm surface roughness). The trends from this table are discussed in the following paragraphs.

Table 7-20 Mean, Individual, LCF Risk per Event (Dimensionless) for Residents within the Specified Radii of the Peach Bottom Site for the Unmitigated STSBO Scenario without RCIC blackstart, which has a Mean CDF of $3x10^{-7}$ pry. Risks are shown for the base case (10 cm surface roughness) and the sensitivity case (60 cm surface roughness)

Radius of Circular Area (mi)	**LNT**		**US BGR**		**HPS**	
	Base Case	**Increased Roughness**	**Base Case**	**Increased Roughness**	**Base Case**	**Increased Roughness**
10	$2.1x10^{-4}$	$2.3x10^{-4}$	$1.2x10^{-5}$	$1.1x10^{-5}$	$1.3x10^{-5}$	$1.2x10^{-5}$
20	$5.7x10^{-4}$	$4.6x10^{-4}$	$3.7x10^{-4}$	$2.7x10^{-4}$	$3.7x10^{-4}$	$2.4x10^{-4}$
30	$3.9x10^{-4}$	$3.2x10^{-4}$	$2.4x10^{-4}$	$1.7x10^{-4}$	$2.2x10^{-4}$	$1.4x10^{-4}$
40	$2.4x10^{-4}$	$2.0x10^{-4}$	$1.3x10^{-4}$	$9.4x10^{-5}$	$1.1x10^{-4}$	$6.4x10^{-5}$
50	$1.9x10^{-4}$	$1.7x10^{-4}$	$9.7x10^{-5}$	$6.9x10^{-5}$	$7.3x10^{-5}$	$4.3x10^{-5}$

A number of factors need to be considered to understand the trends contained in these results. For elevated releases, enhanced vertical dispersion increases the ground-level concentrations close to the point of release because the plume spreads down to the ground more quickly. The MACCS2 results show that ground-level concentrations and resulting doses are greater for the sensitivity case within about 4 miles of the plant; at greater distances the ground-level doses are smaller for the sensitivity case. At intermediate distances, enhanced vertical dispersion reduces ground-level concentrations because the plume spreads more rapidly in the vertical dimension and, as a result, becomes more dilute at ground level. At long distances, the ground-level concentrations are about the same because the plume becomes well mixed within the mixing layer where the plume is confined.

Compounding the effect of increased surface roughness on vertical dispersion, as described above, is the fact that the deposition velocity is also increased. This leads to more deposition at shorter distances and faster depletion of the plume. As a result, doses at short distances are increased and doses at longer distances are diminished.

The trends for the dose-truncation results are similar to the LNT results, but the reductions in risk are generally greater than 20% for the sensitivity case. In contrast to the LNT risk, the risks within 10 miles are slightly lower for the sensitivity case than for the base case when using dose truncation based on either the US background or HPS Position.

Comparing the LNT results, the results at intermediate distances are about 20% lower for the sensitivity case with increased surface roughness. The risk within 10 miles for the sensitivity case is about 10% higher because of the larger ground-level concentrations within 4 miles and because of increased deposition onto the ground. The results within 50 miles are reduced by only 10%. This is because the plume is well mixed between the ground and the top of the mixing layer by 50 miles under many of the prevailing weather conditions.

A general observation based on this sensitivity study is that the specific choice of surface roughness only has a relatively modest effect on LNT predictions of risk; it has a larger, but less than a factor-of-two, effect for the two dose truncation levels considered here.

7.3.8 Importance of Chemical Classes

Each isotope present in the core of a nuclear reactor contributes to the overall risk of an accident; however, the release of some isotopes contributes to risk much more than others. There are three reasons some isotopes are more important than others:

- abundance of an isotope in the inventory in the core at the beginning of an accident,
- release fraction of an isotope into the atmosphere, and
- the dose conversion factors for an isotope, which depends strongly on the type and energy of the radiation produced, the half life of the isotope, and for internal pathways, the biokinetics of the isotope.

There are 69 isotopes in the treatment of consequences considered in the MACCS2 analysis, as described in Appendix A. These isotopes are grouped into a set of 9 chemical classes in the MELCOR analyses that generated the source terms used in the SOARCA analyses. Since release fractions are calculated by MELCOR at the level of chemical classes, it is both reasonable and useful to examine how these same chemical classes influence the evaluation of risk.

One approach to estimate the relative importance of each chemical class on risk is to release one chemical class at a time and evaluate the fraction of the overall risk that results, where overall risk is evaluated by releasing all chemical classes simultaneously. The problem with this approach is that the contributions from the individual chemical classes add up to more than the overall risk. The difference results from the amount of remedial action that is taken to reduce doses to the public. For example, much less remedial action is taken when doses are small, which may be the case when only one chemical class is released at a time, than when doses are large. Because less remedial action is taken, the contribution of an individual chemical group to risk is greater when it is released on its own than when it is part of a larger release. To make the fractional contributions from individual chemical groups add to unity, the contribution from a single chemical class must be normalized by the sum of the individual contributions of the chemical classes rather than the risk calculated for the combined effect of all chemical classes. This inherent nonlinearity tends to diminish the effect of the major contributors and exaggerate the effect of the minor contributors.

To minimize the effect of the nonlinearities described in the previous paragraph, an alternative approach is adopted here. That is to evaluate the contribution of a chemical class by performing calculations with all but that one chemical class. The effect of that chemical class is then calculated by taking the difference between the risk when all chemical classes are included and the risk for all but that one chemical class (i.e., setting the release fractions for that chemical class to zero).

The relative importance of each chemical class was evaluated for all three accident sequences the unmitigated LTSBO, the STSBO with RCIC blackstart, and the unmitigated STSBO without RCIC blackstart. Results were also calculated for each dose response: LNT, US BGR, and HPS. The results for the unmitigated LTSBO scenario for the population within 10 miles are shown in Figure 7-9, Figure 7-10, and Figure 7-11. Results at longer distances are shown in subsequent figures.

The first of these, Figure 7-9, is for LNT. It shows the importance of each chemical group on total risk, on just the emergency-phase risk, and on just the long-term-phase risk. The cesium group dominates the total risk and the long-term phase risk, but contributes only a few percent to the emergency-phase risk owing to the relatively long half lives of the cesium isotopes (e.g., ^{137}Cs has a half life of 30 yrs). Tellurium, barium/strontium, iodine, and cerium contribute most of the emergency-phase risk owing to the short half lives of the isotopes represented by these chemical classes. However, the emergency phase contributes very little to the total risk because 99.5% of the population within 10 miles evacuate and do not receive any dose during the emergency phase.

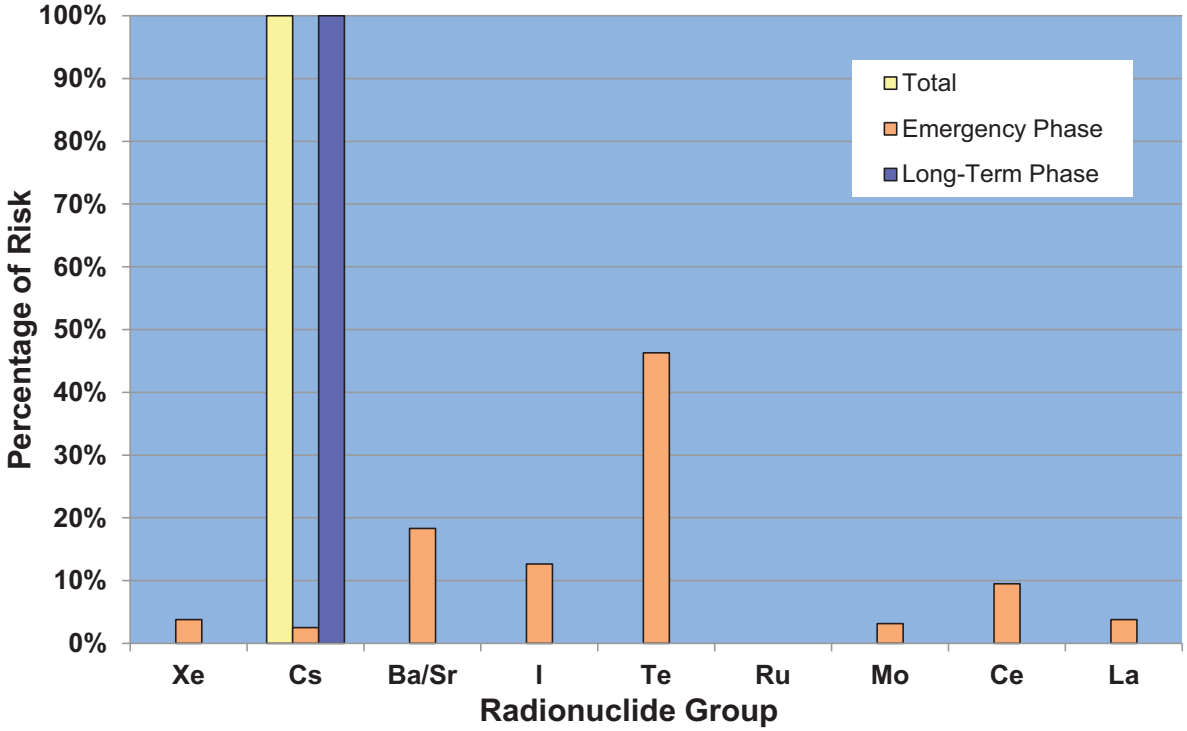

Figure 7-9 Percentage contribution to total, emergency-phase, and long-term-phase, mean, individual risk for the population within 10 miles by chemical class for the Peach Bottom unmitigated LTSBO based on the LNT hypothesis

Figure 7-10 and Figure 7-11 show the total risk contributions of each chemical class for the unmitigated LTSBO using dose truncation based on the US BGR and the HPS Position, respectively. These plots also show risk contributions to the population living within 10 miles of the plant. They only show the total risk contribution because annual doses in the first year are combinations of emergency- and long-term phase doses. As a result of the overlapping contributions to the first year, the individual contributions of the two phases cannot be easily deconvolved from the whole. These figures show that the barium/strontium, cesium, tellurium, and iodine chemical classes contribute most of the risk for these dose truncation criteria, although the order of importance is different in the two figures. Isotopes with relatively short half-lives tend to be more dominate than those with longer half-lives because most of the risk is from doses received during the first year for either of the dose-truncation criteria. Longer-term annual doses are limited by the habitability criterion to values below the dose-truncation levels.

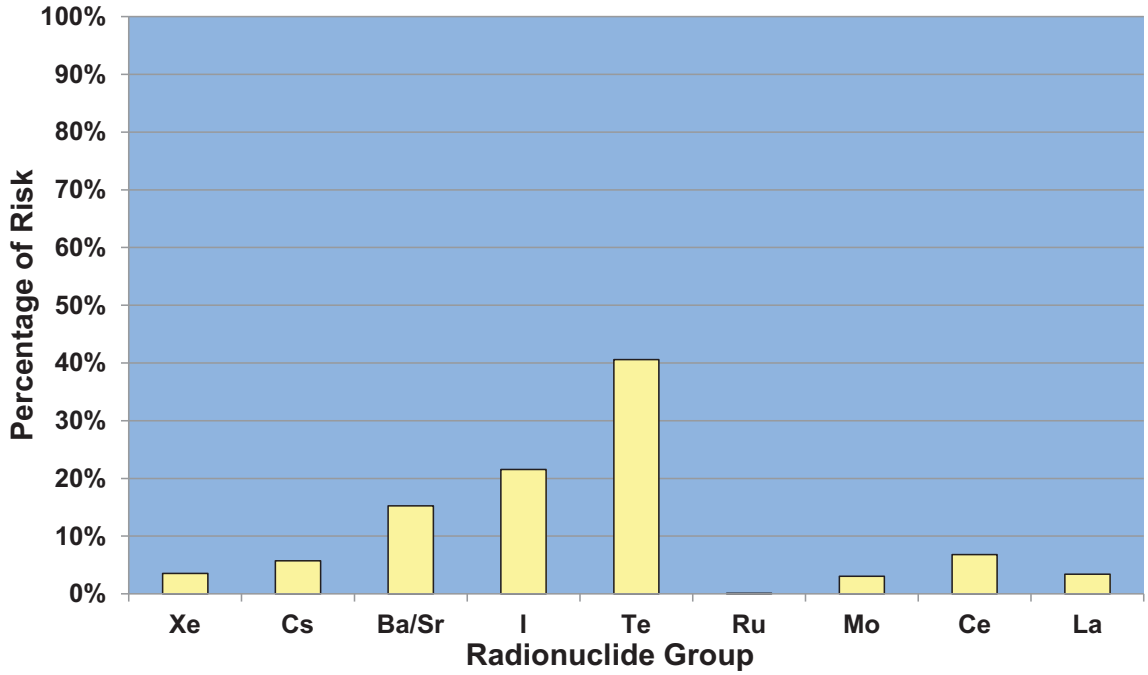

Figure 7-10 Percentage contribution to total, mean, individual risk for the population within 10 miles by chemical class for the Peach Bottom unmitigated LTSBO based on US BGR dose truncation

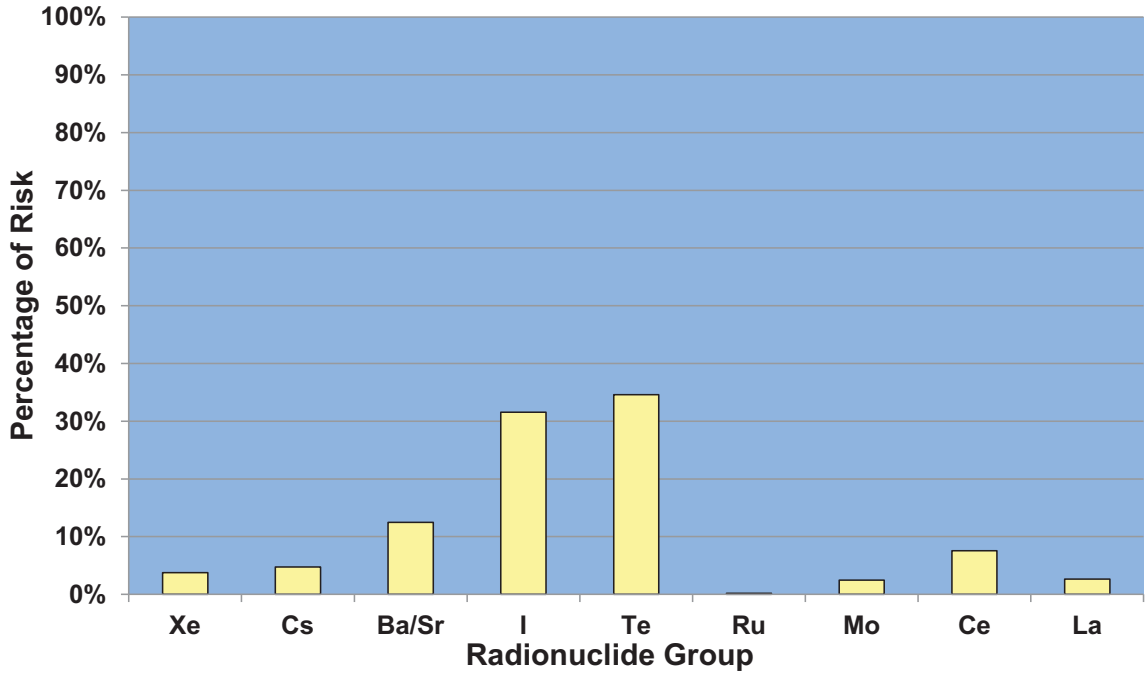

Figure 7-11 Percentage contribution to total, mean, individual risk for the population within 10 miles by chemical class for the Peach Bottom unmitigated LTSBO based on a truncation level reflecting the HPS Position for quantifying health effects

The following figures, Figures 7-12 through 7-17, are analogous to those immediately above but show the relative importance of the chemical classes for the population within 20 and 50 miles. The trends are similar, but the emergency phase plays a larger role because significant portions of the population do not evacuate before the plume arrives and, thereby, receive a dose during the emergency phase. The most important set of chemical classes using the LNT hypothesis is cesium, tellurium, barium/strontium, cerium, and iodine in that order. For the two dose truncation criteria, cesium is less important because of the relatively long half-lives of the dominate isotopes. Generally, the barium/strontium, cesium, tellurium, and iodine classes are the most important chemical classes, although the order of importance differs depending on the choice of radius and dose truncation criterion.

Figure 7-18 through Figure 7-26 show the importance of the chemical classes for the STSBO scenario with RCIC blackstart. These figures are analogous to the ones above. There are a total of nine figures showing the three dose truncation levels at three distances. The LNT figures show that, again, the cesium class is the dominate contributor for the total and long-term phase risk. Following the cesium class are the tellurium, barium/strontium, and cerium classes in terms of importance. For the non-LNT assumptions, the chemical classes that contribute most of the risk are the barium/strontium, tellurium, iodine, cesium, and cerium classes, although the order of importance varies with dose truncation level and distance. The reason that the cesium class is less important for either of the dose-truncation levels considered here than for the LNT is the same as the one given for the unmitigated LTSBO scenario above.

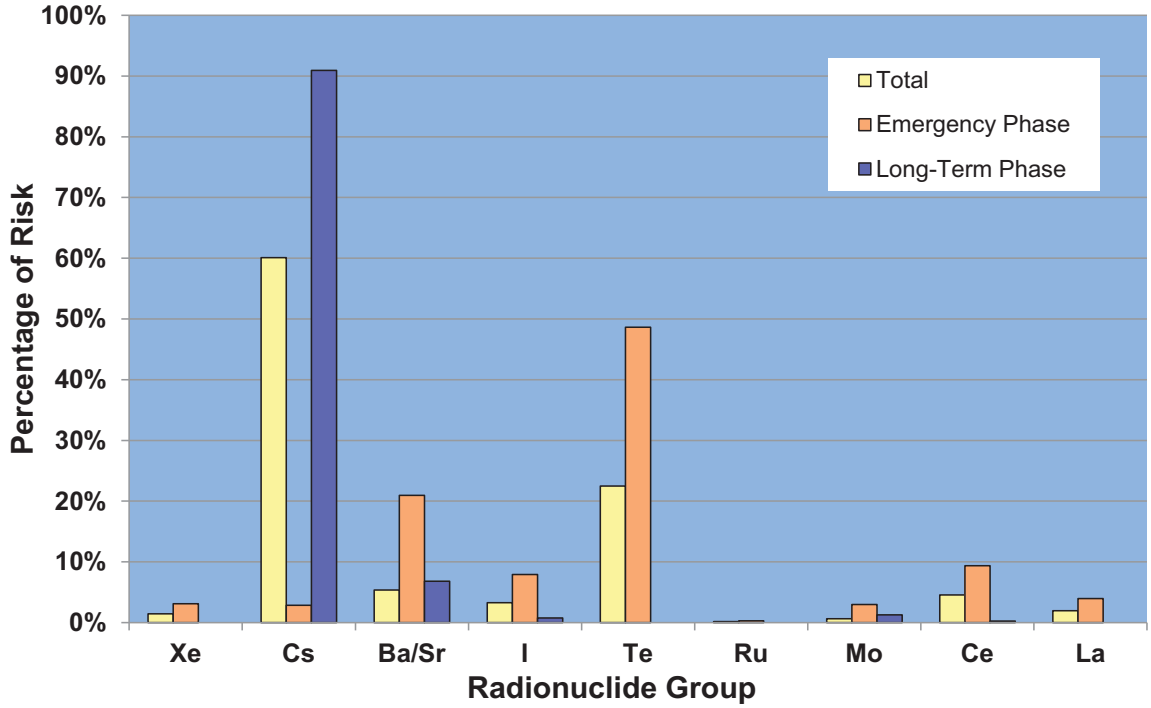

Figure 7-12 Percentage contribution to total, emergency-phase, and long-term-phase, mean, individual risk for the population within 20 miles by chemical class for the Peach Bottom unmitigated LTSBO based on the LNT hypothesis

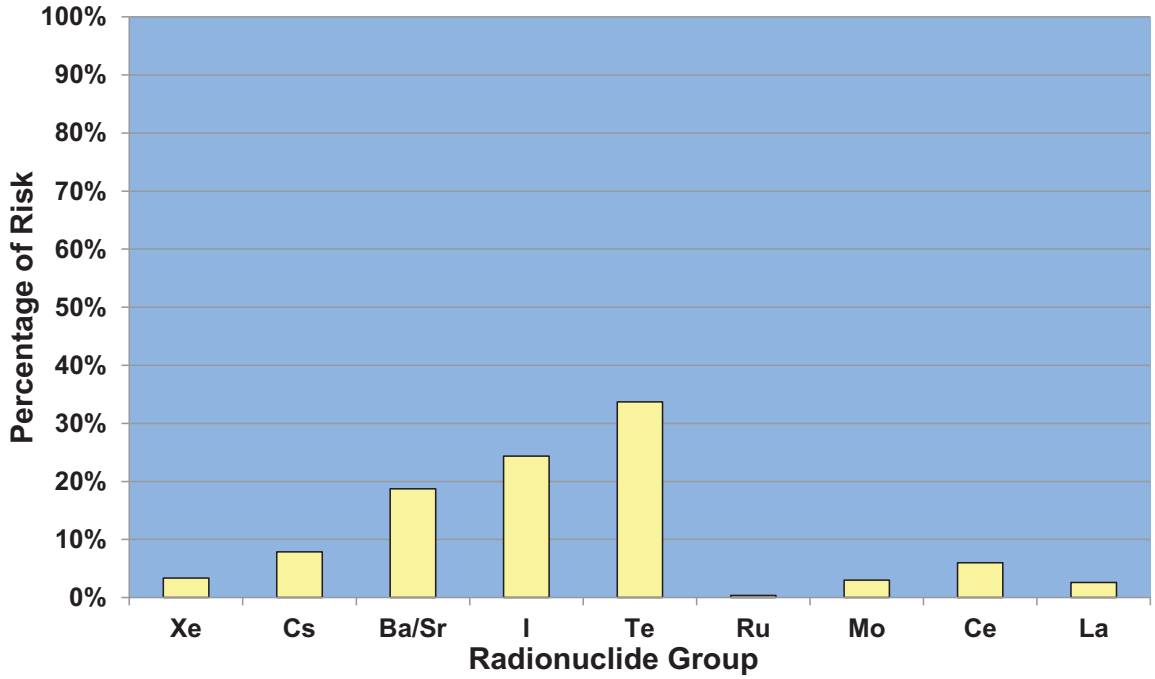

Figure 7-13 Percentage contribution to total, mean, individual risk for the population within 20 miles by chemical class for the Peach Bottom unmitigated LTSBO based on US BGR dose truncation

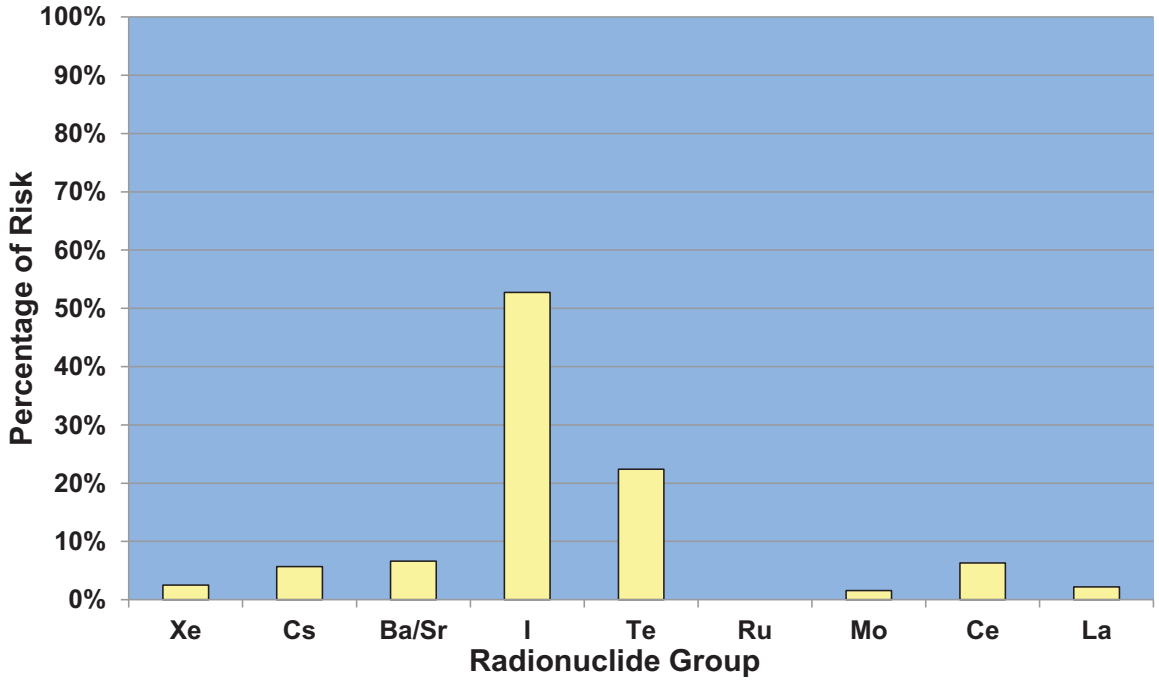

Figure 7-14 Percentage contribution to total, mean, individual risk for the population within 20 miles by chemical class for the Peach Bottom unmitigated LTSBO based on a truncation level reflecting the HPS Position for quantifying health effects

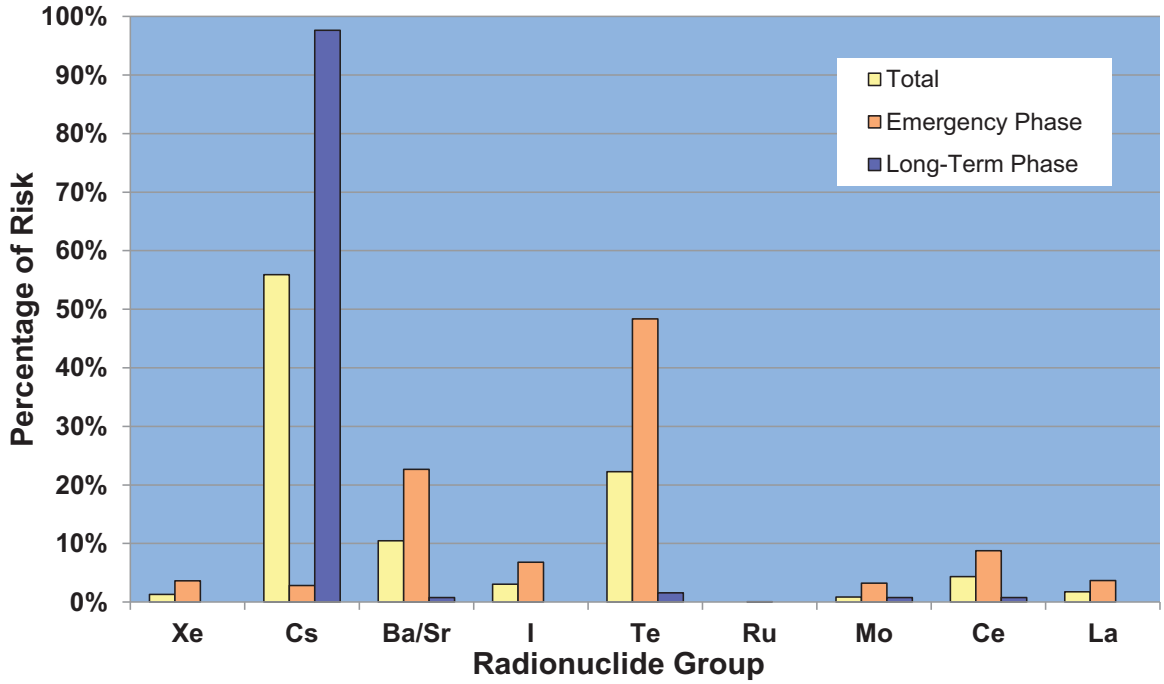

Figure 7-15 Percentage contribution to total, emergency-phase, and long-term-phase, mean, individual risk for the population within 50 miles by chemical class for the Peach Bottom unmitigated LTSBO based on the LNT hypothesis

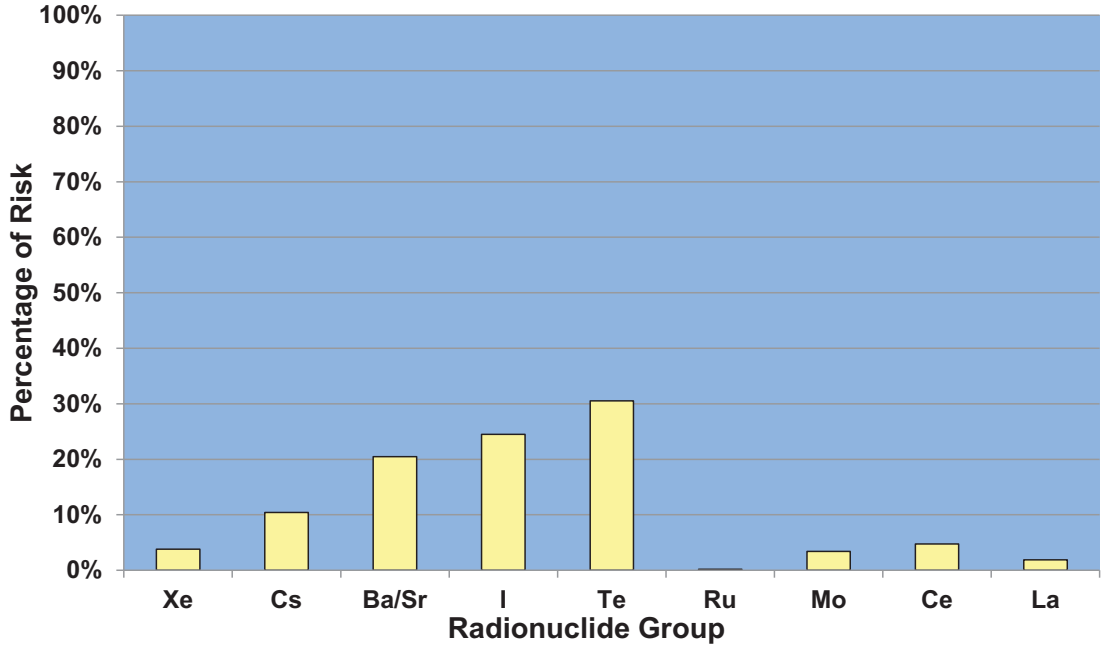

Figure 7-16 Percentage contribution to total, mean, individual risk for the population within 50 miles by chemical class for the Peach Bottom unmitigated LTSBO based on US BGR dose truncation

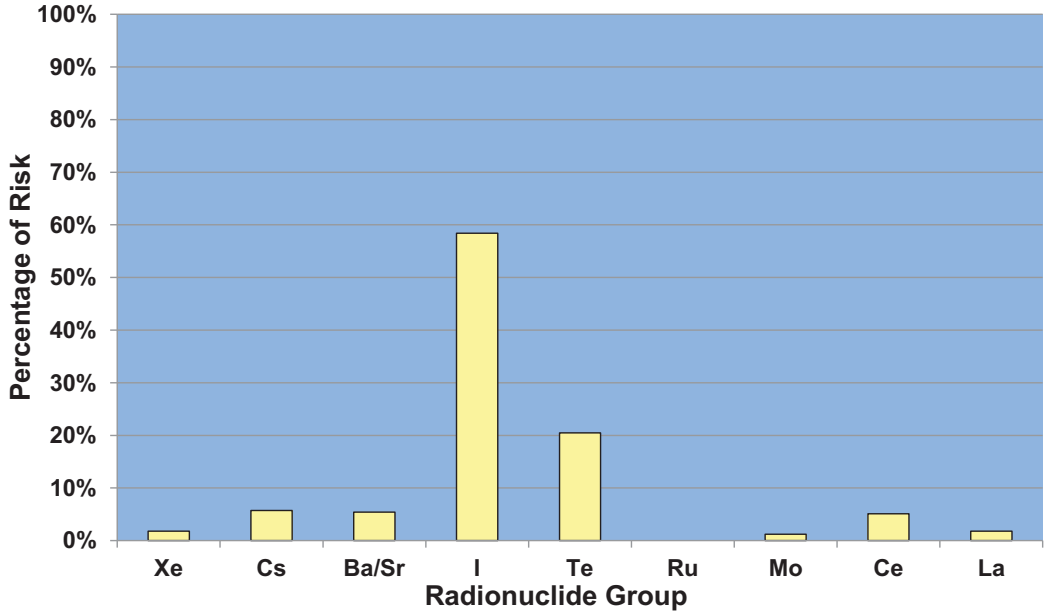

Figure 7-17 Percentage contribution to total, mean, individual risk for the population within 50 miles by chemical class for the Peach Bottom unmitigated LTSBO based on a truncation level reflecting the HPS Position for quantifying health effects

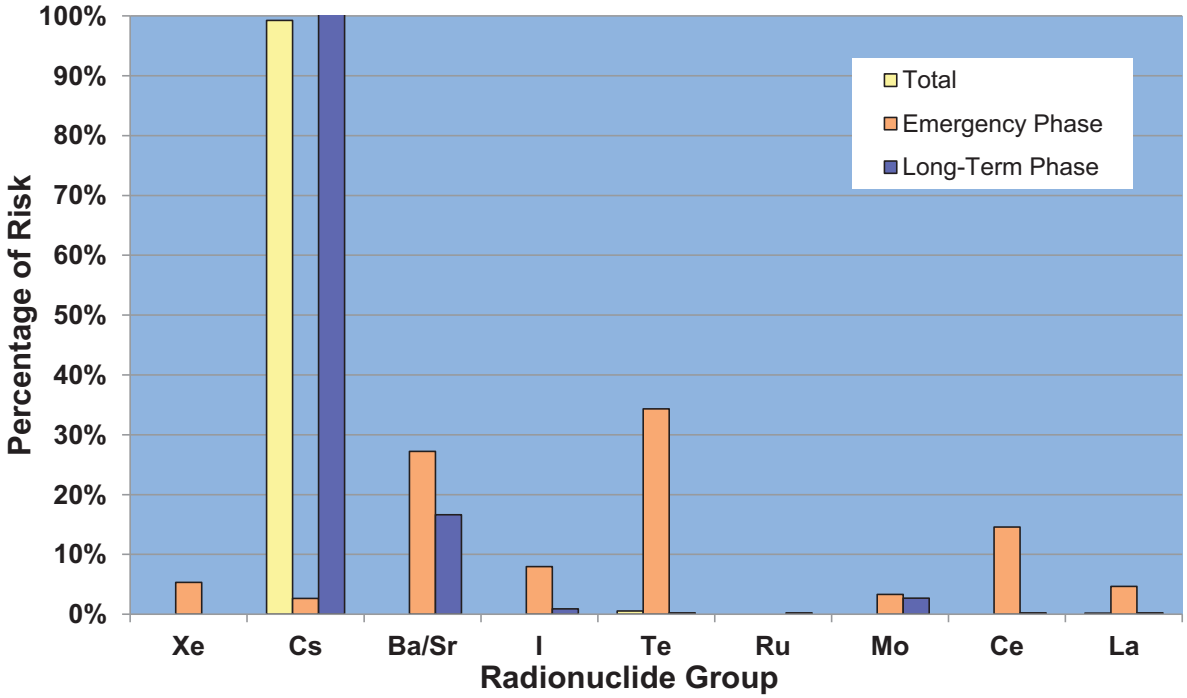

Figure 7-18 Percentage contribution to total, emergency-phase, and long-term-phase, mean, individual risk for the population within 10 miles by chemical class for the Peach Bottom unmitigated STSBO with RCIC blackstart based on the LNT hypothesis

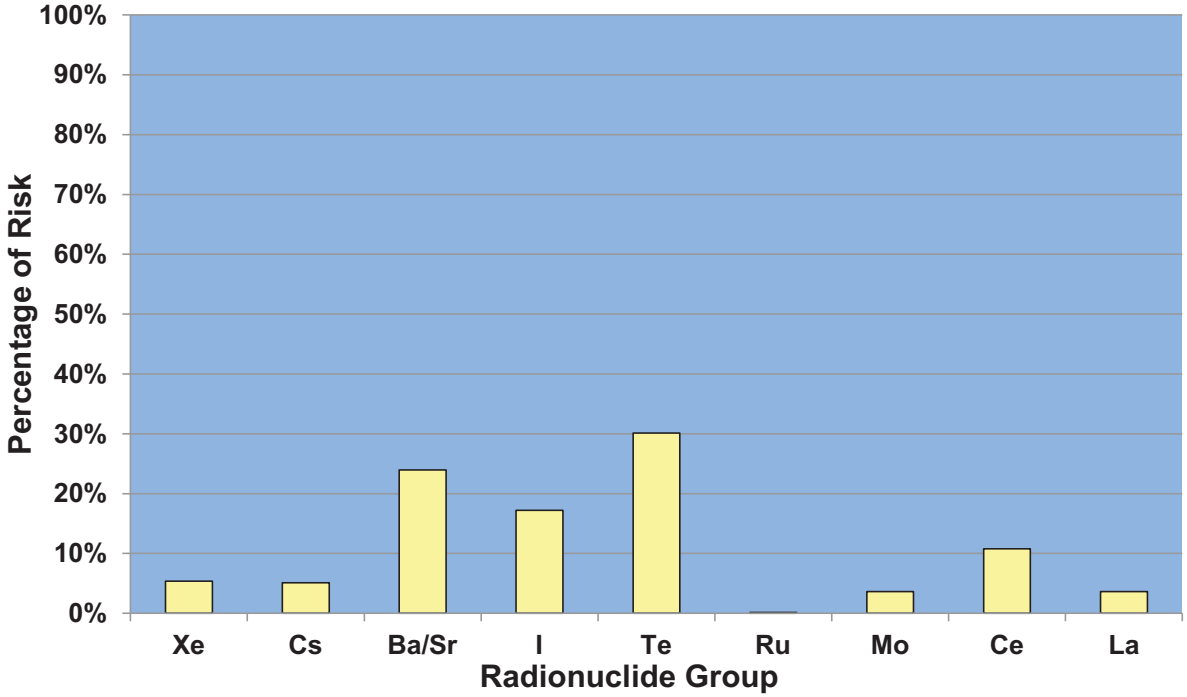

Figure 7-19 Percentage contribution to total, mean, individual risk for the population within 10 miles by chemical class for the Peach Bottom unmitigated STSBO with RCIC blackstart based on US BGR dose truncation

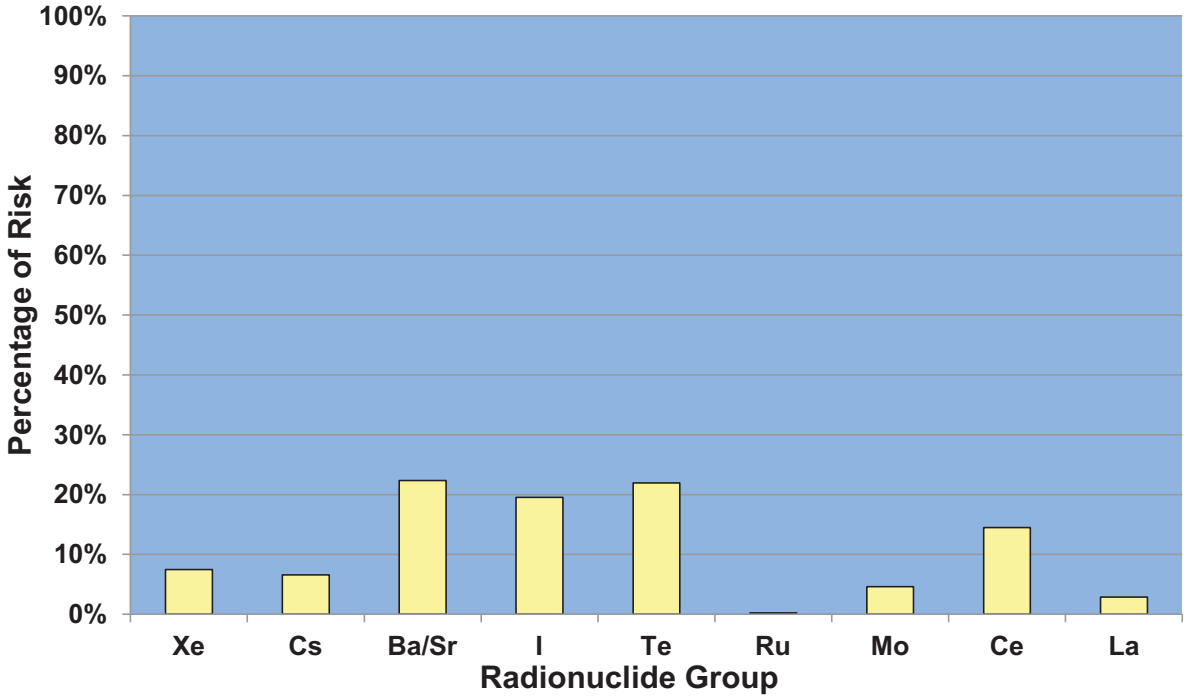

Figure 7-20 Percentage contribution to total, mean, individual risk for the population within 10 miles by chemical class for the Peach Bottom unmitigated STSBO with RCIC blackstart based on a truncation level reflecting the HPS Position for quantifying health effects

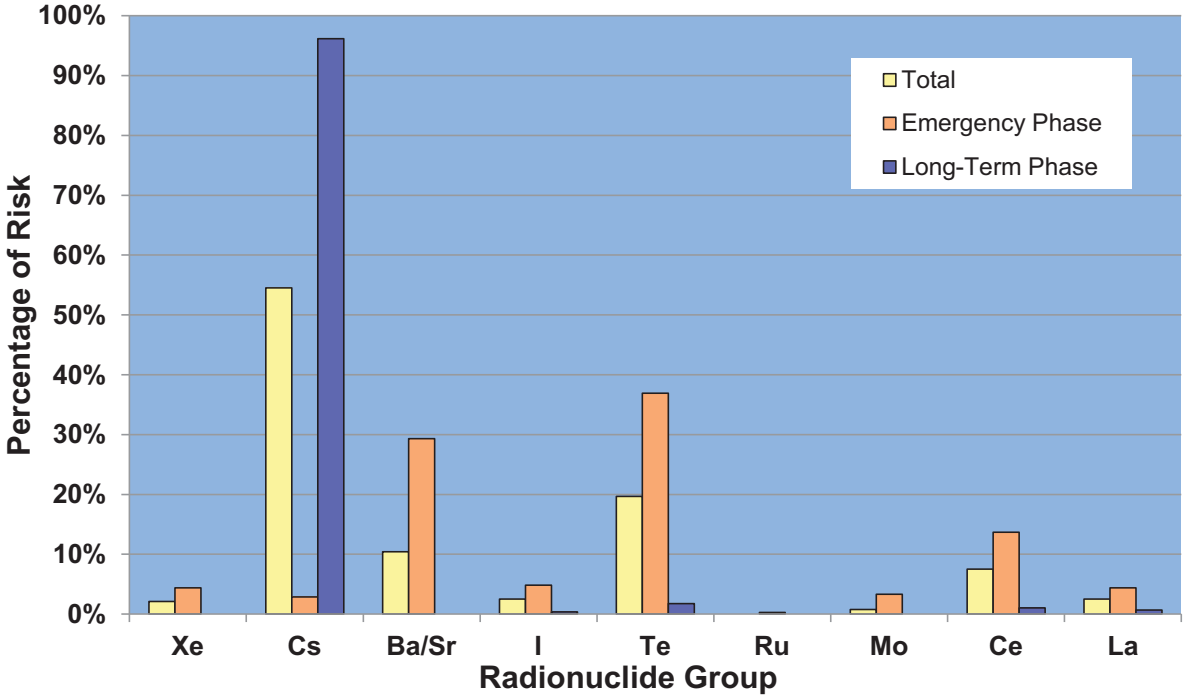

Figure 7-21 Percentage contribution to total, emergency-phase, and long-term-phase, mean, individual risk for the population within 20 miles by chemical class for the Peach Bottom unmitigated STSBO with RCIC blackstart based on the LNT hypothesis

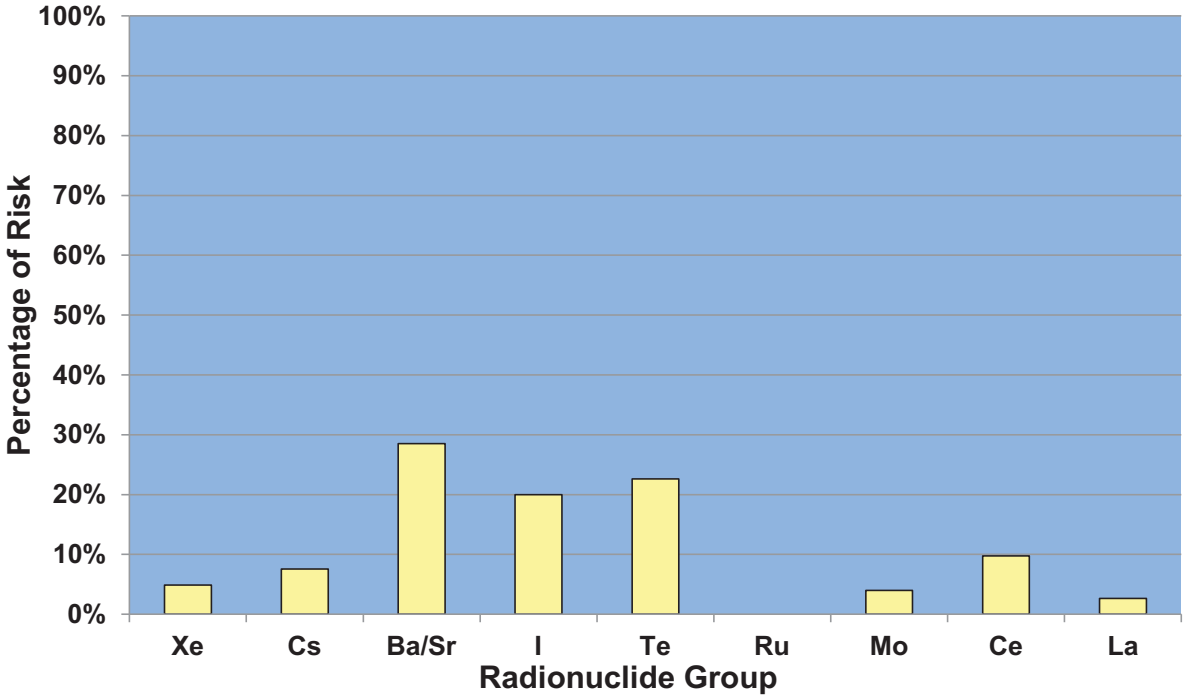

Figure 7-22 Percentage contribution to total, mean, individual risk for the population within 20 miles by chemical class for the Peach Bottom unmitigated STSBO with RCIC blackstart based on US BGR dose truncation

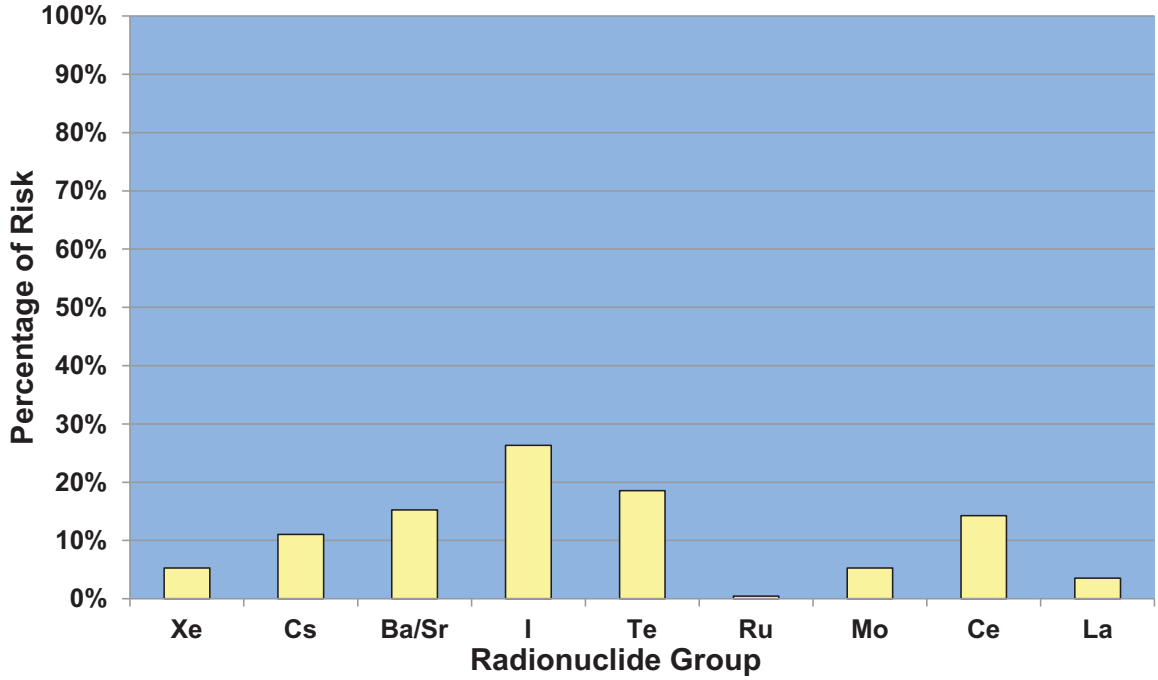

Figure 7-23 Percentage contribution to total, mean, individual risk for the population within 20 miles by chemical class for the Peach Bottom unmitigated STSBO with RCIC blackstart based on a truncation level reflecting the HPS Position for quantifying health effects

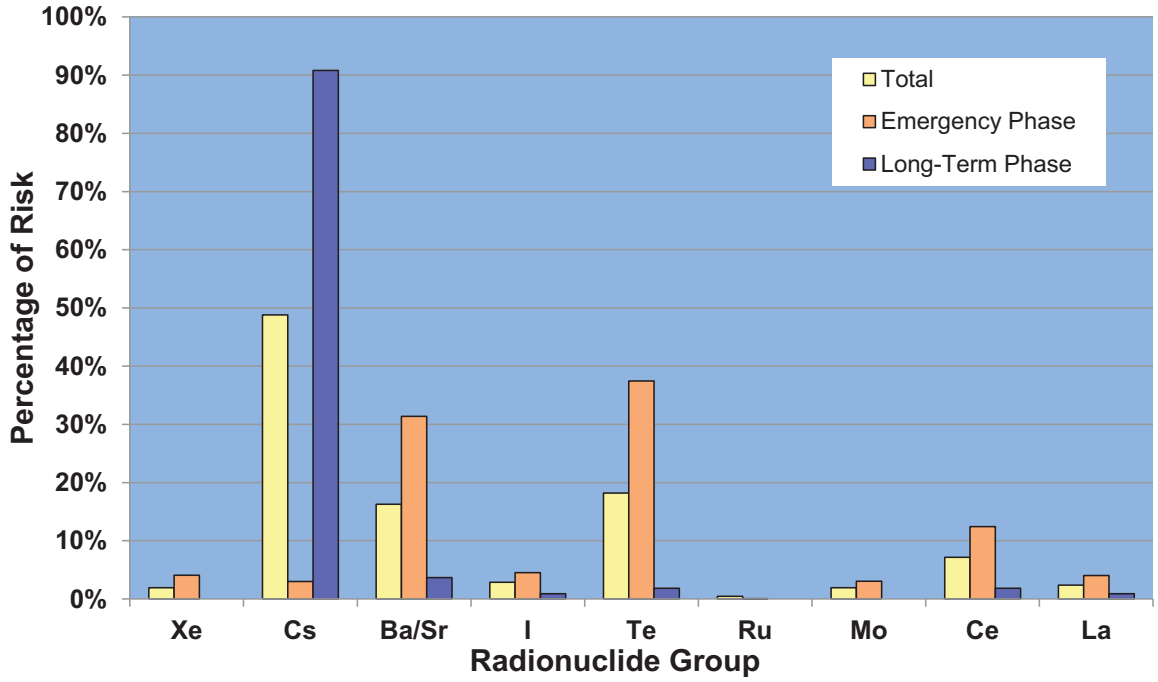

Figure 7-24 Percentage contribution to total, emergency-phase, and long-term-phase, mean, individual risk for the population within 50 miles by chemical class for the Peach Bottom unmitigated STSBO with RCIC blackstart based on the LNT hypothesis

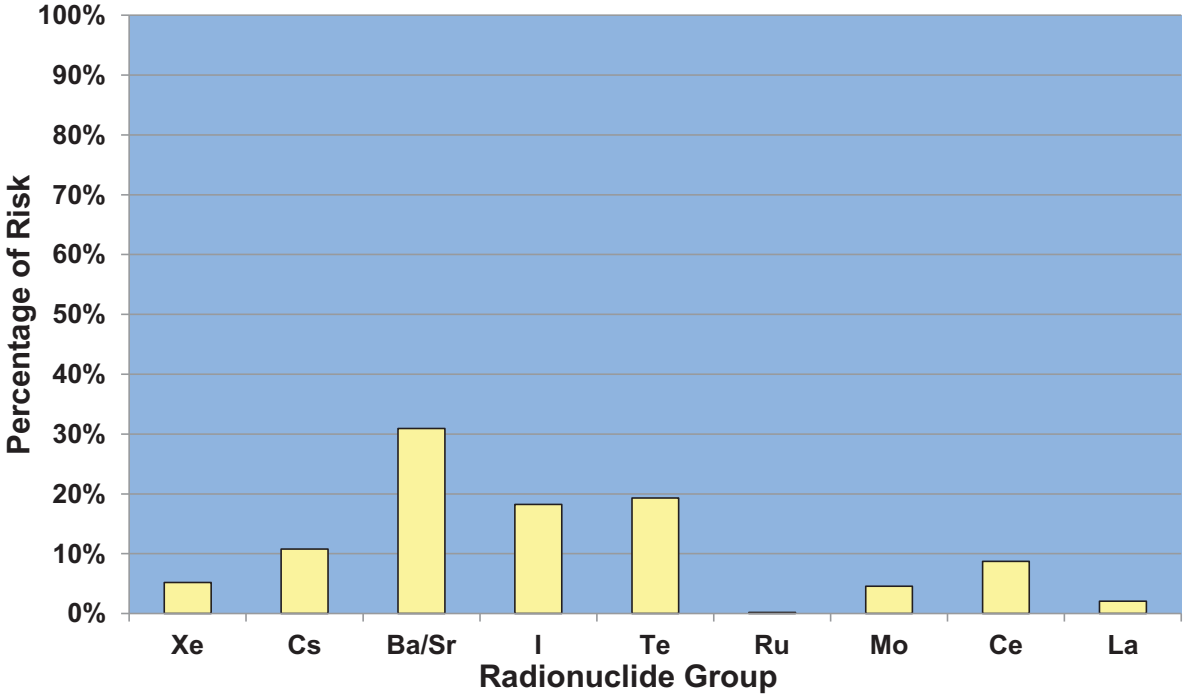

Figure 7-25 Percentage contribution to total, mean, individual risk for the population within 50 miles by chemical class for the Peach Bottom unmitigated STSBO with RCIC blackstart based on US BGR dose truncation

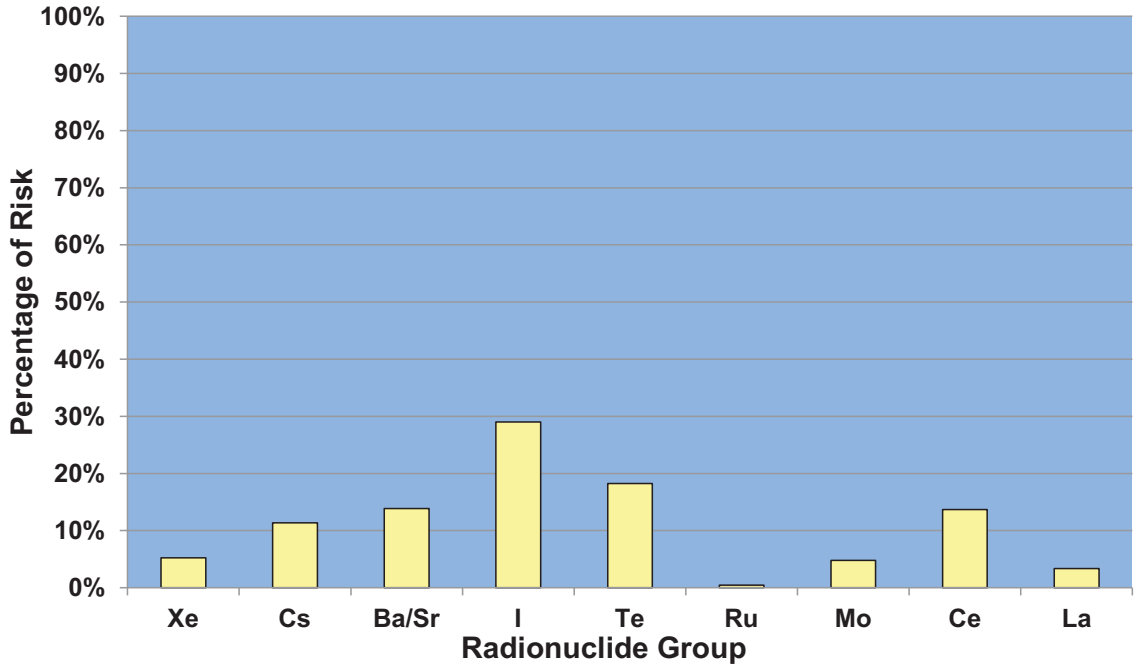

Figure 7-26 Percentage contribution to total, mean, individual risk for the population within 50 miles by chemical class for the Peach Bottom unmitigated STSBO with RCIC blackstart based on a truncation level reflecting the HPS Position for quantifying health effects

Figure 7-27 through Figure 7-35 show the results for the unmitigated STSBO without RCIC blackstart scenario. Comparing these figures with the previous ones for the LTSBO and with the STSBO with RCIC blackstart, two features immediately stand out as distinctly different. First, the risk is dominated by the emergency phase rather than the long-term phase at distances beyond 10 miles. Second and related to the first, the cesium class plays a much smaller role at distances of 20 and 50 miles; the cerium and barium/strontium classes are dominant in terms of contribution to risk even under the LNT hypothesis. The cesium class continues to dominate the risk during the long-term phase under the LNT hypothesis, but the contribution of the long-term phase is diminished for this scenario. The diminished contribution of the cesium class in the unmitigated STSBO without RCIC blackstart scenario is due to the comparatively large release fractions of the barium/strontium and cerium classes, as shown in Table 7-1. The iodine and tellurium release fractions are also large (11.5% and 10.4%, respectively), but most of these releases occur at a later time (about 25 hr for iodine and tellurium as opposed to about 8 hr for barium/strontium and cerium), as shown in Figure 5-43 and Figure 5-44. The late releases of iodine and tellurium diminish the importance of these chemical groups for this scenario, as shown in the following figures.

The release fraction for the cerium class appears small (only 0.7%), as shown in Table 7-1, but this class represents a significant fraction of the overall activity in the core at reactor shutdown. As a result, even this small release fraction provides about half or more of the total risk for distances beyond 10 miles, as shown in the figures below. Cesium remains the dominate contributor to the long-term phase, but both the cerium and barium/strontium classes contribute to doses during the long-term phase as well as during the emergency phase.

The trends for risk within 10 miles are somewhat different than those for the longer distances. Whereas the emergency phase in this accident scenario plays a major role beyond the EPZ (10 miles), it plays a minor role within the EPZ. This is because nearly all of the population are able to evacuate before plume arrival and receive no dose during the emergency phase. Thus, even though the emergency phase dominates beyond 10 miles, the long-term phase dominates for the population within 10 miles from the plant.

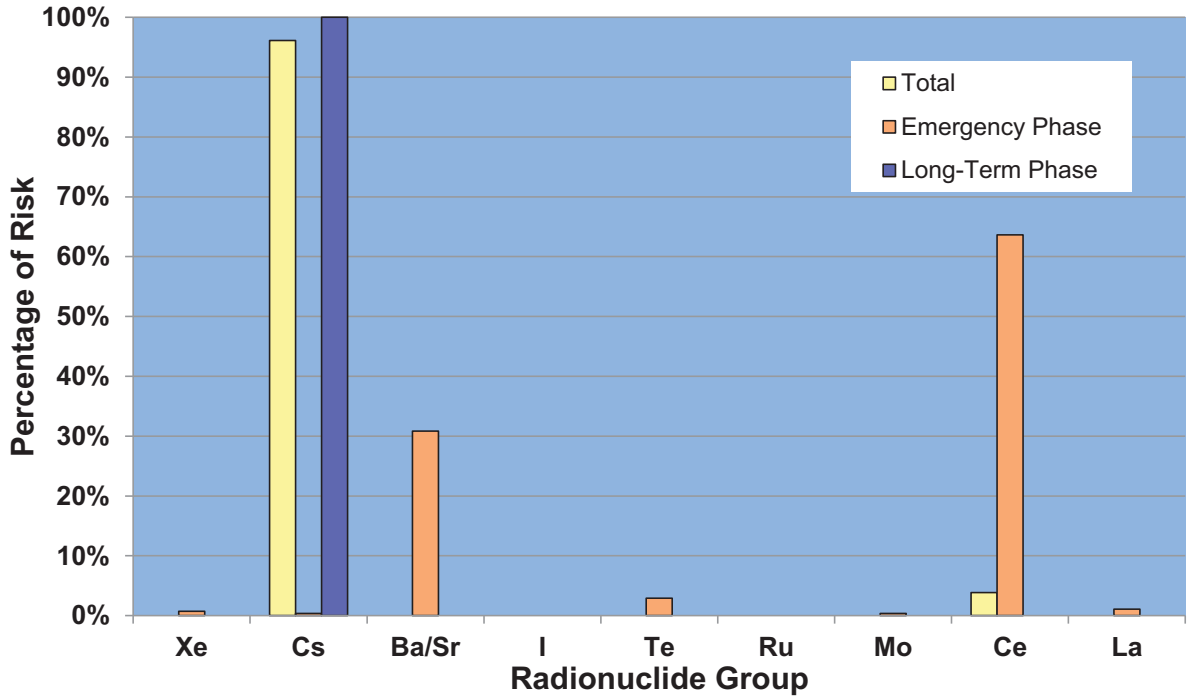

Figure 7-27 Percentage contribution to total, emergency-phase, and long-term-phase, mean, individual risk for the population within 10 miles by chemical class for the Peach Bottom unmitigated STSBO without RCIC blackstart based on the LNT hypothesis

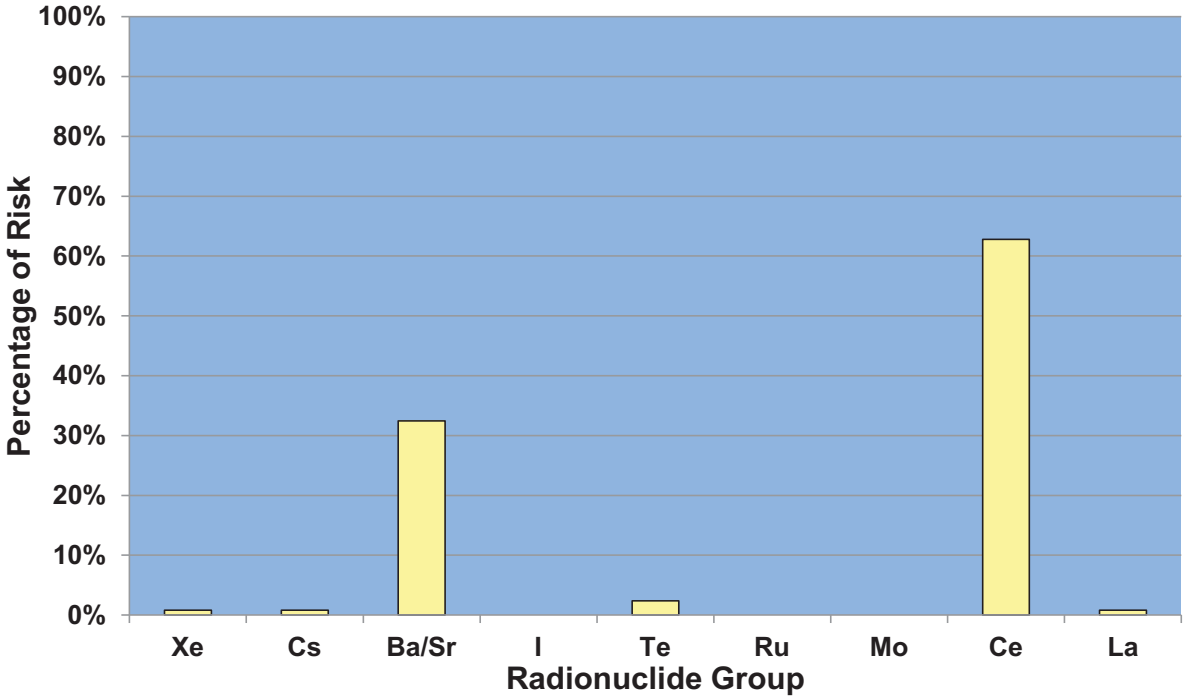

Figure 7-28 Percentage contribution to total, mean, individual risk for the population within 10 miles by chemical class for the Peach Bottom unmitigated STSBO without RCIC blackstart based on US BGR dose truncation

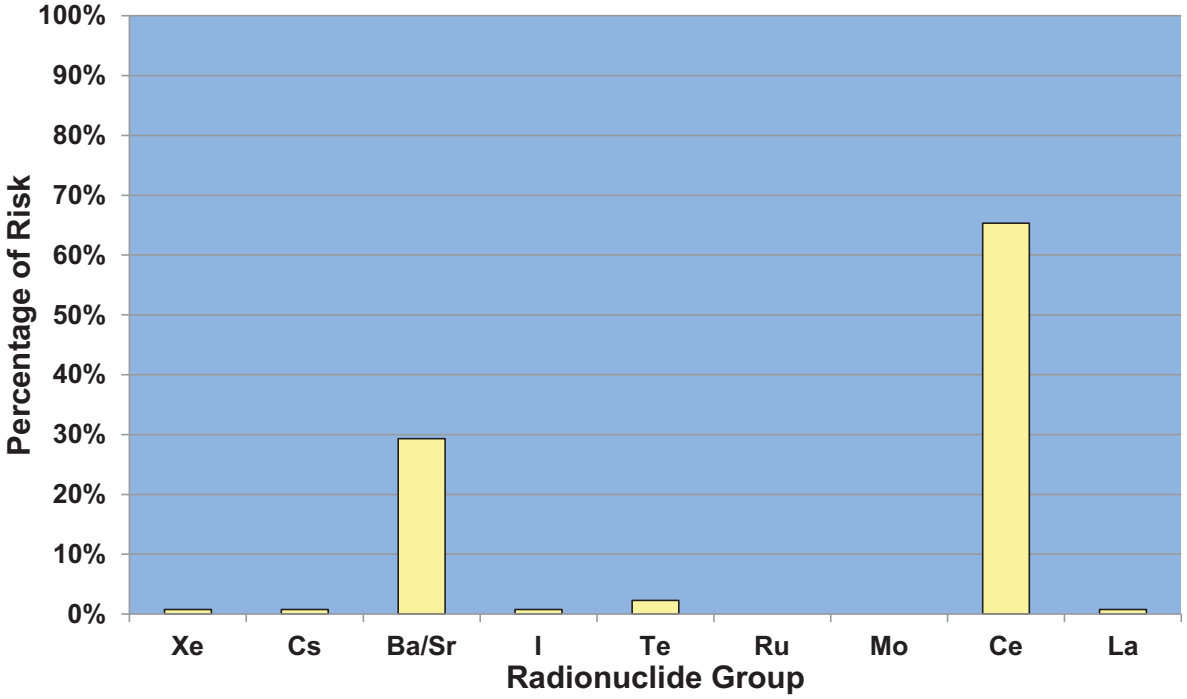

Figure 7-29 Percentage contribution to total, mean, individual risk for the population within 10 miles by chemical class for the Peach Bottom unmitigated STSBO without RCIC blackstart based on a truncation level reflecting the HPS Position for quantifying health effects

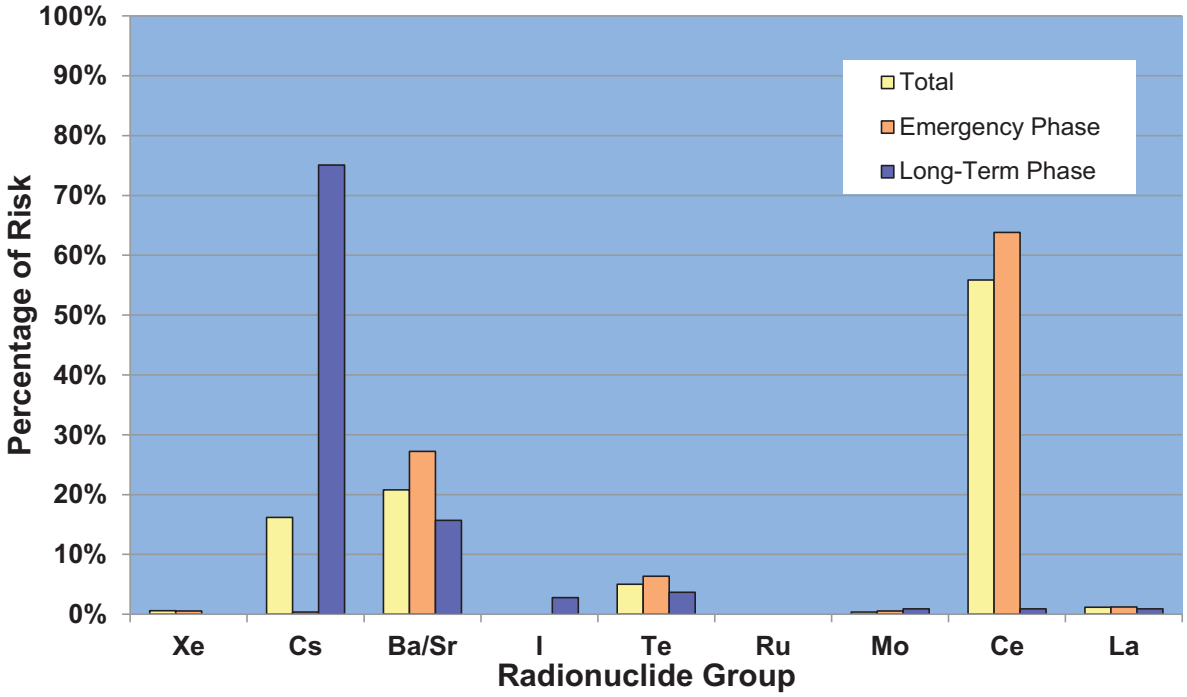

Figure 7-30 Percentage contribution to total, emergency-phase, and long-term-phase, mean, individual risk for the population within 20 miles by chemical class for the Peach Bottom unmitigated STSBO without RCIC blackstart based on the LNT hypothesis

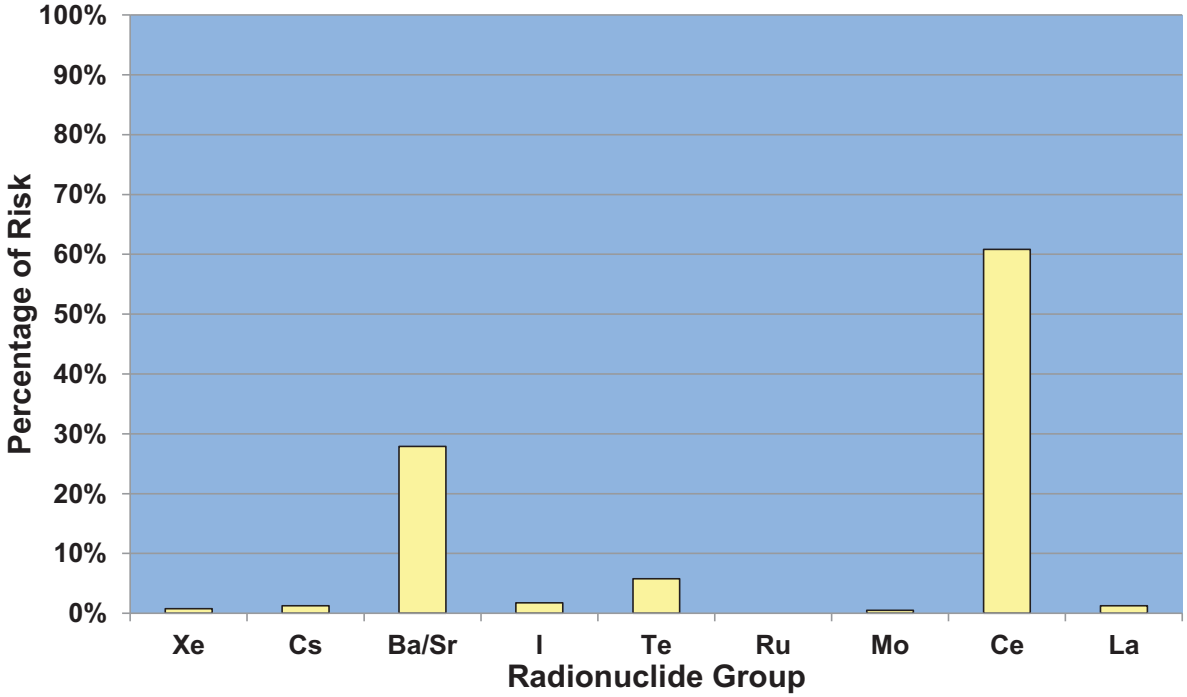

Figure 7-31 Percentage contribution to total, mean, individual risk for the population within 20 miles by chemical class for the Peach Bottom unmitigated STSBO without RCIC blackstart based on US BGR dose truncation

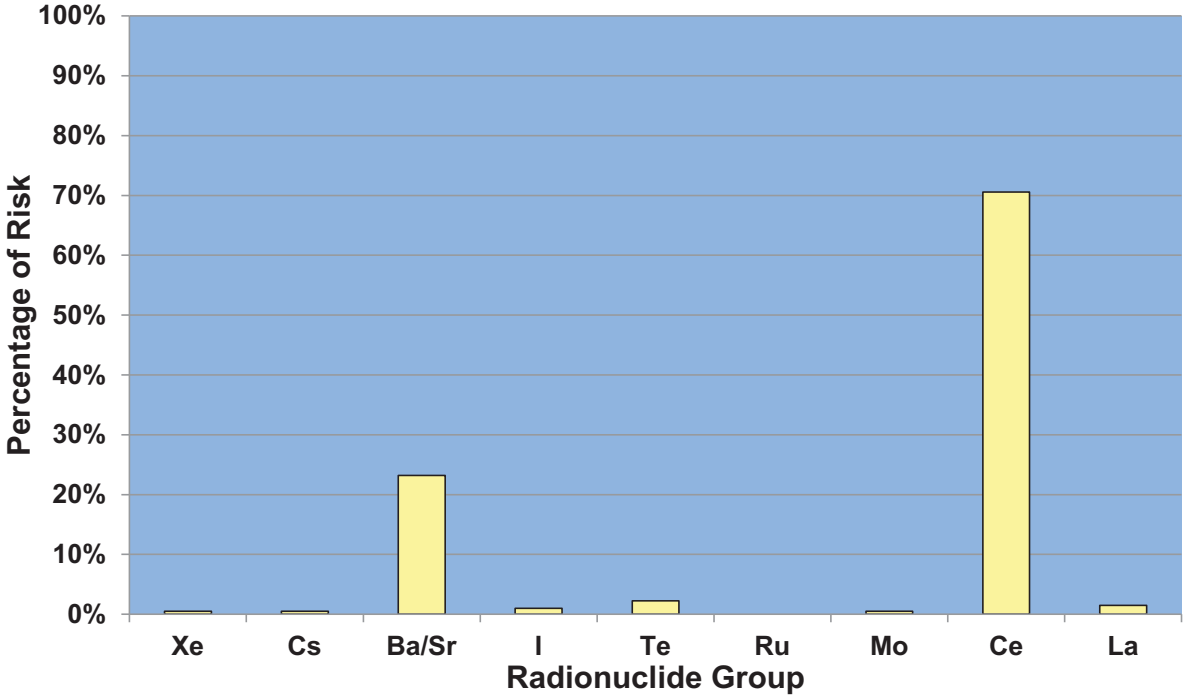

Figure 7-32 Percentage contribution to total, mean, individual risk for the population within 20 miles by chemical class for the Peach Bottom unmitigated STSBO without RCIC blackstart based on a truncation level reflecting the HPS Position for quantifying health effects

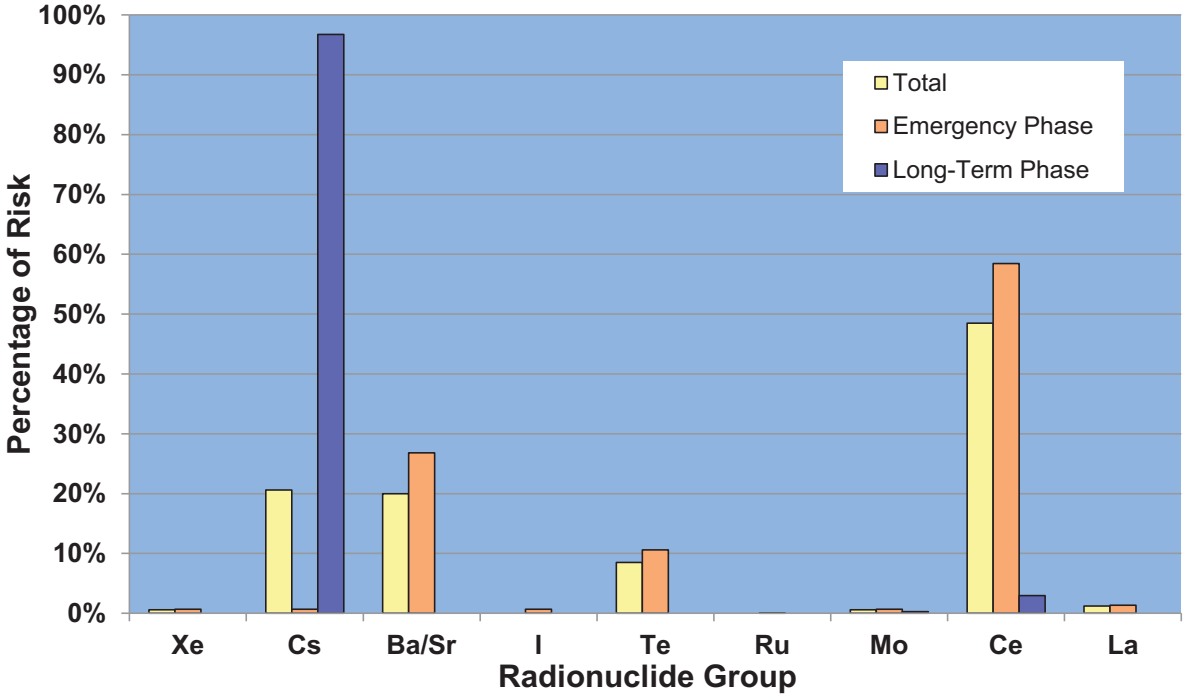

Figure 7-33 Percentage contribution to total, emergency-phase, and long-term-phase, mean, individual risk for population within 50 miles by chemical class for the Peach Bottom unmitigated STSBO without RCIC blackstart based on the LNT hypothesis

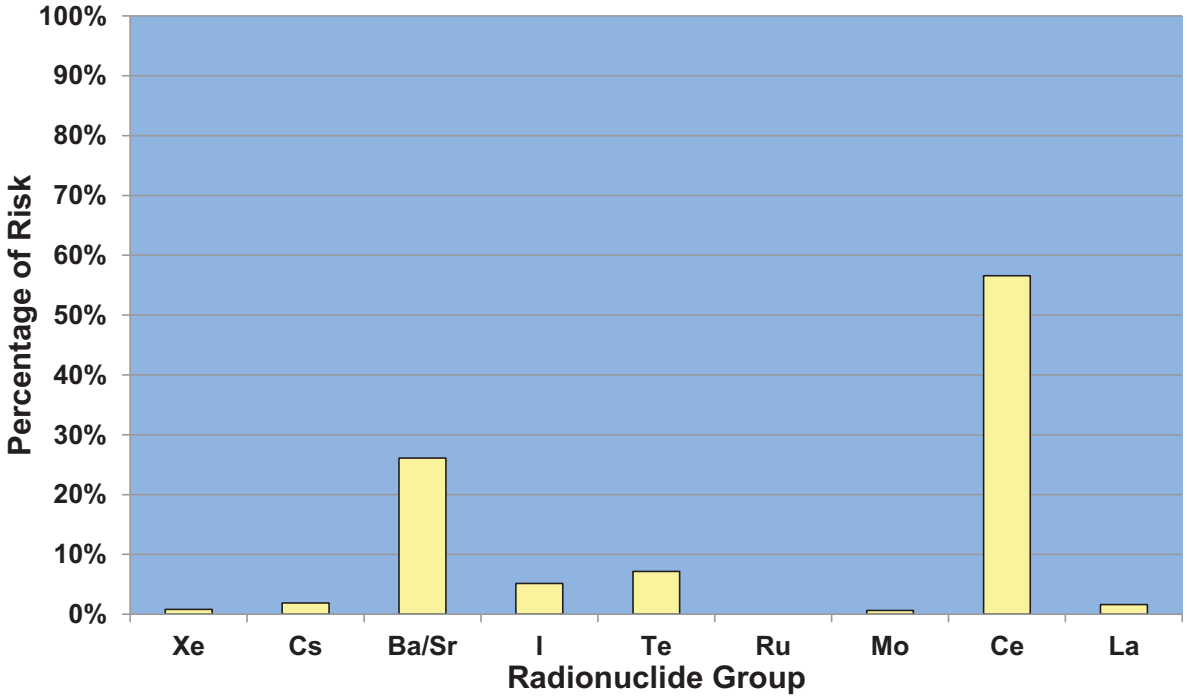

Figure 7-34 Percentage contribution to total, mean, individual risk for the population within 50 miles by chemical class for the Peach Bottom unmitigated STSBO without RCIC blackstart based on US BGR dose truncation

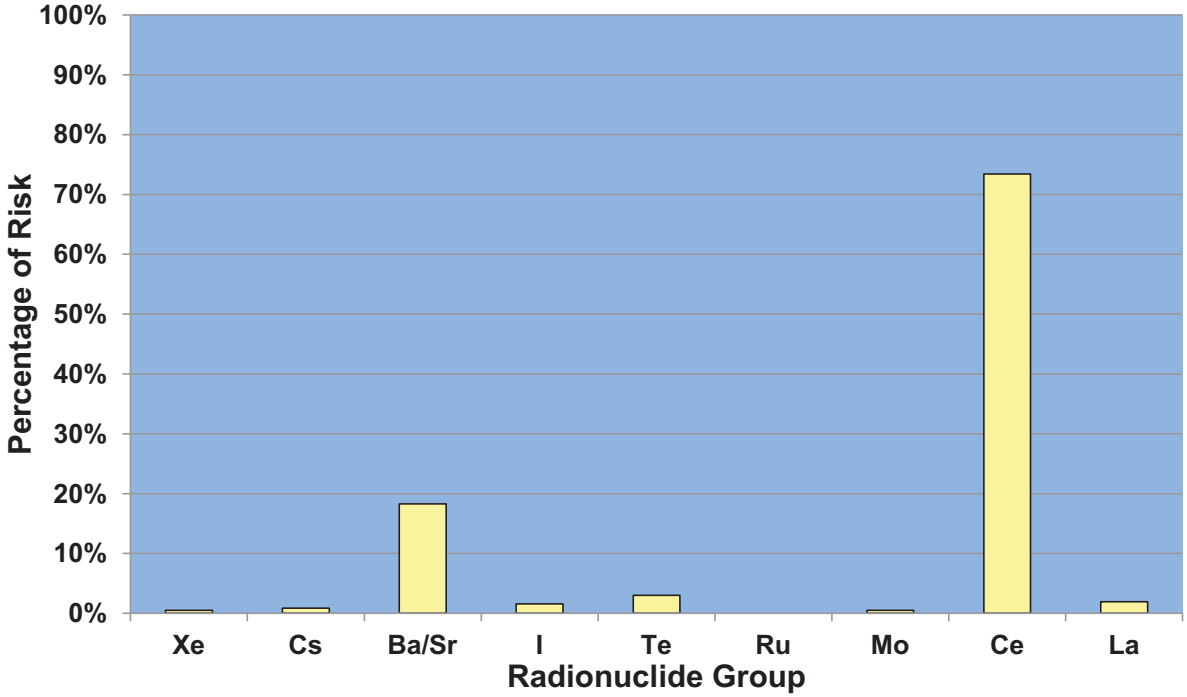

Figure 7-35 Percentage contribution to total, mean, individual risk for the population within 50 miles by chemical class for the Peach Bottom unmitigated STSBO without RCIC blackstart based on a truncation level reflecting the HPS Position for quantifying health effects

8.0 REFERENCES

[1] Carbajo, J.J. "Severe Accident Source Term Characteristics for Selected Peach Bottom Sequences Predicted by the MELCOR Code." NUREG/CR-5942, Oak Ridge National Laboratory: Oak Ridge, TN. July 1993.

[2] Peach Bottom Atomic Power Station, Special Event Procedure – SE-11.

[3] Peach Bottom Atomic Power Station, Trip Procedure T-101.

[4] D.A. Powers, et al., "Accident Source Terms for Light-Water Nuclear Power Plants Using High-Burnup or MOX Fuel," SAND2011-0128, Sandia National Laboratories: Albuquerque, NM. January 2011.

[5] Soffer, L, et al., "Accident Source Terms for Light-Water Nuclear Power Plants," NUREG-1465, Nuclear Regulatory Commission: Washington, DC. February, 1995.

[6] Gauntt, R.O., et al., "MELCOR Computer Code Manuals, Vol. 1: Primer and User's Guide, Version 1.8.6," NUREG/CR 6119, Vol. 1, Rev. 3, Nuclear Regulatory Commission: Washington, DC. 2005.

[7] Laur, M.N., "Meeting with Sandia National Laboratories and an Expert Panel on MELCOR/MACCS Codes in Support of the State of the Art Reactor Consequence Analysis Project," Memo to J.T. Yerokun, Agency Document Access and Management System Accession Number ML062500078, Nuclear Regulatory Commission: Washington, DC. September, 2006.

[8] Nuclear Regulatory Commission, "Severe Accident Risks: An Assessment for Five U.S. Nuclear Power Plants," NUREG 1150, Nuclear Regulatory Commission: Washington, DC. 1990.

[9] Gauntt, R.O., "Synthesis of VERCORS and Phebus Data in Severe Accident Codes and Applications," SAND2010-1633, Sandia National Laboratories: Albuquerque, NM. April 2010.

[10] Harper, F. T., et al., "Evaluation of Severe Accident Risks: Quantification of Major Input Parameters, Experts' Determination of Containment Loads and Molten Core Containment Interaction Issues," NUREG/CR-4551, Sandia National Laboratories: Albuquerque, NM. April 1991.

[11] Theofanous, T.G., et al., "The Probability of Liner Failure in a Mark I Containment," NUREG/CR-5423, Nuclear Regulatory Commission: Washington DC. 1989.

[12] Theofanous, T.G., et al., "The Probability of Mark I Failure by Melt –Attack of the Liner," NUREG/CR-6025, Nuclear Regulatory Commission: Washington DC. November 1993.

[13] Oak Ridge National Laboratory, "SCALE: A Modular Code System for Performing Standardized Computer Analyses for Licensing Evaluations," ORNL/TM-2005/39, Version 5.1, Vols. I-III, Oak Ridge National Laboratory: Oak Ridge, TN. November 2006.

[14] Philadelphia Electric Company, "Individual Plant Examination, Peach Bottom Atomic Power Station, Units 2 and 3," August 1992.

[15] T.Y. Chu, et al., "Lower Head Failure Experiments and Analyses," NUREG/CR-5582, SAND98-2047, Sandia National Laboratories: Albuquerque, NM. October 1998.

[16] J.L. Rempe, et al., "Light Water Reactor Lower Head Failure Analysis," NUREG/CR-5642, EGG-2618, Idaho National Engineering Laboratory: Idaho Falls, ID. September 1993.

[17] Eide, S.A., et al., "Industry-Average Performance for Components and Initiating Events at U.S. Commercial Nuclear Power Plants," NUREG/CR-6928, Idaho National Laboratory: Idaho Falls, ID. February 2007.

[18] Peach Bottom Atomic Power Station Procedure, "Reactor Pressure Vessel Reassembly."

[19] Personal communication from Thomas R. Loomis of Exelon Corporation to Abdul Sheikh of the Nuclear Regulatory Commission about torque value for the 2 ½ inch diameter reactor head flange bolts, October 31, 2006.

[20] Nuclear Regulatory Commission, "Criteria for Preparation and Evaluation of Radiological Emergency Response Plans and Preparedness in Support of Nuclear Power Plants." NUREG-0654/FEMA-REP-1, Rev. 1, Nuclear Regulatory Commission: Washington DC. November 1980.

[21] Nuclear Regulatory Commission, "Identification and Analysis of Factors Affecting Emergency Evacuations," NUREG/CR-6864, Nuclear Regulatory Commission: Washington DC. January 2005.

[22] Nuclear Regulatory Commission, "Review of NUREG-0654, Supplement 3, "Criteria for Protective Action Recommendations for Severe Accidents," NUREG/CR-6953, Vol. I, Nuclear Regulatory Commission: Washington D.C. December 2007.

[23] Nuclear Regulatory Commission, "Development of Evacuation Time Estimate Studies for Nuclear Power Plants," NUREG/CR-6863, Nuclear Regulatory Commission: Washington D.C. January 2005.

[24] Oak Ridge National Laboratory. "Oak Ridge Evacuation Modeling System (OREMS)," Oak Ridge National Laboratory: Oak Ridge, TN. July 2003.

[25] Rogers, G.O., et al., "Evaluating Protective Actions for Chemical Agent Emergencies," ORNL-6615, Oak Ridge National Laboratory: Oak Ridge, TN. April 1990.

[26] Chanin, D.I., and M.L. Young, "Code Manual for MACCS2: Volume 1, User's Guide," NUREG/CR-6613, Nuclear Regulatory Commission: Washington D.C. 1998.

[27] Aldrich, D.C., et al., "Technical Guidance for Siting Criteria Development," NUREG/CR-2239, Nuclear Regulatory Commission: Washington DC. 1982.

[28] Harper, F. T., et al., "Probabilistic Accident Consequence Uncertainty Analysis, Dispersion and Deposition Uncertainty Analysis," NUREG/CR-6244, Nuclear Regulatory Commission: Washington DC. 1994.

[29] Exelon Nuclear, "Evacuation Time Estimates for the Peach Bottom Station Plume Exposure Pathway Emergency Planning Zone," Exelon Corporation: Chicago, IL. August, 2003.

[30] Transportation Research Board, "Highway Capacity Manual," National Research Council: Washington DC. 2000.

[31] Nuclear Regulatory Commission, "Review of NUREG-0654, Supplement 3, 'Criteria for Protective Action Recommendations for Severe Accidents' – Focus Group and Telephone Survey," NUREG/CR-6953, Volume 2, Nuclear Regulatory Commission: Washington DC. October 2008.

[32] Wheeler, T., G. Wyss, and F. Harper, "Cassini Spacecraft Uncertainty Analysis Data and Methodology Review and Update Volume 1: Updated Parameter Uncertainty Models for the Consequence Analysis," SAND2000-2719/1, Sandia National Laboratories: Albuquerque, NM. November, 2000.

[33] Haugen, D. A. (Ed.), "Project Prairie Grass: A Field Program in Diffusion." No. 59, Vol. III, Report AFCRC-TR-58-235, Air Force Cambridge Research Center. 1959.

[34] Bixler, N. E., E. Clauss, C.W. Morrow, and J.A. Mitchell, "Evaluation of Distributions Representing Important Non-Site-Specific Parameters in Offsite Consequence Analysis," to be published as a NUREG Report, Nuclear Regulatory Commission: Washington DC. 2011.

[35] Miller, C. L., et al., "Recommendations for Enhancing Reactor Safety in the 21st Century – The Near-Term Task Force Review of Insights From the Fukushima Dai-Ichi Accident," Nuclear Regulatory Commission: Washington DC. July 2011.

[36] Whelan, G., D.L. Strenge, J.G. Droppo Jr., B.L. Steelman, and J.W. Buck, "The Remedial Action Priority System (RAPS): Mathematical Formulations," DOE/RL-87-09, Pacific Northwest Laboratory: Richland, WA. August 1987.

APPENDIX A
PEACH BOTTOM RADIONUCLIDE INVENTORY

PEACH BOTTOM RADIONUCLIDE INVENTORY

The following tables summarize the radionuclide core inventory for the Peach Bottom plant at the time of shutdown. This isotopic inventory was used in each of the accident progression scenarios considered in this report. This inventory was computed using SCALE to model the specific fuel management strategy used at Peach Bottom for this unit. The SCALE model assumed that the accident occurs mid-cycle and that the peak fuel rod burnup is 49 MWd/kg fuel. Both radial and axial variations in burnup were modeled with SCALE. The inventory given below was calculated by integrating the isotopic inventory over the whole core.

Table A-1 Peach Bottom radionuclide core inventory and class definition

Radionuclide Class Name	Representative Element	Member Elements	Total Mass (kg)
Noble Gas	Xe	He, Ne, Ar, Kr, Xe, Rn, H, N	531.7
Alkali Metals	Cs	Li, Na, K, Rb, Cs, Fr, Cu	323.0
Alkaline Earths	Ba	Be, Mg, Ca, Sr, Ba, Ra, Es, Fm	235.6
Halogens	I	F, Cl, Br, I, At	19.9
Chalcogens	Te	O, S, Se, Te, Po	49.1
Platinoids	Ru	Ru, Rh, Pd, Re, Os, Ir, Pt, Au, Ni	342.8
Early Transition Elements	Mo	V, Cr, Fe, Co, Mn, Nb, Mo, Tc, Ta, W	400.2
Tetravalent	Ce	Ti, Zr, Hf, Ce, Th, Pa, Np, Pu, C	1,555.5
Trivalents	La	Gd, Tb, Dy, Ho, Er, Tm, Yb, Lu, Am, Cm, Bk, Cf	1793.7
Uranium	U	U	132,794.0
More Volatile Main Group	Cd	Cd, Hg, Zn, As, Sb, Pb, Tl, Bi	6.6
Less Volatile Main Group	Sn	Ga, Ge, In, Sn, Ag	9.6

Table A-2 Peach Bottom noble gas radionuclide class specific isotopic activity at the time of reactor shutdown

Isotope	Activity (Bq)
Kr-85	3.79E+16
Kr-85m	1.03E+18
Kr-87	2.05E+18
Kr-88	2.77E+18
Xe-133	7.02E+18
Xe-135	2.58E+18
Xe-135m	1.43E+18

Table A-3 Peach Bottom alkali metals radionuclide class specific isotopic activity at the time of reactor shutdown

Isotope	Activity (Bq)
Cs-134	3.61E+17
Cs-136	1.43E+17
Cs-137	3.74E+17
Rb-86	4.38E+15
Rb-88	2.80E+18

Table A-4 Peach Bottom alkali earths radionuclide class specific isotopic activity at the time of reactor shutdown

Isotope	Activity (Bq)
Ba-139	6.48E+18
Ba-140	6.27E+18
Sr-89	3.79E+18
Sr-90	2.98E+17
Sr-91	4.77E+18
Sr-92	5.02E+18
Ba-137m	3.55E+17

Table A-5 Peach Bottom halogen radionuclide class specific isotopic activity at the time of reactor shutdown

Isotope	Activity (Bq)
I-131	3.38E+18
I-132	4.99E+18
I-133	7.15E+18
I-134	8.14E+18
I-135	6.80E+18

Table A-6 Peach Bottom chalcogen radionuclide class specific isotopic activity at the time of reactor shutdown

Isotope	Activity (Bq)
Te-127	2.71E+17
Te-127m	4.33E+16
Te-129	8.17E+17
Te-129m	1.55E+17
Te-131m	6.03E+17
Te-132	4.85E+18
Te-131	2.89E+18

Table A-7 Peach Bottom platinoid radionuclide class specific isotopic activity at the time of reactor shutdown

Isotope	Activity (Bq)
Rh-105	2.77E+18
Ru-103	4.83E+18
Ru-105	3.03E+18
Ru-106	1.31E+18
Rh-103m	4.82E+18
Rh-106	1.44E+18

Table A-8 Peach Bottom early transition element radionuclide class specific isotopic activity at the time of reactor shutdown

Isotope	Activity (Bq)
Nb-95	6.07E+18
Co-58	0.00E+00
Co-60	0.00E+00
Mo-99	6.52E+18
Tc-99m	5.83E+18
Nb-97	6.11E+18
Nb-97m	5.77E+18

Table A-9 Peach Bottom tetravalent radionuclide class specific isotopic activity at the time of reactor shutdown

Isotope	Activity (Bq)
Ce-141	5.89E+18
Ce-143	5.64E+18
Ce-144	4.19E+18
Np-239	5.61E+19
Pu-238	6.78E+15
Pu-239	1.37E+15
Pu-240	1.13E+15
Pu-241	3.87E+17
Zr-95	6.11E+18
Zr-97	6.08E+18

Table A-10 Peach Bottom trivalent radionuclide class specific isotopic activity at the time of reactor shutdown

Isotope	Activity (Bq)
Am-241	5.23E+14
Cm-242	9.57E+16
Cm-244	4.70E+15
La-140	6.48E+18
La-141	5.86E+18
La-142	5.70E+18
Nd-147	2.32E+18
Pr-143	5.55E+18
Y-90	3.03E+17
Y-91	4.82E+18
Y-92	5.05E+18
Y-93	5.58E+18
Y-91m	2.75E+18
Pr-144	4.20E+18
Pr-144m	5.85E+16

APPENDIX B
INPUT PARAMETERS FOR CONSEQUENCE ANALYSIS

INPUT PARAMETERS FOR CONSEQUENCE ANALYSIS

The input parameters used for the unmitigated LTSBO scenario and the STSBO with and without RCIC blackstart are shown in this appendix in tabular form. Table B-1 contains the more general ATMOS input parameters used for these three scenarios. Table B-2 through Table B-4 contains specific inputs related to the source terms that were extracted from MELCOR results via the MELMACCS code. Table B-5 contains general EARLY input parameters. Table B-6 and Table B-7 contain parameters associated with the network evacuation model that was used to treat emergency response. Table B-8 contains the CHRONC input parameters.

Table B-1 ATMOS Input Parameters Used in the Peach Bottom Unmitigated LTSBO and STSBO with and without RCIC Blackstart scenarios

Variable	Description	LTSBO	STSBO with RCIC Blackstart	STSBO without RCIC Blackstart
APLFRC	Method of Applying Release Fraction	PARENT	PARENT	PARENT
ATNAM1	Title Describing the ATMOS Assumptions	SOARCA PB Source Term Long-Term SBO	SOARCA PB Source Term Short-Term SBO	SOARCA PB Source Term Short-Term SBO
ATNAM2	Title Describing the Source Term	Peach Bottom source term for long term station blackout.	Peach Bottom source term for short term station blackout.	Peach Bottom source term for short term station blackout.
BNDMXH	Boundary Weather Mixing Layer Height	1000	1000	1000
BNDRAN	Boundary Weather Rain Rate	5	5	5
BNDWND	Boundary Wind Speed	2.2	2.2	2.2
BRKPNT	Breakpoint Time for Plume Meander	3600	3600	3600
BUILDH	Building Height for all Plume Segments	50	50	50
CORINV	Isotopic Inventory at Time of Reactor Shutdown	from MELMACCS (see Appendix A)	from MELMACCS (see Appendix A)	from MELMACCS (see Appendix A)
CORSCA	Linear Scaling Factor on Core Inventory	1	1	1
CWASH1	Linear Coefficient for Washout	1.89E-05	1.89E-05	1.89E-05
CWASH2	Exponential Term for Washout	0.664	0.664	0.664
CYSIGA	Linear Coefficient for sigma-y			
	Stability Class A	0.7507	0.7507	0.7507
	Stability Class B	0.7507	0.7507	0.7507
	Stability Class C	0.4063	0.4063	0.4063
	Stability Class D	0.2779	0.2779	0.2779
	Stability Class E	0.2158	0.2158	0.2158
	Stability Class F	0.2158	0.2158	0.2158

Variable	Description	LTSBO	STSBO with RCIC Blackstart	STSBO without RCIC Blackstart
CYSIGB	Exponential Term for sigma-y			
	Stability Class A	0.866	0.866	0.866
	Stability Class B	0.866	0.866	0.866
	Stability Class C	0.865	0.865	0.865
	Stability Class D	0.881	0.881	0.881
	Stability Class E	0.866	0.866	0.866
	Stability Class F	0.866	0.866	0.866
CZSIGA	Linear Coefficient for sigma-z			
	Stability Class A	0.0361	0.0361	0.0361
	Stability Class B	0.0361	0.0361	0.0361
	Stability Class C	0.2036	0.2036	0.2036
	Stability Class D	0.2636	0.2636	0.2636
	Stability Class E	0.2463	0.2463	0.2463
	Stability Class F	0.2463	0.2463	0.2463
CZSIGB	Exponential Term for sigma-z			
	Stability Class A	1.277	1.277	1.277
	Stability Class B	1.277	1.277	1.277
	Stability Class C	0.859	0.859	0.859
	Stability Class D	0.751	0.751	0.751
	Stability Class E	0.619	0.619	0.619
	Stability Class F	0.619	0.619	0.619
DISPMD	Dispersion Model Flag	LRDIST	LRDIST	LRDIST
DRYDEP	Dry Deposition Flag	Xe = .FALSE. Other Groups = .TRUE.	Xe = .FALSE. Other Groups = .TRUE.	Xe = .FALSE. Other Groups = .TRUE.
ENDAT1	Control flag indicating only ATMOS is to be run	.FALSE.	.FALSE.	.FALSE.
GRPNAM	Names of the Chemical Classes (Used by WinMACCS)			
	Chemical Class 1	Xe	Xe	Xe
	Chemical Class 2	Cs	Cs	Cs
	Chemical Class 3	Ba	Ba	Ba
	Chemical Class 4	I	I	I
	Chemical Class 5	Te	Te	Te
	Chemical Class 6	Ru	Ru	Ru
	Chemical Class 7	Mo	Mo	Mo
	Chemical Class 8	Ce	Ce	Ce
	Chemical Class 9	La	La	La
IBDSTB	Boundary Weather Stability Class Index	4	4	4
IDEBUG	Debug Switch for Extra Debugging Print	0	0	0

Variable	Description	LTSBO	STSBO with RCIC Blackstart	STSBO without RCIC Blackstart
IGROUP	Definition of Radionuclide Group Numbers	1 = Xe	1 = Xe	1 = Xe
		2 = Cs	2 = Cs	2 = Cs
		3 = Ba	3 = Ba	3 = Ba
		4 = I	4 = I	4 = I
		5 = Te	5 = Te	5 = Te
		6 = Ru	6 = Ru	6 = Ru
		7 = Mo	7 = Mo	7 = Mo
		8 = Ce	8 = Ce	8 = Ce
		9 = La	9 = La	9 = La
INWGHT	Number of Samples for Each Bin Used for Nonuniform Weather Bin Sampling			
	Bin 1	71	71	71
	Bin 2	42	42	42
	Bin 3	12	12	12
	Bin 4	52	52	52
	Bin 5	57	57	57
	Bin 6	74	74	74
	Bin 7	21	21	21
	Bin 8	12	12	12
	Bin 9	49	49	49
	Bin 10	103	103	103
	Bin 11	77	77	77
	Bin 12	35	35	35
	Bin 13	51	51	51
	Bin 14	75	75	75
	Bin 15	14	14	14
	Bin 16	4	4	4
	Bin 17	44	44	44
	Bin 18	12	12	12
	Bin 19	17	17	17
	Bin 20	24	24	24
	Bin 21	24	24	24
	Bin 22	12	12	12
	Bin 23	4	4	4
	Bin 24	8	8	8
	Bin 25	12	12	12
	Bin 26	12	12	12
	Bin 27	12	12	12
	Bin 28	1	1	1
	Bin 29	3	3	3
	Bin 30	5	5	5
	Bin 31	4	4	4
	Bin 32	12	12	12
	Bin 33	1	1	1
	Bin 34	7	7	7
	Bin 35	9	9	9
	Bin 36	12	12	12

Variable	Description	LTSBO	STSBO with RCIC Blackstart	STSBO without RCIC Blackstart
IRSEED	Seed for Random Number Generator	79	79	79
LATITU	Latitude of Power Plant	39˚ 45' 32"	39˚ 45' 32"	39˚ 45' 32"
LIMSPA	Last Interval for Measured Weather	25	25	25
LONGIT	Longitude of Power Plant	76˚ 16' 09"	76˚ 16' 09"	76˚ 16' 09"
MAXGRP	Number of Radionuclide Groups	9	9	9
MAXHGT	Flag for Mixing Height	DAY_AND_NIGHT	DAY_AND_NIGHT	DAY_AND_NIGHT
MAXRIS	Selection of Risk Dominant Plume	2	1	9
METCOD	Meteorological Sampling Option Code	2	2	2
MNDMOD	Plume Meander Model Flag	OFF	OFF	OFF
NAMSTB	List of Pseudostable Nuclides			
	Isotope 1	I-129	I-129	I-129
	Isotope 2	Xe-131m	Xe-131m	Xe-131m
	Isotope 3	Xe-133m	Xe-133m	Xe-133m
	Isotope 4	Cs-135	Cs-135	Cs-135
	Isotope 5	Sm-147	Sm-147	Sm-147
	Isotope 6	U-234	U-234	U-234
	Isotope 7	U-235	U-235	U-235
	Isotope 8	U-236	U-236	U-236
	Isotope 9	U-237	U-237	U-237
	Isotope 10	Np-237	Np-237	Np-237
	Isotope 11	Rb-87	Rb-87	Rb-87
	Isotope 12	Zr-93	Zr-93	Zr-93
	Isotope 13	Nb-93m	Nb-93m	Nb-93m
	Isotope 14	Nb-95m	Nb-95m	Nb-95m
	Isotope 15	Tc-99	Tc-99	Tc-99
	Isotope 16	Pm-147	Pm-147	Pm-147
NPSGRP	Number of Particle Size Groups	10	10	10
NRINTN	Number of Rain Intensity Breakpoints	3	3	3
NRNINT	Number of Rain Distance Intervals	5	5	5
NSBINS	Number of Weather Bins to Sample	36	36	36
NUCNAM	Radionuclide Names	See Appendix A	See Appendix A	See Appendix A
NUCOUT	Radionuclide Used in Dispersion Print	Cs-137	Cs-137	Cs-137
NUMCOR	Number of Compass Sectors in the Grid	64	64	64
NUMISO	Number of Radionuclides	69	69	69
NUMRAD	Number of Radial Spatial Intervals	26	26	26
NUMREL	Number of Released Plume Segments	29	33	86

Variable	Description	LTSBO	STSBO with RCIC Blackstart	STSBO without RCIC Blackstart
NUMSTB	Number of Defined Pseudostable Radionuclides	16	16	16
OALARM	Time to Reach General Emergency Conditions	0	0	0
PDELAY	Plume Release Times	MELMACCS Data (See Table B-2)	MELMACCS Data (See Table B-2)	MELMACCS Data (See Table B-2)
PLHEAT	Plume Heat Contents	MELMACCS Data (See Table B-2)	MELMACCS Data (See Table B-2)	MELMACCS Data (See Table B-2)
PLHITE	Plume Release Heights	MELMACCS Data (See Table B-2)	MELMACCS Data (See Table B-2)	MELMACCS Data (See Table B-2)
PLMDEN	Plume Mass Density	MELMACCS Data (See Table A.2-2)	MELMACCS Data (See Table A.2-2)	MELMACCS Data (See Table A.2-2)
PLMFLA	Plume Mass Flow Rate	MELMACCS Data (See Table B-2)	MELMACCS Data (See Table B-2)	MELMACCS Data (See Table B-2)
PLMMOD	Flag for Plume Rise Input Option	DENSITY	DENSITY	DENSITY
PLUDUR	Plume Segment Durations	MELMACCS Data (See Table B-2)	MELMACCS Data (See Table B-2)	MELMACCS Data (See Table B-2)
PSDIST	Particle Size Distribution by Group	MELMACCS Data (See Table B-3)	MELMACCS Data (See Table B-3)	MELMACCS Data (See Table B-3)
REFTIM	Plume Reference Time Point	0. for first 0.5 for subsequent	0. for first 0.5 for subsequent	0. for first 0.5 for subsequent
RELFRC	Release Fractions of the Source Term	MELMACCS Data (See Table B-4)	MELMACCS Data (See Table B-4)	MELMACCS Data (See Table B-4)
RNDSTS	Endpoints of Rain Distance Intervals			
	Interval 1	3.22	3.22	3.22
	Interval 2	5.63	5.63	5.63
	Interval 3	11.27	11.27	11.27
	Interval 4	20.92	20.92	20.92
	Interval 5	32.19	32.19	32.19
RNRATE	Rain Intensity Breakpoints for Weather Binning			
	Intensity 1	2	2	2
	Intensity 2	4	4	4
	Intensity 3	6	6	6
SCLADP	Scaling Factor for A-D Plume Rise	1.0	1.0	1.0
SCLCRW	Scaling Factor for Critical Wind Speed	1.0	1.0	1.0
SCLEFP	Scaling Factor for E-F Plume Rise	1.0	1.0	1.0
SIGYINIT	Initial Sigma-y for All Plume Segments	11.6	11.6	11.6
SIGYINIT	Initial Sigma-z for All Plume Segments	23.3	23.3	23.3
SPAEND	Radial distances for grid boundaries			
	Ring 1	0.16	0.16	0.16
	Ring 2	0.52	0.52	0.52

Variable	Description	LTSBO	STSBO with RCIC Blackstart	STSBO without RCIC Blackstart
SPAEND	Ring 3	1.21	1.21	1.21
	Ring 4	1.61	1.61	1.61
	Ring 5	2.13	2.13	2.13
	Ring 6	3.22	3.22	3.22
	Ring 7	4.02	4.02	4.02
	Ring 8	4.83	4.83	4.83
	Ring 9	5.63	5.63	5.63
	Ring 10	8.05	8.05	8.05
	Ring 11	11.27	11.27	11.27
	Ring 12	16.09	16.09	16.09
	Ring 13	20.92	20.92	20.92
	Ring 14	25.75	25.75	25.75
	Ring 15	32.19	32.19	32.19
	Ring 16	40.23	40.23	40.23
	Ring 17	48.28	48.28	48.28
	Ring 18	64.37	64.37	64.37
	Ring 19	80.47	80.47	80.47
	Ring 20	112.65	112.65	112.65
	Ring 21	160.93	160.93	160.93
	Ring 22	241.14	241.14	241.14
	Ring 23	321.87	321.87	321.87
	Ring 24	563.27	563.27	563.27
	Ring 25	804.67	804.67	804.67
	Ring 26	1609.34	1609.34	1609.34
TIMBAS	Time Base for Plume Expansion Factor	600	600	600
VDEPOS	Dry Deposition Velocities			
	Aerosol Bin 1	5.35E-04	5.35E-04	5.35E-04
	Aerosol Bin 2	4.91E-04	4.91E-04	4.91E-04
	Aerosol Bin 3	6.43E-04	6.43E-04	6.43E-04
	Aerosol Bin 4	1.08E-03	1.08E-03	1.08E-03
	Aerosol Bin 5	2.12E-03	2.12E-03	2.12E-03
	Aerosol Bin 6	4.34E-03	4.34E-03	4.34E-03
	Aerosol Bin 7	8.37E-03	8.37E-03	8.37E-03
	Aerosol Bin 8	1.37E-02	1.37E-02	1.37E-02
	Aerosol Bin 9	1.70E-02	1.70E-02	1.70E-02
	Aerosol Bin 10	1.70E-02	1.70E-02	1.70E-02
WETDEP	Wet Deposition Flag	Xe = .FALSE. Other groups = .TRUE.	Xe = .FALSE. Other groups = .TRUE.	Xe = .FALSE. Other groups = .TRUE.
XPFAC1	Base Time for Meander Expansion Factor	0.2	0.2	0.2
XPFAC2	Breakpoint for Expansion Factor Model	0.25	0.25	0.25
YSCALE	Scale Factor for Horizontal Dispersion	1	1	1
ZSCALE	Scale Factor for Vertical Dispersion	1.27	1.27	1.27

Table B-2 Plume Parameters Used in the Peach Bottom Unmitigated LTSBO and STSBO with and without RCIC Blackstart scenarios

Peach Bottom LTSBO					
Plume Segment	**PDELAY**	**PLHITE**	**PLMDEN**	**PLMFLA**	**PLUDUR**
1	7.20E+04	3.96E+01	9.28E-01	1.46E+02	3.60E+03
2	7.22E+04	4.00E+00	5.44E-01	6.87E+00	3.66E+03
3	7.56E+04	3.96E+01	9.84E-01	1.40E+02	3.60E+03
4	7.92E+04	3.96E+01	9.96E-01	1.35E+02	3.60E+03
5	8.28E+04	3.96E+01	1.01E+00	1.29E+02	3.74E+03
6	8.66E+04	3.96E+01	1.03E+00	1.20E+02	3.60E+03
7	9.02E+04	3.96E+01	1.04E+00	1.14E+02	3.60E+03
8	9.38E+04	3.96E+01	1.06E+00	1.08E+02	3.60E+03
9	9.74E+04	3.96E+01	1.06E+00	1.03E+02	3.60E+03
10	1.01E+05	3.96E+01	1.07E+00	9.96E+01	3.60E+03
11	1.05E+05	3.96E+01	1.08E+00	9.63E+01	3.60E+03
12	1.08E+05	3.96E+01	1.08E+00	9.42E+01	3.60E+03
13	1.12E+05	3.96E+01	1.08E+00	9.32E+01	3.60E+03
14	1.15E+05	3.96E+01	1.08E+00	9.20E+01	3.60E+03
15	1.19E+05	3.96E+01	1.09E+00	9.10E+01	3.60E+03
16	1.23E+05	3.96E+01	1.09E+00	9.01E+01	3.60E+03
17	1.26E+05	3.96E+01	1.09E+00	8.95E+01	3.60E+03
18	1.30E+05	3.96E+01	1.09E+00	8.90E+01	3.60E+03
19	1.33E+05	3.96E+01	1.09E+00	8.86E+01	3.60E+03
20	1.37E+05	3.96E+01	1.09E+00	8.83E+01	3.60E+03
21	1.41E+05	3.96E+01	1.09E+00	8.81E+01	3.60E+03
22	1.44E+05	3.96E+01	1.09E+00	8.79E+01	3.60E+03
23	1.48E+05	3.96E+01	1.09E+00	8.79E+01	3.60E+03
24	1.51E+05	3.96E+01	1.09E+00	8.78E+01	3.60E+03
25	1.55E+05	3.96E+01	1.09E+00	8.77E+01	3.60E+03
26	1.59E+05	3.96E+01	1.09E+00	8.76E+01	3.60E+03
27	1.62E+05	3.96E+01	1.09E+00	8.75E+01	3.60E+03
28	1.66E+05	3.96E+01	1.09E+00	8.74E+01	3.60E+03
29	1.69E+05	3.96E+01	1.09E+00	8.73E+01	3.42E+03

Peach Bottom STSBO with RCIC Blackstart					
Plume Segment	PDELAY	PLHITE	PLMDEN	PLMFLA	PLUDUR
1	6.09E+04	3.96E+01	9.42E-01	1.40E+02	3.60E+03
2	6.09E+04	4.00E+00	6.17E-01	6.61E+00	3.60E+03
3	6.45E+04	3.96E+01	1.01E+00	1.29E+02	3.60E+03
4	6.81E+04	3.96E+01	1.02E+00	1.27E+02	3.60E+03
5	7.17E+04	3.96E+01	1.03E+00	1.22E+02	3.63E+03
6	7.54E+04	3.96E+01	1.04E+00	1.17E+02	3.60E+03
7	7.90E+04	3.96E+01	1.05E+00	1.11E+02	3.60E+03
8	8.26E+04	3.96E+01	1.06E+00	1.06E+02	3.60E+03
9	8.62E+04	3.96E+01	1.07E+00	1.03E+02	3.60E+03
10	8.98E+04	3.96E+01	1.07E+00	9.92E+01	3.60E+03
11	9.34E+04	3.96E+01	1.08E+00	9.64E+01	3.60E+03
12	9.70E+04	3.96E+01	1.08E+00	9.43E+01	3.60E+03
13	1.01E+05	3.96E+01	1.08E+00	9.29E+01	3.60E+03
14	1.04E+05	3.96E+01	1.08E+00	9.18E+01	3.60E+03
15	1.08E+05	3.96E+01	1.09E+00	9.09E+01	3.60E+03
16	1.11E+05	3.96E+01	1.09E+00	9.02E+01	3.60E+03
17	1.15E+05	3.96E+01	1.09E+00	9.09E+01	3.60E+03
18	1.19E+05	3.96E+01	1.09E+00	9.11E+01	3.60E+03
19	1.22E+05	3.96E+01	1.09E+00	8.92E+01	3.60E+03
20	1.26E+05	3.96E+01	1.09E+00	8.90E+01	3.60E+03
21	1.29E+05	3.96E+01	1.09E+00	8.87E+01	3.60E+03
22	1.33E+05	3.96E+01	1.09E+00	8.85E+01	3.60E+03
23	1.37E+05	3.96E+01	1.09E+00	8.84E+01	3.60E+03
24	1.40E+05	3.96E+01	1.09E+00	8.83E+01	3.60E+03
25	1.44E+05	3.96E+01	1.09E+00	8.82E+01	3.60E+03
26	1.47E+05	3.96E+01	1.09E+00	8.81E+01	3.60E+03
27	1.51E+05	3.96E+01	1.09E+00	8.80E+01	3.60E+03
28	1.55E+05	3.96E+01	1.09E+00	8.80E+01	3.60E+03
29	1.58E+05	3.96E+01	1.09E+00	8.78E+01	3.60E+03
30	1.62E+05	3.96E+01	1.09E+00	8.78E+01	3.60E+03
31	1.65E+05	3.96E+01	1.09E+00	8.77E+01	3.60E+03
32	1.69E+05	3.96E+01	1.09E+00	8.76E+01	3.60E+03
33	1.73E+05	3.96E+01	1.09E+00	6.56E+01	2.40E+02

Peach Bottom STSBO without RCIC Blackstart					
Plume Segment	PDELAY	PLHITE	PLMDEN	PLMFLA	PLUDUR
1	2.93E+04	1.75E+01	1.11E+00	1.94E+00	3.60E+03
2	3.05E+04	3.96E+01	6.64E-01	4.02E+01	3.60E+03
3	3.05E+04	4.00E+00	6.43E-01	2.17E+01	3.60E+03
4	3.12E+04	3.96E+01	9.81E-01	1.44E+02	3.66E+03
5	3.41E+04	4.00E+00	5.24E-01	8.34E+00	3.62E+03
6	3.48E+04	3.96E+01	1.05E+00	1.18E+02	3.56E+03
7	3.77E+04	4.00E+00	5.49E-01	3.85E+00	3.60E+03
8	3.84E+04	3.96E+01	1.07E+00	1.04E+02	3.60E+03
9	4.01E+04	1.75E+01	1.11E+00	1.75E+00	3.60E+03
10	4.13E+04	4.00E+00	4.72E-01	2.65E+00	3.60E+03
11	4.20E+04	3.96E+01	1.09E+00	9.13E+01	3.60E+03
12	4.37E+04	1.75E+01	1.11E+00	3.34E+00	3.60E+03
13	4.56E+04	3.96E+01	1.11E+00	8.39E+01	3.60E+03
14	4.73E+04	1.75E+01	1.11E+00	3.59E+00	3.60E+03
15	4.92E+04	3.96E+01	1.11E+00	8.17E+01	3.60E+03
16	5.09E+04	1.75E+01	1.11E+00	3.58E+00	3.60E+03
17	5.28E+04	3.96E+01	1.11E+00	8.04E+01	3.60E+03
18	5.45E+04	1.75E+01	1.11E+00	3.51E+00	3.60E+03
19	5.64E+04	3.96E+01	1.12E+00	7.92E+01	3.60E+03
20	5.81E+04	1.75E+01	1.11E+00	3.41E+00	3.60E+03
21	6.00E+04	3.96E+01	1.12E+00	7.82E+01	3.60E+03
22	6.17E+04	1.75E+01	1.12E+00	3.31E+00	3.60E+03
23	6.36E+04	3.96E+01	1.12E+00	7.75E+01	3.60E+03
24	6.53E+04	1.75E+01	1.12E+00	3.21E+00	3.60E+03
25	6.72E+04	3.96E+01	1.12E+00	7.73E+01	3.60E+03
26	6.89E+04	1.75E+01	1.12E+00	3.14E+00	3.63E+03
27	7.08E+04	3.96E+01	1.12E+00	7.77E+01	3.60E+03
28	7.25E+04	1.75E+01	1.12E+00	3.16E+00	3.60E+03
29	7.44E+04	3.96E+01	1.12E+00	7.77E+01	3.60E+03
30	7.61E+04	1.75E+01	1.12E+00	3.22E+00	3.60E+03
31	7.80E+04	3.96E+01	1.12E+00	7.90E+01	3.60E+03
32	7.97E+04	1.75E+01	1.11E+00	3.35E+00	3.60E+03
33	8.16E+04	3.96E+01	1.11E+00	8.60E+01	3.60E+03
34	8.33E+04	1.75E+01	1.11E+00	3.81E+00	3.60E+03
35	8.52E+04	3.96E+01	1.11E+00	8.83E+01	3.72E+03
36	8.69E+04	1.75E+01	1.10E+00	4.19E+00	3.60E+03
37	8.82E+04	3.96E+01	1.11E+00	5.96E-01	3.60E+03
38	8.89E+04	3.96E+01	1.11E+00	8.60E+01	3.60E+03
39	9.05E+04	1.75E+01	1.09E+00	4.47E+00	3.60E+03
40	9.18E+04	3.96E+01	1.11E+00	5.99E-01	3.60E+03
41	9.25E+04	3.96E+01	1.11E+00	8.72E+01	3.60E+03
42	9.41E+04	1.75E+01	1.09E+00	4.68E+00	3.60E+03
43	9.54E+04	3.96E+01	1.11E+00	6.12E-01	3.60E+03

Peach Bottom STSBO without RCIC Blackstart					
Plume Segment	PDELAY	PLHITE	PLMDEN	PLMFLA	PLUDUR
44	9.61E+04	3.96E+01	1.11E+00	8.79E+01	3.60E+03
45	9.77E+04	1.75E+01	1.08E+00	4.89E+00	3.60E+03
46	9.97E+04	3.96E+01	1.11E+00	8.85E+01	3.60E+03
47	1.01E+05	1.75E+01	1.08E+00	5.05E+00	3.60E+03
48	1.03E+05	3.96E+01	1.10E+00	8.89E+01	3.60E+03
49	1.05E+05	1.75E+01	1.08E+00	5.18E+00	3.60E+03
50	1.07E+05	3.96E+01	1.10E+00	8.93E+01	3.60E+03
51	1.09E+05	1.75E+01	1.07E+00	5.28E+00	3.60E+03
52	1.11E+05	3.96E+01	1.10E+00	8.95E+01	3.60E+03
53	1.12E+05	1.75E+01	1.07E+00	5.34E+00	3.60E+03
54	1.14E+05	3.96E+01	1.10E+00	8.97E+01	3.60E+03
55	1.16E+05	1.75E+01	1.07E+00	5.39E+00	3.60E+03
56	1.18E+05	3.96E+01	1.10E+00	8.99E+01	3.60E+03
57	1.19E+05	1.75E+01	1.07E+00	5.44E+00	3.60E+03
58	1.21E+05	3.96E+01	1.10E+00	9.00E+01	3.60E+03
59	1.23E+05	1.75E+01	1.07E+00	5.47E+00	3.60E+03
60	1.25E+05	3.96E+01	1.10E+00	9.01E+01	3.60E+03
61	1.27E+05	1.75E+01	1.07E+00	5.50E+00	3.60E+03
62	1.29E+05	3.96E+01	1.10E+00	9.02E+01	3.60E+03
63	1.30E+05	1.75E+01	1.07E+00	5.53E+00	3.60E+03
64	1.32E+05	3.96E+01	1.10E+00	9.01E+01	3.60E+03
65	1.34E+05	1.75E+01	1.06E+00	5.56E+00	3.60E+03
66	1.36E+05	3.96E+01	1.10E+00	9.02E+01	3.60E+03
67	1.37E+05	1.75E+01	1.06E+00	5.57E+00	3.60E+03
68	1.39E+05	3.96E+01	1.10E+00	9.03E+01	3.60E+03
69	1.41E+05	1.75E+01	1.06E+00	5.59E+00	3.60E+03
70	1.43E+05	3.96E+01	1.10E+00	9.03E+01	3.60E+03
71	1.45E+05	1.75E+01	1.06E+00	5.60E+00	3.60E+03
72	1.47E+05	3.96E+01	1.10E+00	9.03E+01	3.60E+03
73	1.48E+05	1.75E+01	1.06E+00	5.62E+00	3.60E+03
74	1.50E+05	3.96E+01	1.10E+00	9.03E+01	3.60E+03
75	1.52E+05	1.75E+01	1.06E+00	5.63E+00	3.60E+03
76	1.54E+05	3.96E+01	1.10E+00	9.03E+01	3.60E+03
77	1.55E+05	1.75E+01	1.06E+00	5.64E+00	3.60E+03
78	1.57E+05	3.96E+01	1.10E+00	9.02E+01	3.60E+03
79	1.59E+05	1.75E+01	1.06E+00	5.65E+00	3.60E+03
80	1.61E+05	3.96E+01	1.10E+00	9.02E+01	3.60E+03
81	1.63E+05	1.75E+01	1.06E+00	5.66E+00	3.60E+03
82	1.65E+05	3.96E+01	1.10E+00	9.01E+01	3.60E+03
83	1.66E+05	1.75E+01	1.06E+00	5.68E+00	3.60E+03
84	1.68E+05	3.96E+01	1.10E+00	9.00E+01	3.60E+03
85	1.70E+05	1.75E+01	1.06E+00	5.68E+00	3.06E+03
86	1.72E+05	3.96E+01	1.10E+00	8.98E+01	1.08E+03

Table B-3 Plume Parameters Used in the Peach Bottom Unmitigated LTSBO and STSBO with and without RCIC Blackstart scenarios

Peach Bottom LTSBO										
Class	**Bin 1**	**Bin 2**	**Bin 3**	**Bin 4**	**Bin 5**	**Bin 6**	**Bin 7**	**Bin 8**	**Bin 9**	**Bin 10**
Xe	0.1000	0.1000	0.1000	0.1000	0.1000	0.1000	0.1000	0.1000	0.1000	0.1000
Cs	0.1171	0.1602	0.3303	0.3061	0.0575	0.0180	0.0071	0.0025	0.0009	0.0004
Ba	0.0412	0.2230	0.4450	0.2275	0.0486	0.0111	0.0030	0.0005	0.0001	0.0001
I	0.0231	0.1503	0.5219	0.2579	0.0333	0.0102	0.0027	0.0005	0.0001	0.0000
Te	0.0286	0.1370	0.4603	0.2779	0.0643	0.0249	0.0059	0.0009	0.0002	0.0001
Ru	0.0393	0.1512	0.3597	0.2682	0.1214	0.0484	0.0104	0.0011	0.0002	0.0001
Mo	0.1553	0.1638	0.2563	0.3259	0.0649	0.0202	0.0087	0.0033	0.0012	0.0005
Ce	0.0306	0.1930	0.4357	0.2427	0.0708	0.0218	0.0047	0.0005	0.0001	0.0001
La	0.0235	0.1473	0.3990	0.2664	0.1109	0.0433	0.0089	0.0007	0.0000	0.0000

Peach Bottom STSBO with RCIC Blackstart										
Class	**Bin 1**	**Bin 2**	**Bin 3**	**Bin 4**	**Bin 5**	**Bin 6**	**Bin 7**	**Bin 8**	**Bin 9**	**Bin 10**
Xe	0.1000	0.1000	0.1000	0.1000	0.1000	0.1000	0.1000	0.1000	0.1000	0.1000
Cs	0.1704	0.1914	0.2388	0.2874	0.0796	0.0169	0.0094	0.0039	0.0017	0.0005
Ba	0.0303	0.1751	0.4211	0.3035	0.0581	0.0084	0.0023	0.0008	0.0003	0.0001
I	0.0322	0.1958	0.4343	0.2527	0.0634	0.0164	0.0040	0.0008	0.0003	0.0001
Te	0.0499	0.1770	0.3605	0.2675	0.0987	0.0353	0.0088	0.0016	0.0005	0.0001
Ru	0.0501	0.1443	0.2997	0.3035	0.1406	0.0480	0.0114	0.0017	0.0005	0.0001
Mo	0.2081	0.1901	0.1871	0.2966	0.0834	0.0167	0.0108	0.0047	0.0021	0.0006
Ce	0.0188	0.1393	0.4164	0.3264	0.0786	0.0164	0.0034	0.0005	0.0001	0.0001
La	0.0218	0.1333	0.3404	0.3148	0.1352	0.0442	0.0093	0.0008	0.0001	0.0000

Peach Bottom STSBO without RCIC Blackstart										
Class	**Bin 1**	**Bin 2**	**Bin 3**	**Bin 4**	**Bin 5**	**Bin 6**	**Bin 7**	**Bin 8**	**Bin 9**	**Bin 10**
Xe	0.1000	0.1000	0.1000	0.1000	0.1000	0.1000	0.1000	0.1000	0.1000	0.1000
Cs	0.0288	0.2922	0.2076	0.2174	0.1847	0.0587	0.0089	0.0012	0.0002	0.0003
Ba	0.0178	0.0546	0.1120	0.3364	0.3641	0.0994	0.0135	0.0018	0.0002	0.0001
I	0.0282	0.5160	0.2181	0.1261	0.0864	0.0217	0.0023	0.0003	0.0003	0.0006
Te	0.0393	0.3360	0.2596	0.2010	0.1225	0.0376	0.0034	0.0004	0.0001	0.0001
Ru	0.0323	0.0946	0.1503	0.2915	0.2935	0.1127	0.0209	0.0036	0.0005	0.0003
Mo	0.0300	0.1217	0.1995	0.2859	0.2584	0.0880	0.0141	0.0020	0.0002	0.0002
Ce	0.0219	0.0558	0.1024	0.3281	0.3666	0.1076	0.0151	0.0021	0.0002	0.0002
La	0.0203	0.0724	0.1218	0.3231	0.3501	0.0976	0.0127	0.0016	0.0002	0.0002

.

Table B-4 Release Fraction Parameters Used in the Peach Bottom Unmitigated LTSBO and STSBO with and without RCIC Blackstart Scenarios

Peach Bottom LTSBO									
Plume Segment	**Xe**	**Cs**	**Ba**	**I**	**Te**	**Ru**	**Mo**	**Ce**	**La**
1	8.75E-01	2.32E-03	1.17E-03	1.65E-03	1.73E-03	1.31E-06	6.39E-04	1.32E-05	1.91E-06
2	7.93E-02	3.29E-04	2.01E-05	4.99E-05	1.27E-04	9.46E-08	9.48E-05	1.85E-07	2.79E-08
3	1.71E-02	2.47E-04	3.24E-03	2.27E-03	4.00E-04	7.92E-07	2.52E-05	4.90E-05	3.49E-06
4	3.23E-03	1.39E-04	5.75E-04	1.10E-03	3.01E-04	7.10E-07	1.65E-05	1.01E-05	2.83E-06
5	7.40E-04	4.24E-04	1.48E-04	6.08E-03	7.48E-03	4.11E-07	7.67E-06	3.23E-06	2.40E-06
6	9.39E-04	2.61E-04	1.15E-04	3.64E-03	1.76E-03	4.13E-07	6.80E-06	2.46E-06	2.05E-06
7	6.99E-04	1.06E-04	7.24E-05	1.22E-03	2.99E-03	4.31E-07	6.98E-06	2.13E-06	1.95E-06
8	2.97E-04	6.06E-05	6.33E-05	5.46E-04	7.42E-04	4.12E-07	6.36E-06	1.74E-06	1.64E-06
9	1.39E-04	8.02E-05	2.80E-05	8.82E-04	3.63E-04	4.13E-07	5.89E-06	1.23E-06	1.18E-06
10	8.46E-05	7.28E-05	2.15E-05	8.05E-04	4.03E-04	4.21E-07	5.29E-06	1.71E-06	1.69E-06
11	5.97E-05	5.33E-05	1.02E-05	5.08E-04	2.82E-04	4.19E-07	5.07E-06	1.65E-06	1.63E-06
12	4.96E-05	3.33E-05	4.59E-06	1.56E-04	2.06E-04	4.11E-07	5.63E-06	1.57E-06	1.55E-06
13	4.42E-05	3.02E-05	5.34E-06	9.41E-05	2.47E-04	4.01E-07	6.04E-06	1.45E-06	1.44E-06
14	3.96E-05	2.74E-05	1.36E-05	7.53E-05	3.13E-04	3.94E-07	5.77E-06	1.35E-06	1.34E-06
15	3.59E-05	2.63E-05	2.23E-05	6.53E-05	4.07E-04	3.84E-07	5.62E-06	1.26E-06	1.25E-06
16	3.34E-05	2.66E-05	5.12E-06	6.08E-05	3.28E-04	3.78E-07	5.74E-06	1.19E-06	1.18E-06
17	3.06E-05	2.76E-05	4.04E-06	6.02E-05	3.34E-04	3.70E-07	5.98E-06	1.12E-06	1.11E-06
18	2.93E-05	2.85E-05	4.33E-06	5.94E-05	3.93E-04	3.62E-07	6.36E-06	1.05E-06	1.04E-06
19	2.71E-05	3.00E-05	4.34E-06	6.02E-05	3.89E-04	3.53E-07	6.84E-06	9.87E-07	9.83E-07
20	2.55E-05	3.23E-05	8.15E-06	6.31E-05	2.78E-04	3.44E-07	7.41E-06	9.35E-07	9.31E-07
21	2.27E-05	3.47E-05	1.38E-05	6.71E-05	2.68E-04	3.35E-07	8.10E-06	8.90E-07	8.86E-07
22	2.11E-05	3.65E-05	5.32E-06	7.33E-05	2.96E-04	3.07E-07	8.54E-06	8.51E-07	8.47E-07
23	2.05E-05	4.15E-05	5.60E-06	8.51E-05	3.42E-04	3.09E-07	9.73E-06	8.15E-07	8.12E-07
24	1.95E-05	4.67E-05	5.86E-06	1.02E-04	3.42E-04	3.06E-07	1.09E-05	7.82E-07	7.78E-07
25	1.86E-05	5.16E-05	6.03E-06	1.27E-04	3.43E-04	2.99E-07	1.18E-05	7.53E-07	7.50E-07
26	1.82E-05	5.72E-05	6.11E-06	1.61E-04	3.53E-04	2.92E-07	1.28E-05	7.26E-07	7.23E-07
27	1.74E-05	6.10E-05	6.32E-06	2.05E-04	3.79E-04	2.86E-07	1.31E-05	6.99E-07	6.96E-07
28	1.67E-05	3.25E-05	6.38E-06	1.11E-04	3.51E-04	2.79E-07	6.72E-06	6.75E-07	6.72E-07
29	1.54E-05	2.55E-05	6.04E-06	7.60E-05	1.98E-04	2.59E-07	5.37E-06	6.19E-07	6.16E-07

Peach Bottom STSBO with RCIC Blackstart									
Plume Segment	Xe	Cs	Ba	I	Te	Ru	Mo	Ce	La
1	8.60E-01	2.42E-03	1.66E-03	1.90E-03	2.29E-03	1.20E-06	6.56E-04	1.68E-05	2.13E-06
2	8.85E-02	4.22E-04	3.99E-05	7.02E-05	2.09E-04	1.32E-07	1.20E-04	2.40E-07	3.26E-08
3	2.02E-02	2.15E-04	4.28E-03	2.29E-03	8.33E-04	4.01E-07	1.76E-05	7.56E-05	3.61E-06
4	5.32E-03	1.02E-04	5.37E-04	1.07E-03	3.48E-04	3.81E-07	7.97E-06	1.00E-05	2.41E-06
5	1.51E-03	6.39E-05	8.13E-05	6.60E-04	2.14E-04	3.61E-07	5.06E-06	3.33E-06	2.45E-06
6	8.70E-04	1.26E-04	4.44E-05	1.75E-03	1.75E-03	2.84E-07	3.25E-06	2.42E-06	2.15E-06
7	8.32E-04	7.58E-05	5.18E-05	1.05E-03	7.84E-04	2.15E-07	2.03E-06	2.14E-06	1.90E-06
8	4.41E-04	1.04E-04	4.80E-05	1.50E-03	6.51E-04	2.40E-07	1.70E-06	1.28E-06	1.16E-06
9	2.13E-04	4.35E-05	5.05E-05	5.72E-04	1.71E-03	2.57E-07	1.61E-06	1.80E-06	1.75E-06
10	1.20E-04	2.69E-05	5.92E-05	3.06E-04	7.49E-04	2.65E-07	1.71E-06	1.71E-06	1.68E-06
11	7.74E-05	1.51E-05	2.86E-05	9.63E-05	2.02E-04	2.67E-07	2.06E-06	1.61E-06	1.60E-06
12	4.05E-05	1.61E-05	3.02E-05	7.74E-05	1.96E-04	2.66E-07	2.56E-06	1.51E-06	1.50E-06
13	4.17E-05	1.40E-05	2.40E-05	6.22E-05	2.37E-04	2.62E-07	2.53E-06	1.40E-06	1.39E-06
14	5.76E-05	1.33E-05	3.86E-05	5.33E-05	3.01E-04	2.59E-07	2.49E-06	1.31E-06	1.30E-06
15	5.39E-05	1.29E-05	5.58E-05	4.97E-05	3.54E-04	2.56E-07	2.42E-06	1.23E-06	1.22E-06
16	4.91E-05	1.31E-05	1.47E-05	4.81E-05	2.81E-04	2.49E-07	2.49E-06	1.16E-06	1.15E-06
17	4.75E-05	4.58E-05	5.74E-05	3.28E-04	9.72E-04	3.29E-07	6.42E-06	1.09E-06	1.08E-06
18	4.05E-05	2.05E-05	1.58E-05	1.52E-04	5.36E-04	2.12E-07	2.83E-06	1.02E-06	1.01E-06
19	3.79E-05	1.84E-05	6.90E-06	1.27E-04	2.59E-04	2.10E-07	2.71E-06	9.75E-07	9.68E-07
20	3.53E-05	1.56E-05	7.82E-06	6.08E-05	2.72E-04	2.05E-07	3.13E-06	9.28E-07	9.22E-07
21	3.25E-05	1.68E-05	8.97E-06	5.73E-05	1.65E-04	1.88E-07	3.55E-06	8.86E-07	8.80E-07
22	2.99E-05	1.87E-05	7.47E-06	6.39E-05	1.64E-04	1.71E-07	3.99E-06	8.47E-07	8.41E-07
23	2.83E-05	2.15E-05	4.55E-06	7.57E-05	1.81E-04	1.69E-07	4.60E-06	8.11E-07	8.06E-07
24	2.66E-05	2.48E-05	4.35E-06	9.32E-05	2.02E-04	1.65E-07	5.26E-06	7.80E-07	7.75E-07
25	2.49E-05	2.88E-05	4.28E-06	1.17E-04	2.28E-04	1.61E-07	5.96E-06	7.50E-07	7.46E-07
26	2.35E-05	3.33E-05	4.23E-06	1.50E-04	2.59E-04	1.57E-07	6.64E-06	7.22E-07	7.18E-07
27	2.22E-05	3.17E-05	4.17E-06	8.83E-05	2.95E-04	1.54E-07	7.34E-06	6.96E-07	6.92E-07
28	2.09E-05	3.06E-05	4.11E-06	6.29E-05	1.87E-04	1.50E-07	7.47E-06	6.70E-07	6.66E-07
29	1.96E-05	2.42E-05	4.06E-06	7.08E-05	1.19E-04	1.45E-07	5.43E-06	6.45E-07	6.42E-07
30	1.85E-05	2.15E-05	4.01E-06	8.06E-05	1.19E-04	1.42E-07	4.46E-06	6.24E-07	6.21E-07
31	1.76E-05	1.40E-05	3.96E-06	9.33E-05	1.21E-04	1.39E-07	2.02E-06	6.03E-07	6.00E-07
32	1.66E-05	1.50E-05	3.92E-06	1.09E-04	1.22E-04	1.36E-07	2.04E-06	5.83E-07	5.80E-07
33	1.01E-06	1.06E-06	2.59E-07	7.85E-06	8.25E-06	9.00E-09	1.39E-07	3.82E-08	3.80E-08

Peach Bottom STSBO without RCIC Blackstart									
Plume Segment	Xe	Cs	Ba	I	Te	Ru	Mo	Ce	La
1	1.13E-03	5.67E-06	9.10E-05	1.11E-05	9.18E-06	4.79E-09	1.41E-06	8.74E-06	1.16E-07
2	5.21E-01	2.40E-03	2.98E-02	3.75E-03	3.58E-03	2.58E-06	6.15E-04	2.95E-03	3.72E-05
3	7.48E-02	3.61E-04	1.09E-02	1.29E-03	9.89E-04	2.26E-07	7.37E-05	8.41E-04	1.41E-05
4	1.98E-01	8.81E-04	3.80E-02	4.19E-03	3.15E-03	3.02E-07	1.49E-04	2.66E-03	4.90E-05
5	3.70E-03	8.13E-05	1.69E-04	2.12E-04	2.11E-04	8.78E-09	1.58E-05	7.26E-06	4.70E-07
6	2.01E-02	3.61E-04	1.18E-03	8.66E-04	8.98E-04	5.36E-08	7.27E-05	6.02E-05	2.34E-06
7	1.16E-03	5.96E-05	5.39E-04	1.03E-04	7.69E-05	3.28E-09	1.33E-05	2.25E-06	1.84E-07
8	1.08E-02	4.65E-04	3.59E-03	6.22E-04	3.91E-04	3.09E-08	1.09E-04	3.11E-05	1.48E-06
9	1.12E-03	7.34E-06	1.01E-04	1.63E-05	1.36E-05	3.48E-09	1.66E-06	7.42E-06	1.20E-07
10	5.67E-04	3.23E-05	6.83E-05	1.24E-05	3.72E-05	1.82E-09	8.03E-06	1.37E-06	1.05E-07
11	6.67E-03	2.46E-04	5.78E-04	1.27E-04	4.14E-04	1.88E-08	5.93E-05	1.84E-05	9.53E-07
12	1.95E-03	1.55E-05	1.70E-04	2.80E-05	2.78E-05	5.78E-09	3.57E-06	1.20E-05	2.05E-07
13	5.32E-03	2.57E-04	8.56E-04	2.24E-04	1.99E-04	1.34E-08	5.84E-05	1.05E-05	8.08E-07
14	1.95E-03	1.91E-05	1.71E-04	3.02E-05	2.88E-05	5.45E-09	4.37E-06	1.10E-05	2.00E-07
15	5.01E-03	2.81E-04	1.58E-03	4.31E-04	1.25E-04	1.07E-08	6.18E-05	8.28E-06	8.70E-07
16	1.81E-03	2.17E-05	1.76E-04	3.38E-05	2.65E-05	4.75E-09	4.92E-06	9.33E-06	1.85E-07
17	4.78E-03	2.98E-04	1.18E-03	4.10E-04	1.11E-04	9.07E-09	6.94E-05	7.01E-06	1.12E-06
18	1.66E-03	2.39E-05	1.65E-04	3.66E-05	2.39E-05	4.07E-09	5.45E-06	7.79E-06	1.75E-07
19	4.60E-03	3.20E-04	4.99E-04	5.76E-04	1.05E-04	7.47E-09	7.33E-05	5.77E-06	1.05E-06
20	1.51E-03	2.55E-05	1.45E-04	4.10E-05	2.16E-05	3.46E-09	5.82E-06	6.46E-06	1.63E-07
21	4.40E-03	2.53E-04	7.84E-04	5.51E-04	1.00E-04	6.58E-09	5.32E-05	4.84E-06	9.73E-07
22	1.38E-03	2.56E-05	1.34E-04	4.37E-05	1.95E-05	2.95E-09	5.76E-06	5.36E-06	1.51E-07
23	4.23E-03	2.36E-04	1.13E-03	3.10E-04	9.64E-05	5.95E-09	5.24E-05	4.13E-06	9.16E-07
24	1.26E-03	2.51E-05	1.30E-04	4.04E-05	1.77E-05	2.51E-09	5.66E-06	4.45E-06	1.40E-07
25	4.11E-03	2.21E-04	6.95E-04	4.65E-05	1.03E-04	5.46E-09	5.58E-05	3.58E-06	8.67E-07
26	1.17E-03	2.47E-05	1.17E-04	3.42E-05	1.64E-05	2.17E-09	5.66E-06	3.74E-06	1.31E-07
27	3.96E-03	2.34E-04	8.36E-05	4.40E-05	1.19E-04	5.02E-09	5.98E-05	3.10E-06	8.24E-07
28	1.11E-03	2.13E-05	8.54E-05	2.53E-05	1.37E-05	1.63E-09	4.98E-06	2.73E-06	1.06E-07
29	3.89E-03	2.44E-04	5.21E-05	5.61E-05	1.44E-04	4.51E-09	6.33E-05	2.47E-06	7.83E-07
30	1.07E-03	1.91E-05	6.14E-05	1.89E-05	1.21E-05	1.23E-09	4.56E-06	1.97E-06	8.78E-08
31	4.12E-03	2.36E-04	3.97E-05	8.28E-05	1.83E-04	4.41E-09	6.07E-05	2.03E-06	7.60E-07
32	1.07E-03	1.91E-05	4.95E-05	1.80E-05	1.30E-05	1.05E-09	4.62E-06	1.60E-06	8.31E-08
33	9.23E-03	1.43E-04	3.99E-05	5.78E-04	2.49E-04	3.51E-09	2.73E-05	2.15E-06	8.15E-07
34	1.24E-03	2.04E-05	4.70E-05	2.90E-05	1.71E-05	1.04E-09	4.77E-06	1.54E-06	9.33E-08
35	7.72E-03	3.45E-04	7.37E-05	4.52E-03	4.74E-04	3.31E-09	1.42E-05	3.19E-06	7.50E-07
36	1.38E-03	3.17E-05	4.54E-05	2.02E-04	3.07E-05	1.03E-09	4.80E-06	1.48E-06	1.04E-07
37	3.22E-05	9.69E-06	6.78E-07	1.42E-04	9.97E-06	2.30E-11	1.35E-07	2.05E-08	4.80E-09
38	4.20E-03	1.54E-03	8.71E-05	2.28E-02	1.69E-03	3.07E-09	1.89E-05	2.77E-06	6.85E-07
39	1.38E-03	6.87E-05	4.21E-05	7.82E-04	7.56E-05	9.79E-10	4.74E-06	1.36E-06	1.10E-07
40	2.06E-05	1.04E-05	3.48E-07	1.56E-04	1.99E-05	1.55E-11	1.08E-07	1.30E-08	4.52E-09
41	2.80E-03	1.48E-03	4.78E-05	2.21E-02	3.45E-03	2.18E-09	1.55E-05	1.70E-06	6.50E-07
42	1.32E-03	1.02E-04	3.79E-05	1.31E-03	1.79E-04	9.09E-10	4.56E-06	1.22E-06	1.14E-07
43	1.50E-05	8.34E-06	3.61E-07	1.24E-04	4.99E-05	1.48E-11	1.14E-07	9.31E-09	4.34E-09
44	2.02E-03	1.09E-03	5.50E-05	1.61E-02	8.02E-03	2.14E-09	1.68E-05	1.30E-06	6.17E-07
45	1.24E-03	1.20E-04	3.44E-05	1.60E-03	4.07E-04	8.48E-10	4.46E-06	1.09E-06	1.18E-07
46	1.47E-03	6.02E-04	8.16E-05	8.38E-03	9.10E-03	2.10E-09	1.91E-05	1.15E-06	5.85E-07
47	1.14E-03	1.21E-04	3.21E-05	1.63E-03	6.55E-04	7.90E-10	4.44E-06	9.64E-07	1.19E-07

Peach Bottom STSBO without RCIC Blackstart									
Plume Segment	Xe	Cs	Ba	I	Te	Ru	Mo	Ce	La
48	1.09E-03	3.24E-04	1.06E-04	4.00E-03	1.11E-02	1.94E-09	1.95E-05	1.03E-06	5.55E-07
49	1.02E-03	1.13E-04	3.06E-05	1.51E-03	9.56E-04	7.32E-10	4.43E-06	8.44E-07	1.20E-07
50	8.15E-04	1.99E-04	9.58E-05	1.94E-03	1.45E-02	1.92E-09	2.07E-05	9.29E-07	5.30E-07
51	9.09E-04	1.01E-04	2.89E-05	1.32E-03	1.29E-03	6.76E-10	4.43E-06	7.34E-07	1.19E-07
52	6.24E-04	1.37E-04	9.13E-05	1.02E-03	7.55E-03	1.77E-09	1.95E-05	8.48E-07	5.07E-07
53	7.96E-04	8.88E-05	2.73E-05	1.13E-03	1.33E-03	6.23E-10	4.39E-06	6.34E-07	1.17E-07
54	4.85E-04	1.21E-04	1.08E-04	7.21E-04	3.31E-03	1.77E-09	2.02E-05	7.73E-07	4.86E-07
55	6.92E-04	7.77E-05	2.66E-05	9.60E-04	1.22E-03	5.78E-10	4.37E-06	5.48E-07	1.14E-07
56	3.85E-04	1.17E-04	1.29E-04	6.32E-04	1.97E-03	1.74E-09	2.06E-05	7.12E-07	4.67E-07
57	6.00E-04	6.84E-05	2.66E-05	8.14E-04	1.08E-03	5.39E-10	4.37E-06	4.74E-07	1.12E-07
58	3.12E-04	1.16E-04	9.57E-05	6.42E-04	1.57E-03	1.66E-09	1.99E-05	6.61E-07	4.50E-07
59	5.16E-04	6.05E-05	2.53E-05	6.92E-04	9.41E-04	5.04E-10	4.35E-06	4.11E-07	1.09E-07
60	2.58E-04	1.20E-04	4.82E-05	6.56E-04	1.55E-03	1.64E-09	2.08E-05	5.93E-07	4.34E-07
61	4.43E-04	5.39E-05	2.24E-05	5.88E-04	8.29E-04	4.73E-10	4.36E-06	3.56E-07	1.06E-07
62	2.17E-04	8.83E-05	2.79E-05	2.00E-04	1.60E-03	1.59E-09	2.01E-05	5.49E-07	4.19E-07
63	3.80E-04	4.74E-05	1.93E-05	4.89E-04	7.40E-04	4.47E-10	4.34E-06	3.09E-07	1.03E-07
64	1.86E-04	8.44E-05	2.10E-05	1.31E-04	1.72E-03	1.58E-09	2.01E-05	5.17E-07	4.04E-07
65	3.25E-04	4.20E-05	1.65E-05	4.04E-04	6.72E-04	4.25E-10	4.34E-06	2.70E-07	9.95E-08
66	1.62E-04	8.79E-05	1.92E-05	1.06E-04	1.92E-03	1.60E-09	2.15E-05	4.88E-07	3.91E-07
67	2.77E-04	3.76E-05	1.42E-05	3.33E-04	6.24E-04	4.08E-10	4.38E-06	2.37E-07	9.64E-08
68	1.41E-04	8.52E-05	1.77E-05	8.70E-05	1.86E-03	1.51E-09	2.10E-05	4.63E-07	3.79E-07
69	2.36E-04	3.41E-05	1.22E-05	2.74E-04	5.78E-04	3.92E-10	4.42E-06	2.09E-07	9.35E-08
70	1.24E-04	8.90E-05	1.77E-05	7.19E-05	1.22E-03	1.54E-09	2.23E-05	4.38E-07	3.66E-07
71	2.01E-04	3.12E-05	1.06E-05	2.25E-04	5.18E-04	3.79E-10	4.48E-06	1.86E-07	9.06E-08
72	1.11E-04	9.11E-05	1.76E-05	5.95E-05	1.07E-03	1.53E-09	2.30E-05	4.18E-07	3.55E-07
73	1.71E-04	2.90E-05	9.30E-06	1.85E-04	4.61E-04	3.68E-10	4.56E-06	1.66E-07	8.78E-08
74	9.89E-05	9.35E-05	1.73E-05	4.94E-05	6.69E-04	1.55E-09	2.38E-05	4.00E-07	3.46E-07
75	1.46E-04	2.73E-05	8.22E-06	1.52E-04	4.02E-04	3.61E-10	4.67E-06	1.50E-07	8.52E-08
76	8.89E-05	9.70E-05	1.59E-05	4.12E-05	6.33E-04	1.56E-09	2.49E-05	3.85E-07	3.38E-07
77	1.24E-04	2.61E-05	7.29E-06	1.25E-04	3.52E-04	3.55E-10	4.80E-06	1.36E-07	8.28E-08
78	7.95E-05	9.99E-05	1.46E-05	3.43E-05	6.44E-04	1.57E-09	2.58E-05	3.71E-07	3.30E-07
79	1.05E-04	2.52E-05	6.49E-06	1.03E-04	3.12E-04	3.51E-10	4.94E-06	1.24E-07	8.06E-08
80	7.25E-05	9.60E-05	1.36E-05	2.87E-05	6.22E-04	1.50E-09	2.49E-05	3.61E-07	3.26E-07
81	8.96E-05	2.44E-05	5.81E-06	8.46E-05	2.78E-04	3.47E-10	5.04E-06	1.15E-07	7.87E-08
82	6.69E-05	9.50E-05	1.31E-05	2.42E-05	6.00E-04	1.56E-09	2.49E-05	3.55E-07	3.23E-07
83	7.62E-05	2.37E-05	5.24E-06	6.95E-05	2.50E-04	3.45E-10	5.12E-06	1.06E-07	7.71E-08
84	6.12E-05	9.83E-05	1.35E-05	2.04E-05	6.25E-04	1.62E-09	2.67E-05	3.49E-07	3.22E-07
85	5.57E-05	1.98E-05	4.09E-06	4.92E-05	1.96E-04	2.94E-10	4.46E-06	8.52E-08	6.45E-08
86	1.73E-05	3.07E-05	4.19E-06	5.48E-06	1.96E-04	5.06E-10	8.72E-06	1.03E-07	9.65E-08

Table B-5 EARLY Parameters Used in the Peach Bottom Unmitigated LTSBO and STSBO with and without RCIC Blackstart Scenarios

Variable	Description	LTSBO	STSBO with RCIC Blackstart	STSBO without RCIC Blackstart
ACNAME	Latent Cancer Effect			
	Cancer Type 1	LEUKEMIA	LEUKEMIA	LEUKEMIA
	Cancer Type 2	BONE	BONE	BONE
	Cancer Type 3	BREAST	BREAST	BREAST
	Cancer Type 4	LUNG	LUNG	LUNG
	Cancer Type 5	THYROID	THYROID	THYROID
	Cancer Type 6	LIVER	LIVER	LIVER
	Cancer Type 7	COLON	COLON	COLON
	Cancer Type 8	RESIDUAL	RESIDUAL	RESIDUAL
ACSUSC	Population Susceptible to Cancer	1.0 for all cancers	1.0 for all cancers	1.0 for all cancers
ACTHRE	Linear Dose-Response Threshold	0	0	0
BRRATE	Breathing Rate (for all activity types)	0.000266	0.000266	0.000266
CFRISK	Lifetime Cancer Fatality Risk Factors			
	Cancer Type 1	0.0111	0.0111	0.0111
	Cancer Type 2	0.00019	0.00019	0.00019
	Cancer Type 3	0.00506	0.00506	0.00506
	Cancer Type 4	0.0198	0.0198	0.0198
	Cancer Type 5	0.000648	0.000648	0.000648
	Cancer Type 6	0.003	0.003	0.003
	Cancer Type 7	0.0208	0.0208	0.0208
	Cancer Type 8	0.0493	0.0493	0.0493
CIRISK	Lifetime Cancer Injury Risk Factors			
	Cancer Type 1	0.0113	0.0113	0.0113
	Cancer Type 2	0.000271	0.000271	0.000271
	Cancer Type 3	0.0101	0.0101	0.0101
	Cancer Type 4	0.0208	0.0208	0.0208
	Cancer Type 5	0.00648	0.00648	0.00648
	Cancer Type 6	0.00316	0.00316	0.00316
	Cancer Type 7	0.0378	0.0378	0.0378
	Cancer Type 8	0.169	0.169	0.169
CRIORG	Critical Organ for EARLY Phase	L-ICRP60ED	L-ICRP60ED	L-ICRP60ED
CSFACT	Cloudshine Shielding Factors			
	Evacuation Shielding Factor for All but Cohort 4	1	1	1
	Normal Activity Shielding Factor for All but Cohort 4	0.6	0.6	0.6
	Sheltering Shielding Factor for All but Cohort 4	0.5	0.5	0.5

Variable	Description	LTSBO	STSBO with RCIC Blackstart	STSBO without RCIC Blackstart
CSFACT	Evacuation Shielding Factor for Cohort 4	1	1	1
	Normal Activity Shielding Factor for Cohort 4	0.31	0.31	0.31
	Sheltering Shielding Factor for Cohort 4	0.31	0.31	0.31
DCF_FILE	Name of Dose Conversion Factor File	FGR13GyEquivDCF.INP	FGR13GyEquivDCF.INP	FGR13GyEquivDCF.INP
DDREFA	Dose-Dependent Reduction Factor			
	Cancer Type 1	2	2	2
	Cancer Type 2	2	2	2
	Cancer Type 3	1	1	1
	Cancer Type 4	2	2	2
	Cancer Type 5	2	2	2
	Cancer Type 6	2	2	2
	Cancer Type 7	2	2	2
	Cancer Type 8	2	2	2
DDTHRE	Threshold for Applying Dose-Dependent Reduction Factor	0.2	0.2	0.2
DLTSHL	Delay from Alarm Time to Shelter			
	Cohort 1	5400	3600	3600
	Cohort 2	5400	3600	3600
	Cohort 3	900	900	900
	Cohort 4	5400	3600	3600
	Cohort 5	5400	3600	3600
	Cohort 6			
DLTEVA	Delay from Beginning of Shelter to Evacuation			
	Cohort 1	3600	3600	3600
	Cohort 2	3600	3600	3600
	Cohort 3	2700	2700	2700
	Cohort 4	15300	15300	15300
	Cohort 5	15300	15300	15300
	Cohort 6			
DOSEFA	Cancer Dose-Response Linear Factors	1 for all organs	1 for all organs	1 for all organs
DOSEFB	Cancer Dose-Response Quadratic Factors	0 for all organs	0 for all organs	0 for all organs
DOSHOT	Hot-Spot Relocation Dose Threshold	0.05	0.05	0.05
DOSMOD	Dose-Response Model Flag	LNT, AT	LNT, AT	LNT, AT
DOSNRM	Normal Relocation Dose Threshold	0.005	0.005	0.005
DURBEG	Duration of Beginning of Evacuation Phase			
	Cohort 1	900	900	900

Variable	Description	LTSBO	STSBO with RCIC Blackstart	STSBO without RCIC Blackstart
DURBEG	Cohort 2	900	900	900
	Cohort 3	3600	3600	3600
	Cohort 4	1800	1800	1800
	Cohort 5	1800	1800	1800
	Cohort 6	N/A	N/A	N/A
DURMID	Duration of Middle of Evacuation Phase			10800
	Cohort 1	10800	10800	10800
	Cohort 2	10800	10800	10800
	Cohort 3	1800	1800	1800
	Cohort 4	1800	1800	1800
	Cohort 5	1800	1800	1800
	Cohort 6	N/A	N/A	N/A
EANAM1	Text Describing the EARLY Assumptions	SOARCA calculation for Peach Bottom LTSBO, EARLY input	SOARCA calculation for Peach Bottom STSBO, EARLY input	SOARCA calculation for Peach Bottom STSBO, EARLY input
EANAM2	Text Describing the Emergency Response			
	Cohort 1	Group 1	Group 1	Group 1
	Cohort 2	Group 2	Group 2	Group 2
	Cohort 3	Group 3	Group 3	Group 3
	Cohort 4	Group 4	Group 4	Group 4
	Cohort 5	Group 5	Group 5	Group 5
	Cohort 6	Group 6	Group 6	Group 6
EFFACA	LD50 for Early Fatality Types			
	A-RED MARR	5.6	5.6	5.6
	A-LUNGS	23.5	23.5	23.5
	A-STOMACH	12.1	12.1	12.1
EFFACB	Shape Factor for Early Fatality Types			
	A-RED MARR	6.1	6.1	6.1
	A-LUNGS	9.6	9.6	9.6
	A-STOMACH	9.3	9.3	9.3
EFFACY	Efficacy of the KI Ingestion	0.7	0.7	0.7
EFFTHR	Threshold Dose to Target Organ			
	A-RED MARR	2.32	2.32	2.32
	A-LUNGS	13.6	13.6	13.6
	A-STOMACH	6.5	6.5	6.5
EIFACA	D50 For Early Injuries			
	PRODROMAL VOMIT	2	2	2
	DIARRHEA	3	3	3
	PNEUMONITIS	16.6	16.6	16.6
	SKIN ERYTHRMA	6	6	6
	TRANSEPIDERMAL	20	20	20
	THYROIDITIS	240	240	240

Variable	Description	LTSBO	STSBO with RCIC Blackstart	STSBO without RCIC Blackstart
EIFACA	HYPOTHYROIDISM	60	60	60
EIFACB	Shape Factor for Early Injuries			
	PRODROMAL VOMIT	3	3	3
	DIARRHEA	2.5	2.5	2.5
	PNEUMONITIS	7.3	7.3	7.3
	SKIN ERYTHRMA	5	5	5
	TRANSEPIDERMAL	5	5	5
	THYROIDITIS	2	2	2
	HYPOTHYROIDISM	1.3	1.3	1.3
EINAME	Early Injury Effect Names and Corresponding Organ			
	PRODROMAL VOMIT	A-STOMACH	A-STOMACH	A-STOMACH
	DIARRHEA	A-STOMACH	A-STOMACH	A-STOMACH
	PNEUMONITIS	A-LUNGS	A-LUNGS	A-LUNGS
	SKIN ERYTHRMA	A-SKIN	A-SKIN	A-SKIN
	TRANSEPIDERMAL	A-SKIN	A-SKIN	A-SKIN
	THYROIDITIS	A-THYROID	A-THYROID	A-THYROID
	HYPOTHYROIDISM	A-THYROID	A-THYROID	A-THYROID
EISUSC	Susceptible Population Fraction	1. for all health effects	1. for all health effects	1. for all health effects
EITHRE	Early Injury Dose Threshold			
	PRODROMAL VOMIT	0.5	0.5	0.5
	DIARRHEA	1	1	1
	PNEUMONITIS	9.2	9.2	9.2
	SKIN ERYTHRMA	3	3	3
	TRANSEPIDERMAL	10	10	10
	THYROIDITIS	40	40	40
	HYPOTHYROIDISM	2	2	2
ENDAT2	Control flag indicating only ATMOS and EARLY are to be run	.FALSE.	.FALSE.	.FALSE.
ENDEMP	Time Duration for the Emergency Phase	604800	604800	604800
ESPEED	Evaluation Speed			
	Initial Evacuation Phase, Cohort 1	2.235	2.235	2.235
	Middle Evacuation Phase, Cohort 1	1.341	1.341	1.341
	Late Evacuation Phase, Cohort 1	8.941	8.941	8.941
	Initial Evacuation Phase, Cohort 2	2.235	2.235	2.235
	Middle Evacuation Phase, Cohort 2	1.341	1.341	1.341
	Late Evacuation Phase, Cohort 2	8.941	8.941	8.941
	Initial Evacuation Phase, Cohort 3	8.941	8.941	8.941
	Middle Evacuation Phase, Cohort 3	8.941	8.941	8.941

Variable	Description	LTSBO	STSBO with RCIC Blackstart	STSBO without RCIC Blackstart
ESPEED	Late Evacuation Phase, Cohort 3	8.941	8.941	8.941
	Initial Evacuation Phase, Cohort 4	1.341	1.341	1.341
	Middle Evacuation Phase, Cohort 4	8.941	8.941	8.941
	Late Evacuation Phase, Cohort 4	8.941	8.941	8.941
	Initial Evacuation Phase, Cohort 5	1.341	1.341	1.341
	Middle Evacuation Phase, Cohort 5	8.941	8.941	8.941
	Late Evacuation Phase, Cohort 5	8.941	8.941	8.941
	Cohort 6	N/A	N/A	N/A
ESPGRD	Speed Multiplier to Account for Grid-Level Variations in Road Network	Table B-6	Table B-6	Table B-6
ESPMUL	Speed Multiplier Employed During Precipitation	0.7	0.7	0.7
EVATYP	Evacuation Type	NETWORK	NETWORK	NETWORK
GSHFAC	Groundshine Shielding Factors			
	Evacuation Shielding Factor for All but Cohort 4	0.5	0.5	0.5
	Normal Activity Shielding Factor for All but Cohort 4	0.18	0.18	0.18
	Sheltering Shielding Factor for All but Cohort 4	0.1	0.1	0.1
	Evacuation Shielding Factor for Cohort 4	0.5	0.5	0.5
	Normal Activity Shielding Factor for Cohort 4	0.05	0.05	0.05
	Sheltering Shielding Factor for Cohort 4	0.05	0.05	0.05
IDIREC	Direction in Network Evacuation Model	Table B-7	Table B-7	Table B-7
IPLUME	Plume Model Dispersion Code	3	3	3
KIMODL	Model Flag for KI Ingestion	KI	KI	KI
LASMOV	Last Ring in Movement Zone	17	17	17
NUMACA	Number of Latent Cancer Health Effects	8	8	8
NUMEFA	Number of Early Fatality Effects	3	3	3
NUMEIN	Number of Early Injury Effects	7	7	7
NUMEVA	Outer Boundary of Evacuation/Shelter Region	Cohort 1 - 15 Cohorts 2 to 6 - 12	Cohort 1 - 15 Cohorts 2 to 6 - 13	Cohort 1 - 15 Cohorts 2 to 6 - 13
NUMFIN	Number of Fine Grid Subdivisions	7	7	7

Variable	Description	LTSBO	STSBO with RCIC Blackstart	STSBO without RCIC Blackstart
ORGFLG	Doses to be Calculated for Specified Organ	All TRUE	All TRUE	All TRUE
OVRRID	Wind Rose Probability Override	.FALSE.	.FALSE.	.FALSE.
POPFLG	Population Distribution Flag	FILE	FILE	FILE
POPFRAC	Population Fraction Ingesting KI	Cohort 1 and 2 - 1.0 Cohort 3 to 6 - 0.0	Cohort 1 and 2 - 1.0 Cohort 3 to 6 - 0.1	Cohort 1 and 2 - 1.0 Cohort 3 to 6 - 0.1
PROTIN [E]	Inhalation Protection Factor - evacuation	1	1	1
PROTIN [N]	Inhalation Protection Factor - normal activity	0.41	0.41	0.41
PROTIN [S]	Inhalation Protection Factor - sheltering	0.33	0.33	0.33
REFPNT	Reference Time Point (ARRIVAL or SCRAM)	ALARM	ALARM	ALARM
RESCON	Emergency phase resuspension coefficient	0.0001	0.0001	0.0001
RESHAF	Resuspension Concentration Half-Life	182000	182000	182000
RISCAT	Risk by Weather-Category Flag	.FALSE.	.FALSE.	.FALSE.
RISTHR	Risk Threshold for Fatality Radius	NA	NA	NA
SKPFAC [E]	Skin Protection Factors - evacuation	1	1	1
SKPFAC [N]	Skin Protection Factors - normal activity	0.41	0.41	0.41
SKPFAC [S]	Skin Protection Factors - sheltering	0.33	0.33	0.33
TIMHOT	Hot Spot Relocation Time	43200	43200	43200
TIMNRM	Normal Relocation Time	86400	86400	86400
TRAVELP OINT	Evacuee Movement Option	CENTERPOINT	CENTERPOINT	CENTERPOINT
WTFRAC	Weighting Fraction Applicable to this Scenario			
	Cohort 1	0.2	0.2	0.2
	Cohort 2	0.355	0.355	0.355
	Cohort 3	0.372	0.372	0.372
	Cohort 4	0.006	0.006	0.006
	Cohort 5	0.062	0.062	0.062
	Cohort 6	0.005	0.005	0.005
WTNAME	Type of Weighting for Cohorts	PEOPLE	PEOPLE	PEOPLE

Table B-6 Grid-Level Evacuation Speed Multipliers Used in the Peach Bottom Unmitigated LTSBO and STSBO with and without RCIC Blackstart Scenarios

	Compass Sector															
Radial Ring	1	2	3	4	5	6	7	8	9	10	11	12	13	14	15	16
1	0.75	0.75	1.00	1.00	1.00	1.00	1.00	1.00	1.00	1.00	1.00	1.00	1.00	1.00	1.00	1.00
2	0.75	0.75	1.00	1.00	1.00	1.00	1.00	1.00	1.00	1.00	1.00	1.00	1.00	1.00	1.00	1.00
3	0.75	0.75	1.00	1.00	1.00	1.00	1.00	1.00	1.00	1.00	1.00	1.00	1.00	1.00	1.00	1.00
4	0.75	0.75	1.00	1.00	1.00	1.00	1.00	1.00	1.00	1.00	1.00	1.00	1.00	1.00	1.00	1.00
5	0.75	0.75	1.00	1.00	1.00	1.00	1.00	1.00	1.00	1.00	1.00	1.00	1.00	1.00	1.00	1.00
6	0.75	0.75	1.00	1.00	1.00	1.00	1.00	1.00	1.00	1.00	1.00	1.00	1.00	1.00	1.00	1.00
7	0.75	0.75	1.00	1.00	1.00	1.00	1.00	1.00	1.00	1.00	1.00	1.00	1.00	1.00	1.00	1.00
8	0.75	0.75	1.00	1.00	1.00	1.00	1.00	1.00	1.00	1.00	1.00	1.00	1.00	1.00	1.00	1.00
9	0.75	0.75	1.00	1.00	1.00	1.00	1.00	1.00	1.00	1.00	1.00	1.00	1.00	1.00	1.00	1.00
10	0.75	0.75	1.00	1.00	1.00	1.00	1.00	1.00	1.00	1.00	1.00	1.00	1.00	1.00	1.00	1.00
11	0.75	0.75	1.00	1.00	1.00	1.00	1.00	1.00	1.00	1.00	1.00	1.00	1.00	1.00	1.00	1.00
12	0.75	0.75	1.00	1.00	1.00	1.00	1.00	1.00	1.00	1.00	1.00	1.00	1.00	1.00	1.00	1.00
13	0.75	0.75	1.00	1.00	1.00	1.00	1.00	1.00	1.00	1.00	1.00	1.00	1.00	1.00	1.00	1.00
14	0.75	0.75	1.00	1.00	1.00	1.00	1.00	1.00	1.00	1.00	1.00	1.00	1.00	1.00	1.00	1.00
15	0.75	0.75	1.00	1.00	1.00	1.00	1.00	1.00	1.00	1.00	1.00	1.00	1.00	1.00	1.00	1.00
16	0.75	0.75	1.00	1.00	1.00	1.00	1.00	1.00	1.00	1.00	1.00	1.00	1.00	1.00	1.00	1.00
17	0.75	0.75	1.00	1.00	1.00	1.00	1.00	1.00	1.00	1.00	1.00	1.00	1.00	1.00	1.00	1.00

	Compass Sector															
Radial Ring	17	18	19	20	21	22	23	24	25	26	27	28	29	30	31	32
1	1.00	1.00	1.00	1.00	1.00	1.00	1.00	1.00	1.00	1.00	1.00	1.00	1.00	1.00	1.00	1.00
2	1.00	1.00	1.00	1.00	1.00	1.00	1.00	1.00	1.00	1.00	1.00	1.00	1.00	1.00	1.00	1.00
3	1.00	1.00	1.00	1.00	1.00	1.00	1.00	1.00	1.00	1.00	1.00	1.00	1.00	1.00	1.00	1.00
4	1.00	1.00	1.00	1.00	1.00	1.00	1.00	1.00	1.00	1.00	1.00	1.00	1.00	1.00	1.00	1.00
5	1.00	1.00	1.00	1.00	1.00	1.00	1.00	1.00	1.00	1.00	1.00	1.00	1.00	1.00	1.00	1.00
6	1.00	1.00	1.00	1.00	1.00	1.00	1.00	1.00	1.00	1.00	1.00	1.00	1.00	1.00	1.00	1.00
7	1.00	1.00	1.00	1.00	1.00	1.00	1.00	1.00	1.00	1.00	1.00	1.00	1.00	1.00	1.00	1.00
8	1.00	1.00	1.00	1.00	1.00	1.00	1.00	1.00	1.00	1.00	1.00	1.00	1.00	1.00	1.00	1.00
9	1.00	1.00	1.00	1.00	1.00	1.00	1.00	1.00	1.00	1.00	1.00	1.00	1.00	1.00	1.00	1.00
10	1.00	1.00	1.00	1.00	1.00	1.00	1.00	1.00	1.00	1.00	1.00	1.00	1.00	1.00	1.00	1.00
11	1.00	1.00	1.00	1.00	1.00	1.00	1.00	1.00	1.00	1.00	1.00	1.00	1.00	1.00	1.00	1.00
12	1.00	1.00	1.00	1.00	1.00	1.00	1.00	1.00	1.00	1.00	1.00	1.00	1.00	1.00	1.00	1.00
13	1.00	1.00	1.00	1.00	1.00	1.00	1.00	1.00	1.00	1.00	1.00	1.00	1.00	1.00	1.00	1.00
14	1.00	1.00	1.00	1.00	1.00	1.00	1.00	1.00	1.50	1.50	1.50	1.50	1.50	1.50	1.00	1.00
15	1.00	1.00	1.00	1.00	1.00	1.50	1.50	1.50	1.00	1.00	1.00	1.00	1.00	1.50	1.50	1.50
16	1.00	1.00	1.00	1.00	1.00	1.00	1.00	1.00	1.00	1.00	1.00	1.00	1.00	1.00	1.00	1.00
17	1.00	1.00	1.00	1.00	1.00	1.00	1.00	1.00	1.00	1.00	1.00	1.00	1.00	1.00	1.00	1.00

	Compass Sector															
Radial Ring	33	34	35	36	37	38	39	40	41	42	43	44	45	46	47	48
1	1.00	1.00	1.00	1.00	1.00	1.00	1.00	1.00	1.00	1.00	1.00	1.00	1.00	1.00	1.00	1.00
2	1.00	1.00	1.00	1.00	1.00	1.00	1.00	1.00	1.00	1.00	1.00	1.00	1.00	1.00	1.00	1.00
3	1.00	1.00	1.00	1.00	1.00	1.00	1.00	1.00	1.00	1.00	1.00	1.00	1.00	1.00	1.00	1.00
4	1.00	1.00	1.00	1.00	1.00	1.00	1.00	1.00	1.00	1.00	1.00	1.00	1.00	1.00	1.00	1.00
5	1.00	1.00	1.00	1.00	1.00	1.00	1.00	1.00	1.00	1.00	1.00	1.00	1.00	1.00	1.00	1.00
6	1.00	1.00	1.00	1.00	1.00	1.00	1.00	1.00	1.00	1.00	1.00	1.00	1.00	1.00	1.00	1.00
7	1.00	1.00	1.00	1.00	1.00	1.00	1.00	1.00	1.00	1.00	1.00	1.00	1.00	1.00	1.00	1.00
8	1.00	1.00	1.00	1.00	1.00	1.00	1.00	1.00	1.00	1.00	1.00	1.00	1.00	1.00	1.00	1.00
9	1.00	1.00	1.00	1.00	1.00	1.00	1.00	1.00	1.00	1.00	1.00	1.00	1.00	1.00	1.00	1.00
10	1.00	1.00	1.00	1.00	1.00	1.00	1.00	1.00	1.00	1.00	1.00	1.00	1.00	1.00	1.00	1.00
11	1.00	1.00	1.00	1.00	1.00	1.00	1.00	1.00	1.00	1.00	1.00	1.00	1.00	1.00	1.00	1.00
12	1.00	1.00	1.00	1.00	1.00	1.00	1.00	1.00	1.00	1.00	1.00	1.00	1.00	1.00	1.00	1.00
13	1.00	1.00	1.00	1.00	1.00	1.00	1.00	1.00	1.00	1.00	1.00	1.00	1.00	1.00	1.00	1.00
14	1.00	1.00	1.00	1.00	1.00	1.00	1.00	1.00	1.00	1.00	1.00	1.00	1.00	1.00	1.00	1.00
15	1.50	1.00	1.00	1.00	1.00	1.00	1.00	1.00	1.00	1.00	1.00	1.00	1.00	1.00	1.00	1.00
16	1.00	1.00	1.00	1.00	1.00	1.00	1.00	1.00	1.00	1.00	1.00	1.00	1.00	1.00	1.00	1.00
17	1.00	1.00	1.00	1.00	1.00	1.00	1.00	1.00	1.00	1.00	1.00	1.00	1.00	1.00	1.00	1.00

	Compass Sector															
Radial Ring	49	50	51	52	53	54	55	56	57	58	59	60	61	62	63	64
1	100	1.00	1.00	1.00	1.00	1.00	1.00	1.00	1.00	1.00	1.00	1.00	1.00	0.75	0.75	0.75
2	1.00	1.00	1.00	1.00	1.00	1.00	1.00	1.00	1.00	1.00	1.00	1.00	1.00	0.75	0.75	0.75
3	1.00	1.00	1.00	1.00	1.00	1.00	1.00	1.00	1.00	1.00	1.00	1.00	1.00	0.75	0.75	0.75
4	1.00	1.00	1.00	1.00	1.00	1.00	1.00	1.00	1.00	1.00	1.00	1.00	1.00	0.75	0.75	0.75
5	1.00	1.00	1.00	1.00	1.00	1.00	1.00	1.00	1.00	1.00	1.00	1.00	1.00	0.75	0.75	0.75
6	1.00	1.00	1.00	1.00	1.00	1.00	1.00	1.00	1.00	1.00	1.00	1.00	1.00	0.75	0.75	0.75
7	1.00	1.00	1.00	1.00	1.00	1.00	1.00	1.00	1.00	1.00	1.00	1.00	1.00	0.75	0.75	0.75
8	1.00	1.00	1.00	1.00	1.00	1.00	1.00	1.00	1.00	1.00	1.00	1.00	1.00	0.75	0.75	0.75
9	1.00	1.00	1.00	1.00	1.00	1.00	1.00	1.00	1.00	1.00	1.00	1.00	1.00	0.75	0.75	0.75
10	1.00	1.00	1.00	1.00	1.00	1.00	1.00	1.00	1.00	1.00	1.00	1.00	1.00	0.75	0.75	0.75
11	1.00	1.00	1.00	1.00	1.00	1.00	1.00	1.00	1.00	1.00	1.00	1.00	1.00	0.75	0.75	0.75
12	1.00	1.00	1.00	1.00	1.00	1.00	1.00	1.00	1.00	1.00	1.00	1.00	1.00	0.75	0.75	0.75
13	1.00	1.00	1.00	1.00	1.00	1.00	0.75	1.00	1.00	1.00	1.00	1.00	1.00	0.75	0.75	0.75
14	1.00	1.00	1.00	1.00	1.00	1.00	0.75	1.00	1.00	1.00	1.00	1.00	1.00	0.75	0.75	0.75
15	1.00	1.00	1.00	1.00	1.00	1.00	0.75	1.00	1.00	1.00	1.00	1.00	1.00	0.75	0.75	0.75
16	1.00	1.00	1.00	1.00	1.00	1.00	1.00	1.00	1.00	1.00	1.00	1.00	1.00	0.75	0.75	0.75
17	1.00	1.00	1.00	1.00	1.00	1.00	1.00	1.00	1.00	1.00	1.00	1.00	1.00	0.75	0.75	0.75

Table B-7 Evacuation Direction Parameters Used in the Peach Bottom Unmitigated LTSBO and STSBO with and without RCIC Blackstart Scenarios

	Compass Sector															
Radial Ring	1	2	3	4	5	6	7	8	9	10	11	12	13	14	15	16
1	1	1	1	1	1	1	1	1	1	1	1	1	1	1	1	1
2	1	1	1	1	1	1	1	1	1	1	1	1	1	1	1	1
3	1	1	1	1	1	1	1	1	1	1	1	1	1	2	1	1
4	1	1	1	1	1	1	1	1	1	1	1	1	1	1	1	1
5	1	1	1	1	1	1	1	1	1	1	1	1	1	1	1	4
6	1	1	1	1	1	1	1	1	1	1	1	1	1	1	4	1
7	2	2	1	2	2	1	2	2	1	4	2	1	4	2	2	1
8	1	4	1	1	4	2	1	4	2	1	1	4	2	2	1	1
9	1	1	4	2	1	1	2	1	1	4	1	4	1	4	1	1
10	1	1	1	1	1	1	1	1	1	1	1	1	1	1	1	1
11	1	1	4	2	1	4	2	1	4	4	2	1	4	2	1	4
12	2	1	1	4	1	1	4	1	4	4	2	1	4	2	1	1
13	1	1	4	1	4	2	1	1	2	1	4	4	2	2	1	1
14	1	1	4	1	1	1	2	1	2	1	2	1	1	2	1	1
15	1	1	4	2	2	2	1	1	1	1	1	1	1	1	1	1
16	1	1	1	1	1	1	1	1	1	1	1	1	1	1	1	4
17	1	1	1	1	1	1	1	1	1	1	1	1	1	1	1	1

	Compass Sector															
Radial Ring	17	18	19	20	21	22	23	24	25	26	27	28	29	30	31	32
1	1	1	1	1	1	1	1	1	1	1	1	1	1	1	1	1
2	1	1	1	1	1	1	1	1	1	1	1	1	1	1	1	1
3	1	1	1	1	1	1	1	1	2	1	4	4	4	4	2	2
4	1	1	1	1	1	1	1	1	1	1	1	1	1	1	1	1
5	1	1	1	1	1	1	1	1	1	2	2	2	2	2	2	1
6	1	1	1	1	1	1	1	1	1	1	2	2	2	2	2	2
7	1	1	1	1	1	1	1	1	1	1	2	2	1	4	4	2
8	2	1	1	1	4	4	4	1	1	1	1	1	1	4	1	4
9	1	2	1	1	1	4	4	4	1	1	4	1	2	2	2	1
10	1	1	1	1	1	1	1	1	1	1	1	1	1	4	4	4
11	4	2	2	2	2	2	2	1	4	4	1	1	4	2	2	1
12	4	4	2	2	2	1	4	1	2	1	2	2	1	4	4	2
13	1	1	1	1	1	2	1	2	2	1	1	2	1	4	2	2
14	1	1	1	1	1	4	1	1	1	1	2	1	4	1	1	1
15	1	1	1	1	1	1	1	4	4	4	2	2	2	1	1	1
16	1	1	1	1	1	1	1	1	1	1	1	1	1	1	1	1
17	1	1	1	1	1	1	1	1	1	1	1	1	1	1	1	1

	Compass Sector															
Radial Ring	33	34	35	36	37	38	39	40	41	42	43	44	45	46	47	48
1	1	1	1	1	1	1	1	1	1	1	1	1	1	1	1	1
2	1	1	1	1	1	1	1	1	1	1	1	1	1	1	1	1
3	2	2	2	1	1	1	4	4	4	4	2	2	2	1	1	1
4	4	2	2	1	1	1	1	4	4	4	2	2	1	4	4	2
5	1	1	1	1	2	1	4	4	2	2	1	4	4	2	2	1
6	2	2	1	1	1	1	2	1	1	4	2	2	1	2	1	4
7	1	1	1	1	4	4	2	2	1	1	4	4	1	1	4	1
8	2	1	4	4	2	1	2	1	2	1	4	2	1	4	2	1
9	1	2	1	4	2	1	2	1	2	1	1	4	1	4	1	4
10	2	2	2	2	1	2	1	4	2	1	1	1	4	2	1	4
11	1	1	4	2	1	4	1	4	2	1	4	1	1	2	1	1
12	2	1	1	4	4	2	1	1	1	1	4	1	1	1	1	4
13	1	4	2	1	4	4	1	1	4	2	1	1	2	1	2	1
14	1	1	1	1	1	1	1	1	1	1	1	1	1	1	2	1
15	1	1	1	1	1	1	1	1	1	1	1	4	1	2	1	1
16	1	1	1	1	1	1	1	1	1	1	1	1	1	1	1	1
17	1	1	1	1	1	1	1	1	1	1	1	1	1	1	1	1

	Compass Sector															
Radial Ring	49	50	51	52	53	54	55	56	57	58	59	60	61	62	63	64
1	1	1	1	1	1	1	1	1	1	1	1	1	1	1	1	1
2	1	1	1	1	1	1	1	1	1	1	1	1	1	1	1	1
3	1	1	1	1	1	1	1	1	1	1	1	1	1	4	1	1
4	1	4	4	2	1	1	4	2	1	4	4	4	4	4	1	1
5	4	4	2	2	1	4	4	2	1	1	1	1	1	1	1	1
6	4	2	2	1	4	4	4	4	4	4	4	1	1	1	1	1
7	4	2	2	1	4	4	4	4	4	4	1	1	1	1	1	1
8	1	4	2	1	4	4	4	2	2	1	1	1	1	1	2	2
9	4	2	2	1	4	2	1	4	1	4	1	1	1	2	2	2
10	4	2	2	1	1	1	1	1	4	4	1	1	1	1	1	1
11	4	4	4	2	2	2	1	4	4	4	2	2	1	4	2	2
12	4	4	2	2	2	2	1	4	2	1	1	2	2	1	4	2
13	4	4	2	2	2	1	1	4	2	1	4	2	1	4	1	1
14	1	4	4	2	2	1	1	4	1	4	1	1	1	1	1	1
15	1	4	2	1	2	1	1	2	1	1	2	2	2	1	2	1
16	1	1	1	1	1	1	1	1	1	1	1	1	1	1	1	1
17	1	1	1	1	1	1	1	1	1	1	1	1	1	1	1	1

Table B-8 CHRONC Input Parameters Used in the Peach Bottom Unmitigated LTSBO and STSBO with and without RCIC Blackstart Scenarios

Variable	Description	LTSBO	STSBO with RCIC Blackstart	STSBO without RCIC Blackstart
CHNAME	CHRONC Problem Identification	Peach Bottom with no Food-Chain Modeling	Peach Bottom with no Food-Chain Modeling	Peach Bottom with no Food-Chain Modeling
CDFRM	Farmland Decontamination Cost			
	Level 1	1330	1330	1330
	Level 2	2960	2960	2960
CDNFRM	Nonfarmland Decontamination Cost			
	Level 1	7110	7110	7110
	Level 2	19000	19000	19000
CRTOCR	Critical Organ for CHRONC Phase	L-ICRP60ED	L-ICRP60ED	L-ICRP60ED
DPRATE	Property Depreciation Rate	0.2	0.2	0.2
DLBCST	Hourly Labor Cost for Decontamination Worker	84000	84000	84000
DPFRCT	Farm Production Dairy Fraction	0	0	0
DSCRLT	Long-Term Phase Dose Criterion	0.005	0.005	0.005
DSCRTI	Intermediate-Phase Dose Criterion	100000	100000	100000
DSRATE	Societal Discount Rate for Property	0.12	0.12	0.12
DSRFCT	Decontamination Factors			
	Level 1	3	3	3
	Level 2	15	15	15
DUR_INTPHAS	Duration of the Intermediate Phase	0	0	0
EVACST	Emergency Phase Cost of Evac./Reloc.	172	172	172
EXPTIM	Maximum Exposure Time	1580000000	1580000000	1580000000
FDPATH	COMIDA2 vs. MACCS Food Model Switch	OFF	OFF	OFF
FRACLD	Fraction of Area that is Land	1	1	1
FRCFRM	Fraction of Area Used for Farming	1	1	1
FRFDL	Fraction of Decontamination Cost for Labor			
	Level 1	0.3	0.3	0.3
	Level 2	0.35	0.35	0.35
FRFIM	Farm Wealth Improvements Fraction	0.25	0.25	0.25
FRMPRD	Average Annual Farm Production	0	0	0
FRNFIM	Nonfarm Wealth Improvements Fraction	0.8	0.8	0.8
FRNFDL	Nonfarm Labor Cost Fraction			
	Level 1	0.7	0.7	0.7
	Level 2	0.5	0.5	0.5
GWCOEF	Long-Term Groundshine Coefficients			
	Term 1	0.5	0.5	0.5
	Term 2	0.5	0.5	0.5
KSWTCH	Diagnostic Output Option Switch	0	0	0
LBRRATE	Long-Term Breathing Rate	0.000266	0.000266	0.000266
LGSHFAC	Long-Term Groundshine Protection Factor	0.18	0.18	0.18
LPROTIN	Long-Term Inhalation Protection Factor	0.46	0.46	0.46

Variable	Description	LTSBO	STSBO with RCIC Blackstart	STSBO without RCIC Blackstart
LVLDEC	Number of Decontamination Levels	2	2	2
NGWTRM	Number of Terms in Groundshine Weathering Equation	2	2	2
NRWTRM	Number of Terms in Resuspension Weathering Equation	3	3	3
POPCST	Per Capita Cost of Long-Term Relocation	12000	12000	12000
RELCST	Relocation Cost per Person-Day	172	172	172
RWCOEF	Long-Term Resuspension Factor Coefficients			
	Term 1	0.00001	0.00001	0.00001
	Term 2	0.0000001	0.0000001	0.0000001
	Term 3	0.0000009	0.0000009	0.0000009
TFWKF	Fraction Farmland Worker Time in Contaminated Zone			
	Level 1	0.1	0.1	0.1
	Level 2	0.33	0.33	0.33
TFWKNF	Fraction Nonfarmland Worker Time in Contaminated Zone			
	Level 1	0.33	0.33	0.33
	Level 2	0.33	0.33	0.33
TGWHLF	Groundshine Weathering Half-Lives			
	Term 1	16000000	16000000	16000000
	Term 2	2800000000	2800000000	2800000000
TIMDEC	Decontamination Times			
	Level 1	5184000	5184000	5184000
	Level 2	10368000	10368000	10368000
TMPACT	Time Action Period Ends	31600000	31600000	31600000
TRWHLF	Resuspension Weathering Half-Lives			
	Term 1	16000000	16000000	16000000
	Term 2	160000000	160000000	160000000
	Term 3	1600000000	1600000000	1600000000
VALWF	Value of Farm Wealth	9040	9040	9040
VALWNF	Value of Nonfarm Wealth	210000	210000	210000

NRC FORM 335
(12-2010)
NRCMD 3.7

U.S. NUCLEAR REGULATORY COMMISSION

BIBLIOGRAPHIC DATA SHEET

(See instructions on the reverse)

1. REPORT NUMBER
(Assigned by NRC, Add Vol., Supp., Rev., and Addendum Numbers, if any.)

NUREG/CR-7110, Volume 1

2. TITLE AND SUBTITLE

State-of-the-Art Reactor Consequence Analyses Project, Volume 1, Peach Bottom Integrated Analysis

3. DATE REPORT PUBLISHED

MONTH	YEAR
01	2012

4. FIN OR GRANT NUMBER

5. AUTHOR(S)

Nathan Bixler, Randall Gauntt, Joseph Jones, Mark Leonard (dycoda LLC)

6. TYPE OF REPORT

NUREG

7. PERIOD COVERED *(Inclusive Dates)*

8. PERFORMING ORGANIZATION - NAME AND ADDRESS *(If NRC, provide Division, Office or Region, U.S. Nuclear Regulatory Commission, and mailing address; if contractor, provide name and mailing address.)*

Sandia National Laboratories
Albuquerque, New Mexico 87185
Operated for the U.S. Department of Energy

9. SPONSORING ORGANIZATION - NAME AND ADDRESS *(If NRC, type "Same as above"; if contractor, provide NRC Division, Office or Region, U.S. Nuclear Regulatory Commission, and mailing address.)*

Division of Systems Analysis
Office of Nuclear Regulatory Research
U.S. Nuclear Regulatory Commission
Washington DC 20555-0001

10. SUPPLEMENTARY NOTES

11. ABSTRACT *(200 words or less)*

The evaluation of accident phenomena and the offsite consequences of severe rea ctor accidents has been the subject of considerable research by the U.S. Nuclear Regulatory Commission (NRC) over the last several decades. As a consequence of this research focus, analyses of severe accidents at nuclear power reactors are more detailed, integrated, and realistic than at any time in the past. A desire to leverage this capability to address conserva tive aspects of previous reactor accident analysis efforts was a major motivating factor in the genesis of the State of the Art Re actor Consequence Analysis (SOARCA) project. By applying modern analysis tools and techniques, the SOARCA project developed a body of knowledge regarding the realistic outcomes of severe reactor accidents. To accomplish this objective, the SOARCA project used integrated modeling of accident progression and offsite consequences using both state of-the-art computational analysis tools and best modeling practices drawn from the collective wisdom of the severe accident analysis community. Th is study focused on providing a realistic evaluation of accident progression, source term, and offsite consequences for t he Peach Bottom Nuclear Power Station. By using the most current emergency preparedness practices, plant capabilities, an d best available modeling, these analyses are more detailed, integrated, and realistic than past analyses. These analyses a lso consider all mitigative measures, contributing to a more realistic evaluation.

12. KEY WORDS/DESCRIPTORS *(List words or phrases that will assist researchers in locating the report.)*

State-of-the-Art Reactor Consequence Analyses
SOARCA
Severe Reactor Accidents
Peach Bottom Analysis

13. AVAILABILITY STATEMENT

unlimited

14. SECURITY CLASSIFICATION

(This Page)

unclassified

(This Report)

unclassified

15. NUMBER OF PAGES

16. PRICE

Printed
on recycled
paper

Federal Recycling Program

UNITED STATES
NUCLEAR REGULATORY COMMISSION
WASHINGTON, DC 20555-0001

OFFICIAL BUSINESS